Joint Conference of
9th Asia-Pacific EPR/ESR Society Symposium
1st International EPR (ESR) Society Symposium
53rd SEST Annual Meeting

APES - IES - SEST 2014

12-16 November 2014
Todaiji Culture Center
Nara Prefectural New Public Hall
Nara, Japan

Hosted by

Asia-Pacific
EPR/ESR Society

International
EPR (ESR) Society

The Society of
Electron Spin Science
and Technology

NOV.11(TUE)

- 13:00-16:30: SEST Exective Council Meeting @NWU (13:00-16:30)
- 18:00-21:00: APES Council Meeting (18:00-21:00)

NOV.12 (WED)

Kinsyo Hall

- Registration Starts at 11:00-
- 10:30-12:30: SEST Council Meeting (10:30-12:30) @NWU
- 13:00-13:15: Opening of APES-IES-SEST2014 (13:00-13:15)
- 13:15-14:00: PL-1 (Tutorial) K. Möbius (13:15-14:00)
- 14:00-14:45: PL-2 M. Oshikawa (14:00-14:45)
- Break (14:45-15:10)
- 15:10-15:55: PL-3 G. Smith (15:10-15:55)
- 15:55-17:35: SEST Excellent Presentation Award competition (5×20 min.) (15:55-17:35)
- 17:35-18:00: Morino Foundation Presentation (17:35-18:00)
- 18:30-20:30: Welcome reception @ Nara Women's University (18:30-20:30)

NOV.13(THU)

Kinsyo Hall

- 9:00-9:45: PL-4 E.Bagryanskaya (9:00-9:45)
- Break (9:45-10:10)
- 10:10-12:05: Session 1 Spin Chemistry (10:10-12:05)
- 12:05-13:30: ☆ LUNCH ☆ (12:05-13:30)
- 13:30-14:15: PL-5 (Memorial) L. Berliner (13:30- 14:15)
- Break (14:15-14:25)
- 14:25-16:15: Session 3 Quantum Spin System (14:25-16:15)
- Break (16:20-16:45)
- 16:45-17:35: APES Young Scientist Award Presentation (16:45-17:35)
- 17:35-18:10: APES General Meeting (17:35-18:10)
- 18:30-20:30: Bruker Seminar @ Nara Prefectural New Public Hall (18:30-20:30)

Small Hall

- 10:10-12:00: Session 2 Dosimetry & Dating (10:10-12:00)
- 14:25-16:20: Session 4 In vivo imaging (14:25-16:20)

NOV.14 (FRI)

Kinsyo Hall

- 9:00-9:45: PL-6 T. Prisner (9:00-9:45)
- 9:45-10:30: PL-7 J. Freed (9:45-10:30)
- Break (10:30-10:55)
- 10:55-12:50: Session 5 DNP (10:55-12:50)
- 13:00-14:00: ☆ LUNCH ☆ (13:00-14:00)
- 14:00-15:00: SEST General Meeting SEST Award Ceremony (14:00-15:00)
- 15:00-17:10: SEST Award & SEST Young Investigator Award presentation (15:00-17:10)
- 17:30-19:25: Poster Session @ Nara Prefectural New Public Hall (17:30-19:25)
- 19:00-21:00: IES Council Meeting (19:00-21:00)
- 19:40-21:40: SEST + APES Young scientist Meeting (19:40-21:40) @ NWU

Small Hall

- 10:55-13:00: Session 6 Photo synthesis & Protein distance measurement (10:55-13:00)

NOV.15 (SAT)

Kinsyo Hall

- 9:00-9:55: IES General Meeting IES Award Ceremony (9:00-9:55)
- 9:55-10:30: IES Gold Medal D. Britt (9:55-10:30)
- Break (10:30-10:55)
- 10:55-13:00: Session 7 IES Awards Session (10:55-13:00)
- 13:00-19:00: Excursion (13:00-)
- 19:00-21:00: Banquet @ Restaurant Half Time in Nara National Museum (19:00-21:00)

Small Hall

- 10:55-12:45: Session 8 Instrumen tation (10:55-12:45)

NOV.16 (SUN)

Kinsyo Hall

- 9:00-9:45: PL-8 H. Swartz (9:00-9:45)
- Break (9:45-10:10)
- 10:10-12:05: Session 9 Biology (10:10-12:05)
- 12:05-13:30: ☆ LUNCH ☆ (12:05-13:30)
- 13:30-15:20: Session 11 Material Science, Electric Devices, Spintronics (13:30-15:20)
- Award Ceremony Closing (15:30-16:00)

Small Hall

- 10:10-12:10: Session 10 Quantum Computing (10:10-12:10)
- 13:30-15:30: Session 12 Free radicals and Theory (13:30-15:30)

NWU :Nara Women's University

Joint Conference of
9th Asia-Pacific EPR/ESR Society Symposium
1st International EPR (ESR) Society Symposium
53rd SEST Annual Meeting

APES - IES - SEST 2014

12-16 November 2014
Todaiji Culture Center
Nara Prefectural New Public Hall
Nara, Japan

Hosted by

Asia-Pacific
EPR/ESR Society

International
EPR (ESR) Society

The Society of
Electron Spin Science
and Technology

Welcome Address

On behalf of the organizing committee, we would like to welcome all participants for the Joint Conference of APES2014, IES and SEST2014 (APES-IES-SEST2014, Nov. 12 (Wed) - 16 (Sun), 2014 at Todaiji Culture Center in Nara, Japan), where each stands for APES2014: Asia-Pacific EPR/ESR Society (APES) Symposium 2014, IES2014: International EPR(ESR) Society (IES) Symposium, SEST2014: the 53rd The Society of Electron Spin Science and Technology (SEST) Annual Meeting. We would like to express our sincere thanks to APES, IES, SEST and all participants for the supports.

Let us overview the brief history. For APES2014, this is the ninth symposium following the successful APES 1997 (Hong Kong, China), APES 1999 (Hangzhou, China), APES 2001 (Kobe, Japan), APES 2004 (Bangalore, India), APES 2006 (Novosibirsk, Russia), APES 2008 (Cairns, Australia), APES 2010 (Jeju, Korea), and APES 2012 (Beijing, China). APES series is in the second round and it is coming back to Japan again. For International EPR(ESR) Society Symposium, this will be the first symposium hosted by IES and we are very proud to have it in the old capital of Japan. We would like to extend to all IES members our warmest welcome to participate in this exciting event. Finally this is also the 53 rd Anneal Meeting of SEST, and we would like to welcome Japanese EPR/ESR scientists to participate and exchange ideas with scientists from all over the world.

APES-IES-SEST2014 is intended to stimulate discussions on the forefront of research in all aspects of EPR/ESR ranging from theoretical and experimental advances in CW EPR/ESR, pulsed EPR/ESR, high frequency and high field EPR/ESR, ENDOR, time resolved EPR/ESR, FMR, EPRI, CIDEP and ODMR to applications in medicine, biology, chemistry, physics, materials science and nanotechnology.

APES-IES-SEST2014 will be an excellent place for exchanging scientific ideas with strong friendship among the participants from not only Asia-Pacific region but all over the world. We sincerely hope that the scope of the symposium will serve the interest of the scientific community, as well as the industry and the general public. Finally we would like to extend our welcome to all participants and sponsors of the event.

Hitoshi Ohta, Chairperson of APES and IES2014

Atsushi Kajiwara, Chairperson of SEST2014

Message from APES President

Dear friends and colleagues;

On behalf of the Asia-Pacific EPR/ESR Society and the Council, we would like to welcome you all to the Joint Conference of APES2014, IES and SEST2014 in Nara, Japan.

We are proud to continue the APES in a series of former international meetings, starting in 1997 with the first conference held in Hong Kong, China, organized by Founder President, Professor Czeslaw Rudowicz who was Faculty of Department of Physics & Materials Science, City University of Hong Kong. The first conference was followed by APES1999 (Hangzhou, China), APES2001 (Kobe, Japan), APES2004 (Bangalore, India), APES2006 (Novosibirsk, Russia), APES2008 (Cairns, Australia), APES2010 (Jeju, Korea) and the latest APES2012 (Beijing, China). The APES Project underlain by Dr. Rudowicz's idea was in that an international conference organized by APES provides a foundation for the scientific exchange not only among not only Asian countries but also with leading countries in the field of electron magnetic resonance and related field, hoping that the Project helps Asian countries proceeding toward their own goals or aims in terms of scientific promotion. We are still on the way and we will strive to keep going along the line with relying on each other for friendship and mutual support.

In terms of making the joint effort, the Joint Conference reminds us of ISESS2013(2nd SEST Intn'l Conference) held in Sendai, July 23-25, 2013, organized by late Professor Seigo Yamauchi, Tohoku University, who was the last President of IES. Late Professor Yamauchi as the IES President had dreamed on a joint intn'l conference. Of course, such a joint conference won't just happen. In this context, we appreciate all the efforts of IES and Conference Chairpersons to make this happen. Without their efforts and help, the Joint Conference setup wouldn't have been possible.

We note that APES-IES-SEST2014 has been carefully organized and is intended to give stimuli to scientific advance in emerging fields. We are encouraged in seeing many young scientists and students presenting highly interesting work. We look forward to exciting lectures with lively discussions and impressive poster contributions.

Finally, we would like to thank Conference Chairpersons and all the members of Local Organizing Committee for their efforts to make such an impressive setup for the Joint Conference. We are also grateful for all the sponsors generously supporting the Conference.

We are looking forward to meeting you all in Nara, Japan.

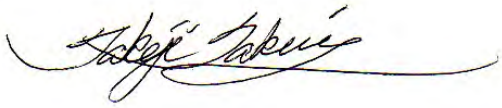

Takeji Takui, APES President 2012-14

Message from IES President

The International EPR (ESR) Society (IES) is extremely grateful to Profs. Hitoshi Ohta and Atsushi Kajiwara for their initiative to integrate IES into the 2014 joint conference of the Asia-Pacific EPR/ESR Society and the Society of Electron Spin Science and Technology. This performance is a premiere in IES history and, on behalf of IES, it is my pleasure to extend a warm welcome to all participants of APES-IES-SEST 2014.

By its very nature, the joint meeting blends together an exciting mixture of EPR topics at the forefront of research areas in physics and chemistry, biology and medicine, material science and nanotechnology. The outstanding program is designed to encourage interaction and discussion among young scientists and prominent contributors from the various fields. I am confident that this 'crossing of borders' will be further intensified by personal contacts between the participants when encountering in the unique environment of Todaiji Culture Center in Nara.

IES is particularly proud that during the APES-IES-SEST 2014 meeting several IES Awards will be presented in dedicated sessions to their winners, such as Poster Awards for Young Scientists, Young Investigator Awards, Gold and Silver Medal Awards, Fellowship Award. I am thankful to the Program Committee that time slots have been reserved in the program for the prize winners to introduce their work.

I wish all of us a stimulating conference with exciting lectures, challenging questions, interesting results, hot discussions during the poster sessions and elsewhere.

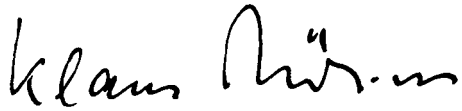

Klaus Möbius, President of IES

Message from SEST President

Welcome to APES-IES-SEST2014, the Joint Conference of Asia-Pacific EPR/ESR Society (APES) Symposium 2014, International EPR(ESR) Society (IES) Symposium, and the 53rd Annual Meeting of The Society of Electron Spin Science and Technology (SEST). As a president of SEST, it is my great pleasure that the 53rd Annual Meeting of SEST (SEST2014) is held in the form of a joint conference with APES2014 and IES Symposium.

SEST is an interdisciplinary society in Japan, which covers wide range of domain related to the electron spin sciences and technology. Since the establishment in 2002, SEST has been played a large role in the progress of this research area and in cultivation of scientists and engineers of next generation through annual domestic meeting, international meeting of every 5 years, commendation of achievements remarkable scientists, bulletin publication of 2 times a year, several educational activities related to ESR, etc. It is a very meaningful thing for SEST members to have an opportunity to present their results internationally in this joint conference. I would like all participants to aggressively discuss about their results each other and get stimulation very much. Furthermore, I hope that everybody obtain a hint to lead to the development of their researches in this conference. I wish this conference is fruitful for all participants and the participants fully enjoy historical place Nara in this nice season.

Finally, I would like to sincerely thank Professor Hitoshi Ohta, Professor Atsushi Kajiwara, and members of organizing committee for preparations of this exciting conference.

Keizo Takeshita
President, The Society of Electron Spin Science and Technology (SEST)

The Morino Foundation for Molecular Science

Koichi M. T. Yamada‡

Professor Yonezo Morino (1908* –1995+), an outstanding molecular scientist in Japan, founded the Morino Foundation for Molecular Science (or expressed simply as "the Morino Foundation") in 1985 donating his personal property. The main intention of the foundation is to encourage young scientists of great promise, in the field of the molecular science, by supporting them financially. On his death in 1995, the fund received a rich legacy. Furthermore his wife, Mrs. Yoshi Morino, donated to the Morino Foundation all her inheritance on her death in 2005. The scientific work of Professor Morino is summarized in a special issue of the *Journal of Molecular Structure* in 1995, by Hirota, Kimura, Kuchitsu, and Tanimoto. The term "**Molecular Science**" was introduced in Japan by Professor Morino and others in early 1960's and the establishment of the Institute of Molecular Science in Okazaki, 1975, is a brilliant result of their endeavor.

Presently, the Morino Foundation supports four kinds of activities. The first one is the **Morino Lecture**. We invite excellent scientists from overseas and give young Japanese scientists chances to discuss directly with them. The first Morino Lecturer was Prof. Polanyi in 1986. We are very proud that we had invited him one year earlier than he got the Novel prize. Since then, we invite a few scientists each year as the Morino Lecturer.

The second activity is to offer **Research Funds** to promising young molecular scientists. Each year two or three awardees are selected.

The third activity is the support for **International Conferences** organized by molecular scientists in Japan.

The fourth activity is the support for **Traveling Expenses** to the molecular scientists in Japan who wish to report their results at the international meetings held abroad.

If you wish to have any support from the Morino Foundation, please contact the steering committee.

‡Chairman of the steering committee of the Morino Foundation; kmt.yamada@aist.go.jp

Committee

Honorary Chairs

Takui, Takeji (Japan)	Utsumi, Hideo (Japan)

Advisory Committee

Anzai, Kazunari (Japan)	Salikhov, Kev (Russia)
Lubitz, Wolfgang (Germany)	Swartz, Harold (USA)
Murai, Hisao (Japan)	Tero-Kubota, Shozo (Japan)
Ozawa, Toshihiko (Japan)	Zhao, Baolu (China)

Organizing Committee

Ohta, Hitoshi (APES & IES chair) (Japan)	Kajiwara, Atsushi (SEST Chair) (Japan)
Tajima, Kunihiko (Treasurer) (Japan)	Okubo, Susumu (Secretary) (Japan)
Hosokoshi, Yuko (Japan)	Matsuoka, Yuki (Japan)
Kobori, Yasuhiro (Japan)	Ohmichi, Eiji (Japan)
Fujiwara, Yasubumi (Japan)	Sakurai, Takahiro (Japan)
Hagiwara, Masayuki (Japan)	Sato, Kazunobu (Japan)
Hara, Shigeo (Japan)	Tominaga, Keisuke (Japan)
Hijii, Keigo (Japan)	

Program Committee

Nakamura, Toshikazu (Program Chair) (Japan)	Kikuchi, Hikomitsu (Japan)
Arata, Toshiaki (Japan)	Kobori, Yasuhiro (Japan)
Demishev, Sergey (Russia)	Kuroda, Shinichi (Japan)
Fujiwara, Toshimichi (Japan)	Lee, Masaichi Chang-il (Japan)
Hanson, Graeme (Australia)	Mino, Hiyoyuki (Japan)
Hirata, Hiroshi (Japan)	Mishra, Kaushala Prasad (India)
Hirayama, Aki (Japan)	Nojiri, Hiroyuki (Japan)
Ichikawa, Kazuhiro (Japan)	Sato, Kazunobu (Japan)
Ikoma, Tadaaki (Japan)	Smith, Graham (UK)
Inanami, Osamu (Japan)	Tajima, Kunihiko (Japan)
Kataev, Vladislav (Germany)	Yamanaka, Chihiro (Japan)

International Committee (APES)

Bagryanskaya, Elena (Russia)	Nakamura, Toshikazu (Japan)
Bhat, Subray (India)	Ohta, Hitoshi (Japan)
Drew, Simon (Australia)	Rudowicz, Czeslaw (Poland)
Dzuba, Sergei (Russia)	Sato, Kazunobu (Japan)
Lee, Hong-In (Korea)	Takui, Takeji (Japan)
Li, Yong (China)	

International Committee (IES)

Berliner, Lawrence (USA)	Möbius, Klaus (Germany)
Freed, Jack (USA)	Ohta, Hitoshi (Japan)
Misra, Sushil (Canada)	Smirnova, Tatyana (USA)

National Committee (SEST)

Hirata, Hiroshi (Japan)	Murai, Hisao (Japan)
Ichikawa, Kazuhiro (Japan)	Nakamura, Toshikazu (Japan)
Kawai, Akio (Japan)	Sato, Kazunobu (Japan)
Kobori, Yasuhiro (Japan)	Takeshita, Keizo (Japan)

Table of Contents

- **Scientific Program**
- **Venue**
- **Events**
- **General Information**
- **Sponsors**

1. Plenary Lecture (PL) 2

(PL-1) **Magic Matrix Effects on Protein Dynamics Decoded by High-Field EPR**

Klaus Möbius

(PL-2) **Recent Progress in Theory of ESR in Strongly Correlated Spin Systems**

Masaki Oshikawa

(PL-3) **Very High Sensitivity Orientational PELDOR**

Graham Smith, Johannes McKay, Claire Motion, Paul Cruickshank, Robert Hunter, David Bolton,Duncan Robertson, Hassane El Mkami, Richard Wylde, Michael Stevens, David Norman

(PL-4) **The New Spin Probes for Biochemical Applications**

Elena Bagryanskaya

(PL-5) **Harden M. McConnell - the Life of a Giant in Magnetic Resonance**

Lawrence J. Berliner

(PL-6) **Overhauser Dynamic Nuclear Polarization at a Magnetic Field of 9.2 T**

Thomas F. Prisner, Vasyl Denysenkov, Petr Neugebauer, Jan Krummenacker

(PL-7) **Protein Dynamic Structure Revealed by High Sensitivity Pulse Dipolar ESR Distance Measurements**

Jack H. Freed

(PL-8) **Clinical Applications of EPR**

Harold M. Swartz, Ann B. Flood, Benjamin B. Williams, Steven G. Swarts, Oleg Grinberg, Jason Sidabras

2. APES Young Scientist Award Lecture (APES YSA) 10

(APES YSA-1) **Nanoscale magnetic resonance with single electron spin sensor under ambient conditions**

Fazhan Shi, Xi Kong, Pengfei Wang, Tobias Staudacher, Friedemann Reinhard, Joerg Wrachtrup and Jiangfeng Du

(APES YSA-2) **Towards the structural design of piperidine nitroxides for in vivo measurement probe**

Toshihide Yamasaki, Kiyoshi Sakai, and Ken-ichi Yamada

3. SEST Award & SEST Young Investigator Award Lecture (SEST AL) 12

(SEST AL-1) **Electron Spin Resonance Studies of Organic Electronic Materials and Devices**

Shin-ichi Kuroda

(SEST AL-2) **In Vivo EPR Imaging Studies of a Brain Disease Mouse Model**

Hirotada Fujii

(SEST AL-3) **High-frequency ESR Studies of Molecule-based Conductors and Magnets**

Yugo Oshima

(SEST AL-4) **Time-Resolved Spectroscopic Study on Paramagnetic Intermediates Generated by Photochemical Reactions**

Tomoaki Yago

4. IES Award Lecture (IES AL) 16

(IES AL-1) **EPR Investigations of Photosynthetic and Bioenergy-Related Enzymes**

R. David Britt

(IES AL-2) **Recent Development of the PELDOR Theory**

Kev M. Salikhov

(IES AL-3) **Ferromagnetic Resonance Studies of Spin-Orbit Effects in Heavy Atom Organic Radical Ferromagnets**

Stephen Hill, Komalavalli Thirunavukkuarasu, Stephen M. Winter and Richard T. Oakley

(IES AL-4) **Quasi-Optical Pulsed EPR and ENDOR at very high Frequencies**

Johan van Tol

(IES AL-5) **The structure of nature's water splitting catalyst prior to O-O bond formation: an EPR and DFT study**

Nicholas Cox, Marius Retegan, Frank Neese, Alain Boussac, Dimitrios A. Pantazis, Wolfgang Lubitz

(IES AL-6) **Dynamic and Electronic Characteristics of Photo-generated Radical Pairs Revealed by Real-time Observation of the Spin Dynamics**

Tomoaki Miura

5. Invited Lecture (IL) 22

(IL-1) **The Spin as Functional Probe in Metal Biocatalysis**

Wolfgang Lubitz

(IL-2) **Progress Toward Spin Teleportation: Reversible Photo-driven Reduction of a Stable BDPA Radical**

Michael R. Wasielewski, Brandon K. Rugg, Kristen E. Brown, and Matthew D. Krzyaniak

(IL-3) **Development of EPR Dosimetry from Micro to Nano-materials**

G.M. Hassan, E. Aboelezz, M.A. Sharaf, and A. El-Khodary

(IL-4) **Application of ESR in Quaternary geological dating**

Masashi Takada

(IL-5) **Probing the Spin Dynamics in Novel Iridium Oxides by sub-THz ESR**

Vladislav Kataev

(IL-6) **Organic Radical Approach to Quantum Spin Systems**

Yuko Hosokoshi, Hironori Yamaguchi, Kenji Iwase, Toshio Ono

(IL-7) **Application of ESR/Spin Trapping for Monitoring Free Radical Formation in Serum of β–Thalassemia with Iron Chelation Therapy**

N. P. Morales, P. Yamanont, S. Fucharoen

(IL-8) **Enhancing cancer treatment in animal models with near absolute O_2 imaging using longitudinal relaxation ratee (R_{1e}) with pulse EPR**

Howard J. Halpern, Gage H. Redler, Boris Epel, Martyna Elas, Eugene D. Barth, Charles A. Pelizzari, Ralph R. Weichselbaum, Victor Tormyshev

(IL-9) **Surface characterization by dynamic nuclear polarization NMR**

Songi Han, Alicia Lund, Ting Ann Siaw, John Franck, Chiyuan Cheng

(IL-10) **The interplay between spectral diffusion and dynamic nuclear polarization**

Akiva Feintuch, Yonatan Hovav, Daphna Shimon, Daniella Goldfarb and Shimon Vega

(IL-11) **Using pulsed and continuous-wave EPR spectroscopy in combination with X-ray crystallography to understand the structure and function of biomolecular machines**

Chris Kay

(IL-12) **Constructing a dynamic picture of Troponin from site directed spin labeling**

Louise J Brown, Phani R Potluri and Nicole M Cordina

(IL-13) **Excited Triplet States of Thiophene-Decorated Phenazines Probed by Time-Resolved EPR**

Hideto Matsuoka, Lisa Röck, Christoph Bannwarth, Stefan Grimme, Sigurd Höger and Olav Schiemann

(IL-14) **Biological Applications of High Sensitivity Electron Spin Resonance with High Spatial Resolution**

Mada Hashem, Avishai Mor, Periannan Kuppusamy, Robert Fluhr, and Aharon Blank

(IL-15) **Development and Applications of Pulsed EPR Oxygen Imaging in Cancer Research**

Shingo Matsumoto, Keita Saito, Chandramouli Gadisetti, Nallathamby Devasahayam, Sankaran Suburamanian, and Murali C. Krishna

(IL-16) **Insights into CO_2 Fixation, Global Warming and Healthy Coral Reefs**

Nina Dovalil, Michael Westphal, Lawrence Gahan, Marcel Maeder, Peter Comba, Graeme R. Hanson

(IL-17) ***In vivo* EPR/NMR Coimaging of Radical Probes: Advances and Challenges**

Jay L. Zweier, Rizwan Ahmad, Yangping Liu and Alexandre Samouilov

(IL-18) **Building up a synthetic quantum system spin by spin**

J. Wrachtrup

(IL-19) **Quantum Computation and Quantum Sensing based on Single Electron Spin in Diamond**

Jiangfeng Du

(IL-20) **Nuclear Hyperpolarization and Spin Entanglement in Phosphorescent Crystals at Level Anti-crossing Conditions**

Gerd Kothe, Tomoaki Yago, Michail Lukaschek, Jörg-Ulrich Weidner, Gerhard Link, David J. Sloop and Tien-Sung Lin

(IL-21) **Magnetoconductance in Photoconductive Thin Films of Perylene Bisimide**

C. E. Ambe, Y. Wakikawa, S. Yagai, and T. Ikoma

(IL-22) **Development of New Analytical Methods for Organic Devices: Applications of ESR to Transistors, Solar Cells and Light-Emitting Diodes**

Kazuhiro Marumoto

(IL-23) **ESR Study on Mechanism of Photocatalytic Synthesis of Phenols without Photosensitizer**

Haijun Yang, Min Jiang, Hua Fu and Yong Li

(IL-24) **Interaction of Cryoprotective Agents with Biological Membranes Studied by Pulsed EPR of Spin Labels**

S.A. Dzuba, N.P. Isaev, K.B. Konov, D.V. Leonov

(IL-25) **Dielectric Constant and Water Penetration Gradients along Transmembrane Peptide-Lipid Bilayer Interface**

Matthew Donohue, Maxim A. Voynov, Alex I. Smirnov, and Tatyana I. Smirnova

6. Oral Presentation (OP) 47

(OP-1) **Photoinitiated Radical Polymerization of Silane Coupling Agents as Studied by Pulsed EPR Spectroscopy**

Hirona Takahashi and Akio Kawai

(OP-2) **Substituent Dependence of Relaxation Processes in the Excited State of Vanadyl Porphyrins : Time-resolved EPR and Luminescence Study**

Motoko S. Asano, Tsubasa Asami, Kazuhito Tomiduka, Ken-ichi Yamashita, Ken-ichi Sugiura and Art van der Est

(OP-3) **Diagnostic of Reactive Oxygen Species (ROS) Induced in Water by Atmospheric Pressure Plasma for Plasma-based Sterilization**

Atsushi Tani, Satoshi Ikawa, Tomoko Ohshima, and Katsuhisa Kitano

(OP-4) **Effects of 0.10−10 Gy X-ray Irradiation on Eggshell Radical Production**

Kouichi Nakagawa

(OP-5) **Singlet-Triplet Transitions of ESR in Gapped Spin Systems**

Toru Sakai, Keigo Hijii, Susumu Okubo and Hitoshi Ohta

(OP-6) **High-field ESR and nuclear polarization of P donors in silicon at ultra-low temperatures**

Sergey Vasiliev, Jarno Järvinen, Janne Ahokas, Sergey Sheludyakov, Denis Zvezdov, Yutaka Fujii, Seitaro Mitsudo, Takao Mizusaki, Minchan Gwak, SangGap Lee, Soonchil Lee and Leonid Vlasenko

(OP-7) **Electron paramagnetic resonance (EPR) oximetry as a future diagnostic tool for head and neck cancer**

Håkan Gustafsson, Ajay Kale, Alexandru Dasu, Anders Lund and Karin Roberg

(OP-8) ***In vivo* imaging of nitroxyl radicals in a mouse using surface coil array and parallel EPR detection**

Ayano Enomoto and Hiroshi Hirata

(OP-9) **Toward applications of DNP using photo-excited triplet electrons**

Makoto Negoro, Kenichiro Tateishi, Shinsuke Nishida, Akinori Kagawa,Yasushi Morita, and Masahiro Kitagawa

(OP-10) **Dynamic Nuclear Polarization for Biological Solid-State NMR at High Fields and Low Temperatures**

Yoh Matsuki, Toshitaka Idehara, Yoshinori Tatematsu, Jagadishwar Sirigiri, Shinji Nakamura, and Toshimichi Fujiwara

(OP-11) **Maltose Binding Protein as Molten Globule and in the Native State**

Mohammed Chakour1, Jörg Reichenwallner, Chen Chen, Bemjamin Selmke, Sandra Theison, Rusha Chakraborty, S. Indu, Raghavan Varadarajan, Dariush Hinderberger, and Wolfgang E.Trommer

(OP-12) **High power Nanosecond Pulse Generation for the Pulsed ESR by using a Gyrotron as a Radiation Source**

S. Mitsudo, C. Umegaki , T. Tanaka and Y. Fujii

(OP-13) **Spectroscopic Investigation of Spin-Dependent Optoelectronic Pathways in Organic Devices**

T. L. Keevers, A. Danos, W. Baker, H. Malissa, C. Boehme and D. R. McCamey

(OP-14) **New Approach to ENDOR Analysis for Manganese(II)-Substituted Soybean Lipoxygenase with A Non-Coordinated Substrate**

Masaki Horitani, George Cutsail III, Cody A. Marcus Carr, Adam R Offenbacher, Judith P. Klinman and Brian M. Hoffman

(OP-15) **EPR elucidation of bacterial terminal oxidase building in multi-heme centers**

Catharina T. Migita, Hiroshi Miura, Norio Miyake, Kouki Kimiya and Kazunobu Matsushita

(OP-16) **Exploiting Quantum Effects Using Electron-Nuclear Coupled Molecular Spin Systems**

Robabeh Rahimi Darabad, Daniel K. Park, Stephane Labruyere, Jonathan Baugh1, Kazunobu Sato, Takeji Takui and Raymond Laflamme

(OP-17) **Electron-Hole Dissociations and Electronic Coupling Influenced by Alkyl Side Chains in the Photovoltaic Polyalkylthiophene:PCBM Interface**

Yasuhiro Kobori, Taku Miura

(OP-18) **Evaluation of Dysprosium(III)-Copper(II) Exchange Coupling Parameters and Relation with the Bridging Geometry**

Yumi Ida, Takayuki Ishida, Soumavo Ghosh, Ashutosh Ghosh, and Hiroyuki Nojiri

(OP-19) **EMR related problems in modeling properties of single-ion and single-molecule magnets (SIM/SMM) - interplay between the crucial notions**

Czesław Rudowicz, and Mirosław Karbowiak

7. SEST Excellent Presentation Award Competition (SEST EPA) 66

(SEST EPA-1) **Er-concentration and charge carrier effects on GaAs;Er,O revealed by X-band ESR**

F. Elmasry, S. Okubo, H. Ohta, and Y. Fujiwara

(SEST EPA-2) **ENDOR Studies on Relationship between the Hydrogen Bonding Network and Ca^{2+} of the Mn Cluster in Photosystem II**

Hiroki Nagashima, Yoshiki Nakajima, Jian-Ren Shen and Hiroyuki Mino

(SEST EPA-3) **Development of fluorescent probe for sensitive detection of ascorbic acid**

Yuta Matsuoka, Kei Ohkubo, Toshihide Yamasaki, Hiroshi Ohtabu, Tomonori Shirouzu, Shunichi Fukuzumi, Ken-ichi Yamada

(SEST EPA-4) **Time-Resolved EPR and Photochemical Study on the Inclusion System of Anthraquinones and Cyclodextrins**

Zhebin Fu, Moe Sasaki, Rina Sato, Akira Naruoka, Akio Kawai and Hisao Murai

(SEST EPA-5) **Magnetoconductance of Pentacene/C60-bilayaer Solar Cell**

T. Omori, Y. Wakikawa, T. Miura, Y. Yamaguchi, K. Nakayama and T. Ikoma

8. Poster Presentation (P) 71

Enclosed poster No. (☐) indicates entry to APES2014 Poster Award and IES Poster Award

(P-1) **EPR Spin Probe Investigation of Surface Structure Analyses of Skin**

Kouichi Nakagawa, S. Minakawa, and D. Sawamura

(P-2) **Localization of EPR probes and labeled drugs in nanocarriers and their penetration and release in skin**

S. B. Lohan, N. Icken, C. Teutloff, R. Bittl, J. Lademann, E. Fleige, M. Unbehauen, R. Haag, S. F. Haag, M. C. Meinke

(P-3) **EPR studies of the conformational states of Aurora-A kinase's activation loop**

Maria Grazia Concilio, Alistair J Fielding

(P-4) **The Cu^{2+} coordination environment of α-synuclein revealed by site-specific isotopic labeling of 56 residue N-terminal peptides**

Simon C. Drew

(P-5) **Investigation of Glass Surface Coating for *In-situ* Electron Paramagnetic Resonance Measurement of Reactive Oxygen Species in Adherent Cells**

Takahiro Ando and Yoshiki Yonamoto

(P-6) **Competitive binding of metal ions to the octarepeat region of human prion protein**

Masahiro Yagi, Kazuya Iwama, Haruto Onda and Wakako Hiraoka

(P-7) **ESR Spectroscopy on Metal binding Sites in Cu^{2+}-Transporting ATPase Protein**

Satoshi Yasuda, Takuya Horimoto, Hiroaki Daimon, Yasuhiro Ueda, Naoyuki Kuwabara, and Toshiaki Arata

(P-8) **Catecholase Activity of a Distant Dicopper Complex and Photodissociation of Ru(III) Nitrosyl Complex: Monitoring by Electron Paramagnetic Resonance**

Shuranjan Sarkar, Jamghoon Cho, and Hong-In Lee

(P-9) **Multi-Frequency, Multi-technique Pulsed EPR Characterization of the Copper-Amyloid Peptides Relevant to Alzheimer's Disease**

Sun Hee Kim

(P-10) **Effects of Nanoscale Curvature on Structure, Dynamics, Phase Properties and Surface Electrostatics of Lipid Bilayers**

Alex I. Smirnov, Amir Koolivand, Antonin Marek, and Maxim A. Voinov

Presentations by High School Students (P-11, P12, P13)

(P-11) **ESR Study by High School Students (1) Evaluation of Ultraviolet (UV)-Protection Properties of Sun Protection Cosmetics**

Hiroki Nakajima, Mai Okahashi, Yuki Shimizu, Atsushi Kajiwara

(P-12) **ESR Study by High School Students (2) Detection of Paramagnetic Species in the Familiar Foods by ESR**

Hiroki Nakajima, Rina Aoi, Asuka Itakura, Yuma Tanaka, Atsushi Kajiwara

(P-13) **ESR Study by High School Students (3) Detection of Paramagnetic Species in the Insects by ESR**

Hiroki Nakajima, Wakana Kakuo, Yuumi Mabuchi, Atsushi Kajiwara

(P-14) **Nitric oxide mediates TLR4-NF-kB signaling in mice with DSS-induced colitis**

Xin Tun, Keiji Yasukawa and Ken-ichi Yamada

(P-15) **High-Frequency ESR Measurements of Shallow Doped Si:P at Low Temperatures and Their Extension to Lower Temperatures for High $\mu_B B/k_B T$**

K. Morimoto, Y. Fujii, S. Mitsudo, T. Mizusaki, H. Kikuchi, A. Fukuda, A. Matsubara, T. Ueno, M. Gwak, S.G. Lee, S. Lee, Tadaaki Saito and S. Vasiliev

(P-16) **Simultaneous and spectroscopic imaging of free radical intermediates using in vivo dynamic nuclear polarization-MRI**

Fuminori Hyodo, Shinji Ito, Keiji Yasukawa, Hinako Eto, Ryoma Kobayashi and Hideo Utsumi

(P-17) **Estimation of relative reaction rate of hydroxy radical with anti-oxidants using ESR spin trapping combined with water radiolysis**

Seiko Nakagawa and Masayuki Sekiguchi

(P-18) **ESR study on thermal metamorphism of kerogen in sedimentary rocks**

Mayu Suzuki, Chihiro Yamanaka

(P-19) **Radiation-induced Defects in Artificially Weathered Quartz and Relation to the OSL (Optically Stimulated Luminescence) Properties**

Chihiro Yamanaka, Akira Osada and Masashi Takada

(P-20) **The decisive factor of clay quality and color of Bizen pottery**

Yuki Matsuoka, Ko Furukawa and Toshikazu Nakamura

(P-21) **EPR-Application in dermatology - in vitro and in vivo investigations**

M. C. Meinke, A. Friedrich, A. C. Lauer, S. Arndt, S. Ahlberg, S. F. Haag, S. B. Lohan, J. Lademann

(P-22) **Mechanism Study on Nitration of Arylboronic Acids with Nitrates by ESR**

Haijun Yang, Min Jiang, Yong Li and Hua Fu

(P-23) **4'-CyanoPLP Presents Better Prospect for the EPR Detection of Elusive Cyclic Intermediate Radical in the Reaction of Lysine 5,6-aminomutase**

Amarendra Nath Maity and Shyue-Chu Ke

(P-24) **Multifrequency (X-band to W-band) CW EPR of the crude oil and by-products**

Eduardo Di Mauro, Marilene Turini Piccinato and Carmen Luisa Barbosa Guedes

(P-25) **Evaluation of Anti-oxidative Materials of 13 Mushrooms by ESR**

Tomomi Kanno, Kumiko Yamamoto, Etsuko Harada, Hiromi Kameya, Mitsuko Ukai and Toshihiko Osawa

(P-26) **Ultrasound-induced activation of caged compounds**

Haruko Koura, Risa Fuji, Asuka Kato, Masato Mutoh and Wakako Hiraoka

(P-27) **Enhancement of vitamin D3-induced differentiation in PLB-985 cells by modulating oxidative stress**

Hiroaki Tanaka, Hiroyuki Kato, Omi Nawa, Asuka Kato, Masato Mutoh and Wakako Hiraoka

(P-28) **Correlation between number of C-C double bonds and relaxation times of polyenyl radicals as studied by CW-ESR spectroscopy**

Takatoshi Sawai, Yoji Yamaguchi

(P-29) **Radical reaction induced by UV-irradiated ketoprofen in liposomal membranes**

Shoko Okazaki, Takuro Nagata, Megumi Takemoto, Yusuke Shogomori, Ayako Hirata and Keizo Takeshita

(P-30) **Measurement of Density of Hydroxyl Radical Generation in Water Induced by Low-LET Radiation**

Yukihiro Ogawa, Ken-ichiro Matsumoto and Shingo Fujisaki

(P-31) **Superoxide radical scavenging activity of cooked rice as studied by HPLC-ESR spin-trapping measurements**

Tomoko Yamaguchi, Gen Httori, Kenji Kanaori, Kunihiko Tajima, Isamu Tachimoto

(P-32) **Direct ESR Observations of Radical Polymerization of N-Vinylcarbazole**

Ryosuke Matoba, Atushi Kajiwara

(P-33) **Electrochemical ESR Cell for Determination of Redox Potentials of Transient Radicals**

Tatsumi Tetsuya and Atsushi Kajiwara

(P-34) **Oxidation mechanism of poly(vinyl alcohol) with persulfate anion radical as studied by spin trapping ESR and LC/MS**

Yuko Nishihara, Toshimitsu Inoue, Tomoko Yamaguchi, Toru Ikegami, Yusuke Miyake, Kenji Kanaori, Kunihiko Tajima

(P-35) **Influence of plasma gas species on bacterial inactivation and reactive species production by plasma-bubbling**

Toshihiro Takamatsu, Yosuke Watanabe, Hidekazu Miyahara, Yuriko Matsumura, Atsuo Iwasawa, Masahiro Kohno and Akitoshi Okino

(P-36) **Investigation of Reactive Species Generated by Various Gas Plasmas using ESR Spin Trapping Method**

Yuriko Matsumura, Toshihiro Takamatsu, Kodai Uehara, Yota Sasaki, Hidekazu Miyahara, Atsuo Iwasawa, Masahiro Kohno and Akitoshi Okino

(P-37) **EPR in the Identification of Fe^{3+} Compounds and Free Radicals of Seeds**

Bruna F. Gazzoni, Daniel F. Valezi, Felipe R. Benatti, Eduardo Di Mauro and Carmen L. B. Guedes

(P-38) **Recent Developments of Multi-Extreme THz ESR in Kobe**

H. Ohta, S. Okubo, E. Ohmichi, T. Sakurai and S. Hara

(P-39) **Improvement of sensitivity on parallel CW-EPR image acquisition system**

Ayano Enomoto and Hiroshi Hirata

(P-40) **Simulation of RF magnetic fields in Crossed loop resonators for 300 MHz Pulsed EPR**

Tatsuya Ishii and Hiroshi Hirata

(P-41) **Bismuth Germanium Oxide as Perspective Material for Dielectric Resonators in EPR Spectroscopy**

Mikhail Ivanov, Sergey Veber, Elena Bagryanskaya, Matvey Fedin, Vladimir Nadolinniy, Gennady Kuznetsov

(P-42) **Quantitative Spin-trapping ESR Investigation of Alkoxyl Radical Thermally Derived from AAPH: Development of a Flow-injection Spin-trapping ESR System for the ORAC-ESR Assay**

Akira Nakajima, Tomoko Yamaguchi, Tomoyuki Yamashita, Naoto Yamamoto, Kenji Kanaori, and Kunihiko Tajima

(P-43) **Development of High Pressure Cyclotron Resonance System and Application to Dirac Fermion System**

Ryosuke Matsui, Takahiro Sakurai, Susumu Okubo, Hitoshi Ohta, Reizo Kato, Masayuki Suda, Kazuyuki Matsubayashi, Yoshiya Uwatoko

(P-44) **Development of High Pressure and Multi-frequency ESR System and Its Application to Quantum Spin System**

Takahiro Sakurai, Ryosuke Matsui, Kohei Kawasaki, Susumu Okubo, Hitoshi Ohta, Kazuyuki Matsubayashi, and Yoshiya Uwatoko

(P-45) **Development of high pressure ESR system using micro-coil**

Kohei Kawasaki, Eiji Ohmichi, Takahiro Sakurai, Hitoshi Ohta, Susumu Okubo, Kazuyuki Matsubayashi, Yoshiya Uwatoko

(P-46) **Application of cantilever-detected ESR to biological systems**

T. Okamoto, E. Ohmichi, and H. Ohta

(P-47) **Artifact suppression in electron paramagnetic resonance imaging of ^{14}N and ^{15}N-labeled nitroxyl radicals with asymmetric absorption spectra**

Wataru Takahashi, Yusuke Miyake and Hiroshi Hirata

(P-48) **Highly sensitive force detection system for high-frequency ESR measurement**

Akiho Ishikawa, Eiji Ohmichi, Hitoshi Ohta

(P-49) **Time-Resolved Faraday Rotation Study on Photo-Excited Triplet State of Organic Molecule in Solutions**

Tomoaki Yago and Masanobu Wakasa

(P-50) **Cantilever-detected ESR measurement using a frequency modulation technique**

R. Tabuse, E. Ohmichi and H. Ohta

(P-51) **Recent advances in cantilever-detected ESR technique**

E. Ohmichi, R. Tabuse, A. Ishikawa, T. Okamoto and H. Ohta

(P-52) **Functional EPR imaging of isolated and perfused rat hearts: monitoring of tissue oxygenation and pH**

Artem A Gorodetsky, Igor A Kirilyuk, Denis A Komarov

(P-53) **Whole-body kinetic images of pyrrolidine redox probes by redox molecular imaging (ReMI)**

Nuttavut Kosem, Fuminori Hyodo, Noppawan Phumala Morales, Kazuhiro Ichikawa, Keiji Yasukawa and Hideo Utsumi

(P-54) **Longitudinal ESR imaging of tumor oxygenation for cancer radiotherapy combined with the metabolic-targeted drug**

Hironobu Yasui, Keita Saito, Naoya Nishida, Shingo Matsumoto, Tohru Yamamori, Murali C. Krishna and Osamu Inanami

(P-55) **Time Course Analysis of Radiation Induced Alteration of Tissue Redox Status Using MR Redox Imaging**

Mizuki Nakamura, Sayaka Shibata, Yoshikazu Ozawa, Megumi Ueno, Ken-ichiro Matsumoto, Ken-ichi Yamada, Tadashi Kamada, and Ichio Aoki

(P-56) **Development of MRI probe linking with nitroxide**

Tomonori Shirouzu, Toshihide Yamasaki, and Ken-ichi Yamada

(P-57) **EPR Spectroscopy and Oxygen Imaging for Evaluation of the Transient Induction of Tumor Hypoxia and Potentiation of Bioreductively Activated Hypoxia-activated Prodrug TH-302**

Yoichi Takakusagi, Shingo Matsumoto, Keita Saito, Masayuki Matsuo, Shun Kishimoto, Jonathan W. Wojtkowiak, Robert J. Gillies, James B. Mitchell, Charles P. Hart and Murali C. Krishna

(P-58) **Combined EPR and Optical Imaging to Reveal Oxidative Stress and Microstructure in Human Atherosclerotic Plaques**

Mikael Lindgren, Pål Ellingsen, Morten Kildemo, Magnus Lilledahl, Martin Hallbeck, Helene Zachrisson and Håkan Gustafsson

(P-59) **Mechanosynthesis of the (α,β)-PbF_2 fine powders doped with rare-earth ions**

I.A. Irisova, A. A. Rodionov, D. A. Tayurskii, and R. V. Yusupov

(P-60) **Structural dynamics in a "breathing" metal-organic framework studied by Electron Paramagnetic Resonance of nitroxide spin probes**

Alena M. Sheveleva, Daniil I. Kolokolov, Anton A. Gabrienko, Alexander G. Stepanov, Sergey A. Gromilov, Inna K. Shundrina, Renad Z. Sagdeev, Matvey V. Fedin, Elena G. Bagryanskaya

(P-61) **Magnetostructural correlations for the $Ni^{2+}(^3A_2$; S=1) ions**

Muhammed Açıkgöz, Paweł Gnutek and Czesław Rudowicz

(P-62) **Temperature dependence of the structural, magnetic and vibrational properties of $KGd(WO_4)_2$ single crystal**

S. M. Kaczmarek, G. Leniec2, L. Macalik, J. Hanuza, A. Pietraszko, T. Bodziony, T. Skibiński

(P-63) **EPR of phosphorus in diamond crystals. An influence of nitrogen impurity, HTHP treatment and high phosphorus concentration**

V. A. Nadolinny, Yu. N. Palyanov, A,Yu. Komarovskikh, I. N. Kupriyanov

(P-64) **Dipolar and Exchange Coupling in (bis-Salicylaldiminatothiocarbhydrazonodicopper(II), A Sulphur Bridged Dimeric Copper(II) Complex**

Rajendra BOSE Muthukumaran, Aditya P. Koley, Balaji Sambandam, and Periyakaruppan T.Manoharan

(P-65) **ESR/CESR and Magnetic Susceptibility Studies of Electronic and Magnetic Structures of Nanographites (withdrawn)**

Albert M. Ziatdinov and Nikita S. Saenko

(P-66) **ESR Signature of Metallic State in Semicrystalline conjugated Polymers Doped with Fluoroalkylsilane Molecules**

Hisaaki Tanaka, ShunWatanabe and Shin-ichi Kuroda

(P-67) (withdrawn)

(P-68) **High frequency ferromagnetic resonance study of Heusler compounds using a micro-cantilever**

Alexey Alfonsov, Eiji Ohmichi, Ahmad Omar, Sabine Wurmehl, Berndt Büchner, Brian Peters, Fengyuan Yang, Hitoshi Ohta

(P-69) **EPR and Magnetic Investigations of Nanoparticles of Colossal Magnetodielectric La_2NiMnO_6**

K. S. Bhagyashree, S. Ranjeet, and S. V. Bhat

(P-70) **Effect of Size Reduction on Magnetic Ordering in $Sm_{1-x}Ca_xMnO3$ (x = 0.35, 0.65 and 0.92) Manganites: Magnetic and EMR Studies**

Lora Rita Goveas, K. S. Bhagyashree, Anuradha K. N., S.V.Bhat

(P-71) **An EPR Study of Magnetic Properties of Polyaniline**

Boris Rakvin

(P-72) **Novel type of organic conductor, self-doped $TTFCOONH_4$ and Its Analogs**

Toshikazu Nakamura, Ko Furukawa, Takeshi Terauchi, Yuka Kobayashi

(P-73) **Antiferromagnetic to Paramagnetic Transition of Goethite (α-FeOOH) by ESR**

Daniel F. Valezi, Marilene T. Piccinato, Paulo W. C. Sarvezuk, Flávio F. Ivashita, Andrea Paesano Jr., J. Varalda, Dante H. Mosca, Carmen L. B. Guedes and Eduardo Di Mauro.

(P-74) **Analysis of polymer degradation by ESR imaging**

Hideyuki HARA

(P-75) **Estimation of Wheat Flour Ash Contents using ESR**

Hiromi Kameya, Mizuki Tsuta, Kaori Fujita, Setsuko Todoriki and Junichi Sugiyama

(P-76) **Electron Magnetic Resonance Studies on Nanosized $Nd_{0.65}Ca_{0.35}$ $Mn_{1-x}Cr_xO_3$ (x=0, 0.06) Manganite**

Daly Paul, K.N. Anuradha, K.S.Bhagyashree and S.V. Bhat

(P-77) **Improper Ferroelastic $MgBF_6 \cdot 6H_2O$ (B-Si, Ge) Crystals in the Incommensurate States: EPR and Group-Theoretical Studies (withdrawn)**

Peter G. Skrylnik and Albert M. Ziatdinov

(P-78) **New Method for Obtaining Highly Resolved ESR spectrum of Aligned Radical**

Masaya Nakamura and Tatsuhisa Kato

(P-79) **Unusual Electric Properties of Binuclear Rhenium Complexes with Biimidazolate Ligands in a Mixed-Valence State as Studied by Single-Crystal ESR Spectroscopy and Quantum Chemical Calculations**

Takeshi Yamane, Kazunobu Sato, Shunsuke Tatsumi, Kenji Sugisaki, Yuki Kanzaki, Kazuo Toyota, Daisuke Shiomi, Makoto Yoshizawa, Makoto Tadokoro and Takeji Takui

(P-80) **Time resolved EPR study on photoinduced intermediates in photoactive interface of the perovskite solar cell**

Kousuke Miyazaki, Taku Miura, Masasi Hasegawa, Yuhei Ogomi, Takashi Tachikawa, Shuji Hayase, Yasuhiro Kobori

(P-81) **Study on Magnetophotoconductance in Fullerene-Based Diode**

Yusuke Wakikawa, Takuya Omori, and Tadaaki Ikoma

(P-82) **Electron spin resonance study of room-temperature ferromagnetism in proton-irradiated fullerene**

Do wan Kim, Kyu Won Lee, Gi Wan Jeon, and Cheol Eui Lee

(P-83) **Electron spin resonance study of thermally treated glassy carbon**

Gi Wan Jeon, Hyun Jin Cho, Do wan Kim, Kyu Won Lee, and Cheol Eui Lee

(P-84) **Morphology effect on the geometry of the photoinduced charge-separated states in RR P3HT:PCBM blend films studied by time-resolved EPR**

Taku Miura, Takashi Tachikawa, Yasuhiro Kobori

(P-85) **Annealing Effect on Photocarrier Dynamics in P3HT Thin Film Studied by Time-resolved Magnetophotoconductance Measurements**

Satomi Akaishi, Christopher E. Ambe, Yusuke Wakikawa, Tomoaki Miura, and Tadaaki Ikoma

(P-86) **Detrapping Reaction of H Atoms From Silsesquioxane Cages in Organic Solvents**

Kenji Komaguchi, Tetsuya Maeda, Ryota Okayama, Ichiro Imae and Yutaka Harima

(P-87) **Spin Dynamics of Photoconductive Donor-Acceptor-type Covalent Organic Framework (COF)**

Ko Furukawa, Toshikazu Nakamura, Shangbin Jin, Long Chen and Donglin Jiang

(P-88) **Pulse EPR detection of UV light generated spins on an Al doped TiO_2 crystal**

Ikuko Akimoto and Takao Sekiya

(P-89) **Electrically Detected Spin Resonance Of Hydrogenated Amorphous Silicon At Room Temperature**

A. M. See, D. R. McCamey and Alex R. Hamilton

(P-90) **Molecular Mechanism of Apoptotic BAX Activation Revealed by Spin-label ESR**

Yun-Wei Chiang, Chia-Jung Tsai, Tai-Ching Sung, and Yei-Chen Lai

(P-91) **Using bound fatty acids to disclose the solution structure of serum albumin**

Jörg Reichenwallner, Dariush Hinderberger

(P-92) **Accurate orientation PELDOR measurements and analysis of the Rx bi-functional spin label for protein structure refinement**

Johannes E. McKay, Michael Stevens, Hassane EL Mkami, David G. Norman and Graham Smith

(P-93) **Time resolved EPR study on photoinduced primary charge-separated state of the PSII reaction center from spinach**

Masashi Hasegawa, Masaki Tsushima, Takashi Tachikawa, Hiroyuki Mino, Yasuhiro Kobori1

(P-94) **Time-resolved EPR Measurements of Y_Z Radical in Photosystem II Detected by High Frequency Magnetic Field Modulation**

Wataru Koinuma and Hiroyuki Mino

(P-95) **Electron Paramagnetic Resonance Lineshape and Spin–spin Interaction of Doubly Labeled Protein in a Denaturation Process**

Yasunori Ohba, Munehito Arai, Tetsuya Itabashi, Jun Abe, Toshikazu Nakamura, Satoshi Takahashi, Seigo Yamauchi

(P-96) **Structural dynamics of cardiac troponin regulated by phosphorylation, as studied by spin-labeling dipolar EPR spectroscopy**

Chenchao Zhao, Takayasu Somiya, Tomoki Aihara, Hiroaki Yamashita, Shoji Ueki, and Toshiaki Arata

(P-97) **Calcium-dependent structural dynamics of actin and tropomyosin in the thin filament with bound myosin heads in rigor state as studied by spin-labeling EPR spectroscopy**

K. Ueda, A. Yamamoto, Y. Ueda, T. Aihara, S. Ueki, M. Miki, and T. Arata

(P-98) **Nucleotide-dependent Displacement and Dynamics of α-1 Helix in Motor Protein Kinesin Superfamily As Revealed by Site Directed Spin Labeling ESR**

S. Yasuda, N. Furutani-Umezu, T. Yanagi, M. Yamada, S. Maruta, and T. Arata

(P-99) **Substrate specificity of the cobalamin uptake system in E. coli studied by EPR spectroscopy**

Benesh Joseph, Arthur Sikora, Katja Barth, Martin Held, Gunnar Jeschke, Enrica Bordignon, David S. Cafiso and Thomas F. Prisner

(P-100) **Arbitrary Waveform Pulse ESR at Very Low Temperatures: Multiple Excitation using Phase-ramped Gaussian Pulses**

Yung Szen Yap, Yutaka Tabuchi, Shuuhei Tanijima, Makoto Negoro, Akinori Kagawa and Masahiro Kitagawa

(P-101) **Molecular Spin Manipulation by Pulsed Electron Multiple Resonance Technique for Molecular Spin Quantum Computers**

Kazunobu Sato, Shigeaki Nakazawa, Ayaka Tanaka, Tomohiro Yoshino, Kenji Sugisaki, Shinsuke Nishida, Tomoaki Ise, Yasushi Morita, Kazuo Toyota, Daisuke Shiomi, Masahiro Kitagawa, and Takeji Takui

(P-102) **Molecular Spin based Adiabatic Quantum Computers: Implementation of Pulse Sequences**

Satoru Yamamoto, Shigeaki Nakazawa, Kenji Sugisaki, Kazunobu Sato, Kazuo Toyota, Daisuke Shiomi Takeji Takui

(P-103) **Determination of the Fine-Structure Tensors and Double Quantum Transitions for Iminonitroxide-Nitroxide Diradicals in Magnetically Diluted Single Crystals as Studied by CW/Pulsed ESR**

S. Nakazawa, M. Kawamori, K. Sugisaki, K. Toyota, D. Shiomi, K. Sato, K. Omukai, T. Furui, M. Kuratsu, S. Suzuki, M. Kozaki, K. Okada and T. Takui

(P-104) **A Nitrogen Nuclear-Spin Manipulation in Single Crystals for the Use of Molecular Spin Qubits by ELDOR-NMR technique**

Ayaka Tanaka, Kazunobu Sato, Tomohiro Yoshino, Shinsuke Nishida, Shigeaki Nakazawa, Robabeh Rahimi, Kazuo Toyota, Daisuke Shiomi, Yasushi Morita, Masahiro Kitagawa and Takeji Takui

(P-105) **Dichotomy of *3d* Electrons in YbT_2Zn_{20} (T=Co; Fe): An ESR Study**

V.A. Ivanshin, T.O. Litvinova, S. Jia, S.L. Bud'ko, P.C. Canfield

(P-106) **DFT-Based Calculations of the Spin–Orbit Term in Zero-Field Splitting Tensors: The Corrected QRO Method**

Kenji Sugisaki, Kazuo Toyota, Kazunobu Sato, Daisuke Shiomi, Masahiro Kitagawa and Takeji Takui

(P-107) **High-Field Multi-Frequency ESR in the Rare-Earth Spinel Compound $CdYb_2S_4$**

Daichi Yoshizawa, Takanori Kida, Satoru Nakatsuji, Kensuke Iritani, Tetsuya Takeuchi, and Masayuki Hagiwara

(P-108) **High-field ESR facility and related research at Wuhan National High Magnetic Field Center**

Z. W. Ouyang, M. Y. Ruan, H. Nojiri, S. Okubo, and H. Ohta

(P-109) **ODMR study of systems with (CdMn)Te/(CdMg)Te quantum wells**

D.O. Tolmachev, A.S. Gurin, N.G. Romanov, B.R. Namozov, Yu.G. Kusrayev, P.G. Baranov

(P-110) **EPR and DFT Investigation of Hydrogen-Producing Bioinspired Catalysts (withdrawn)**

Özlen Ferruh Erdem, Wolfgang Lubitz

(P-111) **Electric Field Effect on Electron-Spin Coherence Time of Single NV center in Diamond**

Satoshi Kobayashi, Hiroki Morishita, Shinji Miwa, Yoshishige Suzuki, Norikazu Mizuochi

(P-112) (withdrawn)

(P-113) **High Field ESR Measurements of the Spin Gap System in Polarized Light**

Shojiro Kimura, Kazuo Watanabe, Takanari Kashiwagi, Hironori Yamaguchi, Masayuki Hagiwara, and Zentaro Honda

(P-114) **Magnetic Anisotropy in Chiral System CuB_2O_4 by ESR**

Sho Arakawa, Susumu Okubo, Hitoshi Ohta, Takahiro Sakurai, Shigeo Hara, Mitsuru Saito, Takahisa Arima

(P-115) **High Field ESR Measurements of Two Dimensional Antiferromagnets Sr_2NiO_3X (X=F,Cl)**

Syota Yoshida, Shigeo Hara, Takahiro Sakurai, Susumu Okubo, Hitoshi Ohta, Yoshihiro Tsujimoto, Kazunari Yamaura, Teturo Uchikoshi

(P-116) **High Field ESR Measurements of Quasi One Dimensional Frustrated Magnet $NaCuMoO_4(OH)$**

Yoko Kitahara, Sihigeo Hara, Takahiro Sakurai, Susumu Okubo, Hitoshi Ohta, Kazuhiro Nawa, Yoshihiro Okamoto, Zenji Hiroi

(P-117) **High-field ESR Measurements of $YCrO_3$ and $YCaCrO_4$**

Shohei Ikeda, Shigeo Hara, Takahiro Sakurai, Susumu Okubo, Hitoshi Ohta, Ting Hui Kao, Hiroya Sakurai, Hung-Duen Yang

(P-118) **Development of Magnetization and XMCD Detection ESR**

Hiroyuki Nojiri and Satoshi Matsuzawa

(P-119) **High-field multi-frequency ESR in the quasi-1D *S*=1/2 Ising-like antiferromagnet $BaCo_2V_2O_8$ in a transverse field**

Akira Okutani, Shojiro Kimura, Tetsuya Takeuchi and Masayuki Hagiwara

(P-120) **The Effective Spin Model and ESR Measurements of an *S* = 1/2 Ferromagnetic Alternating Double Chain, m-Ph-V_2**

Kenji Iwase, Hironori Yamaguchi, Toshio Ono, Takanori Kida, Masayuki Hagiwara and Yuko Hosokoshi

(P-121) **Carbonate Free Radical Production on Addition of Hydrocarbonate to a Weak Acidic Mixture of Rats' Gastric Carcinogen, N-Methyl-N'-Nitro-N-Nitrosoguanidine, and Hydrogenperoxide**

Tomiko Mikuni, Masaharu Tatsuta, Idota Atsushi and Tomoyukieu Yamasaki

(P-122) **High-field ESR Measurements of Low-dimensional Magnets in Natural Minerals**

Susumu Okubo, Yoko Kitahara, Syota Yoshida, Shigeo Hara, Takahiro Sakurai, Hitoshi Ohta, Masashi Fujisawa and Hidekazu Tanaka

(P-123) **ESR Studies of the Molecular Spin Liquid System $EtMe_3Sb[Pd(dmit)_2]_2$**

Yugo Oshima, Takao Tsumuraya and Reizo Kato

(P-124) **Numerical study of dynamical susceptibility in one dimensional trimerized spin systems**

Keigo Hijii, Toru Sakai, Seiji Miyashita and Hitoshi Ohta

(P-125) **Magnetic Anisotropy of the Distorted-Diamond-Chain Compound $Cu_3(MoO_4)_2(OH)_2$**

Shigeo Hara, Hirohiko Sato, Takahiro Sakurai, and Hitoshi Ohta

(P-126) **Molecular orientation and dynamics of NN radicals in organic 1D nanochannels**

Hirokazu Kobayashi

(P-127) **Transient Nutation studies of nitroxide derivatives of fullerene C60**

R. B. Zaripov, G. R. Nureeva, V. K. Voronkova, K. M. Salikhov, V. P. Gubskaya, I. A. Nuretdinov

(P-128) **Time-Resolved and Pulse EPR of Zinc Porphyrin Trimer**

Sukhanov Andrey, Voronkova Violeta, Mikhalitsyna Elena and Tyurin Vladimir

(P-129) **Time-resolved EPR study on the Electronic Structure of the Excited Triplet State of [26] and [28] Hexaphyrins**

Fumitoshi Ema, Atsuhiro Osuka, Mana Tanabe, Seigo Yamauchi, Takashi Tachikawa, and Yasuhiro Kobori

(P-130) **Rate constant measurements for addition reaction of radicals in early photopolymerization processes utilizing pulsed EPR method**

Yusuke Miyake, Hirona Takahashi and Akio Kawai

(P-131) **Reaction Dynamics and Magnetic Field Effects in Cryptochromes and Photolyase**

K. Maeda, J. G. Storey, K. B. Henbest, S. R. T. Neil, D. M. W. Sheppard, T. Biskup, K. Hitomi, E. D. Getzoff, E. Schleicher, S. Weber, S. R. Mackenzie, C. R. Timmel, P. J. Hore

(P-132) **Effect of glycerol concentration on structure of photoinduced chargeseparated states in 9,10-anthraquinone-1-sulfonate-human serum albumin system**

Masaki Tsushima, Masaaki Fuki, Taku Miura, Takashi Tachikawa and Yasuhiro Kobori

(P-133) **Solvent effects on dynamic electron polarization produced through the radical quenching of photoexcited triplet states of organic dyes**

Toshihiro Tamura, Hirona Takahashi and Akio Kawai

(P-134) **Study on Magnetic Anisotropy and Slow Magnetization Relaxation of a Gadolinium(III)-Radical Complex**

Takuya Kanetomo, Hiroyuki Nojiri and Takayuki Ishida

(P-135) **Sub-micron flavin radical and magnetic field effect based imaging**

Jonathan R. Woodward, Joshua P. Beardmore

14. Author Index 206

APES-IES-SEST2014 Scientific Program

November 12 (Wed)			
	Kinsho Hall (1F)		Small Hall (B1F)
11:00~18:00	Registration		
13:00~13:15	Opening of APES-IES-SEST 2014		
13:15~14:00	**(PL-1) Klaus Möbius** Magic Matrix Effects on Protein Dynamics Decoded by High-Field EPR (Chair: T. Ikoma)		
14:00~14:45	**(PL-2) Masaki Oshikawa** Recent Progress in Theory of ESR in Strongly Correlated Spin Systems (Chair: H. Kikuchi)		
14:45~15:10	Break		
15:10~15:55	**(PL-3) Graham Smith** Very High Sensitivity Orientational PELDOR (Chair: H. Ohta)		
	SEST Excellent Presentation Award Competition (Chair: T. Nakamura)		
15:55~16:15	**(SEST EPA-1)** **Fatma Elmasry** Er-concentration and charge carrier effects on GaAs;Er,O revealed by X-band ESR		
16:15~16:35	**(SEST EPA-2)** **Hiroki Nagashima** ENDOR Studies on Relationship between the Hydrogen Bonding Network and Ca^{2+} of the Mn Cluster in Photosystem II		
16:35~16:55	**(SEST EPA-3)** **Yuta Matsuoka** Development of fluorescent probe for sensitive detection of ascorbic acid		

November 12 (Wed)			
16:55~17:15	**(SEST EPA-4)** **Zhebin Fu** Time-Resolved EPR and Photochemical Study on the Inclusion System of Anthraquinones and Cyclodextrins		
17:15~17:35	**(SEST EPA-5)** **Takuya Omori** Magnetoconductance of Pentacene/C60-bilayaer Solar Cell		
17:35~18:00	Morino Foundation Presentation Noboru Hirota		
18:00-18:30	Move to Nara Women's University (about 15 minutes' walk)		
18:30-20:30	**Welcome Reception** (Nara Women's University)		

November 13 (Thu)			
	Kinsho Hall (1F)		Small Hall (B1F)
9:00~9:45	**(PL-4)** **Elena Bagryanskaya** The New Spin Probes for Biochemical Applications (Chair: Y. Kobori)		
9:45~10:10	Break		
	Session 1 **Spin Chemistry** (Chair: Y. Kobori)		**Session 2** **Dosimetry & Dating** (Chair: C. Yamanaka)
10:10~10:15	Opening	10:10~10:15	Opening
10:15~10:50	**(IL-1) Wolfgang Lubitz** The Spin as Functional Probe in Metal Biocatalysis	10:15~10:50	**(IL-3) Gamal Mohamed Hassan** Development of EPR Dosimetry from Micro to Nano-materials
10:50~11:25	**(IL-2) Michael R. Wasielewski** Progress Toward Spin Teleportation: Reversible Photo-driven Reduction of a Stable BDPA Radical	10:50~11:20	**(IL-4) Masashi Takada** Application of ESR in Quaternary geological dating

November 13 (Thu)			
11:25~11:45	**(OP-1) Hirona Takahashi** Photoinitiated Radical Polymerization of Silane Coupling Agents as Studied by Pulsed EPR Spectroscopy	11:20~11:40	**(OP-3) Atsushi Tani** Diagnostic of Reactive Oxygen Species (ROS) Induced in Water by Atmospheric Pressure Plasma for Plasma-based Sterilization
11:45~12:05	**(OP-2) Motoko S. Asano** Substituent Dependence of Relaxation Processes in the Excited State of Vanadyl Porphyrins : Time-resolved EPR and Luminescence Study	11:40~12:00	**(OP-4) Kouichi Nakagawa** Effects of 0.10−10 Gy X-ray Irradiation on Eggshell Radical Production
12:05~13:30	Lunch		
13:30~14:15	Harden M McConnell Memorial Lecture **(PL-5) Lawrence J. Berliner** Harden M. McConnell - the Life of a Giant in Magnetic Resonance (Chair: K. Ichikawa)		
14:15~14:25	Break		
	Session 3 **Quantum Spin System** (Chair: H. Kikuchi, H. Nojiri)		**Session 4** ***In vivo* Imaging** (Chair: K. Ichikawa)
14:25~14:30	Opening	14:25~14:30	Opening
14:30~15:05	**(IL-5) Vladislav Kataev** Probing the Spin Dynamics in Novel Iridium Oxides by sub-THz ESR	14:30~15:05	**(IL-7) Noppawan P. Morales** Application of ESR/Spin Trapping for Monitoring Free Radical Formation in Serum of β−Thalassemia with Iron Chelation Therapy
15:05~15:35	**(IL-6) Yuko Hosokoshi** Organic Radical Approach to Quantum Spin Systems	15:05~15:40	**(IL-8) Howard J. Halpern** Enhancing cancer treatment in animal models with near absolute O_2 imaging using longitudinal relaxation rate (R_{1e}) with pulse EPR
15:35~15:55	**(OP-5) Toru Sakai** Singlet-Triplet Transitions of ESR in Gapped Spin Systems	15:40~16:00	**(OP-7) Håkan Gustafsson** Electron paramagnetic resonance (EPR) oximetry as a future diagnostic tool for head and neck cancer

November 13 (Thu)			
15:55~16:15	**(OP-6) Sergey Vasiliev** High-field ESR and nuclear polarization of P donors in silicon at ultra-low temperatures	16:00~16:20	**(OP-8) Hiroshi Hirata** *In vivo* imaging of nitroxyl radicals in a mouse using surface coil array and parallel EPR detection
16:20~16:45	Break		
	APES Young Scientist Award (Chair: Yong Li)		
16:45~17:10	**(APES YSA-1) Fazhan Shi** Nanoscale magnetic resonance with single electron spin sensor under ambient conditions		
17:10~17:35	**(APES YSA-2) Toshihide Yamasaki** Towards the structural design of piperidine nitroxides for in vivo measurement probe		
17:35~18:10	APES General Meeting		
18:10~18:30	Move to Nara Prefectural New Public Hall (5 minutes' walk)		
18:30~20:30	Bruker Seminar (Nara Prefectural New Public Hall)		

November 14 (Fri)			
	Kinsho Hall (1F)		Small Hall (B1F)
9:00~9:45	**(PL-6) Thomas F. Prisner** Overhauser Dynamic Nuclear Polarization at a Magnetic Field of 9.2 T (Chair: T. Fujiwara)		
9:45~10:30	**(PL-7) Jack H. Freed** Protein Dynamic Structure Revealed by High Sensitivity Pulse Dipolar ESR Distance Measurements (Chair: T. Arata)		
10:30~10:55	Break		
	Session 5 **DNP** (Chair: T. Fujiwara)		**Session 6** **Photo Synthesis & Protein Distance Measurement** (Chair: H. Mino, T. Arata)
10:55~11:00	Opening	10:55~11:00	Opening

November 14 (Fri)			
11:00~11:35	**(IL-9) Songi Han** Surface characterization by dynamic nuclear polarization NMR	11:00~11:35	**(IL-11) Christopher Kay** Using pulsed and continuous-wave EPR spectroscopy in combination with X-ray crystallography to understand the structure and function of biomolecular machines
11:35~12:10	**(IL-10) Akiva Feintuch** The interplay between spectral diffusion and dynamic nuclear polarization	11:35~12:10	**(IL-12) Louise J Brown** Constructing a dynamic picture of Troponin from site directed spin labeling
12:10~12:30	**(OP-9) Makoto Negoro** Toward applications of DNP using photo-excited triplet electrons	12:10~12:40	**(IL-13) Hideto Matsuoka** Excited Triplet States of Thiophene-Decorated Phenazines Probed by Time-Resolved EPR
12:30~12:50	**(OP-10) Yoh Matsuki** Dynamic Nuclear Polarization for Biological Solid-State NMR at High Fields and Low Temperatures	12:40~13:00	**(OP-11) Wolfgang E.Trommer** Maltose Binding Protein as Molten Globule and in the Native State
12:50~14:00	Lunch		
14:00~15:00	SEST General Meeting SEST Award and SEST Young Investigator Award Ceremony		
	SEST Award and SEST Young Investigator Award Session		
15:00~15:40	SEST Award **(SEST AL-1) Shin-ichi Kuroda** Electron Spin Resonance Studies of Organic Electronic Materials and Devices (Chair: K. Marumoto)		
15:40~16:20	SEST Award **(SEST AL-2) Hirotada Fujii** *In Vivo* EPR Imaging Studies of a Brain Disease Mouse Model (Chair: O. Inanami)		

November 14 (Fri)			
16:20~16:45	SEST Young Investigator Award **(SEST AL-3)Yugo Oshima** High-frequency ESR Studies of Molecule-based Conductors and Magnets (Chair: H. Ohta)		
16:45~17:10	SEST Young Investigator Award **(SEST AL-4) Tomoaki Yago** Time-Resolved Spectroscopic Study on Paramagnetic Intermediates Generated by Photochemical Reactions (Chair: T. Ikoma)		
17:10~17:30	Move to Nara Prefectural New Public Hall (5 minutes' walk)		
17:30~19:25	**Poster Session** (Nara Prefectural New Public Hall)		
19:40~21:40	SEST-APES Young Scientists Meeting (Nara Women's University)		

November 15 (Sat)			
	Kinsho Hall (1F)		Small Hall (B1F)
9:00~9:55	IES General Meeting IES Award Ceremony		
9:55~10:30	IES Gold Medal **(IES AL-1) R. David Britt** EPR Investigations of Photosynthetic and Bioenergy-Related Enzymes (Chair: K. Möbius)		
10:30~10:55	Break		
	Session 7 **IES Award Session** (Chair: L. Berliner)		**Session 8** **Instrumentation** (Chair: H. Hirata)
10:55~11:30	IES Fellow **(IES AL-2) Kev M. Salikhov** Recent Development of the PELDOR Theory	10:55~11:00	Opening

November 15 (Sat)			
11:30~11:55	IES Silver Medal **(IES AL-3) Stephen Hill** Ferromagnetic Resonance Studies of Spin-Orbit Effects in Heavy Atom Organic Radical Ferromagnets	11:00~11:35	**(IL-14) Aharon Blank** Biological Applications of High Sensitivity Electron Spin Resonance with High Spatial Resolution
11:55~12:20	IES Silver Medal **(IES AL-4) Johan van Tol** Quasi-Optical Pulsed EPR and ENDOR at very high Frequencies	11:35~12:05	**(IL-15) Shingo Matsumoto** Development and Applications of Pulsed EPR Oxygen Imaging in Cancer Research
12:20~12:40	John Weil Young Investigator Award **(IES AL-5) Nicholas Cox** The structure of nature's water splitting catalyst prior to O-O bond formation: an EPR and DFT study	12:05~12:25	**(OP-12) Seitaro Mitsudo** High power Nanosecond Pulse Generation for the Pulsed ESR by using a Gyrotron as a Radiation Source
12:40~13:00	IES Young Investigator Award **(IES AL-6) Tomoaki Miura** Dynamic and Electronic Characteristics of Photo-generated Radical Pairs Revealed by Real-time Observation of the Spin Dynamics	12:25~12:45	**(OP-13) Dane R. McCamey** Spectroscopic Investigation of Spin-Dependent Optoelectronic Pathways in Organic Devices
13:00~19:00	**Excursion** (Sandwich lunch for bus tour participants)		
19:00~21:00	**Banquet** (Restaurant Half Time at Nara National Museum)		

November 16 (Sun)			
	Kinsho Hall (1F)		Small Hall (B1F)
9:00~9:45	**(PL-8) Harold M. Swartz** Clinical Applications of EPR (Chair: H. Hirata)		
9:45~10:10	Break		
	Session 9 **Biology** (Chair: O. Inanami)		**Session 10** **Quantum Computing** (Chair: K. Sato)
10:10~10:15	Opening	10:10~10:15	Opening

November 16 (Sun)			
10:15~10:50	**(IL-16) Graeme R. Hanson** Insights into CO_2 Fixation, Global Warming and Healthy Coral Reefs	10:15~10:50	**(IL-18) J. Wrachtrup** Building up a synthetic quantum system spin by spin
10:50~11:25	**(IL-17) Jay L. Zweier** *In vivo* EPR/NMR Coimaging of Radical Probes: Advances and Challenges	10:50~11:25	**(IL-19) Jiangfeng Du** Quantum Computation and Quantum Sensing based on Single Electron Spin in Diamond
11:25~11:45	**(OP-14) Masaki Horitani** New Approach to ENDOR Analysis for Manganese(II)-Substituted Soybean Lipoxygenase with A Non-Coordinated Substrate	11:25~11:50	**(IL-20) Gerd Kothe** Nuclear Hyperpolarization and Spin Entanglement in Phosphorescent Crystals at Level Anti-crossing Conditions
11:45~12:05	**(OP-15) Catharina T. Migita** EPR elucidation of bacterial terminal oxidase building in multi-heme centers	11:50~12:10	**(OP-16) Robabeh Rahimi Darabad** Exploiting Quantum Effects Using Electron-Nuclear Coupled Molecular Spin Systems
12:05~13:30	Lunch		
	Session 11 **Material Science, Electric Devices, Spintronics** (Chair:T. Ikoma, S. Kuroda)		**Session 12** **Free Radicals and Theory** (Chair: K. Tajima)
13:30~13:35	Opening	13:30~13:35	Opening
13:35~14:10	**(IL-21) Christpher E. Ambe** Magnetoconductance in Photoconductive Thin Films of Perylene Bisimide	13:35~14:10	**(IL-23) Yong Li** ESR Study on Mechanism of Photocatalytic Synthesis of Phenols without Photosensitizer
14:10~14:40	**(IL-22) Kazuhiro Marumoto** Development of New Analytical Methods for Organic Devices: Applications of ESR to Transistors, Solar Cells and Light-Emitting Diodes	14:10~14:45	**(IL-24) Sergei A. Dzuba** Interaction of Cryoprotective Agents with Biological Membranes Studied by Pulsed EPR of Spin Labels

November 16 (Sun)			
14:40~15:00	**(OP-17) Yasuhiro Kobori** Electron-Hole Dissociations and Electronic Coupling Influenced by Alkyl Side Chains in the Photovoltaic Polyalkylthiophene:PCBM Interface	14:45~15:10	**(IL-25) Tatyana I. Smirnova** Dielectric Constant and Water Penetration Gradients along Transmembrane Peptide-Lipid Bilayer Interface
15:00~15:20	**(OP-18) Takayuki Ishida** Evaluation of Dysprosium(III)-Copper(II) Exchange Coupling Parameters and Relation with the Bridging Geometry	15:10~15:30	**(OP-19) Czesław Rudowicz** EMR related problems in modeling properties of single-ion and single-molecule magnets (SIM/SMM) - interplay between the crucial notions
15:30~16:00	**Closing** APES Young Scientist Award Ceremony SEST Excellent Presentation Award Ceremony APES, IES Poster Award Ceremony Closing Remarks		

Venue

Symposium Venue

Todaiji Culture Center (Address: 100 Suimon-cho, Nara City)

Floor Plan of Todaiji Culture Center

1F

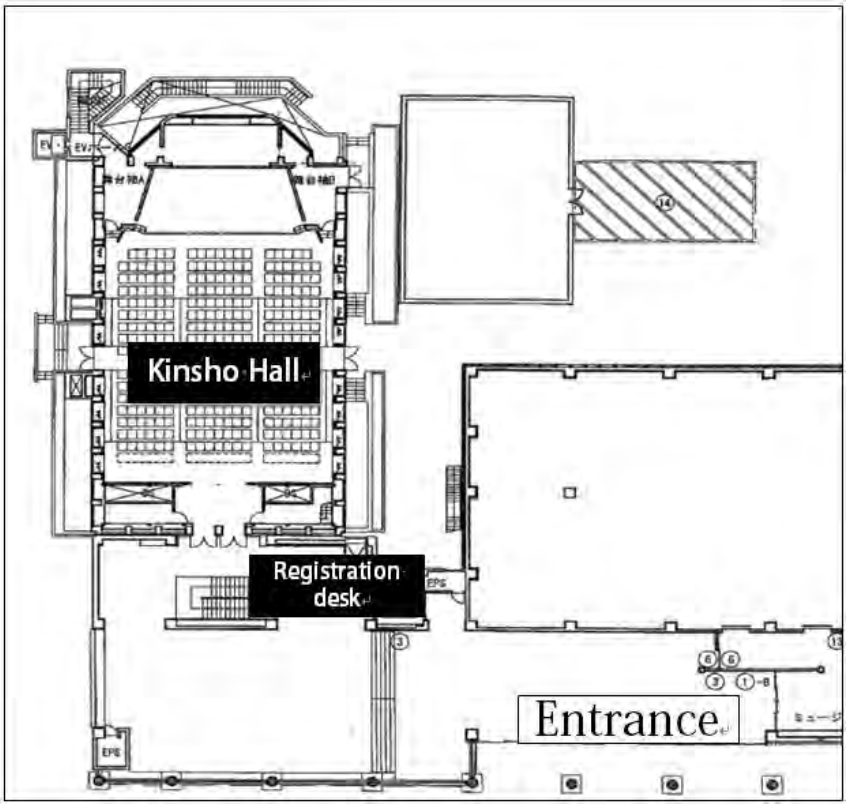

B1F

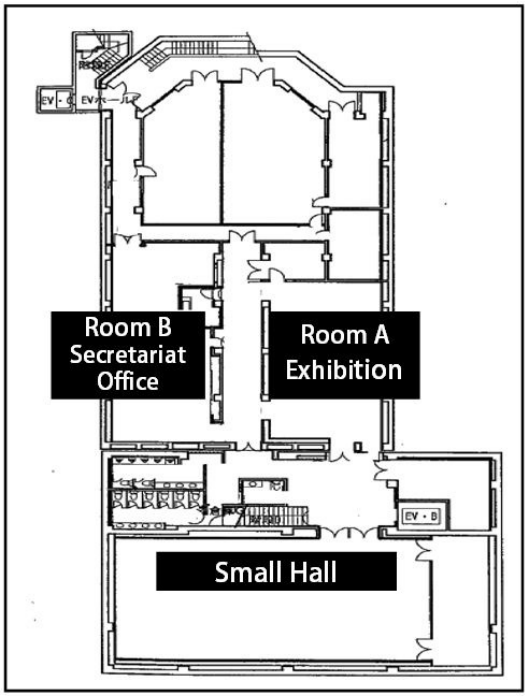

Poster Session Venue

Nara Prefectural New Public Hall (Reception Hall)

(Address: 101 Kasugano-cho, Nara City)

Route to Nara Prefectural Public Hall

(5 minutes' walk from Todaiji Culture Center)

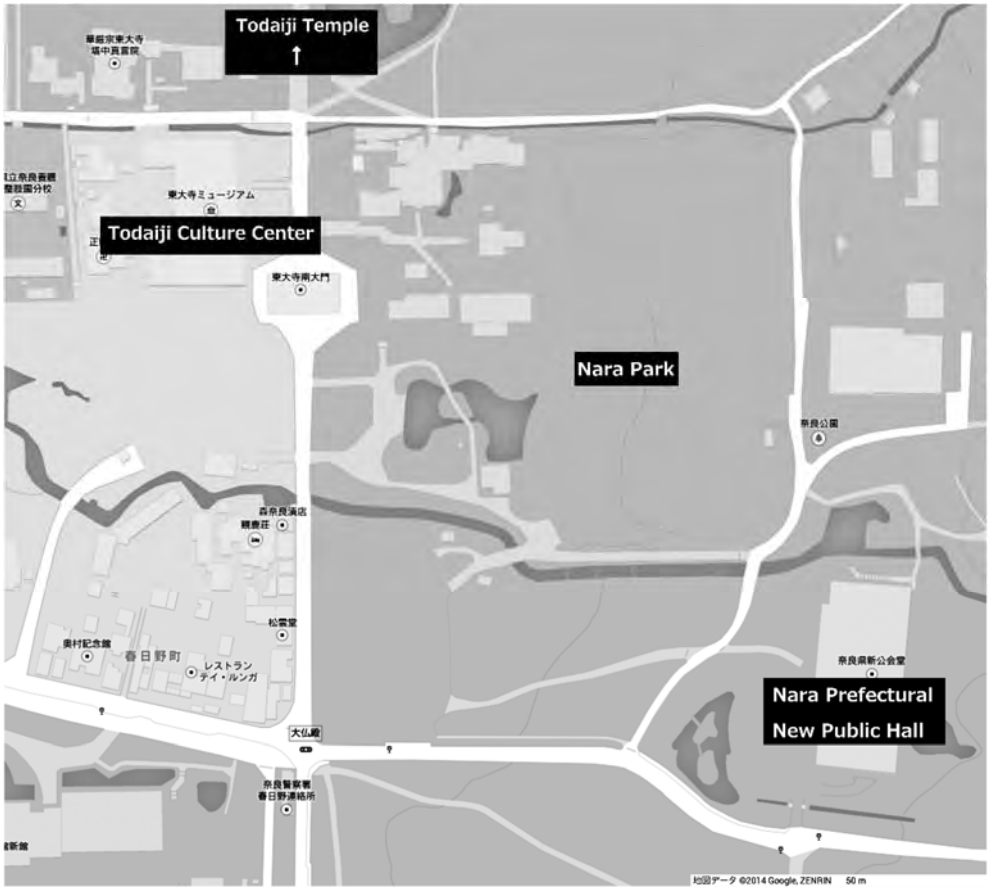

Nara Prefectural New Public Hall

Ceremony and Events

Welcome Reception and SEST-APES Young Scientists Meeting Venue

Welcome Reception and SEST-APES Young Scientists Meeting will be held at Nara Women's University (NWU) near Todaiji Culture Center. It is about 15 minutes' walk to the main gate of NWU.

The route to NWU from Todaiji Culture Center.

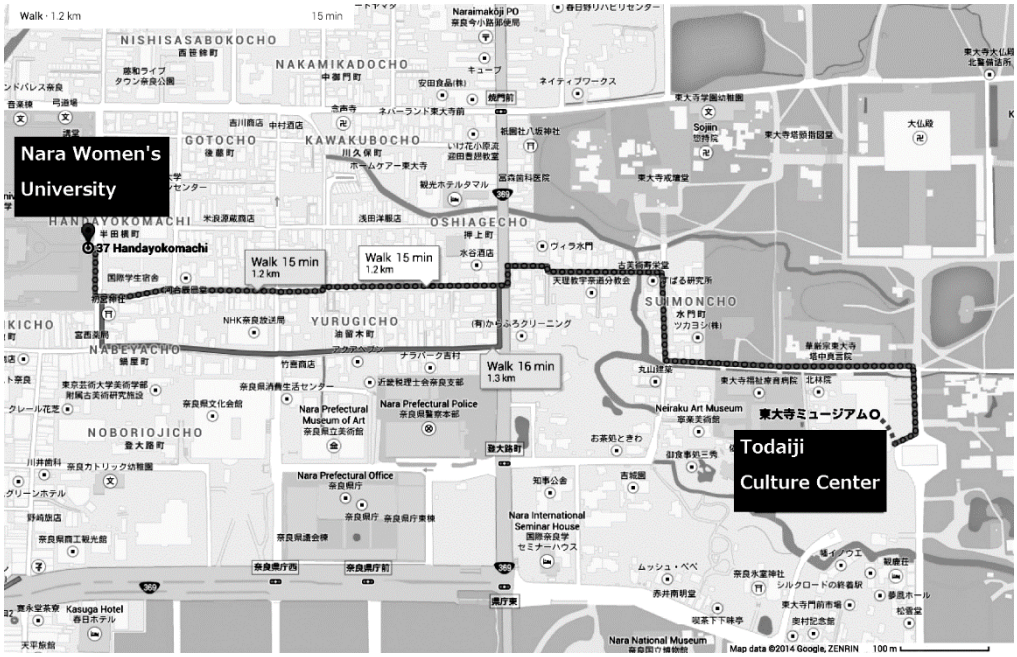

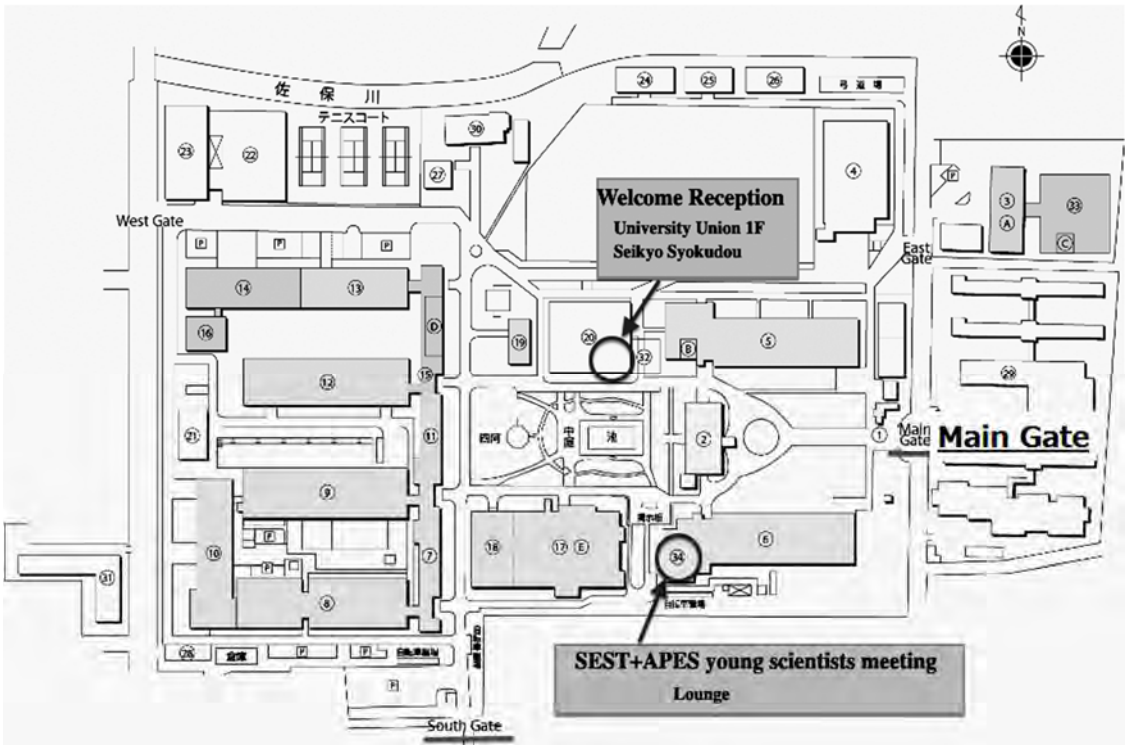

Banquet Venue

Restaurant Half Time “葉風泰夢” (in Nara National Museum)
Address: 50 Noboriooji-cyo, Nara City
Phone : 0742-22-1673

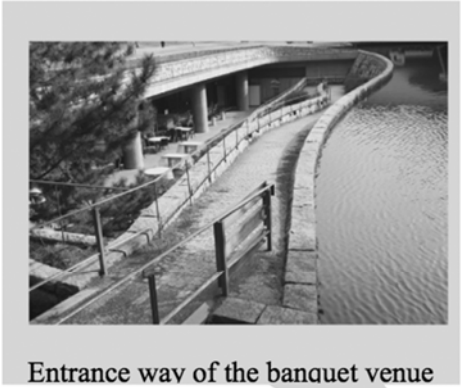
Entrance way of the banquet venue

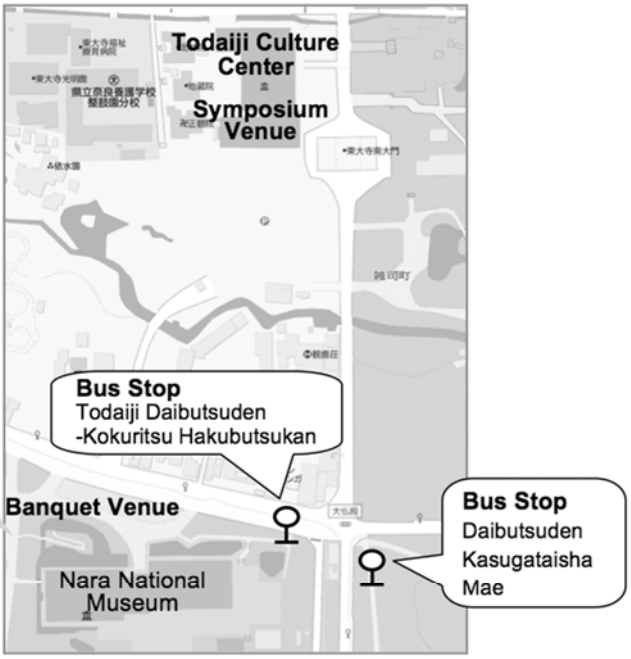

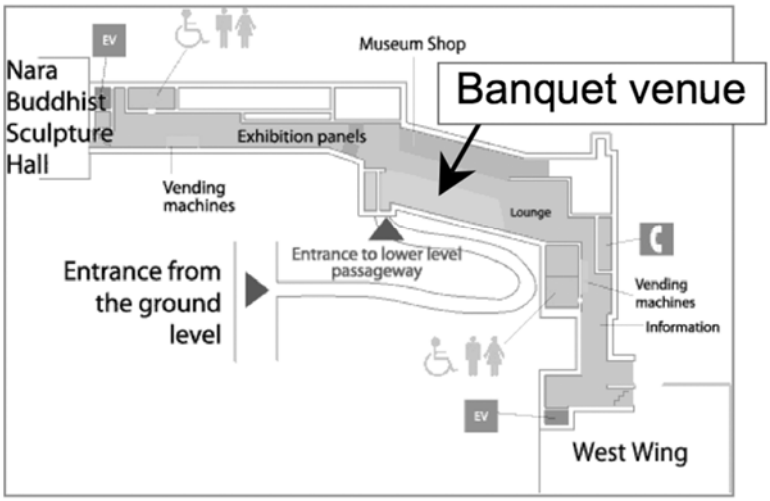

Awards

IES Award:

IES Award will be given to excellent researches having great contributions to EPR/ESR society. Presentations will be given by awardees.

Presentation : Gold medal lecture Nov. 15 (Sat) 9:55~10:30 (Kinsho Hall)

IES award session Nov. 15 (Sat) 10:55~13:00 (Kinsho Hall)

Ceremony : Nov. 15 (Sat) 9:00~9:55 (Kinsho Hall)

SEST Award and SEST Young Investigator Award

SEST Award will be given to excellent and contributory researches in electron spin science and technology. SEST Young Investigator Award will be given to young researchers achieving excellent outcomes in electron spin science and technology.

Presentation : Nov. 14 (Fri) 15:00~17:10 (Kinsho Hall)

Ceremony : Nov. 14 (Fri) 14:00~15:00 (Kinsho Hall)

APES Young Scientist Award:

APES Young Scientist Award will be given to excellent young researches involving EPR in any field covered by physics, materials science, chemistry, biology and medicine.

Presentation : Nov. 13 (Thu) 16:45~17:35 (Kinsho Hall)

Ceremony : Nov. 16 (Sun) 15:30~16:00 (Kinsho Hall)

SEST Excellent Presentation Award Competition:

SEST Excellent Presentation Awards will be given to excellent oral presentations among five presentations applied in advance.

Presentation : Nov. 12 (Wed) 15:55~17:35 (Kinsho Hall)

Ceremony : Nov. 16 (Sun) 15:30~16:00 (Kinsho Hall)

APES2014 Poster Award:

APES2014 Poster Award will be given to excellent poster presentations to encourage students and post-docs. Posters applied in advance are marked for guidance.

Presentation : Nov. 14 (Fri) 17:30~19:25 (Nara Prefectural New Public Hall)

Ceremony : Nov. 16 (Sun) 15:30~16:00 (Kinsho Hall)

IES Poster Award:

IES Poster Award will be given to excellent poster presentations to encourage students and post-docs. Posters applied in advance are marked for guidance.

Presentation : Nov. 14 (Fri) 17:30~19:25 (Nara Prefectural New Public Hall)

Ceremony : Nov. 16 (Sun) 15:30~16:00 (Kinsho Hall)

SEST Student Research Award:

SEST Student Research Award will be given to excellent researches of SEST student members to encourage their research activities.

Ceremony : Nov. 14 (Fri) 14:00~15:00 (Kinsho Hall)

Excursion

Excursion is scheduled on the afternoon of Nov. 15 (Sat). The destination will be Horyuji Temple, oldest wooden temple built in 7th centuries in Japan, and Japanese sake brewery where you can look around how sake is brewed. After coming back to the conference site, you are invited to conference banquet. Details will be announced during the conference.

General Information

Transportation to Nara

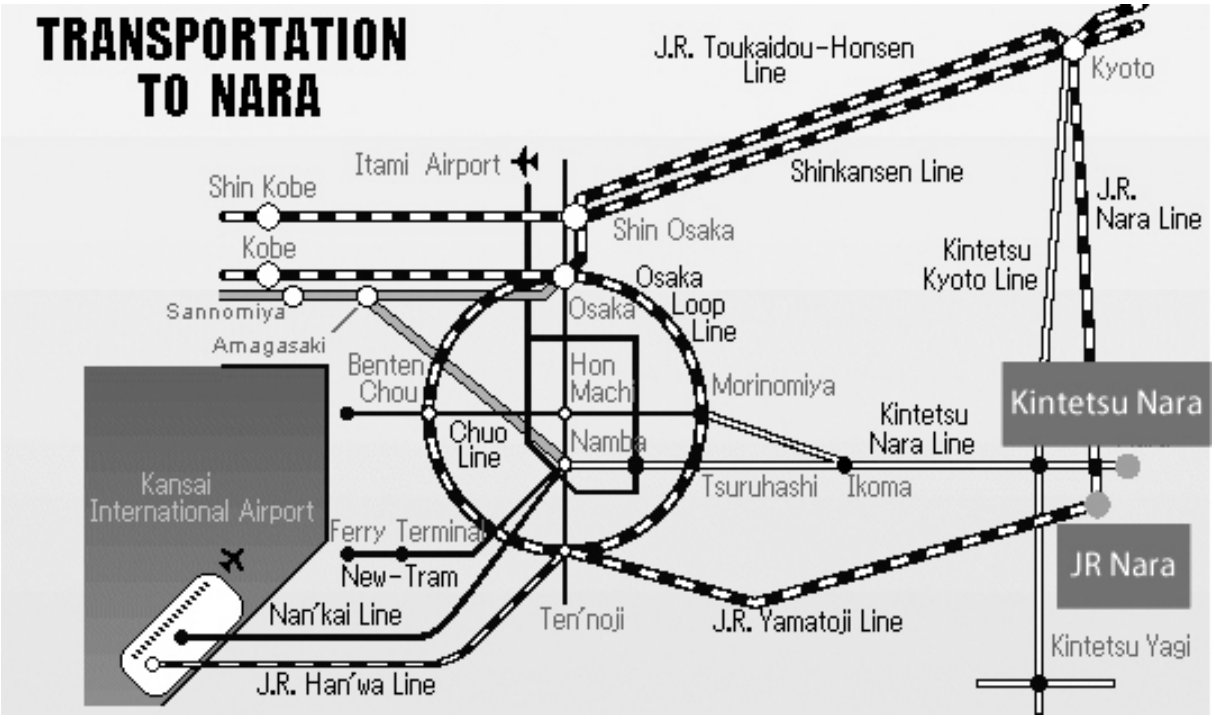

From Osaka

- Kintetsu Namba → Kaisoku-kyuko [Rapid Service Express] → (Kintetsu Nara Line) 32 minutes → Kintetsu Nara
- Hommachi → (Subway / Kintetsu Higashi-osaka Line) 30 minutes → transrate to Kintetsu Nara line at Ikoma , Ikoma → Kaisoku-kyuko (Kintetsu Nara Line) 12 minutes → Kintetsu Nara
- JR Osaka → Nonstop Kaisoku [Rapid Service] (Osaka Loop Line / Yamatoji Line) 48 minutes → JR Nara

From Kansai Airport

- Kansai Airport → (Kansai-kuko Line) 29 minutes → Tennoji → Kaisoku (Yamatoji Line) 29 minutes → JR Nara
- Kansai Airport → Nankai RAPI:T (Nankai Line) 29 minutes → Namba → Limited Express (Kintetsu Nara Line) 31 minutes → Kintetsu Nara
- Kansai Airport → Limousin Bus (about 95minutes) → Bus Stop: JR Nara

From Osaka Airport (Itami Airport)

- Osaka Airport(Itami Airport) → Osaka Airport Limousine Bus(about 65 minutes) → Kintetsu Nara
- Osaka Airport(Itami Airport) → Airport Bus (about 30 minutes) → Kintetsu Uehommachi → Kaisoku kyuko (Kintetsu Nara Line) 29 minutes → Kintetsu Nara

How to get to Todaiji Culture Center

Local buses are a good way to get to the symposium venue.

Buses frequently depart from JR Nara and Kintetsu Nara stations. Take a bus "Nara City Loop Line" from Bus stop No. 1 at JR Nara Station or from Bus stop No. 1 at Kintetsu Nara Station, and get off at Daibutsuden Kasugataisha Mae.

Todaiji Culture Center is a 5-minute walk from the bus stop.

Walk on the approach to the temple among deer and walk past Nan-daimon (Great South Gate). You will see Todaiji Culture Center on your left.

It takes around 20 minutes to walk from Kintetsu Nara Station to the venue.

On the way, you will see a lot of temples and deer.

On your way back, take bus from "Todaiji Daibutsuden-Kokuritsu Hakubutsukan" bus stop bound for JR Nara and Kintetsu stations.

Map of Nara City Loop Line

Take a bus <Loop.2> at "JR Nara Station", <Loop.2> or <Loop.6> at "Kintetsu Nara Station", and get off at Daibutsuden Kasugataisha Mae (the number of the bus stop: N-7).

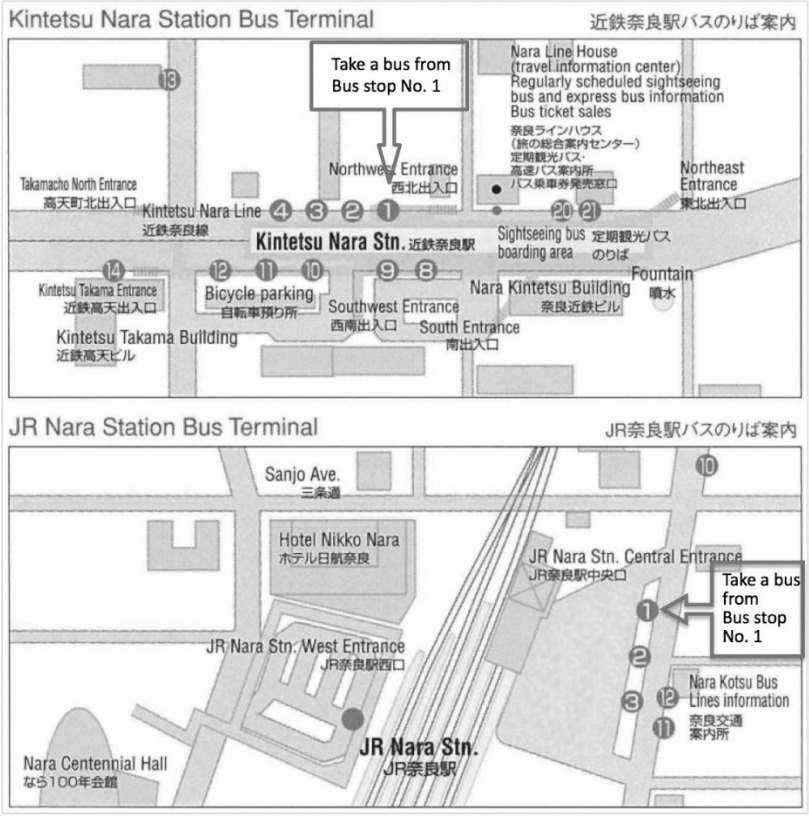

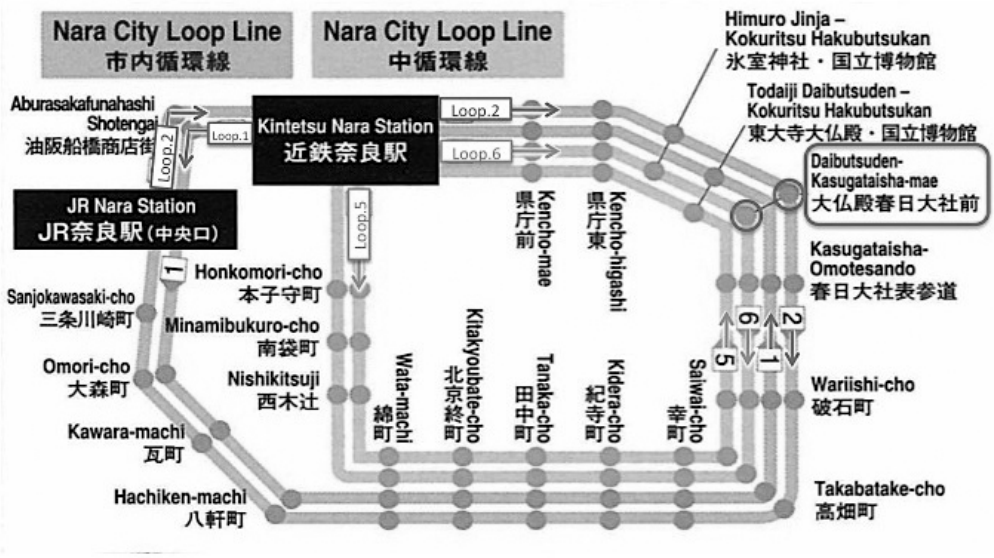

☆ How to get on a bus:

Please get on a bus from the front door, and pay "210 JPY" when you board.
Only 1,000 JPY bill can be exchanged into small changes in the bus (10,000 JPY and 5,000 JPY bills are not available).

Available IC cards: CI-CA, PiTaPa, and ICOCA.
Unavailable IC cards: Suica, Pasmo, Kitaka, SUGOCA, manaca, TOICA, nimoca, and HAYAKAKEN

Publications

Participants of the conference are welcome to submit their contributions to the special issue of Applied Magnetic Resonance (http://www.springer.com/materials/journal/723) under co-guest-editorship of Professors Hitoshi Ohta (Kobe), Elena Bagryanskaya (Novosibirsk), Hong In Lee (Daegu), and Czeslaw Rudowicz (Szczecin). Submission deadline is Nov. 30, 2014.

Internet Connection

Internet connection will be available at both symposium and poster sites. Password will be included in the conference bag.

Oral Presentation Guideline

The bell will ring three times during oral presentation. The first bell rings when the designated time has passed and the second bell notifies that the presentation time is over. The third bell notifies that the scheduled time for presentation including discussions is over.

All oral speakers are strongly recommended to check the display connection at the presentation site before the session.

Poster Presentation Guideline

Poster session is held on Nov. 14 (Thu) at Nara Prefectural New Public Hall. Poster boards will be available after 17:10, and session time is 17:30 – 19:25. Posters should be removed when poster session is closed. Otherwise the posters will be discarded.

Opening Hours of Registration Desk

Nov.	12 (Wed)	11:00 ~ 18:00
	13 (Thu)	9:00 ~ 18:00
	14 (Fri)	9:00 ~ 17:30
	15 (Sat)	9:00 ~ 13:00
	16 (Sun)	9:00 ~ 15:30

APES2014-IES-SEST2014 Secretary

Dr. Susumu Okubo
Molecular Photoscience Research Center, Kobe University
1-1 Rokkodai-cho, Nada, Kobe 657-8501, Japan
E-mail : apes@kobe-u.ac.jp

Exhibitions

Exhibitions are in Room A (B1F) at Todaiji Culture Center.

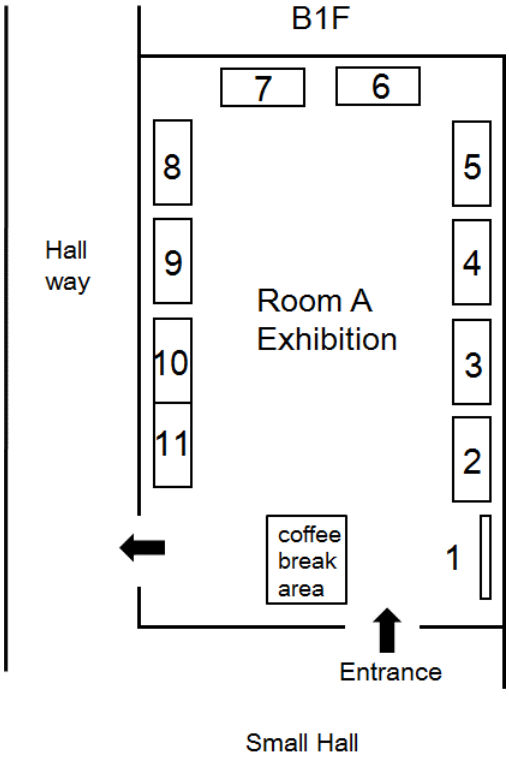

Booth No.	Exhibitor
1	Message board
2	Shizuoka University Center for Doctoral Career Development
3	INFRARED Limited
4	Tokyo Instruments Inc.
5	CORNES Technologies Ltd.
6	JEOL Ltd.
7	Thorlabs Japan Inc.
8	Flex Co., Ltd., KYOTO-SPINLABO LTD., Kimura Giken
9	KEYCOM Corp.
10, 11	Bruker BioSpin K.K.

Sponsors

International EPR(ESR) Society

The Society of Electron Spin Science and Technology (SEST)

Organization of Advanced Science and Technology, Kobe University

Morino Foundation for Molecular Science

Inoue Foundation for Science

Supporting Companies

Bruker BioSpin K.K.

INFRARED Limited

Tokyo Instruments Inc.

KEYCOM Corp.

JEOL Ltd.

Thorlabs Japan Inc.

AIR LIQUIDE Japan Ltd.

AmTechs Corporation

CORNES Technologies Ltd.

Shimadzu Corporation

Shizuoka University Center for Doctoral Career Development

Quantum Design Japan, Inc.

KYOTO-SPINLABO LTD.

Flex Co., Ltd.

Kimura Giken

Gyro Tech Co., Ltd.

SOGO ELECTRONICS,INC.

AILIN VACUUM Co., Ltd.

HAMAMATSU PHOTONICS K.K.

SUZUKI SHOKAN CO., LTD.

JECC TORISHA CO., LTD.

The Nippon Synthetic Chemical Industry Co., Ltd.

DESIGNER FOODS CO., LTD

DELICA FOODS CO., LTD

Nippon Sokki Co., Ltd

KOKENRIKA SEISAKUSYO K. K.

NIPPON AUTOMATIC CONTROL COMPANY

DOJINDO LABORATORIES

LABOTEC LTD.

MATSUO Co., Ltd.

Springer

Hitachi High-Tech Science Corporation

Hiroko Motizuki

Oral Presentations

PL-1

Magic Matrix Effects on Protein Dynamics Decoded by High-Field EPR

Klaus Möbius [1, 2]

[1] *Department of Physics, Free University Berlin, Arnimallee 14, 14195 Berlin, Germany*
[2] *Max Planck Institute for Chemical Energy Conversion, 45470 Mülheim (Ruhr), Germany*
E-mail: moebius@physik.fu-berlin.de

The biological function of many water-soluble and membrane proteins depends not only on the three-dimensional structure of the protein and its cofactors but also on the matrix properties of its micro-environment under the specific conditions of temperature and hydration degree. Remarkably, some organisms in the kingdoms of plants, animals and micro-organisms can survive long periods of complete dehydration and high temperatures transforming into an *anhydrobiotic state* of suspended metabolism. By adding some water they resume their metabolism again (like the "resurrection plants"). In the anhydrobiotic state, the intracellular medium contains large amounts of the non-reducing disaccharides *trehalose* or *sucrose*. Trehalose is most effective also in protecting isolated *in vitro* biostructures [1] which to exploit is a common technique in food preservation. However, the molecular mechanism of the anhydrobiotic biostability is largely unknown up to now.

To clarify the molecular mechanisms of disaccharide bioprotection, we studied the structure and dynamics of spin-labelled molecular systems and photosynthetic reaction centers (RCs) in sucrose and trehalose matrices at different hydration levels by cw and pulse high-field W-band (95 GHz) EPR as well as by FTIR [2,3]. Analysis of the EPR spectra showed that the structural organization and dynamics of the dehydrated matrix as well as their evolution upon re-hydration differ substantially between trehalose and sucrose. The dehydrated trehalose matrix is homogeneous in terms of distribution of the residual water and nitroxide probe molecules, which are equally immobilized at room temperature and at 150 K. In contrast, dehydrated sucrose forms a heterogeneous matrix. The different solvent-solute interaction characteristics account for the different protein-matrix dynamical coupling observed in dried sucrose and trehalose matrices and their different efficacy as a bioprotectant.

We conclude that the anhydrobiotic state of the RC-trehalose system (i) *is not* the result of matrix-induced changes of the local structure of the charge-separated radical-pair cofactors and (ii) *is not* the result of changes of local dynamics and local hydrogen bonding of Q_A in its binding pocket. Rather, the stability of the charge-separated radical-pair state originates in the high rigidity of the dry trehalose glass matrix coating the RC protein surface by hydrogen-bond networks already at room temperature. This shifts the correlation time of thermal conformational fluctuations into the *non-biological* time domain.

This work has been done in collaboration with M. Malferrari, F. Francia and G. Venturoli from the University of Bologna, Italy, and with A. Savitsky, A. Nalepa and W. Lubitz from the Max Planck Institute in Mülheim (Ruhr), Germany.

References

[1] Clegg, J.S., *Comp. Biochem. Physiol., B: Comp. Biochem.*, **2001**, 128, 613.
[2] Savitsky, A., Malferrari, M., Francia, F., Venturoli, G., Möbius, K., *J. Phys. Chem.* B, **2010**, 114, 12729.
[3] Malferrari, M., Nalepa, A., Francia, F., Venturoli, G., Lubitz, W., Möbius, K., Savitsky, A., *Phys. Chem. Chem. Phys.* **2014**, 16, 15910.

PL-2

Recent Progress in Theory of ESR in Strongly Correlated Spin Systems

Masaki Oshikawa

Institute for Solid State Physics, University of Tokyo, Kashiwa 657-8501, Japan

E-mail: oshikawa@issp.u-tokyo.ac.jp

Electron Spin Resonance (ESR) is not only one of the most important experimental probes to magnetic systems, but also a fundamental problem in statistical physics. The linear response theory, which is of ubiquitous importance, is initially developed [1] for treatment of magnetic resonances including ESR. Despite the success of the linear response theory as a general formulation, theory of ESR in strongly correlated systems poses a considerable challenge; the general difficulty of strongly correlated systems is amplified with the subtle nature of ESR. Thus, most of existing theoretical calculations rely on phenomenological assumptions, to some extent. In the low-energy limit of one-dimensional spin systems, however, a systematic formulation of ESR based on field theory is possible [2]. It turns out difficult to extend this to outside the low-energy limit, or to higher dimensions. Nevertheless, there are some encouraging progresses. I will review some of these theoretical developments in the last 10 years or so. The expected topics to be discussed, which are admittedly biased, include

- Kanamori-Tachiki formula [3] for ESR shift: modern interpretation and applications [4]
- Numerical approaches to ESR in strongly correlated spin systems [5]
- Memory-function type hypothesis and quasi-one-dimensional systems [6]
- Impurity effects and boundary resonances [7]

References

[1] Kubo R. and Tomita K., "A General Theory of Magnetic Resonance Absorption", *J. Phys. Soc. Jpn*. **1954**, 9, 888-919.

[2] Oshikawa M. and Affleck I., "Low-Temperature Electron Spin Resonance Theory for Half-Integer Spin Antiferromagnetic Chains", *Phys. Rev. Lett*. **1999**, 82, 5136-5139; "Electron spin resonance in S=1/2 antiferromagnetic chains", *Phys. Rev. B* **2002**, 65, 134410-1-28.

[3] Kanamori J. and Tachiki M., "Collective Motion of Spins in Ferro- and Antiferromagnets", *J. Phys. Soc. Jpn.* **1962**, 17, 1384-1394.

[4] Maeda Y., Sakai K. and Oshikawa M., "Exact Analysis of ESR Shift in the Spin-1/2 Heisenberg Antiferromagnetic Chain", *Phys. Rev. Lett.* **2005**, 95, 037602-1-4; Furuya, S. C., Suzuki, T., Takayoshi, S., Maeda Y. and Oshikawa M., "Single-ion anisotropy in Haldane chains and the form factor of the O(3) nonlinear sigma model", *Phys. Rev. B* **2011**, 84, 180410(R)-1-5; Furuya, S. C., Maeda Y. and Oshikawa M., "Electron spin resonance shifts in S=1 antiferromagnetic chains", *Phys. Rev. B* **2013**, 87, 125122-1-10.

[5] Iitaka T. and Ebisuzaki T., "Algorithm for Linear Response Functions at Finite Temperatures: Application to ESR Spectrum of s=1/2 Antiferromagnet Cu Benzoate", *Phys. Rev. Lett*. **2003**, 90, 047203-1-4; Tiegel A. C., Manmana S. R., Pruschke T. and Honecker A., "Matrix product state formulation of frequency-space dynamics at finite temperatures", *Phys. Rev. B* **2014**, 90, 060406(R)-1-5.

[6] Furuya S. C. and Sato M., "Electron Spin Resonance in Quasi-One-Dimensional Quantum Antiferromagnets: Relevance of Weak Interchain Interactions", e-print arXiv:1308.2714.

[7] Furuya S. C. and Oshikawa M., "Boundary Resonances in S=1/2 Antiferromagnetic Chains Under a Staggered Field", *Phys. Rev. Lett.* **2014**, 109, 247603-1-5.

PL-3

Very High Sensitivity Orientational PELDOR

Graham Smith[1], Johannes McKay[1], Claire Motion[1], Paul Cruickshank[1], Robert Hunter[1], David Bolton[1], Duncan Robertson[1], Hassane El Mkami[1], Richard Wylde[2], Michael Stevens[3], David Norman[3]

[1]School of Physics and Astronomy, University of St Andrews, Scotland
[2]Thomas Keating Ltd., Staton Mills, Billingshurst, England
[3]School of Life Sciences, University of Dundee, Dundee, Scotland
E-mail: gms@st-and.ac.uk

Orientational PELDOR is a technique to determine both the distance and relative orientation between pairs of "highly constrained" spin labels (or other paramagnetic centres). The technique becomes particularly powerful using semi-rigid spin labels such as the RX spin label[1] at W-band frequencies, where the g-factor of nitroxides become fully resolved. Experiments have shown the rigidity of this spin label can allow well defined (narrow) distance and orientation distributions to be measured, and to be directly related to the underlying protein structure. This adds considerable extra information content relative to standard PELDOR measurements using conventional spin labels. But, the Orientational PELDOR technique itself requires multiple selective individual PELDOR measurements over large bandwidths and, for many systems, only becomes practical if concentration sensitivity is relatively high.

However, using the design mantra, "high power, high frequency, high volume" we have constructed a W-band pulse EPR spectrometer that has orders of magnitude more concentration sensitivity than standard commercial X-band instruments, whilst benefiting from very large instantaneous bandwidths low deadtime and high g-factor resolution. The HIPER spectrometer[2] system routinely now offers 20-30 x improvement in sensitivity for PELDOR/DEER measurements, compared to X-band, for the same sample volume, but over greatly increased bandwidth. It is also believed that another order of magnitude improvement in sensitivity is still experimentally possible with relatively modest adaptations. For individual PELDOR measurements, this means, today, that samples can now be measured in minutes rather than days, or concentration levels can be reduced to micro-molar levels, or time windows can be significantly extended to measure longer distances. Orientational PELDOR measurements also become highly practical.

In the talk I will give a number of examples illustrating the potential of both the instrumentation and the Orientational PELDOR technique.

References

[1] Fleissner, M.R., et al., "Structure and dynamics of a conformationally constrained nitroxide side chain and applications in EPR spectroscopy". Proceedings of the National Academy of Sciences of the United States of America, 2011. **108**(39): p. 16241-16246.

[2] Cruickshank, P.A.S., et al., "A kilowatt pulsed 94 GHz electron paramagnetic resonance spectrometer with high concentration sensitivity, high instantaneous bandwidth, and low dead time". Review of Scientific Instruments, 2009. **80**(10): p. 103102

PL-4

THE NEW SPIN PROBES FOR BIOCHEMICAL APPLICATIONS

E. Bagryanskaya

[1]N.N.Vorozhtsov Novosibirsk Institute of Organic Chemistry SB RAS, Pr. Lavrentieva 9, Novosibirsk, 630090, Russia
[2]International Tomography Center SB RAS, Institutskaya 3A, Novosibirsk, 630090, Russia

E-mail: egbagryanskaya@nioch.nsc.ru

The range of applications of stable nitroxides involves living polymerization, magnetic materials, reagents for selective oxidation, functional probes for measurement of oxygen, pH, thiols and NO in various heterogeneous media (including living tissues), structural studies of biological macromolecules, therapeutic agents, MRI contrast agents, electrode active and charge storage materials in rechargeable batteries, etc. The advantages of sterically substituted nitroxide application in material science and biophysics will be demonstrated using our recent results [1-5]. A series of new nitroxides - potential spin probes for EPR and MRI redox status measurements in biomedical research was synthesized and studied using CW and pulse EPR [4]. It is shown that the stability of synthesized nitroxides against reduction by ascorbic acid substantially exceed the same for spirohexasubstituted TEMPO and OXO-TEMPO. The new spin labels demonstrated clear advantages over 2,2,5,5-tetramethylpyrroline nitroxides with respect to electron spin relaxation rates, which should allow PELDOR distance measurements at liquid nitrogen temperature range [3,4].

Resolving the nanometer-scale structure of biomolecules in natural conditions still remains a challenging task. We report the first distance measurement in nucleic acid at room temperature using Electron Paramagnetic Resonance (EPR) using a 10-mer DNA duplex as an example [5]. The essential milestones of this success have been (i) the use of triarylmethyl-based spin labels with long relaxation time, (ii) the development of SDSL strategy for attaching TAM label to nucleotide residue via a rigid piperazine linker, and (iii) the elaboration of the efficient and delicate immobilization procedure using Nucleosil^{TM} sorbent. Simultaneously, these advances allowed us to measure as long distances as ~4.5 nm with high accuracy and in conditions simulating natural ones (water solution at 300 K). The developed approaches are rather flexible and universal. They can be adapted and applied in a broad range of biological studies involving nucleic acids, stimulating further progress in determination of nanometer-scale structure and dynamics of biological systems in natural conditions. The measurements of series of new trityl radicals were performed and peculiarities of electron spin relaxation of trytul radicals of different structure will be under discussion.

References.

[1] E.G.Bagryanskaya, S.R.A.Marque, *Chemical reveiws*, 2014, 114, 5011–5056
[2] M.Edeleva et al., *J.Polym. Scien, Polym.Chem*. 2014, 52, 2014, 929-943.
[3] A. Sheveleva et al., *J. Phys. Chem. Lett.*, 2014, 5, 20–24.
[3] I.Kirilyuk et al., *J. Org. Chem.*, 2012, 77, 8016-8027
[4] E.Babaylova, et al.*Org. Biomol. Chem.*, 2014,12, 3129-3136
[5] G. Yu. Shevelev, et al. *J.Amer.Chem.Soc.*, 2014, submitted.

Acknowledgements

This work was supported by the RFBR (№12-04-01435) and RSF (№14-14-00922).

PL-5

Harden M. McConnell - the life of a giant in magnetic resonance

Lawrence J Berliner[1,2]

[1]*Department of Chemistry and Biochemistry, University of Denver, Denver USA 80208*
[2]*Emeritus Professor, Department of Chemistry, The Ohio State University, Columbus, Ohio USA 43210*

E-mail: berliner@du.edu

Harden Marsden McConnell passed away October 6, 2014 after a struggle with terminal cancer. This lecture covers the life history of McConnell and some of his major contributions to magnetic resonance and, more particularly, EPR from a PhD student of his, an observer and a participant in some of the many developments that he contributed to our field, to science and the world.

With relevance to the International EPR(ESR) Society, he was chosen for the Gold Medal in 1997 – with an emphasis in Biology & Medicine and in 2014 he was elected a Fellow of the IES. In the field of EPR, he was also the 1995 Bruker Award and the 2000 Zavoisky Award recipient. He won many other awards including the 1983 Wolf Prize in Chemistry, 1989 U.S. National Medal of Science for Chemistry, 1988 U.S. National Academy of Sciences Award in Chemical Sciences. The American Chemical Society recognized him several times: 1962 ational ACS Award in Pure Chemistry, 1972 Irving Langmuir Award in Chemical Physics, 1990 Peter Debye Award in Physical Chemistry.

This report is a personal perspective and may occasionally have some omissions of works that the author inadvertently overlooked and offers his deepest apologies.

PL-6

Overhauser Dynamic Nuclear Polarization at a Magnetic Field of 9.2 T

Thomas F. Prisner, Vasyl Denysenkov, Petr Neugebauer, Jan Krummenacker

Department of Physical and Theoretical Chemistry and Center of Biomolecular Magnetic Resonance, Goethe University Frankfurt am Main, Germany

E-mail: prisner@chemie.uni-frankfurt.de

Dynamic Nuclear Polarization (DNP) allows to enhance proton NMR signals more than two orders of magnitude and therefore strongly increase the sensitivity of NMR spectroscopy. Unfortunately the polarization transfer mechanism for solids and liquid samples work best at low magnetic fields (< 1T), where chemical shift resolution is too small for structural studies. Only recently DNP has been applied at high magnetic fields (>3 T), first in the solid state and more recently also in the liquid state [1, 2]. Here we will present major technical requirement for DNP at 9.2 T, which comprises a double resonance structure for EPR excitation at 260 GHz and NMR detection at 400 MHz [3] as well as applications to several different solvents and other target molecules [4-6]. TEMPOL radicals were used as DNP agents in all cases. The observed DNP enhancements are compared with predictions by NMR dispersion measurements [5,6] and with molecular dynamic simulations [7, 8] and discussed with respect to the physical origins of the sub-ps dynamics responsible for the polarization transfer at high magnetic fields

[1] M. J. Prandolini, V. P. Denysenkov, M. Gafurov, B. Endeward and T. F. Prisner, *J. Am. Chem. Soc.*, 2009, **131**, 6090-6092.
[2] C. Griesinger, M. Bennati, H. M. Vieth, C. Luchinat, G. Parigi, P. Höfer, F. Engelke, S. J. Glaser, V. Denysenkov and T. F. Prisner, *Prog. Nucl. Magn. Reson. Spectrosc.*, 2012, **64**, 4-28.
[3] V. Denysenkov and T. Prisner, *J. Magn. Reson.*, 2012, **217**, 1-5.
[4] J. Krummenacker, V. Denysenkov, T. F. Prisner *Appl. Magn. Reson.*, 2012, **43**, 139-146.
[5] P. Neugebauer, J. G. Krummenacker, V. P. Denysenkov, G. Parigi, C. Luchinat and T. F. Prisner, *Physical Chemistry Chemical Physics*, 2013, **15**, 6049-6056
[6] P. Neugebauer, J. Krummenacker, V. Denysenkov, C. Helmling, C. Luchinat, G. Parigi, T. Prisner *Physical Chemistry Chemical Physics* 2014 **DOI: 10.1039/c4cp02451f**
[7] D. Sezer, M. J. Prandolini and T. F. Prisner, *Phys. Chem. Chem. Phys.*, 2009, **11**, 6626-6637.
[8] D. Sezer *Phys. Chem. Chem. Phys.* 2014, **16**, 1022-1032

PL-7

Protein Dynamic Structure Revealed by High Sensitivity Pulse Dipolar ESR Distance Measurements

Jack H. Freed

Department of Chemistry and Chemical Biology, and ACERT - National Biomedical Center for Advanced ESR Technology, Cornell University, Ithaca, New York, USA

jhf3@cornell.edu

Pulse dipolar electron-spin resonance (PDS-ESR) has emerged as a powerful methodology for the study of protein structure and function. This technology, in the form of double quantum coherence (DQC) – ESR and double-electron-electron resonance (DEER) in conjunction with site-directed spin-labeling will be described. It enables the measurement of distances and their distributions in the range of 1-9 nm between pairs of spins labeled at two sites in the protein. Concentrations from micromolar to tens of millimolar are amenable, requiring only small amounts of biomolecules. The distances are quite accurate, so a relatively small number of them are sufficient to reveal structures and functional details. Several examples will be shown. The first is defining the protein complexes that mediate bacterial chemotaxis, which is the process whereby cells modulate their flagella-driven motility in response to environmental cues. It relies on a complex sensory apparatus composed of transmembrane receptors, histidine kinases, and coupling proteins. PDS-based models have captured key architectural features of the receptor kinase arrays and the flagellar motor, and their changes in conformation and dynamics that accompany kinase activation and motor switching. Another example will be determining the conformational states and cycling of a membrane transporter, GltPh, which is a homotrimer, in its apo, substrate-bound, and inhibitor-bound, states in membrane vesicles providing insight into its energetics. In a third example the structureless (in solution) proteins alpha-synuclein and tau, which are important in Parkinson's disease and in neurodegeneration will be described and the structures they take on in contact with membranes will be described. Also the relevance of the protein SOD-1 to Lou Gehrig's disease will be described using Cu^{2+} - Cu^{2+} PDS. The relative virtues of DQC and DEER in these studies are compared, and the new technique of 5-pulse DEER, which can also double acquisition times, will be discussed.

PL-8

Clinical Applications of EPR

Harold M. Swartz[1], Ann B. Flood[1], Benjamin B. Williams[1], Steven G. Swarts[2], Oleg Grinberg[1], Jason Sidabras[3]

[1]*Geisel School of Medicine at Dartmouth, EPR Center for the Study of Viable Solutions, Lebanon, New Hampshire,03766*

[2]*University of Florida, Department of Radiation Oncology, Gainesville, Florida, 32610*

[3]*Medical College of Wisconsin, Department of Biophysics, Milwaukee, Wisconsin,53226*

E-mail: Harold.swartz@dartmouth.edu

The development and use of *in vivo* techniques for experimental applications of EPR in animals has been very successful and now has led to attractive clinical applications. This presentation provides an overview of the challenges, opportunities, and results as *in vivo* EPR is extended into use in human subjects. The most widespread clinical use is oximetry, where EPR can make repeated and accurate measurements of pO_2 in tissues, which provides clinicians with information that bears directly on diagnosis and therapy, especially for oncology, peripheral vascular disease, and wound healing. We have recently shown that it is feasible and effective to repeatedly directly measure pO2 in tumors in human subjects. Our results indicate how this could be used to significantly enhance the effectiveness of cancer therapy (especially Radiation Therapy) including selection of subjects who are likely to benefit from interventions designed to enhance tumor oxygenation.It was shown that: 1. the pO2 in human tumors can be measured under conditions compatible with regular clinical practice; 2. the baseline pO2 in the tumors varied from 0 to 10 torr; 3. Tumors differed as to whether their pO2 was affected by breathing 100% oxygen (40% did not respond at all); 4. The changes in pO2 in individual tumors ranged from 0 to more than 100 torr. Conclusion: EPR oximetry is now poised to be utilized clinically to definitively whether the use of repeated measurements of determine tumor pO2 can be used to select subjects who will benefit from hyperoxygenation interventions and to more optimally time the therapy to exploit clinically the radio sensitizing effect of oxygen.

The other area of importance in human subjects is the ability of *in vivo* EPR to measure clinically significant exposures to ionizing radiation 'after-the-fact', due to accidents, terrorism, or nuclear war. Developments using EPR tooth dosimetry based on measurements of the upper incisors in situ have matured sufficiently such that its development into a deployable device suitable for use by non-expert operators for carrying out initial triage in the field to determine immediately whether an individual has a high probability of having received at least 2 Gray. Complimentary methods based on nails are under way using both nail clippings and measurements of nails in situ. The use of nails provides the additional capability of determining the homogeneity of the exposure. The most likely application of this approach is to measure clipped nails transported to specialized laboratoriesand in vivo EPR using nails in situ to provide information on the hoimogeneity of the exposure, which is a key factor in determining therapy. The key to be able to measure nails in situ is implementaion of new resonator concepts that permit measurements to be made invivo using higher frequency (9 GHz) EPR. **Conclusions:** We conclude that EPR methods are likely to be very useful additions to the methods used for immediate triage in the field and may also be useful in facilitating decisions on treatment.

Nanoscale magnetic resonance with single elecltron spin sensor under ambient conditions

Fazhan Shi[1], Xi Kong[1], Pengfei Wang[1], Tobias Staudacher[2], Friedemann Reinhard[2], Joerg Wrachtrup[2] and Jiangfeng Du[1]

[1]*Hefei National Laboratory for Physical Sciences at the Microscale and Department of Modern Physics, University of Science and Technology of China, Hefei 230026, China*
[2]*3rd Physics Institute and Research Center SCoPE, University of Stuttgart, 70569 Stuttgart, Germany*

E-mail: fzshi@ustc.edu.cn

Current spin-magnetic resonance spectrometers are based on the principle of ensemble detection and the test object is an ensemble sample containing billions of identical spins. However, at room temperature NMR/ESR at nano-scale is still a huge challenge. To achieve the scientific goal, we choose single spins in solids based on NV defect center in diamond - (NV) as the sensitivity magnetic probe. The single NV spin can be easily visualized, polarized and detected with a confocal microscope. Ultra-long spin coherence time for such qubits, even at room temperature, enables it is ultra-sensitivity to external magnetic noise with characteristic frequency. Instead of traditional detection manner, weak magnetic signals generated by the nano-scale spin system is mapped to coherent state phase, so as to realize high sensitivity signal detection.

We designed and constructed the S-band Optical Detected Magnetic Resonance spectrometers to meet the requirement of the quantum manipulation on single NV spin at room temperature. By the quantum interferometer of NV sensor on the home-built setup, we have experimentally realized atomic-scale structure analysis of single nuclear-spin clusters [1] and succeed to detect a single electron spin[2] in diamond. Collaborates with scientists from Germany and America, we succeed in detection of $(5nm)^3$ hydrogen nuclear spin sample using shallow NV probes. It's a "first step toward molecular-scale magnetic resonance imaging". Recently, we have detected ESR spectrum from single proteins [4].

These results indicate that, central spin decoherence under dynamical decoupling control is a useful probe for nuclear magnetic resonance single-molecule spectroscopy and structure analysis. It provides a new method for nano-scale science, including physics, life science and chemistry.

References:

[1] Shi F. Z., Kong X., Wang P. F., Kong F., Zhao N., Liu R-B. and Du J. F. "Sensing and atomic-scale structure analysis of single nuclear spin clusters in diamond", *Nature Physics* **2014**, 10, 21-25.
[2] Shi F. Z., Zhang Q., Naydenov B., Jelezko F., Du J. F., Reinhard F., and Wrachtrup J. "Quantum logic readout and cooling of a single dark electron spin", *Phys. Rev. B* **2013**, 87, 195414.
[3] Staudacher T., Shi F. Z., Pezzagna S., Meijer J., Du J. F., Meriles C. A., Reinhard F., Wrachtrup J. "Nuclear magnetic resonance spectroscopy on a $(5nm)^3$ volume of liquid and solid samples", *Science* **2013**, 339, 561-563.
[4] Shi F. Z., Zhang Q., et al. "Single molecular magnetic resonance spectroscopy under ambient conditions". In preparation (2014).

Towards the structural design of piperidine nitroxides for in vivo measurement probe

Toshihide Yamasaki[1], Kiyoshi Sakai[1], and Ken-ichi Yamada[1,2]

[1]*Department of Bio-functional Science, Faculty of Pharmaceutical Sciences, Kyushu University, Fukuoka 812-8582, Japan*
[2]*JST PRESTO, 4-1-8 Honcho, Kawaguchi, Saitama, 332-0012, Japan*

E-mail: toshihide@pch.phar.kyushu-u.ac.jp

Nitroxides (nitroxyl or aminoxyl radicals) have been widely used in the biological fields to serve as antioxidants, contrast agents, spin labels and spin probes. However nitroxides were immediately reduced to hydroxylamine *in vivo* by reductants such as ascorbate.[1] To overcome this issue, nitroxides having ethyl groups at α-position of the N-O moiety have been reported.[2] This motivated us to control the reactivity with the substituent near the N-O group. However there were no versatie synthetic method to introduce a variety of substituents near the N-O moiety.

Herein, the aim of this study was to develop the new synthetic approach to substitute the four methyl groups of 4-oxo-TEMPO (2,2,6,6-tetramethyl piperidin-4-one-1-oxyl), which is well used for *in vivo* redox status detection, and invastigate the structure-reactivity relationship. These results were that the four methyl groups of TEMPO were easily substituted to afford 2,6-substituted piperidin-4-one nitroxides.[3] And the reactivity toward ascorbate was varied with the substituents proximal to N-O moiety, which was well correlated with the redox potential.[4] Among other reactants such as ROS, the inhibition effect of lipid peroxidation was increased especially with the alkyl substituents and correlated with its alkyl length[5] retaining the resistant to reduction by ascorbate. These results indicated that the reaction specificity of nitroxides would be controlable by introducing the optimal substituents near the N-O moiety.

In conclusion, we succeeded to vary the reactivity toward ascorbate and lipid peroxidation by development of versatile synthetic method for substitution near the N-O moiety. This method can offer the ability to develop novel nitroxides having more effective antioxidant activity by controlling the reactivity.

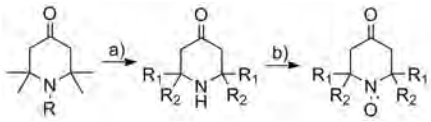

Scheme. Synthetic route for 2,6-substituted piperidine nitroxides. R = H or Me. a) R_1COR_2, NH_4Cl, base; b) H_2O_2, $Na_2WO_4 \cdot 2H_2O$

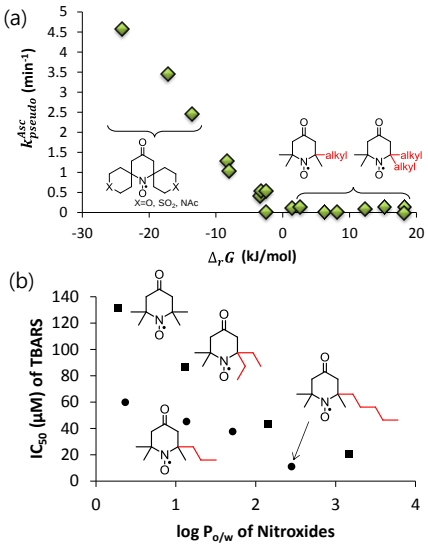

Fig. (a) Plot of pseudo first-order kinetic with $\Delta_r G$. (b) Plot of IC_{50} of TBARS with $\log P_{o/w}$ of nitroxides.

References

[1] Saphier, O., Silberstein, T., Shames, A. I., Likhtenshtein, G. I., Maimon, E., Mankuta, D., Mazor, M., Katz, M., Meyerstein, D., Meyerstein, N., "The Reduction of a Nitroxide Spin Label as a Probe of Human Blood Antioxidant Properties", *Free Radic. Res.* **2003**, 37, 301-8.

[2] Bobko, A., Kirilyuk, I., Grigor'ev, I., Zweier, J., Khramtsov, V., "Reversible reduction of nitroxides to hydroxylamines: roles for ascorbate and glutathione", *Free Radic. Biol. Med.* **2007**, 42, 404-12.

[3] Sakai K., Yamada K., Yamasaki T., Kinoshita Y., Mito F., Utsumi H., "Effective 2,6-substitution of piperidine nitroxyl radical by carbonyl compound", *Tetrahedron* **2010**, 66, 2311-5.

[4] Yamasaki T., Mito F., Ito Y., Pandian S., Kinoshita Y., Nakano K., Murugesan R., Sakai K., Utsumi H., Yamada K., "Structure-reactivity relationship of piperidine nitroxide: electrochemical, ESR and computational studies", *J. Org. Chem.* **2011**, 76, 435-40.

[5] Yamasaki T., Ito Y., Mito F., Kitagawa K., Matsuoka Y., Yamato M., Yamada K., "Structural concept of nitroxide as a lipid peroxidation inhibitor", *J. Org. Chem.* **2011**, 76, 4144-8.

Electron Spin Resonance Studies of Organic Electronic Materials and Devices

Shin-ichi Kuroda

Department of Applied Physics, Nagoya University, Nagoya 464-8603, Japan

E-mail: kuroda@nuap.nagoya-uc.ac.jp

Organic electronic devices such as electroluminescent (EL) displays, field-effect transistors and solar cells attract much attention as low-cost devices with flexibility. Varieties of molecular materials based on π-conjugated polymers and small molecules have been synthesized since the discovery of polyacetylene by Shikarawa, Heeger and MacDiarmid. Unpaired electrons in these materials such as solitons and polarons carry spin and charge and play important roles in manifesting the functions of materials. Based on this understanding, we have been applying electron spin resonance (ESR) spectroscopy as a powerful microscopic tool to investigate the fundamental properties of molecular materials and the electronic processes in the devices by detecting unpaired electron spins.

Initial challenge was the study of the soliton in polyacetylene. By use of stretch-oriented Shirakawa samples, π-electron character of spin center has been successfully confirmed through the characteristic anisotropy of g-value and hyperfine coupling. ENDOR spectra of stretch-oriented samples unambiguously showed the soliton spin distribution close to the theoretical prediction [1]. Second topic was the polaron in EL polymers that have been discovered by R. Friend. First ENDOR spectra of EL polymers were obtained using stretch-oriented samples [2]. After moving to Nagoya, the author carried out international joint research with Friend's group, where polarons in EL polymers were observed by light-induced ESR (LESR) to elucidate their wave functions [3].

Eventually, new regioregular polythiophene (rr-PT) and fullerene composites appeared as solar cell materials. LESR and LENDOR were successfully observed for photoinduced hole polarons. Organic transistors of rr-PT also attracted attention. Direct observation of charges in organic transistors was a big challenge. In 2004, we have developed a new technique, field-induced ESR (FI-ESR) method which can detect charges injected at the interface of organic transistors [4]. The method has proved to be useful in finding electronic states, spin-charge relation, wave functions, dynamics, and local molecular orientations, crucial for device performance [5-7]. In recent thienothiophene-based organic transistors, carrier motion has been directly observed in the crystallites even at 4K, providing evidence for intrinsic high mobility of these molecular materials [7]. At higher doping levels, crossover of polarons with spin to spinless bipolarons (or polaron pairs) has already been observed [4, 6]. Recent high-mobility semicrystalline polymer has shown such tendency of the formation of spinless states and even the metallic states with clear Pauli susceptibility with retaining crystallinity [8]. Such spin and metallic properties now attract significant attention from spintronics and thermoelectric applications.

In conclusion, ESR spectroscopy has provided valuable information of molecular materials and devices and it is further expected to be useful in exploring the nature of molecular systems. Finally, the author expresses his sincere gratitude to all the collaborators for their significant contributions.

References

[1] Kuroda S. and Shirakawa H., *Phys. Rev. B* **1987**, 35, 6471-6474. [2] Kuroda S., Noguchi T. and Ohnishi T., *Phys. Rev. Lett.* **1994**, 72, 286-289. [3] Kuroda S., Marumoto K., Ito H., Greenham N. C., Friend R. H., Shimoi Y. and Abe S., *Chem. Phys. Lett.* **2000**, 325, 183-188. [4] Marumoto K., Muramatsu Y., Ukai S., Ito H. and Kuroda S., *J. Phys. Soc. Jpn.* **2004**, 73 1673-1676. [5] Marumoto K., Kuroda S., Takenobu T. and Iwasa Y., *Phys. Rev. Lett.* **2006**, 97, 256603-1-4. [6] Watanabe S., Tanaka H., Kuroda S. et al., *Appl. Phys. Lett.* **2010**, 96, 173302-1-3. [7] Tanaka H., Kozuka M., Watanabe S., Ito H., Shimoi Y., Takimiya K. and Kuroda S., *Phys. Rev. B* **2011**, 84, 081306-1-4 (R). [8] Tanaka H., Hirate M., Watanabe S. and Kuroda S., *Adv. Mater*. **2014**, 26, 2376-2383.

In Vivo EPR Imaging Studies of a Brain Disease Mouse Model

Hirotada Fujii[1]

[1]*Center for Medical Education, Sapporo Medical University, Sapporo 060-8556, Japan*

E-mail: hgfujii@sapmed.ac.jp

Paramagnetic centers, such as reactive oxygen species (ROS), reactive nitrogen species (RNS) and paramagnetic metal ions, are of crucial importance in many biological functions. Some attempts to detect ROS and RNS produced in biological systems were made at X-band frequency in the early seventies [1], but their works were limited by the size and electronic constraints of the X-band cavity. The conventional X-band EPR spectrometers have several technical limitations to measurements on live animals, thus the requirements for small animal studies are twofold: a resonant device with dimensions suitable to fit a whole animal (mice or rats), and a choice of an operating frequency that does not produce dielectric heating. An important methodological breakthrough was the use of low microwave frequency operating at L-band where dielectric losses were reduced significantly. Second was the newly developed resonant devices, such as surface coils and loop gap resonators. Current in vivo EPR spectroscopy studies began in the early 1980s, working at L-band microwave frequency with home-made cavity systems. The first major success occurred using the loop-gap resonator [2]. Lukiewicz et al. [3] demonstrated the direct in vivo observation of melanin bio-radicals in an implanted melanoma tumor in the mouse tail.

First EPR imaging study has been demonstrated for the visualization of the distribution of paramagnetic centers in materials. The first EPR imaging experiment involving an in vivo model for biological sample with nitroxides was reported in 1985 [4], which monitored the capillary action of plant species when dipped into a solution of TEMPOL. The plant stem with two capillaries was placed in the flat-loop coil under 3mT/cm field gradient. The obtained one-dimensional EPR image indicates several interesting information; (i) speed of a capillary action through the vessel, (ii) homogenous/ inhomogeneous distribution of nitroxides between two vessels, and (iii) reduction of nitroxides dependent on the antioxidants in the plant. Unique capability of EPR imaging to visualize the distribution of nitroxide imaging probes led to the observation of heterogeneous tissue structures in the tumor implanted into the mouse tail [5]. Furthermore, as the bio-reduction of nitroxides has been shown to be dependent on the redox status of the tissue, EPR image is able to visualize the redox information non-invasively.

In this presentation, the basics of the modern EPR imager using recently developed new technology and its applications in experimental animals will be discussed [6, 7].

References

[1] Feldman A., et al., “In vivo electron spin resonance in rats”, *Phys Med Biol* **1975**, 20, 602-612.
[2] Froncisz SJ. and Hyde JS., “The loop-gap resonator. A new microwave lumped circuit ESR sample structure”, *J Magn Reson* **1982**, 47, 515-521.
[3] Lukiewicz SJ. and Lukiewicz SG., “In vivo ESR spectroscopy of large biological objects”, *Magn Reson Med* **1984**, 1, 297.
[4] Berliner LJ. and Fujii H., “Magnetic Resonance Imaging of Biological Specimens by Electron Paramagnetic Resonance of Nitroxide Spin Labels”, *Science* **1985**, 227, 517-519.
[5] Berliner LJ., Fujii H., et al., “Feasibility Study of Imaging a Living Murine Tumor by Electron Paramagnetic Resonance”, *Magn Reson Med* **1987**, 4, 380-384.
[6] Fujii H., et al., “Development of an EPR/MRI Dual-imaging system as a tool to detect bioradicals”, *Magn Reson Med Sci* **2006**, 5, 17-23.
[7] Fujii H., et al., “Mapping of Redox Status in a Brain-Disease Mouse Model by Three-Dimensional EPR Imaging”, *Magn Reson Med* **2011**, 65, 295-303.

High-frequency ESR Studies of Molecule-based Conductors and Magnets

Yugo Oshima[1]

[1]*Condensed Molecular Materials Lab., RIKEN, Wako 351-0198, Japan*

E-mail: yugo@riken.jp

Molecular-based conductors and magnets have attracted broad interests due to characteristic features such as the degree of freedom of the molecular design, flexibility, its wide variety of ground states and so on. In recent years, interesting phenomena such as the giant magnetoresistance or field-induced superconductivity have been observed in molecular conductors where conducting π-electrons interact with localized *d*-electrons. Moreover, nano-scaled magnets such as the single-molecule magnets with unique magnetic network have been synthesized, and its peculiar magnetic properties have been revealed. High-frequency ESR is one of the important methods to clarify the ground states or the magnetic properties of such interesting molecular materials thanks to its high-sensitivity, high-resolution and accessibility to the high-magnetic field. For the past decade, we have developed a high-frequency ESR system optimized for molecular materials with an additional rotation mechanism and simultaneous transport measurement system. The talk will consist of three subjects that we have achieved on molecular materials by the use of our high-frequency ESR system.

(1) *Studies on single-chain magnets and molecular conductors by use of the high-frequency ESR system* [1,2]

Molecule-based single-chain magnet is a good 1D magnetic system with infinitesimal interchain couplings. However, its low energy excitation has never been explored. Thanks to the high-frequency ESR, it is revealed that the observed ESR mode is attributed to the spin wave excitation with strong magnetic anisotropy. Moreover, ESR measurements of π-*d* molecular conductor β-$(BDA\text{-}TTP)_2FeCl_4$ will be presented, and its peculiar antiferromagnetic ground states will be discussed.

(2) *Determination of the exchange energies in the nano-scaled molecular magnets by ESR* [3]

The magnetism of the polyoxometalate cluster $\{Mo_{75}V_{20}\}$, containing a saw-tooth ring of 10 corner-sharing triangles, has remained debatable since it is masked by contribution from impurities as well as van Vleck paramagnetism. Here, we will demonstrate the usefulness of high-frequency ESR in such material, and discuss how to determine the exchange parameters.

(3) *Control of the electronic states by dynamical spin reversal* [4]

The molecular conductor λ-$(BETS)_2FeCl_4$ shows a superconductivity in the high magnetic field. This is due to the compensation effect between the conducting π-electrons and localized *d*-electrons. We have succeeded to destroy the field-induced superconductivity by ESR, namely, by dynamical spin reversals of *d*-electrons.

References

[1] Oshima Y., Nojiri H., Asakura K., Sakai T., Yamashita M. and Miyasaka H., *"Collective magnetic excitation in a single-chain magnet by electron spin resonance measurements"*, Phys. Rev. B, (2006), 73, 214425.

[2] Tokumoto T., Brooks J.S., Oshima Y., Choi E.S., Brunel L.C., Kaihatsu T., Yamada J. and van Tol J., *"Antiferromagnetic d-electron exchange via a spin-singlet pi-electron ground state in an organic conductor"*, Phys. Rev. Lett., (2008), 100, 147602.

[3] Oshima Y., Nojiri H., Schnack J., Koegerler P. and Luban M., *"Determination of exchange energies in the sawtooth spin ring $\{Mo_{75}V_{20}\}$ by ESR"*, Phys. Rev. B, (2012), 85, 024413.

[4] Oshima Y., Nojiri H., Uji S., Brooks J.S., Tokumoto T., Cui H.-B., Kato R., Kobayashi A. and Kobayashi H., *"Breakdown of the field-induced superconductivity by dynamical spin reversal"* Phys. Rev. B, (2012), 86, 024525.

Time-Resolved Spectroscopic Study on Paramagnetic Intermediates Generated by Photochemical Reactions.

Tomoaki Yago

Department of Chemistry, Graduate School of Science and Engineering, Saitama University, 255 Shimo-ohkubo, Sakura-ku, Saitama 338-8570 Japan

E-mail: yago@chem.saitama-u.ac.jp

Photochemical reactions often involve paramagnetic chemical intermediates such as excited triplet state, radicals and radical pairs. The spin dynamics in these intermediates provide the valuable information on the mechanism of the chemical reactions including the environmental effects. The author has studied such spin dynamics in photochemical processes by using time-resolved optical spectroscopy such as EPR and transient absorption. The obtained results were analyzed by using the stochastic Liouville equation (SLE) to extract the dynamical information in the course of the chemical reactions. Here three different researches, in which the author was involved so far, are presented.

"Hydrogen bonding effects on the reorganization energy in electron transfer reactions"
(Time-resolved EPR study at Tohoku University, the Tero group)

Hydrogen bonding is ubiquitous to biological systems and it has been believed that hydrogen bonding plays important roles in biological electron transfer reaction systems. However the details of the hydrogen bonding effects on the ET reactions had not been clarified. The hydrogen bonding effects on the electron transfer were therefore studied by observing the chemically induced dynamic electron polarizations (CIDEPs) generated in the bimolecular ET reactions in polar solvents. The charge transfer interaction, which connects the singlet-triplet energy splitting (J) and the charge recombination reaction rate, was the key to determine the reorganization energies in radical ion pairs. It is shown for the first time that hydrogen bonding increase the reorganization energy in addition to the stabilization of the charge separated states and varies the electron transfer reaction rate.

"Light induced spin coherences in photo-excited triplet state under the external magnetic field"
(Time-resolved EPR study at Freiburg University, the Kothe group)

It is well known that the light induced spin coherences are generated in the spin correlated radical pairs. Such spin coherences can be interpreted by the adiabatic change of the spin Hamiltonian with the photo-induced ET reactions. The detailed theoretical analysis in the Freiburg EPR group suggested that the adiabatic change of the spin Hamiltonian is also involved in the generation of the photo-excited triplet state under the magnetic field. In the photo-excited triplet state, the oscillations of the EPR signals originated from the light-induced nuclear coherences were observed for the first time by using an X-band EPR spectroscopy. The generated nuclear spin coherences were associated with the high spin polarizations created by the intersystem crossing in photo-excited triplet state.

"Magnetic field effects on radical pairs in ionic liquids"
(Transient absorption study at Saitama University, the Wakasa group)

Ionic liquids are liquids solely consisting of caion and anion and are currently recognized as a new class of promising solvents. However the ionic liquids have the complex solvent structures and the mechanisms of the chemical reactions in the ionic liquids are still unknown. The MFEs on the radical pairs were then studied by using a nano-second laser flash photolysis. The detailed analysis indicated that nano-ordering structures are created in ionic liquids and such structures cause the inhomogeneous diffusions of the solute molecules. It was also found that the lifetimes of the radical pairs are prolonged when the radicals have plus or minus charges due to the strong solute-solvent Coulomb interactions.

Finally, the author would like to thank Prof. Tero (Tohoku University), Prof. Kobori (Kobe University), Prof. Kothe (Freiburg University), Prof. Wakasa (Saitama University) and his colleagues for their supports, patience and encouragements.

EPR Investigations of Photosynthetic and Bioenergy-Related Enzymes

R. David Britt[1]

[1]*Department of Chemistry, University of California, Davis CA 95616 U.S.A.*

E-mail: rdbritt@ucdavis.edu

Photosystem II uses visible light to split water into molecular oxygen, protons, and electrons, employing a multinuclear Mn/Ca cluster as the catalyst. This chemistry, which serves as a paradigm for solar energy-to-fuel conversion systems, can be explored in detail with advanced EPR methods. We have targeted this fascinating photosynthetic enzyme system for a number of years, using methods such as multifrequency ESEEM, ENDOR, and parallel polarization EPR (1-4). In the early years of this project most of the work was carried out with "homebuilt" pulse EPR instrumentation (1,5). Currently our CalEPR facility at the University of California, Davis has a blend of homebuilt and commercial instruments covering frequency ranges from 8 to 130 GHz. We are using these EPR instruments to explore a wide variety of enzyme and catalyst mechanisms, with bioenergy remaining at the forefront of our research interests. As a recent example we will discuss recent investigations into the biosynthesis of the active site "H-cluster" of [Fe-Fe] hydrogenase (6,7), in which radical S-adenosylmethionine (SAM) chemistry is directed to cleave tyrosine to form CO and CN^- ligands to an unusual binuclear Fe center.

References

[1] Britt, R. D., Zimmermann, J. L., Sauer, K. and Klein, M. P. "Ammonia Binds to the Catalytic Mn of the Oxygen Evolving Complex of Photosystem II: Evidence by Electron Spin Echo Envelope Modulation Spectroscopy" *J. Am. Chem. Soc.* **1989**, 111, 3522-3532.

[2] Gilchrist, M. L., Ball, J. A., Randall, D. W. and Britt, R. D. "Proximity of the manganese cluster of photosystem II to the redox-active tyrosine Y_Z" *Proc. Natl. Acad. Sci. U.S.A.* **1994**, 92, 9545-9549.

[3] Pelquin, J. M., Campbell, K. A., Randall, D. W., Evanchik, M. A., Pecoraro, V. L., Armstrong, W. H. and Britt, R. D. "^{55}Mn ENDOR of the S_2-state multiline EPR signal of photosystem II: Implications on the structure of the tetranuclear Mn cluster" *J. Am. Chem. Soc.* **2000**, 122, 10926-10942.

[4] Campbell, K. A., Force, D. A., Nixon, P. J., Dole, F., Diner, B. A. and Britt, R. D. "Dual-Mode EPR Detects the Initial Intermediate in Photoassembly of the Photosystem II Mn Cluster: The Influence of Amino Acid Residue 170 of the D1 Polypeptide on Mn Coordination" *J. Am. Chem. Soc.* **2000**, 122, 3754-3761.

[5] Sturgeon, B. E. and Britt, R. D. "Design of a Sensitive Pulsed EPR Spectrometer with an 8 to 18 GHz Frequency Range" *Rev. Sci. Instrum.* **1992**, 63, 2187-2192.

[6] Kuchenreuther, Jon M., Myers, William K., Stich, Troy A., George, Simon J., NajatyJahromy, Yaser, Swartz, James R. and Britt, R. David. "A Radical Intermediate in Tyrosine Scission to the CO and CH^- Ligands of FeFe Hydrogenase" *Science* **2013**, 342, 472-427.

[7] Kuchenreuther, Jon M., Myers, William K., Suess, Daniel L. M., Stich, Troy A., Pelmentschikov, Vladimir, Shiigi, Stacey A., Cramer, Stephen P., Swartz, James R., Britt, R. David and George, Simon J. "A Radical SAM Enzyme HydG Generates an $Fe(CO)_2(CN)$ Synthon in the Biosynthesis of the [FeFe] Hydrogenase H-Cluster" *Science* **2014**, 343, 424-427.

Recent development of the PELDOR theory

K.M. Salikhov

Zavoisky physical-technical institute of Russian academy of sciences, Kazan 420029, Russian Federation

E-mail: salikhov@kfti.knc.ru

The current theory of the pulse electron double resonance (PELDOR) has been generalized to the case, when paramagnetic particles (spin labels) in pairs or groups have the electron paramagnetic resonance (EPR) spectra, which overlap essentially or coincide. The 3-pulse and 4-pulse ELDOR signals modulation (oscillations) induced by the dipole-dipole interaction between paramagnetic spin ½ particles in pairs embedded in disordered systems have been analyzed comprehensively. It has been shown that the PELDOR signal contains additional terms in contrast to the situation considered in the current theory, when the EPR spectra of the spin labels in the pairs do not overlap. These new terms arise as a result of the possible excitation of the same spin by the signal forming microwave (MW) pulses and by the pump MW pulse used during the PELDOR experiment. All terms oscillate with the same frequency, which is the characteristic dipolar interaction frequency. The results of the numerical calculations, which demonstrate the possible scale of the effect of these additional terms on the PELDOR signal are presented.

In disordered systems the pairs of spin labels have the characteristic dipolar interaction frequency. For pairs of spin labels the oscillations of the PELDOR signal reveal this characteristic frequency, which does not depend on the shape of the EPR spectra of spin labels. However, the effective amplitude of the PELDOR signal and of the oscillations of the PELDOR signal depend on the overlapping of the EPR spectra of spin labels. It has been also analyzed how the spin flips and molecular motion or molecular isomerization can affect the manifestation of the spin-spin interaction between the spin labels in the PELDOR experiments.

References

[1] Milov A.D., Salikhov K.M., Schirov M/D., Fiz. Tverd. Tela **23**, pp. 975-982 (1981)
[2] Spiess H.W. J. Magn. Reson.**213**, pp. 326-328 (2011)
[3] Salikhov K.M., I.T. Khairuzhdinov I.T., Zaripov R.B.. Appl. Magn, Reson. **45**, pp. 573-620 (2014)

Ferromagnetic Resonance Studies of Spin-Orbit Effects in Heavy Atom Organic Radical Ferromagnets

Stephen Hill[1], Komalavalli Thirunavukkuarasu[2], Stephen M. Winter[2] and Richard T. Oakley[2]

[1]*Department of Physics and National High Magnetic Field Laboratory, Florida State University, Tallahassee, FL32310, USA*
[2]*Department of Chemistry, University of Waterloo, Waterloo, Ontario, N2L 3G1, Canada*

E-mail: shill@magnet.fsu.edu

The application of high pressure in the study of molecule-based materials has gained considerable recent interest, in part due to their high compressibilities, but also because the relevant electronic/ magnetic degrees of freedom are often very sensitive to pressure. For example, small changes in the coordination environment around a magnetic transition metal ion can produce quite dramatic variations in both the on-site spin-orbit anisotropy as well as the exchange interactions between such ions when assembled into clusters or 3D networks. This has spurred the development of sophisticated spectroscopic tools that can be integrated with high-pressure instrumentation. The study of magnetic structure/property relations requires not only precise crystallographic data, but also detailed spectroscopic information concerning the unpaired electrons that give rise to the magnetic properties.

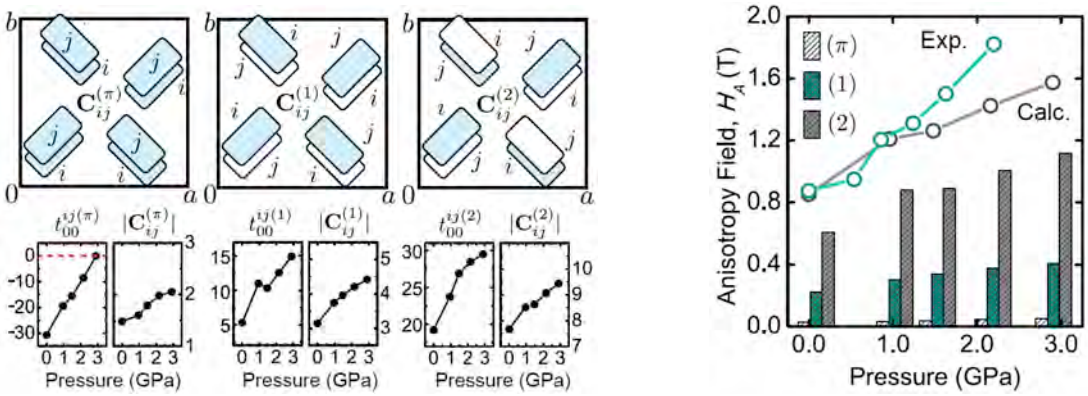

Figure. Contributions of different inter-molecular interactions to the anisotropy field, H_A [4].

This presentation will begin with a brief description of the development and application of methods enabling EPR studies of oriented single-crystal samples subjected to hydrostatic pressures of up to 3.5 GPa. After an introductory example [1], the remainder of the talk will focus on a family of organic radical ferromagnets that hold records for both the highest transition temperature and coercivity (for organic magnets). The latter is the result of an unexpectedly high magnetic anisotropy, attributable to spin-orbit-mediated exchange (hopping) processes [2,3]. Ferromagnetic resonance (FMR) measurements reveal an enhancement of the anisotropy field under applied pressures, which is attributed to increased π-orbital overlap that, in turn, increases the strength of the exchange anisotropy [4].

References

[1] Prescimone A., Hill S. et al., "Pressure-driven orbital reorientations and coordination sphere reconstructions in $[CuF_2(H_2O)_2(pyz)]$", *Angew. Chem. Int. Ed.* **2012**, 51, 7490-7494.

[2] Winter S. M., Datta S., Hill S. and Oakley R. T., "Magnetic Anisotropy in a Heavy Atom Radical Ferromagnet", *J. Am. Chem. Soc.* **2011**, 133, 8126-8129.

[3] Winter S. M., Oakley R. T., Kovalev A. and Hill S., "Spin-Orbit Effects in Heavy Atom Organic Radical Ferromagnets", *Phys. Rev. B* **2012**, 85, 094430.

[4] Winter S. M., Thirunavukkuarasu K., Oakley R. T. and Hill S., submitted to *Phys. Rev. Lett.* **2014**.

Quasi-Optical Pulsed EPR and ENDOR at very high Frequencies

Johan van Tol[1]

[1]*National High Magnetic Field Laboratory, Florida State University, Tallahassee, FL 32310, USA*

E-mail: vantol@magnet.fsu.edu

Quasi-optical techniques have significantly reduced the micro/milli-meter wave losses in high-frequency electron paramagnetic resonance (EPR). That has made very high frequency (>200GHz) pulsed EPR possible even with relatively low available source power, and in this talk various applications of high frequency pulsed EPR will be discussed. In the low temperature limit, the spin-spin relaxation times can be significantly longer than at low frequencies in select systems, as the electron-electron spin dipolar contributions to the de-coherence can be largely quenched, in some cases increasing coherence times by orders of magnitude[1,2]. At the same time, in the majority of spin systems the low-temperature longitudinal relaxation strongly decreases with increasing frequency and field.

One of advantages of high fields is the increased resolution. Examples will be given of pulsed Electron Nuclear Double Resonance (ENDOR) spectroscopy in crystals and frozen solution. The high field enables to better separate the EPR signals of different centers and/or of different orientations while at the same time increasing the ENDOR frequencies to provide better separation of signals from different isotopes (see Fig 1), and enabling ENDOR of isotopes with small magnetic moments like ^{25}Mg or ^{39}K[3].

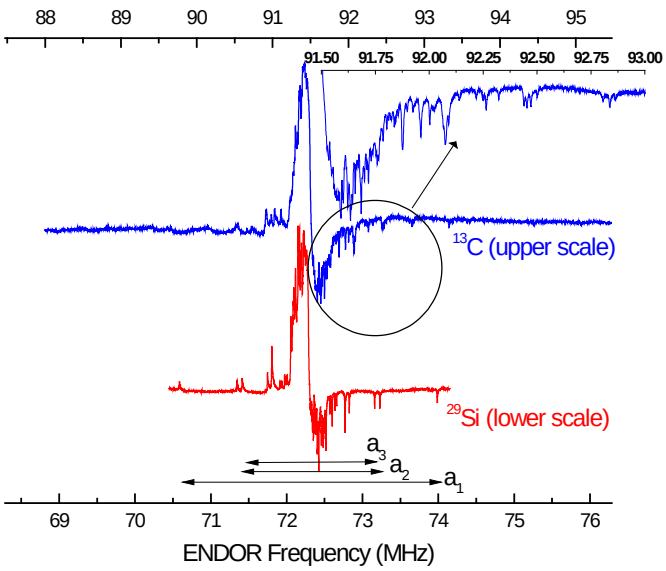

Figure 1 *Pulsed ^{13}C and ^{29}Si ENDOR spectrum at 240.0 GHz in 4H-SiC (natural abundance)*

The manipulation of spins also create great interest in the field of quantum computing, and here high fields can be used to create pure initial electron spin states, and via pulsed ENDOR techniques[4] or only electrical means [5] also pure nuclear spin states. Examples of electrically-detected high-field pulsed EPR of small spin-ensembles will be shown.

References

[1] Takahashi, S.; Tupitsyn, I.S.; van Tol, J. et al., Nature 2011, 476, 76-79.
[2] Takahashi, S.; Hanson, R.; van Tol, J. et al., Phys. Rev. Lett. 2008, 101, 047601.
[3] Nellutla, S.; Morley, G.W.; Pati, M.; Dalal, N.S. and van Tol, J., Phys. Rev. B. 2008, 78, 054426.
[4] McCamey, D.R.; van Tol, J.; Morley, G.W. and Boehme, C., Science 2010, 330, 1652-1656.
[5] Lo, C.C.; Weis, C.D.; van Tol, J.; Bokor, J., and Schenkel, T., Phys. Rev. Lett. 2013, 110, 057601.

The structure of nature's water splitting catalyst prior to O-O bond formation: an EPR and DFT study

Nicholas Cox,[1] Marius Retegan,[1] Frank Neese,[1] Alain Boussac,[2] Dimitrios A. Pantazis,[1] Wolfgang Lubitz[1]

[1]*Max Planck Institute for Chemical Energy Conversion, D-45470 Mülheim (Ruhr) Germany*
[2]*iBiTec-S, CNRS UMR 8221, CEA Saclay, 91191 Gif-sur-Yvette, France*

E-mail: nicholas.cox@cec.mpg.de

Multi-frequency (X-, Q-, W-band) pulse EPR data[1] are reported for the last metastable intermediate of nature's water splitting catalyst, a pentaoxygen, tetramanganese-calcium cofactor.[2,3] Simulations of the entire EPR dataset using the spin Hamiltonian formalism require this intermediate to have a ground electronic state of $S = 3$ and exhibit a small fine structure splitting ($|D| < 0.2$ cm^{-1}), consistent with the cofactor representing an all Mn^{IV} complex in this state.[1] Concomitant double resonance measurements (ELDOR-detected NMR) support this assignment. These measurements allow all manganese nuclear transition of the cofactor to be simultaneously visualized, over the 10-300 MHz range with high sensitivity, allowing the Mn ions that constitute the water splitting catalyst to be examined independently.[1] It is observed that all four Mn ions of the catalyst are structurally and electronically similar in the last intermediate state: they all have the same formal oxidation state of IV+ and an octahedral local geometry ($t_g^3e_g^0$).[1] These results are interpreted with the aid of density functional theory calculations. It is shown that only one structural model is consistent with all magnetic resonance data.[1-4] This model requires the binding of an additional water molecule, possibly the second substrate water, to the manganese cofactor during the formation of the last intermediate[1,5] and assign its binding position. These new experiments resolve the mechanism of the biological water splitting reaction, with the O-O bond forming between two manganese bound oxygens in the transition state, most likely an oxo-bridge and an oxyl radical. It is demonstrated that structural flexibility is important for second substrate inclusion[4,5] and that oxygen-oxygen coupling is facilitated by the spin topology of the cofactor.[1,6]

References

[1] Cox N., Retegan M., Neese F., Pantazis D.A., Boussac A., Lubitz W., Electronic structure of the oxygen-evolving complex in photosystem II prior to O-O bond formation, *Science* **2014**, 345, 804-808

[2] Cox, N., Pantazis, D.A., Neese, F., Lubitz, W., Biological water oxidation *Acc. Chem. Res.*,**2013** 46, 1588.

[3] Umena, Y., Kawakami, K., Shen, J.-R., Kamiya, K., Crystal structure of oxygen-evolving photosystem II at a resolution of 1.9 Å, *Nature* **2011** 473, 55

[4] Pantazis, D. A.; Ames, W.; Cox, N.; Lubitz, W.; Neese, F. Two Interconvertible Structures that Explain the Spectroscopic Properties of the Oxygen‐Evolving Complex of Photosystem II in the S_2 State, *Angew. Chem. Int. Ed.* **2012** 51, 9935

[5] Cox, N.; Messinger, J., Reflections on substrate water, *Biochim. Biophys. Acta* **2013**, 1827, 1020

[6] Siegbahn P.E.M, Structures and Energetics for O_2 Formation in Photosystem II, *Acc. Chem. Res.*, **2009**, 42, 1871–1880

Dynamic and Electronic Characteristics of Photo-generated Radical Pairs Revealed by Real-time Observation of the Spin Dynamics

Tomoaki Miura[1]

[1]*Department of Chemistry, Niigata University, Niigata 950-2181, Japan.*

E-mail: t-miura@chem.sc.niigata-u.ac.jp

The radical pair is one of the most important paramagnetic reaction intermediates seen in various organic molecular systems as natural and artificial photosynthesis, photovoltaics and organic LEDs. The spin selective generation and recombination of the radical pairs are the key processes that govern the total efficiency of these photo-functional materials. Spin scientists have been contributing greatly to elucidation of spin dynamics of the radical pairs for several decades by means of mainly three methodologies; namely 1) Optically detected magnetic field effect (MFE), 2) EPR-based electron spin polarization and 3) NMR-based nuclear spin polarization. It is broadly accepted that these phenomenon results from non-equilibrium quantum mechanical mixing among the spin states, but it is usually difficult to directly monitor the time evolution of the spin state due to interference from other "incoherent" processes as reactions and relaxations. Furthermore, considerably less is known about interplay with dynamic fluctuation of spin-spin interaction with the spin-state mixing processes especially in low magnetic fields comparable to hyperfine interactions.

The author has been studying the spin dynamics of radical pairs by several time-domain detection methods including newly developed pulsed MFE and EPR techniques. Through the analysis of the experimental data with novel theoretical calculations, interplay with molecular and spin dynamics has been clarified, which provides information about dynamic and electronic characteristics of the radical pairs. The following topics will be presented in the talk.

1) Detection and control of spin selective recombination of donor-bridge-acceptor molecules by pulsed EPR.[1]

2) Extraction of motion that gates electronic coupling between the radicals by Monte-Carlo analysis of MFE.

3) Molecular transport and electron transfer dynamics in membrane-like environments studied by static and pulsed MFE. [2]

References

[1] Miura, T. and Wasielewski M. R., "Manipulating Photogenerated Radical Ion Pair Lifetimes in Wire-like Molecules Using Microwave Pulses: Molecular Spintronic Gates", *J. Am. Chem. Soc.* **2011**, 133, 2844-2847.

[2] Miura T. "Supramolecular Control of the Spin-dependent Dynamics of Long-Lived Charge-Separated States at the Micellar Interface as Studied by Magnetic Field Effect" *J. Phys. Chem. B* **2013**, 117, 6443-6454.

IL-1

The Spin as Functional Probe in Metal Biocatalysis

Wolfgang Lubitz

Max Planck Institute for Chemical Energy Conversion, 45470 Muelheim/Ruhr, Germany

wolfgang.lubitz@cec.mpg.de

Many catalytic reactions in biology are performed by metalloenzymes. These are often paramagnetic – at least in some of their intermediate states – and can advantageously be studied by EPR techniques. Metal centers are involved in such interesting processes as catalytic water oxidation and reduction (proton reduction), the conversion of molecular nitrogen to ammonia and carbon dioxide reduction. In this lecture the enzymes wateroxidase and hydrogenase are discussed as examples.

Light-induced water splitting and oxygen release is performed by a protein-bound Mn_4O_5Ca cluster located in photosystem II (PSII) [1] of photosynthetic organisms. The cluster has been energy-minimized using DFT [2] based on the X-ray crystallographic structure of PSII [1]. Details of the cluster's electronic structure in the various states of the enzymatic cycle are available from cw/pulse EPR and double resonance technique like ^{55}Mn ENDOR [3,4]. ELDOR-detected NMR (EDNMR) has been used to detect the binding of the 1st substrate water (using $H_2{}^{17}O$) to the Mn_4O_5Ca cluster [5]. Recently, the state directly preceding the O-O bond formation could also be analyzed by EPR techniques leading to a model for the binding of the 2nd water molecule. Based on these data and together with quantum chemical approaches a robust model for the mechanism of water oxidation in PS II has been developed [6].

The [NiFe] and [FeFe] hydrogenases contain bridged binuclear transition metal cores in their active sites, which are tuned by a special ligand environment to reversibly convert molecular hydrogen to protons with high efficiency via a heterolytic splitting mechanism. The various intermediate states in the catalytic cycle have been investigated by spectroscopic techniques, e.g. EPR [7]. Enzyme activation, inhibition (e.g. by CO or O_2), as well as substrate binding and product formation were studied and led to proposals for the catalytic cycles of these hydrogenases [8].

References

[1] Umena, Y., Kawakami, K., Shen, J.-R., Kamiya, N. "Crystal Structure of Oxygen-Evolving Photosystem II at a Resolution of 1.9Å", *Nature* **2011**, 473, 55-60.

[2] Pantazis, D. A., Ames, W., Cox, N., Lubitz, W., Neese, F. "Two Interconvertible Structures that Explain the Spectroscopic Properties of the Oxygen-Evolving Complex of Photosystem II in the S_2 State", *Angew. Chem., Int. Ed.* **2012**, 51, 9935-9940.

[3] Kulik, L. V., Epel, B., Lubitz, W., Messinger, J. "Electronic Structure of the Mn_4O_xCa Cluster in the S_0 and S_2 States of the Oxygen-evolving Complex of Photosystem II Based on Pulse ^{55}Mn ENDOR and EPR Spectroscopy", *J. Am. Chem. Soc.* **2007**, 129, 13421-13435.

[4] Lohmiller, T., Ames, W., Lubitz, W., Cox, N., Misra, S. K. "EPR Spectroscopy and the Electronic Structure of the Oxygen-Evolving Complex of Photosystem II", *Appl. Magn. Reson.* **2013**, *44*, 691-720.

[5] Rapatskiy, L., Cox, N., Savitsky, A., Ames, W. M., Sander, J., Nowaczyk, M. M., Rögner, M., Boussac, A., Neese, F., Messinger, J., Lubitz, W. "Detection of the Water Binding Sites of the Oxygen-evolving Complex of Photosystem II Using W-band ^{17}O ELDOR-detected NMR Spectroscopy", *J. Am. Chem. Soc.* **2012**, 134, 16619-16634.

[6] Cox, N., Pantazis, D. A., Neese, F., Lubitz, W. "Biological Water Oxidation", *Acc. Chem. Res.* **2013**, 46, 1588-1596.

[7] Lubitz, W., Reijerse, E., van Gastel, M. "[NiFe] and [FeFe] Hydrogenases Studied by Advanced Magnetic Resonance Techniques", *Chem. Rev.* **2007**, 107, 4331-4365.

[8] Lubitz, W., Ogata, H., Rüdiger, O., Reijerse, E. "Hydrogenases", *Chem. Rev.* **2014**, 118, 4081-4148.

Progress Toward Spin Teleportation: Reversible Photo-driven Reduction of a Stable BDPA Radical

Michael R. Wasielewski, Brandon K. Rugg, Kristen E. Brown, and Matthew D. Krzyaniak

Department of Chemistry and Argonne-Northwestern Solar Energy Research (ANSER) Center, Northwestern, Evanston, IL 60208-313, USA

E-mail: m-wasielewski@northwestern.edu

Salikhov et al. have proposed a protocol for spin QT to a distant location in molecules using an electron donor-acceptor (D-A) system coupled to a stable radical ($R^{\bullet}$) to form D-A-$R^{\bullet}$. In this protocol, coherence is introduced on the $R^{\bullet}$ ensemble by applying a $\pi/2$ microwave pulse at a frequency ω_R. Shortly thereafter, laser photoexcitation of D followed by ultrafast electron transfer from D to A is used to produce the singlet spin-correlated radical pair (SCRP): $D^{+\bullet}$-$A^{-\bullet}$. Subsequent thermally-allowed electron transfer $D^{+\bullet}$-$A^{-\bullet}$-$R^{\bullet} \rightarrow D^{+\bullet}$-A-$R^{-}$ constitutes the Bell state measurement. Following delay time τ, a π microwave pulse is applied at a frequency ω_D to refocus the teleported spins (now on $D^{+\bullet}$) to produce an electron spin echo as the readout. Since reduction of $R^{\bullet}$ to R^{-} places both electrons in the same spatial orbital, the reaction only occurs from the singlet configuration of the unpaired spins on $A^{-\bullet}$ and $R^{\bullet}$. It is then assumed that the experiment can distinguish whether electron transfer has occurred from $A^{-\bullet}$ to $R^{\bullet}$ or the two spins remain in a triplet spin configuration. In the former case the donor spin interacts with a singlet acceptor-radical pair, where a π-pulse at the Zeeman frequency of the donor ω_D will refocus the spins.

Using D = perylene (PER), A = pyromellitimide (PI), and $R^{\bullet}$ = the α,γ-bisdiphenylene-β-phenylallyl (BDPA) stable radical, conclusive evidence for the rapid, reversible photo-reduction of BDPA at 295 K has been obtained for **1**. Further improvements to the system are being implemented, such as the synthesis of D = 2,5-di-tert-butylperylene (to prevent aggregation at low temperatures) and deuterated BDPA (to narrow the EPR spectral linewidth of $R^{\bullet}$), both of which can be readily incorporated into the existing molecular design.

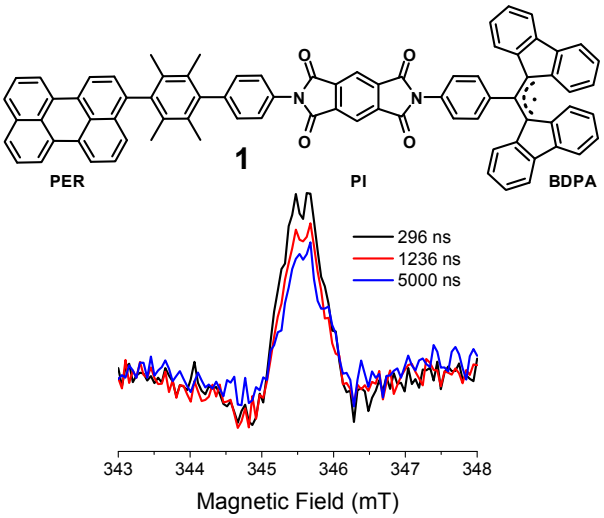

Figure. 2. TREPR spectra of **1** in a frozen toluene glass (85 K) following excitation with a 416 nm pulse. The central absorption is assigned to polarized $BDPA^{\bullet}$, while the wider emission signal is $PER^{\bullet+}$.

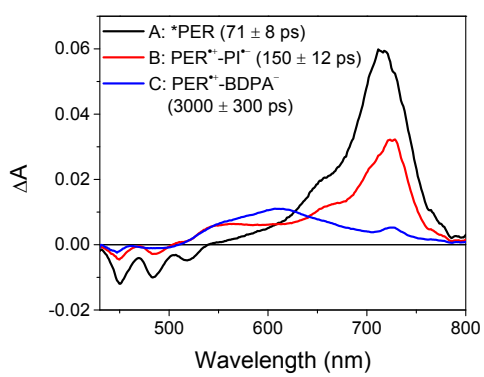

Figure. 1. Global fitting of the fsTA data of **1** based on an A→B→C→ GS model

IL-3

Development of EPR Dosimetry From Micro to Nano-materials

G.M. Hassan[1] , E. Aboelezz[1], M.A. Sharaf[1], and A. El-Khodary[2]

[1] *Department of Ionizing Radiation, National Institute for Standards, El-Giza, Egypt.*

[2] *Department of Physics, Faculty of Science, Mansoura University.*

E-mail: gamalhassn65@hotmail.com

ABSTRACT

A series of studies to find high sensitive dosimeter materials have been made to develop the field of EPR dosimetry. The sensitive organic materials such as alanine, metal ion – organic compound have been studied as EPR dosimeter. Other kind of natural radiation detector using EPR technique such as tooth enamel and coral reef have been known for more than three decades ago. Inorganic barium sulfate ($BaSO_4$) was irradiated by γ-ray to study radiation induced radicals as radiation dosimeter. Growing recognition of the importance of nano-materials in the field of radiation dosimetry has stimulated research focused on the new sensitive nano-materials as EPR dosimeter. Nano & micro $BaSO_4$ were prepared for measuring ionizing radiation doses using EPR technique. EPR dosimetric properties of nano & micro $BaSO_4$ were studied. The prepared micro & nano $BaSO_4$ have the same electron and hole centers, which may be ascribed to SO_3^- and SO_4^-, respectively. The dosimetric signal for micro & nano is characterized by g- factor = 2.0027 ± 0.0006 and 2.0025 ± 0.0006, respectively. The sensitivity of nano $BaSO_4$ to γ-ray is nine times more than that of alanine, the activation energy and lifetime for nano $BaSO_4$ were calculated by conducting a thermal stability study to be 0.73 ± 0.14 eV and 5.7 ± 1.1 x 10^4 years, respectively.

Keywords

Electron Paramagnetic Resonance, $BaSO_4$, Nanomaterials, Dosimetry, Radiation

IL-4

Application of ESR in Quaternary geological dating

TAKADA Masashi[1]

[1]*Research Group of History, Sociology and Geography, Nara Women's University, Nara 630-8506, Japan*

E-mail: takada@cc.nara-wu.ac.jp

The Quaternary, including the Pleistocene and Holocene, is the latest geological age of the human being. There are some dating methods for Quaternary geohistory of the human kind and palaeoenvironment. In particular ^{14}C and K-Ar dating methods have been playing important roles for them. The former and the latter are suitable for dating of younger ages than ca. 50 ka and of older ages than ca. 100 ka respectively. Therefore there are some difficulties for the dating of the above age gap.

Electron spin resonance (ESR) spectroscopy was first successfully employed as a Quaternary dating technique by Ikeya (1975) who showed that it could be used to determine the age of speleothem calcite, but since then its applications have expanded to include the dating particularly of tooth enamel, as well as a range of other media including coral, molluscs, quartz-bearing rocks and sediments, and burnt flint (Rink, 1997). Although ESR dating has a greater time range than most of the other Quaternary dating methods, extending from a few thousand years to about 2 million years in the case of tooth enamel, the most important applications lie in the time range between 40,000 and 200,000 years in general (Walker, 2005). It implies that ESR dating has a great possibility regarding the age gap between ^{14}C and K-Ar ages.

The ESR signal intensity is proportional to the number of the unpaired and trapped electrons in crystal lattices of rocks or sediments and hence it is a reflection of the time that has elapsed since the onset of electron trapping (Ikeya, 1993). This allows evaluation of the equivalent dose, that is, the laboratory dose of nuclear radiation needed to induce ESR signal equal to that acquired subsequent to the most recent event of zeroing the signal intensity. Natural radiation from radionuclides, which are mainly uranium (^{238}U and ^{235}U), thorium (^{232}Th) and their daughter radionuclides, and potassium (^{40}K) in the environment or inside geological materials, produces unpaired electrons in the crystal. Therefore assessing "annual dose rate of natural radiation", we can estimate the ESR age from the equation below;

$$\text{ESR age} = \text{Equivalent dose} / \text{Annual dose rate}$$

In this talk the author present and discuss recent progresses and some subjects of ESR dating for Quaternary geological studies.

References

[1] Ikeya, M., "*New applications of electron spin resonance – Dating, dosimetry and microscopy*", World Scientific, (1993) pp. 500.
[2] Walker, M., "*Quaternary dating methods*", Wiley, (2005) pp. 286.
[3] Rink, W.J., "Electron spin resonance (ESR) dating and ESR applications in Quaternary Science and archaeometry", *Radiation Measurements* **1997**, 27, 975-1025.
[4] Ikeya, M., "Dating a stalactite by electron paramagnetic reasonance", *Nature* **1975**, 255, 48-50.

IL-5

Probing the Spin Dynamics in Novel Iridium Oxides by sub-THz ESR

Vladislav Kataev

Leibniz Institute for Solid State and Materials Research IFW Dresden, D-01069 Dresden, Germany

E-mail:v.kataev@ifw-dresden.de

Complex iridium oxides have attracted recently a lot of attention in the condensed matter community due to the predictions of unusual quantum magnetic phases to occur in these materials. Beyond the physics of the celebrated 3*d* cuprates, such as the parent compound of high temperature superconductors La_2CuO_4, the strong relativistic spin-orbit coupling in 5*d* iridates gives rise to the novel spin-orbital Mott insulating state. Owing to a complex spin-orbital character of the effective spin J_{eff} = 1/2 ground state of Ir^{4+} ions a rich variety of spin structures in iridium oxides, ranging from a Heisenberg to exotic quantum compass and Kitaev models, have been proposed on theoretical grounds.

In the IFW Dresden we have focused on the ESR and NMR studies of the low energy spin dynamics in a number of iridium oxides, such as Na_2IrO_3, Li_2IrO_3, $Na_{1-x}M_{1/3}Ir_{2/3}O_2$ (M = 3*d* metal), Sr_2IrO_4 and others [1,2]. In my talk I shall exemplify our research by discussing our results on Sr_2IrO_4 [2], and if the time allows, will briefly mention our findings on other Ir-based systems.

Sr_2IrO_4 possesses a tetragonal crystallographic structure very similar to La_2CuO_4. At T_N = 230 K the compound experiences a phase transition to a canted antiferromagnetically (AFM) "easy-plane" ordered spin structure with an anomalously large "hidden" ferromagnetic (FM) moment.
We have studied low-energy magnetic excitations at the AFM zone center in a single crystal of Sr_2IrO_4 by high field ESR spectroscopy in the sub-THz frequency domain. We could identify both the "low" frequency mode due to the precession of the FM moments and the "high" frequency modes due to the precession of the AFM sublattices. Surprisingly, despite the spin-orbital entanglement in the ground state, the energy gap for the AFM excitations appears to be very small, amounting to 0.83 meV only. This suggests a rather isotropic Heisenberg dynamics of Ir spins in the AFM ordered state. We compare our ESR data with recent inelastic x-ray scattering and inelastic neutron scattering results on iridium oxides and discuss possible reasons for the smallness of the magnon gap in Sr_2IrO_4.

[1] Baroudi K. *et al.*, "Structure and properties of α-$NaFeO_2$-type ternary sodium iridates", *Journal of Solid State Chemistry* **2014**, 210, 195–205.

[2] Bahr S. *et al.*, "Low-energy magnetic excitations in the spin-orbital Mott insulator Sr_2IrO_4", *Physical Review B* **2014**, 89, 180401(R).

IL-6

Organic Radical Approach to Quantum Spin Systems

Yuko Hosokoshi, Hironori Yamaguchi, Kenji Iwase, Toshio Ono

Department of Physical Science, Osaka Prefecture University, Sakai 599-8531, Japan

E-mail: yhoso@p.s.osakafu-u.ac.jp

Organic radicals bearing ideal Heisenberg spins are attractive because of the emergence of exotic phenomena due to the quantum fluctuation. Quantum spin systems have been studied in several decades both theoretically and experimentally, and the most extensive study was done for one-dimensional antiferromagnets. Recently the quantum states of the magnetic lattices with more complicated magnetic interactions attract interests. Here presented are double chains and honeycomb-based two dimensional lattices by organic radicals. In this study, verdazyl radicals are utilized. They have no bulky substituents and have the wide spin density distribution on the phenyl rings attached to the N atoms of the verdazyl ring. We can expect strong magnetic interaction by their π-π stacking in the crystals. Molecular designing for multidirectional network is described.

A verdazyl biradical *p*-BIP-V_2 [= 4, 4'-bis(1,5-diphenylverdazyl-3-yl)biphenyl] crystallizes to a monoclinic system $P2_1/n$ and each radical site is crystallographically identical due to the inversion symmetry in a molecule. There are two kinds of dominant intermolecular interactions to form a two-dimensional network in the *ab* plane. The magnetization isotherms measured at 1.3 K showed almost linear field dependence up to 70 T at which magnetization reaches about half the value of the full saturation magnetization. This behavior suggests the strong exchange coupling in two-dimension. Molecular orbital calculation using the UB3LYP/6-31G gives that the two kinds of intermolecular interactions are almost the same in magnitude. The temperature dependence of the magnetic susceptibility shows a broad maximum at 25 K and was analyzed by the quantum Monte Carlo method. Satisfactory fit was obtained with the intermolecular interactions of 40 K forming a honeycomb lattice with diagonal bridges by the intramolecular interaction of 8.8 K [1]. Strong intermolecular magnetic interaction of 40 K appears also in another verdazyl biradical with a metaphenylene linkage [2]. The molecular shape is essential for the magnetic network and the effect of halogenation [3] is also presented.

References

[1] Yamaguchi H., Nagata S., Tada M., Iwase K., Ono T., Nishihara S., Hosokoshi Y., Shimokawa T., Nakano H., Nojiri H., Matsuo A., Kindo K., and Kawakami T., *Phys. Rev.B*, **2013**, 87, 25120/1-8.

[2] Iwase K., Yamaguchi H., Ono T., Shimokawa T., Nakano H., Matsuo A., Kindo K., Nojiri H., and Hosokoshi Y., *J. Phys. Soc. Jpn.*, **2013**, 82, 074719/1-6.

[3] Yamaguchi H., Miyagai H., Shimokawa T., Iwase K., Ono T., Kono Y., Kase N., Araki K., Kittaka S., Sakakibara T., Kawakami T., Okunishi K., and Hosokoshi Y., *J. Phys. Soc. Jpn.*, **2014**, 83, 033707/1-4.

Application of ESR/Spin Trapping for Monitoring Free Radical Formation in Serum of β-Thalassemia with Iron Chelation Therapy

N. P. Morales[1], P. Yamanont[1], S. Fucharoen[2]

[1]*Department of Pharmacology, Faculty of Science, Mahidol University, Bangkok 10400, Thailand*
[2]*Thalassemia Research Center, Institute of Molecular Biosciences, Mahidol University, Salaya Campus, Nakhon Pathom, 73170 Thailand*

E-mail: noppawan.phu@mahidol.ac.th

Iron-induced free radical generation contributes systemic organ damages in β-thalassemia, and other forms of iron overload condition. Sufficient chelation therapy is necessary to prevent the fatal complications in the patients. Deferiprone is an orally active iron chelator that has been approved for using in transfusion-dependent patients in several countries. Being the bidentate chelator, deferiprone could form 3:1, 2:1 and 1:1 complex with Fe^{3+} ion. The fully coordinated deferiprone-iron 3:1 is the major form in biological fluid, however, 1:1 and 2:1 chelator-iron complexes could be formed at the low concentration of deferiprone. The unoccupied coordination sites of these complexes catalyze Fenton reaction, and this may be an explanation of deferiprone toxicity in some patients.

Electron spin resonance (ESR) spectroscopy using 5,5-dimethyl-l-pyrroline-N-oxide (DMPO) as a spin trapping agent was employed to monitor free radical formation in serum of β-thalassemia/hemoglobin E (β-thal/Hb E) patients. The study was investigated in the patients who received a single oral dose of deferiprone (25 mg/kg) and also in the patients under long term chelation therapy (75 mg/kg divided for 3 doses daily for 12 months).

ESR spectra demonstrated free radical generation in serum of the patients after addition of ascorbic acid and *tert*-butylhydroperoxide. We proposed that serum non-transferrin bound iron catalyzed free radical reaction thus, produced ascorbyl radical (a_H = 1.8 G) and DMPO-carbon centered adduct (a_H = 23 G, a_N =16.5 G). Shortly after deferiprone administration ESR signal intensities decreased concomitant with an increase in serum levels of deferiprone. Enhanced ESR signal intensities were observed at 300 min after dosing in the patients with serum molar ratio of deferiprone to iron less than 3, suggesting the formation of incomplete iron-deferiprone complexes and consequently free radical formation.

Following 24 patients with long term chelation therapy demonstrated that ESR signal intensities in serum were gradually decreased after 3 months of treatment. The significant decrease in ESR signal intensities were observed at 12 months, corresponding with decreasing of serum non-transferrin iron. No adverse effect of deferiprone was observed in this group of patients.

In conclusion, ESR/spin trapping technique was applicable for monitoring pro-oxidant and anti-oxidant activity of deferiprone in serum of β-thalassemia. ESR signal intensities correlated with levels of serum non-transferrin bound iron. We suggested that a dosage regimen of iron chelator should be designed according to iron status of the patients and aimed to maintain an adequate ratio of serum chelator to iron concentration.

References

[1] Jirasomprasert T., Morales NP., Limenta LMG., et al., “Pharmaco/ferrokinetic-related pro-oxidant activity of deferiprone in β-thalassemia”, Free Radic Res **2009**, 43, 485-491.

IL-8

Enhancing cancer treatment in animal models with near absolute O_2 imaging using longitudinal relaxation ratee (R_{1e}) with pulse EPR

Howard J. Halpern[1,2], Gage H. Redler[1,2], Boris Epel[1,2], Martyna Elas[2,3], Eugene D. Barth[1,2], Charles A. Pelizzari1,[2], Ralph R. Weichselbaum[1,2], Victor Tormyshev[2,4]

[1]*Dept. Radiation and Cellular Oncology, University of Chicago, Chicago, IL, USA,*

[2]*Center for Electron Paramagnetic Resonance Imaging In Vivo Physiology, University of Chicago, Chicago, IL, USA*

[3]*Faculty Bio- chemistry, Biophysics and Biotechnology, Jagiellonian University, Krakow, PO*

[4]*Novosibirsk Institute of Organic Chemistry, Novosibirsk, RU*

E-mail: h-halpern@uchicago.edu

To properly characterize molecular oxygen (O_2) distributions in animal tumors and tissues images of O_2 distributions are required because of tissue O_2 content heterogeneity. Quantitative image assessment of pO_2 assures reproducibility and reliability. We recently demonstrated that image pO_2 quantification with pulse EPR based on the longitudinal electron magnetization relaxation rate, R_{1e} (spin lattice relaxation rate), of narrow spectral linewidth, injected, trityl spin probe provides pO_2 reproducibility unavailable to other imaging modalities.[1] The technique specifically reduces the sensitivity to concentration or self relaxation by nearly an order of magnitude. Historically, linewidth or transverse relaxation based soluble spin probe linewidth oxymetry is more susceptible to self-relaxation. Animal tumors and tissues, because of variable exclusion volumes and variable vascular access, are particularly susceptible to this effect. EPR O_2 images correlate with point Oxylite pO_2 measurements in tumors of living animals. The fraction of tumor image voxels with pO_2 less than 10 torr (HF10) based on EPR O_2 images significantly correlate with tumor cure by a 50% tumor control dose (TCD_{50}) of radiation for mouse MCa4 mammary carcinomas and FSa fibrosarcomas. These pO_2 images challenge the model of tumor treatment based solely on the sensitivity to large radiation dose fractions of a tumor's malignant cells. Our data demonstrate that tumor cure with radiation therapy also depends on the functionality of host blood microvessels supplying the tumor. The response of these vessels to large dose fractions of radiation is remarkably rapid, within 15 minutes. The hypoxia modulated gene BNIP3 product maintains mitochondrial integrity and functionality by autophagy. Mice in whom this gene is has been knocked-out have very hypoxic tumors. We will demonstrate results from the test that treatment beyond 50% control dose of only the portions of a tumor that are hypoxic enhances cure, allowing dose painting and potentially sparing normal tissues from radiation toxicity.

[1] B. Epel, M.Bowman, C. Mailer, H. Halpern. Magn. Reson. Med. e-pub Sept. 4 (2013)

Surface characterization by dynamic nuclear polarization NMR

Songi Han, Alicia Lund, Ting Ann Siaw, John Franck, Chiyuan Cheng

Department of Chemistry and Biochemistry & Department of Chemical Engineering, University of California Santa Barbara, Santa Barbara, CA 93106, USA

E-mail: songi@chem.ucsb.edu

Among the most promising prospect for dynamic nuclear polarization (DNP) is to transform NMR—offering atomistic details, but usually averaged over the entire sample—into a surface sensitive and selective tool. We suggest that the success of this premise will hinge on two key factors, namely to achieve dramatic NMR signal enhancements and to do so while employing site-selective spin label or localized spin probes. Recent innovation in instrument development, mechanistic understanding, experimental design and applications for solid and solution state DNP will be presented.

(1) First, key features of our home-built solid-state DNP instrument will be shown, operating at 7 Tesla, under static and magic angle spinning conditions, and powered by a widely tunable (193-201 GHz) solid-state microwave source, via quasi optics and corrugated waveguide transmission to the sample [1-3]. Crucially, the sample temperature is set to 4-40 K that dramatically enhances the DNP performance compared to at > 90 K, while yielding competitive enhancements for generic mono-nitroxide radicals. The ability to employ mono nitroxie radicals with competitive DNP performance is a significant opportunity to characterize heterogeneous porous materials, as will be showcased for ^{27}Al DNP of Al-substituted SBA-15 alumino-silicate catalysts. Progress in MAS-DNP at >20 K operating temperatures will be presented.

(2) Second, solution-state DNP of local water near nitroxide spin label is used to extract the translational diffusive correlation time of surface water moving with 10s and 100s of picosecond correlation times, via dramatic and selective enhancement of water within 5-10 Angstrom of the spin label. Measurements of surface water diffusion dynamics are exploited to characterize protein, polymer and hard material surfaces, and to sensitively unravel adsorption, wet adhesion, structural motifs, binding events or signatures of protein activation and signaling [4-6].

[1] B. D. Armstrong, D. T. Edwards, R. J. Wylde, S. A. Walker, S. Han, “A 200 GHz dynamic nuclear polarization spectrometer”, *Phys. Chem. Chem. Phys.* 12-22 (**2010**) 5920-5926.

[4] T. Siaw, S. A. Walker, B. D. Armstrong, S. Han, “Inductively coupled NMR probe for versatile dynamic nuclear polarization operation at 7 Tesla: observation of 61 ± 2% 1H polarization at 4 K” *J. Magn. Reson.* 221 (**2012**) 5-10.

[3] T. Siaw, M. Fehr, A. Lund, A. Latimer, S. Walker D. Edwards, S. Han, Role of Electron Spin Dynamics on Solid-State Dynamic Nuclear Polarization Performance, *Phys. Chem. Chem. Phys.* 16 (**2014**) 18694-18706.

[4] J. M. Franck, A. Pavlova, S. Han, Quantitative cw Overhauser DNP for the Analysis of Local Water Dynamics, *Prog. Nucl. Magn. Reson.* 74 (**2013**) 33-56.

[5] J.M Franck, J.A. Scott, S. Han, Nonliner Scaling of Surface Water Diffusion with Bulk Water Viscosity of Crowded Solutions, *J. Am. Chem. Soc.* 135(11) (**2013**) 4175-4178

[6] C.Y. Cheng, J. Varkey, M.R. Ambroso, R. Langen, S. Han, Hydration Dynamics as an Intrinsic Ruler for Refining Protein Structure at Lipid Membrane Interfaces, *Proc. Natl. Acad. Sci.* 110 (42) (**2013**).

IL-10

The interplay between spectral diffusion and dynamic nuclear polarization

Akiva Feintuch[1], Yonatan Hovav[1], Daphna Shimon[1], Daniella Goldfarb[1] and Shimon Vega[1]

[1]*Dept. of Chem. Phys., Weizmann Institute of Science, Rehovot, Israel*
E-mail: akiva.feintuch@Weizmann.ac.il

Dynamic nuclear polarization (DNP) has become in the past few years a widely used method for enhancing NMR signals. In DNP, polarization is transferred from electron spins to adjacent nuclear spin by microwave irradiation. This transfer of polarization has been described traditionally by three mechanisms termed the solid effect (SE) the cross effect (CE) and thermal mixing (TM). In a number of previous publications we demonstrate these mechanisms by quantum simulations on small model systems[1,2,3]. Due to the limited size of the system applicable for such simulations effects of spectral diffusion are not taken into account in these studies. In this talk I will show experimental results demonstrating the broad effect the MW irradiation has on the electron polarization throughout the EPR spectrum due to spectral diffusion. I will then present a model which takes the spectral diffusion into account and will show some surprising effects the spectral diffusion has on the nuclear polarization enhancement.

References

[1] Y. Hovav ; A. Feintuch; S. Vega J. Magn. Reson. (2010), 207(2), 176-189
[2] Y. Hovav; A. Feintuch ; S.Vega J. Magn. Reson. (2012), 214, 29-41
[3] Y. Hovav; A. Feintuch ; S. Vega Phys. Chem. Chem. Phys. (2013), 15, 188-203

IL-11

Using pulsed and continuous-wave EPR spectroscopy in combination with X-ray crystallography to understand the structure and function of biomolecular machines

Chris Kay[1]

[1]*Institute of Structural & Molecular Biology and London Centre for Nanotechnology, University College London, Gower Street, London WC1E 6BT, UK*

E-mail: c.kay@ucl.ac.uk

Structural biology relies on high-resolution methodologies to reveal protein function, mis-function and disease. X-ray crystallography, NMR spectroscopy and electron microscopy are three principal techniques used for this purpose. However, advances in other areas such as Electron Paramagnetic Resonance (EPR) spectroscopy in conjunction with molecular modeling are emerging as complementary approaches for unraveling details of cellular processes at the molecular level.

A form of pulsed EPR spectroscopy known as PELDOR or DEER allows the dipolar interaction between pairs of paramagnetic centers to be determined in frozen solution samples over the range 2-10 nm. In some systems, native centers such as Cu^{2+} [1] or flavin radicals [2] can be used as labels, but because the majority of proteins are diamagnetic, nitroxide spin labels are usually attached to proteins. This approach is now a key tool for structural analysis of proteins and their complexes.

In this talk I will discuss some of recent work on membrane proteins, where we have combined X-ray crystallography, EPR-based distance measurements and molecular modeling/dynamics simulations allowing us to reveal the key role played by dynamics [3,4].

References

[1] Kay C.W.M., Elsässer C., Bittl R., Farrell S.R. and Thorpe,C., “Determination of the Distance between the Two Neutral Flavin Radicals in Augmenter of Liver Regeneration by Pulsed ELDOR”, *Journal of the American Chemical Society* **2006** 128(1), 76-77.

[2] Kay C.W.M., El Mkami E., Cammack R. and Evans,R.W., “Pulsed ELDOR determination of the intramolecular distance between the metal binding sites in Dicupric human serum transferrin and lactoferrin”, *Journal of the American Chemical Society* **2007** 129, 4868-4868.

[3] Phan G., Remaut H., Wang T., Allen W., Pirker K.F., Lebedev A., Henderson N., Geibel S., Volkan E., Yan J., Kunze M.B.A., Pinkner J., Ford B., Kay C.W.M., Li H., Hultgren S., Thanassi D. and Waksman G., “Crystal structure of the FimD usher bound to its cognate FimC–FimH substrate” *Nature*, **2011**, 474, 49-53.

[4] Bagnéris C., DeCaen P.G., Hall B.A., Naylor C.E., Clapham D.E., Kay C.W.M. and Wallace B.A., “Role of the C-terminal domain in the structure and function of tetrameric sodium channels” *Nature Communications* **2013**, 4, 2465.

IL-12

Constructing a dynamic picture of Troponin from site directed spin labeling

Louise J Brown[1], Phani R Potluri[1] and Nicole M Cordina[1]

[1] *Department of Chemistry and Biomolecular Sciences, Macquarie University, 2109, Australia*

E-mail: Louise.Brown@mq.edu.au

Troponin (Tn) is a large (~77 kDa), dynamic protein complex located on the thin filament of striated muscle, responsible for controlling the interaction of myosin with actin. The simple binding of calcium (Ca^{2+}) to troponin initiates a series of protein conformational changes throughout the complex that then alter protein-protein interactions in the muscle filament, leading to contraction. Despite a wealth of structural data on Tn and its subunits from both x-ray crystallography and nuclear magnetic resonance (NMR), defining the molecular details of the conformational changes triggered by Ca^{2+} binding within the intact Tn complex is still needed and experimentally remains a challenge. This is particularly true for the cardiac isoform for which only a single incomplete crystal structure of a Ca^{2+} saturated core complex is available.

Spin labeling of cardiac troponin enables a toolbox of spectroscopic approaches to be used which can provide an insight into the structure and dynamics of key functional domains and thus provide a mechanistic description of muscle regulation. Here we have used both electron paramagnetic resonance (EPR) and nuclear magnetic resonance (NMR) to probe troponin through all its levels of structural complexity; from isolated subunits to whole reconstituted muscle filaments. This has allowed us to answer questions not accessible with other conventional structural methods. Specifically, inter-spin distances between two nitroxide spin labels were obtained using continuous wave (CW) and pulsed (Double Electron Electron Resonance) EPR techniques. Additionally, long-range distance constraints were also derived from the paramagnetic relaxation enhancement (PRE) of the NMR signal in the presence of the nitroxide spin label. Together, these approaches have provided us with a movie detailing the conformational interplay between key regions of cardiac troponin in response to Ca^{2+} binding and phosphorylation. We will also discuss how the complementary approaches of EPR and NMR have revealed the key role that dynamics plays in fine-tuning the Ca^{2+} troponin switch regulatory mechanism in the cardiac isoform[1,2]; and how its structure is perturbed by point mutations linked to hypertrophic cardiomyopathy[2].

References

[1] Cordina N., Liew C-K., Gell D., Fajer P., Mackay J. and Brown L. “Interdomain orientation of cardiac Troponin C characterized by paramagnetic relaxation enhancement NMR reveals a compact state”, *Protein Science* **2012**, 21, 1376-1387.

[2] Cordina N., Liew C-K., Gell D., Fajer P., Mackay J. and Brown L. “Effects of calcium binding and the hypertrophic cardiomyopathy mutation A8V on the dynamic equilibrium between closed and open conformations of the regulatory N-domain of isolated cardiac Troponin C”, *Biochemistry* **2013**, 52, 1950-1962.

Excited Triplet States of Thiophene-Decorated Phenazines Probed by Time-Resolved EPR

Hideto Matsuoka[1], Lisa Röck[2], Christoph Bannwarth[3], Stefan Grimme[3], Sigurd Höger[2] and Olav Schiemann[1]

[1]*Institute for Physical and Theoretical Chemistry, University of Bonn, Germany*
[2]*Kekulé Institute of Organic Chemistry and Biochemistry, University of Bonn, Germany*
[3]*Mulliken Center for Theoretical Chemistry, Institute for Physical and Theoretical Chemistry, University of Bonn, Germany*

E-mail: matsuoka@pc.uni-bonn.de

Organic light-emitting diodes (OLEDs) have attracted significant attention for the application in next generation display technologies. In OLEDs using fluorescent emitters, internal quantum efficiency is limited to about 25%. Introduction of phosphorescent emitters allows to take advantage of spin statistics and to raise this limit. To enhance radiative decay from triplet states via phosphorescence, normally metal–organic emitters are used in OLEDs. In such a device, intersystem crossing is accelerated by the spin-orbit coupling due to the heavy-atom effect. Recently, triplet harvesting without heavy atoms has also been explored, in which the spin-orbit coupling is tuned by molecular design and engineering. Examples for this are thiophene-decorated phenazines shown in Figure, which are promising candidates as metal-free organic compounds for OLEDs. They showed room-temperature electrophosphorescence with millisecond order lifetimes [1].

Here, we present the results of a time-resolved EPR study on the excited triplet state of a series of such phenazines. Molecular properties such as zero-field splittings were characterized in frozen solutions as well as in films. The zero-field splittings, which depend on substituents and sulfur positions in the molecules, were also investigated by DFT calculations. The lifetime of the triplet state determined by time-resolved EPR was strongly influenced by the sulfur positions.

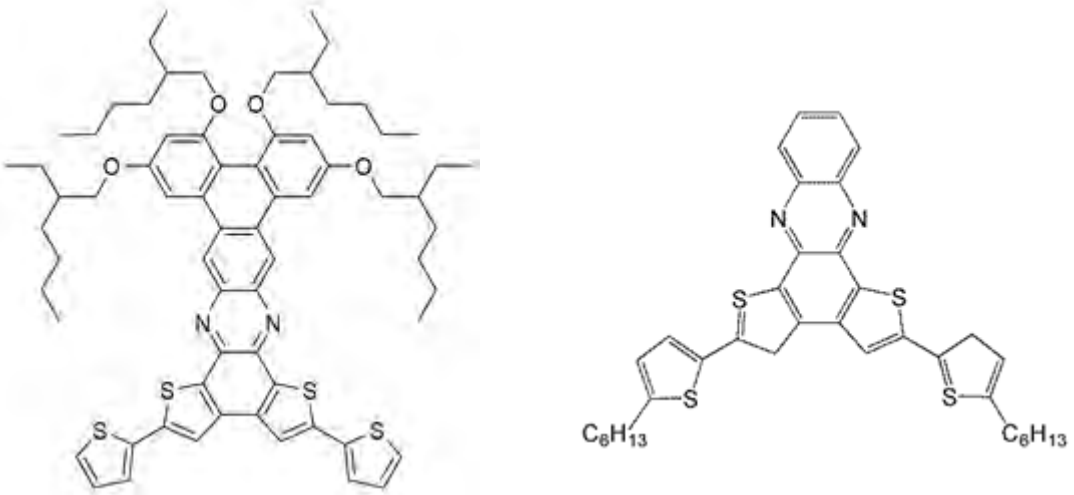

Figure Structures of the thiophene-decorated phenazines.

Reference

[1] D. Chaudhuri, E. Sigmund, A. Meyer, L. Röck, P. Klemm, S. Lautenschlager, A. Schmid, S. R. Yost, T. Van Voorhis, S. Bange, S. Höger, and J. M. Lupton, *Angew. Chem.*, **2013**, *125*, 1-5.

IL-14

Biological Applications of High Sensitivity Electron Spin Resonance with High Spatial Resolution

Mada Hashem,[1] Avishai Mor,[2] Periannan Kuppusamy,[3] Robert Fluhr,[2] and Aharon Blank,[1]

[1]*Schulich Faculty of Chemistry, Technion, Israel Institute of Technology, Haifa, Israel*
[2]*Department of Plant Sciences, Weizmann Institute of Science, Rehovot, Israel*
[3]*EPR Center, Dartmouth College, NH, USA*

E-mail: ab359@tx.technion.ac.il

Electron spin resonance is a well-known method in biology and biomedicine; however, its applicability to very small samples (< mm) with large heterogeneity is very limited. This talk will present two recent examples in which we make use of advanced ESR methodological tools to examine two types of challenging biological samples and obtain important information. The first one is an Arabidopsis Thaliana root, which is very thin (<100 microns) and long (~30 mm), in which we observe through ESR the superoxide levels generated in different regions of the root as a result of wounding the leaves. The study was carried out with a specially-prepared set of CW-ESR resonators that enable the sensitive measurements of the signal along the entire root. Our results show a rapid induction of a superoxide response in root tips but not in the other root regions, indicating that reactive oxygen signaling does not propagate along the root of the wounded seedlings, but rather occurs in the root tip. This contradicts current believes which claimed that superoxide mediates the injury signal all along the root. The second type of sample is a spheroid of Human Colorectal carcinoma cell line, which is ~500 microns in diameter, that serves as an important model system for cancer growth. Here we make use of high-resolution pulsed ESR microimaging to obtain the three-dimensional distribution of the oxygen concentration in the spheroid. This provides unique information about the cells viability and their metabolism in this type of heterogeneous tissue. It is concluded that high-sensitivity/high spatial resolution ESR can be used to answer important biological questions, which are not accessible by other methodologies.

IL-15

Development and Applications of Pulsed EPR Oxygen Imaging in Cancer Research

Shingo Matsumoto[1], Keita Saito[1], Chandramouli Gadisetti[1], Nallathamby Devasahayam[1], Sankaran Suburamanian[1], and Murali C. Krishna[1]

[1]*Radiation Biology Branch, National Cancer Institute, NIH, Bethesda, MD 20852, USA*

E-mail: matsumos@mail.nih.gov

Structural and functional abnormalities of tumor blood vessels cause impaired delivery of nutrients and oxygen, resulting in a low concentration of tissue oxygen, a condition known as tumor hypoxia. This feature of tumors confers resistance to radiation therapy and so carries poor prognosis. Therefore, there is a strong clinical demand for non-invasive imaging techniques to map absolute oxygen concentrations in tissue. Dipolar interaction between molecular oxygen, which is paramagnetic and paramagnetic tracer shortens the relaxation of unpaired electron spin of the paramagnetic tracer, giving a capability of quantitative oxygen mapping.

The emergence of the narrow-line triarylmethyl based, biocompatible paramagnetic tracers has enabled the development of radiofrequency "pulsed" EPR imaging, also known as a time-domain EPR, in living animals, which had been believed impossible/impractical until 2 decades ago. Although still challenging, the pulsed EPR imaging has several significant advantages over conventional continuous wave (CW) mode of EPR to extend it to human use. In this presentation, the development of *in vivo* pulse EPR oxygen imaging technique is traced from its origins with our recent update that includes 1) instrumentation of the scanner, 2) pulse sequences and image reconstruction techniques for T_{1e} and T_{2e} based oxygen mapping, 3) partial k-space strategies for fast image acquisition, 4) co-imaging with MRI or ultrasound for anatomic guidance, 5) applications to predict tumor response to oxygen sensitive anti-cancer therapies.

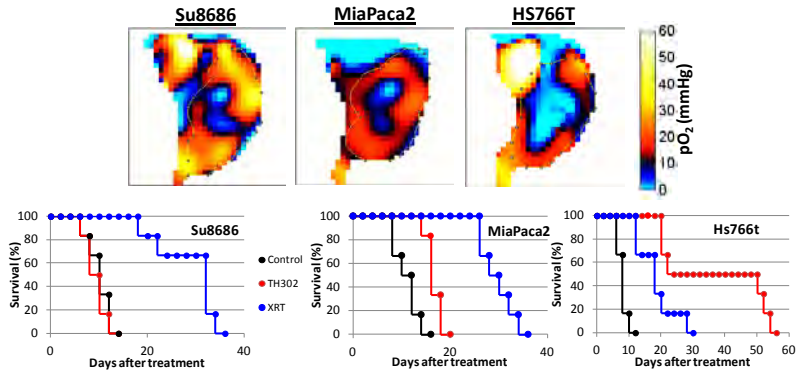

Fig.1 Pulsed EPR oxygen images of three pancreatic tumor xenografts and treatment response to hypoxia activated prodrug TH-302 or fractionated radiation.

References

[1] Murugesan R. et al. "*In vivo* imaging of a stable paramagnetic probe by pulsed-radiofrequency electron paramagnetic resonance spectroscopy", *Magn Reson Med* **1997**, 38, 409-14.

[2] Matsumoto S. et al. "Low-field paramagnetic resonance imaging of tumor oxygenation and glycolytic activity in mice", *J Clin Invest* **2008**, 118, 1965-73.

[3] Jang H. et al. "Accelerated 4D quantitative single point EPR imaging using model-based reconstruction.", *Magn Reson Med* **2014**, doi: 10.1002/mrm.25282. [Epub ahead of print].

Insights into CO_2 Fixation, Global Warming and Healthy Coral Reefs.

Nina Dovalil[1,2,3], Michael Westphal[1,2,3], Lawrence Gahan,[2] Marcel Maeder,[4]
Peter Comba[3], Graeme R. Hanson[1]

[1]Centre for Advanced Imaging, [2]School of Chemistry and Molecular Biosciences,
The University of Queensland, Brisbane, Queensland, 4072, Australia
[3]Anorganisch-Chemishes Insitut, Universitat Heidelberg, 69120 Heidelberg, Germany
[4]Department of Chemistry, The University of Newcastle, Callaghan, NSW 2308, Australia.

E-mail: Graeme.Hanson@cai.uq.edu.au

CO_2 fixation healthy oceans and coral reefs are key issues relevant in global warming and climate change. Our research focus has been on the molecular understanding of CO_2 fixation by marine organisms, such as the ascidians. The *Lissoclinum patella* family of ascidians found on the Great Barrier Reef, live in a symbiotic relationship with the cyanobacterium *prochlorin*, which produces a vast array of 8-azacrown macrocyclic pseudo-octapeptides (H_4PatA-G and ascidiacyclamide, Figure 1). The ascidians are known to concentrate metal ions, particularly Cu^{II} and we have utilized multifrequency EPR in conjunction with UV-vis, circular dichroism and mass spectrometry to show that Cu^{II} forms mononuclear and multiple dinuclear complexes with the symmetric (H_4asc) and asymmetric (H_4patD) cyclic pseudo-octapeptides.[1] The dinuclear Cu^{II} complexes are capable fixing CO_2 producing a μ-CO_3^{2-} bridged complexes.

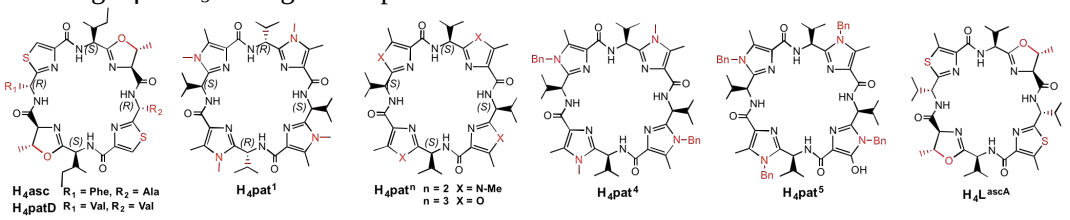

Figure 1: Schematic structures of marine cyclic pseudo-peptides and their synthetic analogues.

To understand how the choice of heterocyclic ring, stereochemistry, bulkiness of substituents (R) and backbone flexibility affect the Cu^{II} coordination chemistry and reactivity (CO_2 fixation), we have prepared a range of synthetic analogues of the marine cyclic pseudo-octapeptides (Figure 1) and structurally characterized their Cu^{II} complexes with EPR spectroscopy in conjunction with computer simulation (Molecular Sophe) and density functional theory calculations.[2] Kinetic studies have shown that the dinuclear Cu^{II} complexes can catalytically hydrolyze CO_2 producing CO_3^{2-}.[3] To date, these are the first examples of copper-based natural carbonic anhydrases (CA) and are the most efficient catalysts known (k_{cat} up to $7.3 \cdot 10^3$ sec^{-1}; uncatalyzed $3.7 \cdot 10^{-2}$ sec^{-1}; CA: $2 \cdot 10^5$ - $1.4 \cdot 10^6$ sec^{-1}; turnover number ≥ 1700). The experimental observations indicate that nucleophilic attack of a Cu^{II}-coordinated hydroxide at the CO_2 carbon center is rate determining, *i.e.* formation of the catalyst-CO_2 adduct and release of carbonate/bicarbonate are relatively fast processes. Thus, CO_2 hydrolysis and CO_3^{2-} transport are plausible biological functions for the native Cu^{II} peptide complexes.

References

[1] (a) van den Brenk A.L., Fairlie D.P., Hanson G.R., Gahan L.R., Hawkins C.J., Jones A. *Inorg. Chem.* **1994,** *33*, 2280-2289. (b) van den Brenk A.L., Byriel K.A., Fairlie D.P. Gahan L.R., Hanson G.R., Hawkins C.J., Jones A., Kennard C.H.L., Moubaraki B., Murray K.S. *Inorg. Chem.* **1994,** *33*, 3549-3557.

[2] (a) Comba P., Dovalil N., Gahan L.R., Hanson G.R., Westphal M. *Dalton Trans.* **2014**, 43, 1935-1956. (b) Comba P., Dovalil N., Gahan L.R., Haberhauer G., Hanson G.R., Noble C.J., Seibold B., Vadivelu P. *Chem. Eur. J.* **2012**, 18, 2578-2590. (c) Comba P., Dovalil N., Hanson G.R., Linti G. *Inorg Chem.* **2011**, 50, 5165–5174.

[3] Comba P., Gahan L.R., Hanson G.R., Maeder M., Westphal M. *Dalton Trans*. **2014**, 43, 3144-3152.

IL-17

In vivo EPR/NMR Coimaging of Radical Probes: Advances and Challenges

Jay L. Zweier, Rizwan Ahmad, Yangping Liu and Alexandre Samouilov

EPR Center and Molecular Imaging Program
The Ohio State University, 473 West, 12th Avenue, Room 0390 BRT,Columbus Ohio 43210

E-mail: Jay.Zweier@osumc.edu

Electron paramagnetic resonance imaging (EPRI) is a powerful technique that enables spatial mapping of free radicals or other paramagnetic molecules; however, it does not in itself provide anatomic visualization of the body. Proton magnetic resonance imaging (MRI) can provide anatomical visualization as well as additional functional information and has been widely used in research and clinical applications.

In this lecture, considerations and approaches for the design of EPR and NMR coimaging systems will be discussed with consideration of two-magnet vs. integrated one-magnet design. The design and construction of an integrated hybrid EPR/NMR coimaging instrument will be described that takes advantage of the complementary capabilities of both techniques superimposing EPR and proton-MR images to provide the distribution of paramagnetic species in the body. This instrument utilizes a common magnet and magnetic field gradient system along with a novel dual EPR and proton NMR resonator assembly, designed for whole-body *in vivo* imaging of living mice. EPR imaging is performed at ~1.2 GHz /~40 mT and proton MRI at 16.18 MHz /~380 mT. The gradient system used for both techniques is calibrated and controlled in a manner that the spatial geometry of the two acquired images is matched enabling their superposition with no additional post-processing or marker-registration.

Applications and performance of the system will be presented in a series of phantoms and *in vivo* applications mapping the location of a paramagnetic contrast material and in measuring redox metabolism. Approaches to accelerate image acquisition, including rapid scan and spinning gradient, will also be presented along with how newly developed trityl and other paramagnetic probes open the way for expanded *in vivo* applications with functional imaging of radical metabolism, oxygenation, thiols, pH and viability.

References

[1] Johnson D.H., Ahmad R., Liu Y., Chen Z., Samouilov A., and Zweier J.L., "Uniform spinning sampling gradient electron paramagnetic resonance imaging", *Magnetic Resonance in Medicine* **2014**, 71, 893-900.

[2] Johnson D.H., Ahmad R., He G., Samouilov A., and Zweier J.L. "Compressed sensing of spatial electron paramagnetic resonance imaging", *Magnetic Resonance in Medicine* **2014**, 72, 893-901

[3] Chen Z., Reyes L.A., Johnson D.H., Velayutham M., Yang C., Samouilov A., and Zweier J.L. "Fast gated EPR imaging of beating heart: Spatiotemporally resolved 3D imaging of free-radical distribution during the cardiac cycle", *Magnetic Resonance in Medicine* **2013**, 69, 594-601.

[4] Samouilov A., Caia G. L., Kesselring E., Petryakov S., Wasowicz T., and Zweier J. L. "Development of a hybrid EPR/NMR" coimaging system. *Magnetic Resonance in Medicine* **2007,** 58, 156-166.

[5] Ahmad R., Caia G., Potter L. C., Petryakov S., Kuppusamy P., and Zweier, J.L., "In vivo multisite oximetry using EPR–NMR coimaging", *Journal of Magnetic Resonance* **2010**, 207, 69-77.

Building up a synthetic quantum system spin by spin

J. Wrachtrup[1]

[1]3rd Institute of Physics, Stuttgart University, Stuttgart
E-mail: wrachtrup@physik.uni-stuttgart.de

Solid state spins are ideal playground for quantum physics. Precision control of spins but also of spin-spin coupling has emerged in a plethora of spectroscopic applications with unprecedented impact in e.g. structure analysis. It is a long sought goal to build up spin system in such a fashion that they can be controlled one by one but also that their interaction can be tuned with high fidelity. Such spin array would have impact as quantum simulators or precision sensing. In my talk I will describe our approach to build interacting electron spin systems in diamond. I will show entanglement generation ion those spin arrays and show the importance of nuclear spins as quantum memory and resource to improve electron spin correlations. I will show how we measure spins one by one, follow their quantum trajectory and apply feedback to extend spin lifetimes beyond their "natural" T_1.

References

[1] Waldherr G., Wrachtrup, J. et al. "Quantum Error Correction in a Solid State Hybrid Quantum Register", *Nature,* **2014**, 506, 204-207.

[2] Dolde F., Wrachtrup, J., et al. "Room temperature entanglement between single defect spins in diamond", *Nature Physics*,**2013**, 3, 139-143.

Quantum Computation and Quantum Sensing based on Single Electron Spin in Diamond

Jiangfeng Du

Hefei National Laboratory for Physical Sciences at the Microscale and Department of Modern Physics, University of Science and Technology of China, No. 96 Jinzhai Road, Hefei 230026, China

E-mail: djf@ustc.edu.cn

One of the key issues in quantum computation is to realize precise control over quantum qubits in the realistic system. The electron spin suffers the noise resulted by the around nuclear spin bath. This noise will not only destroy the quantum states of the electron spin, but also will deteriorate the quality of the quantum gates. It is of great challenge to perform the accurate controlling the electron spin qubits, due to the noises aroused from the nuclear spin bath and the driving field.

In this talk, I will briefly introduce our new researches in the robust quantum control and metrology. Firstly, we adopted a type of dynamically corrected gats to realize robust and high-fidelity quantum gates in the presence of fluctuation of static magnetic field. The results show that the noise was suppressed to 6th order and the quantum gate's performance was pushed to $T_{1\rho}$ limit[1]. On the other hand, we experimentally observed a new Rabi Oscillations (ROs) resulting from more than 100 Landau-Zener (LZ) transitions. The fluctuations of the driving field can be suppressed in the new ROs relative to common ROs under the same driving microwave power[2]. Besides, cooperating with Wrachtrup's group, we have experimentally realized the quantum error correction in diamonds, which is another effective method to overcome the noise effect[3]. Precise quantum control and effectivly supressing noise of the environment are also of great importance for quantum metrology. Cooperating with theory group, we recently succeeded in sensing and atomic-scale analysis of single nuclear spin clusters in diamond at room temperature via quantum interferometer[4]. Besides, we have succeed to detect a few nuclear spins with single spin sensitivity[5].

References:

[1] Rong X., Geng J. P., Wang Z. X, Zhang Q., Ju C. Y., Shi F. Z., Duan C. K., and Du J. F. "Implementation of Dynamically Corrected Gates on a Single Electron Spin in Diamond", *Phys. Rev. Lett.* **2014**, 112, 050503

[2] Zhou J. W., Huang P., Zhang Q., Wang Z. X., Tan T., Xu X. K., Shi F. Z., Rong X., Ashhab S., Du J. F. "Observation of Time-Domain Rabi Oscillations in the Landau-Zener Regime with a Single Electronic Spin", *Phys. Rev. Lett.* **2014**, 112, 010503

[3] Waldhere G., Wang Y., Zaiser S., Jamali M., Schulte-Herbrueggen T., Abe H., Ohshima T., Isoya J., Du J. F., Neumann P. and Wrachtrup J. "Quanutm error correction in a solid-state hybrid spin register", *Nature* **2014**, 506, 204-207

[4] Shi F. Z., Kong X., Wang P. F., Kong F., Zhao N., Liu R-B. and Du J. F. "Sensing and atomic-scale structure analysis of single nuclear spin clusters in diamond", *Nature Physics* **2014**, 10, 21-25.

[5] Mueller C., Kong X., Cai J. M., Melentijevic K., Stacey A., Markham M., Isoya J., Pezzagna S., Meijer J., Du J. F., Plenio M. B., Naydenov B., McGuinness L. P., and Jelezko F. "Nuclear magnetic resonance with single spin sensitivity". *Nature Communications*, **2014**, in press

Nuclear Hyperpolarization and Spin Entanglement in Phosphorescent Crystals at Level Anti-crossing Conditions

Gerd Kothe[1], Tomoaki Yago[1], Michail Lukaschek[1], Jörg-Ulrich Weidner[1], Gerhard Link[1], David J. Sloop[2] and Tien-Sung Lin[2]

[1]*Department of Physical Chemistry, University of Freiburg, Freiburg 79104, Germany*
[2]*Department of Chemistry, Washington University, St. Louis MO 63130, USA*

E-mail: gerd.kothe@physchem.uni-freiburg.de

Huge nuclear spin polarization has been observed in organic triplet states at level anti-crossing (LAC) conditions.[1-3] So far, however, the quantum mechanical mechanism responsible for the nuclear hyperpolarization was not identified. Here, we explore this mechanism using pulsed low-field magnetic resonance in combination with pulsed laser excitation. The model system for our studies is triplet pentacene embedded in a host single crystal. On the basis of an analytical theory, developed for LAC conditions, the results can be summarized as follows: First, a laser pulse generates the triplet state and initiates the formation of multipartite entanglement between the electron spin and 14 hyperfine coupled proton spins. This gives rise to huge oscillatory electron and nuclear spin polarization. Then, by the action of a resonant high-power microwave pulse, the electron spin is disentangled from the nuclear spins. As a result, the longitudinal nuclear magnetization evolves separately under the nuclear spin Hamiltonian. Due to robust entanglement among the 14 proton spins, one observes quantum oscillations[4] at the nuclear Larmor frequency.

Thus, at triplet LAC conditions, a multitude of entangled nuclear spin states is created simply by light excitation. The number of entangled states depends on the type and number of hyperfine coupled nuclei which can be tailored by chemical synthesis. In phosphorescent crystals, the decay of the light-induced nuclear spin polarization is determined by paramagnetic relaxation in solids.[5] Thus, under favorable conditions, we expect ultra-long spin coherence times in the order of milliseconds. Using advanced pulse NMR techniques, the entangled spin states can be addressed and coherently controlled in the time domain.[6] Because of the huge polarization of the nuclear spins, generated at LAC conditions, these quantum systems are capable of room temperature operation. This makes them promising candidates for various applications in quantum information processing.

References

[1] Veeman W. S., van der Poel A. L. J. and van der Waals J. H., "Level anticrossing and cross-relaxation in phosphorescent crystals", *Mol. Phys.* **1975**, 29, 225-248.
[2] Atsarkin V. A. and Morshnev S. K., "Optical polarization of nuclei in molecular crystals at 4.2 K", *Sov. Phys. JETP* **1976**, 44, 795-800.
[3] Colpa J. P. and Stehlik D., "Optical nuclear polarization as a consequence of the non-crossing rule (level-anti-crossing)", *Chem. Phys.* **1977**, 21, 273-288.
[4] Kothe G., Yago T., Weidner J.-U., Link G., Lukaschek M. and Lin T.-S., "Quantum oscillations and polarization of nuclear spins in photoexcited triplet states", *J. Phys. Chem B* **2010,** 114, 14755-14762.
[5] Abragam A., "Principles of Nuclear Magnetism", 2nd edition, Oxford University Press, (1962) pp 378-386.
[6] Vandersypen L. M. K. and Chuang I. L., "NMR techniques for quantum control and computation", *Rev. Mod. Phys.* **2004**, 76, 1037-1069.

Magnetoconductance in Photoconductive Thin Films of Perylene Bisimide

C. E. Ambe[1], Y. Wakikawa[2], S. Yagai[3,4], and T. Ikoma[4,5,6]

[1]*Department of Chemistry, MSU – Iligan Institute of Technology, Iligan City, 9200 Philippines*
[2]*Center for Fostering Innovative Leadership, Niigata University, Niigata 950-2181, Japan.*
[3]*Graduate School of Engineering, Chiba University, Chiba 263-8522, Japan.*
[4]*CREST, Japan Science and Technology Agency, Kawaguchi 332-0012, Japan.*
[5]*Graduate School of Science and Technology, Niigata University, Niigata 950-2181, Japan.*
[6]*Center for Instrumental Analysis, Niigata University, Niigata 950-2181, Japan.*

E-mail: christopher.ambe@g.msuiit.edu.ph

Detailed understanding on the photophysical properties of functionalized organic small molecules and polymers has played an important role in realizing organic electronic devices with higher efficiency. For instance, swallow-tailed perylene tetracarboxylic acid bisimide (ST-PBI, Fig. 1) dyes and other PBI derivatives are gaining much attention as they manifest not only their strong spectral absorption in the visible region [1], but also their thermal and photochemical stability [2, 3]. Together with their high fluorescence quantum yield [4] and n-type conductance [5] related to the high electron affinity, PBIs are well-suited as promising materials for light-emitting diodes (LED), organic field effect transistor (OFET), and organic photovoltaic cell (OPV) applications. One of the key issues concerning the OPV application is the accessibility of long-lived triplet exciton which is known to enhance the photovoltaic process in organic solar cells [6]. Recently we report that magnetoconductance (MC) effect in PCBM film clarifies the carrier detrapping by triplet exciton [7], suggesting the MC measurement is a powerful tool to study on the triplet exciton dynamics. Hence in this paper, the time-resolved MC measurement technique has been applied to the photoconduction in thin films of ST-PBI in order to investigate the mechanisms governing the access and the role of the triplet exciton. In the presentation, we will show the MC effects due to not only the detrapping mechanism of the trapped carriers in ST-PBI with the collision of triplet excitons but also the non-geminate recombination process.

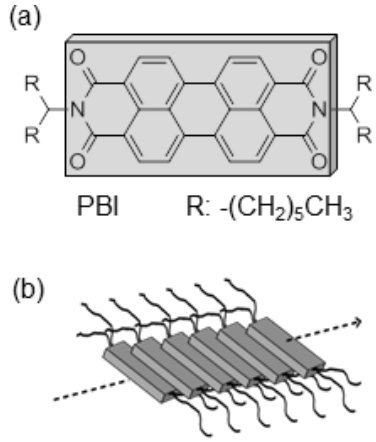

Fig 1. (a) Molecular structure of ST-PBI and (b) a possible assembly in pure ST-PBI film.

References

[1] Flamigni L., et al., "Photophysical and Redox Properties of Perylene Bis- and Tris-Dicarboximide Fluorophores with Triplet State Formation: Transient Absorption and Singlet Oxygen Sensitization". *J. Phys. Chem. A*, **2012**, 116, 1503-1509.

[2] Jancy B. and Asha S. K., "Control of molecular structure in the generation of highly luminescent liquid crystalline perylenebisimide derivatives: Synthesis, liquid crystalline and photophysical properties". *J. Phys. Chem. B*, **2006**, 110, 20937-20947.

[3] Wicklein A., et al., "Swallow-Tail Substituted Liquid Crystalline Perylene Bisimides: Synthesis and Thermotropic Properties". *J. Am. Chem. Soc.*, **2009**, 131, 14442-14453.

[4] Langhals H., et al., "Spectroscopic properties of new and convenient standards for measuring fluorescence quantum yields". *J. Chem. Soc. Faraday T*, **1998**, 94, 2919-2922.

[5] Würthner F. "Perylene bisimide dyes as versatile building blocks for functional supramolecular architectures". *Chem. Commun.*, **2004**, 1564-1579.

[6] Rachford A. A., et al. "Accessing the triplet excited state in perylenediimides". *J. Am. Chem. Soc.*, **2008**, 130, 2766-2767.

[7] Ambe C. E., et al., "Thermal Annealing Effect on Photocarrier Dynamics in PCBM Films", *Bull. Chem. Soc. Jpn.*, **2013**, 86, 1051-1058.

IL-22

Development of New Analytical Methods for Organic Devices: Applications of ESR to Transistors, Solar Cells and Light-Emitting Diodes

Kazuhiro Marumoto[1,2]

[1]*Division of Materials Science, University of Tsukuba, Tsukuba, Ibaraki 305-8573, Japan*
[2]*Research Center for Interdisciplinary Materials Science (TIMS), University of Tsukuba, Tsukuba, Ibaraki 305-8571, Japan*

E-mail: marumoto@ims.tsukuba.ac.jp

Organic devices are promising prospective devices because of their lightweight, printable and flexible device structures. There has been a significant amount of interest in their improvement of device perfromance However, their microscopic properties have not yet been fully understood. Such understanging will be extremely important for further improvements of device performance and durability. Electron spin resonance (ESR) is one promising method for such a microscopic characterization because it is a highly sensitive and powerful approach that is capable of investigating organic materials at the molecular level. The application of the ESR method to organic devices, however, had not yet been conducted because of experimental dificulties such as dielectric loss due to conducting electrodes and wires in an ESR cavity resonator.

In this talk, we report on development of new analytical methods for organic devices with ESR. This development has been recently performed by overcoming the above experimental difficulties. Applications of ESR to organic transistors, organic solar cells (OSCs), and organic light-emitting diodes (LEDs) will be presented. The ESR method was firstly applied to field-effect devices and transistors using poly(3-alkylthiophene) (P3AT) [1] and pentacene [2], where the spin states and the spatial extent of wave function of gate-induced hole carriers (radical cations) were studies. From the studies of the field-induced ESR (FI-ESR) for rubrene single-crystal (RSC) transistors that show highest field-effect motilities in all organic transistors, we clarified microscopic mechanisms behind the very high mobility [3]. The extremely high charge-density states in P3AT and RSC transistors due to electric double layers by ionic liquids were studied by FI-ESR, which shows magnetic interactions between charge carriers and nonmagnetic charge transport [4,5]. The ESR applications were further extended to the investigations of OSCs. We observed charge formation in pentacene layer in pentacene/C_{60} solar cells during solar-cell fabrication, which decreases initial device performance [6]. For P3HT:PCBM polymer solar cells, we directly observed hole accumulation during device operation under simulated solar irradiation, where the hole accumulation can be ascribed as the main mechanism for the reversible initial deterioration of the device performance [7]. Dramatic enhancement of fullerene anion formation by thermal annealing was found to cause the performance degradation [8]. For OLEDs, the ESR method clarified the spin states in OLED materials and devices [9].

In summary, the ESR analysis provides useful knowledge for understanding device operation and improving device performance at the microscopic level. We would like to thank Prof. Kuroda, Dr. Shimoi, Dr. Tanaka, Prof. Takenobu, Prof. Iwasa, Prof. Takeya for their cooperation on the works.

References

[1] Marumoto K., Muramatsu Y., Ukai S., Ito H. and Kuroda S., *J. Phys. Soc. Jpn.* **2005**, 74, 3066.
[2] Marumoto K., Kuroda S., Takenobu T., Iwasa Y., *Phys. Rev. Lett.* **2006**, 97, 256603.
[3] Marumoto K., Takeya J., Shimoi Y., Takenobu T., Iwasa Y., *et al.*, *Phys. Rev. B* **2011**, 83,075302.
[4] Tsuji M., Takenobu T., Iwasa Y., Marumoto K. *et al.*, *Appl. Phys. Lett.* **2013**, 102, 133301.
[5] Takahashi Y., Takenobu T., Iwasa Y., Marumoto K. *et al.*, *Appl. Phys. Express* **2013**, 6, 041603.
[6] Marumoto K., Fujimori T., Ito M. and Mori T., *Adv. Energy Mater.* **2012**, 2, 591.
[7] Nagamori T. and Marumoto K., *Adv. Mater.* **2013**, 25, 2362.
[8] Liu D., Yasuda T., Han L. and Marumoto K. *et al.*, *Appl. Phys. Lett.* **2014**, 104, 243903.
[9] Matsuo Y., Son D., Shimoi Y. and Marumoto K., *Chem. Phys. Lett.* **2014**, 607, 29.

ESR Study on Mechanism of Photocatalytic Synthesis of Phenols without Photosensitizer

Haijun Yang, Min Jiang, Hua Fu and Yong Li

Beijing Key Laboratory for Microanalytical Methods and Instrumentation, Department of Chemistry, Tsinghua University, Beijing 100084, P.R. China

E-mail: hxxly@mail.tsinghua.edu.cn

Photosythesis has shown many advantages in synthesis of organic compounds for its environment friendly and clean. [1] Recently, some progress in synthesis of phenols has been made using arylboronic acids as the substrates. [2,3] The visible-light initiated aerobic oxidative hydroxylation of arylboronic acids has been developed using air as the oxidant in the presence of photosensitizer ($[Ru(bpy)_3Cl_2]\cdot 6H_2O$). [4] As everyone knows, about 8% of solar light is high energy ultroviolet light that can activate organoboron compounds. Based on this point, we applied photocatalysis to our study on transformation of arylboronic acids to phenols without photosensitizer in the quartz tubes instead of the glass tubes, using high pressure mercury lamp with all range of light wavelength as the light source. The present reactions were performed in quartz tubes instead of normal glass tubes because the quartz tubes are of better transmittance than glass tubes for ultraviolet light. Two control experiments were carried out, the reaction from methoxyphenylboronic acid to 4-methoxyphenol in the quartz tube was performed well, but a lower yield (12%) was provided when the experiment was carried out in the glass tube. Therefore, ultraviolet can be a key factor for the reactions. In order to explore the present mechanism, ESR was used to monitor the reaction process, and the spin trap (DMPO) was applied to trap the free radicals generated during the reaction. It was shown that both hydroxyl radical and carbon centered free radical existed in the reaction. Accordding to the simulated spectra of hydroxyl free radical and carbon centered free radical trapped by DMPO, the simulated spectrum was a good agreement with the measured one. The A-values were coincided with the literature reported by Mason and Kalyanaraman (for hydroxyl radical, $A_H = 1.5$ mT, $A_N = 1.5$ mT), and Jones (for phenyl radical which is a carbon central radical, A_N=1.60 mT, A_H=2.46 mT). We supposed that the carbon centered free radical was produced from arylboronic acids. A control experiment was performed by using ^{18}O-labeled water as the solvent. No ^{18}O-labeled product was found with mass spectrometry. The result indicated that oxygen was from O_2 in air (not from water). The similar result was reported by Xiao's group. Water provided proton and hydroxyl anion in the reaction. However, hydroxyl anion didn't take part in the formation of the product. The ESR experiments showed existence of a carbon centered free radical and a hydroxyl free radical in the reactions, which is helpful for interpretation of reaction mechanism. Further investigation on this mechanism is in progress.

References

[1] Ravelli D., Dondi D., Fagnoni M. and Albini A., "Photocatalysis. A multi-faceted concept for green chemistry", *Chem. Soc. Rev.*, **2009**, 38, 1999-2011.

[2] Yang H., Li Y., Jiang M., Wang J., Fu H., "General Copper-Catalyzed Transformations of Functional Groups from Arylboronic Acids in Water", *Chem. Eur. J.*, **2011**,17, 5652-5660.

[3] Jiang M., Yang H., Li Y., Jia Z., Fu H., "Metal-free synthesis of substituted phenols from arylboronic acids in water at room temperature", *Chin. Chem. Lett.*, **2014**, 25,715-719.

[4] Zou Y., Chen J., Liu X., Lu L., Davis R. L., K. Jorgensenand A. and Xiao W., "Highly Efficient Aerobic Oxidative Hydroxylation of ArylboronicAcids: Photoredox Catalysis Using Visible Light", *Angew. Chem., Int. Ed.*, **2012**, 51, 784-788.

Interaction of Cryoprotective Agents with Biological Membranes Studied by Pulsed EPR of Spin Labels

S.A. Dzuba,[1,2] N.P. Isaev,[1] K.B. Konov,[3] D.V. Leonov[2]

[1]*Voevodsky Institute of Chemical Kinetics and Combustion SB RAS, 630090 Novosibirsk, Russia,*
[2]*Novosibirsk State University, 630090 Novosibirsk, Russia*
[3]*Zavoisky Physical-Technical Institute, RAS, Kazan 420029, Russia*

E-mail: dzuba@kinetics.nsc.ru

The transport of small molecules across biological membranes is important for cell regulation. Passive transport occurs by means of diffusion for a wide range of non-ionic species. The transport of water and cryoprotective chemicals, such as sugars and glycerol, across cell membranes is of fundamental importance for cryopreservation processing. A variety of organisms accumulate cryoprotective chemicals to tolerate extreme environmental conditions (e.g., drought, high salinity and freezing temperatures), stabilise the native structures of biomacromolecules, regulate microviscosity, and prevent intracellular ice formation. However, many of the details for these protective molecular mechanisms remain unclear.

To probe the properties of membranes at the molecular level, electron paramagnetic resonance (EPR) employing spin-labelling techniques can be used. Electron spin echo envelope modulation (ESEEM) – see Fig. 1 – allows the direct examination of the accessibilities of deuterium-substituted molecules to spin labels. The amplitude of the ESEEM spectrum depends on the distance to the nuclei. The amplitude decreases rapidly for distances greater than ~ 0.5 nm, which can be considered as the spatial resolution of the method. Thus, the ESEEM amplitudes observed for spin labels attached at different positions along the lipid chain can serve as indicators for the penetration depth of the deuterium-substituted molecules. The use of deuterium has a two-fold purpose: 1) to obtain a pronounced ESEEM signal (protons also cause ESEEM but the amplitude is several times smaller) and 2) to distinguish hydrogen atoms from the molecules penetrating the membrane and from those in the lipid chains. The ESEEM amplitude is proportional to the local concentration of nearby nuclei, and provides information on the spatial location of the matrix nuclei relative to the spin label.

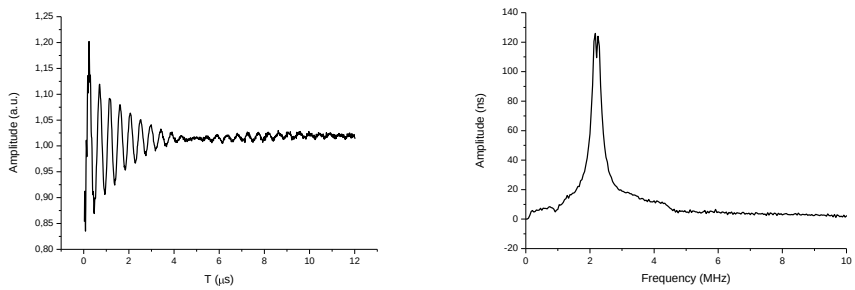

Fig. 1. Time-domain ESEEM (left) and Fourier-transform frequency spectra (right) for spin labels interacting with remote deuterium nuclei

Recent applications of spin-label ESEEM for studying interaction of glycerol and biological sugars with model biological membranes DPPC are discussed. The results obtained provide a detailed profile of the penetration of these cryoprotective agents across the membrane at the molecular level. In the middle of the DPPC bilayer, the glycerol concentration was estimated to be ~ 0.4 M (~ 3 % v/v). These data support a model in which small neutral solutes permeate the membrane by partitioning into the hydrophobic phase of the bilayer.

Three-pulse stimulated electron spin echo spectroscopy is known as an efficient tool of studying molecular dynamics of phospholipids bilayers, at temperatures low enough so the echo signal could be observed. It was applied to spin-labeled phospholipid bilayers DPPC and POPC hydrated in the presence of sucrose and sorbitol, which are known for their cryoprotective action on biological membranes. The results suggest non-specific interactions of sugars with bilayer surface, which are likely to influence only the bulk physical properties of hydrated membranes.

Dielectric Constant and Water Penetration Gradients along Transmembrane Peptide-Lipid Bilayer Interface

Matthew Donohue, Maxim A. Voynov, Alex I. Smirnov, and Tatyana I. Smirnova

North Carolina State University, Raleigh, NC, USA

E-mail: tismirno@ncsu.edu

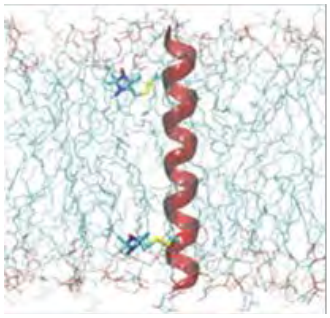

Snapshot of the preliminary molecular dynamics simulations of spin-labeled WALP in lipid membrane.

Local polarity, electric potentials, and hydration are the major physico-chemical characteristics of lipid membranes that govern membrane-protein and protein-protein interactions as well as small molecules transport. Although a relatively good understanding of gradients in polarity, electric potentials, and hydration in model biological membranes exists, very little is known about these properties at the protein-membrane interface. In this work we report on employing pH-sensitive ionizable EPR labels to profile a heterogeneous dielectric environment along the α-helix of a WALP peptide integrated in a lipid bilayer. Labels were attached to two cysteine residues positioned equidistant from the center of the peptide so that the primary sequence of each peptide is palindromic, thus, ensuring symmetric location of the labels with respect to the bilayer center. The change in the protonation state of the nitroxide was directly observed by EPR. Q-band double electron-electron resonance (DEER) experiments were carried out to determine the distance between spin labels when imbedded in lipid bilayers, providing data on the label location with respect to bilayer interface. Thus, for the first time, measurements of local electrostatics at the peptide-bilayer interface were based on direct distance measurements rather than on assumptions regarding the probe location. Displacement of the EPR probe upon protonation, similar to that of the proposed "snorkeling" of the charged sidechains of Lys and Arg, was directly observed by DEER and was shown to depend strongly upon the depth of the label. The experimentally observed dielectric constant at the membarane-protein interface is significantly higher than that which is expected for the same location in the bulk membrane. Two pH-sensitive spin labels, methanethiosulfonic acid S-(1-oxyl-2,2,3,5,5-pentamethyl-imidazolidin-4-ylmethyl) ester (IMTSL) and S-4-(4-(dimethylamino)-2-ethyl-5,5-dimethyl-1-oxyl-2,5-dihydro-1H-imidazol-2-yl) benzylmethanethiosulfonate (IKMTSL), with intrinsic *pKa*'s differing by approximately 2 pH units were used, providing opportunity to vary the lipid composition in order to investigate effect of the surface charge on dielectric profile at peptide-membrane interface. Water penetration at the peptide-membrane interface was assessed by hyperfine sublevel correlation spectroscopy (HYSCORE) experiment in which the hyperfine coupling between the nitroxide label and hydrogen/deuterium atoms of water is measured. Molecular dynamics simulations were conducted to provide further details on conformation of WALP peptides and spin-labels within the lipid bilayer. Supported by NSF-0843632 to TIS.

OP-1

Photoinitiated Radical Polymerization of Silane Coupling Agents as Studied by Pulsed EPR Spectroscopy

Hirona Takahashi and Akio Kawai

Department of Chemistry, Graduate School of Science and Engineering, Tokyo Institute of Technology, Tokyo 152-8551, Japan

E-mail: takahashi.h.ba@m.titech.ac.jp

Phosphinoyl and carbon-centered radicals have been widely used as the initiator of photoinitiated radical polymerization. Addition reaction of the radicals to double bonds of monomers are important to understand polymerization processes. We have determined the rate constants for addition reaction of the phosphinoyl- and carbon-centered radicals to acrylate or methacrylate by pulsed EPR spectroscopy. In this study, we focused on silane coupling agents as monomer. The primary adduct radicals in photoinitiated polymerization were directly detected and assigned by use of time-resolved (TR) EPR spectroscopy. Then, we determined the rate constants for addition reaction of radicals to silane coupling agents by measuring phase memory time of the radicals as a function of the concentration of silane coupling agents.

Figure 1 shows TR EPR spectra measured by 355 nm laser irradiation of α-hydroxylcyclohexylphenylketone (IRG184) in toluene in the presence of 0 M (the upper figure) and 0.2 M silane coupling agent, KBM-1003. The upper spectrum shows emissive singlet near the center field assigned to benzoyl radical and a quintet due to the ketyl radical (R·). In the presence of KBM-1003, the ketyl radical undergoes addition reaction to the unsubstituted carbon of KBM-1003. A prominent feature of the lower spectrum is the presence of the emissive double triplet components. These components are assigned to adduct radical (RM·).

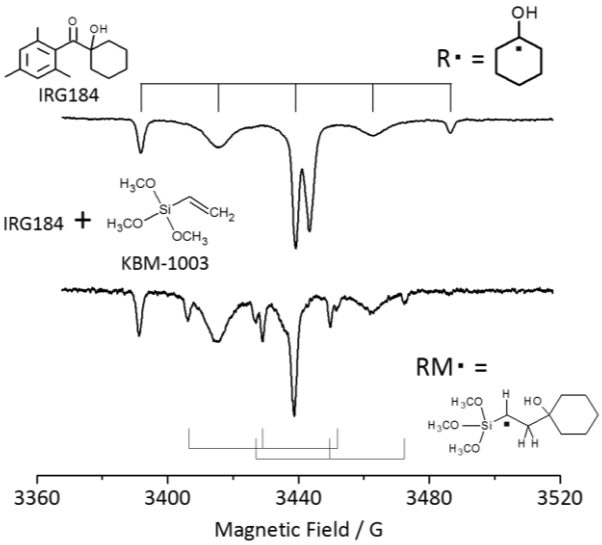

Figure 1 TR-EPR spectra of IRG184 in toluene measured at 2.0~2.5 μs after laser pulse in the presence of 0 M (the upper figure) and 0.2 M (the lower figure) KBM-1003.

Figure 2 shows time profile of spin echo signal of R· in the toluene solution of IRG184 and KBN-1003 mixture. The phase memory time (T_2^*) of radicals were determined by this time profile. Because the T_2^* values depended on the concentration of KBM-1003, the addition rate constants were determined by Stern-Volmer type analyses of the phase memory times.

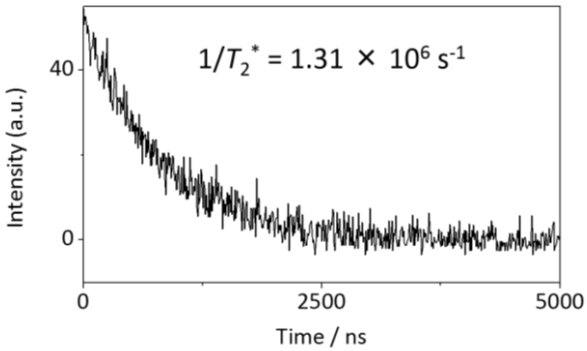

Figure 2 Time profile of spin-echo signal of R· in IRG184 – KBM-1003 toluene solution.

Similar measurements were carried out for several different photo-initiator radical – silane coupling agent systems. The addition rate constants for silane coupling agents and conventional monomers were discussed to understand initial photochemical processes of silane coupling agents.

OP-2

Substituent Dependence of Relaxation Processes in the Excited State of Vanadyl Porphyrins : Time-resolved EPR and Luminescence Study

Motoko S. Asano[1], Tsubasa Asami[1], Kazuhito Tomiduka[1], Ken-ichi Yamashita[1], Ken-ichi Sugiura[1] and Art van der Est[2]

[1]*Department of Chemistry, Tokyo Metropolitan University, Minami-Osawa, Hachiohji, Tokyo 192-0397, Japan*
[2]*Department of Chemistry, Brock University, 500 Glenridge Ave. St. Catharines Ont., Canada L2 S 3A1*

E-mail: motoko@tmu.ac.jp

Vanadyl (V(IV)O) ion has a d-unpaired electron and the excited states of vanadyl porphyrin are spin-coupled system of VO and porphyrin π-electrons spins. Vanadyl porphyrins show luminescence of "porphyrin triplet character" in wide temperature range from room temperature to low temperatures due to exchange coupling with VO unpaired electron. The lowest excited state of VO porphyrins is quartet state, and the doublet state is present upper the quartet state. The energy gaps between the doublet and quartet states are supposed to be several tense cm^{-1}.[1] However, reports on relaxation processes involving the excited doublet and quartet states have been considerably limited, and one of such examples was presented on vanadyl octaethylporphyrin by means of time-resolved EPR (TREPR) technique.[2, 3]

To understand the relaxation processes involving the excited doublet and quartet states as well as relation between luminescence and TREPR behavior, we have performed TREPR and luminescence measurements on three kinds of VO porphyrins as shown below. Peripheral substituents on the porphyrin macrocycle affect the spin density distribution and energy level of the HOMO, and thus changes the energy gap between the doublet and quartet states. For all three VO porphyrins, TREPR signals at 12 K were composed multuplet and net absorption spin-polarization patterns. The decay rates for the multiplet pattern are remarkably substituenet dependent. On the other hands, temperature dependence of TREPR relaxation times as well as luminescence lifetimes between 12 K and 80 K lead to the doublet and quartet energy gaps. The relaxation mechanism of the excited states involving the doublet and quartet states are discussed in relation to the size of coupling between the vanadyl and porphyrin electron spins.

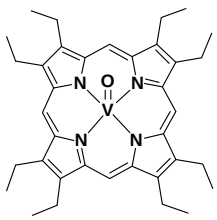

OEPVO

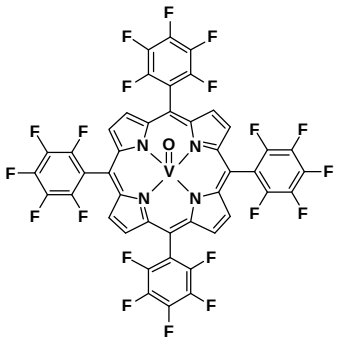

TFPPVO

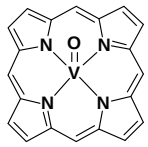

PorVO

References

[1] Gouterman M; Mathies, R. A.; Smith, B. E.; Caughey, W. S. *J. Chem. Phys.* **1970**, *52*, 3795
[2] Kandrashkin, Y. E.; Asano, M. S.; van der Est, A. *Phys. Chem. Chem. Phys.* **2006**, *8*, 2129–2132.
[3] (i) Kandrashkin, Y. E.; Asano, M. S.; van der Est, A. *J. Phys. Chem. A* **2006,** 110(31), 9607-9616, (ii) Kandrashkin, Y. E.; Asano, M. S.; van der Est, A. *J. Phys. Chem. A* **2006,** 110(31), 9617-9626.

OP-3

Diagnostic of Reactive Oxygen Species (ROS) Induced in Water by Atmospheric Pressure Plasma for Plasma-based Sterilization

Atsushi Tani[1], Satoshi Ikawa[2], Tomoko Ohshima[3], and Katsuhisa Kitano[4]

[1]*Graduate School of Science, Osaka University, Osaka 560-0043, Japan*
[2]*Technology Research Institute of Osaka Prefecture, Osaka 594-1157, Japan*
[3]*School of Dental Medicine, Tsurumi University, Yokohama 230-8501, Japan*
[4]*Graduate School of Engineering, Osaka University, Osaka 565-0871, Japan*

E-mail: atani@ess.sci.osaka-u.ac.jp

Considering medical applications of plasmas, which involve disinfection and wound healing, the supply of active species to solution is extremely important. For plasma disinfection, once atmospheric pressure plasma is exposed to aqueous solution, high bactericidal activity is achieved in the solution via "the reduced pH method" where the solution is sufficiently acidic [1]. Superoxide anion radical ($O_2^{-\cdot}$) induced in acidic aqueous solutions (lower than pH 4.8) tends to capture a proton (H^+) to form hydroperoxy radical ($HOO\cdot$), which shows considerably stronger bactericidal activity [2,3]. This indicates that plasma-induced active species in liquid are crucial for medical application of plasmas. Reactive oxygen species (ROS) including hydroperoxy radical is known to cause damages against nucleic acids, proteins, and lipids. For specific medical applications like plasma disinfection, it is necessary to supply desired active species and simultaneously to avoid supplying unnecessary species to reduce unwanted affect to human body.

We investigated formation of ROS including free radicals in water exposed to different types of contact or non-contact atmospheric-pressure helium plasma [4]. In contact plasma, all of those (relatively large amount of $^1O_2$) are induced in the liquid, whereas, in non-contact plasma, $O_2^{-\cdot}$ can be dominantly induced in the solution. Non-contact plasma is one of suitable methods to supply key species for the reduced pH method. We also investigated formation of ROS in plasma treated water (PTW), a pure water exposed to the plasma. Halflife of bactericidal activity in the PTW strongly depends on temperature (4 sec at 37ºC and several hours at 0ºC) and lower temperature brings longer lifetime. These results reveal that this bactericidal effect is not caused by stable active species like O_3, hydrogen peroxide (H_2O_2), or nitrogen oxide (NO_x). ESR (electron spin resonance) measurements with spin trapping method and spin oxidation method show intense signal of $O_2^{-\cdot}$ and no signal of the others like $^1O_2$, O_3, or $OH\cdot$ in the PTW. The activation energy of $O_2^{-\cdot}$ decay is concordant with that of bactericidal activity. Since high bactericidal activity via $O_2^{-\cdot}$ is kept by cryopreservation and deactivated soon at body temperature, PTW is another suitable method for plasma disinfection based on the reduced pH method.

References

[1] Ikawa S., Kitano K. and Hamaguchi S., "Effects of pH on bacterial inactivation in aqueous solutions due to low-temperature atmospheric pressure plasma application", *Plasma Process. Polym.* **2010**, 7 1, 33-42.

[2] Korshunov S.S. and Imlay J.A., "A potential role for periplasmic superoxide dismutase in blocking the penetration of external superoxide into the cytosol of Gram-negative bacteria", *Mol. Microbiol.* **2002**, 43 1, 95-106.

[3] Takai E., Ikawa S., Kitano K., Kuwabara J. and Shiraki K., "Molecular mechanism of plasma sterilization in solution with the reduced pH method: importance of permeation of HOO radicals into the cell membrane", *J. Phys. D: Appl. Phys.* **2013**, 46 29, 295402.

[4] Tani A., Ono Y., Fukui S., Ikawa S. and Kitano K., "Free radicals induced in aqueous solution by non-contact atmospheric-pressure cold plasma", *Appl. Phys. Lett.* **2012**, 100 25, 254103.

OP-4

Effects of 0.10−10 Gy X-ray Irradiation on Eggshell Radical Production

Kouichi Nakagawa

Department of Radiological Life Sciences, Graduate School of Health Sciences, Hirosaki University, 66-1 Hon-cyo, Hirosaki 036-8564, Japan

nakagawa@cc.hirosaki-u.ac.jp

We investigated effects of low dose X-ray irradiation (0.10−10 Gy) on eggshells radical production. Eggshells irradiated by low dose X-ray produced stable radicals [1]. Electron paramagnetic resonance (EPR) was used to measure the radical species. The stable radicals at the central region of the spectrum were the carbonates and $CO_2^{\bullet-}$ signals. The EPR signals increase with increasing absorbed dose. The estimated radical concentration (spin number) at the central region was ~3.6×10^{12} (spins/g) at 10 Gy dose using various known concentrations of TEMPOL (4-hydroxy-2, 2, 6, 6-tretramethyl piperidin-1-oxyl) aqueous solutions.

The stable radicals in irradiated eggshells were recognized at the low-level dose. The 0.10 Gy dose X-ray irradiation of 0.36 g eggshell produces the stable radicals. The carbonates and $CO_2^{\bullet-}$ signals are the same as the carbonates of seashells and other minerals. The stable radicals increase with increasing irradiation dose whereas the Mn^{2+} signals stay at the same intensities.

In addition, the different dose rates produce the same radicals. There was no significant dose rate (0.5−1.5 Gy/min) dependence for the radical production. Therefore, the present EPR results of the low dose X-ray suggest that the irradiation produces stable radicals and the radicals of 0.05 g eggshell can be useful for estimation of radiation exposure such as accidental exposures [1-3].

References

[1] Nakagawa K., *Free Radical Research*, **2014** , 48, 679-683.

[2] Nakagawa K., K. Nakagawa, K. Kobukai, and Y. Sato, *J. Radiation Research*, **2014**, in press.

[3] SatoY., Nakagawa K., and Takahashi T., *Proceeding of the 5th International Symposium on Radiation Emergency*, **2014**, 39-41.

[4] Nakagawa K. and Anzai K., *Appl. Magn. Reson.,* **2010**, 39, 285-293.

OP-5

Singlet-Triplet Transitions of ESR in Gapped Spin Systems

Toru Sakai[1,2], Keigo Hijii[3], Susumu Okubo[3] and Hitoshi Ohta[3]

[1]*JAEA, SPring-8 , Hyogo 679-5148, Japan*
[2]*Graduate School of Materials Science, University of Hyogo, Hyogo 678-1297, Japan*
[3]*Molecular Photoscience Research Center, Kobe University, Kobe 657-8501, Japan*

E-mail: sakai@spring8.or.jp

The spin gap of the low-dimensional quantum spin systems and the strongly correlated electr on systems is one of the interesting macroscopic quantum phenomena. Since the spin gap is t he energy gap between the singlet ground state and the triplet excitation, the ESR direct transi tion is prohibited because of the spin conservation law. Thus the properties of the spin gap sy stems has been observed by some ESR transitions among the triplet excitations. Recently, how ever, the ESR direct transition corresponding to the spin gap was observed in several gapped s pin systems. The mechanism of appearance of these prohibited ESR transition are supposed to be the Dzyaloshinsky-Moriya interaction and/or the staggered g-tensor. In order to identify the origin of the ESR direct transition, we gave some selection rules depending on the relative a ngle among the crystal axes of each material, the polarization of the microwave and the direct ion of external magnetic field. We report the results for the following systems:

(1) Haldane magnet: NENP [1]
(2) Spin Peierls system: $CuGeO_3$ [2]
(3) Shastry-Sutherland $SrCu_2(BO_3)_2$ [3]
(4) Distorted diamond chain: Azurite [4]
(5) Quasi-1D antiferromagnet $Cu_2Cl_4 \cdot H_8C_4SO_2$[5]

In addition possible direct transition in some other systems will be proposed.

References

[1] T. Sakai and H. Shiba: J. Phys. Soc. Jpn. 63 (1994) 867.
[2] T. Sakai, O. Cepas and T. Ziman: J. Phys. Soc. Jpn. 69 (2000) 3521.
[3] T. Sakai: J. Phys. Soc. Jpn. 72 (2003) Suppl. B 53.
[4] S. Okubo et al. : private communications.
[5] M. Fujisawa et al.: Phys. Rev. B 80 (2009) 012408.

OP-6

High-field ESR and nuclear polarization of P donors in silicon at ultra-low temperatures

Sergey Vasiliev[1], Jarno Järvinen[1], Janne Ahokas[1], Sergey Sheludyakov[1], Denis Zvezdov[1,2], Yutaka Fujii[3], Seitaro Mitsudo[3], Takao Mizusaki[3], Minchan Gwak[4], SangGap Lee[4], Soonchil Lee[5] and Leonid Vlasenko[6]

[1]*Wihuri Physical Laboratory, Department of Physics and Astronomy, University of Turku, 20014 Turku, Finland*
[2]*Institute of Physics, Kazan Federal University, 18 Kremlyovskaya St., 420008 Kazan, Russia*
[3]*Research Center for Development of Far-Infrared Region, University of Fukui, 3-9-1Bunkyo, Fukui 910-8507, Japan*
[4]*Division of Materials Science, Korea Basic Science Institute, 169-148 Gwahak-ro, Yuseong-gu, Daejeon 305-806, Korea*
[5]*Department of Physics, Korea Advanced Institute of Science and Technology, 291 Daehak-ro, Yuseong-gu, Daejeon 305-701, Korea*
[6]*A. F. Ioffe Physico-Technical Institute, Russian Academy of Sciences, Russia*

E-mail: servas@utu.fi

We report on experimental studiy of dynamic nuclear polarization (DNP) in P doped silicon (Si:P). The samples of natural Si:P (4.6% of ^{29}Si, I= 1/2) with P concentration of $6.5*10^{16}$ cm^{-3} were studied in a strong 4.6 T magnetic field and temperatures below 1 K, when the donor electron spins are fully polarized and the relaxation times of electrons and nuclei are very long [1].

Utilizing an Overhauser effect for the donor nuclei we obtained DNP of ^{31}P exceeding 98% by saturating the high field ESR line with very low RF powers (<1 μW) in 20 minutes. An inverse sign polarization of ^{31}P was created by pumping the low field line. We observed non-exponential behavior of DNP of ^{31}P with fast initial part followed by slow exponential increase. From the DNP evolution we extracted the data on the relaxation rates of forbidden transitions with simultaneous flips of electron and nuclear spins of ^{31}P. We performed measurement of nuclear relaxation of ^{31}P and found that it follows bi-exponential function of time. We explain these peculiar DNP and relaxation behavior by the influence of ^{29}Si nuclear magnetic moments surrounding ^{31}P donor.

Due to strong interactions of the ^{31}P donors with ^{29}Si nuclei, the electronic polarization of ^{31}P can be effectively transferred to ^{29}Si. We performed classical hole burning experiments in the ESR lines of ^{31}P inhomogeneously broadened due to the interactions with surrounding ^{29}Si nuclei. We obtained very narrow holes with the width defined by the transversal relaxation rate of ^{31}P electrons. In addition to the hole a narrow peak was observed on the right from the hole. We explain the hole and the peak shapes by the nuclear polarization of ^{29}Si via the Overhauser effect. We realized DNP of ^{29}Si via the resolved solid effect by pumping the ^{31}P-^{29}Si forbidden electron-nuclear transitions. A pattern of narrow holes and peaks observed in the ESR spectrum, corresponds to polarization of ^{29}Si in the specific lattice sites, resolved by the strength of the superhyperfine interactions. This opens a way for creating entangled states of ^{29}Si spins, and realization of quantum operations with large ensembles of identical nuclei.

References

[1] Jarno Järvinen, Denis Zvezdov, Janne Ahokas, Sergey Sheludyakov, Otto Vainio, Lauri Lehtonen, Sergey Vasiliev, Yutaka Fujii, Seitaro Mitsudo, Takao Mizusaki, Minchan Gwak, SangGap Lee, Soonchil Lee, Leonid Vlasenko, "Efiicient Dynamic Polarization of Phosphorus Nuclei in Silicon in Strong Magnetic Fields and Low Temperatures", arXiv: 1402.4288, 2014.

OP-7

Electron paramagnetic resonance (EPR) oximetry as a future diagnostic tool for head and neck cancer

Håkan Gustafsson[1,2], Ajay Kale[3], Alexandru Dasu[4], Anders Lund[5] and Karin Roberg[3]

[1] *Department of Medical Technology (MTÖ), Department of Medical and Health Sciences, Linköping University, Linköping, Sweden*
[2] *Center for Medical Image Science and Visualization (CMIV), Linköping University, Sweden*
[3] *Division of Oto-Rhino-Laryngology and Head and Neck Surgery, Department of Clinical and Experimental Medicine, Linköping University, Linköping, Sweden*
[4] *Radiation Physics, Department of Medical and Health Sciences, Linköping University, Linköping, Sweden*
[5] *IFM, Linköping University, Linköping, Sweden*

E-mail: hakan.l.gustafsson@liu.se

Head and neck squamous cell carcinomas (HNSCC) are often associated with poor prognosis, resistance to treatments and low 5-year survival rate. Thus there is a paramount need for assessment of predictive biomarkers, new targets for treatment as well as new diagnostic tools. The majority of all HNSCC have their origin in the mucosa of the oral cavity, pharynx, larynx, and nasal cavity and a combination of radiotherapy and surgery or definitive chemoradiation is currently the primary mode of treatment. Moreover, a monoclonal antibody against the epidermal growth factor receptor (EGFR), cetuximab (Erbitux®), has been approved for the treatment of advanced HNSCC.

While hypoxia imaging using the hypoxic tracer [F-18] fluoromisonidazole (FMISO) and positron emission tomography (PET) is a promising tool to be used in treatment planning in radiation therapy of head and neck cancer [1], PET cannot provide directly quantitative tumor oxygen pressure [2]. Our aim is therefore also to establish the relationship between hypoxia imaging using FMISO-PET and true quantitative tumor oxygen pressure as measured using electron paramagnetic resonance (EPR) oximetry using lithium phthalocyanine (LiPc) probes [3]. Two HNSCC cell lines (UT-SCC-45 and UT-SCC-14) were cultured and injected subcutaneously in BALB/c (nu/nu) nude mice at two positions in each mouse (N = 22). The day after the first cetuximab injection we found that the oxygen pressure varied quite a lot between tumors within the same groups with a tendency of decreased pressure after cetuximab treatment. Using immunohistochemistry we found that the expression of HIF-1α was lower in the cetuximab sensitive tumors (UT-SCC-14) than in the insensitive (UT-SCC-45). After one week with three injections of cetuximab the expression of HIF-1α (a protein often overexpressed during hypoxia) was reduced in the sensitive tumors.

Further experiments are ongoing where tumor oxygen pressure will be established before and after radiotherapy or treatment with cetuximab using L Band EPR oximetry. Immediately after the final EPR oximetry measurements the hypoxia in the tumors will be imaged by FMISO-PET to show the potential of EPR oximetry as a valuable tool in head and neck cancer research.

References

[1] Hendrickson K., Phillips M., Smith W., Peterson L., Krohn K., Rajendran J., "Hypoxia imaging with [F-18] FMISO-PET in head and neck cancer: Potential for guiding intensity modulated radiation therapy in overcoming hypoxia-induced treatment resistance", *Radiotherapy and Oncology* **2011**, 101, 369–375.

[2] Tran L.-B.-A., Bol A., Labar D., Jordan B., Magat J., Mignion L., Grégoire V., Gallez B., "Hypoxia imaging with the nitroimidazole 18F-FAZA PET tracer: A comparison with OxyLite, EPR oximetry and 19F-MRI relaxometry", *Radiotherapy and Oncology* **2012**, 105, 29–35.

[3] Hou H., Abramovic Z., Lariviere J. P., Sentjurc M., Swartz H., Khan N., "Effect of a Topical Vasodilator on Tumor Hypoxia and Tumor Oxygen Guided Radiotherapy using EPR Oximetry", *Radiation Research* **2010**, 173, 651-658.

OP-8

In vivo imaging of nitroxyl radicals in a mouse using surface coil array and parallel EPR detection

Ayano Enomoto and Hiroshi Hirata

Division of Bioengineering and Bioinformatics, Graduate School of Information Science and Technology, Hokkaido University, North 14, West 9, Kita-ku, Sapporo, 060-0814, Japan

E-mail: hhirata@ist.hokudai.ac.jp

In this presentation, we will report the experiments of *in vivo* EPR imaging of nitroxyl radicals using surface coil array and parallel EPR signal detection. We previously reported the feasibility of parallel detection of EPR signals of Tempone radicals *in vitro* using a two-channel surface coil array at 750 MHz [1]. In this parallel EPR detection, we used the surface coil array and two radio-frequency (RF) reflection-type bridges in addition to a 27-mT magnet system. Although *in vivo* mouse imaging of nitroxyl radicals using a sequential acquisition scheme and a four-channel surface coil array was previously reported, it took a longer time to obtain EPR signals from four channels of the surface coil array [2]. To overcome this technical issue, we assessed a parallel detection scheme that uses two different RF frequencies simultaneously to measure EPR signals. To demonstrate the concept of the parallel detection scheme, we measured nitroxyl radicals injected into a subject mouse. The parallel EPR detection scheme is potentially faster than the sequential EPR acquisition with the surface coil array. This feature might be useful for *in vivo* EPR imaging that often has a limitation of the lifetime of exogenously injected nitroxyl radicals as an imaging agent. In this talk, we will show some EPR images of nitroxyl radicals in a subject mouse measured with the two-channel surface coil array in the parallel detection scheme. We will also discuss about technical challenges of parallel EPR detection in small animal imaging.

This work was supported by grants from Japan Society for the Promotion of Science (JSPS) (26249057 and NEXT Program LR002 to H.H.). A.E. was supported by a Research Fellowship for Young Scientists (24-1486) from JSPS.

References

1. A. Enomoto and H. Hirata, *J. Magn. Reson*. 239 (2014) 29–33.
2. A. Enomoto, M. Emoto, H. Fujii, and H. Hirata, *J. Magn. Reson*. 234 (2013) 21–29.

OP-9

Toward applications of DNP using photo-excited triplet electrons

Makoto Negoro[1], Kenichiro Tateishi[1,2], Shinsuke Nishida[3,4], Akinori Kagawa[1], Yasushi Morita[3,4], and Masahiro Kitagawa[1]

[1]*Graduate School of Engineering Science, Osaka University, Toyonaka, Osaka 560-8531, Japan*
[2]*RIKEN Nishina Center for Accelerator-based Science, Wako*
[3]*Graduate School of Science, Osaka University, Toyonaka, Osaka 560-8531, Japan*
[4]*Faculty of Engineering, Aichi Institute of Technology, Toyota, Aichi 470-0392, Japan*

E-mail: negoro@ee.es.osaka-u.ac.jp

Dynamic nuclear polarization (DNP) is a means of transferring spin polarization from electrons to nuclei [1]. As a method to enhance the bulk nuclear polarization, DNP has been successfully applied to areas ranging from fundamental physics [1,2] to materials science [3], biology [4,5], and medical science [6]. As long as electron spins in thermal equilibrium are used as polarizing agents, the upper limit of the polarization enhancement is 660 for ^{1}H spins and cryogenic temperatures of around 4.2 K are required for high polarization in the order of 10% even in strong magnetic fields used for NMR. By using electron spins in photo-excited triplet states instead, DNP can overcome the above limit [7]. DNP will be implemented simply and more economically if the need for cryogenic temperatures is removed. Hyperpolarization of the samples which do not prefer cryogenic temperatures may have many potential applications.

We show the potential of DNP using photo-excited triplet electrons, henceforth we call triplet-DNP. We demonstrate a ^{1}H spin polarization of 34%, which gives an enhancement factor of 250,000 in 0.40 T, while maintaining a bulk sample (~0.6 mg, ~0.7 × 0.7 × 1 mm^3) containing >10^{19} ^{1}H spins at room temperature [8]. We discuss the scalability of triplet-DNP to a larger sample for in-vivo MRI application. Until recently, demonstrations of triplet-DNP were limited to single crystal and polycrystalline samples [9]. In the conventional DNP, a wide variety of samples have been hyperpolarized as a dopant in glassy host materials with polarizing agents [3-6]. In a similar manner, we demonstrate hyperpolarization of molecules, e.g., 5-fluorouracil, used as antimetabolite, doped in a glassy matrix codoped with pentacene at 120 K [10]. To attain a higher polarization at a higher temperature and broaden future applications, we invite contributions from various fields of chemistry and materials science for a suitable glassy host material and polarizing agent with characteristics including high solubility, near unity spin polarization, and harmlessness. Triplet-DNP can be also applied in fundamental physics experiments such as quantum information processing experiments and scattering experiments with unstable nuclei, neutrons, and elementary particles [2]. The low entropic state of a bulk nuclear spin ensemble can be used for quantum sensing toward single nuclear spin detection, quantum computing, and studies on magnetic phase transition, which is presently a hot topic in quantum simulation and was previously investigated by Abragam *et al.* at sub-Kelvin [1].

References

[1] Abragam A, Goldman M (1982) *Nuclear Magnetism: Order and Disorder* (Clarendon, Oxford).
[2] Obertelli A, Uesaka T (2011) *Eur Phys J A* **47**: 105.
[3] Lesage A, *et al.* (2010) *J Am Chem Soc* **132**: 15459.
[4] Ardenkjaer-Larsen JH, *et al.* (2003) *PNAS* **100**: 10158.
[5] Maly T, *et al.* (2008) *J Chem Phys* **128**: 052211.
[6] Gallagher FA, *et al.* (2008) *Nature* **453**: 940.
[7] Henstra A, Lin T-S, Schmidt J, Wenckebach WTh (1990) *Chem Phys Lett* **165**: 6.
[8] Tateishi K, Negoro M, Nishida S, Kagawa A, Morita Y, Masahiro K (2014) *PNAS* **111**: 7527.
[9] Takeda K, Takegoshi K, Terao T (2001) *Chem Phys Lett* **345**: 166.
[10] Tateishi K, Negoro M, Kagawa A, Kitagawa M (2013) *Angew Chem Int Ed* **52**: 13307.

OP-10

Dynamic Nuclear Polarization for Biological Solid-State NMR at High Fields and Low Temperatures

Yoh Matsuki[1], Toshitaka Idehara[2], Yoshinori Tatematsu[2], Jagadishwar Sirigiri[3], Shinji Nakamura[4], and Toshimichi Fujiwara[1]

[1]*Institute for Protein Research, Osaka University, Osaka 565-0871, Japan*
[2]*Research Center for Development of Far-Infrared Region, University of Fukui, Fukui 910-8507, Japan*
[3]*Bridge12 Technologies Inc., Massachusetts 01702, USA*
[4]*JEOL RESONANCE Inc., Tokyo 196-8558, Japan*

E-mail: yoh@protein.osaka-u.ac.jp

Precise information on 3D structure of bio-macromolecules is valuable for elucidating their functions. Magic-angle sample spinning (MAS) solid-state NMR spectroscopy (SSNMR) is suited to study atomic-resolution structure and dynamics of insoluble or non-crystalline molecular systems such as membrane proteins that are difficult to study with conventional structural analysis tools such as X-ray crystallography and solution-state NMR. Although SSNMR is rapidly maturing in its hardware and methodologies, its low sensitivity remains to be the major bottleneck in many studies using SSNMR.

Dynamic nuclear polarization (DNP) is a method for transferring ~660-times larger thermal electron spin polarization to nuclear spin of interest with an irradiation of high-power millimeter waves (in the order of 1W@400GHz), and thereby amplifying NMR signal intensities to the similar extent.

In 2010, we observed ^{1}H polarization enhancement via DNP at world's highest (at the time of report) external field condition (B_0 =14.1 T, i.e. 600 MHz for ^{1}H Larmor frequency and 395 GHz for millimeter wave) at sample temperature of ~90 K [1]. We later observed the enhancement at much lower temperatures (~30 K) using a cryogenic helium gas-driven MAS system [2]. The high field condition is good for spectral resolution, which is crucial for analysis of complex systems such as proteins, and low temperature is good for the DNP efficiency. Using these systems, we have achieved so far ^{1}H polarization enhancement by a factor of more than 500, combining the effect of DNP and low sample temperature. The enhancement should grow further with an optimization of sample and instruments.

Here, we report a development of a new 700MHz/460GHz DNP-SSNMR system which is equipped with a novel closed-cycle helium-gas MAS system that enabled us to sustain MAS (>4 kHz) at cryogenic sample temperatures (<40 K) stably for an extended period of time (basically as long as you want) with low running cost (<5 $/hr for e.g. 24 hrs run, including the helium expense and electricity). We also started assembling/testing two state-of-the-art 460 GHz 2nd-harmonic gyrotrons for a simultaneous use, and a corrugated waveguide system for it. One of the gyrotrons is able to tune the output frequency over a wide range (~1 GHz), and the other is designed to rapidly modulate (tens of kHz) the frequency over the range of tens of MHz, both being helpful for increasing the DNP efficiency. The transmission system for our double-gyrotron setup should include a universal polarizer, variable power attenuator and beam combining structures. In the presentation, we will report on our current status in the above development.

References

[1] Matsuki Y., Takahashi H., Ueda K., Idehara T., Ogawa I., Toda M., Akutsu H., and Fujiwara T., "Dynamic Nuclear Polarization Experiments at 14.1T for Solid-State NMR", *PhysChemChemPhys* **2010**, 12, 5799-5803.

[2] Matsuki Y., Ueda K., Idehara T., Ikeda R., Ogawa I., Nakamura S., Toda M., Anai T., and Fujiwara T., "Heium-Cooling and -Spinning Dynamic Nuclear Polarization for Sensitivity-Enhanced Solid-State NMR at 14T and 30K", *J. Magn. Reson.* **2012**, 225, 1-9.

OP-11

Maltose Binding Protein as Molten Globule and in the Native State

Mohammed Chakour[1], Jörg Reichenwallner[2], Chen Chen[1], Bemjamin Selmke[1], Sandra Theison[1], Rusha Chakraborty[3], S. Indu[3], Raghavan Varadarajan[3], Dariush Hinderberger[2], and Wolfgang E. Trommer[1]

[1] *Department of Chemistry, TU Kaiserslautern, D-67653 Kaiserslautern, Germany*
[2] *Institute for Chemistry, University Halle-Wittenberg, D-06099 Halle, Germany*
[3] *Molecular Biophysics Unit, Indian Institute of Science, Bangalore 560004, India*

E-Mail: trommer@chemie.uni-kl.de

Maltose-binding protein (MBP) is in a molten globule state at pH 3 as characterized by ANS binding [1]. DEER measurements of seven spin-labeled double mutants as shown in Fig. 1a & b in the native state at pH 7 had shown excellent agreement with X-ray data [2]. At pH 3 corresponding DEER measurements of all the mutants yield a broad distribution of distances. This was to be expected if there is no defined tertiary structure and the individual helices pointing into all possible directions.

However, as MBP still binds maltose in the molten globule state although more weakly, the native structure must be retained at or near the active site. This has now been verified with a new set of mutants.

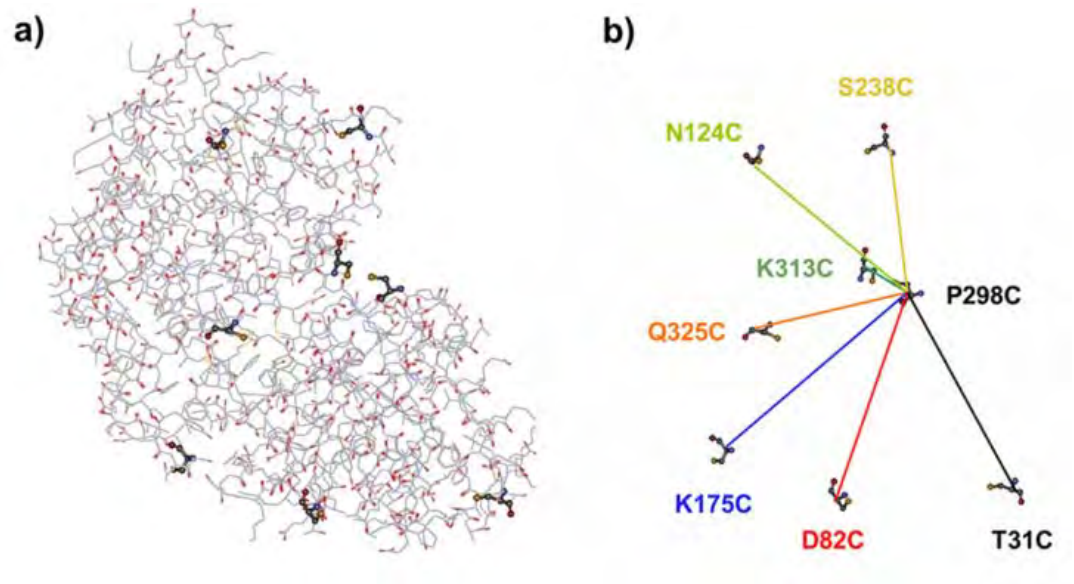

Fig. 1

[1] Prajapati, RS, Indu, S., and Varadarajan, R., *Biochem.* **2007**, 10339-10352.
[2] Reichenwallner, J., Chakour, M., Indu, S., Varadarajan, R. and Trommer, W.E., Maltose binding protein is partially structured in its molten globule state, *Appl. Magn. Reson.* **2013,** 44, 983-995 (2013).

OP-12

High power Nanosecond Pulse Generation for the Pulsed ESR by using a Gyrotron as a Radiation Source

S. Mitsudo, C. Umegaki , T. Tanaka and Y. Fujii

Research Center for Development of Far-Infrared Region, University of Fukui, Fukui, Bunkyou 3-9-1 Japan

E-mail: mitsudo@fir.u-fukui.ac.jp

The electron spin resonance (ESR) spectroscopy is one of the most important methods to investigate microscopic properties in substances [1]. Furthermore, a pulsed ESR method has advantage of measuring relaxation times of electron spins as compared to CW ESR method. One of the most popular pulsed methods is spin echo method, in which subsequent two pulses ($\pi/2$ and π pulses) with a delay time τ are applied to a sample and the echo signal is obtained after another time τ from the end of the second pulse. In general, a pulsed ESR spectroscopy requires a certain pulse duration $\Delta\tau$, then it determines the required strength of the microwave P_{RF} as $\Delta\tau \sim P_{RF}^{-1}$. The higher power means the shorter $\Delta\tau$, which extends the applicability of pulsed ESR methods. To date, the commercial pulsed ESR systems at X-band have been used extensively by researchers. The system with millimeter and/or submillimeter wave region is thought to be more useful. However, its development includes many difficulties in the treatment and development of high power radiation sources. Gyrotron is a high power radiation source in the submillimeter wave region [2-4], which is suitable for the radiation source of a short-pulsed ESR system. The radiation of several kW from a high power gyrotron allows the pulse duration in nanosecond-order. Such system has a potential to develop materials sciences, especially in the subject of substance with short relaxation time.

As the high power millimeter wave source, a CW operated sub-THz Gyrotron (Gyrotron FU CW VIIA) has been developed. We examined many candidate modes and finally selected a TE_{02} mode (154 GHz, 150 W). In order to obtain a Gaussian mode electromagnetic wave beam from a TE_{02} mode, a quasi-optical mode converter was developed. A radius of 9 mm beam waist was obtained at the semiconductor shutter system. This liner polarized millimeter wave beam is incident on Si wafers with an incident angle made to a Brewster angle. In order to realize the intense and short excitation millimeter wave pulses by using a Gyrotron output, a high power millimeter wave pulse forming system has been developed by using light controlled semiconductor shutters. A semiconductor shutter was consisted of a pair of Si wafers. These switches are activated by high energy nanosecond Nd:YAG lasers. A pulse duration $\Delta\tau$ of the millimeter wave is determined by a timing of Nd:YAG laser irradiation to Si wafer pair. This timing is adjusted by an optical delay line at laser transmission system. A delay time τ between $\pi/2$ pulse and π pulse is determined by a timing of firing of Nd:YAG laser for each millimeter wave pulse. This timing of firing is controlled by a digital delay generator. A Gyrotron output was sliced $\pi/2$ pulse (10 ns) and π pulse (20 ns) pair with arbitrary delay time by using a light controlled semiconductor shutters. The repetition cycle of this pulse pair is limited by repetition period of Nd:YAG laser. The maximum repetition cycle is 5 Hz.

References

[1] Charles P. Poole, “Electron Spin Resonance”, John Wiley & Sons Inc, 1983.

[2] T. Idehara, I. Ogawa, S. Mitsudo, M. Pereyaslavets, N. Nishida and K. Yoshida, IEEE Transactions on Plasma Science, 27, (1999) 340-354.

[3] S. Mitsudo, T. Higuchi, K. Kanazawa, T. Idehara, I. Ogawa and M. Chiba, J. Phys. Soc. Jpn., Suppl. B, 72, (2003) 172-176.

[4] S. Mitsudo, H. Hoshizuki, T. Idehara and T. Saito, Journal of Physics: Conference Series, 51, (2006) 549-552.

OP-13

Spectroscopic Investigation of Spin-Dependent Optoelectronic Pathways in Organic Devices

T. L. Keevers[1], A. Danos[2], W. Baker[1], H. Malissa[3], C. Boehme[3] and D. R. McCamey[1]

[1] *School of Physics, UNSW Australia, Sydney NSW 2052, Australia*
[2] *School of Chemistry, UNSW Australia, Sydney NSW 2052, Australia*
[3] *Department of Physics and Astronomy, University of Utah, Salt Lake City Utah 84112, USA*

Email: dane.mccamey@unsw.edu.au

The low cost and flexibility of organic polymers makes them ideal for a range of interesting optoelectronic applications. Device optimization may be assisted through microscopic understanding of spin-dependent pathways. Due to the low spin volumes present in these devices, exploration of spin-dependent pathways through magnetic resonance generally needs to be coupled with electrical or optical detection for sufficient sensitivity [1], and to allow the discrimination of the paramagnetic states which affect the optoelectronic pathways.

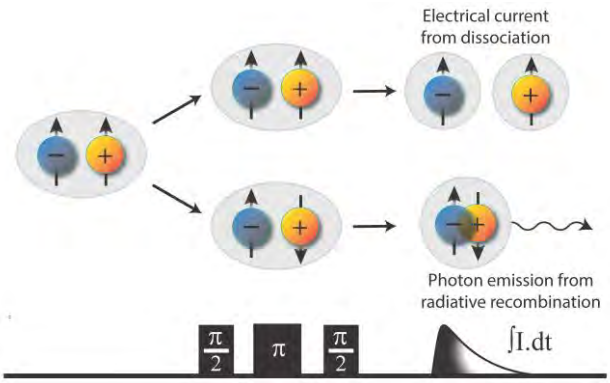

Figure 1. *Polaron pairs may spin-dependently dissociate into free polarons or form excitons and recombine. We can manipulate these rates through resonant excitation.*

The low dielectric constant and highly disordered structure of organic semiconductors may lead to the formation of weakly spin-interacting, coulombically bound polaron pairs. These states can be accessed through resonant changes in luminosity or conductivity due to overall changes in spin-dependent recombination [2].

We use these methods to investigate the spin relaxation and charge transport rates in various organic materials. From these data, we find that polaron-pair hopping is significantly slower than its free carrier counterpart, suggesting Coulombic interactions may inhibit transport [3].

Finally, we develop a framework for the interpretation and prediction of electrically-detected signals in the weakly interacting pair limit and show that simultaneous excitation of the electron and hole can significantly influence the signal seen with electrical detection following complex pulse sequences.

[1] Lupton, J. M., *et al.*, *ChemPhysChem* **11,** 3040-3058 (2010)
[2] McCamey, D. R., *et al.*, *Nature Materials* **7,** 723-728 (2008)
[3] Baker, W. J., *et al.*, *Phys. Rev. Lett.* **108,** 267601 (2012)

OP-14

New Approach to ENDOR Analysis for Manganese(II)-Substituted Soybean Lipoxygenase with A Non-Coordinated Substrate

Masaki Horitani[1], George Cutsail III[1], Cody A. Marcus Carr[2], Adam R Offenbacher[2], Judith P. Klinman[2,3,4] and Brian M. Hoffman[1]

[1]*Department of Chemistry, Northwestern University, Evanston, IL 60208, United States*
[2]*Department of Chemistry,* [3]*Department of Molecular and Cell Biology, and* [4] *California Institute for Quantitative Biosciences (QB3), University of California, Berkeley, California 94720, United States*

E-mail: m-horitani@northwestern.edu

Soybean lipoxgenase-1 (SLO) contains a mono-nuclear Fe center as a cofactor, which catalyzes a proton-coupled electron transfer from C-11 of the bound substrate, linoleic acid (LA), to the Fe^{3+}-OH, producing a substrate-derived free radical and Fe^{2+}-H_2O[1]. However, the mechanism of proton transfer is unknown and no crystal structure has been solved in presence of LA. To investigate the substrate binding to SLO, we utilize ENDOR spectroscopy for Mn^{2+}-substituted SLO and its variants.

The EPR spectrum of Mn^{2+} bound to SLO is characteristic of an ion of S = 5/2 with small zero-field splitting. A conventional 'slow-passage' field-modulated spectrum exhibits the derivative of a sextet centered at g-2 that is associated with transitions within the $m_s = \pm 1/2$ electron-spin manifold, as split into six lines by hyperfine interactions with the ^{55}Mn (I = 5/2) nucleus. Spectra collected by 2 K CW 'rapid passage' spectra instead yield an absorption display. Such spectra show that the sextet $m_s = \pm 1/2$ feature that sits on and is flanked by signals from 'satellite' transitions involving the other electron spin substates ($m_s = \pm 3/2, \pm 5/2$). The overall breadth of the pattern is proportional to the zero-field splitting (ZFS) parameter, D, whose magnitude in-turn increases with deviations of the spherical coordination symmetry of the Mn^{2+} ion. For purposes of this study it is important to note that the EPR intensity and subsequent ENDOR observations near g-2 are a superposition from all manifolds, but the 'wings' of the EPR spectrum derive solely from transitions involving the $m_s = \pm 5/2$ levels, yielding selection of ENDOR transitions.

^{13}C-ENDOR spectra for Mn-SLO with uniformly labeled ^{13}C-LA at g-2 (Fig 1 (left, middle) is uninterpretable because this field contains contribution from all manifolds ($m_s = \pm 1/2, \pm 3/2, \pm 5/2$). For simple analysis, we focused on the ENDOR spectrum at 11000 G, which is derived from only the m_s = -5/2 → -3/2 transition, refining the ν_- ENDOR peaks. Sum of three distinct ^{13}C spectral simulations shows good agreement with experimental spectra at both low and high fields (Fig 1 (right)). In the presentation, I will discuss more about this precise approach to measurements with a ZFS Mn^{2+} ion center.

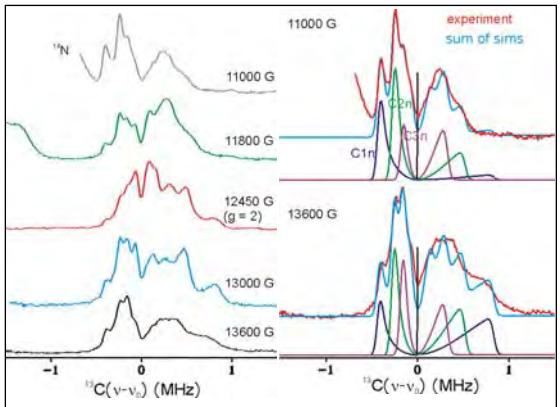

Fig 1 2D-pattern ^{13}C Mims ENDOR spectra (left) and simulation spectra (right) at 11000 G and 13600 G

Reference

[1] Knopp M. J., Seebeck F. P., Klinman J. P., "Steric control of oxygenation regiochemistry in soybean lipoxgenase-1", *J. Am. Chem. Soc.*, 2001, 123, 10319-10320

OP-15

EPR elucidation of bacterial terminal oxidase building in multi-heme centers

Catharina T. Migita, Hiroshi Miura, Norio Miyake, Kouki Kimiya and Kazunobu Matsushita

Department of Biological Chemistry, Faculty of Agriculture, Yamaguchi University, Yamaguchi 753-8515, Japan

E-mail: ctmigita@yamaguchi-u.ac.jp

Bacteria have acquired several branched respiratory chains, as they faced and adopted in various environmental changes, through the course of evolution. They express several kinds of oxidase in response to dynamic variations of their surroundings. Cyanide insensitive quinol oxidase (CIO) is one of the bacterial terminal oxidases and consisting a subfamily of cytochrome bd, a relatively well-characterized oxidase. We have succeeded to purify CIO from *Gluconobacter oxidans* membrane (of Δcyt bd strain, NBRC3172) and examined the multi-heme redox centers [1]. Alternatively, cytochrome bd was purified from *E. coli* ST4533 strain (Δcyt bo, lacking main respiratory terminal oxidase) and applied similar analysis. EPR on these enzymes have revealed that the newly purified CIO contains heme b and heme d as Cyt bd does but the hemes in CIO showed evidently discriminating features from those in Cyt bd. Such differences certainly cause their biochemical uniqueness such in oxygen affinity, optimum pH, and cyanide sensitivity.

The aerobic gram-negative bacteria *G. oxidans* is a member of α-proteobacteria, whereas *E. coli* of facultatively anaerobic rods belongs to the γ-subclass. On the other hand, genome sequence analysis have showed that Cyt bd are expressed in many clades from Archaea to Eubacteria but CIO does only in closely related three sub-clades. Both enzymes reduce molecular oxygen to water by use of electrons from ubiquinol and/or menaquinol to generate proton motive force for the ATP generation. Main terminal oxidase in these bacteria is cytochrome bo_3, a member of the heme-Cu binuclear center super family, and either Cyt bd or CIO, non-Cu binuclear center family members, works in supplementary. In spite of similar protein architecture of hetero-dimer supposed by amino acid sequences, Cyt bd and CIO differ especially in oxygen affinity (K_m: 0.3 μM for Cyt bd vs 21 μM for CIO), cyanide sensitivity (IC_{50}: 4.2 mM for Cyt bd vs 118 mM for CIO), optimum pH (7.0 for Cyt bd vs 5-6 for CIO), and the turn-over number (~10^3 for Cyt bd vs 1.4 x 10^4 for CIO). The X-ray crystal structures of both enzymes have not been available.

EPR on the purified enzymes under aerobic conditions showed signals from both high-spin and low-spin hemes but the number of species as well as their g-values were different. Oxidation by tetrachlorobenzoquinone or ferricyanide revealed that nearly 50% of hemes in CIO were in the ferric state, which is in consistent with much lower oxygen affinity of CIO than Cyt bd, in which only 30% of heme was in the ferric state. The apparent high-spin/low-spin ratio was also different: evidently higher in CIO than in Cyt bd. In Cyt bd, an axial and a rhombic high-spin species were observed and their g-values were slightly different from the reported values. To the contrast, CIO showed three kinds of high-spin signals: one axially symmetric and two rhombic signals were detected and none of their g-values were identical to those of the high-spin species from Cyt bd. The low-spin signals were further strikingly different: Cyt bd showed three incomplete signal sets, similar to the reported ones, whereas CIO exhibited clearly resolved rhombic signals from four species. In addition, ^{15}NO-bound nitrosylheme was purely formed in CIO but that in Cyt bd was inhomogeneous and less stable. Based on these EPR data, characterization of heme b - heme d centers of the two terminal oxidases were performed.

References

[1] Miura H., Migita C.T., Matsutani M., Yakushi T., Kita K., and Matsushita K., "Cyanide-insensitive quinol oxidase (CIO) from *Gluconobacter oxydans* is a unique terminal oxidase subfamily of cytochrome bd", *J. Biochem*, 2013, 153 (6), 535-545.

OP-16

Exploiting Quantum Effects Using Electron-Nuclear Coupled Molecular Spin Systems

Robabeh Rahimi Darabad[1,2], Daniel K. Park[1,2], Stephane Labruyere[1,3], Jonathan Baugh[1,4] , Kazunobu Sato[5], Takeji Takui[5] and Raymond Laflamme[1,2,6]

[1]*Institute for Quantum Computing, University of Waterloo, Waterloo N2L 3G1, Canada*
[2]*Department of Physics and Astronomy, University of Waterloo, Waterloo N2L 3G1, Canada*
[3]*Department of Electrical and Computer Engineering, University of Waterloo, Waterloo N2L 3G1, Canada*
[4]*Department of Chemistry, University of Waterloo, Waterloo N2L 3G1, Canada*
[5]*Department of Chemistry and Materials Science, Osaka City University, Osaka 558-8585, Japan*
[6]*Perimeter Institute for Theoretical Physics, Waterloo N2L 2Y5, Canada*

E-mail: rrahimid@uwaterloo.ca

Electron-nuclear coupled molecular spin systems have intrinsic properties important for exploiting quantum effects. Nuclear spins with typically long coherence times play the role of quantum memories. Fast electron spin manipulation is achieved by applying on-resonance microwave pulses. Couplings between spins make it plausible to speed-up nuclear spins manipulations by using the electron spins as actuators. In addition, flexibilities are offered by synthetic chemistry for designing new molecular materials for quantum applications such as high resolution imaging, molecular sensors and quantum information processing.

One of the main challenges in utilizing the spin systems for quantum practices is the thermal fluctuations of nuclear spins [1]. In principle, a highly pure initial state should be prepared in order to establish a clean start-up. The idea is to employ the coupled spins and take advantage of the electron high spin polarization. Polarization of nuclear spins are enhanced to the electron spin polarization using DNP methods, yet further boosting is achieved by implementing heat-bath algorithmic cooling.

Nonclassical correlation, and specifically entanglement, are generally believed to be the distinctive resources of power for quantum processing to surpass any corresponding classical counterparts. In order to verify this statement, also to characterize the important role of entanglement, and compare it with the general nonclassical correlation, the testing experimental system should have access to all types of correlations. The electron-nuclear coupled system is one of the appropriate systems because it initiates the classical/quantum processing with nuclear spins in thermal polarization (the expected correlations are solely non-entangled), however, by applying DNP followed by heath-bath algorithmic cooling, it changes to an ultimate quantum system (entanglement is generated).

Extracting reliable processing outcome, i.e. robust against noise, is the ultimate goal for every effort relating to engineering a processing system. In quantum context, only few examples are applicable since generally quantum systems are fragile against noise. The electron-nuclear coupled molecular spin system is useful since extra spins can be introduced by appropriate molecular optimization; spins are refreshed by the means mentioned above, and they are controlled by using varieties of tools and techniques adapted from ESR/ENDOR/ELDOR [2]. We emphasize that more powerful experimental techniques based on AWGs are emerging in this field.

References

[1] Rahimi D. R., Takeda K., Ozawa M., and Kitagawa M., "Entanglement witness derived from NMR superdense coding", *Journal of Physics A: Mathematical and General* **2006,** 39, 2151-2159.

[2] Nakazawa S., Nishida S., Ise T., Yoshino T., Mori N., Rahimi D. R., Sato K., Morita Y., Toyota K., Shiomi D., Kitagawa M., Hara H., Carl. P., Höfer P., and Takui T., "A Synthetic Two-Spin Quantum Bit: g-Engineered Exchange-Coupled Biradical Designed for Controlled-NOT Gate Operations", *Angewandte Chemie* **2012**, 124, 9998-10002.

OP-17

Electron-Hole Dissociations and Electronic Coupling Influenced by Alkyl Side Chains in the Photovoltaic Polyalkylthiophene:PCBM Interface

Yasuhiro Kobori, Taku Miura

Department of Chemistry, Graduate School of Science, Kobe University, 1-1 Rokkoudai-cho, Nada-ku, Kobe 657-8501, Japan

E-mail: ykobori@kobe-u.ac.jp

Organic bulkheterojunction (BHJ) thin-films composed of the conjugated polymers as the electron donors (D) and [6,6]-C_{61}-butyric acid methyl ester (PCBM) as the electron acceptor (A) have been regarded as one of the attractive materials for low cost and flexible solar-cell devices. In the photoactive layer of the BHJ film, the polymer-fullerene phase segregation contributes to the efficient photoinduced charge-transfer (CT) reaction at the polymer-fullerene interface. One of the puzzling subjects has been that most of the electrons and holes generated at the interface escape from the CT binding by the Coulomb attraction for the low dielectric environment ($\varepsilon_r \approx 3$) in the solid blends. The molecular motion in the organic semiconductors is a key to the efficient carrier dissociation. The molecular libration in the blend should enhance the entropy of the dissociated charge-separated (CS) state as compared to that of the bound CT state. Numerous studies have been performed to clarify the carrier dissociation mechanism in the organic semiconductors. However, only a few studies have experimentally elucidated effects of the polymer motions on the carrier dissociation. Moreover, despite the importance of the electronic character of the distant CS systems, no study has determined the distance dependence of the electronic coupling (V_{CR}) for understanding the nature of the electron tunneling to contribute to the charge transport at the BHJ domain interface. In the present study, we characterized the nanostructure, the V_{CR} and the motion of the spin correlated radical pair (SCRP) of the photoinduced CS states in the blend materials by poly(3-hexylthiophene-2,5-diyl) (P3HT) and PCBM at 77 K by using time resolved electron paramagnetic resonance (TREPR) spectroscopy.[1] We have examined effects of the alkyl side-chains on the electron-hole dissociation and on the V_{CR} of the transient CS state for the regioregular polyalkylthiophene (RR-P3AT):PCBM blend films fabricated by the spin coating method.[2]

To clarify the electron-hole dissociation mechanism and the electronic property in the photoinduced CS states, the nanostructures and the exchange coupling ($2J$) are determined from the simulation of the TREPR data. Figure 1 shows one of the nanostructures of the CS states for the thermally annealed RR-P3HT:PCBM film. From the $2J$ parameters, one can estimate the electronic coupling values (V_{CR}) for the CS states in Figure 1. From exponential decays of the V_{CR} values with respect to the center-to-center separations between the unpaired orbitals in Figure 1, the attenuation factor (β_e) has been determined to be β_e = 0.2 Å^{-1}. From this β_e, the tunneling barrier from the delocalized holes in the P3AT region of Figure 1 to the highest occupied molecular orbitals (HOMO) of the single P3AT chains has been obtained to be ΔE_{eff} = 0.2 eV, implying that the transient holes in Figure 1 are energetically located at a level very close to the valence band in the P3AT crystalline domain.

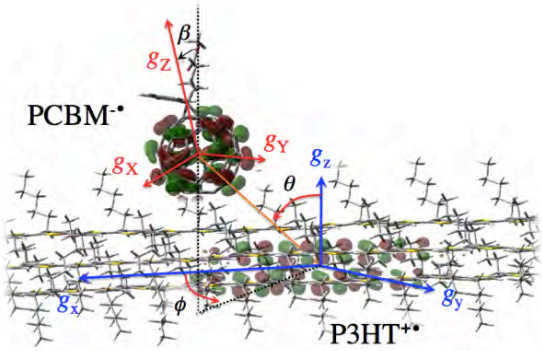

Figure 1. One of the geometries of the interfacial photoinduced CS state to reproduce the TREPR spectra for the thermally annealed film of the RR-P3HT:PCBM blend.

References

[1] Kobori Y., Noji R., Tsuganezawa S., *J. Phys. Chem. C* **2013**, 117, 1589-1599.
[2] Miura T., Aikawa M., Kobori Y., *J. Phys. Chem. Lett.* **2014**, 5, 30-35.

OP-18

Evaluation of Dysprosium(III)-Copper(II) Exchange Coupling Parameters and Relation with the Bridging Geometry

Yumi Ida,[1] Takayuki Ishida,[1] Soumavo Ghosh,[2] Ashutosh Ghosh,[2] and Hiroyuki Nojiri[3]

[1]*Department of Engineering Science, The University of Electro-Communications, Tokyo, Japan*
[2]*Department of Chemistry, University College of Science, University of Calcutta, Kolkata, India*
[3]*Institute of Material Research, Tohoku University, Sendai, Japan*

E-mail: ishi@pc.uec.ac.jp

There have been many 4f-3d heterometallic single-molecule magnets ([Dy_2Cu], [Dy_4Cu] etc.) with various structures and 4f/3d ratios.[1] For such discrete molecules we have recently established a standard method to determine precisely the 4f-3d exchange couplings by means of combined high-frequency electron paramagnetic resonance (HF-EPR) and pulsed-field magnetization techniques.[2] Ferromagnetic 4f-3d compounds show no jump in magnetization, and accordingly the HF-EPR spectroscopy would be an important tool to characterize 4f-3d exchange interaction.

According to the known method for the corresponding $(CuL)_2Tb$ compounds,[3] dimeric $[\{(CuL)_2Dy(H_2O)(NO_3)_3\}_2bpy]\bullet 2MeOH\bullet 4H_2O$ (**1**) and polymeric $[\{(CuL)_2Dy(NO_3)_3bpy\}_\infty]\bullet(MeOH\bullet 2H_2O)_\infty$ (**2**) were synthesized (H_2L = *N,N'*-bis(salicylidene)-1,3-propanediamine or salpn; bpy = 4,4'-bipyridine). The Dy and Cu ions are doubly oxo-bridged in each $(CuL)_2Dy$ unit. We measured the HF-EPR spectra on **1** and **2** (Figure 1), where the signals are assigned to the $\Delta m_S = \pm 1$ transition due to the Cu spins. The number of the signals corresponds to that of the independent Cu sites. Ferromagnetic Dy-Cu exchange couplings are responsible for the negative bias fields observed here. The coupling parameter $J_{Dy\text{-}Cu}$ was estimated as follows, +2.2(2) and +1.7(10) K for **1** and +1.8(5) K for **2**, from the Ising-type spin Hamiltonian:[4] $H = -J_{Dy\text{-}Cu1}J^z_{Dy}\bullet S_{Cu1} - J_{Dy\text{-}Cu2}J^z_{Dy}\bullet S_{Cu2} + \mu_B H^z(g_{Dy}J^z_{Dy} + g_{Cu1}S_{Cu1} + g_{Cu2}S_{Cu2})$.

Since the study on determination of the Dy-Cu exchange coupling is rare, discussion on the magneto-structure relation is unprecedented to our knowledge. The $J_{Dy\text{-}Cu}$ value may be correlated with the "butterfly" angle, ϕ, between the CuO_2 and DyO_2 planes in the DyO_2Cu core and/or with the Dy-O-Cu bond angles. Details will be discussed.

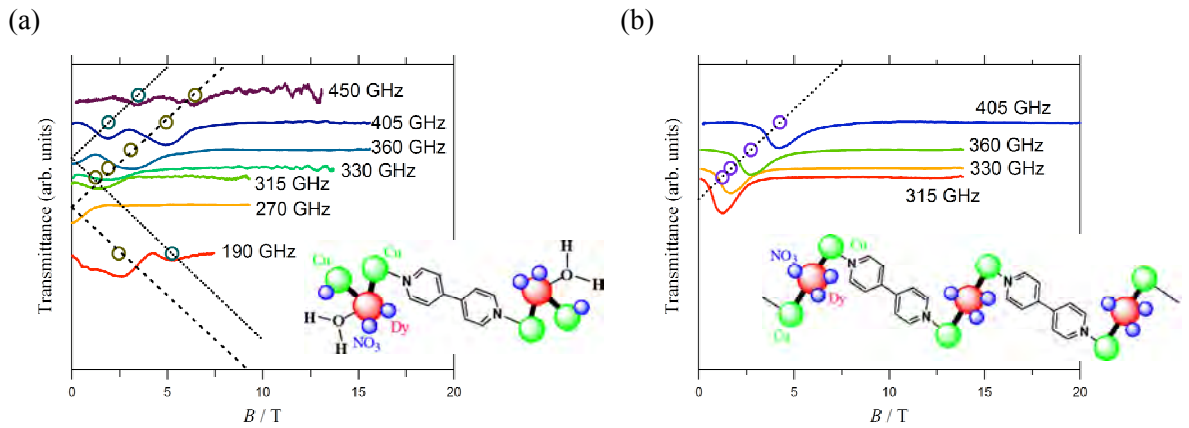

Figure 1. Selected EPR spectra measured at 4.2 K as a function of frequency for (a) **1** and (b) **2**. The spectra are offset in a linear scale of the frequency. Schematic formulas are also drawn.

References

[1] F. Mori et al., *J. Am. Chem. Soc.* **2006**, *128*, 1440; S. Ueki et al., *Chem. Phys. Lett.* **2007**, *440*, 263.
[2] T. Ishida et al., *Dalton Trans.* **2012**, *41*, 13609.
[3] S. Ghosh et al., *Cryst. Growth Des.* **2014**, *14*, 2588.
[4] T. Shimada et al., *Inorg. Chem.* **2011**, *50*, 10555.

OP-19

EMR related problems in modeling properties of single-ion and single-molecule magnets (SIM/SMM) - interplay between the crucial notions

Czesław Rudowicz[1], and Mirosław Karbowiak[2]

[1] *Institute of Physics, West Pomeranian Univ. of Technology, Al. Piastów 17, 70–310 Szczecin, Poland*
[2] *Faculty of Chemistry, University of Wrocław, ul. F. Joliot-Curie 14, 50-383 Wrocław, Poland*

E-mail: crudowicz@zut.edu.pl

Interpretation of magnetic and spectroscopic properties of the single transition-ion complexes and magnetic systems is based on the ***physical*** crystal field (CF) [ligand field (LF)] Hamiltonians [H_{CF} (H_{LF})] and the ***effective*** spin Hamiltonians (SH) including the zero-field splitting (ZFS) terms [H_{SH} (H_{ZFS})]. The Hamiltonians H_{CF} (H_{LF}) underlie the optical spectroscopy, whereas H_{SH} (H_{ZFS}) - EMR and magnetism areas [1, 2, 3]. Our task is to bring order to the zoo of different Hamiltonians and simplify the navigation through the maze of the complex web of interrelated notions involved in the interface CF (LF) ↔ SH (ZFS) between these Hamiltonians, which has become entangled over the years [4, 5]. The focus is on EMR-related problems in modeling properties of single-ion and single-molecule magnets (SIM/SMM) [6, 7]. Using concept maps, the interplay between the crucial notions as well as the operators is elucidated for the benefit of, especially, junior researchers. Terminological confusions have, most recently, resulted in factual and implied usage of the invalid conversion relations. Such pitfalls or errors of substance bear on understanding of physical properties of SIM/SMM.

First, the examples of conceptual problems and related terminological confusions at the interface CF (LF) ↔ SH (ZFS) are surveyed. Then, the notions pertinent for single transition ions and exchange coupled systems are systematically defined and their logical interrelationships outlined. The key aspects pertinent for SIM complexes concern the interplay between the physical and effective Hamiltonians, including: Hamiltonian forms and definitions of the associated parameters, distinct properties of the Stevens and Wybourne CF (LF) parameters and implications for conversion relations, distinctions and interrelationships between the CF (LF) and SH (ZFS) Hamiltonians and parameters, conversion relations for the Stevens and conventional ZFS parameters, and orthorhombic standardization. The key aspects pertinent for SMM complexes concern the interplay between the multispin (or microscopic spin) Hamiltonians and the effective total spin (or giant spin) ones, including: distinction between the single-ion spins S_i and the total spin S_T of SMM, relationships between the respective ZFS parameters, higher-order terms in the generalized spin Hamiltonians (GSH), as well as role of the CF (LF) interactions and the spin-orbit (SO) coupling (SOC) in description of SIM/SMM, which appear to be misinterpreted in some SIM/SMM studies. The elucidation of the problems exposed here should lead to deeper understanding of the intricacies involved in the interface CF (LF) ↔ SH (ZFS) and, in longer terms, prevent proliferation in future literature of terminological confusions and errors of substance.

References

[1] J. Mulak, Z. Gajek, *The Effective Crystal Field Potential*, Elsevier (2000).
[2] S.K. Misra, Ed., *Multifrequency Electron Paramagnetic Resonance*, Wiley-VCH (2011).
[3] K.H.J. Buschow and F.R. de Boer, *Physics of Magnetism and Magnetic Materials*, Kluwer (2003).
[4] C. Rudowicz and S.K. Misra, Spin-hamiltonian formalisms in EMR and related spectroscopies, *Appl. Spectrosc. Rev.* **2001,** 36, 11-63.
[5] C. Rudowicz, Clarification of the confusion concerning the CF quantities vs. the ZFS quantities in magnetism studies: Part I, *Physica B* **2008,** 403, 1882-1897; Part II, **2008,** 403, 2312- 2330.
[6] D. Gatteschi, R. Sessoli, J. Villain, *Molecular Nanomagnets*, Oxford Univ Press (2006).
[7] L. Sorace, C. Benelli, D. Gatteschi, Lanthanides in molecular magnetism: old tools in a new field, *Chem. Soc. Rev.* **2011,** 40, 3092-3104.

Er-concentration and charge carrier effects on GaAs;Er,O revealed by X-band ESR

F. Elmasry[1], S. Okubo[2], H. Ohta[1, 2], and Y. Fujiwara[3]

[1]*Graduate School of Science, Kobe University, Kobe 657-8501, Japan*
[2]*Molecular Photoscience Research Center, Kobe University, Kobe 657-8501, Japan*
[3]*Graduate School of Engineering, Osaka University, Osaka 565-0871, Japan*

E-mail: 108s151s@stu.kobe-u.ac.jp

Er-doped GaAs is expected as one of the promising materials for development of temperature stable light sources, since the Er^{3+} intra-4f shell transition exhibits a temperature stable luminescence around 1.54μm, which matches the minimum loss region of silica-based optical fibers. Oxygen codoping has been recognized to influence sharp simple photoluminescence spectra (PL) due to the local structure, which is an Er^{3+} at Ga-site with two adjacent oxygen atoms (referred to as Er-2O center) [1]. However, the photoluminescence excitation (PLE) spectra due to direct intra 4f-shell excitation revealed that many inactive Er centers exist. This is one of unsolved problem in the luminescence mechanism of GaAs;Er,O. Recently Fujiwara *et al*. performed PL measurements on three GaAs;Er,O samples with different Er concentration and charge carriers. Fujiwara *et al*. observed weak PL emission from p-type sample with the highest Er-concentration [2]. This result can provide additional information to clarify luminescent Er-center in GaAs;Er,O. As electron spin resonance (ESR) measurement has proven to be a powerful method to investigate the local structures of impurities in solids, we have performed ESR measurements on Fujiwara's three GaAs;Er,O samples.

The epitaxial film of GaAs;Er,O were grown by organometallic vapor phase epitaxy (OMVPE) method. The Er concentration in n-type GA040396, high resistance GA050462 and p-type GA050461 samples was estimated to be 7.0×10^{17}, 4.0×10^{18}, 1.0×10^{19} cm^{-3} respectively, by secondary ion mass spectrometer (SIMS). ESR measurements at 9.49 GHz have been performed from T= 4.7K to 18K using Bruker ESR spectrometer EMX081 and Oxford He-flow cryostat ESR 900 at Kobe University.

Previous X-band ESR measurements on GaAs;Er,O samples without charge carrier showed three ESR signals labeled A, B, and C assigned to Er-2O centers [3]. The three types of ESR signals were observed in our samples. The resonance field of these signals is consistent with those reported previously. Furthermore, we found drastic decrease of C-ESR signal intensity as shown in Fig.1. Similar decrease of signal C was also observed in Zn doped GaAs:Er,O with p-type carriers [4]. A suggestion of Er-excitation model to explain this decreases will be discussed. Moreover, effect of Er-concentration and charge carrier on temperature dependence of the integrated intensities, linewidth and line shape analysis of ESR will be discussed in comparison with GaAs;Er,O samples without charge carrier.

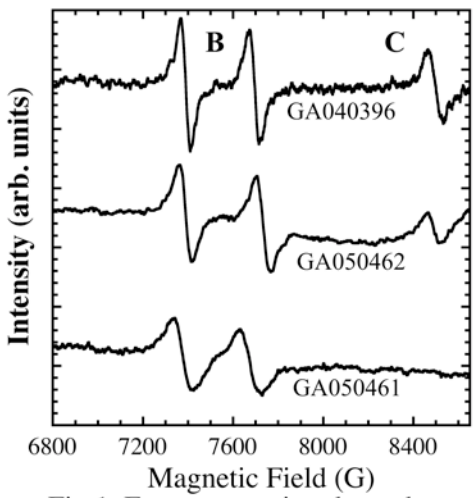

Fig 1. Er concentration dependence of ESR Spectra at T=8.0K, H//001

References

[1] K. Takahei, A. Taguchi, Y. Horikoshi, Atomic configuration of the ErO luminescence center in Erdoped GaAs with oxygen codoping, J. Appl. Phys. **1994,** 76, 4332-4339

[2]Y.Fujiwara, A.Koizumi, Private communication, **2010**

[3] M. Yoshida, K. Hiraka, H. Ohta, ESR study of GaAs:Er,O grown by organometallic vapor phase epitaxy. J. Appl. Phys. **2004,** 96, 4189-4196

[4] M. Yoshida, K. Hiraka, H. Ohta, ESR study of Zn-codoping effect on the local structure of the Er-related centers in GaAs;Er,O, J. Appl. Phys. **2005**, 96, 023909-4

ENDOR Studies on Relationship between the Hydrogen Bonding Network and Ca^{2+} of the Mn Cluster in Photosystem II

Hiroki Nagashima[1], Yoshiki Nakajima[2], Jian-Ren Shen[2] and Hiroyuki Mino[1]

[1]*Graduate School of Science, Nagoya University, Nagoya 464-8601, Japan*
[2]*Graduate School of Natural Science and Technology/Faculty of Science, Okayama University, Okayama 700-8530, Japan*

E-mail: hnagashima@bio.phys.nagoya-u.ac.jp

Mn cluster in photosystem II (PS II) of plants and cyanobacteria catalyzes water splitting and oxygen evolution in the oxygenic photosynthesis. Upon absorption of one photon, charge separation occurs at the reaction center of PS II which is a multi-pigment assembly consisting of six chlorophylls and two pheophytins. The electron is transferred to accepter side of PS II and primary oxidant $P680^+$ oxidizes the Mn cluster through a tyrosine residue, Y_Z. The Mn cluster has five different redox states, called S_n (n=0-4), which is advanced sequentially to higher states (S_n to S_{n+1}) by absorbing one photon. Molecular oxygen is evolved during the transition of $S_3 \rightarrow (S_4) \rightarrow S_0$ state. Recent X-ray crystal structure analysis revealed that the Mn cluster consists of four Mn, five O and one Ca. Additionally, four water molecules, labeled W1-W4, are ligated to the Mn cluster. W1 and W2 are ligated to the Mn4 ion and W3 and W4 are ligated to the Ca^{2+} [1]. The Ca^{2+} is required for oxygen evolution. Oxygen evolving activity is lost by the Ca^{2+} depletion and recovered by reconstitution of Ca^{2+} or Sr^{2+}. EXAFS have shown that distances between Mn ions were not changed by the Ca^{2+} depletion [2]. Thus, the role of Ca^{2+} which has no redox activity in water splitting is still unclear.

Electron nuclear double resonance (ENDOR) is a powerful method to detect hyperfine interaction between electron and nuclei spins. We applied ENDOR to the S_2 state Mn cluster from spinach in order to detect protons surrounding the Mn cluster. To determine precise locations of protons, the oriented PS II membranes were used. Seven pairs of ENDOR signals were detected and analyzed based on the X-ray crystal structure. The signals arising from $^1H/^2H$ exchangeable protons were assigned to W1–W4 protons [3].

In order to clarify the role of Ca^{2+}, based on the assignments of ENDOR signals, we applied ENDOR to the Sr^{2+}-substituted PS II from *T. vulcanus* and Ca^{2+}-depleted PS II from spinach. Similar ENDOR spectra were observed with Ca^{2+}-containing PS II from *T. vulcanus* and spinach, indicating that there is no structural difference in the S_2 state Mn cluster between the two species. ENDOR spectrum of Sr^{2+}- substituted PS II from *T. vulcanus* was also similar to that of the Ca^{2+}-containing PS II, but small difference arising from perturbation of water molecules ligated to Ca^{2+}/Sr^{2+} was detected. On the other hand, the Ca^{2+} depletion resulted in peak shifts and disappearance of ENDOR signals which were assigned to W3 and W4 protons. Additionally, Ca^{2+} depletion modified angular dependence of the ENDOR signals assigned to protons of W2 which is not ligated to the Ca^{2+}. Thus, these results indicate that Ca^{2+} depletion caused disruption of the hydrogen-bonding network surrounding the Mn cluster, and reconstitution of Ca^{2+} or Sr^{2+} restored the hydrogen-bonding network and thereby recovered the oxygen evolving activity.

References

[1] Umena Y., Kawakami K., Shen J.-R. and Kamiya N., ”Crystal structure of oxygen-evolving photosystem II at a resolution of 1.9 Å”, *Nature* **2011**, *463*, 55-60.
[2] Latimer M., Derose V., Yachandra V., Sauer K. and Klein M., “Structural effects of calcium depletion on the Manganese Cluster of Photosystem II: Determination by X-ray Absorption Spectroscopy”, *J. Phys. Chem. B* **1998**, 102, 8257-8265.
[3] Nagashima H. and Mino H., “Highly resolved proton matrix ENDOR of oriented photosystem II membranes in the S_2 state”, *Biochim. Biophys. Acta* ***2013***, *1827, 1165-1173.*

Development of fluorescent probe for sensitive detection of ascorbic acid

Yuta Matsuoka[1], Kei Ohkubo[2,3], Toshihide Yamasaki[1], Hiroshi Ohtabu[1], Tomonori Shirouzu[1], Shunichi Fukuzumi[2,3], Ken-ichi Yamada[1,4]

[1]*Department of Bio-functional Science, Faculty of Pharmaceutical Sciences, Kyushu University*
[2]*Department of Material and Life Science Graduate School of Engineering, Osaka University*
[3]*JST ALCA,* [4]*JST PRESTO*

E-mail: 3PS13010N@s.kyushu-u.ac.jp

【Introduction】Ascorbic acid is a small-molecular reductant with multiple functions *in vivo* and related to disease states. Therefore, the rapid and convenient detection of ascorbic acid is expected to be useful as a diagnostic tool. Nitroxide is reduced to generate the corresponding hydroxylamine by ascorbic acid. In previous work, we developed an ascorbic acid detection probe, Naph-DiPy (15-(naphthyl-1-amino)-3,11-dioxa-7-azadispiro[5.1.5^8.3^6]hexadecan-7-oxyl), which employs covalent coupling of nitroxide with a fluorophore, leading to intramolecular quenching of fluorescence emission. This probe could sensitively detect ascorbic acid in the plasma of ODS rats[1]. However, Naph-DiPy has a short emission wavelength at 430 nm where is overlapped with the other *in vivo* fluorescent substances. To overcome this undesirable property, we focused on Nile-Blue used as a fluorophore and developed a long wavelength fluorescent probe "Nile-DiPy" for detecting ascorbic acid (Figure 1).

【Results and Discussion】 We synthesized Nile-DiPy as a long wavelength fluorescent probe for det ection of ascorbic acid. Nile-DiPy showed the similar photochemical properties to those of Nile-Blue except for the low fluorescence quantum efficiency. The lifetime of the excited state of Nile-DiPy was evaluated by the femtosecond laser transient absorption measurements in a deaerated aqueous solution. The lifetime of the singlet excited state of Nile moiety of Nile-DiPy was much shorter than that of Nile-Blue without linking nitroxide as a reference. The shorter lifetime of the excited state of Nile-Blue moiety in the Nile-DiPy may be ascribed to the electron transfer from nitroxide to the singlet excited state of Nile-Blue to produce the charge-separated state, followed by the faster back electron transfer to the ground state. Next we evaluated the kinetic isotope effect (KIE) using D_2O to determine the rate-determining step. The value of KIE was 9.77. This result suggests that the reaction of Nile-DiPy with ascorbic acid takes place via hydrogen atom transfer to produce a fluorescent OH-form (Figure 1). To confirm the practical usefulness of this probe, we measured the concentration of plasma ascorbic acid of Streptozotocin-induced diabetic mouse using Nile-DiPy. There was good correlation betw een the plasma ascorbic acid levels m easured by the method using Nile-DiP y and by HPLC. This indicates that Nile-DiPy could sensitively and conveniently detect ascorbic acid and be a useful bio-probe for understanding the role of ascorbic acid in disease states.

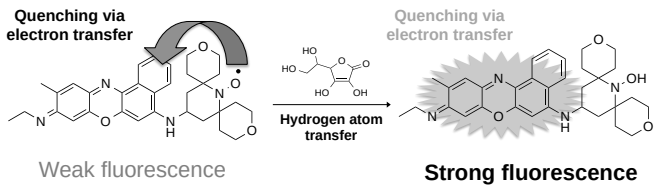

Figure 1. Long wavelength AsA detection probe "Nile-DiPy"

References

[1] Matsuoka, Y. Yamato, M. Yamasaki, T. Mito, F. Yamada, KI. *Free Radical Biol. Med.* **2012**, 53, 2112-8.

Time-Resolved EPR and Photochemical Study on the Inclusion System of Anthraquinones and Cyclodextrins

Zhebin Fu[1,2], Moe Sasaki[2], Rina Sato[2], Akira Naruoka[2], Akio Kawai[1] and Hisao Murai[2]

[1]*Graduate School of Science and Engineering, Tokyo Institute of Technology, Tokyo 152-8551, Japan*
[2]*Graduate School of Science, Shizuoka University, Shizuoka 422-8529, Japan*

E-mail: fu.aa@m.tetich.ac.jp

The photophysics and photochemistry of crown ethers have been extensively studied over several years. Cyclodextrins (CD), as one of them, can be used as model enzymes and their unique reaction cavity provide specific photochemical properties. Their inclusion properties and dynamic behaviors have been studied so far, whereas α–CD who has the smallest cavity has not been well known.

In this study, the photochemical reactions of a series of sulfonated anthraquinones (AQSs) included in α–, β–, γ– CD in aqueous solutions were investigated using a time-resolved electron paramagnetic resonance (tr-EPR) method. The main reaction pathway of the hydrogen abstraction form the CD molecule and the ejection of the transient radical of AQSs were shown. These are tentatively assigned to free radicals of AQSs and CDs formed inside of the CD cavity, where triplet mechanism (TM) and radical pair mechanism (RPM) were observed. The chemically induced dynamic electron polarization (CIDEP) spectra show four groups of CD radicals with specific hyperfine coupling (hfc) constants. The photochemical properties of the included system of AQSs and CD are clarified, and the interaction of AQSs and CDs will discussed.

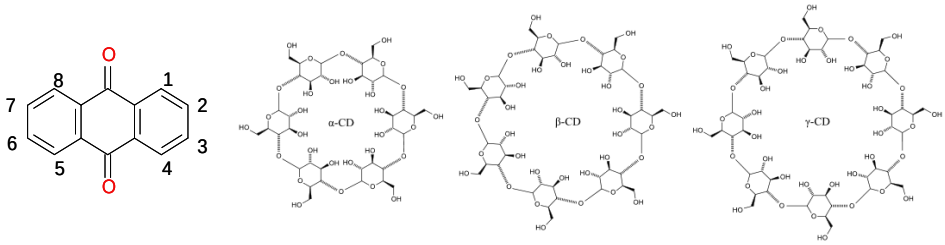

Figure 1. Chemical structure of the Anthraquinones and Cyclodextrins used in this work. The positions of sulfonic groups ($-SO_3^-$) placed at Anthraquinone are shown.

Magnetoconductance of Pentacene/C_{60}-bilayaer Solar Cell

T. Omori[1], Y. Wakikawa[2], T. Miura[1], Y. Yamaguchi[3], K. Nakayama[3,4] and T. Ikoma[1,4,5]

[1]*Graduate School of Science and Technology, Niigata University, Niigata 950-2181, Japan.*
[2]*Center for Fostering Innovative Leadership, Niigata University, Niigata 950-2181, Japan.*
[3]*Graduate School of Science and Engineering, Yamagata University, Yonezawa 992-8510, Japan.*
[4]*CREST, Japan Science and Technology Agency, Kawaguchi 332-0012, Japan.*
[5]*Center for Instrumental Analysis, Niigata University, Niigata 950-2181, Japan.*

E-mail: f13a032h@mail.cc.niigata-u.ac.jp

Organic solar cells (OSCs) have been paid attention from the view point of light-weight, flexible and low-cost solar energy conversion devices. However, the energy conversion efficiency in OSCs is lower than that of silicon-based solar cells, because of short exciton diffusion length, large charge recombination yield and low mobility in organic semiconductors. Recently several concepts for improving the efficiency of OSCs through control of electron spins have been proposed [1-5]. The electron spin dynamics in encounter pair of elementary excitations play an important role in these concepts based on singlet fission, triplet fusion, charge recombination and so on in organic semiconductors. Also the conservation and conversion dynamics of spin angular momentum in the encounter pairs lead to magnetoconductance effects (MC) in organic semiconductors under both dark and light conditions [6-8]. In this paper we will demonstrate that the MC effect provides quantitative information about the singlet fission, the charge recombination and the trap-related dynamics with triplet exciton in a bilayer OSC device of pentacene (Pen) and fullerene (C_{60}).

At room temperature the Pen|C_{60}-device showed totally negative and positive MC effects respectively in dark and light. The magnetic field dependence of the MC effect in dark was fitted with double Gaussians with linewidths of 2.1 (MC_1) and 13 mT (MC_2). The MC effect detected in light was reproduced by triplet Gaussians with 4.1 (MC_1), 20 (MC_2) and 190 mT (MC_2). The multi-components of MC effects indicate several mechanisms originated from different encounter pair dynamics. The ratio between the MC_1 and MC_2 components in dark varied with the bias voltage and the ratio among the three MC components detected in light also depended on the intensity and wavelength of the incident light. Combined with kinetic and quantum mechanical simulations, we will discuss about the recombination, trap and detrapping of carrier and singlet fission in the active layers.

References

[1] Jadhav P. J., et al., “Singlet Exciton Fission in Nanostructured Organic Solar Cells”, *Nano Lett* **2011**, 11, 1495–1498.
[2] Tritsch J. R., et al., “Harvesting singlet fission for solar energy conversion via triplet energy transfer”, *Nature Commun.*, **2013**, 4, 1-7.
[3] Congreve D. N., et al., “External Quantum Efficiency Above 100% in a Singlet Exciton Fission Based Organic Photovoltaic Cell”, *Science*, **2013**, 340, 334-337
[4] Jankus V., et al., “Energy Upconversion via Triplet Fusion in Super Yellow PPV Films Doped with Palladium Tetraphenyltetrabenzoporphyrin: a Comprehensive Investigation of Exciton Dynamics”, *Adv. Funct. Mater.*, **2013**, 23, 384-393
[5] Rao A., et al., “The role of spin in the kinetic control of recombination in organic photovoltaics” *Nature*, **2013**, 500, 435-439.
[6] Janssen P., et al.,“ Tuning organic magnetoresistance in polymer-fullerene blends by controlling spin reaction pathways“ *Nature Commun.*, **2013**, 4, 2286
[7] Ambe C. E., et al., "Thermal Annealing Effect on Photocarrier Dynamics in PCBM Films", *Bull. Chem. Soc. Jpn.*, **2013**, 86, 1051-1058.
[8] Wakikawa Y., et al., "Effect of Acceptor Lamination on PhotoCarrier Dynamics in Hole Transporting Hexabenzocoronene Nanotubular Self-Assembly", *J. Phys. Chem. C*, **2013**, 117, 15295-15305.

Poster Presentations

P-1

EPR Spin Probe Investigation of Surface Structure Analyses of Skin

Kouichi Nakagawa,[1] S. Minakawa[2], and D. Sawamura [2]

[1] *Department of Radiological Life Sciences, Graduate School of Health Sciences, Hirosaki University, 66-1 Hon-cyo, Hirosaki 036-8564, Japan*

[2] *Department of Dermatology, Graduate School of Medicine, Hirosaki University, 5 Zaifu-Cyo, Hirosaki 036-8562, Japan*

nakagawa@cc.hirosaki-u.ac.jp

EPR EPR (electron paramagnetic resonance) spin-probe method along with spectral simulation was used to investigate structural changes of various stratum corneum (SC). The SC was stripped consecutively from one to three or four times using a glass plate coated with a cyanoacrylate resin. Aliphatic spin probes, 5-doxylstearic acid (5-DSA) and 3β-doxyl-5α-cholestane (CHL), were used to evaluate the SC ordering. EPR spectrum of 5-DSA incorporated in the SC demonstrated a characteristic peak for the first strip. A slow-tumbling simulation for 5-DSA showed clear differences in EPR intensities as well as ordering values (S_0) of the SC for control and terpenes treated SC.

In addition, a little, broad three-line pattern of 5-DSA in *psoriasis vulgaris* stratum corneum (pv-SC) was observed. The spectral pattern of pv-SC is quite different from those of control SC reported. The S_0-values obtained for the pv-SC and the control were approximately 0.20 and 0.49, respectively. The statistical analysis suggests that the 0.20 value of pv-SC is significantly smaller than the 0.49 value of the control ($p < 0.01$). The results suggest that the pv-SC is less rigid of the structure than that of the control SC, indicating irregular architecture of pv-SC. Therefore, the present EPR results can be useful for analyses of various SC.

References

[1] Nakagawa K., Minakawa S., and Sawamura D., *J. Dermatological Science*, **2012**, 65, 222-224.

[2] Nakagawa K., Ohba Y., Epel B., and Hirata H., *J. Oleo Science*, **2012**, 61, 451-456.

[3] Nakagawa K., Minakawa S., and Sawamura D., *Appl. Magn. Reson.*, **2013**,44, 941-948.

[4] Nakagawa K., Minakawa S., and Sawamura D., *Skin Research and Technology*, **2013**, 19, 450-453.

P-2

Localization of EPR probes and labeled drugs in nanocarriers and their penetration and release in skin

SB Lohan,[1] N Icken,[1] C Teutloff,[2] R Bittl,[2] J Lademann,[1] E Fleige,[3] M Unbehauen,[3] R Haag,[3] SF Haag,[1] MC Meinke[1]

[1]*Charité-Universitätsmedizin Berlin, Department of Dermatology, Center of Experimental and Applied Cutaneous Physiology, Berlin, Germany*
[2]*Freie Universität Berlin, Fachbereich Physik, Berlin, Germany*
[3]*Freie Universität Berlin, Institut für Chemie und Biochemie, Berlin, Germany*

E-mail: silke.lohan@charite.de

The successful inclusion of active substances into nanocarriers, their penetration into the skin and the release of the drugs at the target sites are essential for effective local therapy approaches. The skin is easily accessible, the transport distances are short and the release of active compounds from the nanocarriers can be triggered by internal and external parameters. The exterior layer of the skin (horny layer, *stratum corneum*) has a distinctive barrier function that protects against environmental influences [1]. As the drugs implemented in the topical treatment of inflammatory skin diseases are usually strongly lipophilic, their penetration into the skin may be impeded. Several techniques and carrier systems are currently being developed to improve the penetration of such active ingredients into the skin, whereby research is focused on the use of promoting solvents and nano transport systems (NTS). Polymer-based carrier systems such as dendric core-multishell (CMS) NTS and nanogels are particularly promising. These organic substances are soluble in water enable the transport of a multitude of different drugs. The application of EPR spectroscopy could show that within the CMS, hydrophilic substances can be localized in the hydrophilic outer shell while lipophilic drugs can be found in the nonpolar inner shell [1, 2].
Multi frequency EPR spectroscopy (W, Q, X band) in combination with 2D-imaging was applied to investigate the localization of the drugs within the carrier, the penetration properties of the carrier and the release of the drug [1, 2].
Stearic acid is often used as an additive in skin creams and oils but its strong hydrophobic character impedes its penetration into the skin. Analysis of CMS NTS, loaded with the spin probe 5-doxyl stearic acid (5DSA), revealed an indication of its localization and mobility within the hydrophobic inner shell of the CMS NTS [3] as well as its release characteristics. Another active substance, dexamethasone, a synthetic member of the glucocorticoid class of steroid drugs with anti-inflammatory and immunosuppressive effects, could be labeled covalently with PCA and was analyzed in regard to its penetration and depot properties when it was loaded into CMS or into thermoresponsive nanogels.
EPR analyses in combination with 2D-imaging provided important information about the localization and release of the active compounds, which is of high value for the optimization of the treatment regimens for inflammatory skin disorders using drug-loaded nanocarrier systems. The work has been partly supported by the collaborative research center 1112, Project B01 of the DFG.

References

[1] Haag SF, Fleige E, Chen M, Fahr A, Teutloff C, Bittl R, Lademann J, Schafer-Korting M, Haag R, Meinke MC: Skin penetration enhancement of core-multishell nanotransporters and invasomes measured by electron paramagnetic resonance spectroscopy. Int J Pharm 2011;416:223-228
[2] Haag SF, Chen M, Peters D, Keck CM, Taskoparan B, Fahr A, Teutloff C, Bittl R, Lademann J, Schafer-Korting M, Meinke MC: Nanostructured lipid carriers as nitroxide depot system measured by electron paramagnetic resonance spectroscopy. Int J Pharm 2011;421:364-369.
[3] Lohan, S, Icken, N, Teutloff, C, Bittl, R, Lademann, J, Fleige E, Haag R, Meinke MC Haag, SF, Investigation of the penetration properties of stearic acid into the skin via „dendritic core-multi-shell“ (CMS) nanocarriers, in preparation

P-3

EPR studies of the conformational states of Aurora-A kinase's activation loop

Maria Grazia Concilio[1], Alistair J Fielding[1]

[1]*Photon Science Institute, University of Manchester, Oxford road, Manchester M13 9PY, United Kingdom.*

E-mail:mariagrazia.concilio@postgrad.manchester.ac.uk

It is well-established that the activity of Aurora-A kinase protein is regulated by conformational transitions of its activation loop. [1] CW EPR studies provided evidences that the activation loop is engaged in different conformational states characterized by different dynamic properties. Prediction of the conformational distribution, based on rotamer library approach for spin label [2], revealed two different environments surrounding the label (Figure 1, A). We assumed a two-state equilibrium between conformations located in the water-exposed region (Figure 1, A, blue circle) and conformations located in the constrained region (Figure 1, A, red circle). The theoretical simulations of the EPR spectra helped to characterize the dynamics of rotational motions of the two conformational states [3] and obtain the fractions of the two conformations. Simulated EPR spectra were added to fit experimental EPR data (Figure 1, B).

The temperature effect on the conformational equilibrium was studied, measuring EPR spectra at different temperature. Data obtained showed an increase of the population of the states characterized by fast motion and a decrease of the population of the state characterized by slow motion, increasing temperature. The equilibrium between the two conformations was restored after decreasing temperature. These studies can shed light on the structure-function relationship of Aurora-A in order to develop Aurora-A inhibitors.

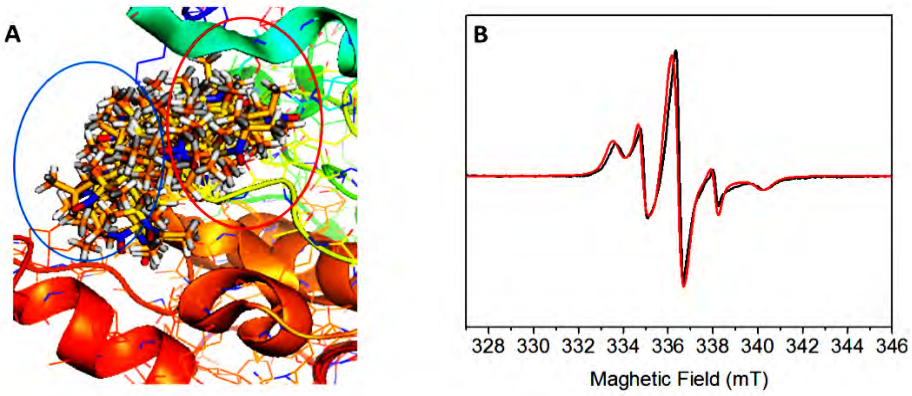

Figure 1: (A) Predicted conformational distribution, (B) Fitting of the simulated EPR data (red trace) to the experimental EPR data (black trace), measured at room temperature.

This work is supported by a studentship from Bruker Ltd. and the authors gratefully acknowledge Dr. Richard Bayliss and Dr. Selena Burgess (Department of Biochemistry, University of Leicester, United Kingdom) for providing the Aurora-A kinase protein.

[1] Rowan F. C., Richards M., Bibby R. A., Thompson A., Bayliss R. and Blagg, J. In-sights into Aurora-A kinase activation using unnatural amino acids incorporated by chemical modification. *ACS Chem. Biol.* 2013, 8, 2184-2191.

[2] Polyhach, Y.; Bordignon, E.; Jeschke, G. Phys Chem Chem Phys. 2011, 13, 2356.

[3] Liang Z. and Freed, J. H. An Assessment of the Applicability of Multifrequency ESR to Study the Complex Dynamics of Biomolecules. *J. Phys. Chem. B.* 1999, 103, 6384-6396.

P-4

The Cu^{2+} coordination environment of α-synuclein revealed by site-specific isotopic labeling of 56-residue N-terminal peptides

Simon C. Drew[1]

[1]*Florey Department of Neuroscience and Mental Health, The University of Melbourne, Victoria 3010, Australia*

E-mail: sdrew@unimelb.edu.au

Aggregation of the presynaptic protein α-synuclein (αSyn) is implicated in the pathogenesis of Parkinson's disease. Physiological concentrations of copper can accelerate the rate of αSyn aggregation *in vitro* and extracellular αSyn aggregates are toxic to neuronal cells. Our previous studies utilised X-band CW and pulsed EPR spectroscopy of recombinant full length αSyn(1–140) to proposed the existence of two coordination modes in equilibrium at pH 7.4, with their coordination spheres comprising $\{NH_2^{M1}, N^{-\,D2}, COO^{-\,D2}, H_2O\}$ (mode 1) and $\{NH_2^{M1}, N^{-\,D2}, COO^{-\,D2}, N_{Im}^{H50}\}$ (mode 2) [1,2] .

Since then numerous studies have proposed a single high affinity coordination mode ion the presence of single equivalent of Cu^{2+} with disagreement as to the role of the amino nitrogen of Met1 and His50 and discounting of the role of pH-dependent equilibrium on the results [3–9].

The present work will present detailed studies of a synthetic αSyn(1–56) peptide, which contains all of the required residues for high affinity Cu^{2+} binding. A combination of site-specific isotopic labelling and multifrequency CW/pulsed EPR spectroscopy will be used to demonstrate the validity of the original proposed coordination modes and their consistency with many of the recent findings.

References

[1] Drew S.C., Leong S.L., Pham C.L.L., Tew D.J., Masters C.L., Miles L.A., Cappai R., Barnham K.J. "Cu^{2+} Binding Modes of Recombinant α-Synuclein – Insights from EPR Spectroscopy", *J. Am. Chem. Soc.* **2008**, 130, 7766–7773.

[2] Copper Coordination by Familial Mutants of Parkinson's Disease-Associated *a*-Synuclein

[3] Drew S.C., Tew D.J., Masters C.L., Cappai R., Barnham K.J. "Copper Coordination by Familial Mutants of Parkinson's Disease-Associated α-Synuclein", *Appl. Magn. Reson.* **2009**, 36, 223–229.

[4] Bortolus M., Bisaglia M., Zoleo A., Fittipaldi M.,Benfatto M., Bubacco L., Maniero A.L. "Structural Characterization of a High Affinity Mononuclear Site in the Copper(II)-α-Synuclein Complex", *J. Am. Chem. Soc.* **2010**, 132, 18057–18066.

[5] Binolfi A1, Rodriguez EE, Valensin D, D'Amelio N, Ippoliti E, Obal G, Duran R, Magistrato A, Pritsch O, Zweckstetter M, Valensin G, Carloni P, Quintanar L, Griesinger C, Fernández CO. "Bioinorganic chemistry of Parkinson's disease: structural determinants for the copper-mediated amyloid formation of alpha-synuclein", *Inorg. Chem.* **2010**, 49, 10668–10679.

[6] Dudzik C.G., Walter E.D., Millhauser G.L. "Coordination Features and Affinity of the Cu^{2+} Site in the α-Synuclein Protein of Parkinson's Disease", *Biochemistry* **2011**, 50, 1771–1777.

[7] Rose F., Hodak M., Miroslav B., Jerzy T.I. "Mechanism of copper(II)-induced misfolding of Parkinson's disease protein , *Scientific Reports* **2011**, 1:11, doi:10.1038/srep00011.

[8] Ahmad A., Burns C.S., Fink A.L., Uversky V.N. "Peculiarities of Copper binding to α-Synuclein", *J. Biomol. Struct. Dyn.* **2012**, 29, 825–842.

[9] Moriarty G.M., Minetti C.A. S. A., Remeta D.P., Baum J. "A Revised Picture of the Cu(II)−α-Synuclein Complex: The Role of N-terminal Acetylation ", *Biochemistry* **2014**, 53, 2815−2817.

P-5

Investigation of Glass Surface Coating for *In-situ* Electron Paramagnetic Resonance Measurement of Reactive Oxygen Species in Adherent Cells

Takahiro Ando[1] and Yoshiki Yonamoto[1]

[1]*Hitachi, Ltd., Yokohama Research Laboratory, 292 Yoshida-cho, Totsuka-ku, Yokohama, Kanagawa, Japan*

E-mail: takahiro.ando.dc@hitachi.com

Since a lot of worldwide attention has focused on cell-based regenerative medicine for the treatment of chronic diseases and for repairing lost tissue and organs, there has been increased interest in the diagnosis of cellular functions. There are currently over 450 regenerative medicine products on the market focused on diverse therapeutic areas, but the diagnosis technologies for fully guaranteeing the safety of biological products including stem cells have not yet been established [1].

An increase in reactive oxygen species (ROS) has long been known as an indicator of inflammatory diseases and cancers. The electron paramagnetic resonance (EPR) method has been recognized as one of the most powerful techniques for directly measuring the ROS in biological cells. The sample holders used in EPR measurements are generally created using quartz glass to avoid the dielectric loss, but living cells cannot easily adhere to naked glass surfaces. Thus, it is standard practice to use the cell suspension after detachment and a thin quartz tube to measure the metabolic products in the cells using an EPR device. In the present study, glass surface coatings were investigated to improve the adhesion efficiency of biological cells in order to create a way to take *in-situ* EPR measurements of ROS in adherent cells.

Mouse fibroblasts (NIH3T3) and human malignant epithelial cells (HeLa) were used. After quartz glass sheets (10 mm×10 mm, t= 0.5 mm) were dry-heat sterilized, the glass surface was treated with collagen, gelatin, fibronectin, or polylysine. Some of the glass sheets were put in a commercially available plastic dish, and then the cell suspension (1×10^5 cells per dish) and culture medium were added into the dish. After incubation at 37°C in a 5% CO_2 atmosphere, the cell density on the dish bottom and the glass surfaces were estimated by counting the number of attached cells.

Figure 1 shows the effects of the surface coating on the adhesion of (a) NIH3T3 and (b) HeLa cells incubated for 24h and 48h. The number of adherent cells on a non-coated glass sheet 24h after seeding decreased to 45% in NIH3T3 and 39% in the HeLa cells as compared with those on a commercially available culture dish. On the other hand, there was a statistically significant increase in the adhesion efficiency for the 24h and 48h post-seeding on a glass surface treated with polylysine relative to those without and with the other coatings, regardless of the cell types used. The cell viabilities were greater than 90%. Moreover, successful cell adhesion was achieved on the surface of a commercially available EPR tube with the polylysine coating.

These findings would be useful for the *in-situ* EPR measurement of the ROS in adherent cells when attempting to determine the precise details of the redox dynamics in cell-based regenerative medicine. In this presentation, our recent developments made using the *in-situ* EPR measurement technique will also be given.

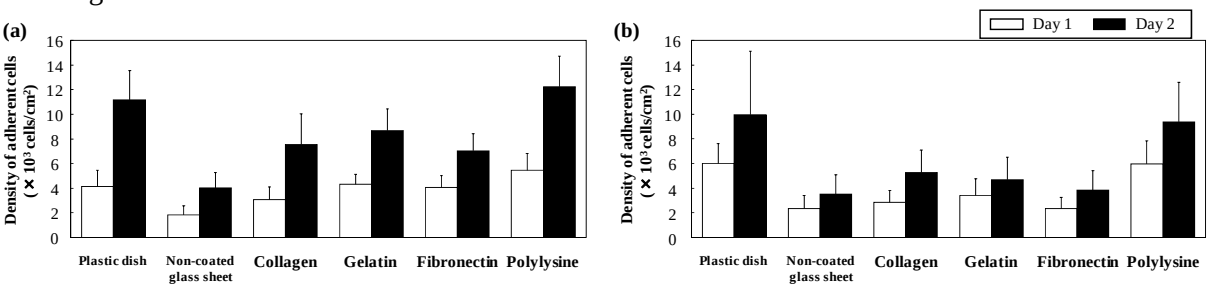

Fig. 1 Effect of surface coating on adhesion of (a) NIH3T3 and (b) HeLa cells (n= 16).

[1] Guthrie K., Bruce A., Sangha N., Rivera E. and Basu J., "Potency evaluation of tissue engineered and regenerative medicine products", *Trends Biotechnol.* **2013**, 31, 505-514.

P-6

Competitive binding of metal ions to the octarepeat region of human prion protein

Masahiro Yagi, Kazuya Iwama, Haruto Onda and Wakako Hiraoka

Graduate School of Science and Technology, Meiji University, Kanagawa 214-8571, Japan

E-mail: hiraoka@isc.meiji.ac.jp

Background. The misfolded form of the prion protein (PrP) causes neurodegenerative diseases. It is believed that the binding of PrP to metal ions results in the misfolding of PrP [1]. The octarepeat in the N-terminal region of PrP constitutes a primary site for Cu^{2+} uptake. To elucidate the process of misfolding and subsequent aggregation, we investigated the structure and stability of the octarepeat peptide of human PrP binding to Cu^{2+}.

Materials and Methods. An eight-regidue octapeptide (PHGGGWGQ) was used for the spectroscopic assay of affinity for metal ions (Cu^{2+}, Ni^{2+}, Co^{2+}, Zn^{2+}, and Mn^{2+}). For electron spin resonance (ESR), the sample was prepared as 0.1 mM octapeptide and 0.1 mM Cu^{2+} in 10 mM HEPES buffer (pH 7.6) containing 30% glycerol. The ESR spectrum was acquired at 20 K. For circular dichroism (CD), the sample was prepared as 0.8 mM octapeptide and 0.8 mM Cu^{2+}in 15 mM HEPES buffer. To verify competitive metal binding, the sample was titirated with other divalent metal ions such as Ni^{2+}, Co^{2+}, Zn^{2+}, and Mn^{2+}.

Result. The ESR of octapeptide-Cu^{2+} yielded a spectrum consisting of hyperfine coupling constants A_1 and A_2. The result indicated two types of coordination modes for the binding of octapeptide-Cu^{2+} (Figure 1). The CD spectrum of octapepide-Cu^{2+} at visible wavelengths showed the characteristic absorbance assigned to Cu^{2+} coordination complexes [2]. Titration with divalent metal ions, such as Ni^{2+}, Co^{2+}, Zn^{2+}, and Mn^{2+}, reduced the molecular ellipticity (θ) of octapeptide-Cu^{2+} (Figure 2).

Conclusion. These results suggest that the binding process of octapeptide-Cu^{2+} is reversible and that other divalent metal ions can partially substitute for Cu^{2+}. The present study indicates that the structure of PrP-Cu^{2+} is possibly affected by the presence of other metal ions.

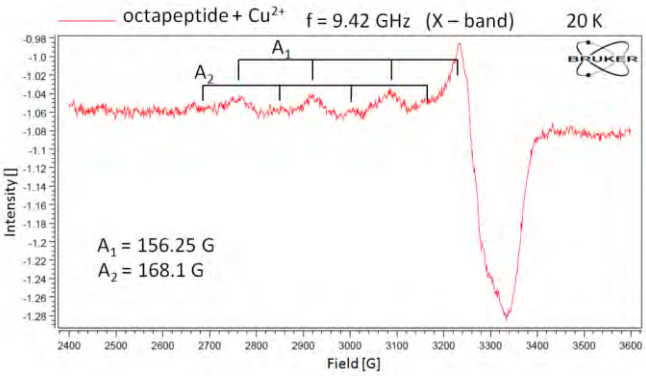

Figure 1. ESR spectrum of octapeptide-Cu^{2+}.

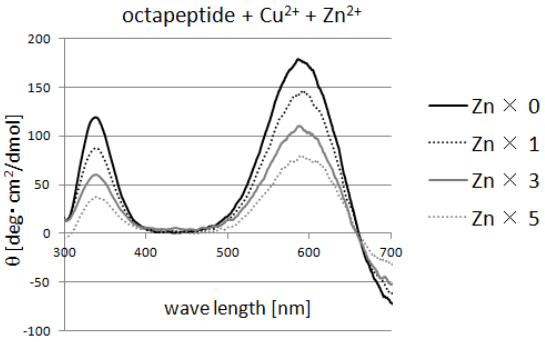

Figure 2. CD spectra of octapeptide-Cu^{2+} titrated with Zn^{2+}.

References.

[1] Singh N., Das D., Singh A. and Mohan M. L., "Prion protein and metal interaction : physiological and pathological implications", *Curr Issues MoL Biol* **2010**, 12(2), 99-107.

[2] Viles J. H., Cohen F. E., Prusiner S. B., Goodin D. B., Wright P. E. and Dyson H. J., "Copper binding to the prion protein: structural implications of four identical cooperative binding sites", *Proc Natl Acad Sci USA* **1999**, 96(5), 2042-2047.

P-7

ESR Spectroscopy on Metal binding Sites in Cu^{2+}-Transporting ATPase Protein

Satoshi Yasuda[1], Takuya Horimoto[1], Hiroaki Daimon[1] ,Yasuhiro Ueda,[1]
Naoyuki Kuwabara,[3] and Toshiaki Arata[1,2]

[1]*Dept. Biol. Sci., and* [2]*Ctr. High Mag, Field Sci., Grad. Sch. Sci., Osaka Univ., Osaka, Japan*
[3]*Photon Factory, KEK, Tsukuba Japan*

E-mail: arata@bio.sci.osaka-u.ac.jp; tetutomo@bio.sci.osaka-u.ac.jp

It is a central problem of biological active pumps how P-type ATPases utilize the energy generated by ATP hydrolysis to drive ion transport across the membrane. All cells have sodium potassium pump ATPase, a member of P-type ATPases, in plasma membrane to maintain ionic conditions inside a cell. Calcium pump ATPase (SERCA) is also studied extensively [1]. The Cu^{2+}-selective CopB (TTHA1733) from thermophilic bacteria (*Thermus thermophiles)* has been investigated to explore the coordination chemistry of the transition metal binding sites in P-typeATPases and to determine the location and pathway of metal, and protein conformational changes. Electron spin resonance (ESR) studies indicate that more than ten Type-2-like Cu^{2+} ions are bound to an ATPase molecule. When 2 moles of Cu^{2+} ions was added to ATPase, the ESR spectra showed the presence of a high-affinity transmembrane Type-2-like Cu^{2+} center in which cupric ions are coordinated in a distorted square pyramidal geometry with nitrogen ligands. When 3-10 moles of Cu^{2+} ions were added, distinct g-value and hyperfine coupling were observed, suggesting the presence of different binding Type-2-like Cu^{2+} centers at low affinity heavy metal binding sites. By using the preparation frozen immediately after ATP addition, ESR studies on Cu^{2+} ion transporting state during ATP hydrolysis are now in progress. Distance measurements between metal and spin label will be also performed to explore the location and pathway of metal, and the protein conformational changes.

[1] Narumi, R., Yamamoto, T., Inoue, A., Arata, T. *FEBS Lett.* **2012,** *586, 3172-3178.*

P-8

Catecholase Activity of a Distant Dicopper Complex and Photodissociation of Ru(III) Nitrosyl Complex: Monitoring by Electron Paramagnetic Resonace

Shuranjan Sarkar, Jamghoon Cho, and Hong-In Lee

Department of Chemistry, Kyungpook National University, Daegu 702-701, Republic of Korea

E-mail: leehi@knu.ac.kr

Multicopper enzymes containing more than one copper ion in their active sites are widely utilized in nature for transporting copper ions, transferring electrons, activating dioxygen molecules, and catalyzing many other reactions. One of the ways to understand the nature of the enzymes is the construction and characterization of model compounds. Recent development of metal-assisted self-assembly has made enormous success in mimicking the multicopper enzymes. In this study, we have synthesized a Schiff-base ligand containing two N-, O-donor groups linked by a spacer. By controlling the length and rigidity of the spacer, we could successfully build a dicopper complex (Cu_2L_2 = bis{*N,N'*-(ethane-1,2-diyldi-*o*-phenylene)-bis(pyridine-2-carboxamido)copper(II)}. Single crystal X-ray crystallography of Cu_2L_2 revealed that the copper sites are distant, however, the complexes showed unexpectedly-high catecholase activity when Cu_2L_2 was treated with 3,5-di-tertbutylcatechol (3,5-DTBC) in the presence of air at basic condition, In this poster, we present electron paramagnetic resonance (EPR) measurements performed during the time course of the oxidation of 3,5-DTBC by Cu_2L_2 to explore the reaction pathway of the catalytic action.

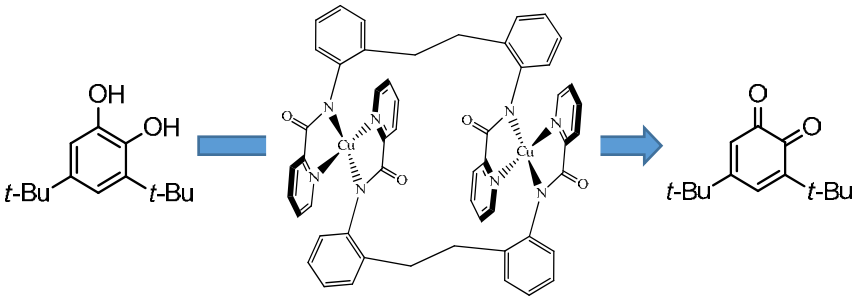

Since the discovery of Nitric Oxide (NO) as one of the major signal-transduction molecules in cells, there have been many attempts to devise acute NO-delivering systems for the purpose of developing disease therapies as well as studying cell functions. Metal-nitrosyl complexes are often releasing NO by light activation. This ability can be adapted to killing cancer cells with high specificity because high concentration of NO in cells induces apoptosis. Ru-NO complexes have been studied for the usages of these photodynamic therapy (PDT) agents for a time. We have developed a new Ru-nitrosyl bis-pyridyl/biscarboxamide compound, [Ru(ebpp)(Cl)(NO)], where H_2ebpp = N,N'-(ethylene di-*p*-phenylene)bis(pyridine-2-carboxamide), to be tested as a model NO-releasing agent. The crystallographic analysis of the complex revealed that the ebpp ligand and its derivative ligands are tetradentately bound to Ru and the remaining two cis sites of the octahedral geometry are occupied by NO and Cl^-. In this poster, we present UV-VIS and EPR data which can be interpreted as that the diamagnetic $[Ru\text{-}NO]^6$ electronic state of the complex becomes low-spin Ru(III) (d^5, S=1/2) state upon losing NO by photoactivation.

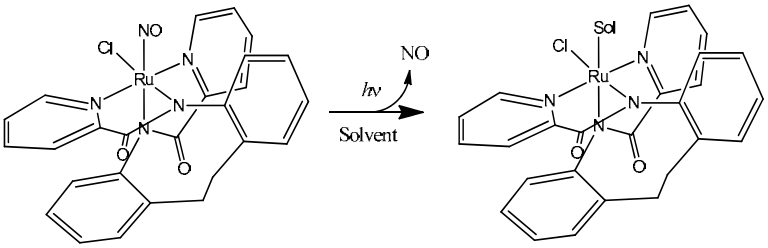

P-9

Multi-frequency, Multi-technique Pulsed EPR Characterization of the Copper-Amyloid Peptides Relevant to Alzheimer's Disease

Sun Hee Kim[1]

[1]*Western Seoul Center, Korea Basic Science Institute, Seoul 120-140, Korea*

E-mail: shkim7@kbsi.re.kr

Due to growing evidence that copper ions play an important role in Alzheimer's disease pathogenesis by an oxidative stress pathway, exploration of the coordination environment of copper ion has been a main theme in this research area. Also the elucidation of the structural details of the copper coordination environment is essential in understanding the molecular mechanisms of amyloid fibrilization. Thus, to characterize the copper coordination mode of amyloid peptide, we employed multi-frequency, multi-technique pulsed EPR. This includes 34 GHz ENDOR (Electron Nuclear Double Resonance), 9 GHz HYSCORE (Hyperfine Sublevel Correlation) and ESEEM (Electron Spin Echo Envelope Modulation) techniques along with various isotopic labelings. The detailed structure of the copper amyloid peptides will be presented.

P-10

Effects of Nanoscale Curvature on Structure, Dynamics, Phase Properties and Surface Electrostatics of Lipid Bilayers

Alex I. Smirnov, Amir Koolivand, Antonin Marek, and Maxim A. Voinov

Department of Chemistry, North Carolina State University, Raleigh, North Carolina, 27695-8204, USA

E-mail: Alex_Smirnov@ncsu.edu

A number of membrane-anchored and membrane-associated proteins are known to be capable of sensing local lipid bilayer curvature. Highly curved lipid bilayers and small vesicles are thought to be involved in such important cellular processes as membrane fusion, endo- and exocytosis, and tubules' formation. While the significance of membrane curvature in cellular regulatory processes is emerging, limited biophysical data for highly curved lipid bilayers can be found in the literature.

Here we summarize the results of spin-probe/spin-labeling multifrequency EPR studies together with solid state NMR and DSC of unilamellar vesicles (SUV) with average diameter ranging from 200 to 30 nm and compare those with tubular bilayers formed inside ceramic nanopores of similar diameters. Analysis of DSC data at multiple scan rates has revealed broadening and shifts of the main phase transition of DMPC. This indicates bilayer compression and an increase in local order parameter – phenomena that are revealed by EPR and oxygen accessibility measurements. The surface electrostatics of lipid vesicles was assessed by EPR of a recently introduced phospholipid (IMTSL-PTE) bearing a pH-sensitive nitroxide covalently attached to the lipid head group [1]. The magnitude of the negative surface electrostatic potential, Ψ, for POPG increased from -137 to -167 mV upon decrease in the vesicle diameter from ca. 110 to 30 nm even though zeta-potentials were nearly identical. This effect could be again rationalized by an increase in lipid packing upon an increase in curvature for the bilayer in fluid phase. However, the effect vanished for the gel phase.

These finding could be rationalized by proposing that highly curved vesicles in the fluid bilayer phase consist of small ordered lipid patches because the bilayer cannot any longer accommodate the hydrophobic forces by continuous rearranging phospholipids. This leads to formation of additional defects in highly curved bilayers that relief the bending stress and provides condition for better local packing of phospholipids. This hypothesis was corroborated by High Field (95 GHz) EPR data on partitioning small molecules and HYSCORE experiments on water penetration into the bilayer. Overall, changes in surface electrostatic could be responsible for preferable binding of some membrane proteins to curved lipid bilayer surfaces.

Supported by U.S. DOE Contract DE-FG02-02ER15354.

References

[1] Maxim A. Voinov, Izarys Rivera, Alex I. Smirnov, "Surface Electrostatics of Anionic Bilayers of Mixed Lipid Composition by EPR of a pH-Sensitive Spin-Labeled Lipid", *Biophysical J.*, **2013**, 104, 106-116.

P-11

ESR Study by High School Students (1) Evaluation of Ultraviolet (UV)-Protection Properties of Sun Protection Cosmetics

Hiroki Nakajima[1], Mai Okahashi[1], Yuki Shimizu[1], Atsushi Kajiwara[2]
[1]*Tezukayama Senior High School, Nara 631-0034, Japan*
[2]*Department of Materials Science, Nara University of Education, Nara 630-8528, Japan*

E-mail: h-nakajima@tezukayama-h.ed.jp

Introduction

Evaluation of ultraviolet (UV)-protection properties of sun protection cosmetics has been conducted using electron spin resonance (ESR) spectroscopy by high school students as a joint project on scientific education between high school and university. The school students have much interest on sun protections especially at physical education and extracurricular activities at outdoors. These students were anxious to know the UV-protection properties of the sun-protection cosmetics for protecting their skin from suntan. ESR detection of radicals from photo-initiators of polymerizations under irradiation through sun-protection cosmetics provided information on their efficiency. Results from the measurements would provide a deeper understanding of chemistry and cosmetics to the high-school students.

Result and Discussion

2, 2'-Azobisisobutyronitrile (AIBN) is a typical initiator for radical polymerizations. It is cleaved homolytically upon heating or under irradiation of UV-light to form two equivalent isobutyronitrile radicals. Stronger light generates larger amount of radicals. By using these properties, photo degradation of AIBN was used for evaluation of properties of sun protection cosmetics.

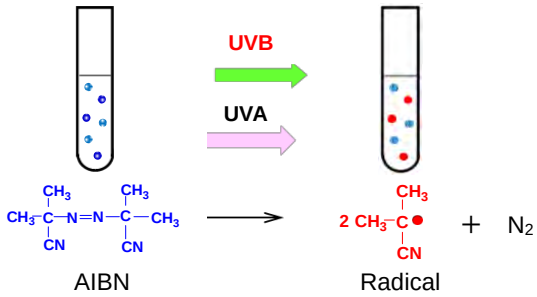

Figure 1 Schematic image of radical generation along with its chemical equation.

The UV protection effect of sun protection cosmetics are classified by the two factors i.e. SPF (Sun Protection Factor) and PA (Protection Grade of UVA). Without any sun-protectors, isobutyronitrile radicals can be observed clearly (Fig. 2 upper). When a sun protection cream put on the surface of a sample cell just like putting on skins, UV-irradiation was inhibited and intensities of the signals turned to weaker according to the SPF (Fig. 2 bottom and Fig. 3). In the case of SPF50, considerable suppression of generation of the radicals was observed.

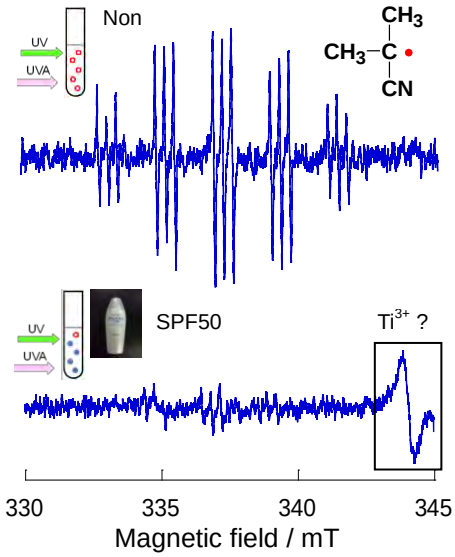

Figure 2 ESR spectra of isobutyronitrile radicals through a sunscreen cream

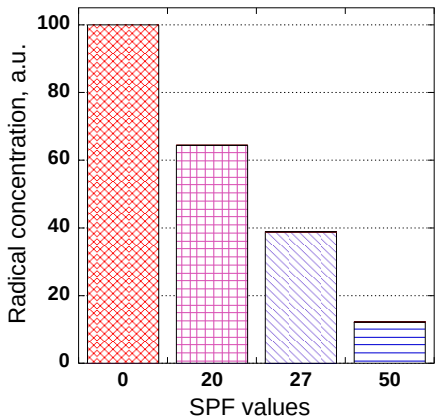

Figure 3 Relative intensities of ESR signals of isobutyronitorile radicals

Acknowledgment

This work was partly supported by JSPS KAKENHI Grant Number 26915003.

References

[1] Nakajima H., *Chemistry & Education* 2013, 60(4), 160-161.
[2] Kajiwara A., Nakajima H., *Chemistry & Education* 2008, 55(12), 620-623.

P-12

ESR Study by High School Students (2)
Detection of Paramagnetic Species in the Familiar Foods by ESR

Hiroki Nakajima[1], Rina Aoi[1], Asuka Itakura[1], Yuma Tanaka[1], Atsushi Kajiwara[2]
[1]*Tezukayama Senior High School, Nara 631-0034, Japan*
[2]*Department of Materials Science, Nara University of Education, Nara 630-8528, Japan*

E-mail: h-nakajima@tezukayama-h.ed.jp

Introduction

High school students investigated various kinds of familiar foods under various conditions by electron spin resonance (ESR) spectroscopy. For example, seafood (shrimp, squid, clam, etc.) and processed foods (chocolates, supplement, etc.), and seeds (sesame, white radish seeds, almond etc.) were investigated. ESR spectra of chocolates showed organic radicals. On the other hand, several kinds of paramagnetic metal ions and organic radicals were detected from white radish sprouts. ESR results of the measurements of the foods would be scientific teaching materials for high-school students.

Experiment of Section

Various kinds of commercially available chocolates from various companies were used. Finely shredded chocolate samples (ca. 20 mg) put into a sample cell (o.d. 5 mm) and measured at various temperatures.

White radish seeds can germinate by the presence of water. Sprouts were grown from the white radish seeds by distilled water and sunlight only. When it grew to 5 cm long, the seed skin, roots, stems, and leaves were separated and measurement.

Result and Discussion

Chocolates: Three kinds of chocolates, “bitter”, “milk”, and “white”, were measured. ESR spectra of these chocolates showed different features. Both bitter and milk chocolates showed signals due to organic radicals (Fig. 1 upper). On the other hand, very weak or no signal was observed in white chocolate (Fig. 1 bottom).

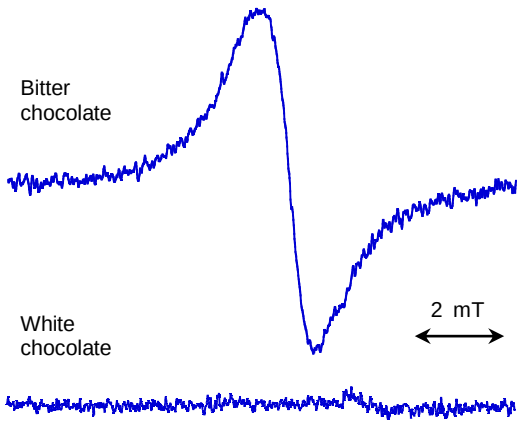

Figure 1 ESR spectra of organic radicals through various chocolates

White radish seeds: ESR spectra of each part of the radish sprouts are shown in Figure 2. In the spectrum of radish seed (before germination), Mn^{2+} ion and metal ion with g = 4.2 (Fe^{3+}?) along with sharp organic radical signal were clearly observed. After germination, Mn^{2+} signals appeared in both leaves and seed skins. Most of organic radical signals were observed in leaves.

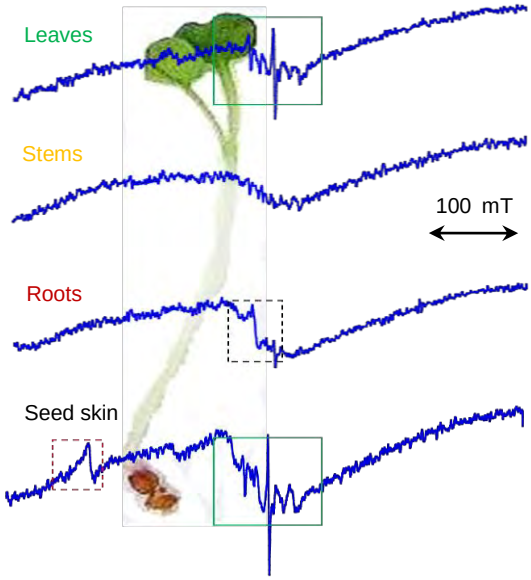

Figure 2 ESR spectra of each part of white radish seeds

Through these education programs, high school students would have much interest about the relationship between science and daily life. Hopefully, they would be a scientist to conduct further investigations in the near future.

Acknowledgment

This work was partly supported by JSPS KAKE NHI Grant Number 26915003.

References

[1] Nakajima H., *Chemistry & Education* 2013, 60(4), 160-161.
[2] Kajiwara A., Nakajima H., *Chemistry & Education* 2008, 55(12), 620-623.

P-13

ESR Study by High School Students (3)
Detection of Paramagnetic Species in the Insects by ESR

Hiroki Nakajima[1], Wakana Kakuo[1], Yuumi Mabuchi[1], Atsushi Kajiwara[2]
[1]*Tezukayama Senior High School, Nara 631-0034, Japan*
[2]*Department of Materials Science, Nara University of Education, Nara 630-8528, Japan*

E-mail: h-nakajima@tezukayama-h.ed.jp

Introduction

ESR study of paramagnetic species in insects has been conducted. This is a part of joint program for scientific education between high-school and university. It is well known that some kinds of insects, birds, fishes and bacteria show magnetotactic nature. ESR has a possibility to detect magnetoactive species from these biological systems. Furthermore, there are trace amounts of essential metal ions in biological systems. Some of these metals can be detected by ESR spectroscopy and the results would be scientific education materials at high-school especially in chemistry class.

Result and Discussion

High-school students measured ESR spectra of honey bee itself. Honey bee showed some ESR signals may be due to ferric oxide (Fe_2O_3) or other metal ions at g = 4.2 and g = 2.0 as shown in Fig.1a. Several kinds of bees like a humble-bee, a hornet, and a giant hornet were measured by ESR for comparison with that of honey bee (Fig.1b, c, and d). Then, a black ant was measured. ESR signal due to Mn^{2+} was clearly observed as shown Fig.2. A bee and an ant is a closely-related species and they showed different feature in ESR spectra.

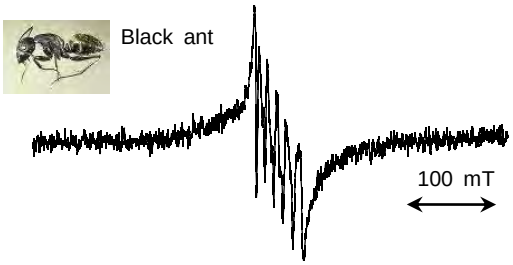

Figure 2 ESR spectrum of a black ant

Through these education programs, high school students would have much interest about the relationship between science and nature. Hopefully, they would be a scientist to conduct further investigations in the near future.

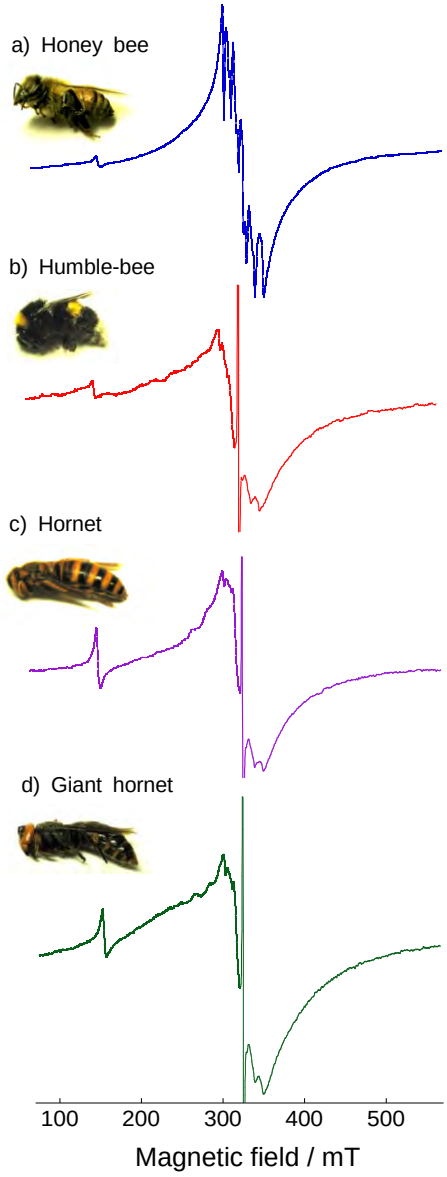

Figure 1 ESR spectra of several kinds of bees

Acknowledgment

This work was partly supported by JSPS KAKENHI Grant Number 26915003.

References

[1] Nakajima H., *Chemistry & Education* 2013, 60(4), 160-161.
[2] Kajiwara A., Nakajima H., *Chemistry & Education* 2008, 55(12), 620-623.

P-14

Nitric oxide mediates TLR4-NF-kB signaling in mice with DSS-induced colitis

Xin Tun[1], Keiji Yasukawa[1,2] and Ken-ichi Yamada[1,3]

[1]*Graduate School of Pharmaceutical Sciences, Kyushu University, Fukuoka 812-8582, Japan*
[2]*Innovation Center for Medical Redox Navigation, Kyushu University, Fukuoka 812-8582, Japan*
[3]*Japan Science and Technology Agency, PRESTO, Saitama 332-0012, Japan*

E-mail: yasukawa@pch.phar.kyushu-u.ac.jp

Ulcerative colitis (UC) is an inflammatory bowel disease characterized by inflammation that occurs selectively at the rectal colon and expands continuously into the large intestine. The number of UC patients in Japan is increasing, but the pathogenesis of the disease is not fully understood. Increases in adhesion molecules in vascular endothelium, and activated neutrophils releasing injurious molecules such as reactive oxygen species, are reportedly associated with the pathogenesis of dextran sodium sulfate (DSS)-induced colitis [1]. Nitric oxide (NO) production derived from inducible NO synthase via activation of nuclear factor kappa B (NF-κB) has been reported [2]. It is also reported that stimulation of Toll-like receptor 4 (TLR4) by lipopolysaccharide can activate NF-κB [3]. In this study, we investigated the involvement of NO production on activation of the TLR4/NF-κB signaling pathway in mice with DSS-induced colitis. The addition of 5% DSS to the drinking water of male ICR mice (4 weeks old; body weight, 18–22 g) resulted in increases in TLR4 protein in colon tissue and NF-κB p65 subunit in the nuclear fraction on day 3, increases in colonic tumor necrosis factor-alpha (TNF-α) on day 4, and P-selectin, intercellular adhesion molecule-1, NO_2^-/NO_3^- and nitrotyrosine in colonic mucosa on day 5. These activated inflammatory mediators and pathology of colitis were completely suppressed by treatment with a NO scavenger, carboxy-PTIO (12 mg/kg/day, s.c.), as well as an iNOS inhibitor (40 mg/kg/day, p.o.), aminoguanidine. Conversely, a NO-releasing compound, NOC-18 (5 mg/kg/day, s.c.), increased TLR4 levels and nuclear translocation of NF-κB p65, and exacerbated mucosal damage induced by DSS challenge. To confirm that NO is really produced in the colon of the DSS-induced colitis mouse, ESR/spin trapping of NO in colon tissue of mice subjected to DSS for 7 days was performed using Fe-$(DTCS)_2$ complex and a NO-releasing compound, NOR-1. When NOR-1 was added to the colon sample, typical triplet ESR spectrum of NO-Fe-$(DTCS)_2$ was observed in both the tap water group and the 7-day DSS group. The increased peak intensity of NO-Fe-$(DTCS)_2$ adduct was significantly suppressed by TLR4 inhibitor VIPER or NF-κB activation inhibitor BMS-345541. These data suggest that increases in TLR4 expression induced by drinking DSS treated water might be directly or indirectly associated with NO overproduction.

References

[1] Yasukawa K., Tokuda H., Tun X., Utsumi H. and Yamada K., "The detrimental effect of nitric oxide on tissue is associated with inflammatory events in the vascular endothelium and neutrophils in mice with dextran sodium sulfate-induced colitis." *Free Radic Res* **2012**, 46, 1427-1436.

[2] Lahde M., Korhonen R. and Moilanen E., "Regulation of nitric oxide production in cultured human T84 intestinal epithelial cells by nuclear factor-kappa B-dependent induction of inducible nitric oxide synthase after exposure to bacterial endotoxin." *Aliment Pharmacol Ther* **2000**, 14, 945-954.

[3] Takeuchi O. and Akira S., "Toll-like receptors; their physiological role and signal transduction system." *Int Immunopharmacol* **2001**, 1, 625-635.

P-15

High-Frequency ESR Measurements of Shallow Doped Si:P at Low Temperatures and Their Extension to Lower Temperatures for High $\mu_B B/k_B T$

K. Morimoto[1], Y. Fujii[2], S. Mitsudo[2], T. Mizusaki[2], H. Kikuchi[1], A. Fukuda[3], A. Matsubara[4], T. Ueno[5], M. Gwak[6], S.G. Lee[6], S. Lee[7], Tadaaki Saito[2] and S. Vasiliev[8]

[1]*Department of Applied Physics, University of Fukui, Fukui 910-8507, Japan*
[2]*Research Center for Development of Far-Infrared Region, Univ. of Fukui, Fukui 910-8507, Japan*
[3]*Department of Physics, Hyogo College of Medicine, Nishinomiya 663-8501, Japan*
[4]*Research Center for Low Temperature and Materials Sciences, Kyoto Univ., Kyoto 606-8501, Japan*
[5]*Graduate School of Medicine, Kyoto University, Kyoto, Kyoto 606-8501, Japan*
[6]*Division of Materials Science, Korea Basic Science Institute (KBSI), 169-148 Gwahak-ro, Yuseong-gu, Daejeon 305-806, Korea*
[7]*Department of Physics, Korea Advanced Institute of Science and Technology, 291 Daehak-ro, Yuseong-gu, Daejeon 305-701, Korea*
[8]*Wihuri Physical Laboratory, Department of Physics and Astronomy, University of Turku, 20014 Turku, Finland*

E-mail: forest.book16@gmail.com

One of the most practical quantum computer designs reported so far is the system consisting of phosphorus (P) atoms in silicon (Si) crystal as proposed by B. Kane [1]. However, experimental demonstration has not been done yet. One of the remaining unknown properties of this device essential for the realization of Kane's model is spin dynamics including dynamic nuclear polarization phenomena at very low temperatures below $T = 0.1$ K and under high magnetic fields above $B = 2$ T. These conditions are required for Kane's model. In order to investigate the feasibility of Kane's model, we have been studying an ensemble of ^{31}P nuclear spins in phosphorous-doped silicon (Si:P) instead of detecting a state of single ^{31}P nuclear spin like in Kane's model. In Si:P, the donor electrons are well localized around the donor ions if the donor concentration is below the critical doping concentration, $n_c = 3.7\times10^{18}$ cm^{-3}, while they are delocalized above n_c. Then, the P atoms in shallow doped Si:P are in the similar environment to those in Kane's model.

We have measured T_1 and T_2 relaxation times of donor electrons in Si:P with the concentration $n = 6.5\times10^{16}$ cm^{-3} with a W-band (94 GHz) pulsed ESR system at KBSI. The spin-lattice relaxation rate $1/T_1$ rapidly decreases with decreasing temperature below 30 K down to approximately 4 K. As lowering the temperature below 4 K, $1/T_1$ decreases nearly proportional to the temperature due to the phonon-direct relaxation mechanism. These behaviors are qualitatively the same as the data extrapolated from X-band ESR data and our previous data from cw-ESR measurements at 80 GHz [2], though the measured values from pulsed ESR are slightly smaller than them.

Because a large value of $\mu_B B/k_B T$ is required for Kane's model in order to quench degree of freedom of electron spins, it is important to study spin dynamics of Si:P in mK region, where μ_B is the Bohr magneton and k_B is the Boltzmann constant. In order to study the spin dynamics of ^{31}P in the mK regime, we are constructing a magnetic resonance system with a ^{3}He/^{4}He dilution refrigerator. We will also present current status of the development of mK ESR and NMR systems.

References

[1] Kane, B.E., "A silicon-based nuclear spin quantum computer" *Nature* **1998**, 393, 133.
[2] Song, M., *et al*., "Spin dynamics of isolated donor electrons in phosphorus-doped silicon from high-frequency electron spin resonance", *J. Phys.: Condens. Matter* **2010**, 22, 206001, and references therein.

P-16

Simultaneous and spectroscopic imaging of free radical intermediates using in vivo dynamic nuclear polarization-MRI

Fuminori Hyodo[1], Shinji Ito[1], Keiji Yasukawa[1,2], Hinako Eto[1], Ryoma Kobayashi[1] and Hideo Utsumi[1]

[1] Innovation Center for Medical Redox Navigation, Kyushu University, 812-8582 Japan
[2] Faculty of Pharmaceutical Sciences, Kyushu University, 812-8582 Japan

E-mail: hyodof@redoxnavi.med.kyushu-u.ac.jp

The in vivo redox reaction plays a central role in living organisms. Mitochondria maintain redox homeostasis via the endogenous molecules such as flavin mononucleotide (FMN), flavin adeninedinucleotide (FAD), and coenzyme Q_{10} (CoQ_{10}), which have flavin or quinone moieties. The obligate one-electron transfer reactions convert FMN, FAD, and CoQ_{10} to the free radical intermediates FMNH and FADH, and $CoQ_{10}H$, respectively. These free radical intermediates, especially $CoQ_{10}H$, produce the superoxide anion radical, which is responsible for various oxidative diseases. The lipophilic vitamin E is a well-known antioxidant against lipid peroxidation in mitochondrial membranes. Vitamin K_1, a fat-soluble derivative of 2-methyl-1,4-naphtoquinone, is a well-known anticoagulant; vitamin K_2 is reportedly involved in redox homeostasis. Both vitamins E and K are converted to free radical intermediates upon oxidation.

In vivo ESR spectroscopy and imaging have revealed how in vivo redox processes are involved in oxidative stress-mediated pathologies, but the spatiotemporal resolution of ESR imaging is much less than that of magnetic resonance imaging (MRI) because of the short T_2 of free radicals. In vivo DNP-MRI, also called proton electron double resonance imaging (PEDRI) or Overhauser-enhanced MRI (OMRI), is a new imaging method for observing free radical species in vivo. Its main advantage is its high spatiotemporal resolution, which rivals that of conventional MRI. Most studies to date have been performed via in vivo DNP-MRI, where obtaining sufficient image intensity requires the use of synthetic stable radicals having simple and narrow resonance lines; nevertheless, these studies have provided unique information regarding redox processes in living animals. However, the ESR spectra of most endogenous free radical intermediates, such as FMNH, FADH, $CoQ_{10}H$, and radicals of vitamin E and K, exhibit multiple hyperfine splitting and inhomogeneous broadening. The imaging of these free radicals has not previously been attempted via in vivo DNP-MRI. If in vivo DNP-MRI offered the possibility of imaging free radical intermediates, it would demonstrate the potential to add metabolic/biochemical information to anatomic images.

Herein, we present a spectroscopic free radical imaging technique using in vivo DNP-MRI, which enables the imaging of multiple free radical intermediates that exhibit multiple hyperfine splitting and broad ESR spectra. DNP-MRI can simultaneously visualize and identify various endogenous free radical intermediates derived from redox transformations.

References

[1] Hyodo F., Ito S., Yasukawa K., Kobayashi R., Utsumi H. "*Simultaneous and spectroscopic redox molecular imaging of multiple free radical intermediates using dynamic nuclear polarization-MRI",* Analytical Chemistry, (2014) in press

P-17

Estimation of relative reaction rate of hydroxy radical with anti-oxidants using ESR spin trapping combined with water radiolysis

Seiko Nakagawa[1] and Masayuki Sekiguchi[1]

[1]*Tokyo Metropolitan Industrial Technology Research Institute, Tokyo 135-0064, Japan*

E-mail: nakagawa.seiko@iri-tokyo.jp

It is known that spin-trapping electron spin resonance (ESR) measurement is one of the techniques to identify the reactive oxygen species (ROS) generated in a biological, medical, and chemical reaction systems. 5,5-Dimethyl-1-pyrroline N-oxide (DMPO) is one of the popular spin traps used in aqueous solutions and some of the rate constants of the scavenging reactions of the ROS including hydroxy radicals have been estimated by the spin-trapping method using DMPO. Photolysis of hydrogen peroxide is often used to produce hydroxy radicals. However, the estimation of the reaction rate of the hydroxy radicals will not be accurate if the competitive scavengers also absorb UV light. In this report, radiolysis of water was employed to generate hydroxy radicals.

The aqueous solutions including DMPO and scavengers were saturated with N_2O gas by bubbling to converse the solvated electrons to hydroxy radicals and flowed. X-ray (YXLON, MG452) irradiation was carried out through a hole with a diameter of 1 cm of Pb-block in front of the flowing sample solution. The voltage and current of X-ray was 450 kV and 10 mA, respectively. The irradiated sample was flowed into a flat-ESR cell. The ESR spectra were recorded by a JEOL FA-200 spectrometer under the following conditions: microwave power of 4 mW, sweep magnetic field of 15 mT, modulation width of 0.3 mT, time constant of 0.03sec, and sweep time of 2 min.

The yield of DMPO-OH decreased with the increasing concentration of scavenger. The reactions of hydroxy radical with DMPO (k_1) and scavenger (k_2) are competition ones. When $[DMPO\text{-}OH]_0$ and $[DMPO\text{-}OH]_t$ refer to the total yield of DMPO-OH in the absence and presence of the scavenger, the relative yield can be written as follows:

$$[DMPO\text{-}OH]_0/[DMPO\text{-}OH]_t \propto 1+k_2[scavenger]/k_1[DMPO]$$

Figure 1 shows the competition plot for p-coumaric acid, mannitol, and thymidine as scavengers. The relative values obtained from the competition plot are listed in Table 1. The relative rates obtained in this study listed in the third column of Table 1are comparable to those of pulse radiolysis studies in the fifth column. The results of some polyphenols will also be discussed.

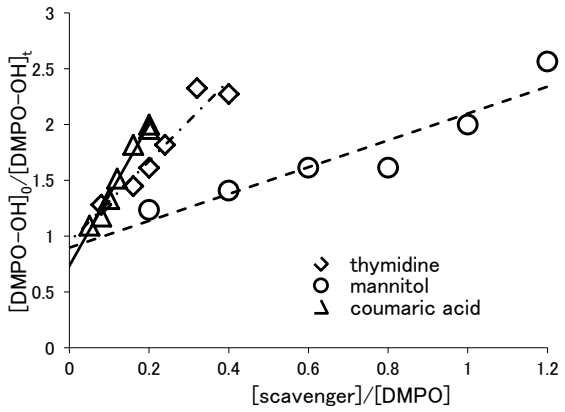

Fig. 1 Competition plot for the reciprocal yield of DMPO-OH

Table 1 Relative rate of the reaction with hydroxy radical

reactant	apparent relative rate constant [a]	relative ratio [b]	rate constant [c] $/10^9 M^{-1}s^{-1}$	relative ratio [d]
p-coumaric acid	6.3	1.00	8.7	1.00
thymidine	3.6	0.57	4.8	0.55
mannitol	1.2	0.19	1.5	0.17

a. The value was obtained as a slope of the competition plot.
b. The apparent rate constant relative to that of p-coumaric acid obtained in this work.
c. The values were obtained by pulse radiolysis. [1)]
d. The rate constant relative to that of p-coumaric acid obtained in the previous studies.

Reference

[1] G. V. Buxton, C. L. Greenstock, W. P. Helman, and A. B. Ross, *J. Phys. Chem. Ref. Data*, **1988**, 17, 513.

P-18

ESR study on thermal metamorphism of kerogen in sedimentary rocks

Mayu Suzuki, Chihiro Yamanaka

Department of Earth and Space Science, Osaka University, Osaka 560-0043, Japan

E-mail:m_suzuki@ess.sci.osaka-u.ac.jp

[Background]
Thermal metamorphism of kerogen which consists of geological organic components is irreversible and applied to a geo-thermometer. Although, vitrinite reflectance, Raman and IR spectroscopy have been used for this purpose, carbon radicals in kerogen, which are produced under thermal cracking process, have a potential to be another unique geological thermometer. Until present, many studies on carbon radicals were accumulated for various coal and oil samples including their pyrolysis experiments. It is known that carbon radicals in kerogen show a broad spectrum at g = 2 by ESR. Bakr et al (1990) reported that the linewidth of ESR spectrum of extracted kerogen decreased as the increase of burial depth[1]. However, such narrowing of ESR spectrum was not observed in laboratory pyrolysis experiments[2][3]. In this research, we have performed isothermal annealing experiments at higher temperature than that previous experiments.

[Sample and Methods]
Asphaltum corrected from Toyokawa oil field in Akita, Japan was used in this study. From this rock, we obtained kerogen by HCl, CsF and HF treatment to remove metal ions and silicates. Atomic H/C in this kerogen was 1.3, which indicated low maturity for this sample. Kerogen samples of 10-30mg were used in ESR experiments. At first, we heated the kerogen samples at 100°C in 10min to remove water under vacuum condition. After that, we performed isothermal annealing experiments under vacuum condition. Heating temperatures of 400, 450, 500, 550, 600°C were selected and each sample was heated for 330 or 390 min. ESR measurements were performed under vacuum condition and at the room temperature with 30-90 min intervals. To study metamorphism in detail, another sample was studied by ESR with heating at 450°C for 110 hours with proper intervals.

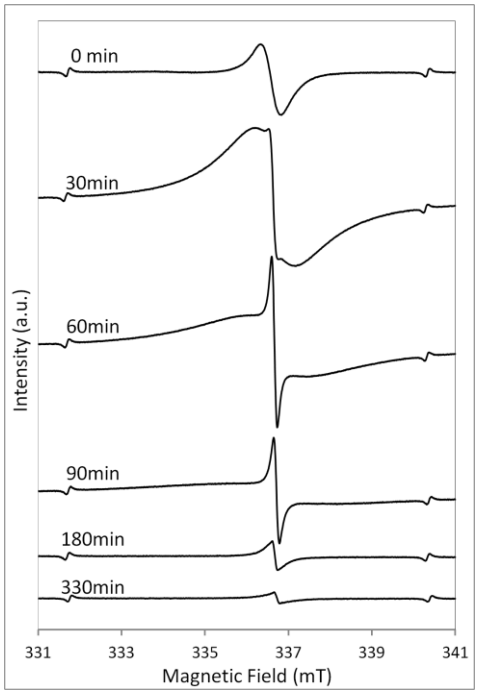

Fig.1. ESR spectra of kerogen extracted from Asphaltum during 600°C heating. (9.45GHz, 1mW, Mod:0.1mT)

[Summary]
Narrowing of ESR spectrum about one-fourth of original was firstly observed for a sample heated at 600°C for 30min (Fig.1.). At 550°C, similar narrow spectrum appeared after 390min. Samples heated at 400-500°C didn't show such narrowing because thermal metamorphism didn't proceeded in experiments. Spin-spin relaxation time for these samples will be discussed.

References

[1] M. Y. Bakr, et al., "ESR assessment of kerogen maturation and its relation with petroleum genesis", *Org. Geochem* **1990**, 15. 595-599.

[2] A. Uesugi and M. Ikeya, "Electron Spin Resonance Measurement of Organic Radical in Petroleum Source Rock Containing Transition Metal Ions", *Jpn. J. Appl. Phys* **2001**, 40, 2251-2254.

[3] N. Qiu, et al., "Temperature and time effects on free radical concentration in organic matter: Evidence from laboratory pyrolysis experimental and geological samples", *Energy Exploration & Exploitation* **2012**, 30, 311-330.

P-19

Radiation-induced Defects in Artificially Weathered Quartz and Relation to the OSL (Optically Stimulated Luminescence) Properties

Chihiro Yamanaka[1], Akira Osada[1] and Masashi Takada[2]

[1]*Department of Earth and Space Science, Osaka University, Osaka 560-0043 Japan*
[2]*Department of Geography, Nara Women's University, Nara 630-8506 Japan*

E-Mail: yamanaka@ess.sci.osaka-u.ac.jp, osada@ess.sci.osaka-u.ac.jp

Optically stimulated luminescence (OSL) using radiation-induced centers has been used for the dating of Quaternary samples. Although the principle is quite similar to that of ESR dating, clear difference exists between them. In OSL dating, luminescence centers easily bleached by light are investigated. Therefore, OSL is used to determine buried ages of samples after resetting OSL signal by exposure to the sunlight. In ESR dating, on the other hand, radiation centers with unpaired electrons are considered. For the ESR centers, usual light bleaching does not affect much but thermal annealing at several hundreds degree in Celsius affects to the centers in spite of higher stimulating energy of photon than temperature.

Usually, Intensity of OSL from a natural sample shows sample-dependence between particles or aliquots. Therefore, a signal regenerating method for the same sample is widely used, which means repeated OSL measurements to the same sample with giving a different dose of γ or β irradiation. Such sample dependence would be attributed to the imperceptible difference of impurities or defects of crystals, but are not fully understood. It is known that quartz from old sediment or from a geological fault shows an intense OSL and specifically shows a quick response for weaker stimulating light known as "the fast component" of OSL. However, quartz from igneous rocks does not show such fast component OSL[1]. Considering these facts, we can assume weathering of materials causes such enhancement of OSL sensitivity.

In this study, we have performed mechanical crushing and α-irradiation on quartz of reagent grade in order to simulate the effects of weathering on the OSL properties. Quartz powder with the grain size of 149-250 μm obtained after the ball-mill operation of 0.5 to 2 hours were used for OSL measurements. Also, α-irradiation at 1.3, 5.5, and 63kGy for powdered quartz was performed at the energy of 1.8MeV. OSL was measured with Risø TL/OSL reader Da-20 at β-irradiation of 50 Gy.

As a result, the OSL intensity increased with the crushing time as shown in Fig. 1. It is considerable that mechanical crushing leads the precursors of OSL centers, although we did not observe the fast component of OSL through this experiment. It is interesting that the α-irradiated quartz samples indicated crucially higher intensity. Considering the range of α-particles, defects near the surface of sample should contribute to the increase of the OSL Intensity. Comparisons with ESR spectra for these samples will be discussed.

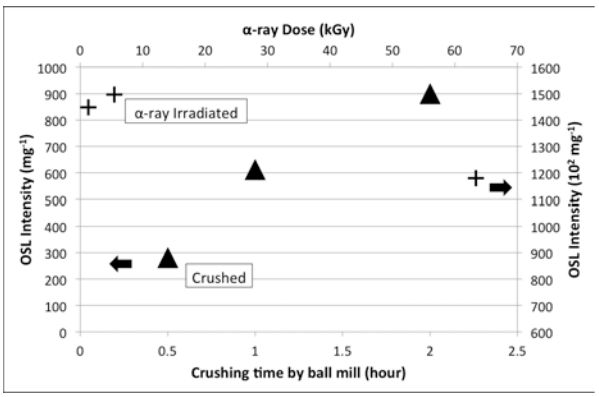

Fig.1 Effects of artificial weathering on OSL

Reference

[1] Tokuyasu K., Tanaka K., Tsukamoto S., and Murray A., "The characteristics of OSL signal from quartz grains extracted from modern sediments in Japan", Geochronometria **2010**, vol.37, pp13-19.

P-20

The decisive factor of clay quality and color of Bizen pottery

Yuki Matsuoka[1], Ko Furukawa[2] and Toshikazu Nakamura[3]

[1]*Faculty Division of Natural Science, Nara Women's University, Kitauoyanishi-machi Nara 630-8506, Japan*
[2]*Center for Instrumental Analysis, Niigata University, Ikarashi-2-nocho 8050 Niigata 950-2181, Japan*
[3]*Department of Materials Molecular Science, Institute for Molecular Science, Nishigou-naka 38 Myoudaiji Okazaki 444-8585, Japan*

E-mail: matsuoka@cc.nara-wu.ac.jp

Bizen pottery is a famous and historical pottery of about 1300 years. This pottery is made without grazing, so quality of material clay directly affects finish. Now, shortage of good quality material clay is serious problem to continue producing Bizen pottery. There are two points to settle the shortage problem. One is "producing area of material clay" and the other is "aging". Typical color of Bizen pottery like perilla frutescens crispa (reddish purple) comes out only in the case of using material clay produced from narrow area of Inbe. The mechanism of coloring is not clarified well. Aging for some years after digging out from field is essential process for material clay. If enough aging is omitted, pottery often cracks in baking process. So substituting clay produced from other area is next to impossible. Elucidating peculiar color system and same effect as aging without taking long time are strongly expected.

We proved that the valency of iron ion deeply contributes the color of pottery, i.e. Fe^{3+} yields reddish purple or reddish brown and Fe^{2+} doesn't form color.[1] In addition, slight difference of environment condition around iron ion is estimated to make delicate difference of color between reddish purple and reddish brown.

To elucidate fine structure of iron ion in clay mineral, ESR measurements were performed. Different quality samples, best quality one collected in Kannonji and poor quality one which collecting site is not specified, were used. In both samples, g = 4.3 and g = 2 signals were observed at room temperature. The spectra of clay have some similarity between Zeolite.[2] The environment of Fe^{3+} in best quality clay is comparatively stable for temperature change. On the other hand, the environment of Fe^{3+} in poor quality clay has remarkable temperature dependence. Interestingly the ground states in both samples seem to be same. From these results, the quality of clay and pottery color are suggested to be affected by the stability of Zeolite framework.

References

[1] Matsuoka Y. and Ikeya M., “Electron Paramagnetic Resonance and Mossbauer Spectra”, *Jpn. J. Appl. Phys.* **1995**, 34, 6068-6072.

[2] Evmiridis N. P., “Effect of Crystal Structure and Percentage of Ion Exchange on ESR Spectra of Hydrated Fe(III) Ion Exchanged Synthetic Zeolites”, *Inorg. Chem.* **1986**, 25, 4362-4369.

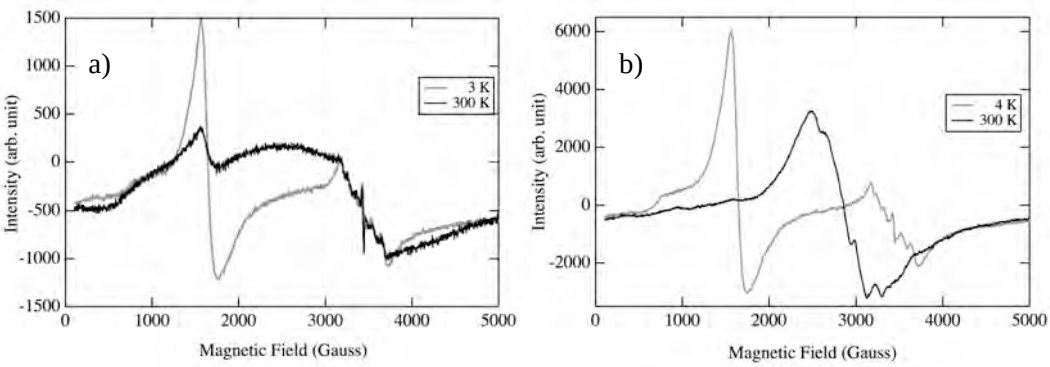

Fig. 1 ESR spectra of a) best quality clay and b) poor quality clay

P-21

EPR-Application in dermatology - in vitro and in vivo investigations

MC Meinke , A Friedrich, AC Lauer, S Arndt, S Ahlberg, SF Haag, SB Lohan, J Lademann

Charité-Universitätsmedizin Berlin, Department of Dermatology, Center of Experimental and Applied Cutaneous Physiology, Berlin, Germany

E-Mail: martina.meinke@charite.de

Enhanced formation of radicals in the skin can lead to premature skin aging and skin cancer. Solar exposure, which is the most harmful noxa, as well as smoking, stress, nanocarriers or xenobiotics can induce the formation of free radicals such as reactive oxygen species. These can result in lipid peroxidation and cell damage. Exogenous antioxidants such as vitamin C, E or carotenoids can prevent cell damage by scavenging the short-lived free radicals. Exogenous antioxidants must be taken up via the diet or can be topically applied. Electron paramagnetic resonance (EPR) spectroscopy can be used to measure the radical scavenging activity of a cream or an extract, as well as its action in the skin. Furthermore, the effect of the above mentioned noxa can be determined. Recent in vivo investigations have shown that the intake and the topical application of antioxidants enhanced the radical scavenging activity of the skin and therefore its antioxidative capacity [1-3]. To investigate the antioxidant capacity of the skin, its radical scavenging activity was measured using in vivo L-band EPR spectroscopy. This method determined the rate constant of a decreasing test radical over time applied on the skin. A high rate constant correlated with a high antioxidant capacity. Furthermore, radical formation after irradiation or nanoparticle application was studied on volunteers and skin cells. The release of the test radical could be delayed using nanocarriers [4]. In vivo studies have shown that the intake of antioxidants such as vitamin C, as well as chokeberry and curly kale extracts enhanced the radical scavenging activity of the skin significantly [1,2]. Furthermore, the selected antioxidants were shown to protect against radical formation in the skin and skin cells subsequent to VIS-NIR irradiation [2]. The protection effect was even more pronounced when antioxidants were topically applied [3]. Nanoparticles such as nanostructured lipid carriers could enhance the action of antioxidants, whereas silver nanoparticles could induce oxidative stress. Interestingly, major differences in radical formation between in vivo and ex vivo investigations were found. As a result of these investigations, we conclude that the EPR technique is a valuable tool for measuring the antioxidant capacity of the skin and the effects of oxidative stress and antioxidant substances and nanoparticles. This will permit specific approaches towards prevention of cell damage, premature skin aging, and skin cancer.
The work has been partly supported by the collaborative research center 1112, Project B01 of the Deutsche Forschungsgemeinschaft (DFG).

References

[1] Lauer AC, Groth N, Haag SF, Darvin ME, Lademann J, Meinke MC, Radical scavenging capacity in human skin before and after vitamin C uptake – measured in vivo with electron paramagnetic resonance spectroscopy , J Invest Dermatol. 2013;133:1102-4
[2] Meinke MC, Friedrich A, Tscherch K, Haag SF, Darvin ME, Vollert H, Groth N, Lademann J, Rohn S: Influence of dietary carotenoids on radical scavenging capacity of the skin and skin lipids. Eur J Pharm Biopharm 2013;84:365-373.
[3] Arndt S, Haag SF, Kleemann A, Lademann J, Meinke MC, Radical protection in the visible and infrared by hyperforin rich cream - in vivo versus ex vivo methods, Exp Dermatol. 2013;22:354-7
[4] Haag SF, Chen M, Peters D, Keck CM, Taskoparan B, Fahr A, Teutloff C, Bittl R, Lademann J, Schäfer-Korting M, Meinke MC, Nanostructured lipid carriers as nitroxide depot system measured by electron paramagnetic resonance spectroscopy. Int J Pharm. 2011;421:364-9.

P-22

Mechanism Study on Nitration of Arylboronic Acids with Nitrates by ESR

Haijun Yang, Min Jiang, Yong Li and Hua Fu

Beijing Key Laboratory for Microanalytical Methods and Instrumentation, Department of Chemistry, Tsinghua University, Beijing 100084, P.R. China

E-mail: cyhj@tsinghua.edu.cn

Arylboronic acids are common and important chemicals, and their nitration attracts much attention.[1] Recently, some methods such as copper-catalyzed,[2] iron-catalyzed[3] nitration of arylboronic acids have been developed. However, the nitration mechanisms are still not clear. One of the key questions is how nitrates work in the reactions. In our present study on transformations of functional groups, arylboronic acids were successfully nitrated with copper nitrate as the nitro source in the absence of catalyst. The target compounds were prepared in high yields and many substrates can be chosen in this method. The corresponding mechanism was investigated with *in situ* ESR without addition of spin trap, and Cu(II) ion and stable free radical signals were observed in toluene at 80℃ under nitrogen atmosphere. In the control experiment, no free radical signal was found for the cupric nitrate in toluene or solvent-free. The nitro radical was speculated based on the ESR information. It was shown that the signal of Cu(II) ion was weakened with the increase of the nitro free radical signal with time, which indicated that the catalysis was performed by variation of copper valence. Various nitrates including $Fe(NO_3)_3$, $Ni(NO_3)_2$, $Zn(NO_3)_2$, $Mg(NO_3)_2$, $AgNO_3$, KNO_3, NH_4NO_3 were used in the nitration of arylboronic acids, and the results showed that only metal ions with variable valence (such as iron, zinc and silver) could work. It is known to all that the solubility of nitrates is very poor in toluene. The nitration provided the similar yields when equivalent of $CuCl_2$ and KNO_3 were added to the reaction system instead of $Cu(NO_3)_2$. Therefore, NO_3^- anion acted as the nitro source and metal ions catalyzed the nitration of arylboronic acids via variation of metal valence . The possible reason is that water was brought in from the metal nitrates with crystal water. It is worthwhile to note that the reaction process could be monitored directly by in situ ESR without addition of spin trapping agent. This study should provide a reliable experimental proof of nitrates as the nitro source in nitration of arylboronics acids.

The financial support of the National Natural Science Foundation of China (Grant No. 21105054) is gratefully acknowledged.

References

[1] Prakash G. K. S. and Mathew T., "*ipso*-Nitration of Arenes", *Angew. Chem. Int. Ed.*, **2010**, 49, 1726-1728.

[2] Yang H., Li Y., Jiang M., Wang J., Fu H., "General Copper-Catalyzed Transformations of Functional Groups from Arylboronic Acids in Water", *Chem. Eur. J.*, **2011**,17, 5652-5660.

[3] Jiang M., Yang H., Li Y., Jia Z., Fu H., "Efficient ipso-Nitration of Arylboronic Acids with Iron Nitrate as the Nitro Source", *RSC Adv.*, **2013**, 3, 25602-25604.

P-23

4′-CyanoPLP Presents Better Prospect for the EPR Detection of Elusive Cyclic Intermediate Radical in the Reaction of Lysine 5,6-aminomutase

Amarendra Nath Maity and Shyue-Chu Ke

Department of Physics, National Dong Hwa University, Hualien, Taiwan 97401

E-mail: anmaity@gmail.com

Lysine 5,6-aminomutase (5,6-LAM) utilizes 5′-deoxyadenosylcobalamin (dAdoCbl) and pyridoxal-5′-phosphate (PLP) to catalyze reversible 1,2-shift of the ε-amino group of D-lysine or L-β-lysine into 2,5- or 3,5-diaminohexanoic acid.[1] 5,6-LAM follows a radical mechanism in which 5′-deoxyadenosyl radical (dAdo$^{\bullet}$) is generated from cleavage of Co-C bond of dAdoCbl. Then a hydrogen atom is transferred from PLP bound substrate to dAdo$^{\bullet}$ and results in the formations of 5′-deoxyadenosine (dAdoH) and substrate-related radical (S$^{\bullet}$). Rearrangement of S$^{\bullet}$ produces product-related radical (P$^{\bullet}$) through a proposed cyclic azacyclopropylcarbinyl radical (I$^{\bullet}$). Another H-atom transfer from dAdoH to P$^{\bullet}$ generates PLP bound product. Corresponding S$^{\bullet}$ has been characterized for 5,6-LAM in the reaction with substrate analogue[2] while analogues of S$^{\bullet}$ and P$^{\bullet}$ have been characterized for a related enzyme lysine 2,3-aminomutase. In contrast, experimental observation of I$^{\bullet}$ is still elusive. However, Radom and coworkers proposed the possible experimental observation of I$^{\bullet}$ if the reaction of 5,6-LAM is performed with either 4′-vinylPLP or 4′-acetylenylPLP.[3] 4′-VinylPLP is relatively more stabilized, and hence more promising, than 4′-acetylenylPLP.

In this work, following the methods established[3] by Radom and co-workers we have performed calculations on 4′-cyanoPLP. The results show that the corresponding I$^{\bullet}$ (4′-cyanoI$^{\bullet}$) is the most stable among the relevant radical intermediates (corresponding S$^{\bullet}$, I$^{\bullet}$, and P$^{\bullet}$). The results also demonstrate that 4′-cyanoI$^{\bullet}$ is relatively more stabilized than 4′-acetylenylI$^{\bullet}$ while less stabilized than 4′-VinylI$^{\bullet}$. Nevertheless, cyano group introduces less perturbation than both vinyl and acetylenyl. Therefore, it would be easier for the enzyme to accommodate 4′-cyanoPLP than 4′-vinylPLP or acetylenylPLP. Furthermore, the presence of nitrogen atom in 4′-cyanoPLP is beneficial as it can act as a magnetic probe for characterization by EPR and ENDOR spectroscopy. We have calculated the corresponding hyperfine coupling constants (HFCCs) for nitrogen atoms using several basis sets. These HFCCs would help to characterize 4′-cyanoI$^{\bullet}$. Taken together, our results suggest that 4′-cyanoPLP promises better prospect for the experimental detection and characterization of elusive I$^{\bullet}$ in the reaction of 5,6-LAM.

References

[1] a) Maity A. N., Chen Y. H. and Ke S. C., "Large-scale domain motions and pyridoxal-5'-phosphate assisted radical catalysis in coenzyme B_{12}-dependent aminomutases". *Int. J. Mol. Sci.* **2014,** 15, 3064-3087; b) Frey P. A. and Reed G. H., "Pyridoxal-5'-phosphate as the catalyst for radical isomerization in reactions of PLP-dependent aminomutases". *Biochim. Biophys. Acta* **2011,** 1814, 1548-1557.

[2] Chen Y. H., Maity A. N., Pan Y. C., Frey P. A. and Ke S. C., "Radical stabilization is crucial in the mechanism of action of lysine 5,6-aminomutase: Role of tyrosine-263α as revealed by electron paramagnetic resonance spectroscopy". *J. Am. Chem. Soc.* **2011,** 133, 17152-17155.

[3] Sandala G. M., Smith D. M. and Radom L., "In search of radical intermediates in the reactions catalyzed by lysine 2,3-aminomutase and lysine 5,6-aminomutase". *J. Am. Chem. Soc.* **2006,** 128, 16004-16005.

Multifrequency (X-band to W-band) CW EPR of the crude oil and by-products

Eduardo Di Mauro, Marilene Turini Piccinato and Carmen Luisa Barbosa Guedes

Fluorescence and Electron Paramagnetic Resonance Laboratory (LAFLURPE), CCE, State University of Londrina, Londrina, PR, 86057-970, Brazil

E-mail: dimauro@uel.br

Our goal was based on environment questions. Environmental accidents involving crude and by-product oils have motivated laboratory research to evaluate photodegradation in monitored environments, as well as the characterization of crude and by-product oils. EPR was the spectroscopic technique used as analysis tool. The samples were measured on EPR spectroscopy at X- (ca. 9 GHz), Q- (ca. 34 GHz) and W-bands (ca. 94 GHz).

The EPR spectra of crude oils show signals of two different paramagnetic centers, namely, the vanadyl group VO^{2+} and free radical (Guedes et al., 2003). These are overlapped in the same magnetic field range (Fig. 1A), being the very intense central line associated with organic free radical (Fig. 1B). This line is interpreted as resulting from the superposition of the signals of the different species of free radicals with very close values of g-factor in crude oil asphaltenes (Guedes et al., 2003).

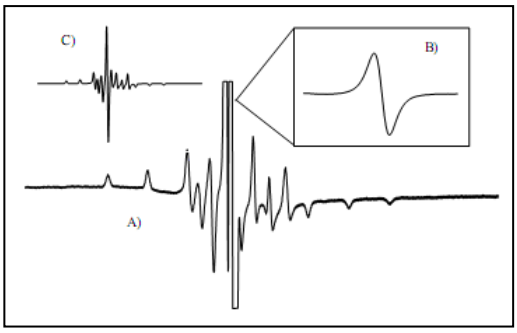

Fig. 1: A) EPR spectrum in X-band for Brazilian oil;
B) Signal of the free radical;
C) Simulated spectrum form VO^{2+}.

The EPR technique proved to be useful in the characterization of the molecular structure of asphaltenes in crude and by-product oil. The EPR parameters are able to reveal changes of the photochemical nature in the oil under the effect of sunlight or in some specific wavelength. This spectroscopy technique can be further explored and, consequently, applied in the monitoring of petroleum weathering and its by-products in environmental matrixes whenever accidents occur or routine operations result in oil spill. The period of permanence of toxic and refractory aromatic components of petroleum in aquatic systems can be evaluated not only through quantitative chromatographic methods, but also using nondestructive and more economical qualitative methods.

References

[1] Guedes, C. L. B., Di Mauro, E., Antunes, V. and Mangrich, A. S., "Photochemical Weathering Study of Brazilian Petroleum by EPR Spectroscopy". *Marine Chemistry* **2003**, Volume 84, No. 1, 105-112.

[2] Di Mauro, E., Guedes, C. L. B. and Piccinato, M. T., "EPR of Marine Diesel", *Applied Magnetic Resonance* **2007**, Volume 32, No. 3, 303-309.

[3] Piccinato, M. T., Guedes, C. L. B. and Di Mauro, E., "EPR Characterization of Organic Free Radicals in Marine Diesel", *Applied Magnetic Resonance* **2009**, Volume 35, No. 3, 379-388.

[4] Piccinato, M. T., Guedes, C. L. B. and Di Mauro, E., "*Crude and by-product oils by EPR In: Crude Oil Emulsions- Composition Stability and Characterization*", 1st edition, InTech, (2012) pp 147-168.

P-25

Evaluation of Anti-oxidative Materials of 13 Mushrooms by ESR

Tomomi Kanno[1], Kumiko Yamamoto[2], Etsuko Harada[3], Hiromi Kameya[4], Mitsuko Ukai[2,4] and Toshihiko Osawa[5]

[1] *Hokkaido University of Education Asahikawa Campus, Hokkaido 070-9621, Japan*
[2] *Hokkaido University of Education Hakodate Campus, Hokkaido 040-8567, Japan*
[3] *Iwade Research Institute of Mycology Co.Ltd., Mie 015-0012, Japan*
[4] *NARO, National Food Research Institute, Ibaraki 305-8642, Japan*
[5] *Aichi Gakuin University, Aichi 470-0195, Japan*

E-mail: kanno.tomomi@a.hokkyodai.ac.jp

We evaluated the radical scavenging abilities of hot water extracts from 13 mushrooms using electron spin resonance (ESR) spin trapping method and oxygen radical absorbance capacity (ORAC) assay[1]. The ESR method was identified hydroxyl radical (·OH), superoxide radical (O_2^-) and alkoxy radical (RO·) scavenging abilities using 5-(2,2-dimethyl-1,3-propoxycyclophosphoryl) -5-methyl-1-pyrroline-*N*-oxide (CYPMPO) as a spin trapping reagent. The ORAC value was largest in *Coprinus comatus*. However the ·OH radical scavenging ability was largest in *Agrocybe cylindracea*, the O_2^- radical scavenging ability was in *Leucopaxillus giganteus* and the RO· radical scavenging ability was in *Pleurotus ostreatus*. The radical scavenging ability of specimens evaluated from ESR did not correlate with the ORAC value. We concluded ESR is useful to evaluate each anti-oxidative materials of mushrooms.

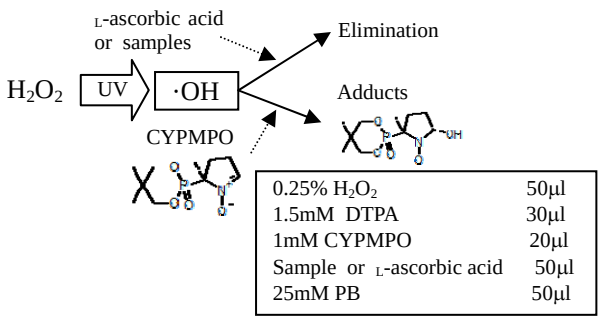

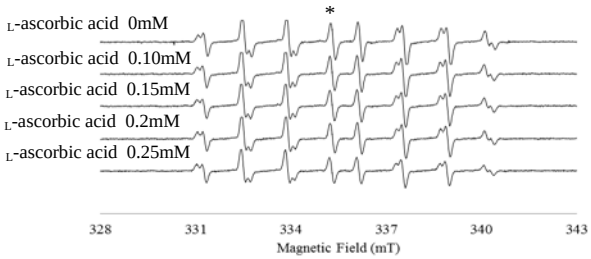

Fig.1 ESR spectra of hydroxyl radical and CYPMPO adduct.

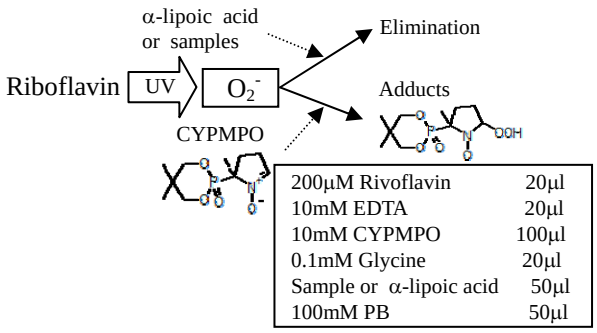

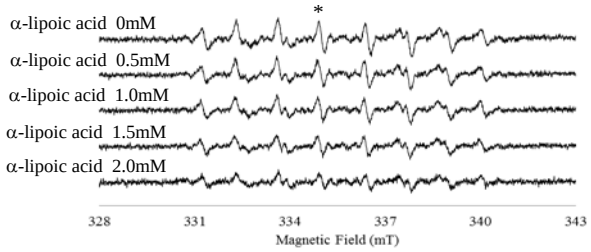

Fig.2 ESR spectra of superoxide radical and CYPMPO adduct.

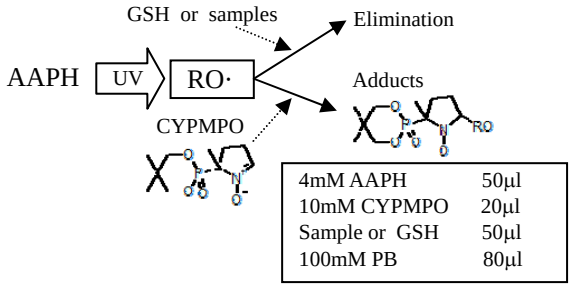

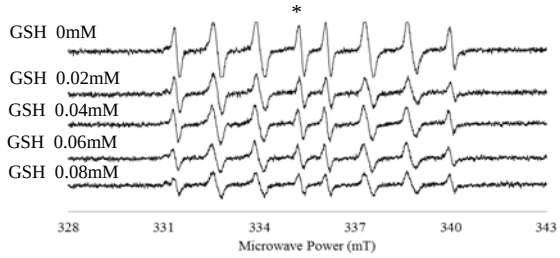

Fig.3 ESR spectra of alkoxy radical and CYPMPO adduct.

References

[1] Kanno T. et al., *Food Science and Technology Research* **2011** 17, 103-110.

P-26

Ultrasound-induced activation of caged compounds

Haruko Koura[1], Risa Fuji[1], Asuka Kato[1], Masato Mutoh[2] and Wakako Hiraoka[1]

[1]*Graduate School of Science and Technology, Meiji University, Kanagawa 214-8571, Japan*
[2] *Department of Materials and Human Environmental Sciences, Shonan Institute of Technology, Kanagawa 251-8511, Japan*

E-mail: hiraoka@isc.meiji.ac.jp

Background. Photoactivatable caged compounds are widely used as tracers and activators in biological systems. The activity or function of caged compounds is masked using a caging moiety, and the release from caging can be controlled both spatially and temporally using a trigger such as flash photolysis. However, photoirradiation may pose a disadvantage in clinical applications. Our laboratory has investigated the potential of ultrasound as a substitute for photoirradiation. The aim of the present study was to determine the mechanism of ultrasound-induced release of an active moiety from caging and to determine whether ultrasound-activatable caged compounds have potential for application in medical therapeutic and diagnostic practice.

Materials and Methods. Fluorescein bis-(5-carboxymethoxy-2-nitrobenzyl) ether (CMNB-caged fluorescein) was used for the activation assay. For activation of caged reagents, we used a super-high-pressure Hg lamp (USH-500D, USHIO, INC., Japan) and 1 MHz continuous-wave ultrasound with variable power. After activation, the released fluorescein and degradation products were analyzed by fluorospectrometry and HPLC. Hydroxyl radicals generated by cavitation were detected by ESR spin trapping.

Results. Figure 1 shows the fluorescence spectra obtained from the CMNB-caged fluorescein solution after ultrasound irradiation for 5 min at 10 W/cm^2. The intensity of fluorescence was proportional to th e length of irradiation but not to the power of ultrasound. The fluorospectrometric and HPLC profiles o f the irradiated sample solution were n ot the same between ultrasound irradia tion and photoirradiation.

Conclusion. In the present study, we showed that fluorescent unmasked molecules were detected in an ultrasound-irradiated caged compound solution. Analysis of the degradation products indicated that the mechanism of release of fluorescein by ultrasound irradiation was distinct from that by photoirradiation. Possible mechanisms, such as mechanical stress, radical production, and sonoluminescence, should be considered.

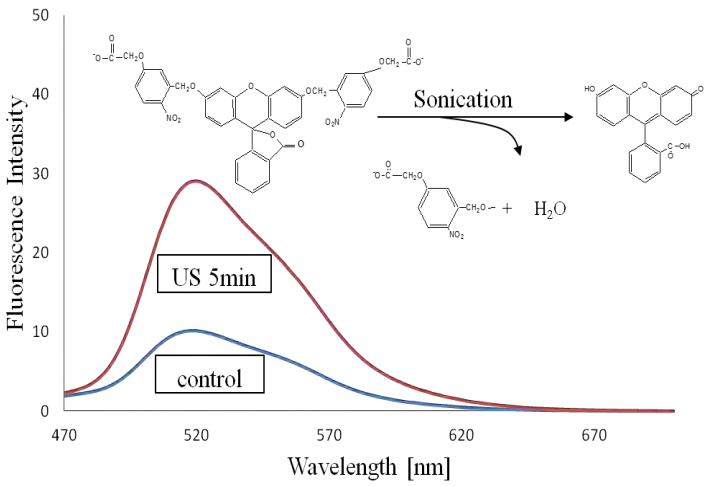

Figure 1. Fluorescence spectra of CMNB-caged fluorescein solutions after ultrasound irradiation.

References.

[1] Feril L. B., Jr. and Kondo T., "Ultrasound liberates nitric oxide (NO) from the caged NO compound N,N′-bis(carboxymethyl)-N,N′-dinitroso-p-phenylenediamine sodium salt", *Ultrasonics sonochemistry* **2006**, 13, 397-400.

[2] Shelby J. P. and Chiu D. T., "Mapping Fast Flows over Micrometer-Length Scales Using Flow-Tagging Velocimetry and Single-Molecule Detection", *Analytical Chemistry* **2003**, 75, 1387-1392.

P-27

Enhancement of vitamin D_3-induced differentiation in PLB-985 cells by modulating oxidative stress

Hiroaki Tanaka[1] , Hiroyuki Kato[1], Omi Nawa[1], Asuka Kato[1], Masato Mutoh[2] and Wakako Hiraoka[1]

[1]*Graduate school of Science and Technology, Meiji University, Kanagawa 214-8571, Japan*
[2]*Department of Materials and Human Environmental Sciences, Shonan Institute of Technology, Kanagawa 251-8511, Japan*

E-mail: hiraoka@isc.meiji.ac.jp

Background. Our laboratory has demonstrated that monocytic differentiation induced by vitamin D_3, an active metabolite of vitamin D_3 in human leukemia (PLB-985 cells) is enhanced by phorbol 12-myristate 13-acetate (PMA) and that PMA-treated PLB-985 cells produce reactive oxygen species (ROS). The aim of the present study was to elucidate the function of ROS in vitamin D_3-induced antineoplastic effects and immune enhancement using myeloid leukemia PLB-985 cells as a test model.

Materials and Methods. PLB-985 cells and $gp91^{phox}$(-) (X-CGD:NADPH oxidase knockout) cells were treated with either 200 nM 1α,25-dihydroxyvitamin D_3 (vitamin D_3), 50 nM PMA, or ROS scavengers (superoxide dismutase or catalase) for 72 h. Expression of Mac-1 alpha (CD11b) was evaluated by flow cytometry and fluorescence microscopy using FITC-conjugated antibodies. ROS was detected by ESR spin trapping. Gene expression of extracted mRNA was assayed with TORAY 3D-Gene®.

Result. Flow cytometry indicated that Mac-1 alpha was present in vitamin D_3-treated PLB-985 cells but not in $gp91^{phox}$(-) cells (Fig. 1). ESR spin trapping showed that ROS was generated in PMA-stimulated PLB-985 cells but not in $gp91^{phox}$(-) cells. Comprehensive gene expression analysis showed that vitamin D_3 enhanced the induction effect of PLB-985 cells for genes involved in the regulation of myeloid cell differentiation, regulation of oxidative stress, and activation of NADPH oxidase (Table 1).

Conclusion. The present study indicates that ROS enhances vitamin D_3-induced cell differentiation. This enhancement is mediated by the expression of genes associated with NADPH oxidase. These findings suggest that the modulation of oxidative stress potentiates the therapeutic effect of vitamin D_3 in neoplasms and immune disorders.

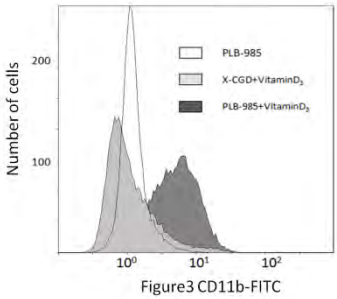

Figure 1. Detection of CD11b by flow cytometry

Factor	Description	UP regulate
Stress Factor	Oxidative stress-induced growth inhibitor 1	*
	Tumor protein p53-inducible nuclear protein 1	*
Differentiation Factor	Monocyte differentiation antigen CD14 Precursor	***
	Differentiation-enhancing factor 1	*
	Cell surface glycoprotein MAC-1 subunit alpha(CD11b)	***
	Interferon-inducible myeloid differentiation transcriptional activator	**
NADPH Factor	Neutrophil NADPH oxidase factor 2(p67-phox)	***
	NADPH oxidase activator 1 (p51-nox)	*
	Cytochrome b-245 heavy chain(gp91-phox)	*
	Neutrophil NADPH oxidase factor 2(p67-phox)	***

Table 1. Up or down-regulation of specific gene-expression of PLB-985 cells stimulated with vitamin D_3 (*: 2-fold,**: 4-fold,***: more than 8-fold)

References.

[1] Deeb K. K., Trump D. L. and Johnson C. S., "Vitamin D signalling pathways in cancer: potential for anticancer therapeutics", *Nature Reviews Cancer* **2007**, 7, 684-700.

[2] Flynn G., Chung I., Yu W. D., Romano M., Modzelewski R. A., Johnson C. S. and Trump D. L., "Calcitriol (1,25-dihydroxycholecalciferol) selectively inhibits proliferation of freshly isolated tumor-derived endothelial cells and induces apoptosis ", *Oncology* **2006**, 70, 447-57.

P-28

Correlation between number of C-C double bonds and relaxation times of polyenyl radicals as studied by CW-ESR spectroscopy

Takatoshi Sawai[1], Yoji Yamaguchi[1]

[1]*Department of Materials Science Laboratory, Toray Research Center, Inc., Shiga, 520-8567, Japan*

E-mail: Takatoshi_Sawai@trc.toray.co.jp

Polyenyl radicals in damaged organic polymers, such as gamma-ray, sunlight irradiated polymers have been detected by ESR spectroscopy. ESR spectroscopy is one of the interesting methods to discuss the origin of discoloration of damaged polymers because conjugation of polyene may absorb visible light depending on number of C-C double bonds. In this work, we focused correlation between number of C-C double bonds of polyenyl radicals predicted by line width and relaxation times determined by CW-ESR saturation method. We believe that a knowledge of relationship between chemical structures and relaxation times of the radicals give us the important basis of practical application of relaxation time measurement.

Table 1. Measurement samples

Sample number	Polymer	Damage
1	polyethylene	ion implantation
2	nylon	sunlight
3	polyvinyl chloride	sunlight
4	polyvinyl chloride	gamma-ray

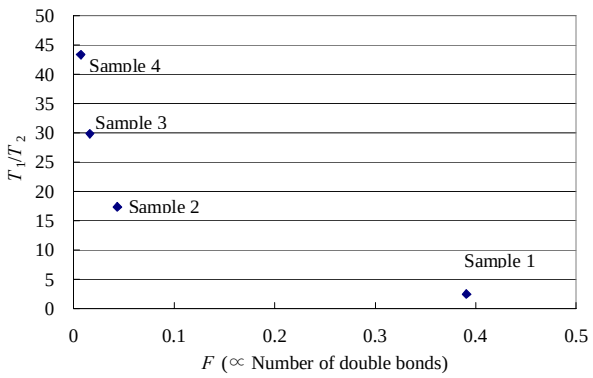

Figure 1. T_1/T_2 vs. number of double bonds.

Polyenyl radicals of some polymers were generated by ion implantation, sunlight and gamma-ray irradiation methods (Table 1). Color of non-damaged polymers changed dramatically after these treatments. CW-ESR spectra of sample1-4 observed at room temperature show poorly resolved or non-resolved hyperfine structures indicated the features of spectra of polyenyl radicals due to *delocalization narrowing* in which spin density is distributed over the polymer chain and ^{1}H hyperfine splitting decrease compared to localized radicals such as alkyl type radicals.

Rough tendency of number of double bonds for sample1-4 were calculated by eq.1 [1]

$$N \propto \left(\frac{1}{\Delta H_{pp}} \right)^2 = F \quad \cdots\cdots \quad (1)$$

where N and ΔH_{pp} are number of double bonds and linewidth of polyenyl radical, respectively. Figure 1 show plot of F-values vs. ratio of relaxation times (T_1/T_2) which determined by Lund's method [2]. In spite of values of different polymers, we can find good correlation between F-values and T_1/T_2, indicating that the relationship is essential for polyenyl radicals. In the poster, we'll discuss the mechanism of the correlation of Fig.1 in terms of temperature dependence of longitudinal relaxation time T_1.

References

[1] Marumoto K., Kuroda S., Takenobu T., Iwasa Y., "Spatial Extent of Wave Functions of Gate-Induced Hole Carriers in Pentacen Field-Effect Devices as Investigated by Electron Spin Resonance", *Physical Review Letters* **2006**, 97, 256603.

[2] Lund A., Sagstuen E., Sanderud A., Maruani J., "Relaxation-Time Determination from Continuous-Microwave Saturation of EPR Spectra", *Radiation Research* **2009**, 172, 753-760.

P-29

Radical reaction induced by UV-irradiated ketoprofen in liposomal membranes

Shoko Okazaki, Takuro Nagata, Megumi Takemoto, Yusuke Shogomori, Ayako Hirata and Keizo Takeshita

[1]*Faculty of pharmaceutical sciences, Sojo University, Kumamoto 860-0082, Japan*

E-mail: o-sho@ph.sojo-u.ac.jp

Ketoprofen (Fig. 1) is one of the popular non-steroidal anti-inflammatory drugs. It induces photosensitivity dermatitis as a side effect. Some researchers have reported that superoxide radical and ketoprofen radicals are produced in the aqueous solution of ketoprofen by UV-irradiation. However, the relationship between these radicals and ketoprofen-related photosensitivity has yet to be revealed. In order to elucidate the mechanisms of the photosensitivity, we examined the radical reaction induced by UV-irradiated ketoprofen in liposomal membranes with electron spin resonance technique.

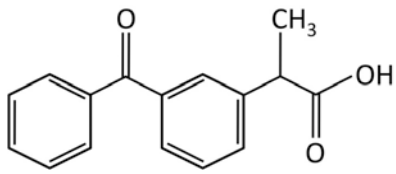

Fig.1 The structure of ketoprofen

Both superoxide anion radical and organic radical (ketoprofen radical) were detected by spin trapping technique, when an aqueous solution of ketoprofen was irradiated with UV. We prepared egg-yolk phosphatidylcholine (egg-PC) liposomes including both 16-doxyl-stearic acid, having doxyl group in hydrophobic region, and ketoprofen in membranes to examine whether ketoprofen induces the radical reaction in liposomal membranes during UV-irradiation. The ESR signal of 16-doxyl-stearic acid in liposomal membranes was decreased by UV-irradiation. It indicates that ketoprofen can induce the radical reaction in liposomal membranes as well as in aqueous solution. The signal decay of 16-doxyl-stearic acid also occurred when a mixture of ketoprofen and liposomes including only 16-doxyl-stearic acid in egg-PC membranes was irradiated with UV. The decay of ESR signal of 5-doxyl-stearic acid, having doxyl group near hydrophilic region of liposomal membranes, was faster than that of 16-doxyl-stearic acid. The signal decay of 5-doxyl-stearic acid increased with an increased in amount of egg-PC in liposomal suspension and was suppressed in liposomal membranes composed of dipalmitoylphosphatidylcholine. The decay was suppressed by POBN, a spin trapping agent, dose-dependently, whereas that was not affected by superoxide dismutase and catalase. These results indicate that (*i*) ketoprofen migrates from water phase to lipid membranes, that (*ii*) the reaction occurs near hydrophilic region of liposomal membranes, and that (*iii*) ketoprofen radical rather than superoxide anion radical is mainly involved in the radical reaction in membranes. The leakage of glucose from liposomes increased in the presence of ketoprofen by UV-irradiation, indicating that disruption of membranes is facilitated by ketoprofen (Fig.2). The relationship between disruption of membranes and radical reaction by UV-irradiated katoprofen is now under investigation.

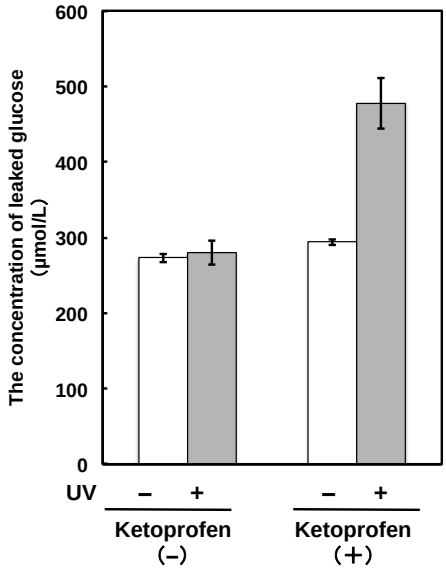

Fig.2 The effect of UV-irradiated ketoprofen on liposomal membrane.

P-30

Measurement of Density of Hydroxyl Radical Generation in Water Induced by Low-LET Radiation

Yukihiro Ogawa[1,2], Ken-ichiro Matsumoto[2] and Shingo Fujisaki[1]

[1] *Department of Biomolecular Science, Toho University Graduate School of Science, Chiba 274-8510, Japan*
[2] *Radio-Redox-Response Research Team, National Institute of Radiological Sciences, Chiba 263-8555, Japan*

E-mail: yukih_o@fml.nirs.go.jp

Secondary radical reactions of the hydroxyl radical ($^{\bullet}$OH) account for 80% of radio-biological effects mediated by the generation of reactive oxygen species (ROS). The regulation of $^{\bullet}$OH is important for suppressing these indirect actions. In this study, by applying the electron paramagnetic resonance (EPR) spin trapping method, we determined the density of $^{\bullet}$OH generation when an aqueous sample was irradiate with low-LET radiation such as X-rays or γ-rays, by using 5,5-dimethyl-1-pyrroline-N-oxid (DMPO) as the spin trapping agent.

Several concentrations (from 0.5 to 1680 mM) of DMPO in aqueous solution were irradiated with 32Gy X-rays (3.2 Gy/min). The amount of hydroxyl radical adduct (DMPO-OH) generated was measured by X-band EPR. The relationship between the concentration of DMPO in the reaction mixture and DMPO-OH generation was analyzed.

The amount of DMPO-OH generated increased linearly and reached an inflexion point where the amount of DMPO-OH formation decreased substantially for a given amount of DMPO added to solution, as the concentration of DMPO was increased above 3 mM, i.e., the inflexion concentration. This observation suggests that the concentration of $^{\bullet}$OH generated was approximately 3.3 mM or more. After the concentration of DMPO-OH formation decreased for a given amount of DMPO added to solution (at approximately 3 mM of DMPO), a linear trend that passed through the origin was observed. From this result, the very high density of $^{\bullet}$OH generation which could be detected by increasing DMPO concentration, was observed. The extremely high-density of $^{\bullet}$OH generation can be very difficult to control, however lower densities of $^{\bullet}$OH generation (~ 3 mM) may well be controlled by antioxidants.

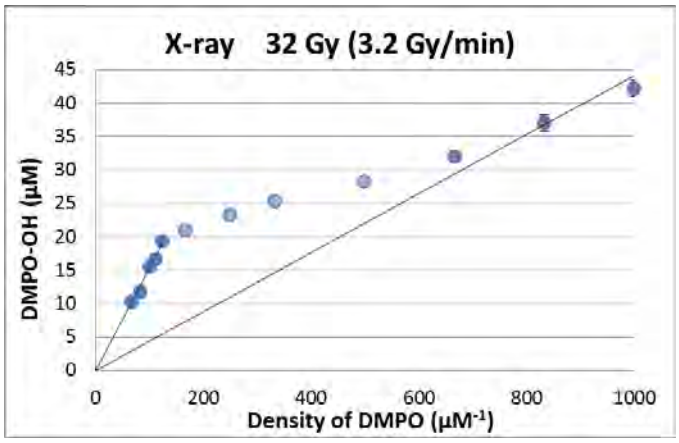

DMPO Conclusi (mM)	Moleclue Distanc (nm)	DMPO Density (μm^{-1})
0.5	15.0	67
0.96	12.0	83
1.65	10.0	100
2.25	9.0	111
3.3	8.0	125
7.7	6.0	167
13.0	5.0	200
26.0	4.0	250
61.6	3.0	333
208	2.0	500
492	1.5	667
961	1.2	833
1661	1.0	1000

References

Ueno M., Nakanishi I., and Matsumoto K., "*Method for X-ray-induced hydroxyl radical-scavenging activity of biological compounds/materials", J. Clin. Biochem. Nutr.*, (2013) 52(2):95-100.

P-31

Superoxide radical scavenging activity of cooked rice as studied by HPLC-ESR spin-trapping measurements

Tomoko Yamaguchi,[1] Gen Httori,[2] Kenji Kanaori,[1] Kunihiko Tajima[1], Isamu Tachimoto[3]
[1]*Bio-molecular Engineering, Kyoto Institute of Technology, Sakyo-ku, Kyoto 606-8585, Japan*
[2]*DESIGNER FOODS CO., Ltd, chikusa-ku, Nagoya 464-0858, Japan*
3 DELICA FOODS CO., Ltd, adachi-ku, Tokyo 121-0073, Japan
E-mail: yamaguchi@kit.ac.jp

Recently, we have developed flow-injection-ESR and HPLC-ESR systems special for quantitative spin-trapping ESR detection of the superoxide radical by using DMPO (5,5-dimethyl-1-pyrroline-*N*-oxide; DMPO/O_2), as a spin-trapping reagent.[1, 2] The flow-ESR techniques were employed to explore potent superoxide radical scavengers involved in cooked white and brown rice. In the present study, HPLC-ESR measurements were made for water-soluble components of several Japanese and imported rice.

A sample solution of a premium-grade Japanese brown-rice (labeled as **k-B**) was obtained by following procedures; 2 g of powder obtained from the cooked brown rice of **k-B** was treated with 18 g of pure water (QII grade), and resulted the suspension was applied for supercentrifuge (Hitachi CP-60) treatment to obtained the water soluble fraction of **k-B**. The sample was suitably diluted by NaH_2PO_4/Na_2HPO_4 buffer solution (0.1 M pH 7.4) for the measurements. The HPLC-ESR system is composed of an X-band ESR spectrometer (TE-30, JEOL), and an HPLC system (Shimadzu LC-10AT) equipped with a TSK-gel size exclusion column (TOSOH, G3000PW, 7.5 mm i.d. × 30 cm). The $O_2^{-\bullet}$ radical was produced by riboflavin (Rf) dependent photo-reduction of oxygen in the presence of EDTA (ethylenediamine-*N,N,N′,N′*-tetraacetic acid), and was detected by ESR as a spin adducts of DMPO (5,5-dimethyl-1-pyrroline-*N*-oxide; DMPO/O_2).

As depicted in Figure 1-1, ESR-chromatogram monitored by signal intensity of the DMPO/O_2 radical showed major five peaks (**A**, 7.7; **B** 8.9; **C**, 11.3; **D**, 12.1; and **E**, 13.2 min), indicating that major superoxide radical scavenger could be involved in strong peaks **A**, **B**, and **D**. Thus, the column eluates from the major peaks were collected and supplied for further ESR and NMR measurements to assign the noble antioxidants. As shown in Figure 1-2, the frozen solution of the mixture of fractions **A** and **B** exhibited typical ESR signals due to the Mn(II) ion, suggesting that the Mn(II) ion played important role for scavenging the superoxide radical. In the case of the peak **D**, NMR signals ascribable to be nicotinic acid derivatives were recognized. Based on the observation results, superoxide radical scavengers involved in cooked brown rice will be discussed.

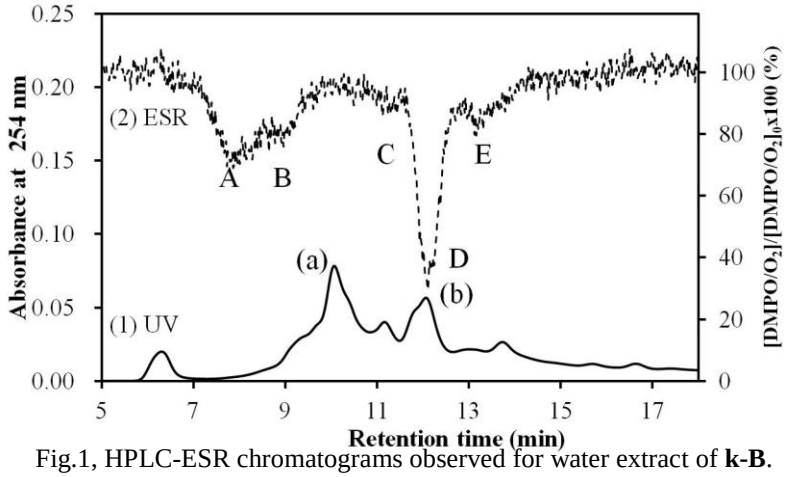

Fig.1, HPLC-ESR chromatograms observed for water extract of **k-B**.
1) UV-chromatogram monitored by absorbance at 254 nm.
2) ESR-chromatogram monitored by relative ESR intensity of the DMPO/O_2 radical.
The final concentration of DMPO, EDTA, and Rf after mixing was adjusted at 20 mM, 1.0 mM and 2.6 μM, respectively.

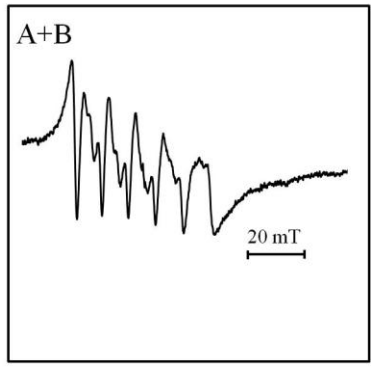

Fig. 2, ESR spectra observed for frozen solution of the fraction **A** and **B**.

References; 1) Y. Sakurai, *et al.*, *Chem. Lett.*, 2009, **38**, 662. 2) K. Kawai, *et al.*, *Applied Magnetic Resonance*, 2011, **40**, 449.

P-32

Direct ESR Observations of Radical Polymerization of *N*-Vinylcarbazole

Ryosuke Matoba[1], Atushi Kajiwara

[1]*Department of Materials Science, Nara University of Education, Nara 630-8528, Japan*

E-mail: a133408@student.nara-edu.ac.jp

Introduction

Elementary processes of radical addition and polymerization reactions during radical polymerization of *N*-vinyl carbazole (*N*VCz) have been investigated by electron spin resonance (ESR) spectroscopy. In our laboratory, various kinds of active species during actual radical polymerizations have been detected by ESR. Among these monomers, observations of ESR spectra of chain initiating and propagating radicals of nitrogen containing monomers like *N*VCz, vinyl pyridines, and (meth)acryl amides were extremely difficult probably due to relatively high reactivity and low steady-state concentrations of the radicals. Combination of time-resolved ESR and steady-state ESR measurements enables us to observe both chain initiating and propagating radicals of *N*VCz after repeated optimization of the measurement conditions. TR ESR showed information on initiation process and SS ESR provided on propagating processes of radical polymerization of *N*VCz.

Experimental

TR-and SS ESR spectra were recorded by JEOL JES RE-2X ESR spectrometer. Measurement temperatures were controlled by DVT2 variable temperature accessory. 3rd harmonic of Nd-YAG laser (Spectra Physics DCR-2, 355 nm) was used as a light souse of TR ESR.

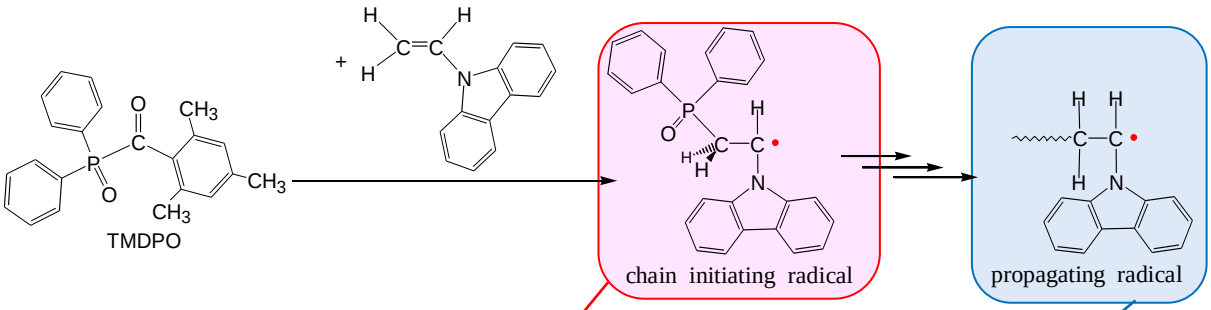

Figure 1. Radical polymerization of *N*-vinylcarbazole

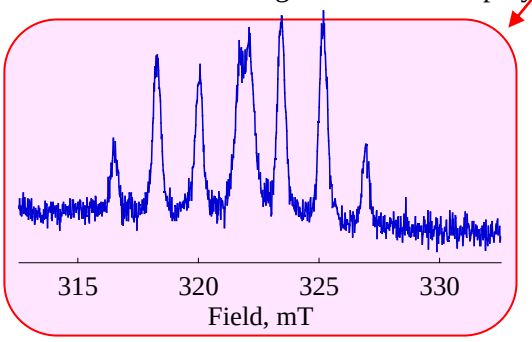

Figure 2. TR ESR spectrum of chain initiating radicals of *N*-vinylcarbazole

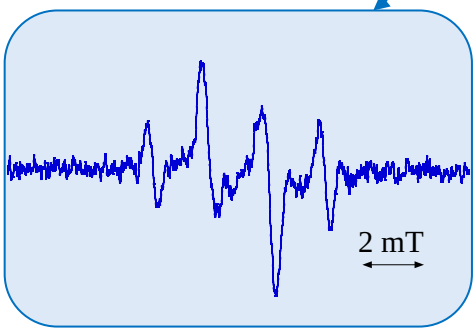

Figure 3. SS ESR spectrum of propagating radical of *N*-vinylcarbazole

Results and Discussion

TR ESR spectra of *N*VCz were clearly observed as shown in Fig. 2. From these spectra, information on both structural and kinetics of the radicals can be obtained. Addition reaction of diphenyl phosphynoyl radical to *N*VCz was estimated to be (1.50 ± 0.08) x 10^6 $M^{-1}s^{-1}$at 20°C.SS ESR spectra clearly showed structure of propagating radicals of *N*VCz as shown in Fig. 3. Propagation rate constants (k_p) for *N*VCz can also be estimated from the SS ESR spectra. For example, value of k_p at 20°C was (1.41 ± 0.12) x 10^3 $M^{-1}s^{-1}$. From these results, we can see what happened during radical polymerizations of *N*VCz from initiation to propagation.

P-33

Electrochemical ESR Cell for Determination of Redox Potentials of Transient Radicals

Tatsumi Tetsuya and Atsushi Kajiwara

Department of Materials Science, Nara University of Education, Nara 630-8528, Japan

E-mail: a133405@student.nara-edu.ac.jp

Introduction

A new type of electrochemical ESR (EC ESR) cell has been developed for determination of redox potential of transient radicals. As far as we know, no one has been directly determined the redox potentials. Measurements of redox potentials of propagating radicals in polymerizations have been extremely difficult even impossible by cyclic voltammetry (CV), probably because concentration of radicals in polymerizations (10^{-6}-10^{-7} M) are much smaller than monomer (10^{-2}-10^{-3} M). Combination of ESR and CV may have a considerable possibility to measure redox potentials of propagating radicals in polymerizations. Attempts for direct determination of redox potentials of transient radicals in actual polymerizations will be presented.

Experimental Section

ESR spectra were recorded on an X-band JEOL JES-TE200 spectrometer, utilizing a 100 kHz modulation and microwave power of 1-5 mW. Temperature was controlled by a JEOL DVT2 variable temperature accessory. Voltammograms were recorded on a BAS CV-50W. Monomers and initiators were purified before use.

Results and discussion

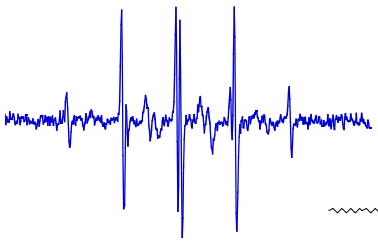

Fig.2 ESR spectrum of *t*BMA Propagating Radical in tolene with ESR cell

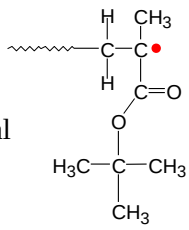

Fig.1 Structure of *tert* butyl methacrylate (*t*BMA) propagating radical

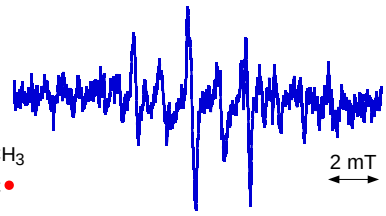

Fig.3 ESR spectrum of *t*BMA Propagating Radical in acetone with EC ESR cell

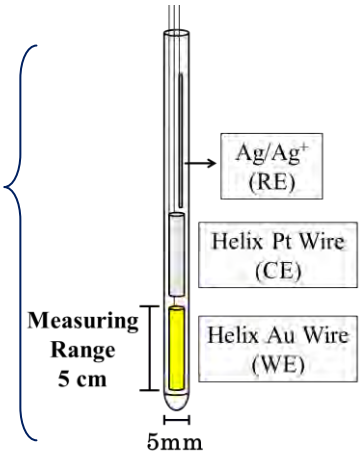

Fig.4 Simplified diagram of Electrochemical ESR Cell

ESR cell with three electrodes (working, counter, and reference) was developed based on commercially available EC ESR cell (Fig.4). Basic topic was that voltammetry during observing ESR spectra of propagating radicals can provide precise redox potentials of the radicals by changing of the signal intensity upon the sweep. Before investigating actual propagating radicals, 2,2,6,6-tetramethylpiperidine 1-oxyl (TEMPO) was used for evaluation of this method. Redox potentials of the TEMPO can also be determined by CV. EC ESR results of the TEMPO can be compared with those from CV results. Clear correspondence between CV and EC ESR was observed. Based on the knowledge and technique of these measurements, application of the method to actual propagating radicals was carried out. Results for various kinds of propagating radicals will be presented.

P-34

Oxidation mechanism of poly(vinyl alcohol) with persulfate anion radical as studied by spin-trapping ESR and LC/MS

Yuko Nishihara[1,2], Toshimitsu Inoue[2], Tomoko Yamaguchi[1], Toru Ikegami[1], Yusuke Miyake[1], Kenji Kanaori[1], Kunihiko Tajima[1]

[1]*Department of Biomolecular Engineering, Kyoto Institute of Technology, Kyoto 606-8585, Japan*
[2]*The Nippon Synthetic Chemical Industry Co., Ltd., Osaka 567-0052, Japan*

E-mail: nishihara.yuuko@mp.nichigo.co.jp

Poly(vinyl alcohol) (PVA) is a well-known water soluble polymer, and it tends to form a stable emulsion in aqueous media. In the hydrophobic phase of the emulsion, the graft polymerization of monomer to PVA proceeds in the presence of ammonium persulfate (APS), as an initiator of the radical reaction. It has been postulated that the hydrogen atom at the methine carbon having hydroxyl group could be abstracted by the persulfate anion radical ($\cdot OSO_3^-$) derived from persulfate anion[1]. So far, however, molecular structure of the radical of PVA is still equivocal, since the life-time of the radical is too short to be detected by ESR spectroscopy. In this study, ESR spin-trapping measurements using DBNBS (3,5-dibromo-4-nitrosobenzene sulfonate) are performed for PVA and related diols (2,3-butanediol, 2,3BD) in order to clarify the structure of the carbon-centered radical of PVA, with the aid of newly developed LC-ESR[2] and LC/MS methods.

As shown in Fig. 1(a), ESR spectrum composed of doublet-triplet hyperfine structure (a(H) = 0.60, and a(N) = 1.29 mT) was observed for reaction mixture containing PVA, APS and DBNBS. Similar ESR spectrum (a(H) = 0.56, and a(N) = 1.33 mT) was also observed for 2,3BD treated by APS, as depicted in Fig. 1(b). By means of LC-ESR (data not shown) and LC/MS (Fig. 2) measurements, the molecular structure of the radical was assigned as methyl-ethyl-ketone radical adduct of DBNBS (m/z = 414.7). Possible radical reaction mechanism of PVA will be discussed by combination of results obtained from related diols.

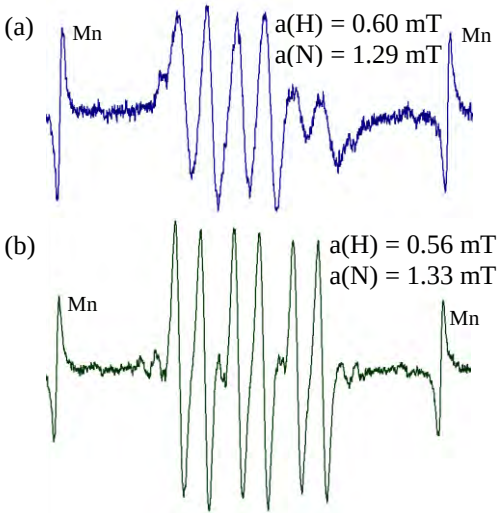

Fig. 1, ESR spectra of DBNBS spin adduct of (a) PVA and (b) 2,3BD in the presence of APS.

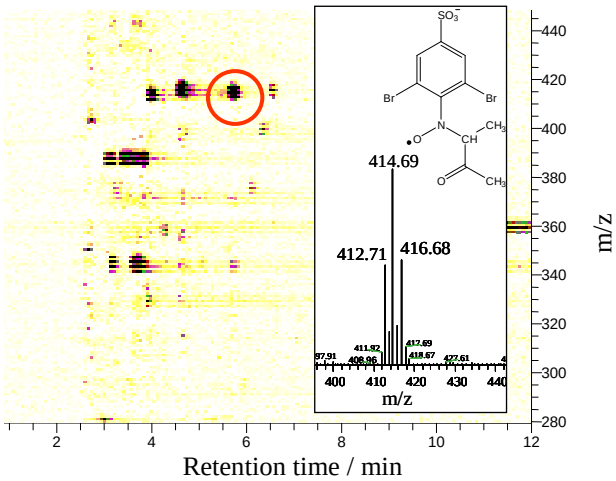

Fig. 2, LC/MS spectrum obtained from oxidation of 2,3BD by APS in the presence of DBNBS. Inset, Mass spectrum of methyl-ethyl-ketone radical adduct of DBNBS.

References

[1] Y. Ikada, Y. Nishizaki, I. Sakurada, "Reaction of Poly(vinyl alcohol) with Potassium Persulfate and Graft Copolymerization'', *J. Polym. Sci. Polym. Chem.*, **1974**, 12, 1829-1839.

1. Y. Sakurai, K. Kawai, R. Komatsu-Watanabe, C. Morimoto, S. Sakamoto, A. Nakajima, K. Kanaori, K. Tajima, "Development of a HPLC-ESR Spin-trapping System for Post-column On-line Detection of Superoxide Radical Scavenging Ability of Column Eluates", *Chem. Lett.*, **2009**, 38, 662-663.

P-35

Influence of plasma gas species on bacterial inactivation and reactive species production by plasma-bubbling

Toshihiro Takamatsu[1,2], Yosuke Watanabe[2], Hidekazu Miyahara[2], Yuriko Matsumura[3], Atsuo Iwasawa[3], Masahiro Kohno[3] and Akitoshi Okino[2]

[1] *Department of Gastroenterology, Kobe University, Kobe, Japan*

[2] *Department of Energy Sciences, Tokyo Institute of Technology, Yokohama, Japan*

[3] *Department of Bioengineering, Tokyo Institute of Technology, Yokohama, Japan*

E-mail: tplasma@med.kobe-u.ac.jp

Recent years, research of sterilization using atmospheric non-thermal plasma has attracted much attention in various fields because it has high processing ability at low temperature. Sterilization effect of plasma is considered to be obtained by oxidant stress by reactive species such as hydroxyl radical (HO・) and singlet oxygen ($^1O_2$). For sterilization in water, plasma is irradiated to bacterial suspension from above. Therefore, amount and kinds of reactive species introduced into water is limited because they depend on atmosphere. In addition, plasma gas species is deeply involved in the amount and kinds of reactive species as well. However, conventional plasma sources have limitation in applicable plasma gas species. In contrast, our multi-gas plasma jet (PCT-DMFJ02, Plasma Concept Tokyo) can generate stable plasma with various gases such as helium, argon, oxygen, nitrogen and their mixed gases. Thus, the various reactive species depending on the gas species could be produced.

In this study, to sterilize bacteria in water efficiently, we used a method to process liquid by plasma bubble using multi-gas plasma jet. In addition, to find the sterilization mechanism, the amount of reactive species generated by various gas plasmas was measured with electron spin resonance(ESR) spin trapping method. As shown Fig. 1, the outlet (1 mm in diameter) of the plasma souce is connected to the bottom of a water-filled container. Then the water was bubbled by the plasma. In this method, the plasma does not contact with atmosphere and so reactive species are transported to water directly. To verify sterilization effect of plasma-bubbling, the effect of bubbled water on *E. coli* and *B. safensis* was investigated. *B. safensis* is spore forming bacterium, and it has very high viability. *E. coli* or *B. safensis* in 200 mL normal saline was bubbled by oxygen(O_2), nitrogen(N_2), carbon dioxide(CO_2), air(N_2+O_2) and argon(Ar) plasma at 3 L/min gas flow rate. As shown in Fig. 2, with O_2, N_2, CO_2 and air plasma processing, *E. coli* was decreased 6-digit within 1, 3, 3 and 10 min respectively. On the other hand, with Ar plasma, the number of the *E. coli* was not changed. These results show that sterilization effect is different by plasma gas species. In the case of *B. safensis*, with oxygen, air and nitrogen plasma processing, it was decreased 5, 2 and 1digit within 10 min respectively. By taking time more than the case of *E. coli*, sterilization effect on *B. safensis* was obtained. To investigate the factor of sterilization, HO・ and $^1O_2$ in bubbled water were measured. 3 mL normal saline including 75 mM of 2,2,5,5-Tetramethyl-3-pyrroline-3-carboxamide (TPC) as $^1O_2$ detector or 100 mM of 5,5-Dimethyl- 1-pyrroline-N-oxide (DMPO) as HO・ detector was bubbled by plasma for 30 sec. The solution sample was measured by ESR. In the normal saline bubbled by O_2, N_2, CO_2, air and Ar, concentrations of $^1O_2$ were μM and 426, 10, 39, 64 and 2 μM, respectively. In terms of concentrations of HO・, N_2, CO_2 and Ar generated HO・ of 126, 3 and 19 μM, respectively. This result shows that $^1O_2$ and HO・ have possibilities of contributing to sterilization effect of plasma-bubbling.

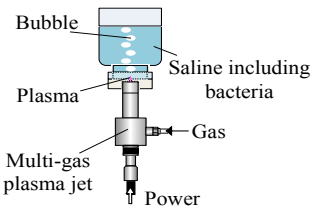

Figure 1: *Device configuration*

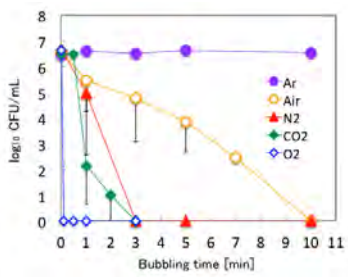

Figure 2: *Survival curve of E.coli*

P-36

Investigation of Reactive Species Generated by Various Gas Plasmas using ESR Spin Trapping Method

Yuriko Matsumura[1], Toshihiro Takamatsu[2,3], Kodai Uehara[3], Yota Sasaki[3], Hidekazu Miyahara[3], Atsuo Iwasawa[1], Masahiro Kohno[1] and Akitoshi Okino[3]

[1]*Department of Bioengineering, Tokyo Institute of Technology, Yokohama, Japan*

[2]*Department of Gastroenterology, Kobe University, Kobe, Japan*

[3]*Department of Energy Sciences, Tokyo Institute of Technology, Yokohama, Japan*

E-mail: matsumura@bio.titech.ac.jp

Atmospheric-pressure plasma shows strong industrial potential because it enables continuous treatment with high-density reactive species without the need for exhaust or pumping devices. Plasma processes have been studied in various fields including semiconductor processing, harmful gas decomposition, toxic degradation, and elemental analysis. In recent years, even heat-sensitive materials such as the human body have been treated with plasma, since argon and helium plasma can be generated at room temperature to 100 °C by nonequilibrium plasma. The use of nonequilibrium plasma has been confirmed to effectively inactivate bacteria, cause blood coagulation and kill cancer cells; therefore, these promising applications have attracted attention in medical fields. Since these effects are observed in the presence of water, discussions only in the case of reactive species generated in the gas phase are insufficient. The reaction of reactive species at the liquid surface is an important consideration. In particular, reactive species such as singlet oxygen, OH radicals, and NO radicals generated by plasma in liquid are considered to have a vital relationship to the mechanisms involved. Therefore, electron spin resonance (ESR) has been used to measure the reactive species generated in liquid[1]. However, conventional plasma sources are limited in their abilities to generate gas species. They can only generate air and argon plasmas, where argon plasma is relatively easy to generate. The reaction processes and production amounts of reactive species are not yet well verified. Our group succeeded in developing a multi-gas plasma jet, which can generate plasma from various gas species. Using this plasma source, reactive species can be investigated in detail, since they can be generated selectively by the supplied gas species. This study aims to clarify the relationships between the amount of reactive species and the gas species, and to consider the reaction process at the gas-liquid interface.

The multi-gas plasma jet can generate stable atmospheric plasma of various types of gas species such as argon, oxygen, nitrogen, carbon dioxide and air at low gas temperatures. The body of the device is grounded and an interior high-voltage electrode is connected to an AC power supply (Plasma Concept Tokyo, Inc.) of 16 kHz and 9 kV. The generated plasma flows through a 1-mm hole with a flow rate of 1 L/min. Each reactive species, which were generated by various gas plasma, reacts with individual spin-trapping agents, and the spin adducts can be identified using Electron Spin Resonance (ESR). The spin-trapping agents include 2,2,5,5-Tetramethyl-3-pyrroline-3-carboxamide (TPC) as the singlet oxygen detector, 5,5-Dimethyl-1-pyrroline-N-oxide (DMPO) as the OH radical and H radical detector, and N-methyl-D-glucamine dithiocarbamate iron (MGD-Fe) as the NO radical detector. These agents were dissolved in a phosphate-buffered saline (PBS)(-) solution, with a pH value of 7.5, and the concentrations of TPC, DMPO, and MGD-Fe were fixed at 75, 200, and 8 mM, respectively. The solutions were treated with various gas plasmas, and spin adducts was measured using ESR. As a result, carbon dioxide plasma generated the largest amount (90 μM) of singlet oxygen at 30 s, and argon-containing vapor gas plasma generated the largest amount (210 μM) of OH radicals. Among the homo-atomic gas species, nitrogen plasma generated the largest amount (130 μM) of OH radicals. In addition, H radicals were generated with argon, helium, and nitrogen plasmas. NO radicals were generated with nitrogen–oxygen plasma. Based on these results, the detailed production processes of reactive species will be presented.

References

[1] Sun Y., Yu S., Sun P., Wu H., Zhu W., Liu W., Zhang J., Fang J. and Li R., “Inactivation of Candida Biofilms by Non-Thermal Plasma and Its Enhancement for Fungistatic Effect of Antifungal Drugs,” PLoS ONE, **2012**, 7, e40629.

P-37

EPR in the Identification of Fe^{3+} Compounds and Free Radicals of Seeds

Bruna F. Gazzoni, Daniel F. Valezi, Felipe R. Benatti, Eduardo Di Mauro and Carmen L. B. Guedes.

Laboratório de Fluorescência e Ressonância Paramagnética Eletrônica (LAFLURPE), CCE, Universidade Estadual de Londrina, C.P. 10.011, 86057-970, Londrina, PR, Brazil

E-mail: carmen@uel.br

Paramagnetic species were characterized in the seeds of mustard, sorghum, sunflower, soybean, cotton, and maize by Electron Paramagnetic Resonance (EPR). Some iron complexes such as goethite (FeOOH), hematite (Fe_2O_3), magnetite (Fe_3O_4), and ferrihydrite ($Fe_5HO_8.4H_2O$), normally present in the soil[1], were also investigated by EPR, since their species can, a priori, be present in the seeds.

The EPR experiments were performed at X-band microwave frequency (9.3 GHz) on the JEOL spectrometer (JES-PE-3X) from 77 to 385 K and on the BRUKER spectrometer (Elexsys E-580) in a temperature range from 30 to 70 K, with the purpose of studying the thermal behavior of the species. In the EPR spectra of the seeds, it was detected the same complex of Fe^{3+} found in goethite, with g=2.0±0.2 in all the investigated seeds[2]. During the temperature variation, changes were observed in the spectra, in a manner that at low temperature (30 K), beyond the higher intensity on signal of the goethite, the spectra of the seeds also detected hematite in small quantities and traces of Mn^{2+}.

In addition, free radicals have also been detected with g=2.004±0.002, on all seeds, due to the unpaired electron interacting with the semiquinone[3,4]. The sunflower seeds showed the highest signal intensity of the free radical.

The goal of this research was to characterize and compare paramagnetic species present in the seeds. In the near future, biodiesel can be used in large scale and these paramagnetic species are of great importance, once they may be present in the vegetable oils, in all the industrial process of the biodiesel and possibly in the air as pollutants.

References [11 points, Times New Roman, bold]

[1] R.E. Siqueira, M.M. Andrade, D.F. Valezi, C.E.A. Carneiro, J.P.P. Pinese, A.C.S. Da Costa, D.A.M. Zaia, R. Ralisch, W. M. Pontuschka, C.L.B. Guedes, E. Di Mauro, "EPR, FT-IR and XRD investigation of soils from Paraná, Brazil", *Applied Clay Science* **2011**, 53, 1, 42-47.

[2] C.A. Ceretta, C. Bayer, D.P. Dick, L. Martin-Neto, L.A. Colnago, *"Fundamentos da matéria orgânica do solo: ecossistemas tropicais e subtropicais",* 1st edition, Gênesis. (1999) p. 293.

[3] M. Kikuchi, M.S. Hussain, N. Morishita, M. Ukai, Y. Kobayashi, Y. Shimoyama, "ESR study of free radicals in mango", *Spectrochim. Acta Part A*, **2010**, 75, 1, 310-313.

[4] R.G. Saifutdinov, L.I. Larina, T.I. Vakul'skaya, M.G. Voronkov, *"Electron paramagnetic resonance in biochemistry and medicine",* 1st edition, Plenum Publishers, (2001) 268 p

P-38

Recent Developments of Multi-Extreme THz ESR in Kobe

H. Ohta[1,2], S. Okubo[1], E. Ohmichi[2] , T. Sakurai[3] and S. Hara[3]

[1]*Molecular Photoscience Research Center, Kobe University, Kobe 657-8501, Japan*
[2]*Graduate School of Science, Kobe University, Kobe 657-8501, Japan*
[3]*Center for Supports to Research and Education Activities, Kobe University, Kobe 657-8501, Japan*

E-mail: hohta@kobe-u.ac.jp

We will present our recent developments of multi-extreme THz ESR in Kobe. THz ESR has several advantages such as the high spectral resolution, ESR measurements beyond the zero field splitting or the magnetic phase transition. Combining extreme conditions such as low temperature, high magnetic field, high pressure and micro-detection, the applications of THz ESR can be expanded. Specifications our multi-extreme THz ESR are the followings: 1) frequency region between 0.03 and 7 THz, 2) temperature region between 1.8 and 300 K [1], 3) magnetic field region up to 55 T using the pulsed magnetic field [1,2], 4) pressure region up to 2.7 GPa [3], 5) measurements of micro-meter size single crystal using a micro-cantilever [4], and magnetization detected ESR using SQUID magnetometer (SQUID ESR) [5]. Some applications will be also shown.

References

[1] H. Ohta, S. Okubo, K. Kawakami, D. Fukuoka, Y. Inagaki, T. Kunimoto and Z. Hiroi, *J. Phys. Soc. Jpn.*: 72, Supplement B pp. 26-35, **2003**; H. Ohta, M. Tomoo, S. Okubo, T. Sakurai, M. Fujisawa, T. Tomita, M. Kimata, T. Yamamoto, M. Kawauchi and K. Kindo: *J. Phys.: Conf. Series*: 51, pp. 611-614, **2006**

[2] H. Ohta, S. Okubo, N. Souda, M. Tomoo, T. Sakurai, T. Yoshida, E. Ohmichi, M. Fujisawa, H. Tanaka, and R. Kato, *Appl. Magn. Reson.*: 35, pp. 399-410, **2009**

[3] T. Sakurai, A. Taketani, T. Tomita, S. Okubo, H. Ohta, Y. Uwatoko, *Rev. Sci. Inst.*: 78, 065107/pp. 1-6, **2007**; T. Sakurai, T. Horie, M. Tomoo, K. Kondo, N. Matsumi, S. Okubo, H. Ohta, Y. Uwatoko, K. Kudo, Y. Koike, H. Tanaka, *J. Phys.: Conf. Series*: 215, 012184/pp. 1-4, **2010**

[4] H. Ohta, M. Kimata, S. Okubo, E. Ohmichi and T. Osada, *AIP Conference Proceedings*: 850 pp. 1643-1644 , **2006**; E. Ohmichi, N. Mizuno, M. Kimata and H. Ohta, *Rev. Sci. Instrum.*: 79, 103903/pp. 1-5, **2008**; E. Ohmichi, N. Mizuno, M. Kimata, H. Ohta and T. Osada, *Rev. Sci. Instrum.*: 80, 013904/pp. 1-5, **2009**; H. Ohta, E. Ohmichi, *Appl. Magn. Reson.*: 37, pp. 881-891, **2010**; E. Ohmichi, N. Mizuno, S. Hirano, H. Ohta, *J. Low Temp. Phys.*: 159, pp. 276-279, **2010**; Y Tokuda, S Hirano, and E Ohmichi, H. Ohta, J. Phys. Conf. 400, 032103/pp. 1-4, **2012**; E. Ohmichi, S. Hirano, H. Ohta, J. Mag. Res. 227, pp.9-13, **2013**.

[5] T. Sakurai, R. Goto, N. Takahashi, S. Okubo, H. Ohta, *J. Phys.: Conf. Series*: 334, 012058/pp. 1-4, **2011;** T. Sakurai, K. Fujimoto, R. Goto, S. Okubo, H. Ohta, Y. Uwatoko, *J. Mag. Res.* 233, pp.41-45 **2012**; K. Fujimoto, T. Sakurai, S. Okubo, H. Ohta, K. Matsubayashi, Y. Uwatoko, K. Kudo, Y. Koike, Appl. Mag. Res. 44, pp. 893-898, **2013**.

P-39

Improvement of sensitivity on parallel CW-EPR image acquisition system

Ayano Enomoto and Hiroshi Hirata

Division of Bioengineering and Bioinformatics, Graduate School of Information Science and Technology, Hokkaido University, North 14, West 9, Kita-ku, Sapporo, 060-0814, Japan

E-mail: a.enomoto@ist.hokudai.ac.jp

For fast image-acquisition of continuous wave (CW)-EPR and EPR imaging for wider area, we previously developed the surface coil array and demonstrated parallel data acquisition by multiplexing of EPR detection in the frequency domain [1]. Although the concept of the parallel data acquisition was proved, the signal-to-noise ratio (SNR) achieved by parallel signal acquisition was decreased to less than half of that under single-resonator feeding due to the saturation of the amplifier in RF bridge. However, a higher EPR signal intensity is desirable for applying parallel EPR imaging to *in vivo* animal measurements. The purpose of this work was to improve the sensitivity of EPR imaging in a parallel detection scheme. To achieve the higher sensitivity, we removed one of the amplifiers from RF bridge to prevent the saturation caused by a leakage of RF signal from the other channel. Moreover, to assess the feasibility of the parallel EPR imaging system for *in vivo* measurement, we demonstrate *in vivo* EPR imaging with a living mouse using the parallel EPR imaging method.

In our experiments, to investigate the effect of removing the saturated amplifier, the signal intensity and the SNR measured by EPR spectra after removal of the amplifier were compared to those before removing. EPR spectra were obtained both of when RF waves were fed to single resonator and both resonators simultaneously. A glass cell filled with 2 mM Tempone aqueous solution was used to obtain EPR spectra. In addition, we obtained three-dimensional (3D) EPR images of a phantom and a living mouse. The phantom was consisted of two quartz tubes placed in parallel with a gap of 6 mm. For *in vivo* EPR imaging, we scanned a subject mouse exogenously injected free radical molecules.

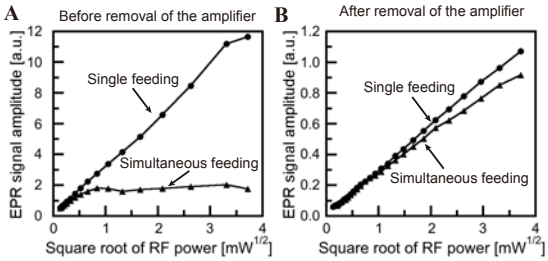

Fig. 1. Relation between the EPR signal intensity and the incident RF power when RF waves were fed to only one resonator or to both resonators simultaneously before and after removal of the amplifier.

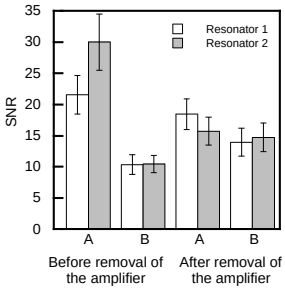

Fig.2. Comparison of SNR before and after removal of the amplifier under the same incident RF power (Error bar shows SD)
A: Single feeding
B: Simultaneous feeding

Figure 1 shows the relation between the EPR signal intensity and the square root of RF input power. From these results, the saturation of the signal amplitude was suppressed after removing the amplifier. Figure 2 shows the comparison of the SNRs measured when the same incident RF power was applied. After removing the amplifier, the SNR under the simultaneous RF feeding was not significantly decreased in comparison to the SNR before the amplifier was removed. Moreover, 3D EPR imaging with a phantom was performed. It was shown that improvement of the EPR signal intensity under the simultaneous feeding was achieved by removing the amplifier that was saturated.

Acknowledgement: This work was supported by Research Fellowship for Young Scientists (24-1486) from Japan society for the promotion of science (JSPS).

Reference

[1] A. Enomoto and H. Hirata, Parallel image-acquisition in continuous-wave electron paramagnetic resonance imaging with a surface coil array: Proof-of-concept experiments, *J. Magn. Reson.*, 239 (2014) 29-33.

P-40

Simulation of RF magnetic fields in Crossed loop resonators for 300 MHz Pulsed EPR

Tatsuya Ishii and Hiroshi Hirata

Division of Bioengineering and Bioinformatics, Graduate School of Information Science, Hokkaido University, North 14, West 9, Kita-ku, Sapporo 060-0814, Japan

E-mail: Tatsuya_0175@bme.ist.hokudai.ac.jp

In low-field pulsed electron paramagnetic resonance (EPR) imaging, a radio-frequency (RF) resonator is used to excite unpaired electrons and to detect EPR signals. After RF excitation of the RF resonator, the dead time of signal detection exists. Ringing down time of the resonator is one of the causes of the dead time. The crossed loop resonators, which consists of a transmit coil and a receive coil, can shorten the dead time and increase the sensitivity of signal detection because of reducing the RF power stored in the receive coil. To suppress mutual inductive coupling between two coils, it needs to cross the directions of RF magnetic fields in two coils orthogonally [1]. In this study, we report the distributions of RF magnetic fields in two coils and mutual coupling of the coils obtained by electromagnetic field simulation.

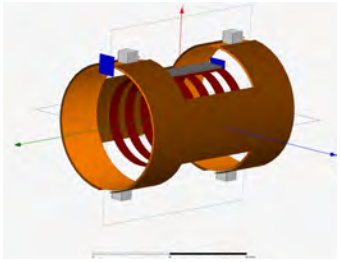

Fig. 1. Simulation model

The simulation model of the crossed loop resonators was made by 3-D electromagnetic wave simulator (HFSS, ANSYS, Inc.). The dimensions of the coils fit to mouse's legs. The transmit coil was Alderman-Grant (AG) coil, and the receive coil was the loop-gap resonator. To suppress electric coupling between two coils, the end rings were inserted between them [2]. Circuits for impedance matching and frequency tuning were designed in RF circuit design environment (Designer, ANSYS, Inc.). Figure 2A shows the magnetic field distribution of the loop-gap resonator when RF power of 100W at 300 MHz was applied to the AG coil. Figure 2B also shows the distribution of magnetic fields in the loop-gap resonator when the loop-gap resonator was fed. Since the direction of magnetic fields in the transmit coil was along the z-axis and that in the receive coil was along with the x-axis, the directions of magnetic fields in coils were orthogonal. We used scattering-matrix parameter S_{21} for investigating the isolation of two coils (Fig. 3). The resonator's quality factor (Q) was adjusted by overcoupling in the matching circuit and inserting dumping resisters in coils. We achieved the isolation of -36 dB between two coils in this simulation. Based on these results of electromagnetic wave simulation, we will physically assemble the prototype resonators for testing.

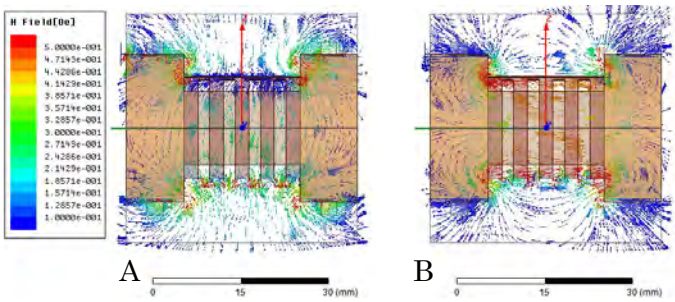

Fig. 2. Magnetic field distribution of crossed loop resonators

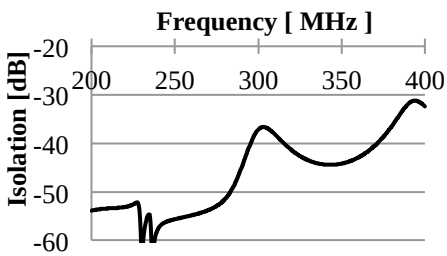

Fig. 3. Isolation of AG/loop-gap coils

Acknowledgements

We thank Drs. Murali C. Krishna and Shingo Matsumoto, NCI/NIH, for their helpful discussion.
This work was supported by JSPS KAKENHI Grant Number. 26249057.

References

[1] G. A. Rinard, R.W. Quine, G. R. Eaton, S. S. Eaton, *Concepts Magn. Reson.* **2002**, 15, 37-46.
[2] S. V. Sundramoorthy, B. Epel, H. J. Halpern, *J. Magn. Reson.* **2014**, 240, 45-51.

P-41

Bismuth Germanium Oxide as Perspective Material for Dielectric Resonators in EPR Spectroscopy

Mikhail Ivanov[1,2], Sergey Veber[1,2], Elena Bagryanskaya[1,2,3], Matvey Fedin[1,2], Vladimir Nadolinniy[4], Gennady Kuznetsov[4]

[1]*International Tomography Center, Novosibirsk 630090, Russia*

[2]*Novosibirsk State University, Novosibirsk 630090, Russia*

[3]*N.N. Vorozhtsov Novosibirsk Institute of Organic Chemistry, SB RAS, Novosibirsk 630090, Russia*

[4]*Nikolaev Institute of Inorganic Chemistry, SB RAS, Novosibirsk 630090, Russia*

E-mail: michael.ivanov@tomo.nsc.ru

Performance of microwave resonator along with microwave source and detector plays important role in the resulting sensitivity of modern electron paramagnetic resonance (EPR) spectrometer. Dielectric microwave cavities became very popular in X- and Q-band due to their compact size, relatively high filling and Q-factors and well space separated E and H components of the electromagnetic field. However, this type of resonators suffers from paramagnetic impurities and defects in dielectric materials which manifest themselves in undesirable background EPR signals. In case of continuous wave (CW) EPR the background signals complicate the analysis of EPR spectra and in some cases limit the resulting sensitivity of the spectrometer.

In this work we investigate bismuth germanium oxide (BGO) as a perspective material for dielectric EPR resonators. In order to compare the performance of BGO with well known sapphire material, we replaced the original sapphire ring by BGO ring in commercially available X-band dielectric resonator Bruker ER 4118 X-MD-5-W1. To avoid any modifications in the resonator itself during the test experiments, the BGO ring had almost the same dimensions as the original sapphire ring. In these conditions we have found that the BGO ring generates the TE_{012} cavity mode in the frequency range of X-band.

The analysis of the properties of two rings (BGO and sapphire) at 5-296 K temperature range revealed that the BGO ring has steeper temperature dependence of Q-factor and resonance frequency at 5-20 K compared to the sapphire ring. The standard "weak pitch" and $CuSO_4$ samples were used as sources of reference signal. At room temperature, the reduction of resulting s/n ratio by a factor of three in comparison with sapphire ring was observed. The disadvantage in sensitivity is expected to be solved in the future when the geometry of the BGO ring will be adjusted for generation of the standard TE_{011} cavity mode. Significantly weaker background signals in the whole temperature range for BGO ring compared to original sapphire ring is an important advantage of BGO material.

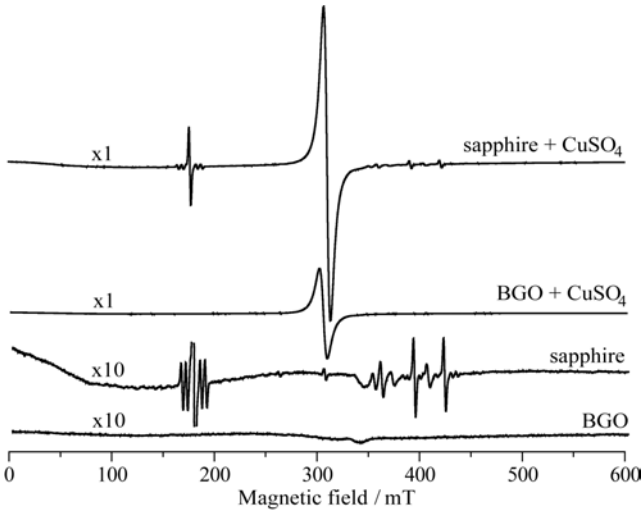

Acknowledgements: This work was supported by the Russian Foundation for Basic Research (Nos. 12-03-31396, 12-04-00737-a and 14-03-00224) and the RF President's Grant (MK-3241.2014.3 and MD-276.2014.3).

P-42

Quantitative Spin-trapping ESR Investigation of Alkoxyl Radical Thermally Derived from AAPH: Development of a Flow-injection Spin-trapping ESR System for the ORAC-ESR Assay

Akira Nakajima[1], Tomoko Yamaguchi[2], Tomoyuki Yamashita,[3] Naoto Yamamoto,[3] Kenji Kanaori,[3] and Kunihiko Tajima [3]

[1]*Frontier Science Research Center, University of Miyazaki, Kiyotake, Miyazaki 889-1692 Japan*
[2] *Venture Laboratory, Kyoto Institute of Technology, Matsugasaki, Sakyo-ku, Kyoto 606-8585 Japan*
[3]*Department of Biomolecular Engineering, Kyoto Institute of Technology, Matsugasaki, Sakyo-ku, Kyoto 606-8585 Japan*

E-mail: akanaka@med.miyazaki-u.ac.jp

The ORAC-fluorescein (FL) assay is a method of evaluating the radical-eliminating capacity of a substrate in the presence of 2,2'-azobis(2-amidino-propane) dihydrochloride (AAPH)-derived free radical and presents as the ORAC values [µmol 6-hydroxy-2,5,7,8-tetramethyl-chroman-2-carboxylic acid (Trolox) equivalent (TE)/g] [1]. The assay, being a non-stoichiometric method, has several demerits. To overcome these demerits, the ORAC-electron spin resonance (ESR) assay, which can evaluate the antioxidant ability as the competitive elimination reaction of the alkoxyl radical derived from AAPH, was developed [2]. As we used the optical irradiation for the produce of free radicals from AAPH, the formation of radicals through the electron transfer after the irradiation affects the kinetics studies on polyphenols, such as Trolox and (+)-catechin [2], the optical method for the alkoxyl radical formation from AAPH should not be adopted for the exact kinetic study of the alkoxyl radical. In this study, therefore, we conducted the quantitative spin-trapping ESR investigation of alkoxyl radical thermally derived from AAPH. We also examined the elimination ability of the radical by Trolox to establish a flow-injection (FI) spin-trapping ESR system for the ORAC-ESR assay.

The FI-ESR system is composed of a HPLC-pumps, a six-port injection valve equipped with a sample loop (inner volume: 200 µL), a micromixer, a syringe pump, a chromato-oven, an ice cooling vessel, and a flow-ESR flat cell. ESR spectra were recorded using an X-band spectrometer (JEOLRESONANCE, TE-100). The spin adduct was assigned to be the alkoxyl radical adduct of DMPO (DMPO/OR) from its hyperfine coupling constants for a nitrogen atom (a^N = 1.42 mT) and a proton (a^H = 1.48) [2]. The FI-ESR signal of the DMPO/OR was recorded by the time-sweep ESR mode by fixing the magnetic field to the top of the second low-field peak.

Spin-trapping reaction is presented as follows:

$$\bullet OR + \text{antioxidants} \rightarrow \text{products} \quad (1) \qquad \bullet OR + DMPO \rightarrow DMPO/OR \quad (2)$$

The second order kinetic constants are k_s and k_1 for eqs 1 and 2. The ratio of the kinetic constants is simplified as

$$k_s/k_1 = [DMPO]/[ID_{50}] \quad (3)$$

where ID_{50} is a median inhibitory dose of antioxidant for alkoxyl-radical-elimination. Solutions containing DMPO (20 - 75 mM) and Trolox (2.4 - 964 µM) were injected (200 µL) into the FI-ESR system. The ESR signal height of the DMPO/OR radical shows concomitant decrease with an increase in the Trolox concentration. The ratio of inhibition, defined as $Y = ([DMPO/OR]_s/[DMPO/OR]_c) \times 100$, is plotted against the [Trolox]. The obtained inhibitory plots shifted to the right with increasing $[DMPO]_0$, indicating that the ID_{50} values significantly varied as a function of the $[DMPO]_0$. From the ratio of $[DMPO]_0$ and ID_{50}, the value, k_s/k_1, for Trolox could be estimated as 0.348. Similar kinetic study of the alkoxyl-radical-elimination was conducted for other antioxidants.

References

[1] Cao G., Prior R.L., “Measurement of oxygen radical absorbance capacity in biological samples”, *Method in Enzymology*, 1999, 299, 50-62.

[2] Nakajima A., Matsuda E., Masuda Y., Sameshima H., .Ikenoue T., “Characteristics of the spin-trapping reaction of a free radical derived from AAPH: further development of the ORAC-ESR assay” *Analytical and Bioanalytical Chemistry*, **2012**, 403, 1961-1970.

P-43

Development of High Pressure Cyclotron Resonance System and Application to Dirac Fermion System

Ryosuke Matsui[1], Takahiro Sakurai[2], Susumu Okubo[3], Hitoshi Ohta[3], Reizo Kato[4], Masayuki Suda[4], Kazuyuki Matsubayashi[5], Yoshiya Uwatoko[5]

[1]*Graduate School of Science, Kobe University, Kobe 657-8501, Japan*
[2]*Center for Supports to Research and Education Activities, Kobe University, Kobe 657-8501, Japan*
[3]*Molecular Photoscience Research Center, Kobe University, Kobe 657-8501, Japan*
[4]*RIKEN, Hirosawa 2-1, Wako-shi, Saitama 351-0198, Japan*
[5]*Institute for Solid State Physics, University of Tokyo, Kashiwa, Chiba 277-8581, Japan*

Pressure as a physical parameter in the study of solid state physics is the few remaining frontier in physical instrumentation. Although many kinds of high-pressure ESR systems have been proposed since the first developed high-pressure ESR equipment in 1957 [1], most of them are limited to fixed frequency such as X-band due to using a special resonator in a pressure cell. Among them, we have developed the multi-frequency and high-pressure ESR system since 2001 [2]. Because the multi-frequency and high-field ESR is powerful method to observe a broad absorption line, ESR with a large zero-field gap, g-values of powder sample with very high-resolution, and so on [3]. In this paper, we will report recent development of our high-pressure ESR system using piston cylinder pressure cell and high-pressure magnetooptical measurements as its application. In our multi-frequency ESR system, transmitted electromagnetic wave through windows and the pistons of pressure cell is detected by InSb detector, which is located at bottom of cryostat. All the internal parts of this pressure cell are made by ZrO_2-Al_2O_3 ceramic, in which Al_2O_3 content affects significantly both its toughness and transmittance of electromagnetic wave. When we use the low Al_2O_3 content ceramic as the inner parts of the pressure cell, we achieve the highest pressure of 2.5 GPa while it loses transmittance significantly in the high-frequency electromagnetic waves more than 400 GHz [4]. On the other hand, for the pure Al_2O_3 ceramic, the transmittance is very high while the toughness is low. We optimize inner parts for the pressure and the transmittance by using both ceramics. The low Al_2O_3 content ceramic is used as the back up to which a load is directly applied and the pure Al_2O_3 ceramic is used for the piston. As a result, we succeed in not only expanding frequency to around 500 GHz but also obtaining the pressure up to 1.5 GPa. A zero-gap semiconducting state with a Dirac-cone-like linear dispersion has attracted much attention since discovery of that state in graphene. The Dirac fermion state is theoretically predicted to realize in the quasi two-dimensional organic conductor α-(BEDT-TTF)$_2$I$_3$ under the hydrostatic pressure more than 1.3 GPa [5]. Landau levels of the Dirac fermion system has a characteristic magnetic field dependence, which leads to the criteria of $\nu \propto B^{1/2}$ relation in the cyclotron resonance (CR). Very wide frequency measurements are required to confirm the criterion. Wide frequency CR measurements to α-(BEDT-TTF)$_2$I$_3$ under high pressure using new improved pressure cell will be reported.

References

[1] Walsh W. M. Jr. and Bloembergen N., "Paramagnetic Resonance of Nickel Fluosilicate under High Hydrostatic Pressure" *Phys. Rev.* **1957**, 107, 904-905.

[2] Ohta H., Okubo S., Sakurai T., Goto T., Kirita K., Ueda K., Uwatoko Y., Saito T., Azuma M., Takano M. and J. Akimitsu., "High-Frequency ESR Measurements Using Pulsed Magnetic Fields in Kobe", *Physica B* **2001**, 294-295, 624-629.

[3] Sakurai T., Fujimoto K., Goto R., Okubo S., Ohta H. and Uwatoko Y., "Development of high-pressure and high-field ESR system using SQUID magnetometer", *J. Magn. Reson.* **2012**, 41, 223.

[4] Fujimoto K., Sakurai T., Okubo S., Ohta H., Matsubayashi K., Uwatoko Y., Kudo K. And Koike Y., "Development of Hybrid-Type Pressure Cell for High-Pressure and High-Field ESR Measurement", Appl. Magn. Reson., **2013**, 44, 893-898.

[5] Katayama S., Kobayashi A. and Suzumura Y., "Pressure-Induced Zero-Gap Semiconducting State in Organic Conductor α-(BEDT-TTF)$_2$I$_3$ Salt", *J. Phys. Soc. Jpn.* **2006**, 75, 054705-6.

P-44

Development of High Pressure and Multi-frequency ESR System and Its Application to Quantum Spin System

Takahiro Sakurai[1], Ryosuke Matsui[2], Kohei Kawasaki[2], Susumu Okubo[3], Hitoshi Ohta[3], Kazuyuki Matsubayashi[4], and Yoshiya Uwatoko[4]

[1]*Center for Supports to Research and Education Activities, Kobe University, Kobe 657-8501, Japan*
[2]*Graduate School of Science, Kobe University, Kobe 657-8501, Japan*
[3]*Molecular Photoscience Research Center, Kobe University, Kobe 657-8501, Japan*
[4]*Institute for Solid State Physics, University of Tokyo, Chiba 277-8581, Japan*

E-mail: tsakurai@kobe-u.ac.jp

High pressure and multi-frequency ESR is a powerful means to study quantum spin systems. Recently, for the antiferromagnetically coupled S = 1/2 spin dimer system, a unique excitation mode was predicted to appear above the quantum critical pressure and it has attracted much attention since this mode is equivalent to the Higgs mode theoretically [1]. We have developed high pressure ESR system using the electromagnetic wave transmission type piston cylinder pressure cell so far [2, 3] and the system is expected to be a promising tool to observe this Higgs mode. In this paper, we show the current stage of our high pressure ESR system and its application to such spin dimer system.

Figure shows the schematic diagram of recently developed high pressure ESR system. The magnetic field is generated by a cryogen-free superconducting magnet whose maximum field is 10 T. Backward wave oscillator (BWO) and Gunn oscillator are used as the light sources and the transmitted light through the pressure cell is detected by InSb detector. The output signal of the detector is amplified by the lock-in amplifier and the optical modulation technique. The pressure cell is a piston cylinder type one whose inner parts are made of ZrO_2-Al_2O_3 ceramic. This ceramic has relatively good transmittance of electromagnetic wave at least up to 500 GHz. It also has toughness and we confirmed that the pressure reaches 1.5 GPa. A spin dimer system $KCuCl_3$, which is one candidate to show the Higgs mode under pressure, is considered to have the quantum critical point around 1 GPa and our high pressure ESR system is very suitable to observe this mode of $KCuCl_3$. We will show our high pressure ESR system in detail together with its application results to $KCuCl_3$.

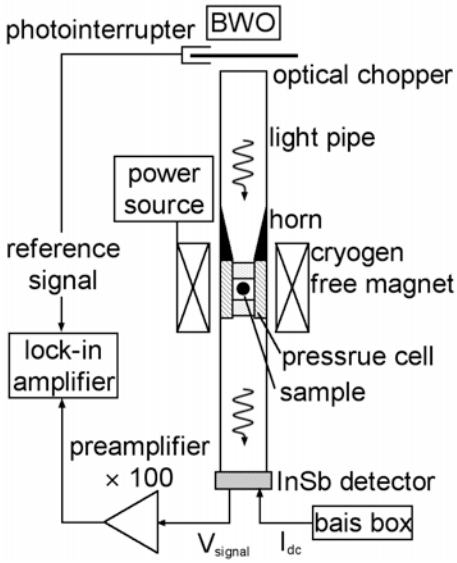

Fig. Schematic diagram of high pressure ESR system using electromagnetic wave transmission type pressure cell.

References

[1] Matsumoto M., Normand B., Rice T. M. and Sigrist M., "Field- and pressure-induced magnetic quantum phase transitions in $TlCuCl_3$", *Phys. Rev. B* **2004**, 69, 054423/1-20.

[2] Sakurai T., Takatani A., Tomita T., Okubo S., Ohta H. and Uwatoko Y., "Development of high-pressure, high-field and mulitifrequency electron spin resonance system", *Rev. Sci. Instrum.* **2007**, 78, 065107/1-6.

[3] Fujimoto K., Sakurai T., Okubo S., Ohta H., Matsubayashi K., Uwatoko Y., Kudo K. and Koike Y., "Development of Hybrid-Type Pressure Cell for High-Pressure and High-Field ESR Measurement", *Appl. Magn. Reson.* **2013**, 44, 893-898.

P-45

Development of high pressure ESR system using micro-coil

Kohei Kawasaki[1], Eiji Ohmichi[1] Takahiro Sakurai[2], Hitoshi Ohta[3], Susumu Okubo[3], Kazuyuki Matsubayashi[4], Yoshiya Uwatoko[4]

[1]*Graduate School of Science, Kobe University, Kobe 657-8501, Japan*
[2]*Center for Supports to Research and Education Activities, Kobe University, Kobe 657-8501, Japan*
[3]*Molecular Photoscience Research Center, Kobe University, Kobe 657-8501, Japan*
[4]*Institute for Solid State Physics, University of Tokyo, Chiba 277-8501, Japan*

E-mail: 141s106s@stu.kobe-u.ac.jp

Pressure can induce interesting physical phenomena through the change of the interaction between electrons. Although ESR is a powerful means to observe the spin states from the microscopic point of view, there are few ESR systems which cover the pressure region above 2 GPa and have enough sensitivity. Therefore, we have developed a new ESR system which achieves both of them in this study.

In order to achieve the pressure above 2 GPa, a hybrid type piston cylinder pressure cell is used. The cylinder consists of NiCrAl inner cylinder and CuBe outer sleeve, and it is known that this type of cylinder can exceed the upper pressure limit for a single layer cylinder (~ 2 GPa) and the maximum pressure is expected to be 4 GPa. The sensitivity can be improved by using micro-coil technique. Although the frequency region is limited up to 10 GHz, the sensitivity is expected to be higher than the cavity method because of high filling factor. The micro-coil is provides the rf field to sample and it is set so that the generating rf field is perpendicular to the external field as shown in Fig. 2 a). ESR signal is obtained by observing the reflection of circuit including the micro-coil under the field sweep at a certain frequency. This coil's length is 2.5 mm and diameter is 1 mm. The pressure calibration is one of the important points in the high pressure ESR system. The AC magnetic susceptibility measurement of Sn is used in this system, which is one of the most popular ways to calibrate the pressure. Figure 2 b) shows the schematic cross section of the coils for AC magnetic susceptibility measurement. The primary and secondary coils are used to pick up the signal and generate the AC magnetic field, respectively. DPPH was used for the test ESR measurements. The sensitivity was estimated to be 1.2×10^{12} spins/G and it is expected to be improved more by the field modulation and the lock-in technique. We will show the detail of the above development and several application results.

References

[1] H. Mahdjour, W. G. clark and K. Baberschke., "High-sensitivity broadband microwave spectr oscopy with small nonresonant coils", Rev. Sci. Instrum. **57** (1986) 1100.

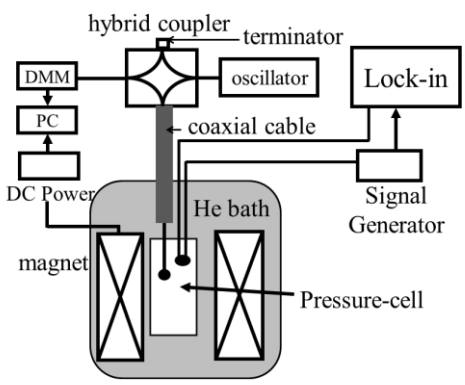

Figure 1. Schematic diagram of high pressure ESR system using micro-coil.

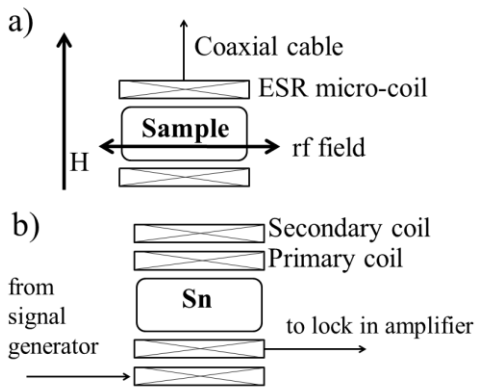

Figure 2. Schematic diagram of micro-coil for ESR measurement a) and AC magnet susceptibility measurement b).

P-46

Application of cantilever-detected ESR to biological systems

T. Okamoto[1], E. Ohmichi[1], and H. Ohta[2]

[1]*Graduate School of Science, Kobe University, Kobe 657-8501, Japan*
[2]*Molecular Photoscience Research Center, Kobe University, Kobe 657-8501, Japan*

144s104s@stu.kobe-u.ac.jp

High-frequency ESR (HFESR) technique is useful to understand microscopic properties of spin systems. In particular, high g-factor resolution and observations of broad ESR lines are unique features of HFESR. HFESR is often carried out with the so-called transmission-type technique. Multi-frequency experiments using the transmission technique allow spectroscopic studies of spin systems. However, such transmission techniques often suffer from low spin sensitivity due the lack of intense light sources. This situation makes biological applications of the technique difficult.

In order to overcome this difficulty, cantilever-detected ESR technique [1-3] will be a promising candidate. In this technique, a tiny sample is mounted on a microcantilever, and an electromagnetic wave is irradiated via oversized waveguide. Magnetization change associated with ESR absorption is sensitively detected as magnetic torque or field-gradient force acting on the sample. So far spin sensitivity as high as 10^{9} spins/G is achieved and multi-frequency ESR of μg-order sample was possible in the terahertz range of up to 370 GHz.

Recently we have developed a new ESR detection system based upon fiber-optic interferometry [4]. This technique is extremely sensitive and we succeeded in ESR detection of hyperfine splitting of Mn^{2+} impurities in MgO. Taking account of low spin concentration of Mn^{2+}<0.2 %, it is motivated to apply our cantilever-detected ESR technique to biological systems. So far large amount of sample is needed for HFESR of biological systems, but if small amount of such samples can be measured, it would have great impact in the research field.

In this study, first attempt was made to detect HFESR signals of biological systems using a microcantilever. Myoglobin was chosen as test sample in this study, since the sample can be easily obtained and a lot of literatures are available. So far, we succeeded in observing preliminary ESR results for myoglobin samples at 4.2 K and further experiments are now undertaken. In the presentation, we will report more detailed analysis of the ESR spectra and future prospects for biological systems are addressed.

References

[1] E. Ohmichi *et al*., “Magnetic detection of high-resolution electron spin resonance using microcantilever in the millimeter-wave region up to 240 GHz”, Rev. Sci. Instrum. **2008**, 79, 103903/1-7
[2] E. Ohmichi *et al*., “High-frequency electron spin resonance system using a microcantilever and a pulsed magnetic field”, Rev. Sci. Instrum. **2009**, 80, 013904/1-6.
[3] E. Ohmichi *et al*, “Design of in situ sample rotation mechanism for angle-dependent study of cantilever-detected high-frequency ESR”, J. Mag. Res. **2013**, 227, 9-13.
[4] Y. Tokuda *et al*., “Development of high-sensitivity cantilever-detected ESR measurement using a fiber-optic interferometer”, J. Magnetics **2013**, 18, 173-177.

P-47

Artifact suppression in electron paramagnetic resonance imaging of ^{14}N- and ^{15}N-labeled nitroxyl radicals with asymmetric absorption spectra

Wataru Takahashi[1], Yusuke Miyake[1] and Hiroshi Hirata[1]

[1]*Division of Bioengineering and Bioinformatics, Graduate School of Information Science and Technology, Hokkaido University, North 14, West 9, Kita-ku, Sapporo 060-0814, Japan*

E-mail: soyori_s63@bme.ist.hokudai.ac.jp

This study shows an improved method for suppressing image artifacts in the visualization of ^{14}N- and ^{15}N-labeled nitroxyl radicals in a single image scan using electron paramagnetic resonance (EPR) [1]. The purpose of this work is to solve the problem of asymmetric EPR absorption spectra in spectral processing. A hybrid function of Gaussian and Lorentzian lineshapes was used to perform spectral line-fitting to successfully separate the two kinds of nitroxyl radicals [2]. This approach can process the asymmetric EPR absorption spectra of the nitroxyl radicals being measured, and can suppress image artifacts due to spectral asymmetry.

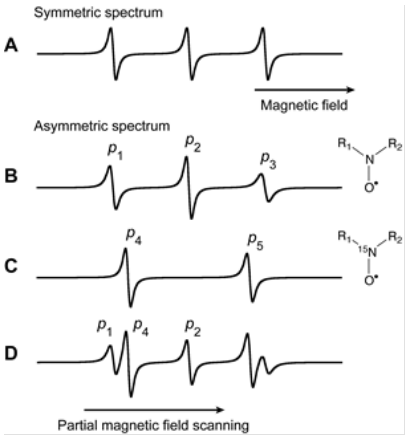

Fig. 1. First-derivative EPR absorption spectral lines of ^{14}N- and ^{15}N-labeled nitroxyl radicals. (A) symmetric spectrum of ^{14}N-labeled nitroxyl radical, (B) asymmetric spectrum of ^{14}N-labeled nitroxyl radical (R: tertiary-alkyl bulky group), (C) spectrum of ^{15}N-labeled nitroxyl radical, and (D) combined asymmetric spectra of ^{14}N- and ^{15}N-labeled nitroxyl radicals.

With this improved visualization method and a 750-MHz continuous-wave EPR imager, a temporal change in the distributions of a two-phase paraffin oil and water/glycerin solution system was visualized using lipophilic and hydrophilic nitroxyl radicals, i.e., 2-(14-carboxytetradecyl)-2-ethyl-4,4-dimethyl-3-oxazolidinyloxy (16-DOXYL stearic acid) and 4-hydroxyl-2,2,6,6-tetramethylpiperidine-d_{17}-1-^{15}N-1-oxyl (TEMPOL-d_{17}-^{15}N). The results of the two-phase separation experiment verified that reasonable artifact suppression could be achieved by the present method that deals with asymmetric absorption spectra in the simultaneous EPR imaging of ^{14}N- and ^{15}N-labeled nitroxyl radicals.

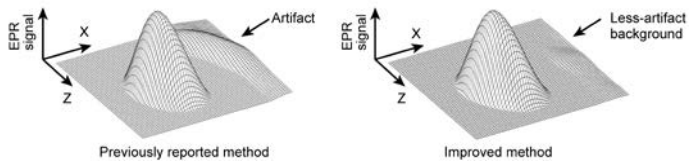

Fig. 2. Wire-mesh plots of the distribution of 16-DOXYL stearic acid in paraffin oil for the comparison of background artifacts obtained with the previously reported method (left) and the reconstructed distribution with the improved method (right).

Acknowledgments

This work was supported by grants from the Japan Society for the Promotion of Science (26249057 and NEXT program LR002 to H.H.).

References

[1] A. Pawlak, R. Ito, H. Fujii, H. Hirata, "Simultaneous molecular imaging based on electron paramagnetic resonance of ^{14}N- and ^{15}N-labelled nitroxyl radicals", *Chem. Commun.* **2011**, 47, 3245-3247.

[2] B.L. Bales, M. Peric M.T. Lamy-Freund, "Contributions to the Gaussian line broadening of the proxyl spin probe EPR spectrum due to magnetic-field modulation and unresolved proton hyperfine structure", *J. Magn. Reson.* **1988**, 132, 279-286.

P-48

Highly sensitive force detection system for high-frequency ESR measurement

Akiho Ishikawa[1], Eiji Ohmichi[1], Hitoshi Ohta[2]

[1]*Graduate School of Science, Kobe Univ.,Kobe 657-8501, Japan*
[2]*Molecular Photosciece Research Center, Kobe Univ., Kobe 657-8501, Japan*

130s104s@stu.kobe-u.ac.jp

Cantilever-detected ESR is a unique technique where a tiny sample on the order of less than 1 μg can be sensitively measured in the high-frequency region. In this method, a magnetic-field-gradient force acting on a sample is measured as cantilever bending. In this sense, in order to increase the sensitivity further, more sensitive force detection is important. Therefore, in this study, we develop a highly sensitive force sensor applicable to versatile experiments such as force detected ESR measurement.

In this study, Fabry-Perot interferometer was used for force detection. Fabry-Perot interferometer is composed of an optical fiber and a cantilever, and the optical fiber end and the cantilever surface form a cavity. A force acting on a sample on the cantilever produces the cantilever displacement, which in turn is measured by the difference in interference. The interference intensity is given as

$$I = I_0\left(1 - A\cos\frac{4\pi\lambda}{d}\right), \qquad (1)$$

Where d is the cavity length, λ is the wavelength, and I_0 and A are constants defined by the respective interferometers. In our setup, cavity length was adjusted at optimum positions with a frequency tunable laser instead of directly moving the fiber end.

A piezo-driven xy stage (Fig. 1) was developed for lateral alignment of the fiber end to the cantilever surface. This actuator is driven by a stick-and-slip motion of the slider on a sapphire rod, and is able to adjust the position with as small steps as 100 nm even at low temperatures.

Thermal vibrational spectrum of the cantilever measured by Fabry-Perot interferometer is shown in Fig. 2, where a peak is clearly observed at 5.2 kHz. This peak is attributable to the cantilever's eigenfrequency. Real-time force resolution is found to be 1 pN for a spring constant of 0.1 N/m. Details of our force det ection system will be presented in the presentation.

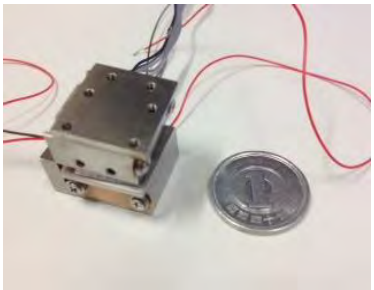

Fig. 1 Piezo-driven xy stage

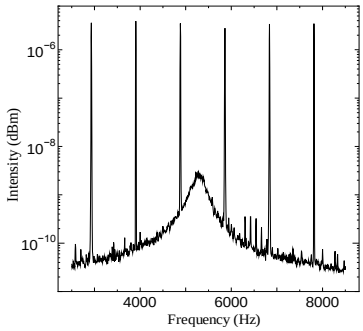

Fig. 2 Thermal vibrational spectrum of the cantilever

P-49

Time-Resolved Faraday Rotation Study on Photo-Excited Triplet State of Organic Molecule in Solutions

Tomoaki Yago and Masanobu Wakasa

Department of Chemistry, Graduate School of Science and Engineering, Saitama University, 255 Shimo-ohkubo, Sakura-ku, Saitama 338-8570 Japan

E-mail: yago@chem.saitama-u.ac.jp

The measurements of the Faraday rotation and the magnetic circular dichroism provide the detailed information on the electronic structures as well as the electron and nuclear spin states in materials [1]. Faraday rotation is a rotation of the plane of probe light after passing the materials in the presence of the magnetic field. In the Faraday rotation measurements, the direction of the magnetic field is parallel to the probe light propagating directions. The large Faraday rotation angles are observed in the presence of the strong magnetic field, the high spin polarizations, and the large spin-orbit coupling.

Chemical reactions can be interpreted as a change of the electronic structures in the reactant molecules. Since the Faraday rotation is sensitive to the electronic structure of the materials, the time-resolved Faraday rotation measurements may provide the useful information on the dynamics of the chemical reactions, which can not be accessed by the ordinal optical measurements such as transient absorption and fluorescence measurements. There are however a few reports on the time resolved Faraday rotation or magnetic circular dichroism measurements [2-5] due to the extremely small signal intensity in the experimental conditions in which the chemical reaction proceed.

In this contribution, we report the time-resolved Faraday rotation measurements on photo-excited triplet state of organic molecule in solutions. The observed time profile of the Faraday rotation signal originating from the photo-excited triplet state was different from that of the transient absorption. The results were interpreted with the change of the electronic structure of the photo-excited triplet state rather than the generation and relaxations of the electron spin polarizations in triplet state. We concluded that the time-resolved Faraday rotation detected the small change of the electronic structure of the chemical intermediate, which cannot be observed by the transient absorption measurements. The present study demonstrated that the time-resolved Faraday rotation measurement is a powerful tool to clarify the mechanism of the complex chemical reactions in solutions. In the presentation, solvents effects on the Faraday rotation measurements will be discussed.

References

[1] Mason W. R., "*A Practical Guide to Magnetic Circular Dichoroism Spectroscopy",* John Wiley & Sons, (2007).

[2] Goldbeck, R. A., Dawes, T. D., Milder S. J., Lewis J. W., and Kliger D. S., "Measurement of Magnetic Circular Dichroism (MCD) on a Nanosecond Timescale", *Chem. Phys. Lett*. **1989**, 156, 6, 545-549.

[3] Xie X., and Simon J. D. "Picosecond Magnetic Circular Dichoism Spectroscopy" *J. Phys. Chem*. **1990**, 94, 8014-8016.

[4] Lewis J. W., Goldbeck R. A., Kliger, D. S., Xie X., Dunn R. C., and Simon J. D. "Time-Resolved Circular Dichroism Spectroscopy: Experiment, Theory, and Application to Biological System", *J. Phys. Chem*. **1992**, 96, 5243-5254.

[5] Chen E., Goldbeck R. A., and Kliger D. S., "Nanosecond Time-Resolved Polarization Spectroscopies: Tools for Protein Reaction Mechanism", *Methods* **2010**, 52, 3-11.

P-50

Cantilever-detected ESR measurement using a frequency modulation technique

R. Tabuse[1], E. Ohmichi[1] and H. Ohta[1,2]

[1]*Graduate School of Science, Kobe University, Kobe 657-8501, Japan*
[2]*Molecular Photoscience Research Center, Kobe University, Kobe 657-8501, Japan*

E-mail: 132s111s@stu.kobe-u.ac.jp

Cantilever-detected ESR [1] is a novel technique to allow high-sensitive and high-frequency ESR measurement. There are several advantages such as high g-factor resolution, observation of broad ESR signal, and high spin sensitivity. Because the intensity of electromagnetic wave is substantially reduced above 100 GHz, it is of particular importance to improve the sensitivity of our cantilever-detected ESR measurement for practical applications in terahertz region. To this end, we develop a frequency modulation (FM) technique combined with Fabry-Perot detection system of the cantilever displacement.

Fabry-Perot detection system consists of an optical fiber and the cantilever. The fiber end and the cantilever surface play a role of a mirror. In standard Fabry-Perot interferometer, an actuator is needed to tune the cavity length at the optimum position where the highest sensitivity is obtained. Instead, a frequency-tunable laser was used in this study to tune the effective cavity length. With this improvement, experimental setup becomes compact and insusceptible to temperature drift and vibration. The real-time resolution is found to be as small as 10 pm. It is demonstrated that ESR signal of Mn^{2+} impurities in MgO, whose concentration was below 0.2 %, was observed at 4.2 K with our detection system.

In the FM mode, ESR signal is detected as eigenfrequency change of the cantilever. The detection scheme is based upon a phase-locked loop (PLL) circuit [2] which drives the cantilever at a constant amplitude. In this setup, the cantilever is excited at its eigenfrequency by a bimorph piezo, and cantilever displacement is monitored by the above-mentioned Fabry-Perot interferometer. It is expected that high Q-factors of a sample-loaded cantilever and highly stable PLL circuit improve the spin detection sensitivity. Figure 1 shows the preliminary result in the FM mode with the Fabry-Perot interferometer. In the presentation, details of the experimental setup and some results will be shown, in comparison with the amplitude detection scheme.

References

[1] E. Ohmichi *et al.*, “Magnetic detection of high-resolution electron spin resonance using a microcantilever in the millimeter-wave region up to 240 GHz”, Rev. Sci. Instrum. **2008**, 79, 103903/1-5.

[2] SangGap Lee *et al.*, “Magnetic resonance force microscopy in fast-relaxing spins using a frequency-modulation mode detection method”, Nanotechnology **2007**, 18, 375505/1-6.

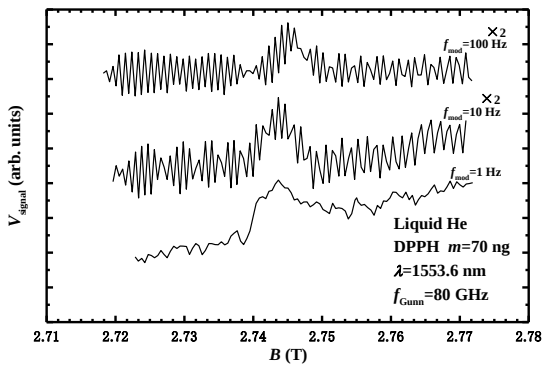

Fig. 1 : ESR signal of DPPH in FM mode with Fabry-Perot interferometer

P-51

Recent advances in cantilever-detected ESR technique

E. Ohmichi[1], R. Tabuse[1], A. Ishikawa[1], T. Okamoto[1] and H. Ohta[2]

[1]*Graduate School of Science, Kobe University, Kobe 657-8501, Japan*
[2]*Molecular Photoscience Research Center, Kobe University, Kobe 657-8501, Japan*

E-mail: ohmichi@harbor.kobe-u.ac.jp

Cantilever-detected ESR [1-3] is known as a novel technique of high-frequency and high-sensitivity ESR measurement. This technique has extremely high sensitivity to a tiny sample on the order of 10 μm, since the cantilever size is typically on the order of 100 μm. In addition, multi-frequency ESR measurement can be carried out in a similar manner to the transmission-type experiments. Therefore, it is expected in the future that cantilever-detected ESR technique can be applied to exotic spin systems such as nanomaterials or biomaterials for which conventional ESR techniques lack the sensitivity.

There are three types of detection modes in cantilever-detected ESR: torque, force and thermal. In the torque mode, which was first developed, ESR signal is obtained as a change of magnetic torque $\boldsymbol{\tau}=\boldsymbol{M}\times\boldsymbol{H}$. This method is useful for a single crystalline sample with anisotropic g factor, and high spectral resolution is obtained due to the absence of field gradient. In the force mode where field-gradient force $F=(\mathrm{d}B_z/\mathrm{d}z)M_z$ is measured, isotropic spin systems such as polycrystals can be measured, though the spectrum is broadened due the local field gradient. In the thermal mode, signals are obtained by thermal displacement of the cantilever caused by relaxation process. Appropriate detection modes are chosen depending on the measurement conditions and magnetic properties of a sample.

In order to increase the sensitivity, two remarkable improvements are recently achieved: fiber-optic detection [4] and customized cantilever fabrication [5]. We developed a detection technique of cantilever displacement based on fiber-optic-based Fabry-Perot interferometer. With use of a frequency-tunable laser, we constructed a compact ESR detection system. The real-time force resolution is as small as 1 pN, and various types of cantilevers can be mounted in this system. We also developed microfabrication technique of customized cantilevers for ESR measurement. Double-side processes are used to fabricate ultra-soft cantilevers with a thickness of 300 nm.

In the presentation, recent advances in cantilever-detected ESR technique are presented together with experimental results demonstrating the feasibility and high-sensitivity of our technique. Special attention was also paid to futuristic applications to biomaterials such as metal protein.

References

[1] E. Ohmichi *et al*., "Magnetic detection of high-resolution electron spin resonance using microcantilever in the millimeter-wave region up to 240 GHz", Rev. Sci. Instrum. **2008**, 79, 103903/1-7
[2] E. Ohmichi *et al*., "High-frequency electron spin resonance system using a microcantilever and a pulsed magnetic field", Rev. Sci. Instrum. **2009**, 80, 013904/1-6.
[3] E. Ohmichi *et al*, "Design of in situ sample rotation mechanism for angle-dependent study of cantilever-detected high-frequency ESR", J. Mag. Res. **2013**, 227, 9-13.
[4] Y. Tokuda *et al*., "Development of high-sensitivity cantilever-detected ESR measurement using a fiber-optic interferometer", J. Magnetics **2013**, 18, 173-177.
[5] E. Ohmichi *et al*., "Microfabrication of MEMS cantilevers for mechanically detected high-frequency ESR measurement", J. Magnetics **2013**, 18, 163-177.

P-52

Functional EPR imaging of isolated and perfused rat hearts: monitoring of tissue oxygenation and pH

Artem A Gorodetsky[1], Igor A Kirilyuk[2], Denis A Komarov[2]

[1]*Novosibirsk State University, Novosibirsk 630090, Russia*
[2]*Novosibirsk institute of Organic Chemistry, Novosibirsk 630090, Russia*

E-mail: dkomarov@nioch.nsc.ru

Ischemic heart disease is the most common type of cardiovascular disease. Deprivation of coronary blood flow results in critical changes in myocardial tissue microenvironment and can cause persistent damage to cardiomyocytes. Reperfusion of ischemic tissue is necessary to prevent myocardium from irreversible damage. However reintroduction of blood flow causes an additional damage to the tissue known as reperfusion injury. Myocardial oxygenation and pH play central roles in the pathology of ischemia and reperfusion and monitoring of these parameters is important for studying the mechanisms of injury and for development of new therapeutic strategies.

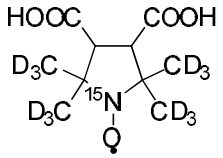

R1

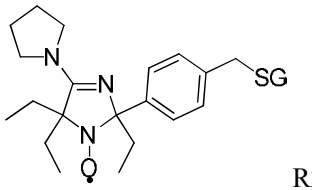

R2

EPR in low magnetic fields with application of exogenous paramagnetic probes provides a unique opportunity for noninvasive monitoring of microenvironment of living tissues and organs. In the present work we applied EPR imaging technique for visualization of myocardial oxygenation and pH during regional ischemia in isolated and perfused rat hearts. For EPR measurements of oxygen concentration a deuterated ^{15}N nitroxide radical (R1) was synthesized. The radical has peak-to-peak EPR linewidth 300 mG and sensitivity to oxygen concentration of about 50 mG/mM. We employed the radical as an oxygen sensitive spin probe for visualization of myocardial tissue oxygenation during ischemia and reperfusion. Isolated rat hearts were perfused directly in resonator of an L-band EPR spectrometer/imager with Krebs buffer containing the spin probe. Regional ischemia was initiated by ligation of left anterior descending coronary artery. A significant decrease in oxygen concentration was observed in the area at the risk during ischemia. After reperfusion the observed concentration of oxygen in the postischemic area was higher than preischemic level. For EPR monitoring of ischemia-induced myocardial acidosis we applied a previously developed pH-sensitive nitroxide radical (R2). A pH map of an isolated and perfused rat heart subjected to regional ischemia was obtained using the radical as a spin probe. The observed pH of normally perfused tissue was about 7.2 –7.4 while pH of ischemic area lowered down to 6.7 – 6.9.

In summary, this work demonstrated great capabilities of low-field EPR for noninvasive imaging of myocardial microenvironment. The applied spin probes revealed no cardiotoxicity and demonstrated good stability and functional sensitivity in myocardial tissue. The developed approaches may become a powerful tool for spatially-resolved measurements of pO_2 and pH of living tissues and organs by EPR imaging technique.

Acknowledgments: This work was supported by RFBR grant 13-04-01258.

P-53

Whole-body kinetic images of pyrrolidine redox probes by redox molecular imaging (ReMI)

Nuttavut Kosem[1], Fuminori Hyodo[1], Noppawan Phumala Morales[2], Kazuhiro Ichikawa[1], Keiji Yasukawa[3] and Hideo Utsumi[1]

[1]*Innovation Center for Medical Redox Navigation, Kyushu University, Japan*
[2]*Department of Pharmacology, Faculty of Science, Mahidol University, Thailand*
[3]*Department of Bio-Functional Science, Faculty of Pharmaceutical Science, Kyushu University, Japan*

E-mail: kosem_k@hotmail.com

Redox molecular imaging (ReMI) as a double resonance technique by coupling the advantages of MRI for spatial resolution and the sensitivity of EPR enables to visualize nitroxyl radicals as redox-sensitive probes in living animals. Redox probes were i.v. injected in female ddY mice (25 g body weight) and placed into a 15-mT ReMI with the following parameters: FOV, 85×85 mm; matrix, 64×64; pixel size, 0.63 × 0.63 mm; slice thickness, 50 mm; time of repetition (TR), 1100 ms; time of echo delay (TE), 25 ms; EPR irradiation time (TEPR), 500 ms; scanning time, 60 s; NMR frequency, 617 kHz; and EPR irradiation frequency, 220.6 MHz.

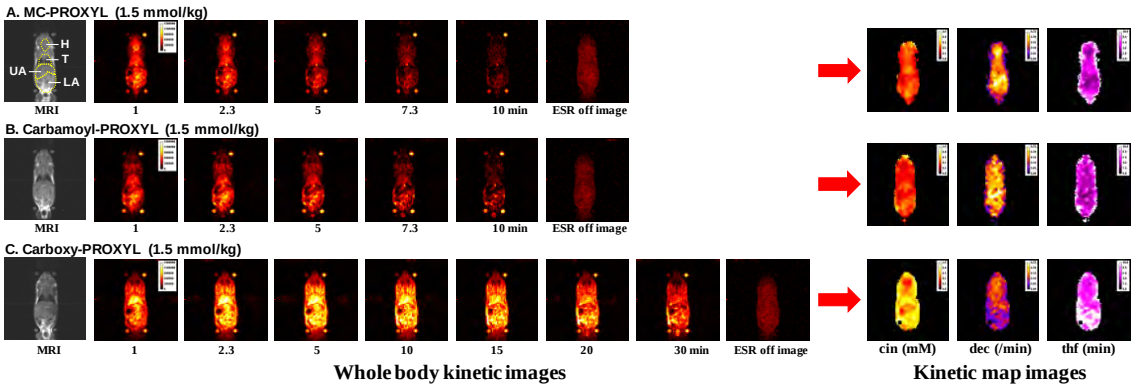

ReMI shows the unique whole-body kinetic images of MC-PROXYL, carbamoyl-PROXYL and carboxy-PROXYL depend on their lipophilicity and membrane permeability. The distribution of these probes was simultaneously visualized in various body regions. All probes initially distributed in the thoracic (T), upper (UA) and lower (LA) abdominal regions. Only MC-PROXYL with a blood-brain permeability penetrated into the brain of head region (H). Evaluated kinetic map images show that carboxy-PROXYL (a non-membrane permeable probe) possesses the highest concentration at time 0 (cin) in thoracic and abdominal regions with very low reduction rate (dec) and long half-life (thf), whereas carbamoyl-PROXYL (a partial membrane permeable probe) and MC-PROXYL (a high membrane permeable probe) show faster reduction rate and shorter half-life. Liver in the upper abdominal region is a main organ of reduction metabolism of all probes. However, the high reduction rate of MC-PROXYL was also observed in the brain. As a noninvasive imaging modality, ReMI allows us to understand and distinguish real-time kinetic behaviors of redox probes in different body regions that might be useful to directly estimate redox status of specific organs and tissues.

References

[1] Kosem N., Naganuma T., Ichikawa K., Morales N.P., Yasukawa K., Hyodo F., Yamada K. and Utsumi H., Whole-body kinetic image of a redox probe in mice using Overhauser-enhanced MRI. *Free Radic. Biol. Med.* **2012**, 53, 328-336.

[2] Utsumi H., Yamada K., Ichikawa K., Sakai K., Kinoshita Y., Matsumoto S. and Nagai M., Simultaneous molecular imaging of redox reactions monitored by Overhauser-enhanced MRI with ^{14}N- and ^{15}N-labeled nitroxyl radicals. *Proc. Natl. Acad. Sci. USA* **2006**, 99, 2216-2221.

P-54

Longitudinal ESR imaging of tumor oxygenation for cancer radiotherapy combined with the metabolic-targeted drug

Hironobu Yasui[1], Keita Saito[2], Naoya Nishida[1], Shingo Matsumoto[2], Tohru Yamamori[1], Murali C. Krishna[2] and Osamu Inanami[1]

[1]*Laboratory of Radiation Biology, Department of Environmental Veterinary Sciences, Graduate School of Veterinary Medicine, Hokkaido University, Sapporo 060-0818, Japan*
[2] *Radiation Biology Branch, Center for Cancer Research, National Cancer Institute, Bethesda, MD 20892, U.S.A*

E-mail: yassan@vetmed.hokudai.ac.jp

It is well-known that cancer cells rely on glycolysis for ATP production even in the presence of oxygen. Recently, there are continued interests in the drugs targeting this aerobic glycolysis in cancer therapy. We also demonstrated that dichloroacetate (DCA), a inhibitor of pyruvate dehydrogenase kinase, increased the radiosensitivity of cancer cells. In this study, we aimed to clarify the mechanism of DCA-induced radiosensitization in vitro, and to investigate whether this potent strategy can work in vivo focusing on the influence of DCA on tumor oxygenation status.

Real-time measurements of oxygen consumption rate (OCR: an indicator of mitochondrial respiration) and extracellular acidification rate (ECAR: an indicator of glycolysis) were performed by a XF24 Extracellular Flux Analyzer. Mice with squamous cell carcinoma SCCVII tumor were administered i.v. with 100 mg/kg DCA. For the combined treatment, X-irradiation was performed at 4 Gy in various timings. The spatial changes of partial pressure of oxygen (pO_2) was analyzed by pulsed electron spin resonance (ESR) imaging using triarylmethyl radicals [1].

DCA increased OCR and suppressed ECAR, suggesting the shift of cellular energy metabolism from aerobic glycolysis to mitochondrial oxidative phosphorylation. ESR imaging revealed that tumor pO_2 decreased for 4 h after DCA administration and recovered to preinjection levels after 10 h (Figure 1). Efficacy of radiotherapy was suppressed when X-irradiation was delivered during this DCA-induced transient hypoxia.

This result suggested that DCA induced development of hypoxia by modifying cellular metabolism, rendering negative influence on radiation effect. Longitudinal monitoring of tumor oxygenation by ESR imaging could provide the optimal timing for the combination of radiation and the metabolic-targeted drugs.

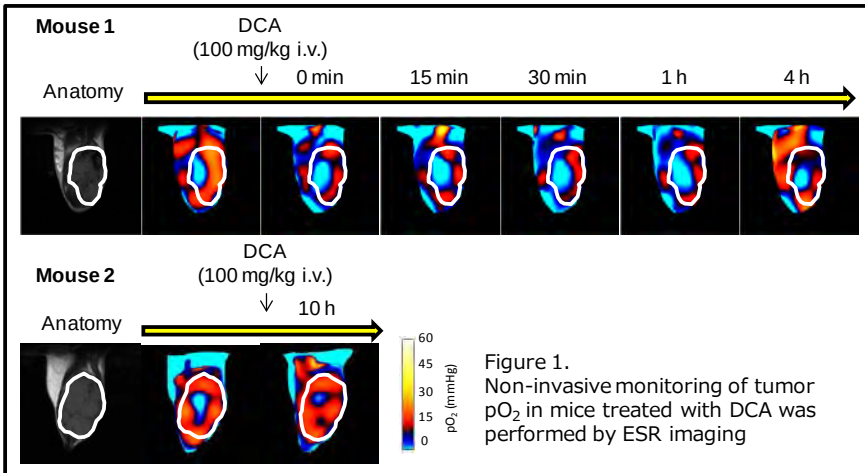

Figure 1.
Non-invasive monitoring of tumor pO_2 in mice treated with DCA was performed by ESR imaging

Reference

[1] Krishna MC., Matsumoto S., Yasui H., Saito K., Devasahayam N., Subramanian S. and Mitchell JB., "Electron paramagnetic resonance imaging of tumor pO_2", *Radiat Res* **2012**, 177(4), 376-386.

P-55

Time Course Analysis of Radiation Induced Alteration of Tissue Redox Status Using MR Redox Imaging

Mizuki Nakamura,[1,2] Sayaka Shibata,[3] Yoshikazu Ozawa,[3] Megumi Ueno,[2] Ken-ichiro Matsumoto,[2] Ken-ichi Yamada,[4,5] Tadashi Kamada,[1,2] and Ichio Aoki [3]

[1] Graduate School of Medical and Pharmaceutical Science, Chiba University, [2] Research Center for Charged Particle Therapy, National Institute of Radiological Science, [3] Molecular Imaging Center, National Institute of Radiological Science, [4] Faculty of Pharmaceutical Sciences, Kyusyu University, [5] PRESTO, Japan Science and Technology Agency

E-mail: nakami@fml.nirs.go.jp

Theranostics is being highlighted in fields of radiotherapy. Theranostics is a combination term of diagnostics and therapeutics, provides optimization of individualized medicine status based on the pathophysiological conditions. For cancer radiotherapy, theranostics is important for selection of efficient therapy and protection of normal tissues. Optimum timing of using radio protector or sensitizer with sufficient dose was required for a radiotherapy irradiating individual tissues. Time course of brain tissue redox status of normal mouse after X-ray and carbon-ion beam irradiation was studied.

Heads of mice were irradiated by 8 Gy X-ray or 16 Gy carbon-ion beam. The bragg peak was planned to hit cortex area. The mice were conducted to take a redox imaging 1, 2, 4, 8 days later from irradiation by 7 T MRI using T_1 weighted gradient echo. The decay rate of nitroxyl induced signal was analyzed. Non-irradiation mice were also taken redox imaging. This study used nitroxyl contrast agent, MC-PROXYL (3-Methoxycarbonyl-2,2,5,5-tetramethylpyrrolidine-1-yloxy) all experiments.

MC-PROXYL was immediately distributed in entire brain after injection and T_1-weighted signal enhancement increased both groups of irradiation and non-irradiation. It showed 2-phase decay curve, which has initial fast phase and later slow phase. Decay rate of fast phase (k) was not so different between cortex area and medulla area; however ventricle area showed slight slow decay rate k. Decay rate k was slightly faster in non-irradiated group than irradiated group. In addition, decay rate k was faster in entire brain 2 days after irradiation compare to that 1 day after irradiation. No clear difference was observed between X-ray and carbon-ion beam in this case.

The result suggested that redox status was changed by irradiation because decay curve of nitroxyl-induced T_1 signal had a difference between irradiated and non-irradiated groups. We will plan advanced experiments to consider changing redox status in tissues by irradiation X-ray and carbon-ion beam to mice.

P-56

Development of MRI probe linking with nitroxide

Tomonori Shirouzu[1], Toshihide Yamasaki[1], and Ken-ichi Yamada[1,2]

[1]*Department of Bio-functional Science, Faculty of Pharmaceutical Sciences, Kyushu University, Fukuoka 812-8582, Japan*
[2]*JST PRESTO, 4-1-8 Honcho, Kawaguchi, Saitama, 332-0012, Japan*

E-mail: yamada@pch.phar.kyushu-u.ac.jp

Nitroxides have been known to react with radical species and have been widely used to serve as antioxidants and spin probes in the biological fields. Especially nitroxides reacted with carbon centered radical and covalent bonding was formed[1]. The radical species are known to damage small molecule and protein to form repeatedly other radical species. These radicals produced *in vivo* are relevant with various diseases such as arteriosclerosis[2], and it would be useful to image these species for clinical prevention. Some of its detection method, fluorometry[3] and electron paramagnetic resonance[4], have been reported, however, these method had disadvantages in invasiveness and spatial resolution. Therefore we focused on 1) reactivity of nitroxides to form covalent bonding and 2) high spin number and many clinical application of Gd-complex, we designed MRI contrast agent probe for detection of radical species linking Gd-complex and nitroxides.

TEMPO derivatives and Gd-chelating agent were linked with alkyl chain spacer. To this compound, Gd ion was added and intended product was obtained, confirmed by HRMS. Its t_1 relaxivities (r_1) were measured in MRI. The r_1 value of Gd-complex with nitroxide probe was increased compared with nitroxide having no Gd-complex.We have already established the synthetic method of six-membered nitroxides. These nitroxides had various characteristics such as reactivity toward ascorbate and solubility. For example, 2-alkyl-2,6,6-trimethyl substituted TEMPO derivatives had low reactivity with ascorbate[5], also had high reactivity with lipid radical[6]. These nitroxides would be adequate in point of reactivity and hereafter would be linked with Gd-complex for optimization of MRI probe. This probe could detect the focus of disease accumulating radical molecule also terminate the radical chain reaction, thereafter it would also be useful for both early detection and therapeutic effect.

References

[1] Chateauneuf, J., Lusztyk, J., Ingold, K. U., “Absolute rate constants for the reactions of some carbon-centered radicals with 2,2,6,6-tetramethyl-1-piperidinoxyl”, *J. Org. Chem.* **1988**, 53, 1629-32.

[2] Esterbauer, H., Gebicki, J., Puhl, H., Juergens, G., “The role of lipid peroxidation and antioxidants in oxidative modification of LDL”, *Free Radic. Biol. Med.* **1992**, 13, 341-90.

[3] Wardman, P., “Fluorescent and luminescent probes for measurement of oxidative and nitrosative species in cells and tissues: Progress, pitfalls, and prospects”, *Free Radic. Biol. Med.* **2007**, 43, 995-1022.

[4] Herrling, T., Fuchs, J., Rehberg, J., Groth, N., “UV-induced free radicals in the skin detected by ESR spectroscopy and imaging using nitroxides”, *Free Radic. Biol. Med.* **2003**, 35, 59-67.

[5] Yamasaki T., Mito F., Ito Y., Pandian S., Kinoshita Y., Nakano K., Murugesan R., Sakai K., Utsumi H., Yamada K., “Structure-reactivity relationship of piperidine nitroxide: electrochemical, ESR and computational studies”, *J. Org. Chem.* **2011**, 76, 435-40.

[6] Yamasaki T., Ito Y., Mito F., Kitagawa K., Matsuoka Y., Yamato M., Yamada K., “Structural concept of nitroxide as a lipid peroxidation inhibitor”, *J. Org. Chem.* **2011**, 76, 4144-8.

P-57

EPR Spectroscopy and Oxygen Imaging for Evaluation of the Transient Induction of Tumor Hypoxia and Potentiation of Bioreductively Activated Hypoxia-activated Prodrug TH-302

Yoichi Takakusagi[1,2,3], Shingo Matsumoto[3], Keita Saito[3], Masayuki Matsuo[3], Shun Kishimoto[3], Jonathan W. Wojtkowiak[4], Robert J. Gillies[4], James B. Mitchell[3], Charles P. Hart[5] and Murali C. Krishna[2,3]

[1]*Incubation Center for Advanced Medical Science (ICAMS), Kyushu University, Fukuoka 812-8582, Japan*
[2]*CREST, Japan Science and Technology Agency (JST), Kawaguchi, Saitama 332-0012, Japan*
[3]*Radiation Biology Branch (RBB), Center for Cancer Research (CCR), NCI/NIH, Bethesda, MD 20892, USA*
[4]*H. Lee Moffitt Cancer Center and Research Institute, Tampa, FL 33612, USA*
[5]*Threshold Pharmaceuticals, South San Francisco, CA 94080, USA*

E-mail: takakusagi.y.452@m.kyushu-u.ac.jp

PURPOSE: TH-302 is a hypoxia-activated prodrug that is selectively activated within hypoxic regions in solid tumors when the redox-sensitive 2-nitroimidazole trigger is reduced to release the bromo isophosphoramide mustard effector moiety. The present study evaluated the oxygen-dependent redox-activation of TH-302 *in vitro* and the pyruvate-mediated potentiation of the therapeutic efficacy of TH-302 *in vivo* by transient induction of hypoxia.

EXPERIMENTAL DESIGN: Superoxide radicals, produced during redox cycling of TH-302 in enzymatic incubation at different oxygen levels, were monitored by electron paramagnetic resonance (EPR) spectroscopy. Pyruvate-induced transient hypoxia in murine SCCVII or human HT29 tumor-bearing mice (500-1500 mm^3) was monitored by *in vivo* EPR oxygen imaging. The potentiation of TH-302 was then evaluated using magnetic resonance imaging (MRI), immunohistochemical analysis and immunoblotting.

RESULTS: The redox cycling of TH-302, reflected by superoxide flux, was reduced substantially with decreasing oxygen levels. Drug incubations at different oxygen levels (0-21%) showed an inverse relationship with the hypoxic cytotoxicity ratio (HCR) on cell survival. *In vivo* EPR oxygen imaging and MRI showed that intravenously administrated pyruvate globally induced transient hypoxia 30 min after injection at all sizes of tumors tested, which was due to the enhancement of the mitochondrial respiration to consume excess cellular oxygen. Pretreatment of SCCVII tumor bearing mice with pyruvate 30 min prior to TH-302 administration, initiated with small sizes (~550 mm^3), significantly delayed tumor growth.

CONCLUSIONS: Our *in vitro* and *in vivo* studies showed that the efficacy of TH-302 is potentiated by pyruvate-induced transient hypoxia.

References

[1] Sun, J.D. *et al.*, *"Selective tumor hypoxia targeting by hypoxia-activated prodrug TH-302 inhibits tumor growth in preclinical models of cancer"*, *Clin Cancer Res* **2012**, 18, 758-770.
[2] Meng, F. *et al.*, *"Molecular and cellular pharmacology of the hypoxia-activated prodrug TH-302"*, *Mol Cancer Ther* **2012**, 11, 740-751.
[3] Duan, J.X. *et al.*, *"Potent and highly selective hypoxia-activated achiral phosphoramidate mustards as anticancer drugs"*, *J Med Chem* **2008**, 51, 2412-2420.
[4] Matsumoto, S. *et al.*, *"Low-field paramagnetic resonance imaging of tumor oxygenation and glycolytic activity in mice"*, *J Clin Invest* **2008**, 118, 1965-1973.

P-58

Combined EPR and Optical Imaging to Reveal Oxidative Stress and Microstructure in Human Atherosclerotic Plaques

Mikael Lindgren[1,2], Pål Ellingsen[1], Morten Kildemo[1], Magnus Lilledahl[1], Martin Hallbeck[3], Helene Zachrisson[4] and Håkan Gustafsson[5]

[1]*Department of Physics, Norwegian University of Science and Technology, Trondheim, Norway*
[2]*IFM-Department of Chemistry, Linköping University, Sweden*
[3]*Department of Clinical Pathology and Clinical Genetics, and Department of Clinical and Experimental Medicine, Linköping University, Linköping, Sweden.*
[4]*Department of Clinical Physiology, Division of Cardiovascular Medicine, and Department of Medical and Health Sciences, Linköping University, Linköping, Sweden.*
[5] *Department of Medical Technology (MTÖ), Radiation Physics, Department of Medical and Health Sciences, Linköping University, Linköping, Sweden*

E-mail: mikael.lindgren@ntnu.no

The development of atherosclerosis is driven by inflammation in combination with structural changes and aggregation of certain tissue, ultimately resulting in a plaque. There is an intricate interplay between the structural changes, characterized by the many different structures seen in a plaque, and the inflammation and ensuing cellular responses. To better understand the etiology of atherosclerosis it is necessary to have methods which elucidate the interplay between the structural and inflammatory features. The main aim of this study is to present the combination of electron paramagnetic resonance imaging (EPRI), which images the oxidative stress and compare this with modern optical imaging techniques that can reveal property and microstructure of a variety of biological tissue. Thus, we compare images mapping the inflammatory locations as detected by ROS trapping and EPRI [1] with images obtained from the adjacent sections as obtained by optical methods such as second harmonic generation (SHG), two-photon excitation fluorescence (TPEF) [2] and imaging based on transmission Mueller Matrix Ellipsometry (MME) [3]. The combined images reveal the presence and location of calcified regions, accumulation of cholesterol crystals within the section of the carotid artery. It is concluded that regions of high oxidative stress appears to be associated with regions of calcification and high concentration of cholesterol crystals, and that the combination of the optical and EPR imaging techniques appears to be useful for investigating the spatial and causal relationships between inflammation and structural modifications.

References

[1] Gustafsson, H., Hallbeck, M., Lindgren, M., Kolbun, N., Jonson, M., Engström, M., de Muinck, E. and Zachrisson, H.; Visualisation of oxidative stress in ex vivo biopsies using electron paramagnetic resonance imaging (EPRI). *Magnetic Resonance in Medicine* **2014**, In Press.

[2] Lilledahl, M. B., Haugen, O. A., de Lange Davies, C. and Svaasand, L. O., Characterization of vulnerable plaques by multiphoton microscopy. *J. Biomed. Opt.* **2007**, 12(4), 044005-. doi:10.1117/1.2772652

[3] Ellingsen, P. G., Lilledahl, M. B.; Aas, L. M. S., Davies, C. D. L. and Kildemo, M.; Quantitative characterization of articular cartilage using Mueller matrix imaging and multiphoton microscopy, *J. Biomed. Opt.*, **2011**, 16, 116002-.

Mechanosynthesis of the (α,β)-PbF_2 fine powders doped with rare-earth ions

I.A. Irisova, A. A. Rodionov, D. A. Tayurskii, and R. V. Yusupov

Kazan Federal University, 420008, Kremlevskaya 18, Kazan, Russia

E-mail: IAIrisova@kpfu.ru

Trivalent rare-earth (RE) ion doped β-PbF_2 single crystals have been extensively studied due to their optical properties and laser applications. Transparent glass-ceramics based on β-PbF_2 doped with Er^{3+} and Yb^{3+} are widely studied now as an alternative to bulk single crystals and glasses for optical applications. Glass-ceramics are much easier to be synthesized and to be shaped than single crystals while optical properties may be very similar to the latter [1, 2]. In order to understand better the optical properties of the glass–ceramics containing RE-doped β-PbF_2 nanocrystals, the situation that occurs in the bulk RE-doped single crystals should be clearly realized. However, papers [3, 4] devoted to β-PbF_2 crystals doped with Er^{3+} ions report on various results showing thus that β-PbF_2:Er is still not perfectly understood. Mechanochemical synthesis can serve as an alternative and effective way of embedding the RE ions into the crystal structure. Term "mechanoactivation" means the processes of changing the energetic state of a material under conditions of the mechanical energy delivery. Moreover, since PbF_2 has the same fluorite structure as MF_2 (M = Ca^{2+}, Sr^{2+} and Ba^{2+}), it is interesting to consider the problem of evaluating the generality of the observed previously phenomenon of mechanosynthesis of the fine powders doped with rare-earth ions [5].

In the present work using the EPR spectroscopy we show that in the course of mechanochemical doping of the (α- and β-) PbF_2 fine powders with Er^{3+} ions the impurity centers of single erbium ions with cubic and orthorhombic symmetry are formed. Investigations of the dependences of the EPR spectra intensities on particle size show that in β-PbF_2 impurities are distributed over the whole volume of the particles. Thus, the main mechanism of the mechanochemical doping of (α- and β-) PbF_2 fine particles with Er^{3+} ions is the mechanoactivated diffusion. We find that grinding of the β-PbF_2 leads to partial phase transformation from metastable cubic (β) to the equilibrium orthorhombic (α) phase of PbF_2. The anisotropic powder spectrum of Er^{3+} ions observed in the as-prepared mechanochemically doped PbF_2:Er^{3+} originates from the centers in the orthorhombic α-PbF_2 phase: after the annealing at 650^0C the majority of the α-phase present in the specimens is transformed to the cubic phase and only the spectrum of the cubic symmetry Er^{3+} centers is observed. Thus, we show that mechanochemical doping is an effective way of obtaining the RE-doped PbF_2, however the situation is more complicated than for CaF_2, SrF_2 and BaF_2 [5] due to the phase transformations.

References

[1] Dantelle G., Mortier M. and Vivien D., "EPR and optical studies of erbium-doped β-PbF_2 single-crystals and nanocrystals in transparent glass–ceramics", Phys. Chem. Chem. Phys., 2007, 9, 5591–5598.

[2] Dantelle G., Mortier M., Goldner Ph. and Vivien D., "EPR and optical study of Yb^{3+}-doped β-PbF_2 single crystals and nanocrystals of glass-ceramics", J. Phys.: Condens. Matter., 2006, 18, 7905–7922.

[3] Rodriguez V., Tikhomirov V., Mendez-Ramos J. and Seddon A. B., "The shape of the 1.55 μm emission band of the Er^{3+}-dopant in oxyfluoride nano-scaled glass-ceramics", Europhys. Lett., 2005, 69, 128-134.

[4] Mho S. and Wright J., "Site selective laser spectroscopy of defects in PbF_2, a superionic conductor", J. Chem. Phys., 1983, 79, 3962 - 3975.

[5] Irisova I., Rodionov A., Tayurskii D. and Yusupov R., "A study of mechanochemical doping of fluoride crystals with a fluorite structure by Er^{3+} ions via electron paramagnetic resonance spectra", Optics and Spectroscopy, 2014, 116, 5, 783–789.

P-60

Structural dynamics in a "breathing" metal-organic framework studied by Electron Paramagnetic Resonance of nitroxide spin probes

Alena M. Sheveleva,[1,2] Daniil I. Kolokolov,[3,2] Anton A. Gabrienko,[3] Alexander G. Stepanov,[3,2] Sergey A. Gromilov,[4] Inna K. Shundrina,[5] Renad Z. Sagdeev,[1] Matvey V. Fedin,[1] Elena G. Bagryanskaya [1,5]

[1]*International Tomography Center SB RAS, Institutskaya 3a, 630090, Novosibirsk, Russia*

[2]*Novosibirsk State University, Pirogova 2, 630090, Novosibirsk, Russia*

[3]*Boreskov Institute of Catalysis SB RAS, Lavrentiev av. 5, 630090, Novosibirsk, Russia*

[4]*Nikolaev Insititute of Inorganic Chemistry SB RAS, Lavrentiev av. 3, 630090, Novosibirsk, Russia*

[5]*N.N. Vorozhtsov Novosibirsk Institute of Organic Chemistry SB RAS, Lavrentiev av. 9, 630090, Novosibirsk, Russia*

E-mail: alena@tomo.nsc.ru

Metal−organic frameworks (MOFs) made up of clusters or chains of metal ions connected by organic linkers have been intensively studied over the past decade. Threedimensional (3D) porous frameworks, which may include 1D, 2D, and 3D channel systems, have intriguing structures, diverse topologies, and many potential applications, such as gas separation and storage, catalysis, ion exchange, microelectronics, health care, and so forth. Among others, a special interest has been drawn to flexible MOFs capable of reversible structural rearrangements ("breathing") under external stimuli, for example, temperature or guest−host interactions with adsorbed molecules. These are interesting and complex phenomena with many potential applications.

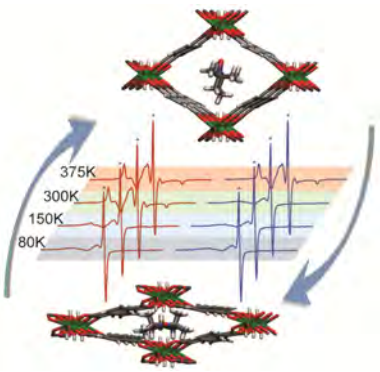

Figure 1. "Breathing" effect of MIL-53(Al) structure.

MIL-53(Al) built of the aluminum terephthalates is one of the impressive representatives of flexible MOFs, known to undergo temperature-induced structural transition with a significant hysteresis. The reversible changes occur between large-pore (LP) and narrow-pore (NP) crystalline states with the cell volumes being 1427.5(3) and 863.9(2) Å, respectively [1].

Due to the sensitivity limitations, most analytical methods require relatively high concentrations of guests in these studies. However, because guest molecules are not "innocent", breathing behavior may become suppressed and unperturbed structural states inaccessible. We propose here the use of guest nitroxide molecules in tiny concentrations (such as 1 molecule per 1000 unit cells), which serve as spin probes for electron paramagnetic resonance (EPR), for effective study of breathing phenomena in MOFs.

In this work, we investigate structural dynamics and guest−host interactions in MIL-53(Al) using multifrequency (9/34 GHz) EPR of nitroxide spin probes. We demonstrate the great advantage of this approach, which combines the use of tiny concentrations of probe molecules and high sensitivity of EPR and thus allows the investigation of unperturbed MOF structure and guest−host interactions in the breathing mode [2].

References

[1] Liu Y., Her J. H., Dailly A., Ramirez-Cuesta A. J., Neumann D. A., Brown C. M., *J. Am. Chem. Soc.,* (2008) pp 11813−11818.

[2] Sheveleva A.M., Kolokolov D.I., Gabrienko A.A., Stepanov A.G., Gromilov S.A., Shundrina I.K., Sagdeev R.Z., Fedin M.V., Bagryanskaya E. G., *J. Phys. Chem. Lett.,* (2014) pp 20−24.

P-61

Magnetostructural correlations for the $Ni^{2+}(^3A_2; S=1)$ ions

Muhammed Açıkgöz[1], Paweł Gnutek[2] and Czesław Rudowicz[2]

[1]*Bahcesehir University, Faculty of Art and Sciences, Beşiktaş, Istanbul, Turkey*
[2]*Institute of Physics, West Pomeranian University of Technology, Szczecin, Poland*

E-mail: macikgoz@bahcesehir.edu.tr

Two procedures may be employed for magnetostructural correlations for transition ions. The ***analytical*** procedure finds semiempirical relations between the zero-field splitting (ZFS) parameters (ZFSPs) determined by electron magnetic resonance (EMR) [1] and some structural ones [2]. The ***computational*** procedure models the ZFSPs using the microscopic spin Hamiltonian (MSH) approaches. For the $3d^8(^3A_2; S=1)$ ions at axial and orthorhombic sites three MSH approaches exist: (i) the higher-order perturbation theory (PT) of the MSH parameters, (ii) the crystal field (CF) analysis (CFA) within all $3d^8$ states combined with the superposition model (SPM) calculations [3,4] of CF parameters (CFPs), and (iii) the second-order PT of MSH parameters. These approaches were employed for $Ni^{2+}(S=1)$ ions in the Haldane gap system Y_2BaNiO_5 [5]. Here an extension of the study [5] is presented. First, a comparative analysis is carried out to assess the merit of each modeling approach. The contributions to the ZFSPs due to the spin-spin and spin-other-orbit interactions are considered using the approach (ii). The results indicate that the approach (i), after corrections, and (iii) may be employed only as an approximation. The approaches (i) - (iii) are applied for $Ni^{2+}(S=1)$ ions in Y_2BaNiO_5 and Nd_2BaNiO_5. Second, the SPM analysis of ZFSPs is considered. Due to the lack of proper intrinsic parameters (IPs) and the power law exponents, which differ from those in SPM/CFP analysis, we determine the IPs from experimental data on the uniaxial-stress parameters for Ni^{2+} ions in six-fold oxygen coordination [6]. The preliminary results of this study are presented together with applications of the so-determined IPs for the SPM/ZFSP calculations for Ni^{2+} ions at different sites.

In summary, the proposed tools for magnetostructural correlations may also enable better understanding of the spectroscopic properties of Ni^{2+} ions in other crystals as well as facilitate applications of high pressure and/or high-magnetic-field and high-frequency EMR (HMF-EMR) techniques [7] in studies of Haldane gap systems [8]. Additional motivation for this study arises from realization that the Ni^{2+}-based compounds may be suitable as high-pressure sensors for HMF-EMR measurements [9].

References

[1] Misra S.K., (Ed.), "*Multifrequency Electron Paramagnetic Resonance*", Wiley-VCH (2011).
[2] Titiš J., Miklovič J., Boča R., "Magnetostructural study of tetracoordinate cobalt(II) complexes", *Inorg. Chem. Commun*. **2013**, 35, 72-75.
[3] Andrut M., Wildner M., Rudowicz C., "*Optical absorption spectroscopy in geosciences. Part II, Quantitative aspects of crystal fields*", in A. Beran and E. Libowitzky (Eds) Spectroscopic Methods in Mineralogy, Vol. 6, Eötvös University Press, Budapest, Ch. 4, (2004), pp 145.
[4] Karbowiak M., Rudowicz C., Gnutek P., "Energy levels and crystal-field parameters for Pr^{3+} and Nd^{3+} ions in rare earth (RE) tellurium oxides $RE_2Te_4O_{11}$ revisited - Ascent/descent in symmetry method applied for triclinic site symmetry", *Opt. Mat*. **2011**, 33, 1147-1161.
[5] Rudowicz C., Gnutek P., Kimura S., Açıkgöz M., Yeung Y.Y., "Modeling Spectroscopic Properties of Ni^{2+} Ions in Y_2BaNiO_5", *Appl. Mag. Res*. **2013**, 44, 899-915.
[6] Siegel E., Muller K.A., "Structure of transition-metal-oxygen-vacancy pair centers", *Phys. Rev.* B **1979**, 19, 109-120.
[7] Sakurai T., Taketani A., Tomita T., Okubo S., Ohta H., Uwatoko Y., "Development of high-pressure, high-field and multifrequency ESR system", *Rev. Sci. Inst.* **2007,** 78, 065107-6.
[8] Mito M., et al. "Pressure Effects on an S = 1 Haldane Compound $Ni(C_5H_{14}N_2)_2N_3(PF_6)$", *J. Phys. Soc. Jpn.* **2003,** 72, 399-404.
[9] Ohta H. and Sakurai T., private communication (2012).

P-62

Temperature dependence of the structural, magnetic and vibrational properties of $KGd(WO_4)_2$ single crystal

S.M. Kaczmarek[2], G. Leniec[2], L. Macalik[1], J. Hanuza[1], A. Pietraszko[1], T. Bodziony[2], T. Skibiński[2]

[1] *Institute of Low Temperature and Structure Research PAS, Okólna 2, 50-422 Wrocław, Poland*

[2] *Institute of Physics, West Pomeranian University of Technology, Al. Piastów 48,*

70-311 Szczecin, Poland

skaczmarek@zut.edu.pl

Abstract

Crystal structure, magnetic and vibrational properties of $KGd(WO_4)_2$ single crystal in dependence on temperature were studied. EPR and Raman spectroscopy as well as crystallographic measurements were used. Results of the Raman and crystallographic measurements do not point out any structural transition up to 4 K. The EPR spectra of $KGd(WO_4)_2$ single crystal recorded in ***ab***, ***bc*** and ***ac*** planes in temperature range 8-300 K are broad and reveal a complex shape. We predicted existing of at least three asymmetric lines and the EPR spectrum of $KGd(WO_4)_2$ was well described by a superposition of the three lines using a relation:

$$\frac{d}{dB}P_{abs} \approx \frac{d}{dB}\sum_i \left(\frac{\Delta B + \alpha(B - B_{res})}{(B - B_{res})^2 + \Delta B^2} + \frac{\Delta B + \alpha(B + B_{res})}{(B + B_{res})^2 + \Delta B^2} \right) \qquad (1)$$

where B – applied magnetic induction, α describes the asymmetry of ESR line (anisotropy factor). P_{abs} is the power absorbed in the EPR experiment, ΔB is a linewidth, α<<1 represents an asymmetry parameter describing an admixture of dispersion, B_{res} is a resonance induction and the index i refers to the i-th line. Figures presented below show the full angular dependences of the resonance field, g-factor and a linewidth calculated in a temperature of 10,6 K for ***ab***, ***bc*** and ***ac*** planes, respectively.

Angular dependences of g-factors were analyzed using a standard relation:

$$g^2 = g_1^2 \cos^2(\theta + \delta) + g_2^2 \sin^2(\theta + \delta) \qquad (2)$$

where θ represents an angle between the magnetic field and crystallographic axis, δ is a tilting angle between a local symmetry axis and a crystallographic axis and $g_{1,2}$ represent extreme values of g-factors in a given plane. Parameters of g-factor and tilt for three of recognized centers are presented in Table.

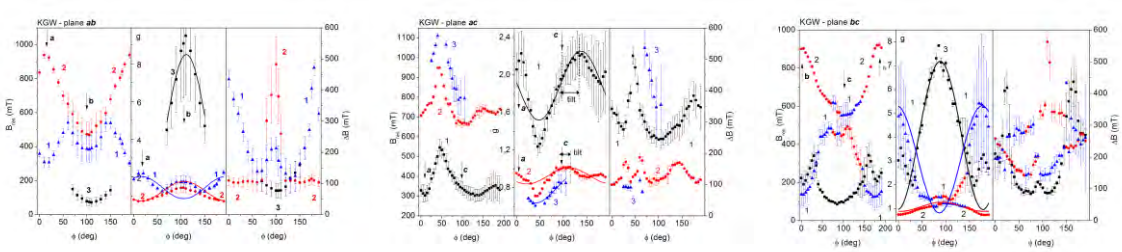

g-factor	Center No 1	Center No 2	Center No 3
g_x	1.86	0.71	0.65
g_y	0.85	1.77	7.83
g_z	1.28	7.18	0.82
tilt	42.6°	21.4°	-

P-63

EPR of phosphorus in diamond crystals. An influence of nitrogen impurity, HTHP treatment and high phosphorus concentration

V.A. Nadolinny[1], Yu.N. Palyanov[2,3], A,Yu. Komarovskikh[1], I.N. Kupriyanov[2,3]

[1]*Nikolaev Institute of Inorganic Chemistry SBRAS, Novosibirsk 630090, Russia,*
[2]*Sobolev Institute of Geology and Mineralogy SBRAS, Novosibirsk 630090, Russia,*
[3]*Novosibirsk State University, Novosibirsk 630090, Russia*

E-mail: spectr@niic.nsc.ru

The creation of semiconductor diamond devices is one of the important research directions in the field of diamond application. Many research groups working in this direction introduce phosphorus impurity in order to obtain *n* type conductive diamond, but up to the present there was no data about structure of phosphorus containing defects determining *n* type conductivity.

In our talk we present experimental data about the role of nitrogen impurity in the process of defect formation when phosphorus atoms are incorporated in diamond structure. In HTHP diamond crystals grown at 1600 ^{o}C, phosphorus atoms replace carbon atoms in the diamond lattice and organize MA1 paramagnetic centers. Spin density of unpaired electron of MA1 center is located mostly on the carbon atom separated by two carbon atoms from phosphorus atom. When annealing of as grown diamond at 1700 ^{o}C during two hours this center captures one nitrogen atom and creates nitrogen – phosphorus NP1 (NIRIM8) center. Nitrogen and phosphorus HFS parameters of this center are close to them of P1 and MA1 centers. Phosphorus and nitrogen atoms are separated in NP1 center by two carbon atoms. When annealing at 1800 ^{o}C NP1 center transforms into NP2 center containing nitrogen and phosphorus atoms separated by one carbon atom. At the next step of annealing at 1900 ^{o}C NP2 center transforms into NP3 center with close pair of phosphorus and nitrogen atoms in diamond lattice [1]. The electron spin of these three centers is equal to 1/2. And an experiment with electron irradiation has shown that substitutional nitrogen is a charge compensator of these centers. The experiment with electron irradiation gave direct evidence of N^- charge state of nitrogen in diamond. With the increasing of annealing temperature up to 2300 ^{o}C phosphorus atoms in the structure of NP1, NP2 and NP3 centers transform symmetry of nearest environment to octahedral one and produce three new NP4, NP5 and NP6 centers. These centers have HFS from one phosphorus atom and electron spin S=1/2. Differences of NP4, NP5 and NP6 centers are due to the different positions of nitrogen atoms in the defect structure [2].

The increasing of phosphorus concentration in diamond crystal produces new types of defects and new properties. EPR study of as-grown diamond crystals containing up to 1 weight % of phosphorus has shown the appearance of new NP8 and NP9 centers, containing one and two phosphorus atoms, and single line with Dyson shape. It means that in local domains of crystals the phosphorus energy levels degenerate into band and Dyson line characters the appearance of electron conductivity.

References

[1] Nadolinny V.A., Palyanov Yu.N., Kupriyanov I.N., Newton M.J., Kryukov E., Sokol. A.G., “A New EPR Data on the MA1 and NIRIM8 (NP1) Phosphorus-Related Centers in Synthetic 1b Diamonds”, *Appl. Mag. Res*. **2012**, V. 42, N 2, 179-186

[2] Nadolinny V.A., Pal’yanov Yu.N., Kalinin A.A., Kupriyanov I.N., Veber S.L., Newton M.J, “Transformation of As-Grown Phosphorus-Related Centers in HPHT Treated Synthetic Diamonds”, *Appl. Mag. Res*. **2011**, V. 41, 371-382.

P-64

Dipolar and Exchange Coupling in (bis-Salicylaldiminatothiocarbhydrazono-dicopper(II), A Sulphur Bridged Dimeric Copper(II) Complex

Rajendra BOSE Muthukumaran [1], Aditya P. Koley[2], Balaji Sambandam[3], and Periyakaruppan T. Manoharan[3]

[1] Department of Chemistry, Mizoram University, Aizawl, India; [2] Department of Chemistry, Birla Institute of Technology and Sciences, Goa, India ; [3] Sophisticated Analytical Instrumentation Centre, Indian Institute of Technology-Madras, Chennai, India.

Email: *rsic15@gmail.com*

Synthesis and the EPR spectroscopic investigations of the magnetic interactions of a Schiff base [1] dimeric copper complex, (bis-salicylaldiminatothiocarbhydrazono-dicopper(II), [Cu_2L], with a bridging sulphur ligand was undertaken. Variable temperature polycrystalline EPR studies of [Cu_2L] has indicated the presence of a weak ferromagnetic coupling (intramolecular interactions) between the copper(II) ions in the dimer. The EPR spectral data were simulated using a FORTRAN program based on the perturbation theory in the Zeeman representation [2]. In addition, EPR spectral analysis has also helped in understanding various types of interactions present in [Cu_2L]. The spin Hamiltonian parameters that were obtained from the EPR spectral simulation studies will be discussed.

Reference:

[1] Gupta, S., Pal, S., Barik, A. K., Hazra, A., Roy, S., Mandal, T. N., Peng, S.-M., Lee, G. H., Fallah, M. S. E., Tercero, J., and Kar, S. K., Synthesis, characterization and magneto-structural correlation studies on three binuclear copper complexes of pyrimidine derived Schiff base ligands, *Polyhedron*, (2008), **27**, 2519–2528.

[2] Smith, T. D. and Pilbrow, J. R., The determination of structural properties of dimeric transition metal ion complexes from EPR spetra, *Coord. Chem. Rev.*, (1974), **13**, 171-279.

P-66

ESR Signature of Metallic State in Semicrystalline conjugated Polymers Doped with Fluoroalkylsilane Molecules

Hisaaki Tanaka[1], Shun Watanabe[2] and Shin-ichi Kuroda[1,]

[1]*Department of Applied Physics, Nagoya University, Nagoya 464-8603, Japan*
[2]*Cavendish Laboratory, University of Cambridge, Cambridge CB30HE, United Kingdom*

E-mail: htanaka@nuap.nagoya-u.ac.jp

Conducting polymers (CPs) are promising candidates for active layers of organic devices such as organic transistors or solar cells. The electronic state of charge carriers in CPs is one of the key issues to be clarified. In particular, formation of the metallic state in semicrystalline CPs which are developed for the recent high-mobility transistors is a fascinating subject both in terms of scientific and technological points of view. Recently, a novel approach to achieve high p-type carrier doping in CP films has been proposed using fluoroalkylsilane (FTS) as a dopant [1]. Based on the efficient interfacial charge transfer between the CP and self-organized FTS layers, which is schematically illustrated in Fig. 1(a), highly conductive state of CPs is realized. In this study, we demonstrate that the highly FTS-doped semicrystalline polymer (PBTTT) exhibits a metallic nature within the crystalline grains having edge-on molecular orientations, which is clarified by using electron spin resonance (ESR) spectroscopy, combined with conductivity measurements [2].

The highly doped films exhibit the room temperature conductivity reaching as high as 50 S/cm, following two-dimensional variable-range-hopping model down to 4 K. These films exhibit clear ESR signals of π-electrons, which consist of two components as shown in Fig. 1(b); the major one arises from the crystalline domains with edge-on molecular orientation and the minor one from the flat-on oriented regions due to the FTS-induced disorder. These orientations are schematically shown in Fig. 1(c). Temperature dependence of the spin susceptibility (χ) has revealed that only the edge-on component exhibits temperature-independent Pauli spin susceptibility expected for metals, whereas the flat-on component follows the Curie law for localized polarons as shown in Fig. 1(d). The metallic nature of edge-on oriented regions is also confirmed from the prominent line broadening for higher temperatures as shown in Fig. 1(e), consistent with the Elliott mechanism for conduction electrons. The present results clearly demonstrate the correlation between the polymer crystallinity and the formation of the metallic state in semicrystalline CPs.

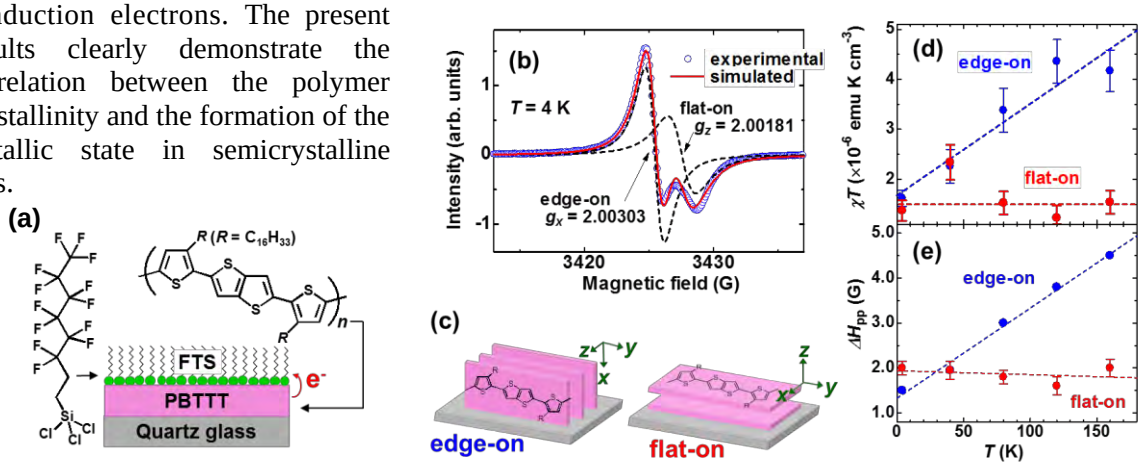

Fig. 1 (a) Schematic illustration of FTS doping on PBTTT films. (b) ESR spectrum of the doped film obtained at 4 K with the external field perpendicular to the substrate. (c) Schematic illustration of the edge-on and flat-on orientations. (d) Temperature dependence of the spin susceptibility (χT vs. T plot) and (e) that of peak-to-peak linewidth obtained for each orientation components.

References

[1] Kao C. Y. et al., *Adv. Funct. Mater.* **2009**, 19, 1906-1911.
[2] Tanaka H., Hirate M., Watanabe S., and Kuroda S., *Adv. Mater*. **2014**, 26 2376-2383.

P-68

High frequency ferromagnetic resonance study of Heusler compounds using a micro-cantilever

Alexey Alfonsov[1], Eiji Ohmichi[2], Ahmad Omar[3], Sabine Wurmehl[3,4], Berndt Büchner[3,4], Brian Peters[5], Fengyuan Yang[5], Hitoshi Ohta[1,2]

[1]*Molecular Photoscience Research Center, Kobe University, Kobe 657-8501, Japan*
[2]*Graduate School of Science, Kobe University, 1-1 Rokkodai-cho, Nada, Kobe 657-8501, Japan*
[3]*Leibniz Institute for Solid State and Materials Research Dresden, IFW, D-01171 Dresden, Germany*
[4]*Institut fur Festkörperphysik, Technische Universität Dresden, D-01062 Dresden, Germany*
[5]*Department of Physics, The Ohio State University, Columbus, Ohio 43210, USA*

E-mail: a.alfonsov@ifw-dresden.de

Heusler alloys have attracted a considerable attention in recent years since they are predicted to be halfmetallic ferromagnets. Possible 100% spin polarization of their conduction electrons together with high magnetic moments and high values of the Curie temperature give them a significant potential for spintronics applications, namely as the spin injection devices, read heads, magnetic random access memory etc. In order to create a fast switching and thermally stable spintronic device one should be able to control a magneto-crystalline anisotropy and a Gilbert damping of the used material. On one hand the anisotropy together with the saturation magnetic moment has to be small in order to reduce the critical current density [1], but on the other hand the anisotropy has to be big enough to ensure that the direction of the magnetization is thermally stable [2]. The viscous Gilbert damping mechanism has its microscopic origin in the spin–orbit interaction, which couples the spin to the lattice. If we consider the device with fast switching of the magnetization, then the Gilbert damping will play a major role in the change of the magnetization direction. In order to create materials with properties suitable for the fast switching one has to minimize this damping [3]. One of the most informative experimental methods to study magneto-crystalline anisotropy and Gilbert damping is frequency tunable ferromagnetic resonance (FMR). Here the resonance field of the FMR line gives information about the magneto-crystalline anisotropy and the linewidth provides information about Gilbert damping [4]. In this work we present a first study of magneto-crystalline anisotropy and Gilbert damping using a unique high frequency FMR technique where the response is detected by the micro-cantilever. Its high sensitivity, possibility to perform experiments at different microwave frequencies and in high magnetic fields together with the ability to change the angle between the sample and magnetic field makes this technique a promising tool for accessing magneto-crystalline anisotropy and Gilbert damping.

References

[1] Yilgin R., Sakuraba Y., Oogane M., Mizukami S., Ando Y. and Miyazaki T., "Anisotropic intrinsic damping constant in epitaxial Co_2MnSi Heusler alloy films", *Japanese Journal of Applied Physics* **2007,** 46, L205.

[2] Balke B., Fecher G. H., Winterlik J. and Felser C., "Mn_3Ga, a compensated ferrimagnet with high Curie temperature and low magnetic moment for spin torque transfer applications", *Appl. Phys. Lett.* **2007,** 90, 152504.

[3] Slonczewski J. C., "Current-driven excitation of magnetic multilayers", *J. Magn. Magn. Mater.* **1996**, 159, L1.

[4] Farle M., "Ferromagnetic resonance of ultrathin metallic layers", *Rep. Prog. Phys.* **1998**, 61, 755.

EPR and Magnetic Investigations of Nanoparticles of Colossal Magnetodielectric La_2NiMnO_6

K. S. Bhagyashree, **S. Ranjeet, and S. V. Bhat**

Department of Physics, Indian Institute of Science, Bangalore-560012, India

bhagyashree@physics.iisc.ernet.in

The double perovskite La_2NiMnO_6 (LNMO) has attracted significant, recent scientific interest due to its near room temperature ferromagnetism[1] (T_C ~ 280 K) and colossal magnetodielectricity (MD)[2], properties important for device applications such as capacitive magnetic field sensors and tunable high frequency filters. The role of antisite disorder[2] and possible extrinsic origin of the MD effect[3] are focus of attention in literature on LNMO. An early electron paramagnetic resonance (EPR) study[4] showed the presence of short range ferromagnetic ordering in bulk samples of LNMO up to a temperature as high as 390 K. In this work we report results of our EPR and magnetic studies on nanoparticles of LNMO. The EPR behavior of the nano LNMO is found to be quite different from that of the bulk sample.

Nano particles of La_2NiMnO_6 were prepared by the citrate-gel method starting with highly pure (> 99.9%) $La(NO_3)_3$, $Ni(NO_3)_2$ and $MnCO_3$ converted into the corresponding nitrate, in stoichiometric ratio. A final annealing at 600^0 C gave particles of the size d ~ 12 nm. The powder XRD pattern recorded at room temperature was fitted to an orthorhombic (Pbnm) structure. Dc magnetization measured using a SQUID magnetometer in the temperature range 5 – 300 K showed that the nanoparticles had a lower T_c (~ 200 K) and a slightly reduced magnetization.

EPR experiments were carried out on a sample consisting of loosely packed nanoparticles using a commercial X-band EPR spectrometer in the temperature range 5 – 300 K. A few typical EPR signals are presented in the inset to figure 1. Main panel of Fig. 1 shows the temperature dependence of the resonance field H_0 and figure 2 that of the linewidth. Inset to Fig. 2 presents the dependence of resonance field shift δH_0 ($H_0(RT) - H_0(T)$) on the linewidth ΔH_{pp} in the light of Nagata-Ishihara phenomenological theory[5] according to which δH_0 should vary as the third power of ΔH_{pp} for randomly distributed nanoparticles. We obtain a slope of 3.44 for the slope which is considerably higher than the expected value. We discuss this difference in terms of possible effects of magnetic anisotropy.

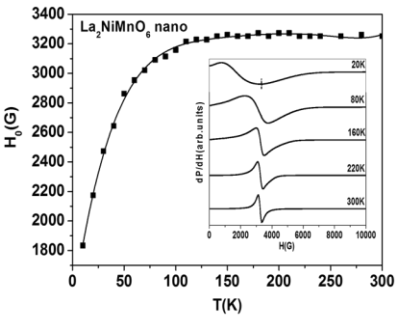

Fig.1: Temperature dependence of resonance field; line is a guide to the eye inset: a few typical ESR signals

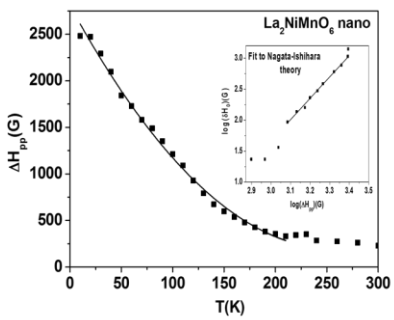

Fig.2: Temperature dependence of peak to peak linewidth; line is a guide to the eye; inset: log-log fit to linewidth dependence of δH_0

References

1. N. S. Rogado, Jun Li, A. W. Sleight, M. A. Subramanyan, "Magnetocapacitance and magnetoresistance near room temperature in a ferromagnetic semiconductor: La_2NiMnO_6", *Adv. Mater.* **2005**,17, 2225
2. D. Choudhury et al. "Near room temperature colossal magnetodielectricity and multiglass properties in partially disordered La_2NiMnO_6" *Phys. Rev. Lett*. **2012**, 108, 127201
3. K Devi Chandrasekhar, A K Das, A Venimadhav, "Spin glass behaviour and extrinsic origin of magnetodielectric effect in non-multiferroic La_2NiMnO_6 nanoparticles", *J. Phys.: Condens. Matter*, **2012**, 24, 376003
4. Shiming Zhou, Lei Shi, Haipeng Yang, and Jiyin Zhao, "Evidence of short-range magnetic ordering above *TC* in the double perovskite La_2NiMnO_6", *Appl.Phys.Lett*, **2007**, 91, 172505
5. K. Nagata and A. Ishihara "ESR of ultrafine magnetic particles", *JMMM*, **1992**, 104-107, 1571

Effect of Size Reduction on Magnetic Ordering in $Sm_{1-x}Ca_xMnO_3$ (x = 0.35, 0.65 and 0.92) Manganites: Magnetic and EMR Studies

Lora Rita Goveas[1,3], K. S. Bhagyashree[2], Anuradha K.N.[1], S.V.Bhat[2]

[1]*Department of Physics, Dr. Ambedkar Institute of Technology, Bangalore-560056, India*
[2]*Department of Physics, Indian Institute of Science, Bangalore-560012, India.*
[3]*St. Joseph's College of Arts and Science, Bangalore-560027, India*
Email:loragoveas@gmail.com

It is well known that electron magnetic resonance (combining ferromagnetic resonance in the ferromagnetic phase and electron paramagnetic resonance in the paramagnetic phase) provides benchmark signatures of the charge ordered phase and ferromagnetic transitions in doped rare earth manganites[1]. Size reduction to nanoscale has been shown to lead to drastic changes in the properties of the manganites leading to disappearance of the charge ordered state and emergence of a ferromagnetic phase[2]. We have employed the highly sensitive EMR technique complimented by the magnetization measurements to study the impact of size reduction on the magnetic ordering in bulk and nanosized $Sm_{1-x}Ca_xMnO_3$ (x = 0.35, 0.65 and 0.92) which are labelled further as Ca0.35, Ca0.65 and Ca0.92 respectively. The bulk Ca0.35 shows a charge ordering transition at 240 K and a ferromagnetic insulator phase below 50 K. Bulk Ca0.65 exhibits charge order below 275 K and shows an antiferromagnetic insulator phase below 135 K while Ca0.92 has a ferromagnetic-cluster glass ground state[3]. Thus, comparative study of magnetic ground state in Ca0.35, Ca0.65 and Ca0.92 bulk and nanoparticles enables us to study the size-induced effects on different types of magnetic ordering.

The nanoparticles (of mean dia ≈ 27nm) were prepared by sol-gel method and the bulk samples were obtained by sintering the nanoparticles at high temperature. Magnetic and X-band EPR measurements were carried out on all the samples in the temperature range 10-300 K. EPR signals were analysed by line shape fitting using double Lorentzian function accounting for both clockwise and anticlockwise rotating components of the microwave field. Magnetization measurements and the extracted EPR parameters, namely, the line width, intensity and the resonance field indicate that in nanoparticles of Ca0.35 and Ca0.65 weakening of the charge order is observed with the occurrence of a ferromagnetic transition around 100 K. In Ca0.92, existence of ferromagnetism with weakened strength is confirmed. Figures 1 and 2 present the temperature dependences of the EMR line width for bulk and naoparticles respectively. It is seen that in the bulk samples the temperature dependences of the linewidth for Ca0.35, Ca0.65 and Ca0.92 samples are quite different from each other. This difference is seen to have reduced in the nanosamples where all the three samples show qualitatively similar behaviour. We discuss the origin of these effects in terms of the presently existing models.

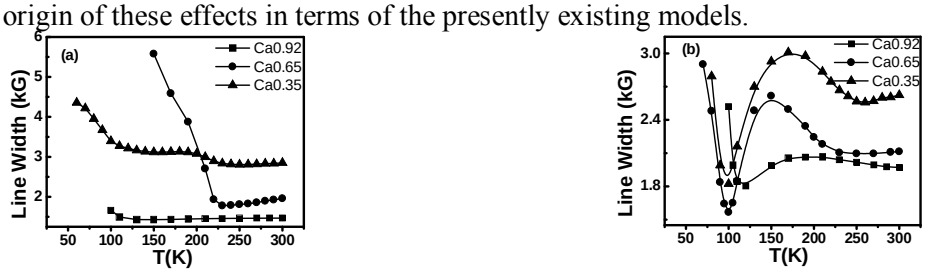

Temperature variation of EMR Line Width in (a) bulk samples (b) nanosamples

References

[1] Joshi J. P., Gupta R., Sood A. K., Bhat S. V., Raju A. R. and Rao C. N. R. "Temperature-dependent electron paramagnetic resonance studies of charge-ordered $Nd_{0.5}Ca_{0.5}MnO_3$" *Phys. Rev. B* **2001**, 65, 24410.

[2] Rao S. S., Tripathi S., Pandey D. and Bhat S. V., "Suppression of charge order, disappearance of antiferromagnetism, and emergence of ferromagnetism in $Nd_{0.5}Ca_{0.5}MnO_3$ nanoparticles" *Phys. Rev. B* **2006,** 74, 144416.

[3] Martin C., Maignan A., Hervieu M., and Raveau B., "Magnetic phase diagrams of $L_{1-x}A_xMnO_3$ manganites (L=Pr,Sm; A=Ca,Sr)" *Phys. Rev. B* **1999**, 60, 17.

P-71

An EPR Study of Magnetic Properties of Polyaniline

Boris Rakvin

Ruđer Bošković Institute, Division of Physical Chemistry, Bijenička c. 54, 10002 Zagreb, Croatia.

E-mail: rakvin@irb.hr

The magnetic properties of the conductive polymer polyaniline (PANI) and its derivatives have been studied extensively during the past decades. These properties are relevant for a better understanding of the nature of the charge carriers in the polymer structure. It can be noted that most of the studied PANI derivatives showed a nearly linear temperature dependence of the magnetic susceptibility multiplied by temperature (χT *vs* T) which was attributed to disorder-induced localised polaron pairs (radical cation with S=1/2). A slight deviation from the linear dependence of χT *vs* T usually was detected by SQUID at low temperature intervals, at $T < 10$K, for various PANI samples. In this low temperature region, the presence of magnetic field dependence of the magnetic moment was also noted. Both of these magnetic properties were described by employing a "triplet" model which used the distribution of the singlet-triplet splitting (E) with the density distribution function having a narrow peak near E=0. Recently, the EPR obtained orientation dependent susceptibility of the polymer film was described by localised state in which spin ½ polarons behave as spin ½ dimmers.

In this presentation local triplet states in two different types of PANI samples (commercial PANI emeraldine salt sample (PANI ES) and newly enzymatically synthesized polymer samples obtained in the presence of submicrometer-sized vesicles formed from sodium bis(2-ethylhexyl)sulphosuccinate (AOT) as templates for polymerisation[1]) will be addressed in order to more closely examine the nature of their distribution in these samples. It was expected that a characteristic EPR spectrum could be found and attributed to the excited triplet state with corresponding energy at low temperatures. Evidence for the presence of thermally activated states was obtained by studying the temperature dependence of EPR spectral intensities and line widths in the low temperature region[2]. The obtained activation energies for the thermally activated process are discussed in terms of expected energies for single-triplet transitions and possible exchange interactions. The obtained exchange interactions are correlated with different distributions of the polaron pairs in the PANI samples.

References

[1] Junker, K., Kissner, R., Rakvin, B., Guo, Z., Willeke, M., Busato, S., Weber, T., Walde, P., "The use of Trametes versicolor laccase for the polymerization of aniline in the presence of vesicles as templates", *Enzyme and Microbial Technology*, **2014,** 55, 72-84.

[2] Rakvin, B., Carić, D., Andreis, M., Junker, K., Walde, P., "EPR Study of Polyaniline Synthesized Enzymatically in the Presence of Submicrometer-Sized AOT Vesicles", *The Journal of Physical Chemistry B*, **2014,** 118, 2205-2213.

P-72

Novel type of organic conductor, self-doped $TTFCOONH_4$ and Its Analogs

Toshikazu Nakamura[1,2] , Ko Furukawa[1,2,*], Takeshi Terauchi[3], Yuka Kobayashi[3]

[1]*Institute for Molecular Science, Okazaki 444-8585, Japan*
[2]*The Graduate University for Advanced Studies, Okazaki 444-8585, Japan*
[3]*National Institute for Materials Science, Tsukuba 305-0047, Japan*
** Present Address: Center for Instrumental Analysis, Niigata University, Niigata 950-2181, Japan*

E-mail: t-nk@ims.ac.jp

We investigated the electronic structure of novel type of organic conductors, ammonium tetrathiafulvalene carboxylate $(TTFCOO)_2[(NH_4^{+1})_{1-x}(NH_3^0)_x]$ (Fig. 1) and its tetrathiapentalene derivative (TTPCOO) by High-Field ESR and ^{1}H-NMR spectroscopy measurements. The pristine TTFCOOH and TTPCOOH molecules are closed-shell. Kobayashi and coworkers found that self-doped type carrier was generated by substitution of the end group of (NH_3^0) with (NH_4^{+1}), which is regarded as a charge-reservoir, and they developed a variety of self-doped organic conductor families [1-5]. Because of sample limitation (powder), the detailed electronic state (anisotropic g-tenor and linewidth) was not clarified within the framework of conventional X-band ESR spectroscopy. In order to investigate the electronic structure from the microscopic point of view, we use the high-field W-band (94GHz) ESR spectrometer. As seen in Fig. 2, a clear powder pattern structure could be found [4]. We can evaluate the principal values of the *g*-tensor for theses salts, assuming anisotropic g-values. As seen in Fig. 1, TTFCOO system shows 1D column structure. On the other hand, the TTPCOO derivative system seems to be isotropic structure within 2D layer. As a result, TTFCOO system is a narrow-gap semiconductor because of 1D instability, while TTPCOO shows a stable metallic state down to 2K. Detailed discussion including ^{1}H-NMR results is presented.

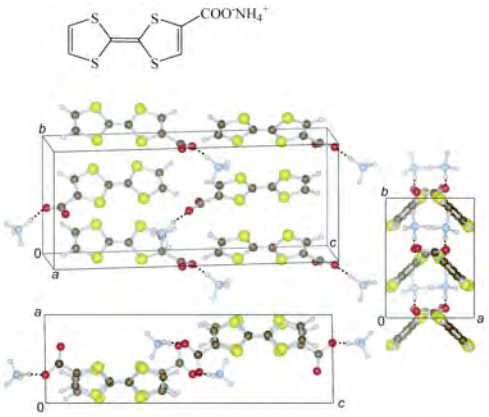

Fig.1 Molecural and Crystal tructure of $(TTFCOO)[(NH_4)_{1-x}(NH_3)_x]$

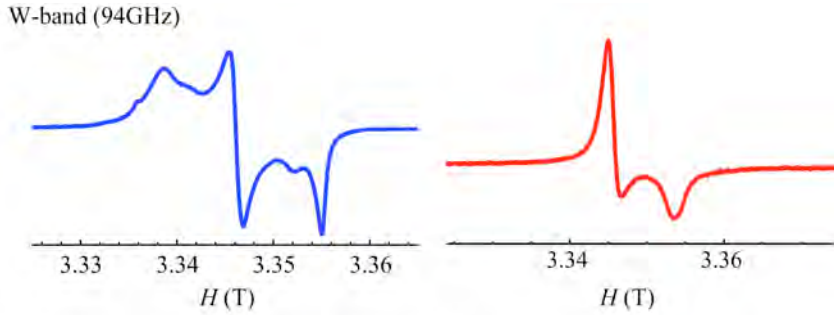

Fig. 2 W-band ESR spectra for 1D TTFCOO (left) and 2D TTPCOO (right) systems.

References

[1] Y. Kobayashi, M. Yoshioka, K. Saigo, D. Hashizume, and T. Ogura, *J. Am. Chem. Soc.* **2009**, 131, 9995.

[2] T. Terauchi, Y. Kobayashi and Y. Misaki, *Tetrahedron Lett.* **2012**, 53, 3277.

[3] Y. Kobayashi, T. Fujii, I. Terasaki, H. Kino, Y. Jin, T. Hibino, T. Kobayashi, E. Nishibori, H. Sawa, H. Yoshikawa, T. Terauchi and S. Sumi, *J. Mater. Chem.* A. **2013**, 1, 5089.

[4] K. Furukawa, T. Nakamura, Y. Kobayashi and T. Ogura, *J. Phys. Soc. Jpn.* **2010**, 79, 053701 (4 pages).

[5] T. Terauchi, S. Sumi, Y. Kobayashi, T. Nakamura, K. Furukawa and Y. Misaki, *Chem. Com.* 2014 50, 7111.

P-73

Antiferromagnetic to Paramagnetic Transition of Goethite (α-FeOOH) by ESR

Daniel F. Valezi[1], Marilene T. Piccinato[1], Paulo W. C. Sarvezuk[2], Flávio F. Ivashita[2], Andrea Paesano Jr.[2], J. Varalda[3], Dante H. Mosca[3], Carmen L. B. Guedes[1] and Eduardo Di Mauro[1].

[1]*LAFLURPE, Department of Physics, CCE, State University of Londrina, 86051-990, Londrina, PR, Brazil*
[2]*Department of Physics, State University of Maringá, 87020-900, Maringá, PR, Brazil*
[3]*Department of Physics, Federal University of Paraná, 81531-990, Curitiba, PR, Brazil*

Email: danieltds@hotmail.com

Electron Spin Resonance (ESR) was applied in the study of magnetic behavior of the mineral goethite with temperature variation, more specifically in the range that the mineral undergoes the transition from antiferromagnetic to paramagnetic state. The study was made with both natural and synthetic sample. Although it was not expected ESR signal in goethite samples at room temperature, due to its antiferromagnetic arrangement, a resonance line was observed in all spectra. This behavior was attributed to the existence of vacancies in the mineral structure [1-3]. Increasing the temperature from 352 K the goethite spectrum showed an additional ESR line, which intensity grows up until it stabilizes around 444 K. The appearance of this resonance line was attributed to the tendency of the magnetic moments align with the applied magnetic field, due to the thermal energy overcoming local exchange interactions and thereafter the transition to the paramagnetic state. Simulations of the goethite ESR spectra in both antiferromagnetic and paramagnetic state were performed, for the first time, by deconvolution of the resonance lines into two contributions, one from species with vacancies in their vicinity, and other ones with complete vicinity. Analyzing the growth rate of the ESR signal it was possible to determine the Néel temperature of the sample (T_N = 372 K). Vibrating sample magnetometry and Mössbauer spectroscopy techniques were used as auxiliary techniques and corroborate such assumption with the transition temperature identified as T_N = 370 K (in magnetometry case) Thereby, it was possible to identify the magnetic transition and the Néel temperature of goethite using the ESR technique and confirm the results with auxiliary techniques.

References

[1] Banerjee S. K. Origin of thermoremanence in goethite, *Earth and Planetary Science Letters* **1970**, 8, 197-201.
[2] Özdemir Ö. and Dulonp D. J. Thermoremanence and Néel temperature of goethite, *Geophysical Research Letters* **1996**, 23, 921-24.
[3] Liu Q., Yu Y., Torrent J., Roberts A., Pan Y. and Zhu R. Characteristic low-temperature magnetic properties of aluminous goethite [α-(Fe, Al)OOH)] explained, *Journal of Geophysical Research* **2006**, 111, B12S34.

P-74

Analysis of polymer degradation by ESR imaging

Hideyuki HARA
ESR Application, Bruker BioSpin K.K.,3-9Moriya-cho, Kanagawa-ku, Yokohama-shi, Kanagawa 221-0022, JAPAN

E-mail: Hideyuki.hara@bruker.com

ESR imaging is widely used for in-vivo samples such as mouse or rat with L-band or lower frequency. However using strong field gradient coil, material imaging at X-band became possible. At X-band imaging, we could not measure large sample volume but could high sensitivity measurements with small sample.

In this work, we show some X-band imaging data of polymer samples. ESR imaging were acquired at RT on an ELEXSYS E580 X-band CW spectrometer (Bruker BioSpin) equipped with 2D 200G/cm filed gradient coil and TMHS cavity. UV light was irradiated to the polymer samples with optical fiber from bottom of the resonator.

We applied it to investigate the degradation of polystyrene and PMMA. In polystyrene, the alkyl radical is generated due to UV irradiation. The alkyl radial was observed in whole sample (fig.1 left) However, we could not observe alkyl radical in the polystyrene with HALS (Hindered Amine Light Stabilizer) because nitro oxide radical were generated due to UV irradiation. The radical were observed only bottom of the polymer and this shows that the polymer degradation was suppressed by HALS (fig.1 right). In PMMA(Poly methyl methacrylate), ESR signal with 9 lines was observed by UV irradiation. But radical distribution with HALS was different to polystyrene. In the presentation, we will report the polymer degradation behavior with various HALS.

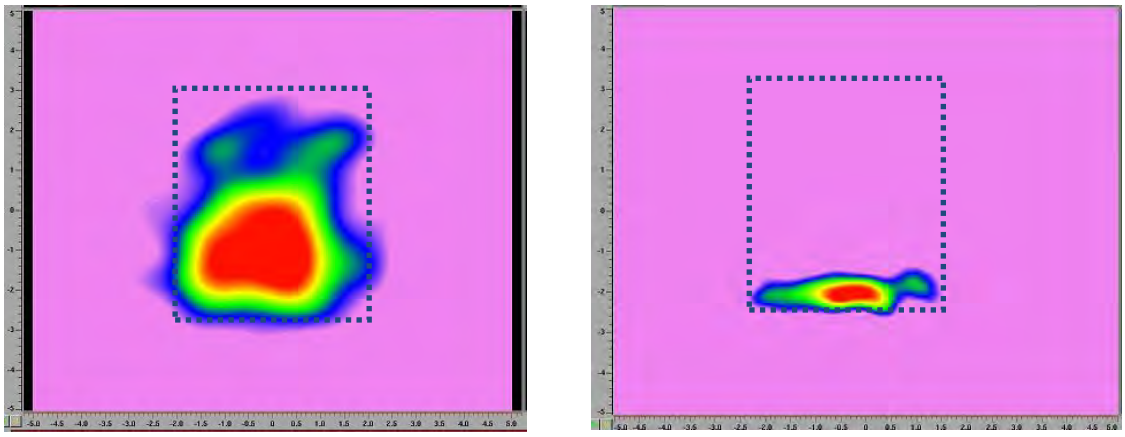

Fig. 1 Radical distribution of polystyrene with (right) and without (left) HALS.

P-75

Estimation of Wheat Flour Ash Contents using ESR

Hiromi Kameya[1], Mizuki Tsuta[1], Kaori Fujita[1], Setsuko Todoriki[1] and Junichi Sugiyama[1]

[1] *NARO, National Food Research Institute, Ibaraki 305-8642, Japan*

E-mail: hkameya@affrc.go.jp

The classification of wheat flours correlate to their ash content: 0.3–0.35% for patent flour, 0.35–0.45% for straight flour, 0.45–0.65% for first clear flour, 0.7–1.0% for second clear flour, and 1.2–2.0% for low-grade flour. The combustion method with a muffle furnace is used to determine ash content, which is a time-consuming process requiring 24–48 h. Ash is considered to have mineral constituents, including calcium, iron, and sodium, which could be detected by the electron spin resonance (ESR) spectroscopy as transition metal ions. The purpose of this study was to investigate the potential of ESR for the easy and quick estimation of the ash content in wheat flour.

ESR measurements were performed with the EMX-Plus by Bruker BioSpin, Inc. Six samples from the distributed Japanese "*Kita Honami*" wheat were used for the measurement, and each sample measurement was conducted with three replications. A partial least squares regression (PLSR) analysis was performed using the obtained ESR spectrum as an independent variable and the ash content value obtained from combustion methods as a dependent variable.

The ESR spectral data for wheat flour showed a single sharp signal due to organic-free radical at g = 2.00 and a six-line signal due to the hyperfine structure of manganese ions (Fig. 1). The correlation coefficients between measured and predicted ash content by the PLSR analysis were 0.5–0.7. Further investigations on measurement conditions and analysis parameters are necessary for the ESR spectroscopy to be a practical method of ash content measurement.

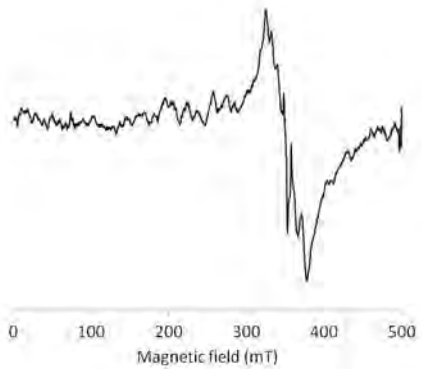

Fig. 1 ESR spectrum of wheat flour

Acknowledgement
We would like to express our sincere appreciation to the Hokuren Federation of Agricultural Cooperatives for providing the wheat samples used in this study.

P-76

Electron Magnetic Resonance Studies on Nanosized $Nd_{0.65}Ca_{0.35}$ $Mn_{1-x}Cr_xO_3$ (x=0, 0.06) Manganite

Daly Paul[1], K.N. Anuradha [2], K.S.Bhagyashree[3] and S.V. Bhat [3]

[1] *Department of Physics, RNS Institute of Technology, Bangalore, India*
[2]*Department of Physics, Dr. Ambedkar Institute of Technology, Bangalore, India*
[3]*Department of Physics, Indian Institute of Science, Bangalore, India*
E-mail:dalypaul9@gmail.com

Electron magnetic resonance spectroscopy (EMR/EPR) is a powerful technique which allows one to study the static and dynamic magnetic correlations on a microscopic level. The temperature dependence of the EMR line width gives information on dynamics/relaxation of electrons and EMR intensity is usually proportional to the static susceptibility. Doped manganites of general formula $R_{1-x}A_xMnO_3$ (where R is trivalent rare earth ion and A is divalent ion) have been found to exhibit remarkable properties such as charge order/orbital order, colossal magnetoresistance etc. Manganites contain Mn^{3+} and Mn^{4+} ions which are in the high spin state and thus EPR active.

Here we report a systematic investigation of the temperature dependence of EMR line width and intensity for ~ 25 nm $Nd_{0.65}Ca_{0.35}$ MnO_3 (NCMO1) and $Nd_{0.65}Ca_{0.35}$ $Mn_{0.94}Cr_{0.06}O_3$ (NCMO2) nanoparticles prepared by sol-gel method. The EMR line width for the two samples is significantly different below a temperature T_{min} where the EMR line width has a local minimum. T_{min} for NCMO1 was found to be 128K and 100K for NCMO2(figure1). Well above T_{min} the linewidths for the two samples have a small difference. The sharp upturn of EMR line width below T_{min} might be due to the formation of short range ferromagnetic ordered clusters. Temperature dependence of EMR intensity shows no sign of charge order and shows the onset ferromagnetic transition around 120K and 70K for NCMO1and NCMO2 respectively(figure2). The decrease in T_c in $Nd_{0.65}Ca_{0.35}$ $Mn_{0.94}Cr_{0.06}O_3$ nanoparticles may be due to the destruction of the double exchange interaction by chromium doping. In addition the magnitude of the intensity decreases for Cr doped nanoparticles. The possible reasons for the change in linewidth behavior and intensity will be discussed.

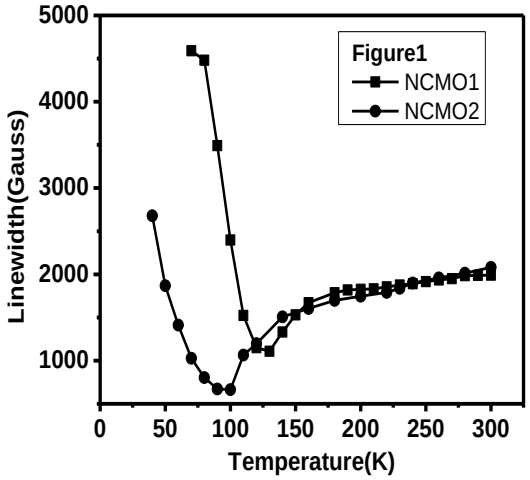

Fig1: Temperature dependence of EMR linewidth

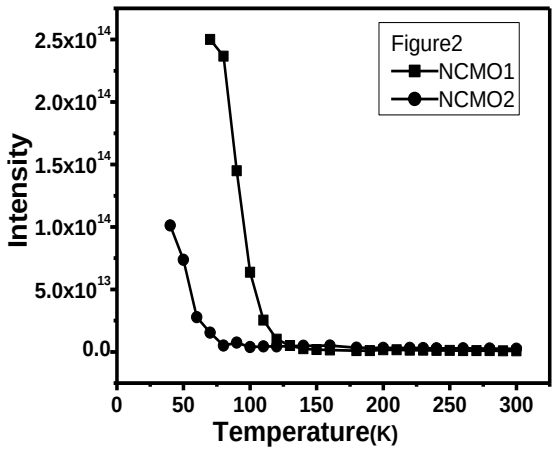

Fig2: Temperature dependence of EMR intensity

P-78

New Method for Obtaining Highly Resolved ESR spectrum of Aligned Radical

Masaya Nakamura[1] and Tatsuhisa Kato[1,2]

[1] *Department of Interdisciplinary Environment, Graduate School of Human and Environmental Studies, Kyoto University, Kyoto 606-8501, Japan*
[2]*Institute for Liberal Arts and Sciences, Kyoto University, Kyoto 606-8501, Japan*

E-mail: kato.tatsuhisa.6e@kyoto-u.ac.jp

We report here the new method for obtaining well-resolved electron spin resonance (ESR) spectra of radicals in the aligned orientation. We used a host crystal of the porous complex, which was soaked in the solution of the target guest radical. The guest molecules were absorbed and oriented in the crystal pores and can be observed by an angle-dependent ESR measurement.

The ESR observation in solid state has an advantage over that in solution to obtain the oriented information. The anisotropic ESR parameters of g- and hyperfine tensors can be directly determined by the measurement in solid state. However a solid state ESR measurement generally exhibits a shapeless spectrum due to broadening by the magnetic dipole interaction with adjacent radicals, or by hopping movement of excited spin state over sample. The fine structures of ESR spectra disappear as a result of the effects, and the oriented information is smeared out. It is necessary to align radical molecules keeping them apart for getting resolved ESR spectra.

We followed the Fujita's production method for the crystal of porous complex absorbing the target guest molecules. [1] Their aim was the 'crystal-free' crystallography and the nanogram scale single-crystal diffraction analysis. We applied their method to ESR spectroscopy. The host porous crystal was grown from layered solution of the two components: ZnI_2 in methanol and 2,4,6-tri(4-pyridyl)-1,3,5-triazine in nitrobenzene/methanol. After the solvent exchange from nitrobenzene to cyclohexane, the host crystal was soaked in the cyclohexane solution of 2-phenyl-4,4,5,5-tetramethylimidazoline-3-oxide-1-oxyl (PTIO) radical. The single crystal absorbing PTIO was obtained after the slow evaporation of the solvent for a several days.

The blue colored single crystal with PTIO was obtained. The crystal structure with the space group of C2/c was observed by X-ray diffraction analysis. And well-resolved angle dependent ESR spectra were obtained for the single crystal as shown in Figure 1.

[1] Inakuma Y., Yoshioka S., Ariyoshi J., Arai T., Hitora Y., Takada K.. Matsunag S., Rissanen K., and Fujita M., "X-ray analysis on the nanogram to microgram scale using porous complexes", *Nature* **2013**, 495, 461-466.

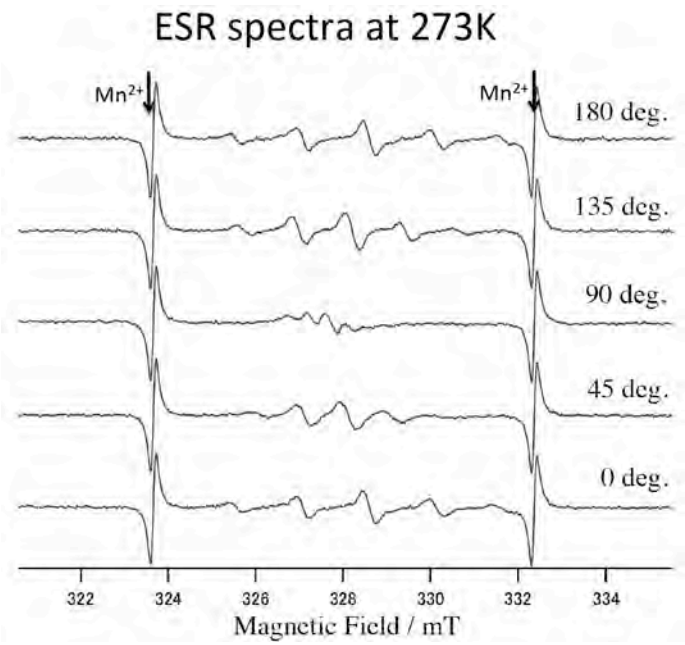

Figure 1. ESR spectra of PTIO radical at the aligned angles measured at 273K.

P-79

Unusual Electric Properties of Binuclear Rhenium Complexes with Biimidazolate Ligands in a Mixed-Valence State as Studied by Single-Crystal ESR Spectroscopy and Quantum Chemical Calculations

Takeshi Yamane[1], Kazunobu Sato[1,3], Shunsuke Tatsumi[1], Kenji Sugisaki[1,3], Yuki Kanzaki[1,3], Kazuo Toyota[1,3], Daisuke Shiomi[1,3], Makoto Yoshizawa[2], Makoto Tadokoro[2] and Takeji Takui[1,3]

[1]*Graduate School of Science, Osaka City University, Osaka 558-8585, Japan*
[2]*Faculty of Science, Tokyo University of Science, Tokyo 162-8601, Japan*
[3]*FIRST-Quantum Information Processing Project, JSPS, Tokyo 101-8430, Japan*

E-mail: yamane@sci.osaka-cu.ac.jp

The synchronized motion between protons and electrons is an important event in chemistry and recognized as a key step in certain biological molecular systems that perform ATP syntheses by using active proton pumps as well as through the conduction of electrons by cytochrome *c* in living matter[1-3]. In such biological systems, the driving mechanism of the synchronized motion has not been well understood, and thus relevant dynamics has been the focus of current topics in both biological and materials science. Many researches on this phenomenon have done in solution systems whereas very few examples are found in solid state[4]. Mixed-valence complexes with multifunctional ligands could be candidate materials for revealing the mechanism of proton-electron synchronized transfer not only in solution but also in solid.

Here, we focus on single-crystal ESR spectra of two rhenium binuclear complexes **1-Cl** and **1-Br**. These complexes have different structures from previously synthesized biimidazolate rhenium dimer **2**, in which the 2,2'-biimidazolate ligands are connected by two hydrogen bonding[5]. ESR spectra observed in helium temperature show a superposition of the two complexes arising from magnetically nonequivalent metal centers, as given in Figure 1, suggesting that both systems are in the mixed-valence state involving both Re^{III} and Re^{IV}. The single crystal ESR spectra can be interpreted by incorporating the contribution from the **D** tensor with its sizable zero-field splitting parameters. The ESR spectra were subject to line broadening with increasing temperature, and the distinct ESR signals merged into one hyperfine structure. We will discuss the paramagnetic and ferroelectric property of **1-Cl** and **1-Br** with the help of the quantum chemical calculations.

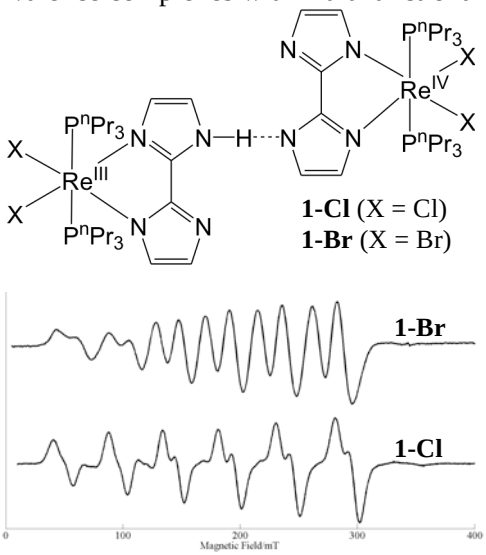

Fig. 1 Single-crystal ESR spectra of **1-Cl** and **1-Br**; (**1-Cl**) Temperature 3.2 K, Microwave frequency 9.62526 GHz; (**1-Br**) Temperature 3.4 K, Microwave frequency 9.62900 GHz; Both spectra was observed at the same degree in the same plane.

References

[1] M. Y. Okamura, and G. Feher, "Proton transfer in reaction centers from photosynthetic bacteria", *Annu. Rev. Biochem.* **1992**, 61, 861-896.

[2] P. J. P. Williams, "Bioenergetics: Purpose of proton pathways", *Nature* **1995**, 376, 643.

[3] S. Iwata, C. Ostermelter, B. Ludwig, and H. Michel, "Structure at 2.8 Å resolution of cytochrome c oxidase from Paracoccus denitrificans", *Nature* **1995**, 376, 660-669.

[4] P. Higel, F. Villain, M. Verdaguer, E. Rivière and A. Bleuzen, "Solid-State Magnetic Switching Triggered by Proton-Coupled Electron-Transfer Assisted by Long-Distance Proton-Alkali Cation Transport" *J. Am. Chem. Soc.* **2014**, 136, 6231−6234

[5] M. Tadokoro, K. Nakasuji et al., "Mixed-valence states stabilized by proton transfer in a hydrogen-bonded biimidazolate rhenium dimer", *Angew. Chem. Int. Ed.* **2007**, 46, 5938-5942.

P-80

Time resolved EPR study on photoinduced intermediates in photoactive interface of the perovskite solar cell

Kousuke Miyazaki[1], Taku Miura[1], Masasi Hasegawa[1], Yuhei Ogomi[2], Takashi Tachikawa[1], Shuji Hayase[2], Yasuhiro Kobori[1]

[1] *Kobe University, Kobe 657-8501, Japan*

[2]*Kyushu Instisute of Technology, Kitakyushu 804-0015, Japan*

E-mail: 143s225s@stu.kobe-u.ac.jp

In recent years, inorganic-organic hybrid soar cells employing $RPbX_3$ (R; monovalent organic cation, X; halide anion) perovskite as light absorber have been reported to have high energy-conversion efficiencies, exceeding 15 %.[1] However, no studies have clarified the detailed conversion mechanism yet. To characterize photoinduced intermediates in the photoactive layer at nanosecond time scale, we have performed time-resolved electron paramagnetic resonance (TREPR) measurements on thin layers composed of mesoporous TiO_2, $CH_3NH_3PbI_3$ perovskite, and Spiro-OMeTAD. The structure of perovskite is shown in Figure 1 where six A cations occupy vertexes of the cubic crystal, centered Pb^{2+} cation and six X^- anions form octahedral geometry.[2]

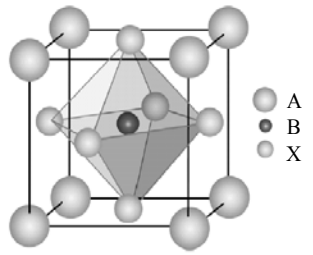

Figure 1. Perovskite structure (BX_6 octahedral)

The TiO_2/ $CH_3NH_3PbI_3$ / Spiro-OMeTAD thin film has been produced as follows. Mesoporous TiO_2 thin film was obtained by spin-coating of TiO_2 (anatase) nanoparticles onto clean glass substrate and subsequent thermal annealing at 773 K for 30 min in air. PbI_2 in dimethylformamide solution was spin-coated on the mesoporous substrate and was annealed at 343 K for 30 min in N_2 atmosphere. The film was immersed in CH_3NH_3I solution in 2-propanol and the color of the film changed from yellow to dark brown, which indicates the formation of $CH_3NH_3PbI_3$, followed by annealing at 343 K for 30 min in N_2 atmosphere. Spiro-OMeTAD in chlorobenzene solution was spin-coated on this film. This film was cut out in a glovebox filled with N_2 gass and the fragments of thin film were inserted into an EPR sample tube. This sample tube was once deaerated by a vacuum pump and then filled with the N_2 gas.

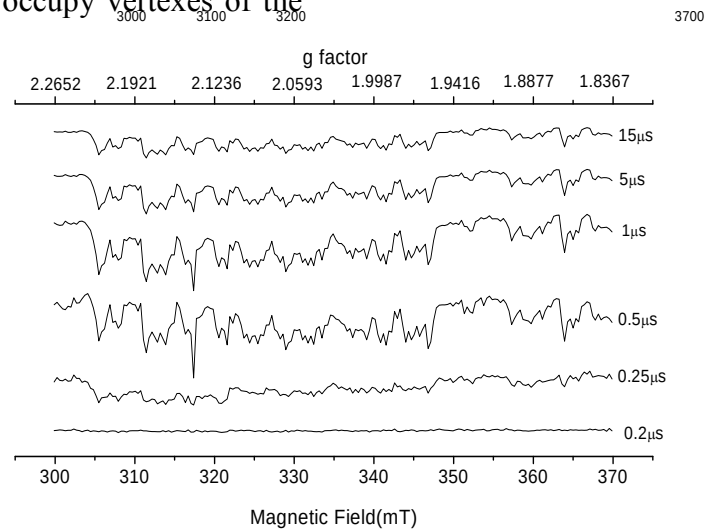

Figure 2. TR-EPR spectra of $TiO_2/CH_3NH_3PbI_3$/Spiro-OMeTAD film on a glass substrate in N_2 atmosphere after 532 nm laser irradiation at 110 K.

Figure 2 shows TREPR spectra of the $TiO_2/CH_3NH_3PbI_3$/Spiro-OMeTAD film obtained by nanosecond Nd:YAG laser (532 nm) irradiation at 110 K. The spectra are composed of the signals exhibiting structured peaks at the lower magnetic field and of the broad signals at the higher field. The assignments of the peaks and the interpretation of the emissive spin polarization are now in progress.

[1]Liu, M. *Nature 2013, 501, 395-398*

[2]Hui- Seon Kim, *J. Phhys. Chem. C 2014, 118, 5615-5625*

P-81

Study on Magnetophotoconductance in Fullerene-Based Diode

Yusuke Wakikawa[1], Takuya Omori[2], and Tadaaki Ikoma[2,3,4]

[1]*Center for Fostering Innovative Leadership, Niigata University, Niigata 950-2181, Japan.*
[2]*Graduate School of Science and Technology, Niigata University, Niigata 950-2181, Japan.*
[3]*CREST, Japan Science and Technology Agency, Kawaguchi 332-0012, Japan.*
[4]*Center for Instrumental Analysis, Niigata University, Niigata 950-2181, Japan.*

E-mail: ywakikawa@gs.niigata-u.ac.jp

Magnetic field effects on dynamics via the paired states involving triplet excitons in organic solids, such as triplet fusion, singlet fission and so on, have been studied for a long time. [1] Recent device development of organic optoelectronics along with the triplet harvest reminds us of the importance of magnetic field effects due to the triplet-triplet and triplet-doublet (TD) pair mechanisms. Last year, we have reported a broad negative magnetophotoconductance (MPC) effect in annealed film of [6,6]-phenyl-C61-butyric acid methyl ester (PCBM, inset of Fig. 1), which is assigned to the carrier detrapping by the triplet exciton and is categorized into the TD-pair mechanism. [2] In order to obtain deeper insight about the carrier detrapping mechanism, in this paper, we study on the MPC effect in a single layer diode comprised of PCBM sandwiched between aluminum (Al) and indium tin oxide electrodes, by means of not only the measurements of transient and steady state photocurrent under external magnetic fields [3] but also the method of photo-charge-carrier extraction by linearly increasing voltage (photo-CELIV).

As shown in Fig. 1, a positive MPC effect on steady state photocurrent (I) generated by photoinjection of carrier under a built-in potential was observed under a short circuit condition (V = 0.0 V) at 298 K, indicating a spin selective recombination in electron-hole pair. In addition to the positive MPC, a broad negative one clearly appeared under V = 1.2 V where the carrier density was high due to the effective carrier injection from the Al cathode. Combined the results obtained by the time-resolved MPC and photo-CELIV measurements, it was concluded that the negative broad MPC effect arose from a carrier detrapping by the collision between a triplet exciton (^{3}ex) and a trapped carrier injected from the electrode (c_t). With decreasing temperature (T) a half-width at half-height ($B_{1/2}$) of negative MPC effect became sharp. Below 100 K, $B_{1/2}$ converged with 10 mT that is comparable to the zero-field splitting of the triplet exciton of PCBM. [4] In the presentation we will discuss about the dynamics of the spin selective detrapping in PCBM together with simulations using a density matrix method based on the TD-pair (^{3}ex-c_t) mechanism.

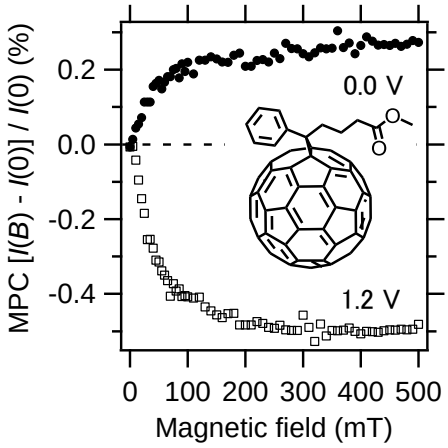

Fig. 1 MPC effect on steady state photocurrent at 298K under the applied voltage (V) of 0.0 V (●) and 1.2 V (□). Inset is molecular structure of PCBM

References

[1] U. E. Steiner, et al, "Magnetic Field Effect in chemical kinetics and related phenomena", *Chem. Rev.* **1989**, 89, 51-147.

[2] C. E. Ambe, et al. "Thermal Annealing Effects on the Photocarrier Dynamics in PCBM Films", *Bull. Chem. Soc. Jpn*, **2013**, 86, 1051-1058.

[3] Y. Wakikawa, et al., "Effect of Acceptor Lamination Effect on Photocarrier Dynamics in Hole Transporting Hexabenzocoronene Nanotubular Self-assembly", *J. Phys. Chem. C.*, **2013**, 117, 15925-15305.

[4] O. G. Poluektov, et al, "Electronic Structure of Fullerene Heterodimer in Bulk-Heterojunction Blends", *Adv. Energy Mater.* **2014**, doi: 10.1002/aenm.201301517.

P-82

Electron spin resonance study of room-temperature ferromagnetism in proton-irradiated fullerene

Do wan Kim, Kyu Won Lee, Gi Wan Jeon, and Cheol Eui Lee

Department of Physics, Korea University, Seoul 136-713, Republic of Korea

e-mail : dowankim@korea.ac.kr

Fullerene proton-irradiated with various irradiation energies and doses was observed to be ferromagnetic at room-temperature. Electron spin resonance (ESR) measurements were employed in order to understand the origin of ferromagnetism in proton-irradiated fullerene. Temperature-dependent ESR parameters were measured and discussed in this work. As a result, abrupt changes in the spin susceptibility, reflecting structural phase transition, were found to depend on the irradiation dose.

Acknowledgments: This work was supported by the National Research Foundation of Korea (Proton Users Program 2014M2B2A4030835 and Project No. 2014028954).

References

[1] Kyu Won Lee, Hyocheon Kweon and Cheol Eui Lee, "Field-induced Transition from Room-Temperature Ferromagnetism to Diamagnetism in Proton-irradiatied Fullerene", *Advanced Materials* 2013, 25, 5663-5667.

[2] Paul A. Heiney, John E. Fischer, Andrew R. McGhie, William J. Romanow, "Orientational Ordering Transition in Solid C_{60}", *Physical Review Letters* **1991**, 66, 2911-2914.

P-83

Electron spin resonance study of thermally treated glassy carbon

Gi Wan Jeon, Hyun Jin Cho, Do wan Kim, Kyu Won Lee, and Cheol Eui Lee*

Department of Physics, Korea University, Seoul 136-713, Republic of Korea

E-mail: jgw23@korea.ac.kr

Water-treated graphite powder has recently exhibited extraordinary ferromagnetism at room temperature, as has been the case in hydrothermally treated glassy carbon systems. In particular, ethanol has been found to give rise to defects in hydrothermally treated glassy carbon and ferromagnetic properties at room-temperature. In this work, we present electron spin resonance (ESR) results from hydrothermally treated glassy carbons with various treatment conditions including solvents and treatment time. Our results demonstrate that the ferromagnetism sensitively depends on the treatment time. The temperature-dependent ESR parameters have been measured and studied in order to understand the magnetism in the hydrothermally treated glassy carbon systems.

Acknowledgments: This work was supported by the National Research Foundation of Korea (Proton Users Program 2014M2B2A4030835 and Project No. 2014028954).

Reference

[1] Scheike. T., Böhlmann. W., Esquinazi. P., Barzola-Quiquia. J., Ballestar. A. and Setzer. A., Can Doping Graphite Trigger Room Temperature Superconductivity? Evidence for Granular High-Temperature Superconductivity in Water-Treated Graphite Powder, ADVANCED MATERIALS 2012, **24**, 5826-5831.

[2] Cho. H. J., Lee. K. W., Lee, C. E., Room-temperature ferromagnetism in hydrothermally treated glassy carbon, Current Applied Physics **2013**, 13 2055-2058

P-84

Morphology effect on the geometry of the photoinduced charge-separated states in RR-P3HT:PCBM blend films studied by time-resolved EPR

Taku Miura, Takashi Tachikawa, Yasuhiro Kobori

Department of Chemistry, Graduate School of Science, Kobe University, Japan

E-mail: 133s231s@stu.kobe-u.ac.jp

Blend films composed of the conjugated polymer of poly(3-hexylthiophene)(P3HT) and the fullerene derivative of [6,6]-phenyl-C61-butyric acid ester (PCBM) have attracted attention as a model system for the study of photoactive bulkheterojunction layer in the organic thin-film solar cells. Only a few studies have directly characterized the orientation of photoinduced charge-separated (CS) state at the domain interface of blend films[1,2]. The mechanisms of photoelectric conversions have not been fully understood. In this study, we have directly observed the photoinduced CS state for the regioregular (RR)-P3HT:PCBM blend films fabricated by the spin-coating method using time-resolved EPR to characterize the morphology effect on the orientational structure and the charge-dissociation dynamics following the primary CS process.

The mixed solutions of the RR-P3HT:PCBM (weight ratio = 2:8 and 8:2) were prepared by dissolving them in 1,2-dichlorobenzene (ODCB). Blend films were fabricated by the spin-coating method on the cleaned cover-glasses at 3000 rpm for 30 s. Morphologies of the thin films were checked by the optical absorption bands of the RR-P3HT domain using the UV-vis spectrometer. The films in EPR quartz tubes were deaerated using a vacuum line to remove ODCB and oxygen. 8:2 grycerol/water (v:v) mixture which has been deoxygenated by the vacuum line were added to the EPR tubes to ensure the EPR-measurement temperature and to avoid film exfoliations by the laser irradiations. The X-band TREPR measurements were carried out using a Bruker EMX system at T = 77 K. Light excitations were performed by the second harmonics (532 nm) of a Nd;YAG laser (Continuum, Minilite II, fwhm ～5 ns) with a laser depolarizer.

UV-vis absorption spectrum of the 2:8 blend films showed a maximum absorption band around 450 nm, which is characteristic of the monomer P3HT. In contrast, the 8:2 blend films showed the bands around 600 nm by the crystalline phase. The above results denote that the lamella stacking by the P3HT molecules is disrupted in the 2:8 system. Figure 1 shows TREPR spectra of the films measured at 77 K. The signals have been explained by the spin correlated radical pair (SCRP) model using the g-factors of the P3HT polaron and of the PCBM anion radical[1,2], denoting that the photoinduced CS states are generated via the excited singlet P3HT. In the 2:8 system, initial narrow A/E/A components (Figure.1a-b) and broad A/E/A/E components are observed, indicating that both of short-range and long-range CS states are generated in the disordered structure of PCBM-rich environment. The narrow signal has been changed to absorptive signals in Figure1.c-e at the later delay times by the spin lattice relaxation to generate thermally equilibrium spin state. On the other hand, broad A/E/A/E pattern is quickly deactivated by the charge recombination. In the 8:2 system, sharper CS state-signals are observed and survived more than 10 μs, indicating that the crystallinity contributes the efficient charge dissociation. The molecular geometries of the CS states have been determined using the SCRP model[1,2].

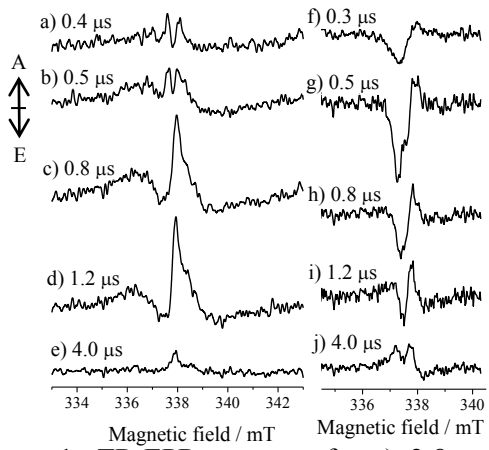

Figure 1: TR-EPR spectra of a-e) 2:8 and f-j) 8:2 P3HT:PCBM blend films. A and E denote the microwave absorption and emission, respectively.

References

[1] Y. Kobori, R. Noji, S. Tsuganezawa, *J. Phys. Chem. C* 117, (2013) pp 1589-1599.

[2] T. Miura, M. Aikawa, Y. Kobori, *J. Phys. Chem. Lett*. 5. (2014) pp 30-35.

P-85

Annealing Effect on Photocarrier Dynamics in P3HT Thin Film Studied by Time-resolved Magnetophotoconductance Measurements

Satomi Akaishi[1], Christopher E. Ambe[2], Yusuke Wakikawa[3], Tomoaki Miura[1], and Tadaaki Ikoma[1,4,5]

[1]*Graduate School of Science and Technology, Niigata University, Niigata 950-2181, Japan*
[2]*Department of Chemistry, MSU – Iligan Institute of Technology, Iligan City, 9200, Philippines*
[3]*Center for Fostering Innovative Leadership, Niigata University, Niigata 950-2181, Japan*
[4]*CREST, Japan Science and Technology Agency, Kawaguchi 332-0012, Japan.*
[5]*Center of Instrumental Analysis, Niigata University, Niigata 950-2181, Japan*

E-mail: f13a027a@mail.cc.niigata-u.ac.jp

Thermal annealing of organic films is practically the most convenient way to effectively enhance the device performance of solar cell. Therefore there are a lot of studies on the post-annealing effect using bulk heterojunction (BHJ) solar cell of blend film consisted of Poly[3-hexylthiophene-2,5-diyl] (P3HT) and [6,6]-Phenyl-C61-Butyric-Acid-Methyl Ester (PCBM).[1] However, little is known about the annealing effect on the carrier dynamics in pure films blended with nothing. Time-resolved magnetophotoconductance (MPC) measurements recently clarified that in contrast to the blend film the photocarrier generation efficiency in pure film of PCBM as an n-type semiconductor is drastically reduced by the annealing, which is related with the crystallization of PCBM film accompanied with deep trap formation. [2] In this paper we have examined pure film of regioregular P3HT by the MPC method,[3] in order to elucidate the annealing effect on the photocarrier dynamics in a p-type polymer.

Fig. 1a shows time profiles of the transient photocharge detected by a pulse light excitation at 532 nm. A fast rising component (Q_f) until 10 ns corresponding to the carrier generation and a slow glowing component (Q_s) reflecting the carrier transport are observed. The annealing at 156 °C lower than the melting point reduces the Q_f component by about one-fifth and induces early saturation behavior of the Q_s component. Fitting the Q_s component by a function considering the first (k_1) and second order (k_2) decays of the carrier density (n), $dn/dt = -k_1n - k_2n^2$, clarified that the channel of k_2-decay is dominant and the annealing increases the k_2-decay rate (k_2n_0) in spite of one-fifth of the initial carrier density (n_0). The fitting also elucidated that the drift mobility is doubled by the annealing. On the other hand, the time profiles of magnetophotoconductance (MPC) effect for the non- and 156 °C-annealed films positively grow with the delay time as depicted in Fig. 1b, indicating the non-geminate recombination. The rise time of the MPC becomes short by the annealing. These facts observed in the carrier transport indicate that the annealing enhances Langevin type of recombination by the increase of mobility due to self-organization of P3HT. In the presentation, we will discuss about the difference from PCBM.

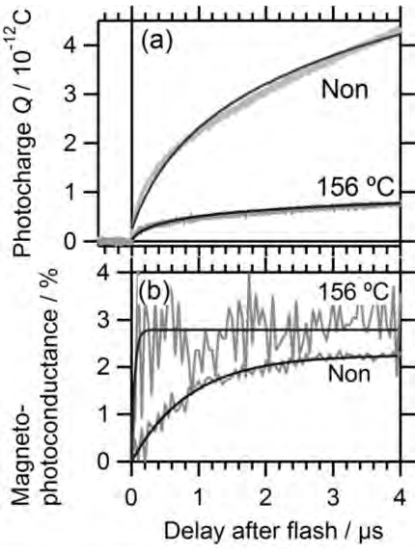

Fig.1 Time profiles of the photocharge (a) and magnetophotoconductance effect (b). Gray and black are respectively the experimental and the fitted curves.

References

[1] Verploegen, E. *et al*. "Effects of Thermal Annealing Upon the Morphology of Polymer–Fullerene Blends" *Adv. Funct. Mater.* **2010**, 20, 3519-3529.
[2] Ambe C. E., *et al*., "Thermal Annealing Effect on Photocarrier Dynamics in PCBM Films", *Bull. Chem. Soc. Jpn.*, **2013**, 86, 1051-1058.
[3] Wakikawa, Y. *et al*. "Effect of Acceptor Lamination on Photocarrier Dynamics in Hole Transporting Hexabenzocoronene Nanotubular Self-Assembly" *J. Chem. Phys. C* **2013**, 117, 15295-15305.

P-86

Detrapping Reaction of H Atoms From Silsesquioxane Cages in Organic Solvents

Kenji Komaguchi, Tetsuya Maeda, Ryota Okayama, Ichiro Imae and Yutaka Harima

Graduate School of Engineering, Hiroshima University, Higashi-Hiroshima 739-8527, Japan

E-mail: okoma@hiroshima-u.ac.jp

Octahedral silsesquioxanes (RT_8: $R_8(SiO_{1.5})_8$) have drawn much attention, since the H atoms trapped in RT_8 cages were generated by glow discharge [1] and γ-ray irradiation [2] of RT_8 powders. The H atom is stabilized in the cage for more than one year at room temperature, and the thermal decay behavior of the trapped H atoms has been studied. [1,2,3] In contrast to the powder sample, there is no report on the detrapping process in solution. In this work, the detrapping of H atoms encapsulated in RT_8 (R: *iso*-butyl) cages was observed in organic solvents and analyzed kinetically by ESR spectroscopy (Scheme 1).

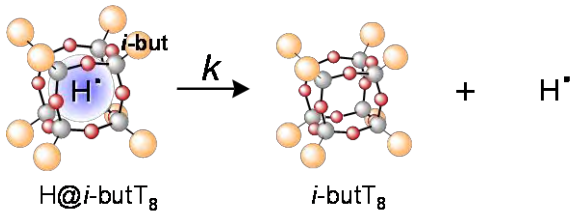

Scheme 1

The H atoms trapped in *i*-butT_8 were generated by glow discharge or γ-ray irradiation of *i*-butT_8 powders [1]. Irradiation of γ-ray (^{60}Co) to the powder was performed in air at room temperature at Radiation Research Facility, Hiroshima University. The γ-irradiated or glow discharged *i*-butT_8 powder (15 mg) was dissolved in solvent (400 μL) and a proper amount of the solution was placed into a Suprasil quartz tube (ϕ = 2 mm). Quantitative measurements were performed for trapped H-atoms by ESR spectroscopy.

Time courses of the ESR signal intensity of the trapped H-atoms were measured at a constant temperature of 30°C for *i*-butT_8 irradiated with γ-ray to a dose of 200 kGy. Logarithmic plots of the intensity against time showed that the decay process fits a straight line, suggesting the detrapping process follows first-order kinetics with a rate constant, *k*. The rate constant was evaluated to be 4.4 x 10^{-6} s^{-1} (life-time: 64 hours) for the γ-irradiated *i*-butT_8 in THF at 30°C. The *k* values significantly varied depending on the sorts of solvents (THF, 2-methyl THF, cyclopentyl methyl ether, diethyl ether, chloroform, benzene). It was found that the larger the dipole moment of the solvent is, the faster the H atom escaped from the cage. On the other hand, in benzene as nonpolar solvent, the life-time was longest among all the solvents tested in this study, which was comparable to that of the crystalline powder. To evaluate Arrhenius parameters for the detrapping reaction, temperature dependence of the rate constants was measured. The activation energies for the reaction were 105.4 kJ mol^{-1} in THF and 119.3 kJ mol^{-1} in benzene. The results suggest that the transition state for detrapping is more stabilized in THF than in benzene in accord with a shorter life-time of the trapped H-atoms in THF. However, in fact, the ESR signal intensity does not decay monotonously at the initial stage. This is because minor components with faster decay rates are included in the sample. On the basis of ESI-MS analysis of γ-irradiated or glow discharged *i*-butT_8, it was suggested that the molecular framework remains undamaged and *iso*-butyl substituents are simply modified by the addition of oxygen atom(s). The detrapping mechanisms of the H atoms in solution are discussed in terms of the O-atom incorporation into the *iso*-butyl substituents and the solvation effects.

References

[1] Y. Harima, K. Komaguchi, et al., *Chem. Commun.* **2010**, 46, 2076-2078.
[2] R. Sasamori, Y. Okaue, T. Isobe, Y. Matsuda, *Science*, **1994**, 265, 1691-1693.
[3] M. Päch, R. Stösser, *J. Phys. Chem. A* **1997**, 101, 8360-8365.

Spin Dynamics of Photoconductive Donor-Acceptor-type Covalent Organic Framework (COF)

Ko Furukawa[1], Toshikazu Nakamura[2], Shangbin Jin,[2] Long Chen[2] and Donglin Jiang[2]

[1]*Center for Instrumental Analysis, Niigata University, Niigata 950-2181, Japan*
[2]*Institute for Molecular Science, Aichi 444-8585, Japan*

E-mail: kou-f@chem.sc.niigata-u.ac.jp

Covalent organic framework (COF) materials, which are crystalline materials with the stacking structure of two-dimensional COFs, attracted much attention because of their photo-functionality, and so on.[1] A variety of photoconductive COF materials based on the Donor-Acceptor (D-A) system have been developed.[2] Recently, the Zn-phthalocyanine (ZnPc) COF materials which encapsulated C_{60} molecules was developed. (Fig. 1) Novel type photoconductivity using the pore of COF materials could be expected. The photoconductive mechanism, which was possibly induced by an electron transfer between donor (ZnPc) and acceptor (C_{60}), has not been clarified yet. In this paper, spin dynamics for the donor-acceptor-type COF, **C_{60}@ZnPc-COF** and **ZnPc-COF** was examined by using time-resolved ESR spectroscopy.

Figure 2 shows the time-resolved ESR spectrum for **C_{60}@ZnPC-COF** at 40 K. The observed spectrum could be expressed as an emission-type single Lorentz signal with 16 G linewidth. The TR-ESR spectrum for ZnPC has been reported as the excited triplet state under 680 nm excitation. Therefore, the observed ESR signal originates in the charge separated state induced by the electron transfer from the ZnPc to the C_{60} in **C_{60}@ZnPC-COF**. Now, we examine the correlation between the lifetime and the molecular structure. We will discuss the photoconduction mechanism of the D-A type COF materials.

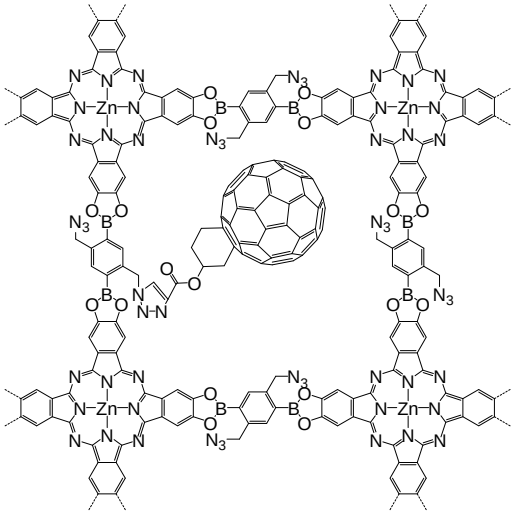

Fig. 1 Molecular structure for C_{60}@ZnPc-COF.

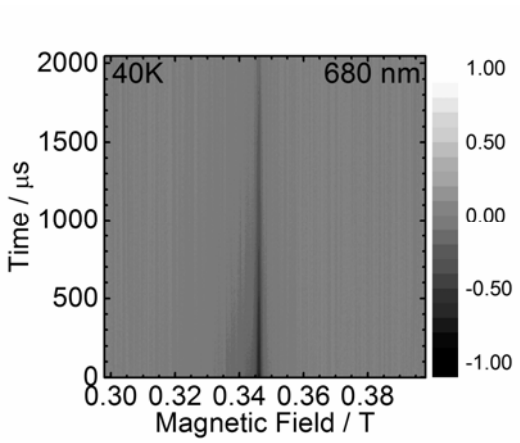

Fig.2 Time-resolved ESR spectrum for C_{60}@ZnPc-COF at 40 K.

References

[1] A. P. Côté, A. I. Benin, N. W. Ockwig, M. O'Keeffe, A. J. Matzger, and O. M. Yaghi, *Science*, **2005**, 310, 1166 – 1170.

[2] X. Ding, L. Chen, Y. Honsho, X. Feng, O. Saengsawang, J. Guo, A. Saeki, S. Seki, S. Irle, S. Nagase , V. Parasuk , and D. Jiang, *J. Am. Chem. Soc.* **2011**, 133, 14510 – 14513.

[3] S. Jin, X. Ding, X. Feng, M. Supur, K. Furukawa, S. Takahashi, M. Addicoat, M. E. El-Khouly, T. Nakamura, S. Irle, S. Fukuzumi, A. Nagai, and D. Jiang, *Angew. Chem. Int. Ed.*, **2013**, 52, 2017 – 2021.

P-88

Pulse EPR detection of UV light generated spins on an Al doped TiO_2 crystal

Ikuko Akimoto[1] and Takao Sekiya[2]

[1]*Faculty of Systems Engineering, Wakayama University, Wakayama 640-8510, Japan*
[2]*Graduate School of Engineering, Yokohama National University, Yokoyama 240-8501, Japan*

E-mail: akimoto@sys.wakayama-u.ac.jp

In some of luminous insulators or semiconductors, luminescence is emitted by recombination of free electrons and holes generated by optical excitation. When electrons and holes are trapped in deep levels inside energy gap, tunneling recombination occurs or thermal/low-energy-optical excitations release trapped ones into mobile ones, and then lead to recombination luminescence. Such a phenomenon has been applied for scintillators and imaging plates. As the recombination pairs of electron and hole switch from nearby pair to distant pair during the stimulation [1], such a system is suitable to explore the temporal change of separately distributed electron and hole pairs.

We measured UV light-generated spins by cw/pulse EPR detection at 93 and 20 K on an Al-doped (5 mol%) TiO_2 crystal. This system exhibits thermally activated recombination luminescence (thermo-luminescence) below 70 K and trapped electrons and holes are known to be EPR active [2, 3]. Electrons are trapped at Ti^{4+} nearby oxygen vacancy and indicate a single sharp line signal, whereas holes are trapped at Al^{3+} sites substituted to Ti^{3+} and indicate HFI split sharp signals. These EPR signal intensities are reduced by thermal or red-light optical excitation due to release of trapped ones. Here, we present preliminary results for the spin system detected by FID and primary echo combined with various optical excitations.

References

[1] C. J. Delbecq, Y. Toyozawa, and P. H. Yuster, *Phys. Rev. B* **1974**, 9, 4497.

[2] T. Sekiya, Y. Takeda, S. Ohya, and T. Kodaira, *Phys. Status Solidi C* **2011**, 8, 173.

[3] I. Nakagawa, Y. Uchiyama, T, Sekiya, Proc. 23rd Symposium of Association for Condensed Matter Photophysics, (2012) p.133 (in Japanese).

Electrically Detected Spin Resonance Of Hydrogenated Amorphous Silicon At Room Temperature

A. M. See[1], D. R. McCamey[1] and Alex R. Hamilton[1]

[1]*School of Physics, University of New South Wales, Sydney NSW 2052, Australia*

Email: a.see@unsw.edu.au

Spin resonance is a power technique [1] which has been utilized in a wide range of applications such as Magnetic Resonance Imaging, where a spatially varying magnetic field is used to measure the location of spins. However, conventional magnetic induction based spin resonance techniques require a large ensemble of spins (10^{10} – 10^{13}), which are not suitable for investigating nanoscale systems where the number of spins is small. In comparison, Electrically Detected Spin Resonance (EDSR) techniques have been demonstrated to have spin sensitivity up to 11 orders of magnitude high than those in the conventional techniques [2]. EDSR works by probing changes in the electrical conductivity that are spin-dependent. To explore the application of EDSR in nanoscale devices and materials, we will first demonstrate EDSR using hydrogenated amorphous silicon a-Si:H as a prototypical test bed since a-Si:H is one of the most widely used materials for photovoltaic applications and other electronic devices ranging from thin-film transistors to radiation detectors [3].

Our device uses thin p-doped and n-doped layers on either side of the intrinsic a-Si:H forming an operational solar cell device similar to those used in commercial applications (see Fig. 1a inset). In order to minimize microwave field distortion from the contacts, sample contacts are made of thin film aluminum approximately 100 nm thick. Electrical connections are made via SMA connectors mounted on a PCB outside the microwave cavity (see Fig. 1b). At this stage, we have fabricated a working a-Si:H device with a photocurrent of about 10 μA at zero bias. An *I-V* characteristic plot is shown in Fig. 1(a). The next step is to place the brass sample holder in a magnetic field and performance spins resonance measurements where spin dependent electrical conductivity change will be measured at room temperature.

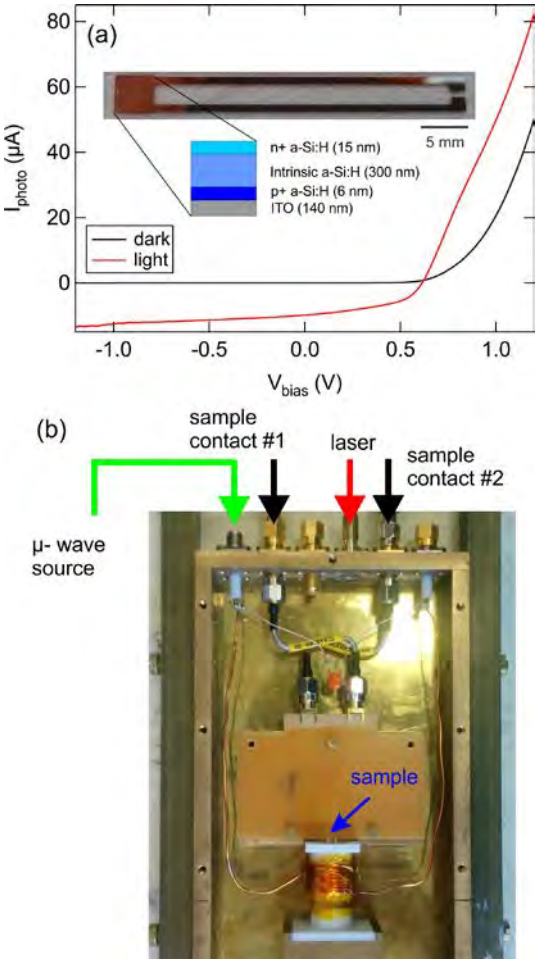

FIGURE 1(a): I-V characteristics of a typical a-Si:H sample. In this setup, a 670 nm laser is used to illuminate the sample where a photocurrent of 10 μA is obtained at zero bias. The active region of the device measures 3.4 mm by 3.4 mm, and is located on the left hand side of the device as shown in the inset. (b) A photograph of the sample holder showing the electrical connections between the sample, the PCB, SMA connectors and the microwave coils.

[1] A. Schweiger & G. Jeschke., "*Principles of Pulse Electron Paramagnetic Resonance*", Oxford University Press (2001).

[2] D. R. McCamey, H. Huebl, M. S. Brandt, W. D. Hutchison, J. C. McCallum, R. G. Clark and A. R. Hamilton, *Appl. Phys. Lett.*, 2006, 89 182115.

[3] R. A. Street., "*Hydrogenated Amorphous Silicon*", Cambridge University Press, Cambridge, England (1991).

P-90

Molecular Mechanism of Apoptotic BAX Activation Revealed by Spin-label ESR

Yun-Wei Chiang*, Chia-Jung Tsai, Tai-Ching Sung, and Yei-Chen Lai

Department of Chemistry and Frontier Research Center on Fundamental and Applied Sciences of Matters, National Tsing Hua University, Hsinchu 30013, Taiwan

**E-mail: ywchiang@mx.nthu.edu.tw*

BAX protein plays a key role in the mitochondria-mediated apoptosis. However, it remains unclear by what mechanism BAX is triggered to form an oligomer and initiate apoptosis. In this talk, we present our recent study on the activation mechanism of BAX proteins using spin-label ESR techniques and confocal fluorescence microscopy. The results of pulsed dipolar spectroscopy show that an inactive BAX monomer actually exist in two distinct conformations at equilibrium, one of which has never been reported. We show that upon apoptotic stimulus by BH3-only peptides, BAX can be induced to convert into either a ligand-bound monomeric state or a ligand-bound oligomeric state through a conformational selection mechanism. The less abundant native conformation exhibits greater accessibility of the BH3 domain to available substrates and is identified to be an on-pathway intermediate between the abundant native state and the oligomeric state. The immunoblotting results of mitochondrial cytochrome *c* release as well as the GUV results of the confocal fluorescence microscopy provide further discrimination between the proposed BAX states, thereby revealing a population-shift allosteric mechanism in the process. The conformation heterogeneity is proven to be an intrinsic property of BAX necessary for modulating the BAX-induced apoptosis.

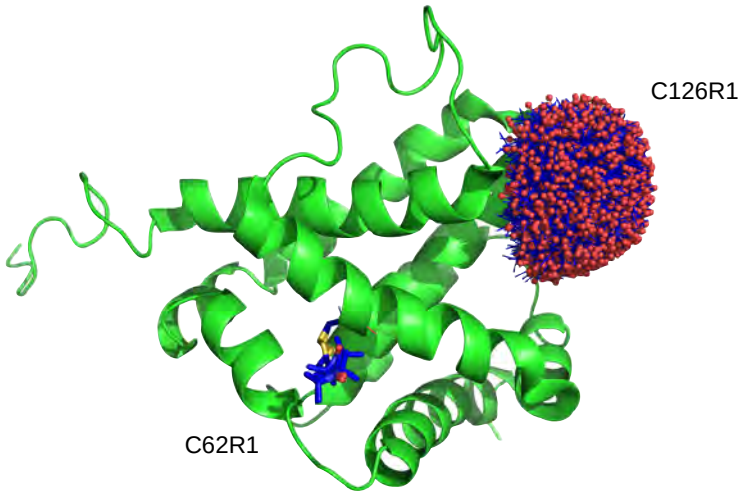

Using bound fatty acids to disclose the solution structure of serum albumin

Jörg Reichenwallner[1,2], Dariush Hinderberger[2]

[1]*Max Planck Institute for Polymer Research, Ackermannweg 10, 55128 Mainz, Germany*
[2]*Institute for Chemistry, Physical and Theoretical Chemistry, MLU Halle-Wittenberg, Von-Danckelmann-Platz 4, 06120 Halle, Germany*

E-mail: joerg.reichenwallner@chemie.uni-halle.de

Serum albumin is a major transport protein in mammals and is known to bind to a wide variety of small molecules [1] such as long-chain fatty acids (FAs). Using a new electron paramagnetic resonance (EPR) spectroscopic approach [2], we aim to gain information on the functional structure of serum albumin in solution as a "coarse-grained" picture from the ligands' point of view. This approach is based on using spin-labeled (paramagnetic) stearic acids self-assembled with albumin and subsequent nanoscale distance measurements between a combination of up to seven diamagnetic (reduced) and paramagnetic FAs using double electron–electron resonance spectroscopy (DEER). Continuous wave (CW) EPR spectroscopy complements our studies, e.g. by quantification and characterization of bound ligands [3].

Based on DEER distance measurements, nanoscale differences in the functional solution structures between different albumins can be revealed with the aid of crystal structure and hydropathy evaluation. Hence, symmetry and flexibility of the proteins' ligand alignment in its interior and its surface can be mapped [4]. This approach allows us to expand structural and functional differences of various albumins to a molecular level. Going beyond fundamental structural studies, we are able to establish a research platform utilizing the albumin model system for general physicochemical studies of proteins or protein-based hybrid materials and their corresponding ligand interactions [5].

References

[1] Peters Jr. T., "*All about albumin: biochemistry, genetics and medical applications*", 1st edition, Academic Press, Inc., San Diego, **(1996)**.

[2] Junk M.J.N., Spiess H.W. and Hinderberger D., "The Distribution of Fatty Acids Reveals the Functional Structure of Human Serum Albumin", *Angew. Chem. Int. Ed.* **(2010)**, 49, 8755-8759.

[3] Rehfeld S.J., Eatough D.J. and Plachy W.Z., "The binding isotherms for the interaction of 5-doxyl stearic acid with bovine and human albumin", *J. Lipid Res.* (**1978)**, 19, 841-849.

[4] Akdogan Y., Reichenwallner J. and Hinderberger D., "Evidence for Water-Tuned Structural Differences in Proteins: An Approach Emphasizing Variations in local Hydrophilicity", *PLoS One* **(2012)**, 7, e45681.

[5] Reichenwallner J., Hinderberger D., "Using Bound Fatty Acids to Disclose the Functional Structure of Serum Albumin". *Biochim. Biophys. Acta, Gen. Subj.* **(2013)**, 1830 (12), 5382-5393.

Accurate orientation PELDOR measurements and analysis of the Rx bi-functional spin label for protein structure refinement

Johannes E. McKay[1], Michael Stevens[2], Hassane EL Mkami[1], David G. Norman[2] and Graham Smith[1]

[1]*The Millimetre Wave & EPR Group, University of St Andrews, St Andrews, United Kingdom*
[2]*Nucleic Acid Structure Research Group, The University of Dundee, Dundee, United Kingdom*

E-mail: jem74@st-andrews.ac.uk

It has been shown that it is possible to use high-field EPR (Electron Paramagnetic Resonance) measurements to obtain accurate long range angular and distance constraints which could be used to build structural models of large biomolecular structures. By using the conformationally constrained nitroxide side chain RX [1] as a spin label it is possible to label secondary structure reliably such that the side chain conformation can be correlated to the underlying structure.

In this paper we describe a reliable library method for measuring and extracting the relative orientation and distance between pairs of RX spin labels using PELDOR (Pulsed Electron-Electron Double Resonance) at W-band using the HiPER spectrometer at St Andrews [2]. As part of collaboration with Nucleic Acids Research Group, University of Dundee samples have been prepared with the RX side chain attached to alpha helix and beta sheet secondary structure. Analysis results for PELDOR measurements of these different pairs of spin labels are presented and compared to existing structural models. A study into the angular resolution of the PELDOR measurements of spin labels with the conformational constraints found in the RX side chain will be presented.

By combining angular and distance constraints derived from conformationally constrained side chains measured with high-field EPR it is hoped that it will be possible to build structural models of large biomolecular systems in a general way.

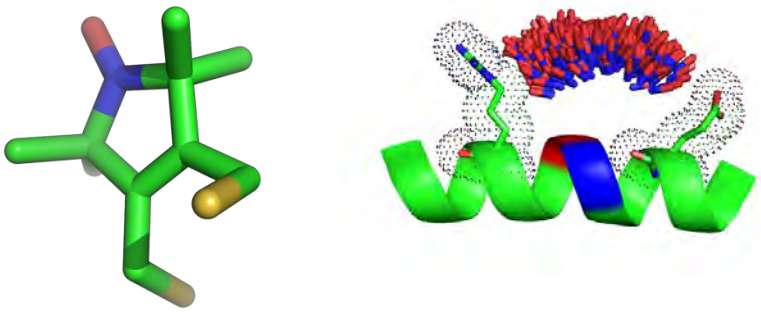

Fig 1 Left: Nitroxide side chain RX. Right: Nitrogen and Oxygen atoms for RX side chain on an α helix
Diagram showing Left: The RX side chain molecule Right: The measured conformation of the side chain RX when attached to an α helix showing the nitrogen and oxygen atoms.

References [11 points, Times New Roman, bold]

[1] Fleissner, M.R., et al., "Structure and dynamics of a conformationally constrained nitroxide side chain and applications in EPR spectroscopy", *Proceedings of the National Academy of Sciences*, **2011**, 108(39), p. 16241.

[2] Cruickshank, P.A.S., et al., "A kilowatt pulsed 94 GHz electron paramagnetic resonance spectrometer with high concentration sensitivity, high instantaneous bandwidth, and low dead time", *Review of Scientific Instruments*, **2009**, 80(10), p. 103102.

P-93

Time resolved EPR study on photoinduced primary charge-separated state of the PSII reaction center from spinach

Masashi Hasegawa[1], Masaki Tsushima[1], Takashi Tachikawa[1], Hiroyuki Mino[2], Yasuhiro Kobori[1]

[1]*Department of Chemistry, Graduate School of Science, Kobe University, Kobe 657-8501, Japan*
[2]*Division of Materials Science (Physics), Graduate School of Science, Nagoya University, Nagoya 464-8602, Japan*

E-mail: 149s222s@stu.kobe-u.ac.jp

【Introduction】In the initial of stage of the photosynthesis of the plants, photoreactions are known to take place in the photosystem II (PSII) reaction center. It is suggested that the photoinduced charge-separated (CS) state composed of P_{D1} radical cation in the special pair and pheophytin radical anion is generated via the excited singlet state of the accessory chlorophyll (Fig.1). However, no experimental studies have been performed to determine the structure of the primary CS state in the PSII. We have employed the time-resolved EPR (TREPR) method to determine the orientational structure of the initial CS state.

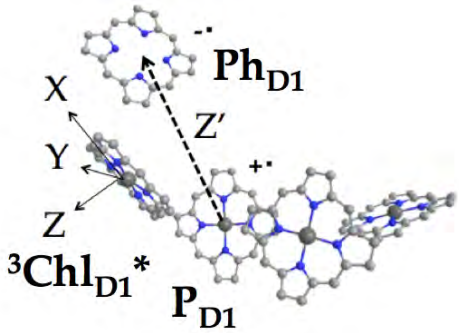

Figure 1. X-ray structure of the cofactors in the photosystem II reaction center.

【Results and Discussion】TREPR spectra have been obtained by nanosecond 532 nm laser irradiations of quinone-prereduced PSII reaction center from spinach at 77 K as shown at the left of Fig. 2. At 0.5 μs, we observed a narrow spectrum with a spin polarization pattern of absorption (A) / emission (E) around 339 mT together with the broad spectrum by the excited triplet of the accessory chlorophyll. Fig. 2 right exhibits the contribution from the A/E polarized signal around the center field region (339 mT) at 500 ns. At the later delay time of 1.5 μs (Fig. 2 left), this narrow spectrum is deactivated while a broad A/E/E/A/A/E pattern is prominent. Since this broad signal is assigned to the excited triplet state of Chl_{D1} generated by the triplet charge recombination via S-T_0 mixing, the center signal can be assigned to the initial CS state. We have modeled the time-evolutions of the transverse magnetizations both of the CS state and the $^3Chl_{D1}$* using the stochastic-Liouville equation[1] to determine the orientational structure of the initial CS state composed of P_{D1} radial cation and Ph_{D1} radical anion.

[1] Kobori, Y. Noji, R. Tsuganezawa, S. *J. Phys. Chem. C* **2013**, *117*, 1589-1599.

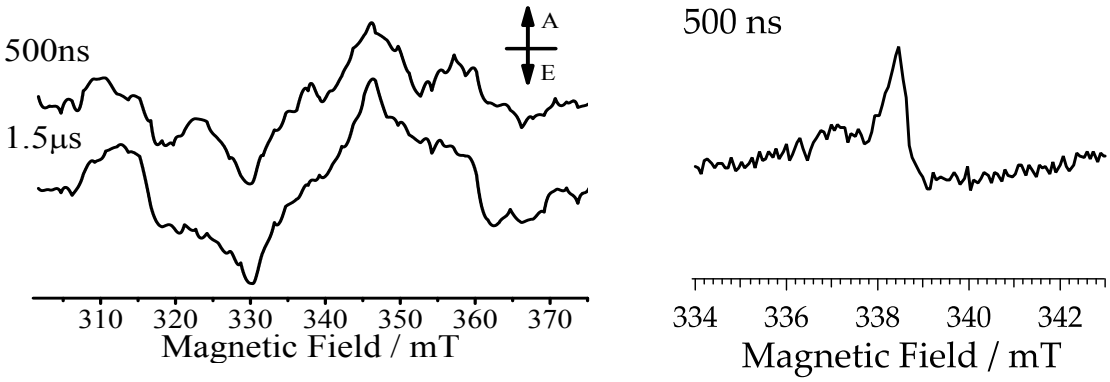

Figure 2. (left): Time resolved EPR spectra of the quinone-prereduced PSII reaction center obtained by the 532 nm irradiation at 77 K. (right): Enlarged EPR spectrum around the center field region (339 mT) at 500 ns, representing the primary charge-separated state.

P-94

Time-resolved EPR Measurements of Y_Z Radical in Photosystem II Detected by High Frequency Magnetic Field Modulation

Wataru Koinuma and Hiroyuki Mino

Graduate School of Science, Nagoya University, Nagoya 464-8602, Japan

E-mail: wkoinuma@bio.phys.nagoya-u.ac.jp

The photosystem II (PS II), protein complex drives oxidation reaction by using light energy. Mn cluster in PS II catalyzes water oxidation reaction through five intermediates states labeled S_i (i = 0-4). Y_Z residue works as an intermediate redox-active component for electron transfer between reaction center chlorophyll P680 and Mn-cluster in PS II (Fig. 1). It is proposed that Y_Z works not only as an electron transfer intermediate but also as a proton transfer intermediate. However conclusive evidences about its relation to proton transfer are not found.

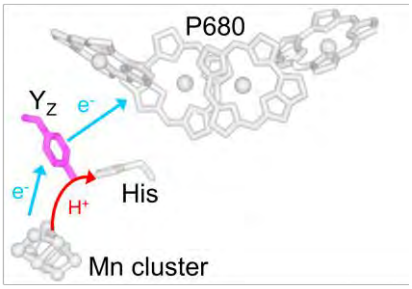

Fig. 1. Redox components, Y_Z, P680 and Mn cluster in PS II

In order to clarify the role of Y_Z, time-resolved EPR measurement was performed. Up to now, $Y_Z^{\bullet}$ transient EPR signal has been not well-resolved because of short lifetime and weak intensities. Such a weak EPR signal has been detected by Lock-in amplifier with magnetic field modulation. In commercial system, maximum modulation frequency is 100 kHz, because higher modulation frequency is difficult to supply to the cavity. Therefore, time resolution is limited by the modulation frequency of 100 kHz. In this work, we have achieved 500 kHz modulation frequency and improved time resolution of the EPR system by using high frequency Lock-in amplifier. We applied the new system to the detection of transient $Y_Z^{\bullet}$ signal in the presence of oxygen evolving complex. By using the system, we obtained four kinds of $Y_Z^{\bullet}$ decay components, depending on S_n/S_{n+1} state transitions. The four decay components have range from several tens of μs to several ms. Fig. 2 shows the time resolved $Y_Z^{\bullet}$ signal in $S_1 \rightarrow S_2$ transition. The result shows that the life time of $Y_Z^{\bullet}$ is less than 100 μs in $S_1 \rightarrow S_2$ transition.

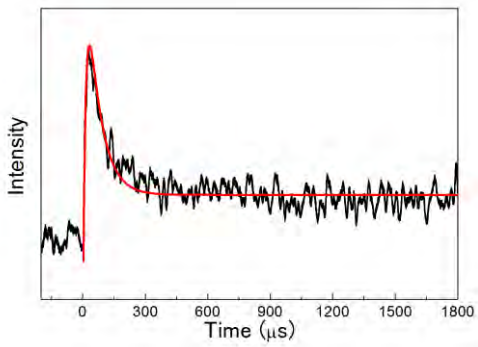

Fig. 2. The $Y_Z^{\bullet}$ transient signal in $S_1 \rightarrow S_2$ transition. Experiment (black) and fitting(red).

P-95

Electron Paramagnetic Resonance Lineshape and Spin–spin Interaction of Doubly Labeled Protein in a Denaturation Process

Yasunori Ohba [1], Munehito Arai [2], Tetsuya Itabashi [1], Jun Abe [3], Toshikazu Nakamura [3], Satoshi Takahashi [1], Seigo Yamauchi [1]

[1]*Institute of Multidiciplinary Research for Advanced Materials, Tohoku University, Sendai 980-8577, Japan*
[2]*Graduate School of Art and Science, Tokyo University, Tokyo 153-8902, Japan*
[3]*Institue of Molecular Science, Okazaki 444-8585, Japan*

E-mail: yohba@tagen.tohoku.ac.jp

Protein's local structures such as helices, sheets, and loops are folded in natural (native) form. The folding is necessary for protein to be active. Denaturation of protein is loss of the folded structure that results in a loss of protein's activity and caused by temperature change, pH change, and addition of chemicals. Folding/denaturation processes is important in studies of functions of protein and has been studied by various methods [1,2].

Combination of the site-directed spin-labeling (SDSL) technique and electron paramagnetic resonance (EPR) is a powerful method to study protein structures. We applied the SDSL-EPR method to a denaturation process of small model-protein focusing on changes of inter helices distances. We choose BDPA (the B domain of protein A) as model protein that consists of 60 aminoacids and has three helices, H1, H2 and H3. BDPA shows rapid transition between the native and denatured structures on addition/removal of guanidinium chloride (GdmCl) which is convenient in experiments [3].

BDPA is labeled at the 22nd (H2) and 55th (H3) residue with nitroxide radical (MTSL) to study the inter-helices distance during the denaturation process, Fig. 1. The spin-spin distance is measured by a DQC (double quantum coherence) method for solution that contains 50 μM doubly labeled BDPA. Denaturation is caused by addition of 5 M GdmCl. Previous DQC results showed that there is wide range of distribution of the spin-spin distance even in the native form that contains rather short distance less than 2 nm for which the analysis of the dipolar interaction is not appropriate. We will discuss effects of the short distance on the fitting of DQC signals modulated by dipolar interaction.

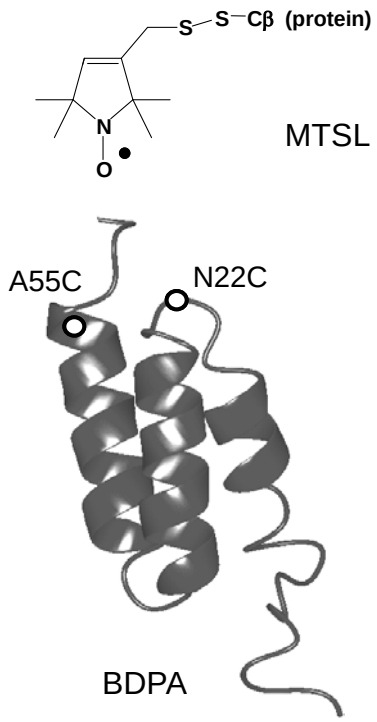

Fig. 1 The structure and labeling positions (22 and 55) of BDPA. The Cα-Cα distance for the 55th and 22nd residues is 0.87 ~ 1.04 nm [4].

References

[1] Sherman, E. and Haran, G., Coil-globule transition in the denatured state of a small protein, *PNAS*, **2006**, 103, 11539.

[2] K. W. Plaxco *et al.*, *Chain collapse can occur concomitantly with the rate-limiting step in protein folding*, *Nat. Struct. Biol.*, **1999**, 6, 554.

[3] Huang F., et al., Time-Resolved Fluorescence Resonance Energy Transfer Study Shows a Compact Denatured State of the B Domain of Protein A, *Biochemistry* **20091999**, 48, 3468

[4] S.Sato, et al., Testing protein-folding simulations by experiment: B domain of protein A, *Proc. Natl. Acad. Sci. USA*, **2004**, 101, 6952; PDB 1SS1.

P-96

Structural dynamics of cardiac troponin regulated by phosphorylation, as studied by spin-labeling dipolar EPR spectroscopy

Chenchao Zhao[1], Takayasu Somiya[1], Tomoki Aihara[1], Hiroaki Yamashita[1], Shoji Ueki[3], and Toshiaki Arata[1,2]

[1]Dept. Biol. Sci. and [2]Ctr. High Mag. Field Sci., Grad. Sch. Sci., Osaka Univ., Osaka 560-0043, Japan
[3]Kagawa Sch. Pharm. Sci., Tokushima Bunri Univ., Kagawa 769-2193, Japan

E-mail: arata@bio.sci.osaka-u.ac.jp

CW[1] and pulse dipolar EPR, PELDOR[2,3,5] and DQC[4], can determine a distribution of the distance 0.8-8.0 nm between two spin labels attached to protein or protein complex by site-directed genetic mutagenesis. Immobilization of spin label can identify tertiary contact sites [6,7]. Using site-directed spin labeling CW-EPR spectroscopy we have determined how major protein actin and Ca^{2+}-binding protein troponin (Tn) C-I-T complex from heart muscle.

Heart muscle beating is regulated by phosphorylation of cardiac troponin I (cTnI). As the switch action of skeletal muscle TnI-TnC was previously detected [5], we measured the distance between N-lobe of cTnC and regulatory region of cTnI both spin labeled, and found that cTnI binding to cTnC was loosened by ~0.2 nm after PKA phosphorylation of cTnI which causes Ca^{2+} desensitization of heart muscle.

We have determined the secondary structure of N-terminal phosphorylatable extension of cTnI by measuring the distance distribution between two spin labels attached on i and i+4 residues [8]. Upon binding with cTnC, PKA- and PKC-phosphorylatable regions formed more stable conformations whereas the other regions still exhibited unstable conformations.

References

[1] Ueki S., Nakamura M., Komori T. and Arata T., *Biochemistry* **2005,** 44, 411-416.
[2] Nakamura M., Ueki S., Hara H. and Arata T., *J. Mol. Biol.* **2005**, 348,127-137
[3] Sugata K., Song L., Nakamura M., Ueki S., Fajer P.G. and Arata T., *J Mol. Biol.* **2009**, 386, 626-636.
[4] Abe J., Ueki S., Arata T., Nakazawa S. Yamauchi S. and Ohba Y., *Appl. Mag. Reson.* **2012**, 42, 273-285.
[5] Aihara T., Nakamura M., Ueki S., Hara H., Miki M. and Arata T., *J. Biol. Chem.* **2010**, 285, 10671-10677.
[6] Ueda K., Kimura-Sakiyama C., Aihara T., Miki M. and Arata T., *Biophys. J.* **2011**, 100, 2432-2439.
[7] Ueda K., Kimura-Sakiyama C., Aihara T., Miki M. and Arata T., *Biophys. J.* **2013**, 105, 2366-2373.
[8] Zhao C., Takai S., Somiya T. and Arata T., *Biophys. J.* **2012**, 102, 406a.

P-97

Calcium-dependent structural dynamics of actin and tropomyosin in the thin filament with bound myosin heads in rigor state as studied by spin-labeling EPR spectroscopy

K. Ueda[1,3], A. Yamamoto[1], Y. Ueda[1], T. Aihara[1], S. Ueki[4], M. Miki[5], and T. Arata[1,2]

[1]Dept. Biol. Sci. and [2]Ctr. High Mag. Field Sci., Grad. Sch. Sci., Osaka Univ., Osaka 560-0043, Japan
[3]Div. Struct. Synth. Biol., RIKEN-Yokohama, Kanagawa 230-0045, Japan
[4]Kagawa Sch. Pharm. Sci., Tokushima Bunri Univ., Kagawa 769-2193, Japan
[5]Div. Appl. Chem. Biotech., Grad. Sch. Eng. Sci., Univ. Fukui, Fukui 910-8507, Japan

E-mail: arata@bio.sci.osaka-u.ac.jp

CW[1] and pulse dipolar EPR, PELDOR[2,3,5] and DQC[4], can determine a distribution of the distance 0.8-8.0 nm between two spin labels attached to protein or protein complex by site-directed genetic mutagenesis. Immobilization of spin label can identify tertiary contact sites [6,7]. Using EPR spectroscopy we have determined how major protein actin and regulatory proteins troponin (Tn) C-I-T complex and tropomyosin (Tm) move in the thin filament in response to myosin and Ca2+ binding. We previously detected the switch action of TnI-TnC complex in response to Ca2+ by measuring the distance between N-lobe of cTnC and regulatory region of cTnI both spin labeled [5]. In this study, we found that the distance between spin label at Cys374 and Mn^{2+} in F-actin increased by ~0.3 nm maximally at 30-60% occupancy by myosin-S1, suggesting structural cooperativity along filament like Tm does [2]. The distance also increased by ~0.3 nm when F-actin was decorated with Tm-Tn complex but returned to the original level upon further S1 binding at >60% occupancy as in the absence of Tm-Tn. However, no Ca^{2+} effect was observed in the actin distance.

We measured the rotational motion of a spin-label covalently bound to the side chain of a cysteine that was genetically incorporated into Tm in the thin filament. Previously, we did not detect Ca^{2+}-induced mobility changes in the absence of myosin [6]. Most of the Tm residues were immobilized on actin filaments with myosin-S1 bound to them and were mobilized when the Tn complex bound to the actin-Tm-S1 filaments. Surprisingly, the addition of Ca^{2+} partially reversed the Tn-induced mobilization of Tm residues on the S1-bound thin filaments [7]. These findings suggest that even in the myosin-bound rigor (open) state, Ca^{2+} may regulate actomyosin contractile properties via Tm.

References

[1] Ueki S., Nakamura M., Komori T. and Arata T., *Biochemistry* **2005,** 44, 411-416.
[2] Nakamura M., Ueki S., Hara H. and Arata T., *J. Mol. Biol.* **2005**, 348,127-137
[3] Sugata K., Song L., Nakamura M., Ueki S., Fajer P.G. and Arata T., *J Mol. Biol.* **2009**, 386, 626-636.
[4] Abe J., Ueki S., Arata T., Nakazawa S. Yamauchi S. and Ohba Y., *Appl. Mag. Reson.* **2012**, 42, 273-285.
[5] Aihara T., Nakamura M., Ueki S., Hara H., Miki M. and Arata T., *J. Biol. Chem.* **2010**, 285, 10671-10677.
[6] Ueda K., Kimura-Sakiyama C., Aihara T., Miki M. and Arata T., *Biophys. J.* **2011**, 100, 2432-2439.
[7] Ueda K., Kimura-Sakiyama C., Aihara T., Miki M. and Arata T., *Biophys. J.* **2013**, 105, 2366-2373.

P-98

Nucleotide-dependent Displacement and Dynamics of α-1 Helix in Motor Protein Kinesin Superfamily As Revealed by Site Directed Spin Labeling ESR

S. Yasuda[1], N. Furutani-Umezu[1], T. Yanagi[1], M. Yamada[3], S. Maruta[3], and T. Arata[1,2]
[1]*Dept. Biol. Sci. and* [2]*Ctr. High Mag. Field Sci., Grad. Sch. Sci., Osaka Univ., Osaka 560-0043, Japan*
[3]*Soka Univ. Hachioji, Japan*

E-mail: arata@bio.sci.osaka-u.ac.jp; tetutomo@bio.sci.osaka-u.ac.jp; furu-ume@bio.sci.osaka-u.ac.jp

Kinesin is a "motor" protein that moves uni-directionally along a microtubule (MT, tubulin polymer) hydrolyzing adenosine triphosphate (ATP to ADP+Pi) in an animal or plant cell. We previously measured the interspin distances between flexible neck linker (NL) and motor core on MT as well as between two NLs in dimeric kinesin on MT [1], and found that the transition of NL from undock to dock conformation occurred in the ATP state but not in ADP state or no nucleotide state, suggesting that NL is an ATP-dependent "actuator" and that two NLs could be pulled by the strain imposed by two docked NLs (Takai et al., unpublished results). Therefore, it is important to know how nucleotide species (ATP or ADP) in active catalytic site can communicate with NL and control NL docking on kinesin core domain. In kinesin x-ray crystal structures, N-terminal region of the α-1 helix is found to be adjacent to the adenine ring of nucleotide and the C-terminal region to the NL. Here, we show the displacement of the α-1 helix of kinesin monomer on MT in the presence and absence of nucleotides by using site directed spin labeling EPR. Kinesin which was doubly spin-labeled at α-1 and α-2 showed an broadening of the CW-ESR spectrum. The inter-helix distance distribution showed that 20% of spins have a peak at 1.4-1.7 nm which is close to that from the x-ray crystal structure but 80% beyond sensitivity (>2.5 nm). Upon MT binding, the fraction of 1.4-1.7 was 20 and 25% in the presence of AMPPNP (non-hydrolysable ATP analog) and ADP, respectively, whereas it increased to 40-50% in the absence of nucleotide. These nucleotide-induced changes in the fraction of defined peak were found to be related to those in the undocking fraction of NL from motor core. An attractive communication or transmission mechanism was therefore postulated that shift of the equilibrium between the α-1 helix positions occurs upon nucleotide binding and release and controls NL docking on motor core [2]. Using this mechanism we will understand how unique rice plant kinesin exhibits very slow ATPase rate [3,4] and probably slow movement like highly resembled mitotic kinesin. We are analyzing the nucleotide dependent distance between two helices in the rice kinesin.

References

[1] Sugata K., Song L., Nakamura M., Ueki S., Fajer P. G. and Arata T., *J. Mol. Biol.* **2009**, 386, 626-636.
[2] Yasuda S., Yanagi T., Yamada M. D., Ueki S., Maruta S., Inoue A. and Arata T., *Biochem. Biophys. Res. Commun.* **2014**, 443, 911-916.
[3] Tanaka K, Umeki N, Mitsui T, Fujimoto Z, and Maruta S., *J. Biochem.* **2011,** 149, 91-101.
[4] Umezu N., Hanzawa N., Yamada M. D., Kondo K., Mitsui T. and Maruta S., *J. Biochem.* **2011**, 149, 539-550.

P-99

Substrate specificity of the cobalamin uptake system in *E. coli* studied by EPR spectroscopy

Benesh Joseph[1], Arthur Sikora[2], Katja Barth[1], Martin Held[3], Gunnar Jeschke[4], Enrica Bordignon[5], David S. Cafiso[2] and Thomas F. Prisner[1]

1. *Institute of Physical and Theoretical Chemistry, Max-von-Laue-Strasse 7, Goethe University, 60438, Frankfurt am Main, Germany*
2. *Department of Chemistry, University of Virginia, McCormick Road, Charlottesville VA22904-4319, USA*
3. *Institute of Organic Chemistry and Chemical Biology, Max-von-Laue-Strasse 7, Goethe University, 60438, Frankfurt am Main, Germany*
4. *Laboratory for Physical Chemistry, ETH Zurich, Vladimir-Prelog-Weg 2, 8093 Zürich, Switzerland*
5. *Department of Physics, Free University of Berlin, Arnimallee 14, 14195 Berlin, Germany*

joseph@prisner.de

In bacteria, cobalamin-containing enzymes function in amino acid synthesis, nucleotide synthesis and metabolism [1]. The various forms of cobalamins like adenosyl-, hydroxyl- or methylcobalamin are derived inside the cell from cyanocobalalamin (vitamin B_{12}) metabolism. In *E. coli*, vitamin B_{12} is transported across the outer membrane into the periplasm by BtuB. For substrate transport into periplasm, it is proposed that BtuB uses the proton motive force existing across the inner membrane through interaction with the TonB-ExbB-ExbD complex. In the periplasm the binding protein BtuF binds free vitamin B_{12} and forms a complex with the inner membrane ATP-Binding Cassette (ABC) transporter BtuCD. The BtuCD-F complex couples ATP hydrolysis at the Nucleotide Binding Domains (NBDs) to transmembrane rearrangements [2,3,4] to transport vitamin B_{12} into the cytoplasm. Crystallographic and biochemical data show that BtuB, BtuF and BtuCD [4,5] can bind cyanocobalamin. Though adenosyl-, hydroxyl- and methylcobalamin are structurally similar to cyanocobalamin, it remains unknown whether any of them could be transported through the BtuB-BtuF-BtuCD system. To further elucidate the specificity of substrate binding and the details of the transport mechanism both *in vivo* and *in vitro*, we synthesized and characterized spin-labeled (4-amino TEMPO) forms of cyano, hydroxyl and methyl cobalamins. Both BtuB and BtuF bind the spin-labeled cobalamins, suggesting that the BtuB-BtuF-BtuCD system is flexible in terms of substrate specificity. Further, we provide the details of cobalamin(s)-BtuB/BtuF binding and the associated conformational changes through distance measurements using Pulsed Electron Double Resonance (PELDOR or DEER).

References

[1] Roth JR, Lawrence JG and Bobik TA., "Cobalamin (coenzyme B_{12}): synthesis and biological significance", *Annual Review of Microbiology* **1996**, 50, 137-181.

[2] Joseph B, Jeschke G, Goetz BA, Locher KP and Bordignon, E., "Transmembrane gate movements in the type II ATP-binding cassette (ABC) importer BtuCD-F during nucleotide cycle", *Journal of Biological Chemistry* **2011,** 286, 41008-41017.

[3] Joseph B, Korkhov VM, Yulikov M, Jeschke G and Bordignon, E., "Conformational cycle of the vitamin B_{12} ABC importer in liposomes detected by double electron-electron resonance (DEER)", *Journal of Biological Chemistry* **2014**, 289, 3176-3185.

[4] Korkhov VM, Mireku SA and Locher KP., "Structure of AMP-PNP-bound vitamin B_{12} transporter BtuCD-F", *Nature* **2012**, 490, 367-372.

[5] Shultis DD, Purdy MD, Banchs CN and Wiener MC., "Outer membrane active transport: structure of BtuB:TonB complex", **2006**, *Science*, 312, 1396-1399.

P-100

Arbitrary Waveform Pulse ESR at Very Low Temperatures: Multiple Excitation using Phase-ramped Gaussian Pulses

Yung Szen Yap[1,2], Yutaka Tabuchi[3], Shuuhei Tanijima[1], Makoto Negoro[1], Akinori Kagawa[1] and Masahiro Kitagawa[1]

[1]*Graduate School of Engineering Science, Osaka University, Toyonaka, Osaka 560-8531, Japan*
[2] *Faculty of Science, Universiti Teknologi Malaysia, 81310 Johor Bahru, Johor, Malaysia*
[3]*Research Center for Advanced Science and Technology, University of Tokyo, Meguro, Tokyo 153-8904, Japan*

E-mails: yungszen@utm.my, kitagawa@ee.es.osaka-u.ac.jp

We have been working on hyper-precise hyperpolarized ESR experiments primarily for quantum optics and quantum information processing such as quantum computation and simulation. Hyperpolarization of electron spins is required for initialization of spin qubit. We demonstrate pulsed ESR experiments at temperatures of the order of 100 mK at 0.6 T, where the electron spin polarization is near unity. The experimental setup using a dilution refrigerator and an arbitrary waveform generator (AWG) is shown in Fig. 1. The AWG-based spectrometer allows advanced pulse techniques with waveform modulation e.g. Gaussian pulses, composite pulses and numerically optimized pulse waveforms [1], which have already been used for precise spin control of nuclear spin qubits [2]. By combining different phase-ramped Gaussian pulses, we demonstrate multiple excitations at low temperatures. We will also introduce our composite pulse experiments carried out at 150 mK.

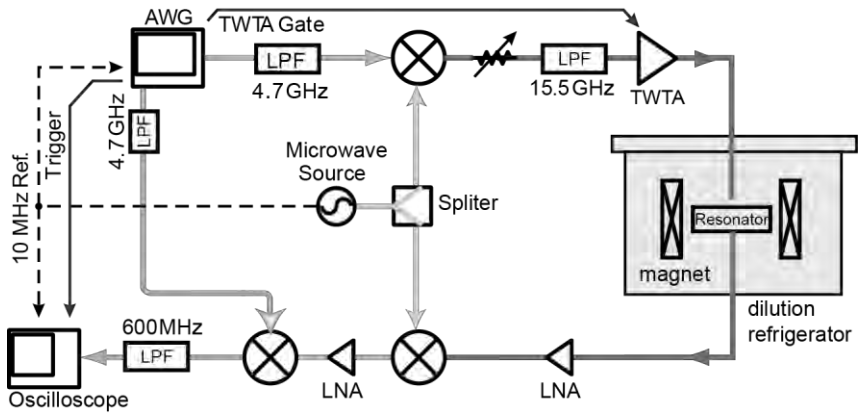

Fig. 1: Experimental setup for pulse ESR at very low temperature.

References

[1] Y. Tabuchi and M. Kitagawa, "Design method of dynamical decoupling sequences integrated with optimal control theory", *arXiv preprint* **2012**, arXiv:1208.5218v1 [quant-ph].

[2] L. M. K. Vandersypen and I. L. Chuang, "NMR techniques for quantum control and comp utation", Rev. Mod. Phys. **76**, 1037 (2004).

P-101

Molecular Spin Manipulation by Pulsed Electron Multiple Resonance Technique for Molecular Spin Quantum Computers

Kazunobu Sato,[1,4] Shigeaki Nakazawa,[1,4] Ayaka Tanaka,[1] Tomohiro Yoshino,[1,4] Kenji Sugisaki,[1,4] Shinsuke Nishida,[2,4] Tomoaki Ise,[1,4] Yasushi Morita,[2,4] Kazuo Toyota,[1,4] Daisuke Shiomi,[1,4] Masahiro Kitagawa,[3,4] and Takeji Takui[1,4]

[1]*Graduate School of Science, Osaka City University, Osaka 558-8585, Japan*
[2]*Faculty of Engineering, Aichi Institute of Technology, Toyota 470-0392, Japan*
[3]*Graduate School of Engineering Science, Osaka University, Toyonaka 560-8531, Japan*
[4]*FIRST-Quantum Information Processing Project, JSPS, Tokyo 101-8430, Japan*

E-mail:sato@sci.osaka-cu.ac.jp

Realization of practical quantum computing and quantum information processing (QC/QIP) has been challenging topics in advanced scientific fields. Among physically realized qubits, molecular electron spin-qubits have been the latest arrival, although electron spins have naturally been anticipated as typical matter spin-qubits. We have studied electronic structures of molecular spin qubit systems for QC/QIP and manipulated electron and nuclear spins in the molecular spin systems by pulse-based Electron Magnetic Resonance spectroscopy [1-4]. Recently, we have implemented an electron spin technique with arbitrary wave generators (AWGs) for precise manipulation of molecular spins. Microwave pulses with an arbitrary X-band frequency, its strength and phase generated by the AWG have been utilized for pulsed ESR experiments. The new AWG-based spectrometer can widely be applied to various sophisticated pulsed-ESR experiments.

In this paper, we present typical spin manipulations of organic stable radicals by pulsed ENDOR/ELDOR spectroscopy. The phase interferogram signals of electron and nuclear spins of the radical, partially deuterated diphenylnitroxide (DPNO), were observed by the time-proportional phase incrementation (TPPI) technique in ENDOR spectroscopy [5]. An interconversion process for transforming one electronic state to the other states is performed by introducing the MW or RF pulse. The observation of the interconversion enables us to directly prove four-π periodicity due to the spinor property of electron or nuclear spin-1/2. We have observed the spinor of the electron in a malonyl radical for the first time [2]. We have also applied pulsed ELDOR-NMR technique to DPNO in order to manipulate nuclear spins with small nuclear *g* factors such as nitrogen nucleus, illustrating that the ELDOR effects depend on which the hyperfine ESR transition is selectively excited. We have successfully analyzed the single-crystal ELDOR-NMR spectra of DPNO based on the ENDOR frequencies calculated.

In addition, we present an AWG-based electron-spin technology for molecular-spin quantum computers, demonstrating phase rotation and amplitude increment experiments with arbitrary microwaves, indicating that the electron spin state is controlled on the Bloch sphere without any limitations. A wide variety of applications of the AWG-based spin technology to quantum information science as well as high-sensitivity pulsed ESR spectroscopy are discussed for the implementation of molecular spin quantum simulators/computers. We will discuss how we can design arbitrary microwave pulses which serve as quantum gates for molecular spin systems.

References

[1] R. Rahimi, K. Sato, T. Takui et al., *Int. J. Quantum Inf.* **3**, 197 (2005).
[2] K. Sato, R. Rahimi, T. Takui et al., *Physica E* **40**, 363 (2007).
[3] K. Sato, S. Nakazawa, Y. Morita, T. Takui et al., *J. Mater. Chem.* **19**, 3739 (2009).
[4] S. Nakazawa, K. Sato, Y. Morita, T. Takui et al., *Angew. Chem. Int. Ed.* **51**, 9860 (2012).
[5] P. Höfer, *Appl. Magn. Reson.* **11**, 375 (1996).

P-102

Molecular Spin based Adiabatic Quantum Computers: Implementation of Pulse Sequences

Satoru Yamamoto, Shigeaki Nakazawa, Kenji Sugisaki, Kazunobu Sato, Kazuo Toyota, Daisuke Shiomi Takeji Takui

Graduate School of Science, Osaka City University, Japan

E-mail: satoru-y@sci.osaka-cu.ac.jp

Implementation of molecular spin quantum computers is an emerging issue in the field of quantum computation and quantum information processing. Molecular spin quantum computers utilize both electron spins and nuclear spins as qubits in open-shell entities. In this work, we have focused on molecular spin mediated adiabatic quantum computations (AQCs) [1], manipulating electronic spin states as a function of time evolution. In AQCs, quantum operations are described by the time evolutions of a ground state in a suitable quantum system. AQC algorithms can afford to transform time evolution operators into a series of pulse sequences to control both spin qubits.

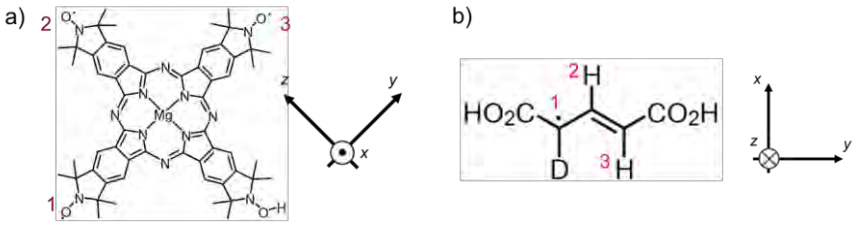

Figure 1. Molecular spins for AQC and the principal axis systems
a) a phthalocyanine derivative, b) a radical from glutaconic acid.

Here, we have calculated the pulse sequence of AQC factorization problems of 21 for molecular spins [2]. The time evolution unitary operator was calculated by Eq. 1, where $H(0)$ is an initial Hamiltonian consistent with the initial state and $H(1)$ is a final Hamiltonian depending on the adiabatic problem to solve. In this algorithm, the final Hamiltonian can be written as Eq. 2.

$$U(g_n: 0 \to 1) \approx \prod_{n=1}^{N} \exp(-iH(g_n)\Delta t_n) = \prod_{n=1}^{N} U_n \qquad \text{Eq. 1}$$

$$H(1) = (21 - \hat{x}\hat{y}), \hat{x} = (I - \sigma_z^1) + I, \hat{y} = 2(I - \sigma_z^2) + (I - \sigma_z^3) + I \qquad \text{Eq. 2}$$

For implementing the pulse sequences, we adopted two molecular spins in single crystals, a phthalocyanine derivative for a three-electron-qubit system and a radical from glutaconic acid for one electron (bus qubit) system with two nuclear client qubits (Fig. 1a and 1b, respectively). The effective Hamiltonians of these systems are calculated by adopting individual rotating frames in terms of a secular averaging approach, following their spin dynamics. The static magnetic field is assumed to apply along the z-direction as depicted in Fig. 1, which fulfils experimental conditions for AQ C.

The conquered pulse sequences in the molecular spins give shorter operation times than an NMR study [2], which depend on spin interaction strengths under study. Especially, the glutaconic acid radical system requires the longest pulse sequence. This is because this system needs three-qubit interaction terms [3] between the nuclei.

References

[1] Farhi E., Goldstone J., Gutman S., Sipser M., "Quantum Computation by Adiabatic Evolution" arXiv:quant-ph/0001106

[2] Peng X.-H., Liao Z., Xu N., Qin G., Zhou X., Suter D., Du J., "Quantum Adiabatic Algorithm for Factorization and Its Experimental Implementation" *Phys. Rev. Lett.* **2008**, 101, 220405.

[3] Tseng C. H., Somaroo S., Sharf Y., Knill E., Laflamme R., Havel T. F., Cory D. G., "Quantum simulation of a three-body-interaction Hamiltonian on an NMR quantum computer" *Phys. Rev. A.* **1993**, 61, 012302.

P-103

Determination of the Fine-Structure Tensors and Double Quantum Transitions for Iminonitroxide-Nitroxide Diradicals in Magnetically Diluted Single Crystals as Studied by CW/Pulsed ESR

S. Nakazawa, M. Kawamori, K. Sugisaki, K. Toyota, D. Shiomi, K. Sato, K. Omukai, T. Furui, M. Kuratsu, S. Suzuki, M. Kozaki, K. Okada and T. Takui

Graduate School of Science, Osaka City University, Osaka 558-8585, JAPAN

s-nakaza@sci.osaka-cu.ac.jp

Recently, quantum computing/quantum information processing (QC/QIP) by using pulsed ESR spectroscopy has attracted much attention, being underlain by novel molecular spins and implementation of sophisticated pulse-microwave spin technology. Extremely stable and highly compact nitoroxide-substituted iminonitroxide **1** was synthesized [1], which serves for not only a building block for organic molecular magnetic materials but also an ensemble electron spin-qubit for memory devices coupled with SC qubit systems for gate operations of QC/QIP. Triplet diradical **1** in the ground state has a large D value (-0.0655 cm^{-1}), the largest among the ground-state triplet (S = 1) nitroxide diradicals documented so far. We made magnetically diluted single crystals which are able to serve as the quantum spin memory. Molecular crystal engineering was exploited for the preparation. Temperature dependence of the D value was observed and was interpreted as the change of the molecular structure in the diamagnetic host single crystal with changing temperature. The structural change resulting in the modulation of the D value was explained in terms of quantum chemical calculations.

During the temperature dependence experiments, we observed the disappearance of the fine-structure ESR signal associated with a catastrophic change of the spin-spin relaxation time at around 25 K, suggesting the occurrence of softening crystal lattice modes. We also observed double quantum (DQ) transitions in the fine-structure ESR spectra in both organic glasses and the single crystal at low temperatures. Two types of the mechanism for the DQ transition have been proposed in the literature [2]. In our case at 50 K in glasses, the power dependence of the DQ signal is indicative of the mechanism of the consecutive absorption of microwave quanta. Avoiding saturation effects, pulsed ESR spectroscopy was used below 50 K. The power dependence of the DQ nutation frequency at 10 K also suggested the occurrence of the consecutive absorption.

In order to study the DQ mechanism in microsopic terms, the Q-band CW single-crystal ESR and pulse based nutation spectroscopy of diradical **1** were carried out. Microscopic origins of the DQ transitions in the present system are proposed, focusing on the possible fluctuation of energy sublevels arising from many component nitrogen nuclei.

[1] S. Suzuki, T. Furui, M. Kuratsu, M. Kozaki, D. Shiomi, K. Sato, T. Takui and K. Okada, *J. Am. Chem. Soc.* **2010 (**132*)* 15908-15910.

[2] D. Collison, M. Helliwell, V.M. Jones, F.E. Mabbs, E.J.L. McInnes, P.C. Riedi, G.M. Smith, R.G. Pritchard and W.I. Cross, *J. Chem. Soc., Faraday Trans*. **1998** (94) 3019-3025.

P-104

A Nitrogen Nuclear-Spin Manipulation in Single Crystals for the Use of Molecular Spin Qubits by ELDOR-NMR technique

Ayaka Tanaka[1], Kazunobu Sato[1,4], Tomohiro Yoshino[1], Shinsuke Nishida[2,4], Shigeaki Nakazawa[1,4], Robabeh Rahimi[1], Kazuo Toyota[1,4], Daisuke Shiomi[1,4], Yasushi Morita[2,4], Masahiro Kitagawa[3,4] and Takeji Takui[1,4]

[1]*Graduate School of Science, Osaka City University, Osaka 558-8585, Japan*
[2]*Faculty of Engineering, Aichi Institute of Technology, Toyota 470-0392, Japan*
[3]*Graduate School of Engineering Science, Osaka University, Toyonaka 560-8531, Japan*
[4]*FIRST-Quantum Information Processing Project, Tokyo 101-8430, Japan*

E-mail: tnkyk-a@sci.osaka-cu.ac.jp

Implementation of quantum computers (QCs) has been the focus of the contemporary issues in quantum science and related fields[1]. We have applied pulse-based Electron- Nuclear DOuble Resonance (ENDOR) and ELectron-electron DOuble Resonance (ELDOR) techniques to molecular spin-based qubits from the experimental side[2-5]. In this paper, we present an application of pulse-based ELDOR-NMR technique to a stable organic radical in order to manipulate the molecular spin-qubits. We also show the potential of pulse-based ELDOR-NMR spectroscopy applied to single crystals which incorporate stable organic radicals with nitrogen nuclei as particular client qubits. The ELDOR-NMR technique reduces operation time for manipulating nuclear spin qubits compared with the ENDOR technique.

The ELDOR measurements have been carried out on a Bruker BioSpin Elexsys E580 spectrometer with a laboratory-designed Oxford Optistat SXM cryostat. Echo-detected field-swept ELDOR-NMR spectra of the stable organic radical have been observed in the single crystal. Typical ELDOR- NMR spectra were shown in Fig.1. The positions of the ELDOR-signals are almost independent on the static magnetic field. The ELDOR effect observed varies when sweeping the frequency of the second MW pulse. The ELDOR effects are attributed to the occurrence of the NMR forbidden transitions related to the Nitrogen nuclear spin. We discuss the manipulation of the electron and nuclear spin qubits by the use of the ELDOR technique and coherent dual ELDOR effects in the molecular qubit system.

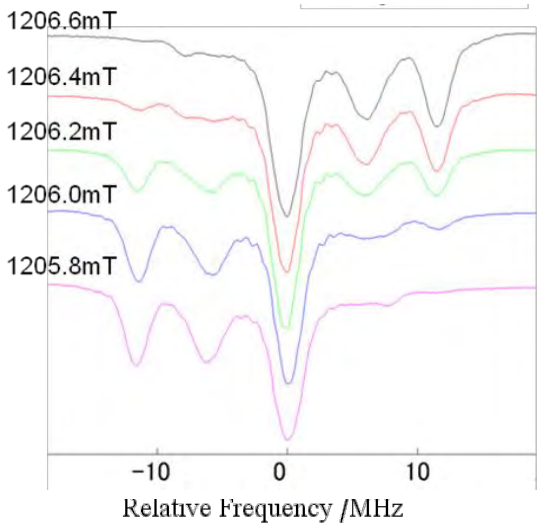

Fig.1 The single-crystal field-dependent ELDOR-NMR spectra of isotope-labeled diphenyl nitroxide observed at ν_1 = 33.814004GHz, T = 100 K with $B_0 \| b$ axis.

[1] E. Coronado, A. J. Epstein, eds., "Molecular spintronics and quantum computing", *J. Mater. Chem.*, **2009**, *19*, 1661-1768.
[2] R. Rahimi, K. Sato, T. Takui et al., "PULSED ENDOR-BASED QUANTUM INFORMATION PROCESSING", *Int. J. Quantum Inf.*, **2005**, *3*, 197-204.
[3] K. Sato, R. Rahimi, T. Takui et al., "Implementation of molecular spin quantum computing by pulsed ENDOR technique: Direct observation of quantum entanglement and spinor", *Physica E*, **2007**, *40*, 363-366.
[4] K. Sato, S. Nakazawa, Y. Morita, T. Takui et al., "Molecular electron-spin quantum computers and quantum information processing: pulse-based electron magnetic resonance spin technology applied to matter spin-qubits", *J. Mater. Chem.*, 2009, *19*, 3739-3754.
[5] T. Yoshino, K. Sato, Y. Morita, T. Takui et al., "ESR and ^{1}H-,^{19}F-ENDOR/TRIPLE Study of Fluorinated Diphenylnitroxides as Synthetic Bus Spin-Qubit Radicals with Client Qubits in Solution", *J. Phys. Chem. Lett.*, **2011**, *2*, 449-453.

P-105

Dichotomy of *3d* Electrons in YbT_2Zn_{20} (T=Co; Fe): An ESR Study

V.A. Ivanshin[1], T.O. Litvinova[1], S. Jia[2], S.L. Bud'ko[2], P.C. Canfield[2]

[1]*Institute of Physics, Kazan Federal (Volga region) University, 420008 Kazan, Russia*
[2]*Ames Laboratory, U.S. Department of Energy, and Department of Physics and Astronomy, Iowa State University, Ames, IA 50011, USA*

E-mail: Vladimir.Ivanshin@kpfu.ru

The essential physics of strongly correlated electron systems is related to the competition of Coulomb repulsion and following localization of *d* or *f* electrons with hybridization of neighboring ligands which causes a *d*- or *f*-itineracy. Both the localized magnetic moments and itinerant electrons can cause the electron spin resonance (ESR) signals. Recently, the series of compounds RT_2Zn_{20} (R is rare earth ion or actinoid and T is *d*-electron transition metal) has attracted considerable attention due to a large span of intriguing physical properties.

We report a remarkable and unprecedented co-existence of the strongly anisotropic ESR spectra from the localized Co *3d* electrons and conduction electrons in the high-quality $YbCo_2Zn_{20}$ single crystals in a broad temperature range between 4 and 300 K [1]. Our results provide the first direct evidence that ESR in a dense heavy-fermion compound with ferromagnetic (FM) correlations or static FM order originates both from localized and conducting states. It is shown that the relative contribution of itinerant electrons to the total magnetization does not exceed 9%. We show that magnetic behavior in YbT_2Zn_{20} (T=Co; Fe) and YbCuAl [2] is strongly influenced by the *3d* magnetic moments, and a weak itinerant ferromagnetism from the 3*d* sublattice only determines ESR spin dynamics at the microscopic level. Our findings on a close interplay between the valence instability of the *4f* electrons and magnetic instability of the *3d* electrons are compared with very similar results in UFe_2Zn_{20} [3], $YbFe_2Al_{10}$ [4], $YbMn_6Ge_{6-x}Sn_x$ [5], and $YbFe_4Sb_{12}$ [6] obtained by different other methods.

We argue that the ESR technique has emerged as a fascinating tool to probe the low energy paramagnetic fluctuations in dense FM *4f* and *5f* intermetallics and can be used as a rapid marker of the IV behaviour and proximity to a quantum criticality [7].

[1] V.A. Ivanshin et al., "Dual nature of electron spin resonance in $YbCo_2Zn_{20}$ intermetallic compound", *JETP Lett.* **2014,** Vol. 99, 153-157.
[2] C. Tien, J.-T. Yu, and H.-M. Duh, "Electron spin resonance in intermediate ytterbium valent compound YbCuAl", *Jpn. J. Appl. Phys.* **1993**, Vol. 32, 2658-2664.
[3] P. Swatek and D. Kaczorowski, "Magnetic behaviour in UFe_2Zn_{20} and URu_2Zn_{20} single crystals", *J. Phys.: Condens. Matter* **2011**, Vol. 23, 466001.
[4] P. Khuntia et al., "Contiguous 3d− and 4f−magnetism: towards strongly correlated 3d−electrons in $YbFe_2Al_{10}$", *arXiv cond-mat/1402.4701v2*.
[5] T. Mazet et al., "Nonpareil Yb behavior in $YbMn_6Ge_{6-x}Sn_x$", *Phys. Rev. Lett.* **2013**, Vol. 111, 096402.
[6] M. Koza et al., "Vibrational dynamics of the filled skutterudite $Yb_{1-x}Fe_4Sb_{12}$: Debye-Waller factor, generalized density of states, and elastic structure factor", *Phys. Rev. B* **2014**, Vol. 89, 014302.
[7] A. Ramires and P. Coleman, "Theory of the electron spin resonance in the heavy fermion metal β−$YbAlB_4$", *Phys. Rev. Lett.* **2014,** Vol. 112, 116405.

P-106

DFT-Based Calculations of the Spin–Orbit Term in Zero-Field Splitting Tensors: The Corrected QRO Method

Kenji Sugisaki[1], Kazuo Toyota[1], Kazunobu Sato[1], Daisuke Shiomi[1], Masahiro Kitagawa[2] and Takeji Takui[1]

[1] *Department of Chemistry and Molecular Materials Science, Graduate School of Science,Osaka City University, 3-3-138 Sugimoto, Sumiyoshi-ku, Osaka 558-8585, Japan*
[2] *Department of System Innovation, Graduate School of Engineering Science, Osaka University, 1-3 Machikaneyama, Toyonaka, Osaka 560-8531, Japan*

E-mail: sugisaki@sci.osaka-cu.ac.jp

Zero-field splitting (ZFS) tensors (**D** tensors) are one of the most important physical quantities which characterize the electronic spin structures of open-shell systems having spin quantum number $S > 1/2$. Major origins of ZFS are spin–spin dipolar (SS) and spin–orbit (SO) couplings appearing as the first- and second-order terms, respectively, in the perturbation expansion starting from the non-relativistic Schrödinger equations.

In transition metal complexes and molecules containing heavy atoms, the SO terms of the **D** tensors ($\mathbf{D}^{SO}$ tensors) are generally more important than the SS terms ($\mathbf{D}^{SS}$ tensors). The DFT-based theoretical approaches for the $\mathbf{D}^{SS}$ and $\mathbf{D}^{SO}$ tensors have attracted attention owing to their low computational costs and the availability of the published quantum chemical calculation software. However, some difficulties intrinsic to the DFT-based approaches have been pointed out by several groups and sophisticated ab initio methods usually give more reliable results than DFT.[1,2] In this context, the improvement of the DFT-based approaches for **D** tensors is of significant importance.

The quasi-restricted orbital (QRO) method for the $\mathbf{D}^{SO}$ tensor calculations utilizes a sum-over-states equation used for the CI-type wave function theory, in conjunction with the single Slater determinant consisting of natural orbitals.[3] The important feature of the QRO method is that it utilizes spin eigenfunctions as the zeroth order wave functions and therefore it is free of spin contamination. However, Schmitt and coworkers pointed out that the "distance" closed-shell subsystems give a spurious contribution to the $\mathbf{D}^{SO}$ tensor in the QRO approach because only a few classes of excitations have been selected.[4]

In this work, we have revisited the derivation of the QRO working equation and modified it, making it include all possible types of excitations in the sum-over-states procedure. Some preliminary calculations of transition metal complexes will be given.

[1] Sugisaki K., Toyota K., Sato K., Shiomi D., Kitagawa M. and Takui T., "Quantum Chemical Calculations of the Zero-Field Splitting Tensors for Organic Spin Multiplets", in *EPR of Free Radicals in Solids I*, Springer, (2013) pp. 363-392., and references therein.

[2] Sugisaki K., Toyota K., Sato K., Shiomi D., Kitagawa M. and Takui T., "An ab initio MO study of heavy atom effects on the zero-field splitting tensors of high-spin nitrenes: how the spin–orbit contributions are affected", *Phys. Chem. Chem. Phys.* **2014**, *16*, 9171-9181.

[3] Neese F., "Importance of direct spin–spin coupling and spin-flip excitations for the zero-field splittings of transition metal complexes: A case study", *J. Am. Chem. Soc.* **2006**, *128*, 10213-10222.

[4] Schmitt S., Jost P. and van Wüllen C., "Zero-field splittings from density functional calculations: Analysis and improvement of known methods", *J. Chem. Phys.* **2011**, *134*, 194113.

P-107

High-Field Multi-Frequency ESR in the Rare-Earth Spinel Compound $CdYb_2S_4$

Daichi Yoshizawa[1], Takanori Kida[1], Satoru Nakatsuji[2], Kensuke Iritani[2], Tetsuya Takeuchi[3], and Masayuki Hagiwara[1]

[1]*Center for Advanced High Magnetic Field Science, Graduate School of Science, Osaka University, Osaka 560-0043, Japan*
[2]*Institute for Solid State Physics, The University of Tokyo, Chiba 277-8581, Japan*
[3]*Low Temperature Center, Osaka University, Osaka 560-0043, Japan*

E-mail: yoshizawa@mag.ahmf.sci.osaka-u.ac.jp

Geometrically frustrated systems sometimes exhibit attractive features such as a spin liquid, spin ice, and chiral order. Recently, rare-earth compounds with a pyrochlore lattice have attracted much attention because of their anomalous magnetic structures and interesting features. Four types of magnetically ordered states are theoretically predicted. The spin ice state, namely two-in-two-out state, in $Dy_2Ti_2O_7$ and $Ho_2Ti_2O_7$ is one of the typical examples [1,2], and magnetic structures with the ψ_2-state and the Palmer-Chalker state were observed in $Er_2Ti_2O_7$ and $Er_2Sn_2O_7$ [3,4], respectively.

Most studies on rare-earth compounds with the pyrochlore lattice have been conducted on pyrochlore compounds $R_2M_2O_7$ (R : rare-earth, M : transition metal). In contrast, spinel rare-earth compound AR_2X_4 (A : 2+ cation, R : rare-earth, X : O, S , Se or Te), where R sites form the pyrochlore lattice, has been merely studied. Exchange interactions and magnetic anisotropy are expected to be different between pyrochlore and spinel compounds due to different local configurations around magnetic ions and exchange pathways. Thus, it is important to study spinel compounds to compare the features in two-kinds of rare-earth compounds with the pyrochlore lattice.

From this point of view, we focus on the rare-earth spinel compound $CdYb_2S_4$. In this material, Yb^{3+} ions form the pyrochlore lattice. Recentry, $Yb_2Ti_2O_7$ has been studied actively as a model compound of the quantum spin ice [5]. Thus, it is conceivable that $CdYb_2S_4$ may show interesting features as in $Yb_2Ti_2O_7$. In previous studies, a sharp peak of the specific heat was observed at T=1.8 K, indicating an antiferromagnetic transition. In the present study, we have performed electron spin resonance (ESR) and magnetization measurements in pulsed magnetic fields of up to 55 T. From the complementary analysis of ESR and magnetization results, we have found three transitions at H_1=2.6 T, H_2=7.7 T, H_3=21.5 T. In addition, we observed an ESR mode which shows a gapless feature of $CdYb_2S_4$ at $H < H_1$ and $T < T_N$. This finding indicates that $CdYb_2S_4$ has the ψ_2-state magnetic structure below T_N. This must be the first observation of the ψ_2-state magnetic structure in the rare-earth spinel compound. The ψ_2-state magnetic structure has been observed so far only in rare-earth pyrochlore compound $Er_2Ti_2O_7$.

References

[1] Ramirez A. P., Hayashi A., Cava R. J., Siddharthan R., and Shastry B. S., "Zero-point entropy in 'spin ice'", *Nature* **1999**, 399, 333.

[2] Fennell T., Deen P. P., Wildes A. R., Schmalzl K., Prabhakaran D., Boothroyd A. T., Aldus R. J., McMorrow D. F., and Bramwell S. T., "Magnetic Coulomb Phase in the Spin Ice $Ho_2Ti_2O_7$", *Science* **2009**, 326, 415.

[3] Savary L., Ross K. A., Gaulin B. D., Ruff J. P. C., and Balents L., "Order by Quantum Disorder in $Er_2Ti_2O_7$", *Phys. Rev. Lett.* **2012**, 109, 167201.

[4] Guitteny S., Petit S., Lhotel E., Robert J., Bonville P., Forget A., and Mirebeau I., "Palmer-Chalker correlations in the *XY* pyrochlore antiferromagnet $Er_2Sn_2O_7$", *Phys. Rev. B* **2013**, 88, 134408.

[5] Ross K. A., Savary L., Gaulin B. D., and Balents L., "Quantum Excitations in Quantum Spin Ice", *Phys. Rev. X* **2011**, 1, 021002.

P-108

High-field ESR facility and related research at Wuhan National High Magnetic Field Center

Z. W. Ouyang,[1] M. Y. Ruan,[1] H. Nojiri[2] S. Okubo,[3] H. Ohta[3]

[1]*Wuhan National High Magnetic Field Center, Huazhong University of Sciences & Technology, Wuhan 430074, P. R. China.*

[2]*Institute for Materials Research, Tohoku University, Sendai 980-8577, Japan*

[3]*Molecular Photoscience Research Center, Kobe University, 1-1 Rokkodai, Nada, Kobe, 657-8501, Japan*

Email: zwouyang@mail.hust.edu.cn

High-field high-frequency electron spin resonance (ESR) facility has been developed in Wuhan National High Magnetic Field Center [1]. The magnetic field up to 30 T is generated by a pulsed magnet driven by a 0.8 MJ capacitor band. Electromagnetic waves from 60 to 520 GHz are available by combining Backward wave oscillators and Guan Oscillators. As examples of its application, we performed the high-field ESR measurements of spin-chain compounds Ca_3ZnMnO_6 [2] and Gd_2BaNiO_5, and triangular-lattice antiferromagnet $Ba_3MnSb_2O_9$. The ESR spectra correlate strongly with magnetization. The observed resonances modes below the ordering temperature T_N are discussed based on the well-developed antiferromagnetic resonance theory.

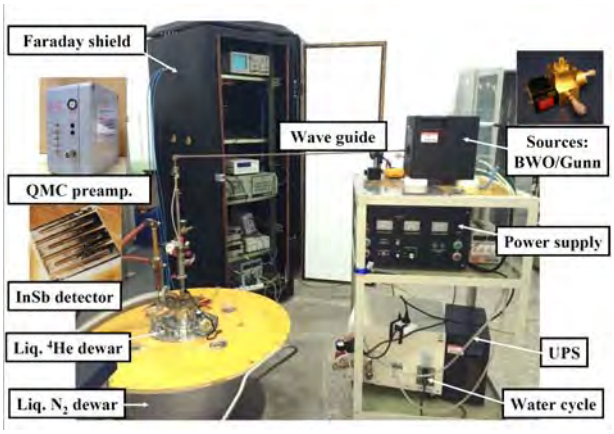

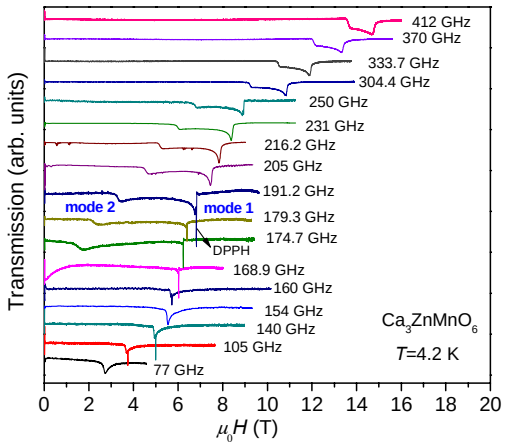

[1] S.L. Wang, L. Li, Z.W. Ouyang, Z.C. Xia, N.M. Xia, T. Peng and K.B. Zhang, "Development of high-magnetic-field, high frequency electronic spin resonance system", Acta Phys. Sin. 61, 107601 (2012).

[2] M.Y. Ruan, Z.W. Ouyang, Y.M. Guo, J.J. Cheng, Y.C. Sun, Z.C. Xia, G.H. Rao, S. Okubo, and H. Ohta, "Disappearance of Ising nature in Ca_3ZnMnO_6 studied by high-field ESR", J. Phys.: Condens. Matter 26, 236001 (2014).

P-109

ODMR study of systems with (CdMn)Te/(CdMg)Te quantum wells

D.O. Tolmachev, A.S. Gurin, N.G. Romanov, B.R. Namozov, Yu.G. Kusrayev, P.G. Baranov

Physical-Technical Institute, Russian Academy of Sciences, 194021 St. Petersburg, Russia

E-mail: Daniel.Tolmachev@gmail.com

Optically detected magnetic resonance (ODMR) has been intensively applied for studying diluted magnetic semiconductors (DMSs). An ODMR of Mn^{2+} ion was measured as a variation of photoluminescence intensity for CdMnSe/ZnSe quantum dots under 35 GHz microwave irradiation [1]. In spite of isotropic *g*-factor of Mn^{2+}, the anisotropic behavior of the center of gravity of the EPR spectra has been observed. It was found that the EPR lines corresponding to the lowest $M_S = -5/2 \rightarrow M_S = -3/2$ transition dominate the spectrum because of the high Boltzmann factor at 35 GHz and 2 K. The axial fine structure with strong positive zero-field splitting in CdMnSe quantum dots was concluded to be caused by their low dimensionality. Fine structure of isolated Mn^{2+} ions in CdMnSe/ZnSe quantum wells (QWs) was revealed by ODMR recorded by monitoring both exciton emission and intra-Mn luminescence in the presence of simultaneous microwave irradiation [2]. A large decrease of photoluminescence (PL) intensity of excitons and an increase of PL intensity of Mn^{2+} ions is observed when an applied magnetic field satisfies the Mn^{2+} electron paramagnetic resonance (EPR) condition. This suggests that a spin-dependent energy transfer from excitons to intra-Mn excitations occurs at the EPR condition.

In system with (Cd,Mn)Te quantum wells containing 2D hole gas exchange interaction effects between Mn^{2+} ions and confined holes were revealed by ODMR [3]. Two anisotropic ODMR signals with different angular variations are observed and ascribed to isolated manganese ions and to exchange-coupled complexes consisting of manganese and holes. It is shown that calculations on the basis of spin Hamiltonian for these systems are in agreement with the experimental data.

In this work, we study structure consisting of three (CdMn)Te/(CdMg)Te QWs where we observe ODMR signals with different structure and anisotropy. The (CdMn)Te/(CdMg)Te heterostructures under study were grown by molecular-beam epitaxy and contained three quantum wells with the widths of 4 nm, 6 nm and 10 nm. The QWs were separated by the 30 nm CdMgTe barriers and cowered by 100 nm CdMgTe cap layer. The Mn content was 1% and 4 %.

In 4 nm and 6 nm QWs there is signal with properties similar to that observed in Ref. [3] for (CdMn)Te QWs containing excess holes. It can be explained as superposition of two lines originating from isolated Mn ions and from complexes formed by Mn ions and localized holes. Observation of ODMR spectra of Mn-hole complexes in 4 nm and 6 nm QWs implies the existence of excess hole concentration in these QWs. This can be proved by detection of ODMR by recording transformations of complete spectra. The PL spectrum in each QW consists of two emission lines - excitons and charged excitons (trions). These lines manifest similar shifts to lower wavelengths with increasing magnetic field. However this ODMR is present only in trion band. That also proves presence of excess holes that can exist due to directional tunneling of photo-created electrons towards wider wells.

In conclusion, using ODMR technique for studying structure with triple (CdMn)Te QWs it is possible to observe signals from exchange-coupled complexes formed by Mn and localized holes and from isolated Mn^{2+} ions. Analysis of recorded signals and angular dependencies allows to assume existence of a directional electron tunneling from narrower towards wider wells.

References

[1] P. G. Baranov, N. G. Romanov, D. O. Tolmachev et al., "Evidence for Mn^{2+} fine structure in CdMnSe/ZnSe quantum dots caused by their low dimensionality", JETP Lett. **2008**, 88, 631.

[2] D.O. Tolmachev et al., "Optically detected magnetic resonance in CdMnSe/ZnSe submonolayer quantum wells", Phys. Status Solidi B-Basic Res. **2010**, 247, 1511-1513

[3] D.O. Tolmachev et al., "ODMR of Mn-related excitations in (Cd,Mn)Te quantum wells", JETP Lett. **2012**, 96, 231-235

P-111

Electric Field Effect on Electron-Spin Coherence Time of Single NV center in Diamond

Satoshi Kobayashi, Hiroki Morishita, Shinji Miwa, Yoshishige Suzuki, Norikazu Mizuochi

Graduate School of Engineering Science, Osaka University, Toyonaka, Osaka 560-8531, Japan

E-mail: kobayashi@spin.mp.es.osaka-u.ac.jp

Nitrogen-vacancy (NV) centers in diamond (see Fig. (a)) utilize a wide range of novel applications; nano-magnetometry [1], electrometry [2], thermometry [3], quantum information processing [4], electrically driven single photon source [5], and bio-imaging [6]. The NV centers in diamond has following remarkable properties for realizing such applications: they have strong enough fluorescence to detect atomic single centers, spin-decedent fluorescence for readout of single-spin states and optical-spin initialization, and long coherence time. However, the performances of the applications are limited by decoherence processes of the NV-electron spin, and hence an enhancement of coherence time of the NV-electron spin (T_{e2}) is essential. Here we present electric field effects on T_{e2}.

Figure (b) illustrates a schematic image of our home-made confocal microscope and sample structure to measure T_{e2} of the single NV centers in an externally applied electrical field. Single NV centers were created in a natural abundance diamond substrate by nitrogen ion-implantation and annealing. The electrodes for applying electric field to the single NV centers were fabricated on the diamond substrate by electron beam lithography and metal deposition. The electrodes have a gap of ~10 μm. The Hahn-echo sequence under electrical field was applied to investigate effects on the T_{e2} of the electrical field.

We succeeded the enhancement of T_{e2} by applying electrical field. It was reported that the T_{e2} in natural abundance diamond is limited by surrounding ^{13}C nuclear spins [7]. The electrical field can reduce the adverse impact of magnetic-field fluctuation generated by the ^{13}C nuclear spins. The T_{e2} therefore was increased 45 μsec at 0 kV/cm to 82 μsec at 70 kV/cm.

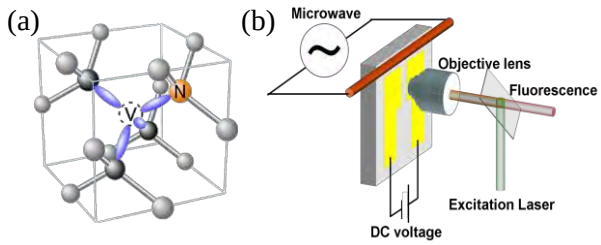

Fig. (a) A nitrogen vacancy center in a diamond crystal. (b) Schematic image of our measurements setup. Electrodes were fabricated on a diamond substrate to apply strong electric field. The distance between the electrodes is about 10 μm.

References

[1] G. Waldherr *et al.*, "High-dynamic-range magnetometry with a single nuclear spin in diamond", *Nature Nanotechnology* **2012**, 7, 105-108.

[2] F. Dolde *et al.*, "Electric-field sensing using single diamond spins", *Nature Physics* **2011**, 7, 459-463.

[3] D. M. Toyli *et al.*, "Fluorescence thermometry enhanced by the quantum coherence of single spins in diamond", *Proceedings of the National Academy of Sciences* **2013**, 110, 8417–8421.

[4] P. Neumann, N. Mizuochi, *et al.*, "Multipartite Entanglement Among Single Spins in Diamond", *Science* **2008**, 320, 1326-1329.

[5] N. Mizuochi *et al.*, "Electrically driven single photon source at room temperature in diamond", *Nature Photonics* **2012**, 6, 299-303.

[6] L. P. McGuinness *et al.*, "Quantum measurement and orientation tracking of fluorescent nanodiamonds inside living cells", *Nature Nanotechnology* **2011**, 6, 358-363.

[7] N. Mizuochi *et al.*, "Coherence of single spins coupled to a nuclear spin bath of varying density", *Physical Review B* **2009**, 80, 041201(R).

P-113

High Field ESR Measurements of the Spin Gap System in Polarized Light

Shojiro Kimura[1], Kazuo Watanabe[1], Takanari Kashiwagi[2],
Hironori Yamaguchi[3], Masayuki Hagiwara[4], and Zentaro Honda[5]

[1]*Institute for Materials Research, Tohoku University, Sendai 980-8577, Japan*
[2] *Graduate School of Pure and Applied Sciences, University of Tsukuba, Tsukuba 305-8573, Japan*
[3] *College of Integrated Arts and Science, Osaka Prefecture University, Sakai 588-8531, Japan*
[4] *Center for Advanced High Magnetic Field Science, Graduate School of Science, Osaka University, Osaka 560-0043, Japan*
[5] *Graduate School of Science and Engineering, Saitama University, Saitama 338-8570, Japan*

E-mail: shkimura@imr.tohoku.ac.jp

The spin gap system $Na_2Co_2(C_2O_4)_3(H_2O)_2$ is known to behave as an isolated antiferromagnetic dimer, composed of two effective spins S = 1/2 [1]. From the previous ESR measurements, the direct transition from the singlet ground state to the excited triplet state of this compound was observed [1]. Such a direct transition is forbidden for usual magnetic dipole transition, because of difference in parity between the singlet and triplet states. The parity in the singlet and triplet states of the S = 1/2 dimer are odd and even, respectively, whereas that of the magnetic field is even. Therefore, to induce the direct transition by oscillating magnetic fields of light, some interaction, which breaks the symmetry of parity, is required. Examples of such an interaction are the Dzyaloshinskii-Moriya interaction and the staggered magnetic field. However, $Na_2Co_2(C_2O_4)_3(H_2O)_2$ has an inversion center between two magnetic Co^{2+} ions in the dimer structure. In this case, the parity breaking cannot take place. Thus, the direct transition seems not to be magnetic dipole active in $Na_2Co_2(C_2O_4)_3(H_2O)_2$. In this study, we have carried out the high field ESR measurements by illuminating circularly polarized light at 162 GHz, to clarify the selection rule of the direct transition in $Na_2Co_2(C_2O_4)_3(H_2O)_2$. The measurements are performed by putting a linear-to-circular polarizer (POL-06-R059R, Millitech Inc.) above the sample in the Faraday configuration. The external magnetic field is applied along both the same and opposite directions to the propagation vector of light. In the case of the usual magnetic dipole transition, the magnetic resonance signal is abruptly changed by reverse of the direction of the external field, because the spin system couples with either left or right handed circularly polarized light. However, the observed change in the signal intensity of the direct transition by the reverse of the field is very little in $Na_2Co_2(C_2O_4)_3(H_2O)_2$. From this result, we consider that the direct transition in this compound is caused by the electric dipole transition. We propose that the spin current mechanism [3], which gives rise to a spin-driven ferroelectricity in multiferroic materials, is responsible to induce a finite probability for the electric dipole active transition between the singlet and the triplet states in $Na_2Co_2(C_2O_4)_3(H_2O)_2$.

References

[1] Nakagawa Y., Kashiwagi T., Yamaguchi H., Kimura S., Honda Z., Yamada K., Kindo K. and Hagiwara M., "High field ESR and magnetization in $Na_2Co_2(C_2O_4)_3(H_2O)_2$", *J. Phys. Soc. Jpn.* 2006, **75**, 124708 (1-5).

[2] Price D. J., Powell A. K. and Wood P. T., "Hydrothermal synthesis, structure, stability and magnetism of $Na_2Co_2(C_2O_4)_3(H_2O)_2$: a new metal oxalate ladder", *J. Chem. Soc., Dalton Trans.* 2000, 3566-3569.

[3] Katsura H., Nagaosa. N. and Balatsky A. V., "Spin current and magnetoelectric effect in noncollinear magnets", *Phys. Rev. Lett.* **95** (2005) 057205 (1-4)

P-114

Magnetic Anisotropy in Chiral System CuB_2O_4 by ESR

Sho Arakawa[1], Susumu Okubo[2], Hitoshi Ohta[2], Takahiro Sakurai[3], Shigeo.Hara[3], Mitsuru Saito[4], Takahisa Arima[5]

[1]*Graduate School of Science, Kobe Univ., Kobe 657-8501, Japan*
[2]*Molecular Photoscience Research Center, Kobe Univ., Kobe 657-8501, Japan*
[3]*Center for Supports to Research and Education Activities, Kobe Univ., Kobe 657-8501, Japan*
[4]*Institute of Multidisciplinary Research for Advanced Materials, Tohoku Univ., Sendai 980-8577, Japan*
[5]*Department of Advanced Materials Science, Univ. of Tokyo, Chiba 277-8561, Japan*

E-mail:133s102s@stu.kobe-u.ac.jp

CuB_2O_4 has a tetragonal space group *I42d* [1]. And magnetic Cu^{2+} ions which are located of square planar Cu (A) site and distorted octahedral Cu (B) site, as shown in Fig.1. Successive magnetic transitions at 21K and 10K were observed by petrakovsky in the magnetic susceptibility and the specific heat measurements [2]. Further investigation, this compound turns out be a weak ferromagnetic state of Cu (A) sites due to the Dzyialonshinskii-Moriya (DM) interaction. Further decreasing temperture, the system goes to a helimagnetic state with a propagation vector along *c* axis at 9K [3]. The helimagnetic state is confirmed also by polarize neuton measurements. For the last decade, ESR reports have been concentrated in the magnetic anisotropy of the ground stete of helical spin structure [4, 5] without few reports of spin dynamics [4]. Since discovery of gigantic optical magnetoelectric effect in a weak ferromagnetic state (canted spin phase) [6], investigation of canted spin phase becomes important issue, because of the possibility of the magnetic controlling the chirality However, there is only one incomplete report of ESR investigation for the magnetic anisotropy in canted spin phase [5]. Therefore, to investigate the magnetic anisotropy in the canted spin phase, X-band and submillimeter wave ESR measurements of the CuB_2O_4 single have been performed. The angular dependence of ESR spectra shows the critical angular divergence. Angular dependence measurements show easy plane anisotropy in ab plane. From AFMR analysis, absolute value of D vector of DM interaction is estimated.

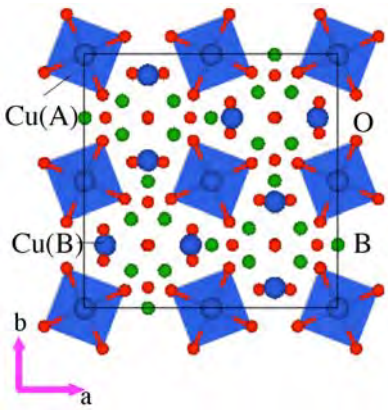

Fig. 1: The crystal structure of CuB_2O_4

References

[1] Martinez-Ripoll M., Martinez-Garrera S., and Garcia-Blanco S., "The Crystal Structure of Copper Metaborate, CuB_2O_4", *Acta Crystallogr*. B **1971**, 27, 677-681.
[2] Petrakovskii G., Velikanov D., Vorotinov A., Balaev A., Sablina K., Amato A., Roessli B., Schefer J., and Staub U., "Weak ferromagnetism in CuB_2O_4 copper metaborate", *J. Magn. Magn. Mater* **1999**, 205, 105-109.
[3] Kousaka Y., Yano S., Kishine J., Yoshida Y., Inoue K., Kikuchi K., and Akimitsu J., "Chiral Magnetic Ordering and Commensurate-to-Incommensurate Transition in CuB_2O_4", *J. Phys. Soc. Jpn.* **2007**, 76, 123709-4.
[4] Fujita T., Fujimoto Y., Mitsudo S., Idehara T., Saito T., Kousaka Y., Yano S., Akimitsu J., Kishine J., Inoue K., and Motokawa M., "Commensurate to Incommensurate Transition in the Chiral Helimagnet CuB_2O_4", *J. Phys. Soc. Jpn*. **2008**, 77, 053702-2.
[5] Pankrat A.I., Petrakovskii G.A., and Vollkov N.V., "Antiferromagnetic Resonance in CuB_2O_4 Single Crystal", *Phys. Solid State* **2000**, 42, pp93-99.
[6] Saito M., Takaniguchi K., and Arima T., "Gigantic Optical Magnetoelectric Effect in CuB_2O_4", *J. Phys. Soc. Jpn.* **2008**, 77, 013705-4.

P-115

High Field ESR Measurements of Two Dimensional Antiferromagnets Sr_2NiO_3X (X=F,Cl)

Syota Yoshida[1], Shigeo Hara[2], Takahiro Sakurai[2], Susumu Okubo[3], Hitoshi Ohta[3], Yoshihiro Tsujimoto[4], Kazunari Yamaura[4], Teturo Uchikoshi[4]

[1]*Graduate School of Science, Kobe University, Kobe 657-8501, Japan*
[2]*Center for Supports to Research and Education Activities, Kobe University, Kobe 657-8501, Japan*
[3]*Molecular Photoscience Research Center, Kobe University, Kobe 657-8501, Japan*
[4]*National Institute for Material Science, Sengen Tsukuba Ibaraki 305-0047, Japan*

140s129s@stu.kobe-u.ac.jp

Low-dimensional magnetic materials have been interested for the quantum-mechanical effect. Plenty of theoretical and experimental works on one-dimensional spin systems including spin ladder systems have been performed for last several decades. On the other hand, investigations of two-dimensional spin systems have been performed in less numbers than that of one-dimensional systems even if it is theoretical work [1, 2]. Moreover experimental study of two-dimensional systems is known only in the orthogonal dimmer system $SrCu_2(BO_3)_2$. In particularly, study of rectangular system does not develop experimentally due to a lack of model substances. Recently, candidate substances for two-dimensional rectangular antiferromagnets Sr_2NiO_3X (X=F, Cl) are synthesized. Magnetic ions Ni^{3+} ($3d^7$) of Sr_2NiO_3X (X=F, Cl) are located at center of NiO_5 O/X octahedron, which forms rectangular square lattice in *ab* plane. According to the Curie-Weiss fitting of the temperature dependence of the magnetic susceptibility, estimated Weiss temperature θ=21.3K and 24.2K for X=F and Cl, respectively, indicate that ferromagnetic interaction is dominant. Although the crystal structure of both fluoride and chloride systems are same, the magnetic susceptibility behave differently at low temperature. The fluoride system shows the spin glass behavior below T_{sg}=11K. On the other hand, the chloride system shows a broad peak at 50K due to low-dimensionality [3]. To investigate the effect of the difference of the halogen ions, the high field ESR measurements of Sr_2NiO_3X (X=F, Cl) powder have been performed in the temperature range from 265K to 1.9K and the frequency range from 60GHz to 160GHz using the pulsed magnetic field up to 16T. Figure 1 shows the temperature dependence of ESR spectra for 160GHz in Sr_2NiO_3Cl. Sharp absorption lines are the absorption of DPPH for the field marker of g=2. The absorption lines are broaden below 24K, which consists with reported Néel temperature T_N=33K [3]. Moreover, another absorption appears at around 4T at 4.2K. We will report also results of the fluoride system and discuss the effect of the difference of the halogen ions.

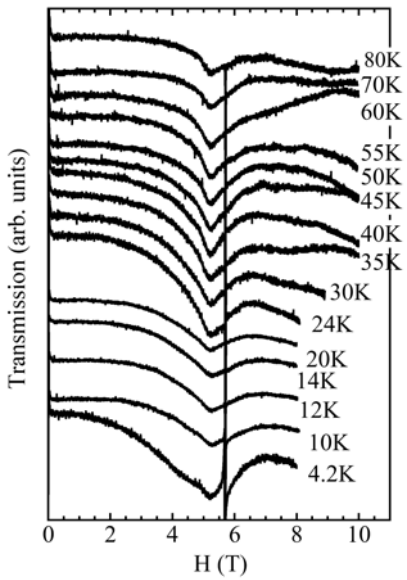

Fig. 1 Temperature dependence of ESR spectra for 160GHz in Sr_2NiO_3Cl.

References

[1] Manousakis E., "The spin-1/2 Heisenberg antiferromagnet on a square lattice and its application to the cuprous oxides" *Rev. Mod. Phys*. **1991**, 63, 1-62

[2] Yasuda C., Todo S., Hukushima K., Alet F., Keller M., Troyer M., and Takayama H., "Néel Temperature of Quasi-Low-Dimensional Heisenberg Antiferromagnets" *Phys. Rev. Lett*. **2005**, 94, 217201-217204

[3] Tsujimoto Y., Yamaura K., Uchikoshi T., "Extended Ni(III) Oxyhalide Perovskite Derivatives: Sr_2NiO_3X (X = F, Cl) ", *Inorg. Chem*. **2013** , 52, 10211-10216

P-116

High Field ESR Measurements of Quasi One Dimensional Frustrated Magnet $NaCuMoO_4(OH)$

Yoko Kitahara[1], Sihigeo Hara[2], Takahiro Sakurai[2], Susumu Okubo[3], Hitoshi Ohta[3], Kazuhiro Nawa[4], Yoshihiro Okamoto[5], Zenji Hiroi[4]

[1]*Graduate School for Science, Kobe University, Kobe 657-8501, Japan*
[2]*Center for Supports to Research and Education Activities, Kobe University, Kobe 657-8501, Japan*
[3]*Molecular Photoscience Research Center, Kobe University, Kobe 657-8501, Japan*
[4]*Institute for Solid State Physics, The University of Tokyo, Chiba 277-8581, Japan*
[5]*Department of Applied Physics, Nagoya University, Nagoya 464-8603, Japan*

E-mail: rebot2x8@gmail.com

Recently, an existence of the new quantum state, called as the spin nematic phase in analogy of the nematic liquid crystal, in the magnetic field of just below the saturation field is proposed theoretically for quasi one dimensional frustrated magnet, which has a ferromagnetic interaction in the nearest neighbor and an antiferromagnetic interaction in the next-nearest neighbor [1]. Experimental studies of the spin nematic phase have been performed intensively in $LiCuVO_4$ [2]. However, the spin nematic state is still unclear until now. Because the saturation field is rather higher fields to observe spin nematic phase. Therefore, we focus on $NaCuMoO_4(OH)$ as a model substance for the J_1-J_2 one-dimensional frustrated magnet. Cu^{2+} ($3d^9$, S=1/2) ions of $NaCuMoO_4(OH)$ form one-dimensional chain along the *b*-axis. The magnetic susceptibility shows a broad peak at 15K reflecting nature of low-dimensionality. The Weiss temperature is reported θ=-5K. Nawa propose that $NaCuMoO_4(OH)$ is the J_1-J_2 model substance having stronger antiferromagnetic interaction [3, 4] .

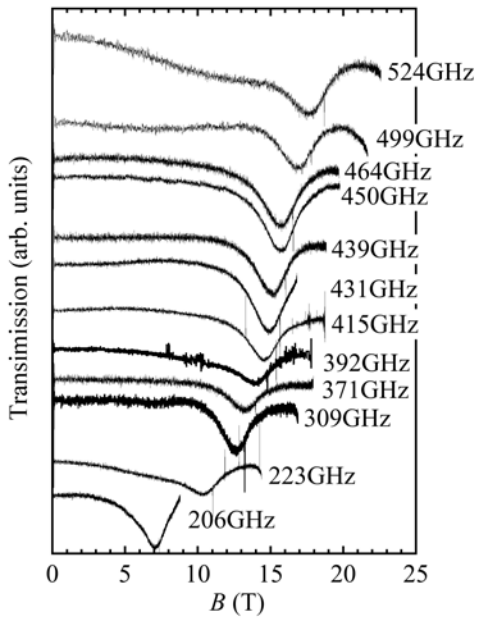

Fig. 1 The frequency dependence of ESR spectra at 173K

To investigate magnetic properties from a microscopic perspective, high field ESR measurements of fine crystal sample have been performed using pulsed magnetic field up to 25T. The measurement temperature range is from 1.9K to 265K, and the frequency range is from 140GHz to 330GHz. To obtain the g-values of paramagnetic state of $NaCuMoO_4(OH)$ have been performed at 173K. Because EPR signal can not be obtained in conventional X-band due to a broad absorption. Obtained EPR spectra at high frequency of 500GHz can be fitted by the single Lorentzian line shape. This result suggests that an anisotropy of the g-values is essentially small or single absorption line is observed due to exchange narrowing between spins with different g-values. From frequency field diagram at 175K, the g-value is estimated to be 2.11, which corresponds to that of standard Cu^{2+} ions. The temperature dependence ESR measurements are also performed. ESR spectra changes from a single absorption lines to complicated absorption lines blow 3K.

References

[1] Zhitomirsky M. E. and Tsunetsugu H., "Magnon pairing in quantum spin nematic", *Europhys. Lett.* **2007**, 92, 37001-3

[2] Detail references of $LiCuVO_4$ are shown in : Nawa K., Takigawa M. Yoshida M. and Yoshimura K., "Anisotropic Spin Fluctuations in the Quasi One-Dimensional Frustrated Magnet $LiCuVO_4$", *J. Phys. Soc. Jpn* . **2013**, 82, 094709-13

[3] Nawa K., *Abs. Meet. Phys. Soc. Jpn. (69th Annual Meeting, Tokyo, March, 2014)* Part3, 345, 30aAF-1

[4] Nawa K. prepare a paper.

P-117

High-field ESR Measurements of $YCrO_3$ and $YCaCrO_4$

Shohei Ikeda[1], Shigeo Hara[2], Takahiro Sakurai[2], Susumu Okubo[3], Hitoshi Ohta[3], Ting Hui Kao[4, 5], Hiroya Sakurai[4], Hung-Duen Yang[5]

[1]*Graduate School of Science, Kobe University, Kobe 657-8501, Japan*
[2]*Center for Supports to Research and Education Activities, Kobe University, Kobe 657-8501, Japan*
[3]*Molecular Photoscience Research Center, Kobe University, Kobe 657-8501, Japan*
[4]*National Institute for Materials Science, Tsukuba 305-0047, Japan*
[5]*Department of Physics, National Sun Yet-sen University, Kaohsiung 804, Taiwan*

E-mail: 131s103s@stu.kobe-u.ac.jp

Perovskite compounds have attracted much attention as functional properties such as a ferroelectricity ($BaTiO_3$), an antiferromagnetism, a ferromagnetism ($BiMnO_3$) and a conductivity (high-T_C cuprates). In this paper, we focus on a conventional three-dimensional and a layered two dimensional Cr-perovsikte antiferromagnets $YCrO_3$ and $YCaCrO_4$. The crystal structures of $YCrO_3$ are shown in fig. 1. Cr^{3+} ion of $YCrO_3$ and $YCaCrO_4$, which has spin S=3/2, is located in a CrO_6 octahedron [1,2]. Although temperature dependence of the magnetic susceptibility of both substances shows an antiferromagnetic transition with weak-ferromagnetism at 140 K [3], whole temperature behaviors are different in both substances. Estimated Weiss temperature are -325 K and -282.6K for $YCrO_3$ and $YCaCrO_4$, respectively, and it indicates the existence of strong antiferromagnetic interaction between Cr ions. However, the magnetization curve at 5 K shows a characteristic hysteresis of the ferromanetism [4].

To investigate magnetic anisotropy, high-field ESR measurements of $YCrO_3$ and $YCaCrO_4$ powder have been performed using the pulsed magnetic field up to 35 T in the frequency region from 40 GHz to 722 GHz using Gunn Oscillators, BWO and FIR laser. Measured temperature range is from 1.9 K to 265 K. Powder patterns of antiferromagnetic resonance with a large antiferromagnetic gap for $YCrO_3$ are observed at 1.9K as shown in fig.2. An antiferromagnetic gaps at zero field are estimated to be 181GHz (6.5T) and 338GHz (12.1T). Although obtained AFMR modes seem to be conventional AFMR modes of two sublattice antiferromagnet, obtained zero field gap is more than twice times lager than expected spin flop transition field.

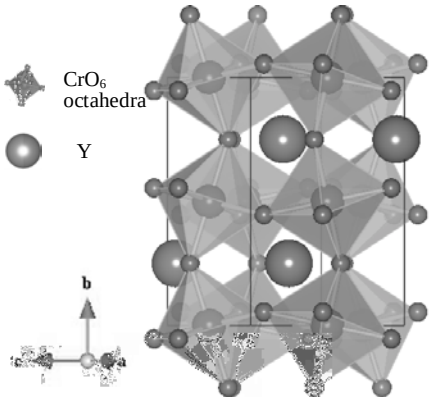

Figure. 1 The crystal structure of $YCrO_3$

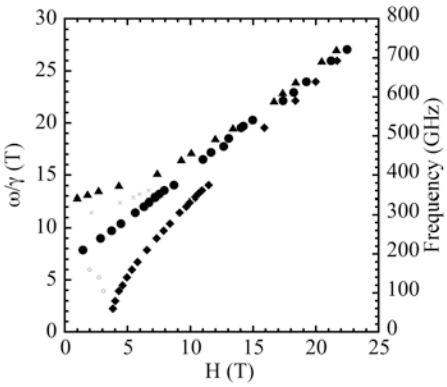

Figure. 2 Frequency – field diagram of $YCrO_3$ at 1.9K

References

[1] Ramesha K., Llobet A., Proffen Th., Serrao C.R., and Rao C.N.R., "Observation of local non-centrosymmetry in weakly biferroic $YCrO_3$" *J. Phys.: Cond. Matter* **2007**, 19, 102202 (8pp).

[2] Berjoan R., Coutures J.P., Le Flem G., and Saux M., "Structural and Magnetic Study of the $Ca_{1-x}Y_xCrO_4$ System" *J. Solid State Chem.* **1982**, 42, 75.

[3] Serrao C.R., Kundu A.K., Krupanidhi S.B., Waghmare U.V., and Rao C.N.R.., "Biferroic $YCrO_3$" *Phys. Rev. B* **2005**, 72, 220101(R).

[4] Tiwari B., Surendra M.K., and Ramachandra Rao M.S.., "$HoCrO_3$ and $YCrO_3$: a comparative study" *J. Phys.: Cond. Matter* **2013**, 25, 216004 (7pp) .

P-118

Development of Magnetization and XMCD Detection ESR

Hiroyuki Nojiri[1] and Satoshi Matsuzawa[1]

[1]*Institute for Materials Research, Tohoku University, Sendai 980-8577, Japan*

E-mail:nojiri@imr.tohoku.ac.jp

We have developed two types of magnetization detection type ESR techniques. The first one is the SQUID detection ESR and the second one is the XMCD detection ESR. It is well known that the ESR absorption is associated with the population change among multiplets. This enables us to evaluate the ESR intensity by measuring magnetization in resonant state, which is the basis of the magnetization detection ESR. As the magnetization detection probe, several methods can be employed such as pickup coil, SQUID and XMCD:X-ray magnetic circular dichroism.

One of the advantages of this method is the measurement of absolute intensity of ESR absorption. It is very powerful in examining a system with a variable spin concentration such as spin-crossover system. Another feature of the magnetization detection ESR is the capability of EPR of surface area by using XMCD technique. XMCD is the element and orbital specific magnetization probe and the intensity is linear to the contribution of bulk magnetization from a specific orbital of each element. The sensitivity is extremely high and the magnetization of a few atomic layers can be detected.

(1) SQUID detection

A conventional SQUID detection type ESR has been developed by Sakurai *et al.* [1] They use a commercial SQUID magnetometer for the magnetization measurement. The waveguide is a simple circular light pipe and no resonant cavity is used. The light pipe does not cover around the sample and thus the SQUID chamber wall replaces the light pipe. To improve the capability of a smaller volume sample measurement, we have put an extension of the light pipe around the sample. By testing Cu, Al and Au as the material, we found that Cu works reasonably fine with low background. The effect of the extension pipe depends on the frequency because the SQUID chamber works as a kind of very loose resonant cavity in which the radiation is confined. The composition of the line shapes for different materials such as Ruby, Cu-doped glass and Gd complex will be reported in details.

(2) XMCD detection[2]

We have developed a XMCD detection type probes for soft-X-ray resume. There are two different types of resonant cavities. One is the TE102 cavity of WR137 waveguide. A Vector network analyzer is used as a source and detection unit. The other is the Q-band reflection type probe with TE102 cavity with a conventional Gunn oscillator source. A pin-hole for the X-ray injection is made on the resonant cavity wall and the sample is mounted on the isolated electrode for total electron yield method.

In the presentations, the design, the characterization and the results of the experiments will be presented and their application will be discussed.

References

[1] T. Sakuraia, K. Fujimoto, R. Goto, S. Okubo, H. Ohtab and Y. Uwatoko, *J Magn Reson.* 2012 **223**:41-5.

Jos´e Goulon 1,*, Andrei Rogalev 1, G´erard Goujon 1, FabriceWilhelm 1, Jamal Ben Youssef

[2] Claude Gros, Jean-Michel Barbe and Roger Guilard, *Int. J. Mol. Sci.* 2011, **12**, 8797-8835.

P-119

High-field multi-frequency ESR in the quasi-1D S=1/2 Ising-like antiferromagnet $BaCo_2V_2O_8$ in a transverse field

Akira Okutani[1], Shojiro Kimura[2], Tetsuya Takeuchi[3] and Masayuki Hagiwara[1]

[1]*Center for Advanced High Magnetic Field Science, Graduate School of Science Osaka University, Osaka 560-0043, Japan*
[2]*Institute for Materials Research, Tohoku University, Miyagi 980-8577, Japan*
[3]*Low temperature center, Osaka University, Osaka 560-0043, Japan*

E-mail: okutani@mag.ahmf.sci.osaka-u.ac.jp

$BaCo_2V_2O_8$ (BCVO) is a good realization of the quasi-one-dimensional (1D) antiferromagnet with Ising-like anisotropy (Co^{2+} ions, $3d^7$), and has a tetragonal crystal structure (space group $I4_1/_{acd}$) at room temperature, in which edge-sharing CoO_6 octahedra form a screw-chain structure along the c-axis. BCVO shows a long-range antiferromagnetic ordering at T_N=5.4 K in zero field. In a longitudinal magnetic field (parallel to the c-axis), a quantum phase transition from the Neel ordered phase to a quantum disordered phase inherent in the S=1/2 1D Ising-like antiferromagnet occurs at a critical field around 3.9 T [1]. The magnetization curve is well fitted to that for an S=1/2 1D antiferromagnetic XXZ model. In a tranverse field (perpendicular to the c-axis), it was theoretically suggested that the Neel order remains up to the saturation field. However, for the field applied along [100] direction, it was reported from recent thermal expansion and magnetostriction measurements that the Neel order is completely suppressed by magnetic fields above 10 T [2]. Magnetization curves for H || [100] and [110] are largely different, and the difference in their magnetization curves was explained by the staggered field caused by a characteristic screw chain structure in BCVO [3]. In order to investigate the in-plane difference from the view point of magnetic excitation, we have performed high-field multi-frequency ESR measurements of $BaCo_2V_2O_8$ in a transverse magnetic field.

In this presentation, the ESR results of $BaCo_2V_2O_8$ for H || [100] and H || [110] will be reported. Figure 1(a) shows the ESR spectra of $BaCo_2V_2O_8$ for H || [100]. The two ESR modes (split signals caused by the domains below T_N due to the structural phase transition) in Fig. 1(b) appear from 400 GHz at zero magnetic field. The lower mode shows a softening around 10 T, and a new ESR mode with an energy gap of 160 GHz was observed above 10 T. In contrast, no softening was observed below the saturation field for H || [110].

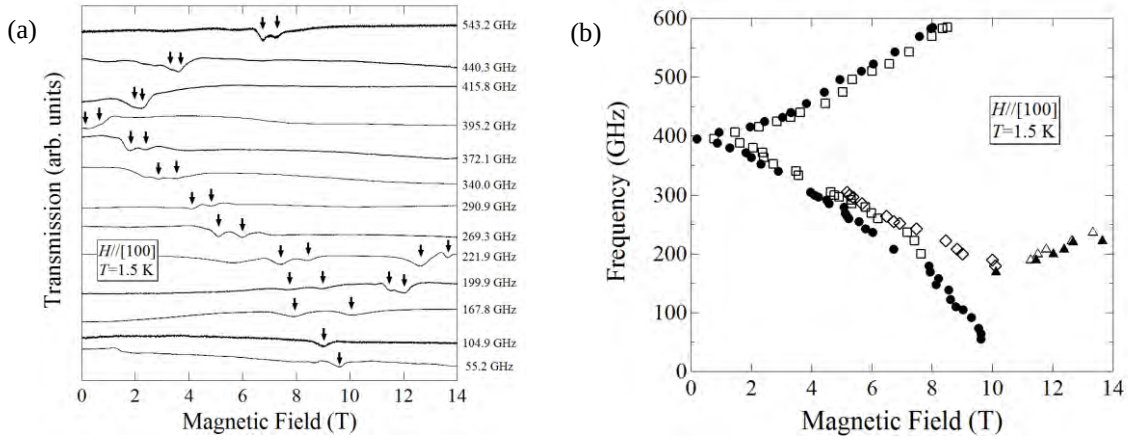

Fig. 1 (a) ESR spectra for H || [100] and (b) Frequency-field plot of resonance fields

References

[1] Z. He, T. Taniyama, T. Kyomen, and M. Itoh, *Phys. Rev. B*, **2005**, 72 172403-1-4.

[2] S. K. Niesen, G. Kolland, M. Seher, O. Breunig, M. Valldor, M. Braden, B. Grenier, and T. Lorentz, *Phys. Rev. B*, **2013,** 87, 224413-1-9.

[3] S. Kimura, K. Okunishi, M. Hagiwara, K. Kindo, Z. He, T. Taniyama, M. Itoh, K. Koyama, and K. Watanabe, *J. Phys. Soc. Jpn*., **2013,** 82, 033706-1-4.

P-120

The Effective Spin Model and ESR Measurements of an S = 1/2 Ferromagnetic Alternating Double Chain, m-Ph-V_2

Kenji Iwase[1], Hironori Yamaguchi[1], Toshio Ono[1], Takanori Kida[2], Masayuki Hagiwara[2] and Yuko Hosokoshi[1]

[1]*Department of Physical Science, Osaka Prefecture University, Sakai 599-8531, Japan*
[2]*AHMF, Graduate School of Science, Osaka University, Toyanaka, Osaka 560-8531, Japan*

E-mail: s_k.iwase@p.s.osakafu-u.ac.jp

Recently, we have succeeded in synthesizing verdazyl biradical m-Ph-V_2. The intra and intermolecular interactions are considered to form an S = 1/2 ferromagnetic (FM) alternating double chain with three types of interactions J_0/k_B = - 28.5 K, J_1/k_B = 42.8 K, and J_2/k_B = - 7.1 K [1], as shown in Fig. 2(a). The magnetic susceptibility shows a shoulder at about 10 K and a magnetic phase transition to an ordered state occurs at T_N = 1.9 K, as shown Fig. 1, which is confirmed by the specific heat result. In addition, about 50% of the total magnetic entropy S_{total} = 2Rln2 is consumed above 10 K, as shown in the upper inset of Fig.1. These behaviors are expected to originate from partially formed singlet state coupled by a strong antiferromagnetic (AF) interaction J_1. Correspondingly, the magnetization curve shows 1/2 magnetization plateau in the field range of 5 to 20 T. In the present work, we examined the ground state of this unconventional quantum spin model from the perturbation treatment of the spin Hamiltonian and ESR measurement.

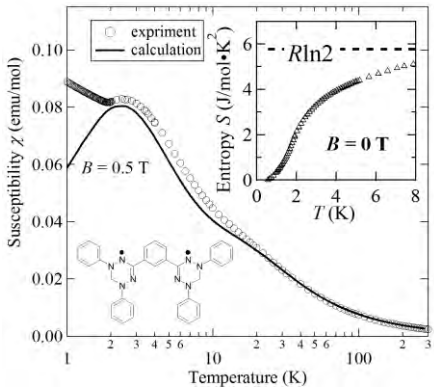

Fig.1. Temperature dependence of magnetic susceptibility. The upper and lower insets show the temperature dependence of the magnetic entropy calculated by the magnetic specific heat at zero field and the molecular structure of m-Ph-V_2, respectively.

We discuss the ground state of the S=1/2 alternating double chain in the low-field region below the 1/2-plateau phase. For $T \ll J_1/k_B$, two spins connected by the strongest AF interaction J_1 form a nonmagnetic singlet dimer. However, an effective interaction exists between the remaining spins through the triplet excited states of the singlet dimer as is shown in Fig.2(b). Consequently, the ground state can be regarded as an effective S = 1/2 Heisenberg AF alternating chain consisting of J_{eff1} and J_{eff2} with the next nearest ferromagnetic interaction J_{eff3} from the second-order perturbation treatment in the spin Hamiltonian. Thus, the observed magnetic order at low temperatures is a long-range order (LRO) of the effective alternating chain, which is a cooperative phenomenon caused by the magnetic order and quantum fluctuation originating from the singlet dimmer.

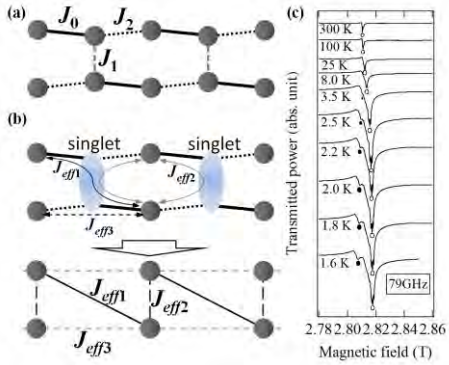

Fig.2.(a) Magnetic lattice of m-Ph-V_2. (b) The effective model at $T \ll J_1/k_B$. The closed circles and ellipses indicate an S = 1/2 and singlet dimers, respectively. (c) Temperature evolution of the ESR spectra at 79 GHz by using polycrystals. The open and close circles indicate the resonance signals.

Temperature dependence of the ESR absorption spectra at 79 GHz is shown in Fig.2(c). Below 10 K, an additional signal appears in the low field region, which comes from the correlations associated with the effective S = 1/2 alternating chain above mentioned. Therefore, the observed ESR signals below 10 K indicate the excitation of magnons associated with the LRO of the effective S = 1/2 chain.

References

[1] Iwase K., Yamaguchi H., T. Ono, Shimokawa T., Nakano H., Matsuo A., Kindo K., Nojiri H., and Hosokoshi Y., *J. Phys. Soc. Jpn.* **2013**, 82, 074719

P-121

Carbonate Free Radical Production on Addition of Hydrocarbonate to a Weak Acidic Mixture of Rats' Gastric Carcinogen, N-Methyl-N'-Nitro-N-Nitrosoguanidine, and Hydrogenperoxide

Tomiko Mikuni[1], Masaharu Tatsuta[2], Idota Atsushi[1] and Tomoyukieu Yamasaki[1]

Clinical Laboratory[1], and Department of Gastric Oncolology[2], Osaka Medical Center for Cancer and Cardiovascular Diseases, Osaka 537-8511, Japan

E-mail: mikuni-to@nifty.com

Introduction Hydroxyl radical(・OH) has been regarded as the most potent carcinogen for its high reactivity. But its reactivity is too high to react with the substances over the solvent, so the possibility of ・OH as a potent carcinogen is recently doubted. Carbonate radical anion(CO_3^-・), which is derived from the reaction of carbon dioxide(CO_2) and a kind of reactive nitrogen species, peroxynitrite/peroxynitrate ($ONOO^-$/HONOO), is as much as reactive as・OH and still has much longer half-life than it. So CO_3^-・is now being considered as the most potent carcinogen. Here, using a kind of rats' gastric carcinogen,N-methyl-N'-nitro-N-nitrosoguanidine (MNNG), a possible production of CO_3^-・was examined in the presence of HCO_3^- and H_2O_2 as shown below. That is, on addition of 2.5mM HCO_3^- to a weak acidic mixture, pH value is increased to a neutral one①. resulting in the reaction of MNNG and H_2O_2.②. The product of $ONOO^-$/HONOO could further react with CO_2 to form CO_3^-・③. The possibility of CO_3^-・production in the gastric mucosa administrated MNNG was examined.

$2HCO_3^- + H^+ \longrightarrow H_2O + 2CO_2 + OH^-$ ①

$2MNNG + H_2O_2 \longrightarrow ONOO^-/HONOO + 2MNG$ ②

$ONOO^- + CO_2 \longrightarrow \underline{CO_3^-\cdot} + NO_2$ ③ (MNG: N-methyl- N'-nitro-N-guanidine)

Methods. Using X-band ESR with a spin trapping agent, DMPO(50mM), the production of CO_3^-・ was examined on addition of 2.5mM HCO_3^- to the MNNG(2.5mM)-H_2O_2(3mM) mixture at pH 6.6 .

Results. The EER spectra of HCO_3^- -added MNNG-H_2O_2- DMPO mixture showed a new signal with a_N=14.0, a_H=9 , corresponding to DMPO adduct of $\underline{CO_3^-\cdot}$ with the signal of・OH.

Conclusion. CO_3^-・could be derived from rats gastric carcinogen, MNNG.

P-122

High-field ESR Measurements of Low-dimensional Magnets in Natural Minerals

Susumu Okubo[1], Yoko Kitahara[2], Syota Yoshida[2], Shigeo Hara[3], Takahiro Sakurai[3], Hitoshi Ohta[1, 2], Masashi Fujisawa[4] and Hidekazu Tanaka[5]

[1]*Molecular Photoscience Research Center, Kobe University, Kobe 657-8501, Japan*
[2]*Graduate School of Science, Kobe University, Kobe 657-8501, Japan*
[3]*Center for Supports to Research and Education Activities, Kobe University, Kobe 657-8501, Japan*
[4]*Technical Department, Tokyo Institute of Technology, Tokyo 152-8551, Japan*
[5]*Department of Physics, Tokyo Institute of Technology, Meguro-ku, Tokyo 152-8551, Japan*

E-mail: sokubo@kobe-u.ac.jp

Natural mineral often has a unique crystal structure, which consists with low-dimensional system. And it grows up in peculiarly complex environments such as hydrostatic high-pressure, high-temperature and long-time growth. Among them, many kinds of minerals cannot be synthesized even still today. Many quantum spin systems is known as minerals. For example, azurite $Cu_3(CO_3)_2(OH)_2$ is known as S=1/2 diamond chain [1]. In this paper, two candidate low-dimensional spin systems of natural minerals will be introduced and it's magnetic properties will be reported from microscopic viewpoint. Henmilite $Ca_2Cu(OH)_4B_2(OH)_8$ has quasi two-dimensional structure of CuO_4 square in *ac*-plane as shown in fig. 1 [2]. From the magnetic susceptibility measurements, the Weiss temperature is estimated to be -3.7K, which suggests existence of dominant antiferromagnetic interaction [3]. A broad peak due to low-dimensionality was observed in the magnetic susceptibility at around 3 K [3]. Cavancite $Ca(VO)Si_4O_{10}\cdot 4H_2O$ has one-dimensional network of VO_4 along *c*-axis as shown in fig. 2 [4]. From X-band ESR measurements the magnetic ion in cavancite is expected to be V^{4+} ($3d^1$, S=1/2). Submillimeter wave and X-band ESR measurements of henmilite and cavancite single crystal have been performed in the temperature range from 265 K to 4.2 K at first time. Dimensionalities of spin-spin correlation in those minerals have been investigated by angular dependence ESR measurements of X-band ESR. Spin dynamics will discuss in connection with the magnetic susceptibility and theoretical prediction.

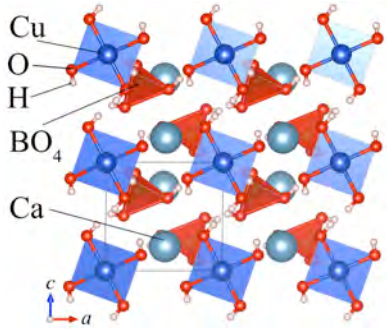

Fig. 1. The crystal structure of $Ca_2Cu(OH)_4B_2(OH)_8$ along *ac* plane.

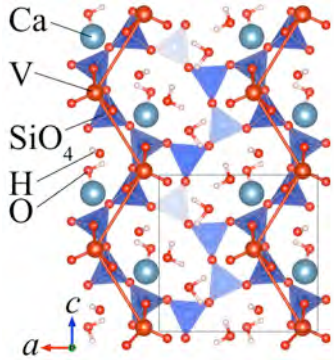

Fig. 2. The crystal structure of $Ca(VO)Si_4O_{10}\cdot 4H_2O$

References

[1] Kikuchi H., Fujii Y., Chiba M., Mitsudo S., Idehara T., Tonegawa T., Okamoto K., Sakai T., Kuwai T. and Ohta H., "Experimental Observation of the 1/3 Magnetization Plateau in the Diamond-Chain Compound $Cu_3(CO_3)_2(OH)_2$", *Phys. Rev. Lett.* **2005**, 94, 227201-4

[2] Nakai I., "Henmilite, $Ca_2Cu(OH)_4[B(OH)_4]_2$, a new mineral from Fuka, Okayama Prefecture, Japan. II. Crystal structure" *Am. Mineral.* **1986**, 71, 1236-1239.

[3] Fujisawa M., Tanaka H., *Abst. Meet. Phys. Soc. Jpn. (67th Annual Meeting, Nishinomiya, March, 2012)* Part 3, p. 493, 24pPS79

[4] Ishida N., Kimata M., Nishida N., Hatta T., Shimizu M. and Akasaka T. "Polymorphic relation between cavansite and pentagonite: Genetic implications of oxonium ion in cavansite", *J. Mineral. Petrol. Sci.* **2009**, 104 241-252.

P-123

ESR Studies of the Molecular Spin Liquid System $EtMe_3Sb[Pd(dmit)_2]_2$

Yugo Oshima[1] , Takao Tsumuraya[1] and Reizo Kato[1]

[1]*Condensed Molecular Materials Lab., RIKEN, Wako 351-0198, Japan*

E-mail: yugo@riken.jp

The magnetic properties of the molecular spin liquid system $EtMe_3Sb[Pd(dmit)_2]_2$, where dmit denotes for 1,3-dithiol-2-thione-4,5dithiolate, is studied by ESR measurements. The anion radical salts $X[Pd(dmit)_2]_2$, where X is a monovalent cation, show a variety of ground states at low temperature depending on the cation X. [1] These salts are basically a Mott insulator that forms a two-dimensional triangular lattice of dimer units $[Pd(dmit)_2]_2^-$ (S=1/2), and most of them show an antiferromagnetic order at low temperature. Meanwhile, other interesting ground state such as a non-magnetic charge ordered state is observed for the $X=Et_2Me_2Sb$ salts, and a valence bond solid state is also observed for $X=EtMe_3P$ salts. On the other hand, the title compound: $EtMe_3Sb[Pd(dmit)_2]_2$ does not show any long range order down to 30 mK, and it is considered as a candidate material for the quantum spin liquid state. [2] Although the specific heat, thermal conductivity and magnetic torque measurements show a gapless excitation, NMR indicates a gapped-like behavior. [2-4] Moreover, the triangular lattice of this salt is strongly distorted at low temperature, and the nature of the ground state is still unclear.

Therefore, to have more microscopic information about the ground state of this salt, we have performed X-band and High-field ESR measurements. As shown in the figure below, a relatively large g-anisotropy was observed due to the *d*-orbit of Pd, and we have also observed the splitting of two EPR spectra coming from two different layers in which the stacking direction of the dimer of $Pd(dmit)_2$ is different. The splitting of the EPR signals suggests that the interlayer exchange interaction is infinitesimal. Moreover, a *g*-shift is observed for *B*//c-axis in the temperature region where a crossover behavior is observed in the specific heat measurement. [3] Detailed 'in-plane' angular dependence and the temperature dependence will be presented, and its characteristic ESR behavior will be discussed in contrast with other $[Pd(dmit)_2]$ salts that have different ground state.

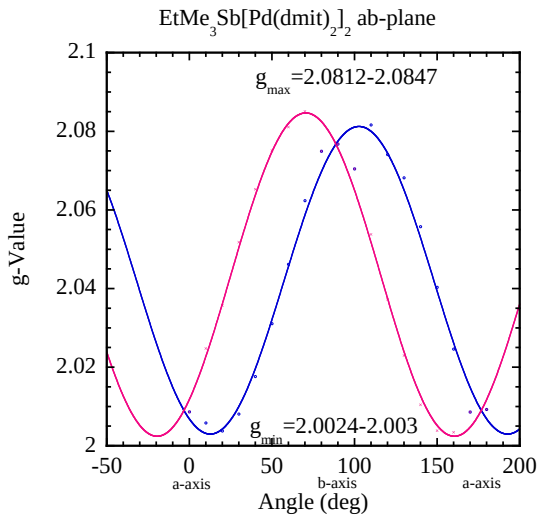

References

[1] Tamura M. and Kato R., "*Variety of valence bond states formed of frustrated spins on triangular lattices based on a two-level system Pd(dmit)2*", Sci. Technol. Adv. Mater., (2009), 10, 024304.

[2] Watanabe D., Yamashita M., Tonegawa S., Oshima Y., Yamamoto H. M., Kato R., Sheikin I., Behnia K., Terashima T., Uji S., Shibauchi T. and Matsuda Y., "*Novel Pauli-paramagnetic quantum phase in a Mott insulator*", Nature Commun., (2012), 3, 1090.

[3] Yamashita S., Yamamoto T., Nakazawa Y., Tamura M. and Kato R., Nature Commun., (2011), 2, 275.

[4] Itou T., Oyamada A., Maegawa S. and Kato R., Nature Phys., (2010), 6, 673.

P-124

Numerical study of dynamical susceptibility in one dimensional trimerized spin systems

Keigo Hijii[1], Toru Sakai[2], Seiji Miyashita[3] and Hitoshi Ohta[1]

[1]*Molecular Photoscience Research Center, Kobe University, Kobe 657-8501, Japan*
[2]*Japan Atomic Energy Agency, Spring-8, Sayo, Hyogo, 679-5148, Japan*
[3]*Department of Physics, University of Tokyo, Bunkyo-ku, Tokyo, 113-0033, Japan*

E-mail: hijiik5@amethyst.kobe-u.ac.jp

Low dimensional quantum spin systems in low temperatures have attracted much attention in statistical, condensed matter physics and other research fields from both theoretical and experimental points of view, because, for example, their ground states are not necessarily ordered and sometimes have an exotic order because of quantum fluctuations and low dimensionalities. ESR is one of the most powerful experimental tools in such systems [1,2]. An advantage of ESR experiments is that ESR can determine an effective g-value. Recently, for ESR, not only experiments but also theories have progress. Theoretically there are mainly two developments. One is a direct numerical calculation based on the exact full diagonalization [3] and another is a field theoretical approach based on bosonization [4].

Composite quantum spin systems in low dimensions are interesting subjects related with novel quantum spin effects due to quantum fluctuations and low dimensionalities. Experimental results for $3CuCl_2$•2dx, which is a model material for S=1/2 trimerized chain [5], have been reported. Its magnetization curve is similar to one of the S=3/2 chain, however it shows a discrepancy from the S=3/2 chain [6,7]. This means that a composite spin system consisting three S=1/2 spins have more quantum nature than a simple S=3/2 system. And a temperature dependence of an effective g-value has been reported in high field ESR experiment [8]. This experiment suggests that this S=1/2 composite spin system is different from the genuine S=3/2 spin system. In order to understand this experimental prediction, we investigate a temperature dependence of the effective g-value within the linear response theory for the small cluster using direct numerical calculations aimed by the exact full diagonalization.

References

[1] Motokawa M., Ohta H., Nojiri N. and Kimura S., “The role of ESR in research of low-dimensional antiferromagnets”, J.Phys.Soc.Jpn. Suppl. B **2003**, 72, 1-11.
[2] Ajiro Y., “ESR Experiments on Quantum Spin Systems”, J.Phys.Soc.Jpn. Suppl. B **2003**, 72, 12-25.
[3] Miyashita S., Yoshino T. and Ogasawara A., “Direct Calculation of Dynamical Susceptibility in Strongly Fluctuating Quantum Spin Systems”, J.Phys.Soc.Jpn. **1999**, 68, 655-661.
[4] Oshikawa M. and Affleck I., “Low-Temperature Electron Spin Resonance Theory for Half-Integer Spin Antiferromagnetic Chains”, Phys.Rev.Lett. **1999**, 82, 5136-5139.
[5] Livermore J.C., Willett R.D., “Magnetic Exchange and Structure Relationships in Polymer Copper(II) Chloride-1,4-Dioxane (3:2)”, Gaura R.M. and Landee C.P., Inorg. Chem. **1982**, 21, 1403-1405.
[6] Zaspel C.E., “EXCHANGE CONSTANTS IN THE COPPER TRIMER SYSTEM $3CuCl_2$•2dx”, J.Mag.Mag.Mat. **1990**, 87, 90-92.
[7] Ajiro Y., Asano T., Inami T., Aruga-Katori H. and Goto T., “High-Field Magnetization of One-Dimensional S=1/2 Trimer System $3CuCl_2$•2dioxane”, J.Phys.Soc.Jpn. **1994**, 63, 859-862.
[8] Ajiro Y., Asano T., Nojiri H. and Motokawa M., “High Frequency ESR in Quantum Spin Trimer System”, JPS Meetings **1997**.

P-125

Magnetic Anisotropy of the Distorted-Diamond-Chain Compound $Cu_3(MoO_4)_2(OH)_2$

Shigeo Hara[1], Hirohiko Sato[2], Takahiro Sakurai[1], and Hitoshi Ohta[3]

[1]*Center for Supports to Research and Education Activities, Kobe University, Kobe 657-8501, Japan*
[2]*Department of Physics, Chuo University, Bunkyo-ku, Tokyo 112-8551, Japan*
[3]*Molecular Photoscience Research Center, Kobe University, Kobe 657-8501, Japan*

E-mail: hrsgo@crystal.kobe-u.ac.jp

Quantum spin system have been attracted the attention for a few decades. Especially, low dimensional quantum spin systems have been at the center of attention. We focus on a distorted diamond chain, which is one of the quasi one - dimensional chain systems formed corner sharing parallelogram plate, shown in Fig. 1. From the theoretical study suggests that there are three type ground stats, dimer, spin-fluid and ferrimagnetic are predicted by the difference in exchange interaction of J_i (i = 1, 2 or 3), on the S = 1/2 antiferromagnetic distorted diamond chain system [1]. In fact, on the study of typical S = 1/2 distorted diamond chain system of $Cu_3(CO_3)_2(OH)_2$ so called azurute one of the mineral, the report shows the experimental results on the magnetic and thermal properties, and this material has a spin-flued ground state and also a wide magnetization plateau at $M = M_s/3$ [2].

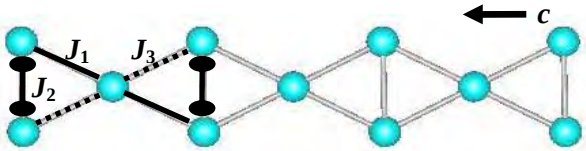

Fig. 1. Structure of the distorted diamond chain. There are three kinds of exchange interactions. Full lines denote the coupling J_1, dumbbell like lines the coupling J_2 and dotted lines the coupling J_3 [2].

Another typical distorted diamond chain system, containing S = 1/2 spins (Cu^{2+}) with antiferromagnetic exchange interaction, is $Cu_3(MoO_4)_2(OH)_2$ so called lindgrenite. This material is also one of the mineral. In our studies, Single crystals of $Cu_3(MoO_4)_2(OH)_2$ were synthesized by a hydrothermal method. The magnetic susceptibility detects a ferrimagnetic transition at approximately T_C = 12.5 K, below which a large anisotropy appears. Unlike the magnetic structure predicted from the neutron studies [3], the spin-easy axis slightly deviates from the c axis. The magnetization curves reveal that the magnetization plateaus appear on approximately forty percent of the saturated magnetization at 1.8 K. Furthermore, a step field-induced magnetic transition occurs in the magnetization curve under magnetic fields along the b axis. To investigate spin dynamics, X-band ESR measurements of single crystal $Cu_3(MoO_4)_2(OH)_2$ have been performed in the wide temperature range.

Fig. 2. Photo of single crystal s of $Cu_3(MoO_4)_2(OH)_2$.

References

[1] Okamoto K., Tonegawa T. and Kaburagi M., "Magnetic properties of the S = 1/2 distorted diamond chain at T = 0", J. Phys.: Condens. Matter **2003**, 15, 5979-5995.

[2] Kikuchi H., Fujii Y., Chiba M., Mitsudo S., Idehara T., Tonegawa T., Okamoto K., Sakai T., Kuwai T. and Ohta H., "Experimental Observation of the 1/3 Magnetization Plateau in theDiamond-Chain Compound $Cu_3(CO_3)_2(OH)_2$", Phys. Rev. Lett. **2005**, 94, 227201-4.

[3] Vilminot S., André G., Richard-Plouet M., Bouré-Vigneron F. and Kurmoo M., "Magnetic Structure and Magnetic Properties of Synthetic Lindgrenite, $Cu_3(MoO_4)_2(OH)_2$", Inorg. Chem. **2006**, 45, 10938-10946.

P-126

Molecular orientation and dynamics of NN radicals in organic 1D nanochannels

Hirokazu Kobayashi[1]

[1]*Department of Chemistry, College of Humanities and Sciences, Nihon University, Tokyo 156-8550, Japan*

E-mail:hirawk@chs.nihon-u.ac.jp

New inclusion compounds (ICs) were prepared using the organic 1D nanochannels of 2,4,6-tris(4-chlorophenoxy)-1,3,5-triazine (CLPOT) [1] as a nanosized template and nitronyl nitroxide (NN) radicals such as phenylnitronylnitroxide (PhNN) and *p*-nitrophenylnitronylnitroxide (*p*-NPNN) [2].

ESR measurements below 255 K for the CLPOT ICs diluted with spacer molecules such as *N*-phenyl maleimide (*N*-PhMI) gave rigid limit spectra (see Figure 1) similar to that for PhNN molecules in a glassy ethanol matrix at low temperature, which suggests isolation of the radical molecules. ESR measurements for them in the range of 290-400 K gave a modulated quintet ESR signal (Fig. 1), which suggested uniaxial rotational diffusion of NN radicals in the CLPOT nanochannels approximately around the principal *y*-axis of the *g*-tensors.

On the other hand, in the ESR measurements to 430 K for the [$(CLPOT)_2$-$(p\text{-NPNN})_{0.07}$] IC without spacers, the broader line width than the case in dilution was observed. This is assumed to be caused by inter-radical dipolar interaction in the CLPOT nanochannels.

In every case, the rotational diffusion activation energies of NN radicals in the CLPOT nanochannels were several times larger than those of 2,2,6,6-tetramethyl-1-piperidinyloxyl (TEMPO) radical derivatives (4-X-TEMPO) in CLPOT nanochannels [3]. This is expected due to the larger molecular size of NN radicals than 4-X-TEMPO or stronger interaction between NN radicals and the surrounding host or guest molecules.

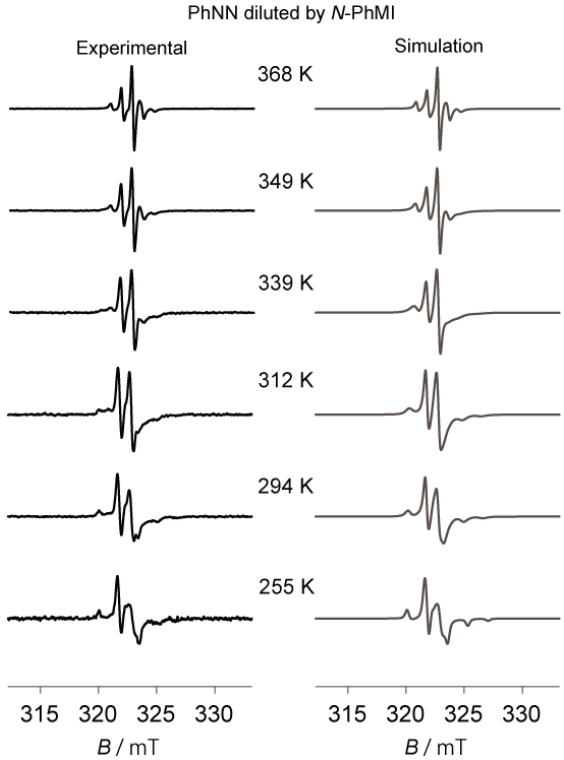

Figure 1.
Temperature dependence of experimental and reproduced ESR spectra (left and right, respectively) for [$(CLPOT)_2$-$(PhNN)_{0.01}$/$(N\text{-PhMI})_{0.50}$].

References

[1] Jetti R. K. R., Thallapally P. K., Xue F., Mak T. C. W. and Nangia A., "Hexagonal nanoporous host structures based on 2,4,6-tris-4-(halo-phenoxy)-1,3,5-triazines (halo = chloro, bromo), *Tetrahedron* **2000**, 56, 6707-6719.

[2] Kobayashi H., Morinaga Y., Fujimori E. and Asaji T., "ESR study of molecular orientation and dynamics of nitronyl nitroxide radicals in CLPOT 1D nanochannels", *to be submitted*.

[3] Kobayashi H., Asaji T. and Tani A., ESR study of the molecular orientation and dynamics of stable organic radicals included in the 1-D organic nanochannels of 2,4,6-tris-4-(chlorophenoxy)-1,3,5-triazine. *Magn. Reson. Chem.* **2012**, 50, 221-228.

P-127

Transient Nutation studies of nitroxide derivatives of fullerene C60

R.B. Zaripov[1], G.R. Nureeva[1,2], V.K. Voronkova[1], K.M. Salikhov[1], V.P. Gubskaya[3], I.A. Nuretdinov[3]

[1]*Zavoisky Physical-Technical Institute, Kazan, 420021, Russia*
[2]*Kazan Federal University, Kazan, 420008, Russia*
[3] *Arbuzov Institute of Organic and Physical Chemistry, Kazan, 420088, Russia*

E-mail: zaripov.ruslan@gmail.com

It is well known that nutation spectroscopy is a powerful technique to identify spin multiplicity. There are a few works were nutation spectroscopy help to obtain spin state of polyradical systems [1] and derivatives of fullerene [2].

In this work we start to study of a new kind of tetraradical derivatives of methano[60]fullerene. We apply pulse EPR technique in particular nutation spectroscopy to its study. Studies were provided at X and Q-bands with photo excitation and without it. At picture is shown two studied isomers of tetraradical adducts of methano[60]fullerene: equatorial (R1) and trans-3 (R2) (by Hirsh classification).

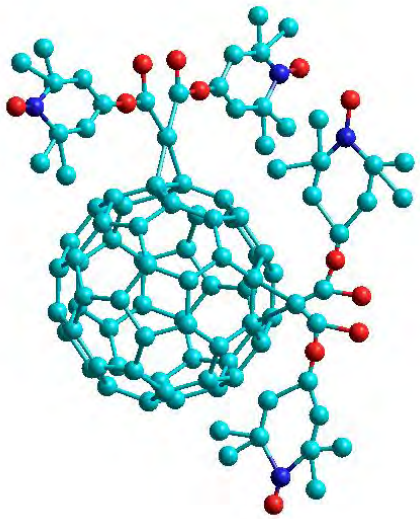

Equatorial isomer – R1

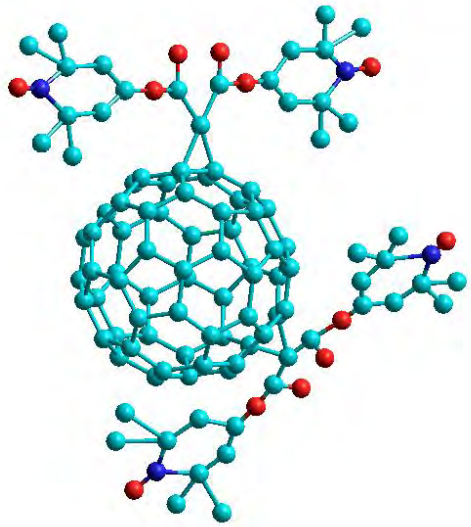

Trans-3 isomer – R2

Authors are grateful in part to the Russian Foundation for Basic Research (grant №. 12-03-97078) and President Grant for Government Support of Young Russian Scientists (grant №14.120.14.4957-MK) for financial support.

References

[1] Sawai T., Sato K., Ise T., Shiomi D., Toyota K., Morita Y., Takui T., “Macrocyclic High-Spin (S=2) Molecule: Spin Identification of a Sterically Rigid Metacyclophane-Based Nitroxide Tetraradical by Two-Dimensional Electron Spin Transient Nutation Spectroscopy”, Angew. Chem. Int. Ed. **2008**, V. 47, 3988-3990.

[2] Mizuochi N., Ohba Y. and Yamauchi S., “First Observation of the Photoexcited Quintet State in Fullerene Linked with Two Nitroxide Radicals”, *J. Phys. Chem. A* **1999**, 103, 7749-7752.

P-128

Time-Resolved and Pulse EPR of Zinc Porphyrin Trimer

Sukhanov Andrey[1], Voronkova Violeta[1], Mikhalitsyna Elena[2] and Tyurin Vladimir[2]

[1]*E. K. Zavoisky Physical -Technical Institute RAS, Sibirsky tract 10/7, Kazan, Russia*
[2]*A.N. Frumkin Institute of Physical Chemistry and Electrochemistry RAS, Leninskiy prospect 31-4, Moscow, Russia*

E-mail: ansukhanov@mail.ru

Conjugated porphyrin oligomers are one of the most extensively studied molecular systems due to their high chemical stabilities, strong electronic absorptions in the visible region, emissive properties of certain porphyrins, efficient energy and electron transfer reactions, nonlinear optical properties, and easily tunable optical properties [1-2]. In nature, the photosynthetic light-harvesting systems consist of well-organized porphyrin antennas in sophisticated three-dimensional structures.

The result of study of a molecular new system consisting of three conjugated molecules of zinc porphyrin is presented.

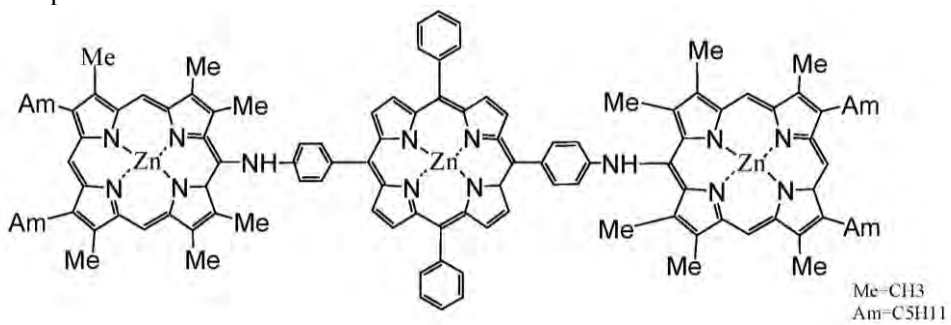

Three zinc porphyrin molecules located in one plane and two extreme molecules differ from the center molecule. Study was carried out for the frozen solution of this compound by CW time resolved (TR) and pulse EPR in X-and Q-bands after laser irradiation at a wavelength of 532 nm. EPR spectrum of this system differs from the characteristic spectrum of the zinc porphyrin monomer. This difference is especially observed in echo detected EPR spectra. Experimental CW TR EPR spectra were described by two triplet states with different values of zero field splitting parameters. Simulation of the EPR spectra was performed using Matlab toolbox 'EasySpin' [3].

References

[1] Aratani N., Kim D. and Osuka A., “Discrete cyclic porphyrin arrays as artificial light-harvesting antenna”, *Acc. Chem. Res.*, **2009**, 42, 1922-1934.
[2] Iyoda M., Yamakawa J.and Rahman M. J., “Conjugated macrocycles: concepts and applications” *Angew. Chem.: Int. Ed.*, **2011**, 50, 10522-10553
[3] Stoll S., Schweiger A., “EasySpin, a comprehensive software package for spectral simulation and analysis in EPR”, *J. Magn. Reson.*, **2006**, 178, 42-55.

Acknowledgments
We are grateful to *the Russian Foundation for Basic Research (project no.* 12-03-97078-p*)* and Division of Physical Science, RAS (II.4) for partial financial support.

P-129

Time-resolved EPR study on the Electronic Structure of the Excited Triplet State of [26] and [28]Hexaphyrins

Fumitoshi Ema[1], Atsuhiro Osuka[2], Mana Tanabe[3], Seigo Yamauchi[4], Takashi Tachikawa[1], and Yasuhiro Kobori[1]

[1]*Graduate School of Science, Kobe University, Kobe 657-8501, Japan*

[2]*Graduate School of Science, Kyoto University, Kyoto 606-8501, Japan*

[3]*Graduate School of Science, Tohoku University, Sendai 980-8578, Japan*

[4]*Institute of Multidisciplinary Research for Advanced Materials, Tohoku University, Sendai 980-8577, Japan*

E-mail: 145s207s@stu.kobe-u.ac.jp

【Abstract】Hexaphyrins are expanded porphyrins having larger macrocyclic structure with large expanded π-conjugated systems and are known to possess various redox states[1]. Especially, molecular structures and photophysical properties of the molecules with twisted Möbius topology have become of great interested in recent years. The electronic states of these molecules have been reported by theoretical methods to be influenced by their conformations. However, the photophysical properties based on the Hückel aromaticity and Möbius aromaticuty have not been investigated so much[2], and then the electronic structure of the excited states of molecules with twisted Möbius topology have not been clarified yet. In this study, the excited triplet states of Hückel aromatic planar rectangular [26]Hexaphyrin and Möbius aromatic twisted rectangular [28]Hexaphyrin were observed by using an X-band time-resolved EPR (TR-EPR) method. The spin distributions and the electronic structures of the excited triplet states will be experimentally clarified with respect to the directions of transition dipole moments of [26]Hexaphyrin and of [28]Hexaphyrin molecules, respectively.

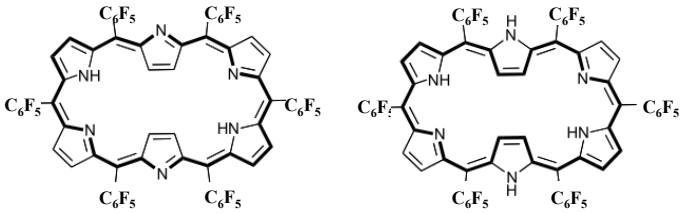

Figure 1. Molecular structures of (left) [26]Hexaphyrin and [28]Hexaphyrin, respectively.

【Experiment】[26]Hexaphyrin and [28]Hexaphyrin were dissolved in 2-Methyltetrahydrofuran (MTHF) and Toluene (Tol), respectively. These solutions were deoxygenated by the freeze-pump-thaw-cycle and were sealed in EPR sample tubes before the X-band TR-EPR measurements. These samples were excited by the nanosecond-pulsed OPO laser pumped by the 355 nm Nd:YAG laser system. The TR-EPR measurements were conducted without magnetic field modulation at 77 K. Excitation wavelengths were set from 568 nm to 635 nm by considering the directions of transition dipole moments of [26] and [28]Hexaphyrin molecules and their absorption wavelength.

【Results and Discussion】TR-EPR spectra shown in Figure 2 were obtained by exciting a transition dipole moment along the short axis of [28]Hexaphyrin molecule. These spectra show typical spectrum splitting (about 40 mT) due to spin dipole-dipole interaction and thus are assigned to the excited triplet state of [28]Hexaphyrin. Figure 2b and 2c exhibit the light-polarization effect on the fine structure. Spectrum simulation will be conducted to clarify the electronic structure of Hexaphyrin excited triplet states.

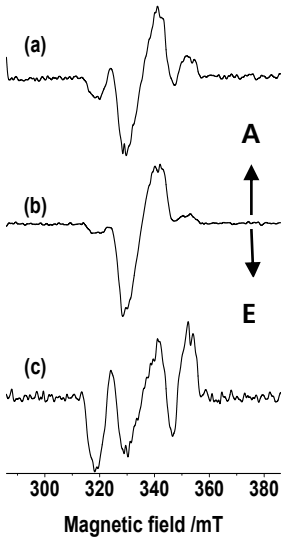

Figure 2. TR-EPR spectra of [28]Hexaphyrin observed in MTHF at 0.5 μs after 635 nm laser irradiation at 77 K. The laser light was (a) depolarized, (b) parallel, and (c) perpendicular to the external magnetic field, respectively.

[1] K. S. Kim, et al, *J. Phys. Chem. A*. **2009**, 113, 4498-4506

[2] M-C. Yoon, et al, *J. Phys. Chem. B*. **2011**, 115, 14928-14937

P-130

Rate constant measurements for addition reaction of radicals in early photopolymerization processes utilizing pulsed EPR method

Yusuke Miyake[1,2], Hirona Takahashi[1] and Akio Kawai[1]

[1]*Graduate School of Science and Technology, Tokyo Institute of Technology, Tokyo 152-8551, Japan*
[2] *Department of Biomolecular Engineering, Kyoto Institute of Technology, Kyoto 606-8585, Japan*

E-mail: y277miyake@gmail.com

Photopolymerization is initiated by the generation of radicals (R) from photoinitiators followed by subsequent addition reaction of R to monomers (M). For the development of useful radical photoinitiators, it is important to understand the dissociation processes of photoinitiators as well as the reactivity of radicals. In order to understand the reactivity of the radical photoinitiators, it is important to know rate constants for addition reactions of early photopolymerization processes. It has been reported that electron spin echo detection is a powerful method to determine rate constants of reaction between monomers and radicals generated by initial photodissociation.[1] In this study, rate constants k_1 and k_2 of two addition reactions in early processes, R + M → R-M$_1$ and R-M$_1$ + M → R-M$_2$, respectively, were determined for several pairs of photoinitiators and monomers by a pulsed EPR method with electron spin echo detection.

Figure (a) shows time-resolved EPR spectra recorded at 0.7 ～ 1.3 μs following laser excitation of an initiator, α-hydroxylcyclohexylphenylketone in toluene solution in the presence of a monomer, *tert*-butylacrylate (tBA) at different concentration. Peaks were assigned to ketyl radical (Ke) and benzoyl radical generated from photodissociation of the initiator, and Ke-(tBA)$_1$ radical generated from the first addition reaction. Intensity of the peaks assigned to the Ke-(tBA)$_1$ radical increase as tBA concentration becomes higher. In addition, peaks of Ke-(tBA)$_2$ radical generated from the secondary addition reaction were observed. This means peaks assigned to Ke, Ke-(tBA)$_1$ and Ke-(tBA)$_2$ radicals can be observed separately using EPR spectroscopy. The magnetic field was fixed at the field of the peak assigned to Ke-(tBA)$_1$, and echo signals were observed. Figure (b) shows echo signal decay for Ke-(tBA)$_1$ in the presence of 0.5 M tBA as a function of time delay between $\pi/2$ and π pulses observed by the electron spin echo method. Phase memory time (T_M) was determined by analysis of the decay curves. Dependence of T_M on concentration of tBA was analyzed according to Stern-Volmer plot, and the k_2 value for the addition reaction between Ke-(tBA)$_1$ and tBA was determined. The k_1 values for the addition reaction of Ke to other monomers were also determined in the similar procedure. At the conference, k_1 and k_2 values determined for several photoinitiators and monomers are compared. We will discuss how structures of the photoinitiators and monomers affect the first and secondary addition reactions.

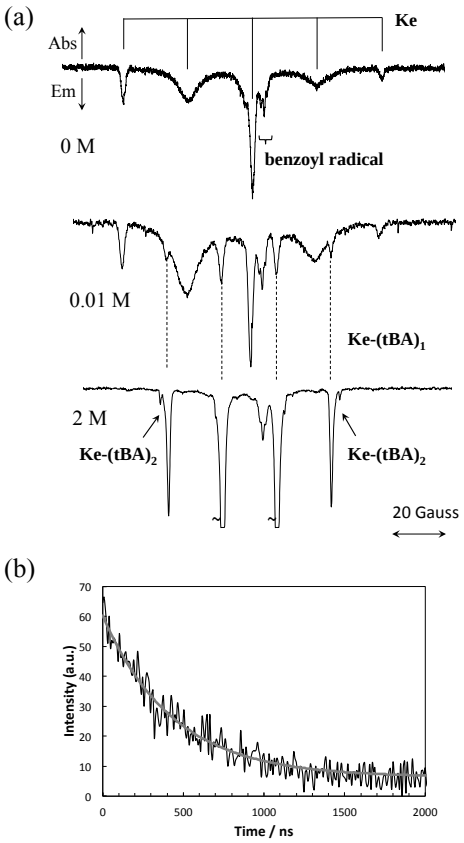

Figure (a) Time resolved EPR spectra for Ke in the presence of tBA at different concentration. (b) Temporal decay of electron spin echo signal for Ke-(tBA)$_1$.

References

[1] Weber A. and Turro N. J., "A Novel Approach for Measuring Absolute Rate Constants by Pulsed Electron Spin Resonance: Addition of Phosphinoyl and 2-Hydroxy-2-propyl Radicals to Several Alkenes", *J. Phys. Chem. A* **2003**, 107, 3326-3334.

P-131

Reaction Dynamics and Magnetic Field Effects in Cryptochromes and Photolyase

K. Maeda[1], J. G. Storey[2], K. B. Henbest[2], S. R. T. Neil[3], D. M. W. Sheppard[3], T. Biskup[4], K. Hitomi[5], E. D. Getzoff[5], E. Schleicher[4], S. Weber[4], S. R. Mackenzie[3], C. R. Timmel[2], P. J. Hore[3]

[1]*Department of Chemistry, Graduate School of Science and Engineering, Saitama University, Saitama 338-8570, Japan.*
[2]*Centre for Advanced Electron Spin Resonance & Inorganic Chemistry Laboratory, University of Oxford.*
[3]*Physical and Theoretical Chemistry Laboratory, University of Oxford.*
[4]*Institut für Physikalische Chemie, Albert-Ludwigs-Universität Freiburg.*
[5]*Department of Molecular Biology and the Skaggs Institute for Chemical Biology, The Scripps Research Institute.*
E-mail:kiminorimaeda @mail.saitama-u.ac.jp.

Blue-light photo-receptor proteins, in particular cryptochromes, have received attention recently as the most likely magnetoreceptors for the behavioral responses of various creatures to magnetic field. Here, we describe recent *in vitro* spectroscopic studies of the magnetic field effects (MFEs) on photochemically formed radicals in cryptochrome/photolyase family proteins, focusing on radical pair (RP) kinetics optimal for magnetoreception.

1) MFEs were observed for *E. coli* photolyase (*Ec*-PL), *Drosophila* Cryptochrome (*Dm*-CRY), and *Xenopus laevis* DASH-cryptochrome (*Xl*-CRY) using laser flash photolysis [1]. In all of the photoreactions, the transformation of [$FAD^{\bullet-}$ $TrpH^{\bullet+}$] (referred to as RP1) into [$FAD^{\bullet-}$ $Trp^{\bullet}$] (RP2) was identified. The RP1 is crucial for MFEs because it has active spin-selective back-electron transfer and RP2 lives long enough to preserve the MFE.

2) Recently we have developed cavity-based methods for measuring MFEs: cavity ring-down (CRD) and cavity enhanced (CE) spectroscopy [2]. The powerful capabilities of this technique, which includes sub-microsecond time-resolution, high sensitivity and small (μL) sample volumes, have the potential to allow studies of the magnetic sensitivity of highly dilute bio molecular samples.

3) The combined technique of CRD spectroscopy and nanosecond magnetic field switching (MFS) was applied to *Xl*-CRY [3]. CRD spectroscopy and MFS showed a much shorter lifetime (~100 ns) for RP1 than in *Dm*-CRY or *Ec*-PL. From a precise analysis, the singlet recombination rate constant (k_S) was found to be about 40 times faster than that of *Ec*-PL. This result indicates the remarkably wide tuning range of the reaction kinetics in different cryptochrome/photolyase proteins.

This work was funded in part by the EMF Biological Research Trust and DARPA.

References.

[1] Maeda, K.; Robinson, A.J.; et al. *Proc. Natl. Acad. Sci. USA* **2012,** *109,* 4774-4779.
[2] Maeda, K.; Neil, S.R.T.; et al. *J. Am. Chem. Soc.* **2011,** *133,* 17807-17815.
Neil, S.R.T.;Jing Li; et al. *J. Phys. Chem. B.* **2014,** 118 (15), 4177-4184.
[3] Biskup, T.; et al. *Ang. Chem. Int. Ed. Engl.* **2008,** *47,* 1-5.

P-132

Effect of glycerol concentration on structure of photoinduced charge-separated states in 9,10-anthraquinone-1-sulfonate-human serum albumin system

Masaki Tsushima[1], Masaaki Fuki[2], Taku Miura[1], Takashi Tachikawa [1]and Yasuhiro Kobori[1]

[1]*Graduarte School of Science, Kobe University, Kobe 657-8501, Japan*
[2] *Graduarte School of Science, Shizuoka University, Shizuoka 422-8017, Japan*

E-mail: 135s230s@stu.kobe-u.ac.jp

In photosynthesis and DNA restoration, proteins play crucial roles on the light-energy conversions to generate the reaction intermediates that transfer electrons or holes. It is therefore important to analyze the conformations of these intermediates. For the analysis, we have used time-resolved electron paramagnetic resonance (TREPR) method[1]. For the low-temperature analysis, glycerol has often been added to the protein solutions. It is known that glycerol prevents a protein denaturation or aggregation. However it is not well known how the glycerol affects the conformations and the hydration structure of proteins. In this study, we prepared protein-ligand solutions of 9,10-anthraquinone-sulfonate ion ($AQ1S^-$ in Figure 1a) bound to human serum albumin (HSA) to clarify the glycerol concentration effect on the conformation of the photoinduced charge-separate state.

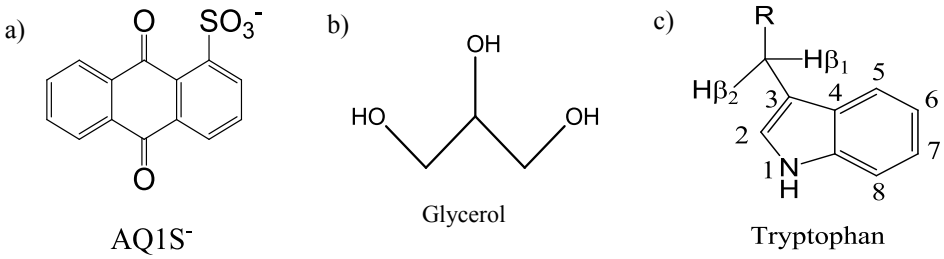

Figure 1. Structure formula of a) 9,10-anthraquinone-1-sulfonate (AQ1S), b) glycerol and c) tryptophan

HSA-$AQ1S^-$ aqueous solution and glycerol were mixed with volume ratios of 3:7 5:5 and 7:3. Concentrations of $AQ1S^-$ and HSA were 3 mM for each. Figure 2 shows enlarged TREPR spectra at the center-field region for each sample at 77 K. These signals are mainly contributed from the distant charge-separated states of $AQ1S^{2-\cdot}$-$Trp214^{+\cdot}$. It has been seen that, as the glycerol concentration is increased, the peak width of the central signal becomes sharper. This means that the spin-spin dipole coupling (*D*) is decreased, denoting that the distance between $AQ1S^{2-\cdot}$ and $Trp214^{+\cdot}$ becomes larger by the glycerol addition. It is known that glycerol molecules surround the protein molecules and stabilize the protein hydration structure. It is thus concluded that the hydration structure is modulated by the glycerol concentration. To obtain details of the structures, we have observed the magnetophotoselection effects on the TPEPR spectra. We simulated the TREPR spectra by the triplet spin polarization transfer model[1,2] and analyzed the conformation of the charge-separated states.

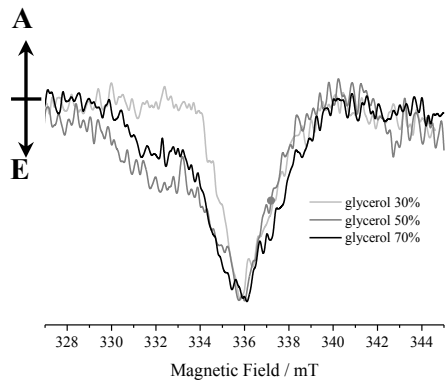

Figure 2. Effect of the glycerol concentration on the TREPR spectra of the $AQ1S^-$-HSA systems at 1 μs after laser irradiation at 77 K. Glycerol concentrations are 30 % (light gray), 50 % (gray) and 70 % (black) with the volume ratios..

[1] Y.Kobori, M.Fuki, *J. Am. Chem. Soc*. **2011**, 133, 16770-16773.
[2] Y. Kobori, M. Fuki, H. Murai, *J. Phys. Chem. B*, **2010**, 114, 14621-14630.

P-133

Solvent effects on dynamic electron polarization produced through the radical quenching of photoexcited triplet states of organic dyes

Toshihiro Tamura, Hirona Takahashi and Akio Kawai

Department of Chemistry, Graduate School of Science and Engineering, Tokyo Institute of Technology, Tokyo 152-8551, Japan

E-mail: tamura.t.af@m.titech.ac.jp

Nitroxide radicals have been widely used for spin probe method in EPR spectroscopy. Although spin probing is powerful in various applications, low sensitivity in aqueous solutions due to dielectric loss gives serious disadvantage. We pay attention to making use of dynamic electron polarization (DEP), which is produced through the relaxation of photoexcited triplet state by radical, for light control of EPR signal intensity. For this purpose, it is of great importance to understand what factors contribute to DEP generation. Previously, we found EPR signal deviation in water due to large DEP generated by the light irradiation towards xanthene dye in the presence of nitroxide. In this study, we determined the DEP magnitude for various triplet dyes－TEMPO systems in water and alcohol solvents by using pulsed and time-resolved (TR) EPR technique and discuss the solvent effects on DEP generation.

Figure 1 shows time profiles of FID intensity observed under 355 nm laser irradiation to Rose bengal － 2,2,6,6-tetramethylpiperidine 1-oxyl (TEMPO) mixture in solutions. In water, dynamical change of intensity was observed immediately after laser shot at time=0. This originates from DEP of TEMPO due to photophysical events including quenching process. This large signal deviation indicates a potential to control EPR signal by light irradiation. In contrast to this observation, the present study found no DEP generation in ethanol as shown in Figure 1. To confirm the DEP of TEMPO in ethanol is small, TR EPR measurements, which is suitable for detecting small DEP signal, was carried out. As a result, small DEP was indeed observed in ethanol, although its quantitative evaluation is difficult.

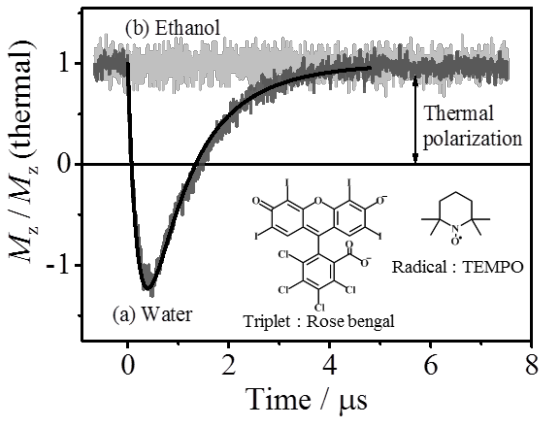

Figure 1 Time profiles of FID intensity measured under 355 nm laser irradiation to Rose Bengal (1.0 mM)－TEMPO (0.2 mM) system in two solvents, (a) water (b)ethanol

Figure 2 shows Stern-Volmer plots for decay of triplet Rose Bengal in each solvents determined by transient absorption spectroscopy. Slope of the best-fitted linear line gives quenching rate constant (k_q). The k_q in ethanol is 38 times smaller than that in water. This indicates dominant quenching mechanism must be different, which can also influence DEP generation.

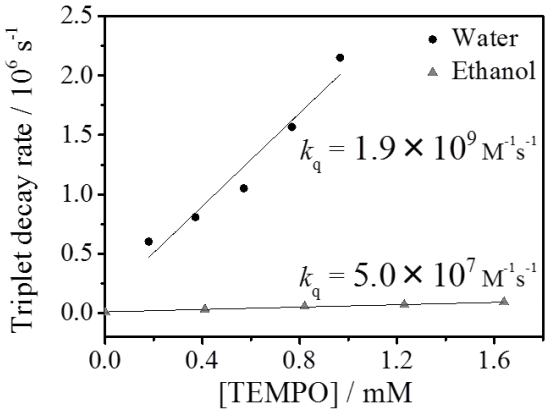

Figure 2 Stern-Volmer plots for water and ethanol solutions for Rose bengal－TEMPO system.

Similar measurements were carried out for several organic dyes and solvent effects on DEP generation are discussed in terms of the free energy change of intermediate states of dye－TEMPO pairs.

P-134

Study on Magnetic Anisotropy and Slow Magnetization Relaxation of a Gadolinium(III)-Radical Complex

Takuya Kanetomo[1], Hiroyuki Nojiri[2] and Takayuki Ishida[1]

[1]*Department of Engineering Science, The University of Electro-Communications, Tokyo, Japan*
[2]*Institute of Materials Research, Tohoku University, Sendai, Japan*

E-mail: ishi@pc.uec.ac.jp

The Gd^{III} compounds rarely exhibit magnetic anisotropy [1], because Gd^{III} ions have the isotropic electron configuration ($^8F_{7/2}$). In this work, we prepared a Gd^{III}-radical compound (a 4f-2p spin system). The Gd^{III}-radical family is expected to show strong exchange coupling in comparison with those of any other 4f-based coordination compounds. No Gd^{III} compound has been reported so far, where strong exchange coupling and magnetic anisotropy are both involved. Our purpose is to investigate a possible relation between the magnetic anisotropy and exchange coupling in Gd^{III}–radical compounds.

We selected the bipyridine(bpy)-based nitroxide radical, 6bpyNO (2,2'-bipyridin-6-yl *t*-butyl nitroxide), and actually $[Gd^{III}(hfac)_3(6bpyNO)]$ (**Gd-6bpyNO**, Fig.1) exhibited considerably strong exchange coupling with $2J/k_B$ = -15.9(2) K [2]. We measured HF-EPR and alternating current (AC) magnetic susceptibility. Fig. 2(a) shows selected EPR spectra. We can find the zero-field splitting of **Gd-6bpyNO**, owing to the anisotropy of the Gd^{III} ion regulated with crystal field and/or exchange coupling. We also found slow magnetization relaxation of **Gd-6bpyNO** (Fig. 2(b)). However, the frequency dependence of the out-of-phase component (χ_m") is not typical of 4f-based SMMs. The peak positions are almost constant in a high frequency region (10000 – 3000 Hz). We will discuss possible origin of the unusual χ_m" frequency dependence.

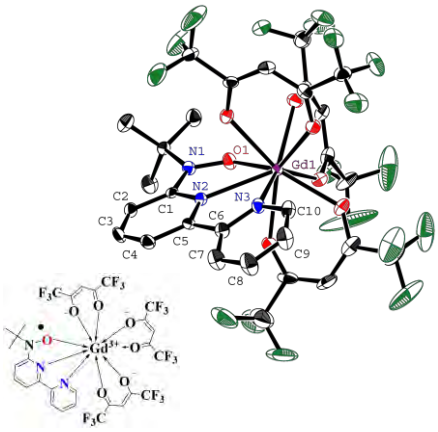

Fig. 1. X-ray structure of **Gd-6bpyNO**.

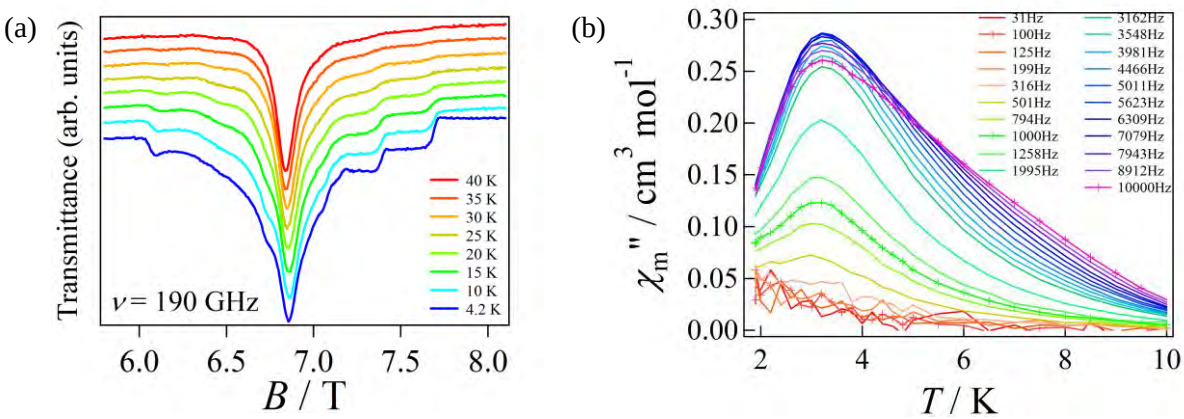

Fig. 2. (a) Temperature dependence of EPR spectra of **Gd-6bpyNO** measured at 190 GHz. (b) AC susceptibility of **Gd-6bpyNO** measured at H_{DC} = 2000 Oe. χ" represents the out-of-phase component.

References

[1] M. J. Martinez-Pérez, S. Cardona-Serra, C. Schlegel, F. Moro, P. J. Alonso, H. Prima-Garcia, J. M. Clemente-Juan, M. Evangelisti, A. Gaita-Ariño, J. Sesé, J. van Sigeren, E. Coronado and F. Luis, *Phys. Rev. Lett.* **2012**, *108*, 247213.

[2] T. Kanetomo and T. Ishida, *Inorg. Chem.* submitted.

P-135

Sub-micron flavin radical and magnetic field effect based imaging

Jonathan R. Woodward, Joshua P. Beardmore

Graduate School of Arts and Sciences, University of Tokyo,
3-8-1 Komaba, Meguro, Tokyo 153-8902, Japan

E-mail: woodward@global.c.u-tokyo.ac.jp

Magnetic Field Effects (MFEs) on the rates and yields of reactions involving radical pairs have been extensively studied (e.g. [1,2]). In recent years, there has been considerable interest in MFEs in biological systems, particularly in the context of animal navigation where cryptochrome photochemistry is strongly implicated [3]. We present here preliminary results from our newly constructed Magnetic Field Effect Microscope (MFEM), which is capable of observing magnetic fields on photochemical reactions with submicron spatial resolution and can be used to study MFEs in living cells.

The photoreaction of flavin adenine dinucleotide (FAD) at low pH is employed as a benchmark system, as it displays a magnetic field sensitive concentration of flavin semiquinone radicals when irradiated with blue light [4]. FAD molecules are photoexcited using a diode laser at 449 nm and the resulting flavin semiquinone radicals, which result from an intramolecular electron transfer from the adenine moiety of the same molecule, can be monitored by their optical absorbance at 532 nm, by means of a second diode laser. Spatial resolution is obtained through the use of twin apochromatic objective lenses of high numerical aperture in a transmission confocal arrangement. Methods employed to achieve high levels of sensitivity in an absorption based microscope are presented along with the challenges of incorporating magnetic field coils capable of providing AC+DC magnetic fields to the sample.

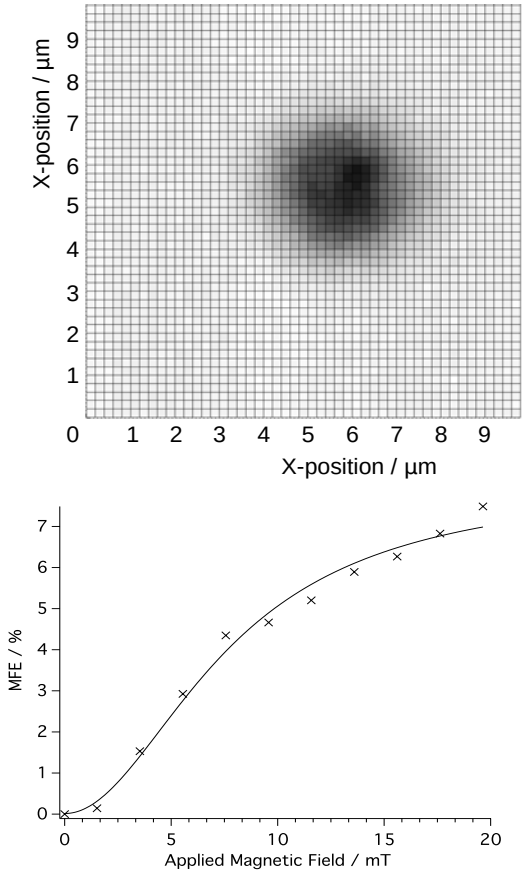

Figure 1. a) Flavin semiquinone radical signal image of a 2.5 µm polystyrene bead in a 0.2 mM solution of FAD in pH3.3 buffer. b) Magnetic field dependence of the signal in the light region of figure 1a.

Figure 1a is an image obtained using the absorption signal from transient flavin semiquinone radicals produced by the photoexcitation of FAD in a 125 µm thick sample. The dark region of the image is a coated 2.5 µm polystyrene bead. Figure 1b shows the magnetic field dependence of the signal obtained from the light region of the image in figure 1a.

References

[1] Steiner, U. E. and T. Ulrich, T., "Magnetic field effects in chemical kinetics and related phenomena", *Chem. Rev.* **1989**, 89, 51-147.

[2] Woodward, J. R., Foster, T. J., Jones, A. R., Salaoru, A. T., and Scrutton, N. S., "Time-resolved studies of radical pairs", *Biochem. Soc. Trans.*, **2009**, *37*, 358–362.

[3] Dodson, C. A., Hore, P. J., & Wallace, M. I., "A radical sense of direction: signalling and mechanism in cryptochrome magnetoreception", *TIBS*, **2013**, *38*(9), 435–446.

[4] Murakami, M., Maeda, K., & Arai, T., "Dynamics of intramolecular electron transfer reaction of FAD studied by magnetic field effects on transient absorption spectra", *J. Phys. Chem. A.*, **2005**, *109*(26), 5793–5800.

Author Index

ABE	Jun	P-95
ABOELEZZ	Eslam	IL-3
AÇıKGÖZ	Muhammed	P-61
AHLBERG	Sebastian	P-21
AHMAD	Rizwan	IL-16
AHOKAS	Janne	OP-6
AIHARA	Tomoki	P-96, P-97
AKAISHI	Satomi	P-85
AKIMOYO	Ikuko	P-88
ALFONSOV	Alexey	P-68
AMBE	Christopher	IL-21, P-85
ANURADHA	K.N.	P-67, P-70, P-76
AOI	Rina	P-12
AOKI	Ichio	P-55
ARAI	Munehito	P-95
ARAKAWA	Sho	P-114
ARATA	Toshiaki	P-7, P-96, P-97 P-98
ARIMA	Takahisa	P-114
ARNDT	Sophia	P-21
ASAMI	Tsubasa	OP-2
ASANO	Motoko	OP-2
BAGRYANSKAYA	Elena	PL-4, P-41, P-60
BAKER	William	OP-13
BANNWARTH	Christoph	IL-13
BARANOV	Pavel	P-109
BARTH	Eugene	IL-8
BARTH	Katja	P-99
BEARDMORE	Joshua	P-135
BERLINER	Lawrence	PL-5
BHAGYASHREE	K.S.	P-67, P-69, P-70, P-76
BHAT	S.V.	P-67, P-69, P-70, P-76
BISKUP	Till	P-131
BITTL	Robert	P-2
BLANK	Aharon	IL-14
BODZIONY	Tomasz	P-62
BOEHME	Christoph	OP-13
BOLTON	David	PL-3
BOSE	Muthukumaran	P-64
BOUSSAC	Alain	IES-AL-5
BRITT	Ralph	IES-AL-1
BROWN	Kristen	IL-2
BROWN	Louise	IL-12
BÜCHNER	Berndt	P-68
BUD'KO	Sergey	P-105
CAFISO	David	P-99
CANFIELD	Paul	P-105
CARR	Cody	OP-14
CHAKOUR	Mohammed	OP-11
CHAKRABORTY	Rusha	OP-11
CHEN	Chen	OP-11
CHEN	Long	P-87
CHENG	Chiyuan	IL-9
CHIANG	Yun-Wei	P-90
CHO	Hyun Jin	P-83
CHO	Jamghoon	P-8
COMBA	Peter	IL-17
CONCILIO	Maria Grazia	P-3
CORDINA	Nicole	IL-12
COX	Nicholas	IES-AL-5
CRUICKSHANK	Paul	PL-3
CUTSAIL	George	OP-14
DAIMON	Hiroki	P-7
DANOS	Andrew	OP-13
DASU	Alexandru	OP-7
DENYSENKOV	Vasyl	PL-6
DEVASAHAYAM	Nallathamby	IL-15
DI MAURO	Eduardo	P-24, P-73
DONAHUE	Matthew	IL-25
DOVALIL	Nina	IL-17
DREW	Simon	P-4
DU	Jiangfeng	APES-YSA-1
DZUBA	Sergei	IL-24
EDUARDO	Di Mauro	P-37
EL MKAMI	Hassane	PL-3, P-92
ELAS	Martyna	IL-8
EL-KHODARY	Alaa	IL-3
ELLINGSEN	Pål	P-58
ELMASRY	Fatma	SEST-EPA-1
EMA	Fumitoshi	P-129
ENOMOTO	Ayano	OP-8, P-39
ENRICA	Bordignon	P-99
EPEL	Boris	IL-8
ERDEM	Oezlen	P-110
ETO	Hinako	P-16
FEDIN	Matvey	P-41, P-60
FEINTUCH	Akiva	IL-10
FELIPE	Benatti	P-37
FIELDING	Alistair	P-3
FLEIGE	Emanuel	P-2
FLOOD	Ann	PL-8
FLUHR	Robert	IL-14
FRANCK	John	IL-9
FREED	Jack	PL-7
FRIEDRICH	Annette	P-21
FU	Hua	IL-23, P-22
FU	Zhebin	SEST-EPA-4
FUCHAROEN	Suthat	IL-7
FUJI	Risa	P-26

FUJII	Hirotada	SEST-AL-2
FUJII	Yutaka	OP-6, P-15, OP-12
FUJISAKI	Shingo	P-30
FUJISAWA	Masashi	P-122
FUJITA	Kaori	P-75
FUJIWARA	Toshimichi	OP-10
FUJIWARA	Yasufumi	SEST-EPA-1
FUKI	Masaaki	P-132
FUKUDA	Akira	P-15
FUKUZUMI	Shunichi	SEST-EPA-3
FURUI	Takanori	P-103
FURUKAWA	Ko	P-20, P-72, P-87
FURUTANI-UMEZU	Nozomi	P-98
GABRIENKO	Anton	P-60
GADISETTI	Chandramouli	IL-15
GAHAN	Lawrence	IL-17
GAZZONI	Bruna	P-37
GETZOFF	Elizabeth	P-131
GHOSH	Ashutosh	OP-18
GHOSH	Soumavo	OP-18
GILLIES	Robert	P-57
GNUTEK	Paweł	P-61
GOLDFARB	Daniella	IL-10
GORODETSKY	Artem	P-52
GOVEAS	Lora	P-67, P-70
GRIMME	Stefan	IL-13
GRINBERG	Oleg	PL-8
GROMILOV	Sergey	P-60
GUBSKAYA	Valentina	P-127
GUEDES	Carmen	P-24, P-37, P-73
GURIN	Alexander	P-109
GUSTAFSSON	Håkan	OP-7, P-58
GWAK	Minchan	OP-6, P-15
HAAG	Rainer	P-2
HAAG	Stefan	P-2, P-21
HAGIWARA	Masayuki	P-107, P-113, P-119, P-120
HALLBECK	Martin	P-58
HALPERN	Howard	IL-8
HAMILTON	Alex	P-89
HAN	Songi	IL-9
HANSON	Graeme	IL-17
HANUZA	Jerzy	P-62
HARA	Hideyuki	P-74
HARA	Shigeo	P-38, P-114, P-115, P-116, P-117, P-122, P-125
HARADA	Etsuko	P-25
HARIMA	Yutaka	P-86
HART	Charles	P-57
HASEGAWA	Masashi	P-80, P-93
HASHEM	Mada	IL-14
HASSAN	Gamal	IL-3
HATTORI	Gen	P-31
HAYASE	Shuji	P-80
HELD	Martin	P-99
HIJII	Keigo	OP-5, P-124
HILL	Stephen	IES-AL-3
HINDERBERGER	Dariush	OP-11, P-91
HIRAOKA	Wakako	P-6, P-26 P-27
HIRATA	Ayako	P-29
HIRATA	Hiroshi	OP-8, P-39, P-40, P-47
HIROI	Zenji	P-116
HITOMI	Kenichi	P-131
HOFFMAN	Brian	OP-14
HÖGER	Sigurd	IL-13
HONDA	Zentaro	P-113
HORE	Peter	P-131
HORIMOTO	Takuya	P-7
HORITANI	Masaki	OP-14
HOSOKOSHI	Yuko	IL-6, P-120
HOVAV	Yonatan	IL-10
HUNG	Yang	P-117
HUNTER	Robert	PL-3
HYODO	Fuminori	P-16, P-53
ICHIKAWA	Kazuhiro	P-53
ICKEN	Niels	P-2
IDA	Yumi	OP-18
IDEHARA	Toshitaka	OP-10
IDOTA	Eiji	P-121
IKAWA	Satoshi	OP-3
IKEDA	Shohei	P-117
IKEGAMI	Toru	P-34
IKOMA	Tadaaki	IL-21, SEST-EPA-5, P-81, P-85
IMAE	Ichiro	P-86
INANAMI	Osamu	P-54
INDU	S.	OP-11
INOUE	Toshimitsu	P-34
IRISOVA	Irina	P-59
IRITANI	Kensuke	P-107
ISAEV	Nicolay	IL-24
ISE	Tomoaki	P-101
ISHIDA	Takayuki	OP-18, P-134
ISHII	Tatsuya	P-40
ISHIKAWA	Akiho	P-48, P-51
ITABASHI	Tetsuya	P-95
ITAKURA	Asuka	P-12
ITO	Shinji	P-16
IVANOV	Mikhail	P-41
IVANSHIN	Vladimir	P-105
IVASHITA	Flávio	P-73

IWAMA	Kazuya	P-6
IWASAWA	Atsuo	P-35, P-36
IWASE	Kenji	IL-6, P-120
JÄRVINEN	Jarno	OP-6
JEON	Gi Wan	P-82, P-83
JESCHKE	Gunnar	P-99
JIA	Shuang	P-105
JIANG	Donglin	P-87
JIANG	Min	IL-23, P-22
JIN	Shangbin	P-87
JOSEPH	Benesh	P-99
KACZMAREK	Sławomir	P-62
KAGAWA	Akinori	OP-9, P-100
KAJIWARA	Atsushi	P-11, P-12, P-13, P-32, P-33
KAKUO	Wakana	P-13
KALE	Ajay	OP-7
KAMADA	Tadashi	P-55
KAMEYA	Hiromi	P-25, P-75
KANAORI	Kenji	P-31, P-34, P-42
KANETOMO	Takuya	P-134
KANNO	Tomomi	P-25
KANZAKI	Yuki	P-79
KARBOWIAK	Mirosław	OP-19
KASHIWAGI	Takanari	P-113
KATAEV	Vladislav	IL-5
KATO	Asuka	P-26, P-27
KATO	Hiroyuki	P-27
KATO	Reizo	P-43, P-123
KATO	Tatsuhisa	P-78
KAWAI	Akio	OP-1, SEST-EPA-4, P-130, P-133
KAWAMORI	Moeko	P-103
KAWASAKI	Kohei	P-44, P-45
KAY	Christopher	IL-11
KE	Shyue-Chu	P-23
KEEVERS	Thomas	OP-13
KIDA	Takanori	P-107
KIDA	Takashi	P-120
KIHATARA	Yoko	P-116
KIKUCHI	Hikomitsu	P-15
KILDEMO	Morten	P-58
KIM	Do Wan	P-82, P-83
KIM	Sun Hee	P-9
KIMIYA	Kouki	OP-15
KIMURA	Shojiro	P-113, P-119
KIRILYUK	Igor	P-52
KISHIMOTO	Shun	P-57
KITAGAWA	Masahiro	OP-9, P-100, P-101, P-104, P-106
KITAHARA	Yoko	P-122
KITANO	Katsuhisa	OP-3
KLINMAN	Judith	OP-14
KOBAYASHI	Hirokazu	P-126
KOBAYASHI	Ryoma	P-16
KOBAYASHI	Satoshi	P-111
KOBAYASHI	Yuka	P-72
KOBORI	Yasuhiro	OP-17, P-80, P-84, P-93, P-129, P-132
KOHNO	Masahiro	P-35, P-36
KOINUMA	Wataru	P-94
KOLEY	Aditya	P-64
KOLOKOLOV	Daniil	P-60
KOMAGUCHI	Kenji	P-86
KOMAROV	Denis	P-52
KOMAROVSKIKH	Andrey	P-63
KONG	Xi	APES-YSA-1
KONOV	Konstantin	IL-24
KOOLIVAND	Amir	P-10
KOSEM	Nuttavut	P-53
KOTHE	Gerd	IL-20
KOURA	Haruko	P-26
KOZAKI	Masatoshi	P-103
KRISHNA	Murali	IL-15, P-54, P-57
KRUMMENACKER	Jan	PL-6
KRZYANIAK	Matthew	IL-2
KUPPUSAMY	Periannan	IL-14
KUPRIYANOV	Igor	P-63
KURATSU	Masato	P-103
KURODA	Shin-ichi	SEST-AL-1, P-66
KUSRAYEV	Yurij	P-109
KUWABARA	Naoyuki	P-7
KUZNETSOV	Gennady	P-41
LABRUYERE	Stephane	OP-16
LADEMANN	Jürgen	P-2, P-21
LAFLAMME	Raymond	OP-16
LAI	Yei-Chen	P-90
LALMUANPUII	Rebecca	P-112
LAUER	Anna	P-21
LEE	Cheol Eui	P-82, P-83
LEE	Hong-In	P-8
LEE	Kyu Won	P-82, P-83
LEE	SangGap	OP-6, P-15
LEE	Soonchil	OP-6, P-15
LENIEC	Grzegorz	P-62
LEONOV	Dmitry	IL-24
LI	Yong	IL-23, P-22
LILLEDAHL	Magnus	P-58
LIN	Tien-Sung	IL-20
LINDGREN	Mikael	P-58
LINK	Gerhard	IL-20
LITVINOVA	Tatyana	P-105
LIU	Yangping	IL-16

LOHAN	Silke	P-2, P-21
LUBITZ	Wolfgang	IL-1, IES-AL-5, P-110
LUKASCHEK	Michail	IL-20
LUND	Anders	OP-7
MABUCHI	Yuumi	P-13
MACALIK	Lucyna	P-62
MACKENZIE	Stuart	P-131
MAEDA	KIMINORI	P-131
MAEDA	Tetsuya	P-86
MAEDER	Marcel	IL-17
MAITY	Amarendra	P-23
MALISSA	Hans	OP-13
MAREK	Antonin	P-10
MARUMOTO	Kazuhiro	IL-22
MARUTA	Shinsaku	P-98
MATOBA	Ryosuke	P-32
MATSUBARA	Akira	P-15
MATSUBAYASHI	Kazuyuki	P-43, P-44, P-45
MATSUI	Ryosuke	P-43, P-44
MATSUKI	Yoh	OP-10
MATSUMOTO	Ken-ichiro	P-30, P-55
MATSUMOTO	Shingo	IL-15, P-54, P-57
MATSUMURA	Yuriko	P-35, P-36
MATSUO	Masayuki	P-57
MATSUOKA	Hideto	IL-13
MATSUOKA	Yuki	P-20
MATSUOKA	Yuta	SEST-EPA-3
MATSUSHITA	Kazunobu	OP-15
MATSUZAWA	Satoshi	P-118
MCCAMEY	Dane	OP-13, P-89
MCCRAKEN	John	P-112
MCKAY	Johannes	PL-3, P-92
MEINKE	Martina	P-2, P-21
MICHAEL	Stevens	PL-3
MIGITA	Catharina	OP-15
MIKHALITSYNA	Elena	P-128
MIKI	Masao	P-97
MIKUNI	Susumu	P-121
MINAKAWA	Satoko	P-1
MINO	Hiroyuki	SEST-EPA-2,P-93, P-94
MITCHELL	James	P-57
MITSUDO	Seitaro	OP-6, OP-12, P-15
MIURA	Hiroshi	OP-15
MIURA	Taku	P-80, P-84, P-132
MIURA	Tomoaki	IES-AL-6, OP-17, SEST-EPA-5, P-85
MIWA	Shinji	P-111
MIYAHARA	Hidekazu	P-35, P-36
MIYAKE	Norio	OP-15
MIYAKE	Yusuke	P-34, P-47, P-130
MIYASHITA	Seiji	P-124
MIYAZAKI	Kousuke	P-80
MIZUOCHI	Norikazu	P-111
MIZUSAKI	Takao	OP-6, P-15
MOEBIUS	Klaus	PL-1
MOR	Avishai	IL-14
MORALES	Noppawan	IL-7, P-53
MORIMOTO	Kazuya	P-15
MORISHITA	Hiroki	P-111
MORITA	Yasushi	OP-9, P-101, P-104
MOSCA	Dante	P-73
MOTION	Claire	PL-3
MURAI	Hisao	SEST-EPA-4
MURUGESAN	Velayutham	P-112
MUTOH	Masato	P-26, P-27
NADOLINNY	Vladimir	P-41, P-63
NAGASHIMA	Hiroki	SEST-EPA-2
NAGATA	Takuro	P-29
NAKAGAWA	Kouichi	OP-4, P-1
NAKAGAWA	Seiko	P-17
NAKAJIMA	Akira	P-42
NAKAJIMA	Hiroki	P-11, P-12, P-13
NAKAJIMA	Yoshiki	SEST-EPA-2
NAKAMURA	Masaya	P-78
NAKAMURA	Mizuki	P-55
NAKAMURA	Shinji	OP-10
NAKAMURA	Toshikazu	P-20, P-72, P-87, P-95
NAKATSUJI	Satoru	P-107
NAKAYAMA	Ken-ichi	SEST-EPA-5
NAKAZAWA	Shigeaki	P-101, P-102, P-103, P-104
NAMOZOV	Barot	P-109
NARUOKA	Akira	SEST-EPA-4
NAWA	Kazuhiro	P-116
NAWA	Omi	P-27
NEESE	Frank	IES-AL-5
NEGORO	Makoto	OP-9, P-100
NEIL	Simon	P-131
NEUGEBAUER	Petr	PL-6
NISHIDA	Naoya	P-54
NISHIDA	Shinsuke	OP-9, P-101, P-104
NISHIHARA	Yuko	P-34
NOJIRI	Hiroyuki	OP-18, P-108, P-118, P-134
NORMAN	David	PL-3, P-92
NUREEVA	Gulina	P-127
NURETDINOV	Ildus	P-127
OAKLEY	Richard	IES-AL-3
OFFENBACHER	Adam	OP-14
OGAWA	Yukihiro	P-30
OGOMI	Yuhei	P-80
OHBA	Yasunori	P-95

OHKUBO	Kei	SEST-EPA-3
OHMICHI	Eiji	P-38, P-45, P-46, P-48, P-50, P-51, P-68
OHSHIMA	Tomoko	OP-3
OHSUKA	Atsuhiro	P-129
OHTA	Hitoshi	SEST-EPA-1, OP-5, P-38, P-43, P-44, P-45, P-46, P-48, P-50, P-51, P-68, P-108, P-114, P-115, P-116, P-117, P-122, P-124, P-125
OHTABU	Hiroshi	SEST-EPA-3
OKADA	Keiji	P-103
OKAHASHI	Mai	P-11
OKAMOTO	Tsubasa	P-46, P-51
OKAMOTO	Yoshihiro	P-116
OKAYAMA	Ryota	P-86
OKAZAKI	Shoko	P-29
OKINO	Akitoshi	P-35, P-36
OKUBO	Susumu	SEST-EPA-1, OP-5, P-38, P-43, P-44, P-45, P-108, P-114, P-115, P-116, P-117, P-122
OKUTANI	Akira	P-119
OMAR	Ahmad	P-68
OMORI	Takuya	SEST-EPA-5, P-81
OMUKAI	Kosuke	P-103
ONDA	Haruto	P-6
ONO	Toshio	IL-6, P-120
OSADA	Akira	P-19
OSAWA	Toshihiko	P-25
OSHIKAWA	Masaki	PL-2
OSHIMA	Yugo	SEST-AL-3, P-123
OUYANG	Z. W.	P-108
OZAWA	Yoshikazu	P-55
PAESANO JR.	Andrea	P-73
PALYANOV	Yury	P-63
PANTAZIS	Dimitrios	IES-AL-5
PARK	Daniel	OP-16
PAUL	Daly	P-76
PELIZZARI	Charles	IL-8
PERIYAKARUPPAN	Manoharan	P-64
PETERS	Brian	P-68
PICCINATO	Marilene	P-24, P-73
PIETRASZKO	Adam	P-62
POTLURI	Phani	IL-12
PRISNER	Thomas	PL-6, P-99
RAHIMI DARABAD	Robabeh	OP-16
RAHIMI	Robabeh	P-104
RAJENDRA	Muthukumaran	P-112
RAKVIN	Boris	P-71
RANJITH	S	P-69
REDLER	Gage	IL-8
REICHENWALLNER	Jörg	OP-11, P-91
REINHARD	Friedemann	APES-YSA-1
RETEGAN	Marius	IES-AL-5
ROBERG	Karin	OP-7
ROBERTSON	Duncan	PL-3
RÖCK	Lisa	IL-13
RODIONOV	Aleksander	P-59
ROMANOV	Nikolay	P-109
RUAN	M. Y.	P-108
RUDOWICZ	Czesław	OP-19, P-61
RUGG	Brandon	IL-2
SAENKO	Nikita	P-65
SAGDEEV	Renad	P-60
SAITO	Keita	IL-15
SAITO	Keita	P-54, P-57
SAITO	Mitsuru	P-114
SAITO	Tadaaki	P-15
SAKAI	Kiyoshi	APES-YSA-2
SAKAI	Toru	OP-5, P-124
SAKURAI	Hiroya	P-117
SAKURAI	Takahiro	P-38, P-43, P-44, P-45, P-114, P-115, P-116, P-117, P-122, P-125
SALIKHOV	Kev	IES-AL-2, P-127
SAMBANDAM	Balaji	P-64
SAMOUILOV	Alexandre	IL-16
SARKAR	Shuranjan	P-8
SARVEZUK	Paulo	P-73
SASAKI	Moe	SEST-EPA-4
SASAKI	Yota	P-36
SATO	Hirohiko	P-125
SATO	Kazunobu	OP-16, P-101, P-102, P-103, P-104, P-106, P-79
SATO	Rina	SEST-EPA-4
SAWAI	Takatoshi	P-28
SAWAMURA	Daisuke	P-1
SCHIEMANN	Olav	IL-13
SCHLEICHER	Erik	P-131
SEE	Andrew	P-89
SEKIGUCHI	Masayuki	P-17
SEKIYA	Takao	P-88
SELMKE	Benjamin	OP-11
SHARAF	Mokhtar	IL-3
SHELUDYAKOV	Sergey	OP-6
SHEN	Jian-Ren	SEST-EPA-2
SHEPPARD	Dean	P-131
SHEVELEVA	Alena	P-60

SHI	Fazhan	APES-YSA-1
SHIBATA	Sayaka	P-55
SHIMIZU	Yuki	P-11
SHIMON	Daphna	IL-10
SHIOMI	Daisuke	P-79, P-101, P-102, P-103, P-104, P-106
SHIROUZU	Tomonori	SEST-EPA-3, P-56
SHOGOMORI	Yusuke	P-29
SHUNDRINA	Inna	P-60
SHUNSUKE	Tatsumi	P-79
SIAW	Tingann	IL-9
SIDABRAS	Jason	PL-8
SIKORA	Arthur	P-99
SIRIGIRI	Jagadishwar	OP-10
SKIBIŃSKI	Tomasz	P-62
SKRYLNIK	Peter	P-77
SLOOP	David	IL-20
SMIRNOV	Alex	IL-25, P-10
SMIRNOVA	Tatyana	IL-25
SMITH	Graham	PL-3, P-92
SMITH	Lund	IL-9
SOMIYA	Takakazu	P-96
STAUDACHER	Tobias	APES-YSA-1
STEPANOV	Alexander	P-60
STEVENS	Michael	P-92
STOREY	Jonathan	P-131
SUBRAMANIAN	Sankaran	IL-15
SUDA	Masayuki	P-43
SUGISAKI	Kenji	P-79, P-101, P-102, P-103, P-106
SUGIURA	Ken-ichi	OP-2
SUGIYAMA	Junichi	P-75
SUKHANOV	Andrey	P-128
SUNG	Tai-Ching	P-90
SUZUKI	Mayu	P-18
SUZUKI	Shuichi	P-103
SUZUKI	Yoshishige	P-111
SWARTS	Steven	PL-8
SWARTZ	Harold	PL-8
TABUCHI	Yutaka	P-100
TABUSE	Ryo	P-50, P-51
TACHIKAWA	Takashi	P-80, P-84, P-93
TACHIMOTO	Isamu	P-31
TADOKORO	Makoto	P-79
TAJIMA	Kunihiko	P-31, P-34, P-42
TAKADA	Masashi	IL-4, P-19
TAKAHASHI	Hirona	OP-1, P-130, P-133
TAKAHASHI	Satoshi	P-95
TAKAHASHI	Wataru	P-47
TAKAKUSAGI	Yoichi	P-57
TAKAMATSU	Toshihiro	P-35, P-36
TAKEMOTO	Megumi	P-29
TAKESHITA	Keizo	P-29
TAKEUCHI	Tetsuya	P-107, P-119
TAKUI	Takeji	OP-16, P-79, P-101, P-102, P-103, P-104, P-106
TAMURA	Toshihiro	P-133
TANABE	Mana	P-129
TANAKA	Ayaka	P-101, P-104
TANAKA	Hidekazu	P-122
TANAKA	Hiroaki	P-27
TANAKA	Hisaaki	P-66
TANAKA	Toshihiro	OP-12
TANAKA	Yuma	P-12
TANI	Atsushi	OP-3
TANIJIMA	Shuuhei	P-100
TATEISHI	Kenichiro	OP-9
TATEMATSU	Yoshinori	OP-10
TATSUMI	Tetsuya	P-33
TATSUTA	Takahiro	P-121
TAYURSKII	Dmitry	P-59
TERAUCHI	Takeshi	P-72
TEUTLOFF	Christian	P-2
THEISON	Sandra	OP-11
THIRUNAVUKKUARASU	Komalavalli	IES-AL-3
TIMMEL	Christiane	P-131
TING	Kao	P-117
TODORIKI	Setsuko	P-75
TOLMACHEV	Danil	P-109
TOMIDUKA	Kazuhito	OP-2
TORMYSHEV	Victor	IL-8
TOYOTA	Kazuo	P-79, P-101, P-102, P-103, P-104, P-106
TROMMER	Wolfgang	OP-11
TSAI	Chia-Jung	P-90
TSUMURAYA	Takao	P-123
TSUSHIMA	Masaki	P-93, P-132
TSUTA	Mizuki	P-75
TUN	Xin	P-14
TUSIMOTO	Yoshihiro	P-115
TYURIN	Vladimir	P-128
UCHIKOSHI	Teturo	P-115
UEDA	Keisuke	P-97
UEDA	Yasuhiro	P-7, P-97
UEHARA	Kodai	P-36
UEKI	Shoji	P-96, P-97
UENO	Megumi	P-55
UENO	Tomohiro	P-15
UKAI	Mitsuko	P-25
UMEGAKI	Chihiro	OP-12
UNBEHAUEN	Michael	P-2

UTSUMI	Hideo	P-16, P-53
UWATOKO	Yoshiya	P-43, P-44, P-45
VALEZI	Daniel	P-37, P-73
VAN DER EST	Art	OP-2
VAN TOL	Johan	IES-AL-4
VARADARAJAN	Raghavan	OP-11
VARALDA	J	P-73
VASILIEV	Sergey	OP-6, P-15
VEBER	Sergey	P-41
VEGA	Shimon	IL-10
VLASENKO	Leonid	OP-6
VORONKOVA	Violeta	P-127, P-128
VOYNOV	Maxim	IL-25, P-10
WAKASA	Masanobu	P-49
WAKIKAWA	Yusuke	IL-21, SEST-EPA-5, P-81, P-85
WANG	Pengfei	APES-YSA-1
WASIELEWSKI	Michael	IL-2
WATANABE	Kazuo	P-113
WATANABE	Shun	P-66
WATANABE	Yosuke	P-35
WEBER	Stefan	P-131
WEICHSELBAUM	Ralph	IL-8
WEIDNER	Jörg-Ulrich	IL-20
WESTPHAL	Michael	IL-17
WILLIAMS	Benjamin	PL-8
WINTER	Stephen	IES-AL-3
WOJTKOWIAK	Jonathan	P-57
WOODWARD	Jonathan	P-135
WRACHTRUP	Joerg	IL-18, APES-YSA-1
WURMEHL	Sabine	P-68
WYLDE	Richard	PL-3
YAGAI	Shiki	IL-21
YAGI	Masahiro	P-6
YAGO	Tomoaki	IL-20, SEST-AL-4, P-49
YAMADA	Ken-ichi	APES-YSA-2, SEST-EPA-3, P-14, P-55, P-56
YAMADA	Masafumi	P-98
YAMAGUCHI	Hironori	IL-6, P-113, P-120
YAMAGUCHI	Tomoko	P-31, P-34, P-42
YAMAGUCHI	Yoji	P-28
YAMAGUCHI	Yuji	SEST-EPA-5
YAMAMORI	Tohru	P-54
YAMAMOTO	Akie	P-97
YAMAMOTO	Kumiko	P-25
YAMAMOTO	Naoto	P-42
YAMAMOTO	Satoru	P-102
YAMANAKA	Chihiro	P-18, P-19
YAMANE	Takeshi	P-79
YAMANONT	Paveena	IL-7
YAMASAKI	Hitoshi	P-121
YAMASAKI	Toshihide	APES-YSA-2, SEST-EPA-3, P-56
YAMASHITA	Hiroaki	P-96
YAMASHITA	Ken-ichi	OP-2
YAMASHITA	Tomoyuki	P-42
YAMAUCHI	Seigo	P-95, P-129
YAMAURA	Kazunari	P-115
YANAGI	Takanori	P-98
YANG	Fengyuan	P-68
YANG	Haijun	IL-23, P-22
YAP	Yung Szen	P-100
YASUDA	Satoshi	P-7, P-98
YASUI	Hironobu	P-54
YASUKAWA	Keiji	P-14, P-16, P-53
YONAMOTO	Yoshiki	P-5
YOSHIDA	Syota	P-115, P-122
YOSHINO	Tomohiro	P-101, P-104
YOSHIZAWA	Daichi	P-107
YOSHIZAWA	Makoto	P-79
YUSUPOV	Roman	P-59
ZACHRISSON	Helene	P-58
ZARIPOV	Ruslan	P-127
ZHAO	Chenchao	P-96
ZIATDINOV	Albert	P-65, P-77
ZVEZDOV	Denis	OP-6
ZWEIER	Jay	IL-16